LNCIS
Lecture Notes in Control and Information Sciences
352

John Chiasson
Jean Jacques Loiseau (Eds.)

Applications of Time Delay Systems

Springer

Lecture Notes
in Control and Information Sciences 352

Editors: M. Thoma, M. Morari

John Chiasson, Jean Jacques Loiseau (Eds.)

Applications of Time Delay Systems

Springer

Editors

John Chiasson

ECE Department
Boise State University
1910 University Dr.
Boise ID 83725-2100
USA
Email: johnchiasson@boisestate.edu

Jean Jacques Loiseau

IRCCyN, UMR CNRS 6597
Ecole Centrale de Nantes
1 rue de la Noë, BP 92101
44321 Nantes
France
Email: Jean-Jacques.Loiseau@irccyn.ec-nantes.fr

Library of Congress Control Number: 2006938337

ISSN print edition: 0170-8643
ISSN electronic edition: 1610-7411
ISBN-10 3-540-49555-X Springer Berlin Heidelberg New York
ISBN-13 978-3-540-49555-0 Springer Berlin Heidelberg New York

Typesetting: by the authors and SPS using a Springer LaTeX macro package

Printed on acid-free paper SPIN: 11596882 89/SPS 5 4 3 2 1 0

Aux gens qui sont toujours en retard

Preface

Delays are very important for the modeling of networks, occuring both in the control of networks and in the control over networks. The main objective is to develop feedback control strategies for minimizing the overall task completion time in the presence of delays. Such applications include load balancing, teleoperation, and congestion control. As a result, research on time-delay systems and their control has been very active in the last decade. This interest has led to many sessions in control conferences (ACC, CDC, IFAC), workshops, special issues in control and systems journals, books and edited books, all being devoted to time-delay systems. Nowadays, a lot of material is available. The properties of differential time-delay systems, including stability, robust stability, controllability, and observability have been thoroughly examined. Many different methods for the design of controllers in the presence of time-delays have also been developed to meet various kinds of specifications such as tracking, disturbance rejection, H_∞/H_2-optimization, and robust stabilization. These approaches were formulated for various classes of time-delay systems, including linear time-invariant systems, nonlinear systems, retarded and neutral type systems, localized and distributed delay systems, and systems with input/state saturation. It is fair to say that the applications of these methods are not as developed as are the theoretical foundations. Numerical tools are still under development (e.g. there is no matlab toolbox devoted to time-delay systems), and the adaptation of models and methods to specific applications is now an active area of research. The aim of this book is to give an update of the latest research in this direction.

The book is organized into six parts: Network control, Teleoperation, Emerging methodologies, New computational methods, Predictors, inversion and filtering, and Merging saturations and input delays.

Boise, Nantes,
September 2006

John Chiasson
Jean Jacques Loiseau

Contents

Part I

Network Control

Delay–Based Non–linear Observers for Congestion Control in Communication Networks

Henri-François Raynaud, Fabienne Floret, and Caroline Kulcsár

L2TI – Institut Galilée, Université Paris 13, 99 Av. J.-B. Clément,
93430 Villetaneuse, France
{raynaud,fabienne.floret,caroline.kulcsar}@l2ti.univ-paris13.fr

1 Introduction

The purpose of this contribution is to investigate the construction and use of delay-based observers in communication networks, starting from a state-space model of an elementary network configuration. This work is a step towards the design of a source-rate congestion and delay control algorithm adapted to applications with real-time constraints, such as video streaming. Our ultimate aim is to design an "end to end" control scheme implemented at source level, using only feedback information from the destinations transmitted through the network as part of the general "best effort" data stream, and which could therefore be deployed on essentially every existing network infrastructure, especially those ruled by the Internet Protocol. Obviously, observer-based control structures provide an appropriate conceptual framework to deal with such measurement constraints. In this particular application, we propose to combine a linear state-feedback plus disturbance feedforward control with a non-linear observer of network congestion fed with measurements of source-to-destination transmission delay.

Before explaining in more details the specific challenge which applications with real-time constraints pose for congestion control design, we would like to point out that our approach to transmission delays in communication networks is somewhat at variance with the traditional treatment of delays in control theory, and therefore in most of the other contributions in this book. In the traditional control-theory approach, delays are regarded as intrinsic features of the dynamic systems under consideration. As a consequence, delays can be modelled as linear, albeit somewhat complicated and possibly time-varying, subsystems inserted into the control loop – to which are then applied appropriate extensions of standard control theory tools and procedures. This most convenient arrangement is of course predicated upon the assumption that delays are not affected by control inputs.

This critical assumption no longer holds true in digital packet-switching communication networks. In this class of applications, the transmission delays experienced by data packets *en route* through various network sections depend both on the congestion of associated buffers and on the history of source data rates. Clearly, modelling such "congestion delays" as distinct linear subsystems would

J. Chiasson and J.J. Loiseau (Eds.): Appl. of Time Delay Systems, LNCIS 352, pp. 3–15 , 2007.
springerlink.com

be, at best, a rough approximation. Instead, pursuing the approach in [9, 10, 11], we choose here to model them as system outputs, *i.e.* as deterministic functions of some suitably defined internal state.

2 Congestion Control for Network Applications with Real-Time Constraints

Managing congestion by rationing available bandwidth between competing users is a critical part of operating all communication networks. In telephone networks, the main mechanism for managing congestion is admission control: only when enough bandwidth is available along the way up to the destination does your call "get through" – a familiar memory for people old enough to remember the days where bandwidth was really scarce. However, the introduction of packet-switching technology, where data streams are broken into autonomous packets which are then tossed separately, and possibly through different routes, into the network, rendered admission control both largely impractical and inefficient. Instead, network designers quickly realized that the proper way to manage congestion was through source rate control, which can be broadly defined as mechanisms compelling sources to respond to relevant congestion signals transmitted back from the network by lowering their data throughput.

Source control should obviously take into account the specifics of those applications the network is designed to support. In computer networks such as Internet, an application of special importance is file transfer, where data integrity is paramount. As a result, any data transfer protocol designed for file transfer needs to include an acknowledgement and re–emission procedure which, in turn, induces a positive (*i.e.* perverse) feedback loop, possibly leading to total "congestion collapse". The most popular source rate control procedure for file transfer is the Transport Control Protocol (TCP), designed in the late 1980's by Van Jacobson [7], which is a critical part of the Internet machinery.

However, TCP is notoriously ill–suited to applications with real–time constraints, such as video streaming, see [6]. Indeed, to avoid network congestions, the TCP sender adjusts its rate according to the AIMD strategy (Additive Increase/Multiplicative Decrease), [7]. As a consequence, the sending rate computed by AIMD undergoes high variations, incompatible with a suitable video streaming. Therefore, video streaming is usually based on UDP (User Data Protocol). An UDP sender keeps its sending rate constant even in a congested environment while a TCP sender decreases its rate in an attempt to eliminate congestion. This predicament is thus unfair for the TCP stream and can lead to its depletion, hindering the coexistence of the two classes of data streams over the same network. To solve this TCP–friendliness problem, it is necessary to define appropriate rules for sending rates in non–TCP sources. One possible approach is to modify the AIMD mechanism by adjusting the rate for a video stream. The Rate Adaptation Protocol (RAP) [12] is computed as the AIMD protocol. The RAP source receives feedback information on congestion in the bottleneck and makes decision about its sending rate. In the spirit of RAP, the

control of the SR–RTP [4] reduces the window size proportionally to the Square Root of its value. The Stream Control Transmission Protocol – SCTP [16] – supporting multi-streaming is also based on the classical AIMD strategy. The Loss-Delay Based Adaptation Algorithm – LDA$^+$ [14] – relies on the RTCP feedback messages based on the RTP protocol [13]. LDA$^+$ uses the AIMD strategy but decrease and increase of the window size are dynamically adjusted to network conditions thanks to feedback information. The TCP–Friendly Rate Control Protocol – TFRC [5], [8] – is derived from the TCP New Reno in particular. This algorithm maintains the sending rate at the level of a TCP flow under the same conditions while providing sufficient responsiveness to competing traffic. Thus, the congestion control procedures in [4], [12], [14], [16] propose to adjust the congestion window size with respect to this kind of application. But TCP could be unfair in the case of large RTTs (Round Trip Time), as shown in [1].

Alternatively, some recent works propose to add over the UDP protocol a congestion control layer, not directly derived from the AIMD strategy. In [2], the Video Transport Protocol (VTP) is proposed in order to adapt the outgoing video stream to the network and to maximize the quality of the MPEG-4 video. VTP is based on bandwidth estimation which is transmitted to the sender to adapt its sending rate.

Another approach consists in modelling the TCP flow by differential equations. The network could be considered as an input/output system where the inputs are the sending rates and the outputs are the effective streams. Since a congestion implies a delay, one obtains a dynamical system where classical control theory can be used. To highlight the relevance of applying control theory to congested communication networks, [15] and all references therein propose a state-of-the-art of this recent research field.

3 State-Space Model and "Full Information" Control for a Simple Network

This contribution will focus on an elementary network building block made up of a single router connected to a buffered link, with one source S and one destination D (Fig. 1). Defining t as the number of some fixed sampling period ΔT, the discrete-time model for this system is

$$c(t+1) = c(t) + \Delta T \left(u(t) - l(t) - b(t) \right) \ , \tag{1}$$

where $c\,(t)$ is the buffer congestion at time t, $b(t)$ the average effective link bandwidth over the sampling interval $[t\Delta T, (t+1)\Delta T]$, while $u\,(t)$ and $l\,(t)$ denote respectively the average rates of packet emission by the source and packet loss rate during $[t\Delta T, (t+1)\Delta T]$.

It should be noted that this balance sheet equation provides an *exact* description of this discrete time system's dynamics. (On the other hand, it obviously does not enable to predict what happens *between* two sampling instants.) In addition, it is assumed that the packets are stored in a First–In, First–Out (FIFO)

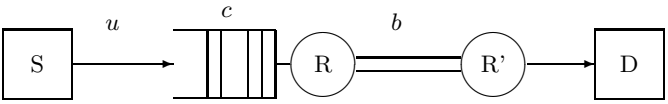

Fig. 1. Single link network topology

buffer. In that case, packets cannot be lost once they have managed to enter the buffer, through which they are then pushed in a orderly, piston-like manner, until they eventually exit. As a result, the effective rate of packet admission in the buffer during $[t\Delta T, (t+1)\Delta T]$ is

$$e\,(t) = u(t) - l(t)\,, \tag{2}$$

and the congestion delay $d\,(t)$, which is defined as the total time packets exiting at time t have spent into the buffer, can be computed from

$$d(t) = \min\left\{ d > 0 \text{ such that } \Delta T \sum_{s=1}^{d} e(t-s) \geq c(t) \right\}\,. \tag{3}$$

We now proceed to define the state of the system as the collection of all the information that, together with $u\,(t)$, $b\,(t)$ and $l\,(t)$, needs to be stored at time t in order to compute both $c\,(t+1)$ and $d\,(t)$. Assuming with no loss of generality that $d \leq d_M$, an adequate choice of state is the vector with $n = d_M + 1$ coordinates

$$x\,(t) = \begin{pmatrix} x_1\,(t) \\ x_2\,(t) \\ x_3\,(t) \\ \vdots \\ x_n\,(t) \end{pmatrix} = \begin{pmatrix} c\,(t) \\ e\,(t-1) \\ e\,(t-2) \\ \vdots \\ e\,(t+1-n) \end{pmatrix} = \begin{pmatrix} c\,(t) \\ u(t-1) - l(t-1) \\ u(t-2) - l(t-2) \\ \vdots \\ u(t+1-n) - l(t+1-n) \end{pmatrix}\,. \tag{4}$$

It is immediately checked that equations (1) and (3) can be rewritten as a *linear state transition* with control u, where b and l appear as disturbance inputs, coupled with a *non-linear observation* equation:

$$x\,(t+1) = Ax\,(t) + B\,(u\,(t) - l\,(t)) + \Gamma b\,(t)\,, \tag{5}$$

$$d\,(t) = h\,(x\,(t))\;, \tag{6}$$

where

$$A = \begin{pmatrix} 1\,0\,0\cdots 0\,0 \\ 0\,0\,0\cdots 0\,0 \\ 0\,1\,0\cdots 0\,0 \\ 0\,0\,1\cdots 0\,0 \\ \vdots\;\vdots\;\vdots\;\ddots\;\vdots\;\vdots \\ 0\,0\,0\cdots 1\,0 \end{pmatrix}\,, \qquad B = \begin{pmatrix} \Delta T \\ 1 \\ 0 \\ \vdots \\ 0 \end{pmatrix}\,, \qquad \Gamma = \begin{pmatrix} -\Delta T \\ 0 \\ 0 \\ \vdots \\ 0 \end{pmatrix}\,, \tag{7}$$

$$h\left(x\right) = \min\left\{ d > 0 \text{ such that } \Delta T \sum_{s=1}^{d} x_{s+1}(t) \geq x_1(t) \right\} . \tag{8}$$

Clearly, in the "full information" scenario where measurements of b, l and x are assumed to be available in real time, this system with linear dynamics could be controlled by applying standard linear state–space procedures. More precisely, if (u^r, x^r) is a reference trajectory for the state transition equation (5), *i.e.* a solution of

$$x^r\left(t+1\right) = Ax^r\left(t\right) + B\left(u^r\left(t\right) - l\left(t\right)\right) + \Gamma b\left(t\right) , \tag{9}$$

then a feedforward plus feedback control in the form

$$u = u^r - K\left(x - x^r\right) , \tag{10}$$

where $(A - BK)$ is a stability matrix, would drive the tracking error $\Delta x = x - x^r$ towards zero. When the loss rate l and the effective link bandwidth b can be predicted with sufficient accuracy, it follows immediately from (9) that a control reference u^r can be constructed from any buffer congestion trajectory c^r by setting

$$u^r(t) = \frac{c^r(t+1) - c^r(t)}{\Delta T} + l(t) + b(t) . \tag{11}$$

As for the control gain K, a simple choice is of course

$$K = \begin{pmatrix} k & 0 & \cdots & 0 \end{pmatrix} , \tag{12}$$

with $0 < k < 1$, which yields for the tracking error $\Delta c = c - c^r$ the closed-loop dynamics

$$\Delta c\left(t+1\right) = \left(1-k\right)\Delta c\left(t\right) . \tag{13}$$

Several corollaries and extensions can be derived from this basic result, and have been presented in [11]. To quote but the most important:

- For a suitable choice of the feedback gain K, convergence of the tracking error can be guaranteed in the presence of input saturation;
- When future values of b are available at time t, the reference trajectory can be constructed in order to achieve constant transmission delay d;
- All convergence results extend to the case where a fixed control delay is inserted into the loop;
- When only delayed measurements of the buffer congestion c are available in real time, the state feedback plus feedforward control can be replaced by a standard linear observer-based output feedback.

4 Delay-Based Observer of Buffer Congestion: Simple Case

In practice, standard network protocols are not designed to relay even delayed measurements of buffer congestion. However, it is always possible to instruct the destination to send acknowledgement messages back to the source. In the sequel,

we shall make the additional assumption that the source and the destination can agree on a sufficiently precise common time reference (that is, sufficiently precise relatively to the sampling period at which the controller is designed to operate). This can be achieved either through direct access to an external time reference (for example through the GPS system), or by a synchronization mechanism embedded in the network itself, such as the Network Time Protocol (for a discussion of recent developments around this clock synchronization problem over the Internet, see [17] and the references therein).

Under these assumptions, a sensible way to estimate buffer congestion is to construct an observer using the delay as the measured output. For the sake of clarity, we shall deal first with the (unrealistic) case where measurements of d, b and l are available at source level in real time. In this case, such an observer would be in the form

$$\widehat{c}(t+1) = \widehat{c}(t) + \Delta T\left(u\left(t\right) - l\left(t\right) - b\left(t\right)\right) + \lambda\left(t\right)\left(d\left(t\right) - \widehat{d}\left(t\right)\right) \tag{14}$$

$$= \widehat{c}(t) + \Delta T\left(e\left(t\right) - b\left(t\right)\right) + \lambda\left(t\right)\left(d\left(t\right) - \widehat{d}\left(t\right)\right) \ , \tag{15}$$

where $\widehat{d}$ is the predicted value of d obtained by plugging $\widehat{c}$ and the past measurements of e into the observation equation (3), *i.e.*

$$\widehat{d}\left(t\right) = h_t\left(\widehat{c}(t)\right) = \min\left\{d > 0 \text{ such that } \Delta T\sum_{s=1}^{d} e\left(t-s\right) \geq \widehat{c}\left(t\right)\right\} \ . \tag{16}$$

Proceeding from now on in the customary fashion, we introduce the estimation and prediction errors as

$$\widetilde{c}(t) = c\left(t\right) - \widehat{c}(t) \ , \tag{17}$$

$$\widetilde{d}(t) = d\left(t\right) - \widehat{d}(t) \ . \tag{18}$$

Since the state transition equation (1) is linear, the dynamics of the estimation error are given by

$$\widetilde{c}(t+1) = \widetilde{c}(t) - \lambda\left(t\right)\widetilde{d}(t) \ . \tag{19}$$

The next question is how to select the observer gain $\lambda\left(t\right)$ so that the estimation error decreases, hopefully toward zero. Because the observation function h_t is piecewise constant, it turns out that the best that can be achieved is to make $\widetilde{c}$ decrease only up to a threshold which depends on the "effective" source rate $e = u - l$. More precisely, we prove the following proposition:

Proposition 1. *Let $\lambda^*\left(t\right) \geq 0$ be defined as*

$$\lambda^*\left(t\right) = 0 \quad \textit{if } \left|\widetilde{d}(t)\right| \leq 1 \ , \tag{20}$$

$$\lambda^*\left(t\right) = \frac{2\left(\widetilde{d}(t) - 1\right)\Delta T e_m}{\widetilde{d}(t)} \quad \textit{if } \widetilde{d}(t) \geq 2 \ , \tag{21}$$

$$\lambda^*\left(t\right) = \frac{2\left(\widetilde{d}(t) + 1\right)\Delta T e_M}{\widetilde{d}(t)} \quad \textit{if } \widetilde{d}(t) \leq -2 \ . \tag{22}$$

Assume that the effective admission rate $e(t)$ verifies a condition in the form

$$e_m \leq e(t) \leq e_M \ . \tag{23}$$

Then for all $\lambda\,(t)$ in the range $0 < \lambda\,(t) \leq \lambda^*\,(t)$ (with $\lambda(t) = 0$ when $\lambda^*(t) = 0$), the estimation error $\widetilde{c}\,(t)$ decreases monotonously towards the neighbourhood of zero $[-2\Delta T e_M, 2\Delta T e_M]$.

Proof of Proposition 1
The proof is conducted in two parts. In the first step, we proceed to derive appropriate lower and upper bounds for the estimation error $\widetilde{c}(t)$ depending on whether $\widetilde{d}(t)$ takes positive or negative values or is close to zero. In a second part, we prove that the estimation error $\widetilde{c}(t)$ is non–increasing for all possible values of the prediction error $\widetilde{d}$ by using an appropriate Lyapunov function.

One can notice that the prediction error $\widetilde{d}(t)$ can only be equal to integer values (positive or negative). To obtain some bounds of the observation error $\widetilde{c}(t)$, assume first that the prediction error $\widetilde{d}(t)$ is greater than one (in other words $\widetilde{d}(t) \geq 2$).

Regarding the observation function $h_t(t)$ (16), we obtain for $c(t)$ and $\hat{c}(t)$

$$\Delta T \sum_{s=1}^{s=d(t)-1} e(t-s) < c(t) \leq \Delta T \sum_{s=1}^{d(t)} e(t-s) \ , \tag{24}$$

$$\Delta T \sum_{s=1}^{s=\hat{d}(t)-1} e(t-s) < \hat{c}(t) \leq \Delta T \sum_{s=1}^{\hat{d}(t)} e(t-s) \ . \tag{25}$$

This translates into a relation in the form

$$m_p(t) < \widetilde{c}(t) < M_p(t) \ , \tag{26}$$

where the time-dependent lower and upper bounds $m_p(t)$ and $M_p(t)$ are given by

$$m_p(t) = \Delta T \sum_{s=\hat{d}(t)+1}^{d(t)-1} e(t-s), \qquad M_p(t) = \Delta T \sum_{s=\hat{d}(t)}^{d(t)} e(t-s) \ . \tag{27}$$

Let us now assume that $\widetilde{d}(t) < -1$.

With the same thought process used in the case $\widetilde{d}(t) > 1$, we obtain a similar inequality, namely

$$-M_n(t) < \widetilde{c}(t) < -m_n(t) \ , \tag{28}$$

with $m_n(t)$ and $M_n(t)$ defined by

$$m_n(t) = \Delta T \sum_{s=d(t)+1}^{\hat{d}(t)-1} e(t-s), \qquad M_n(t) = \Delta T \sum_{s=d(t)}^{\hat{d}(t)} e(t-s) \ . \tag{29}$$

Working along similar lines, it is easily checked that for the remaining values of the prediction error, *i.e.* $\widetilde{d}(t) = 1$, $\widetilde{d}(t) = -1$ or $\widetilde{d}(t) = 0$, the estimation error $\widetilde{c}(t)$ verifies

$$0 < \widetilde{c}(t) < \Delta T e\left(t - d(t)\right) + \Delta T e\left(t - d(t) + 1\right) \ , \qquad \text{for } \widetilde{d}(t) = 1 \tag{30}$$

$$\Delta T e\left(t - d(t)\right) + \Delta T e\left(t - d(t) - 1\right) < \widetilde{c}(t) < 0 \ , \qquad \text{for } \widetilde{d}(t) = -1 \tag{31}$$

$$-\Delta T e\left(t - d(t)\right) < \widetilde{c}(t) < \Delta T e\left(t - d(t)\right) \ , \qquad \text{for } \widetilde{d}(t) = 0 \tag{32}$$

Now, we use Lyapunov's direct method to prove the convergence of the observer introduced in (14), (15) and (16). Let us define

$$V(t) = \widetilde{c}(t)^2 \ . \tag{33}$$

This candidate Lyapunov function obviously verifies $V(t) > 0$ for all non–zero $\widetilde{c}(t)$. We now proceed to establish that, for a suitable choice of the observer gain λ, V can be made non–increasing, *i.e.* $V(t+1) \leq V(t)$. In order to achieve this, we shall deal separately with the three cases

- $\widetilde{d}(t) \geq 2$,
- $\widetilde{d}(t) \leq -2$,
- $\widetilde{d}(t) = 1$ or $\widetilde{d}(t) = -1$ or $\widetilde{d}(t) = 0$.

First case: $\widetilde{d}(t) \geq 2$

By using (19), we obtain

$$V(t+1) - V(t) = \lambda \widetilde{d} \left(\lambda \widetilde{d} - 2\widetilde{c} \right) \ . \tag{34}$$

(For the sake of simplicity, we omit the time arguments where there is no ambiguity in equations.)

Because the observation function h_t is non–decreasing, the observer gain λ needs to be non–negative. When the inequality $\widetilde{d} \geq 2$ holds, the condition needed to insure that V is non–increasing is

$$\lambda \widetilde{d} - 2\widetilde{c} < 0 \ . \tag{35}$$

By assumption (26), the observer error verifies $\widetilde{c}(t) > m_p$. In addition, because $e_m \leq e(t)$ (see (23)), $m_p(t)$ satisfies

$$m_p(t) = \Delta T \sum_{s=\hat{d}(t)+1}^{d(t)-1} e(t-s) \geq \Delta T (\widetilde{d} - 1) e_m \ . \tag{36}$$

Then, inequality (35) could be rewritten

$$\lambda \widetilde{d} - 2\widetilde{c} < \lambda \widetilde{d} - 2m_p \ , \tag{37}$$

$$< \lambda \widetilde{d} - 2\Delta T (\widetilde{d} - 1) e_m \ . \tag{38}$$

If the observer gain λ is taken anywhere in the range $0 < \lambda \leq \lambda^*$, with λ^* given by (21), this guarantees that $V(t+1) < V(t)$. Also, note that the choice $\lambda = \lambda^*$ is optimal in the sense that it maximizes the guaranteed rate of decrease for V.

Second Case: $\widetilde{d}(t) \leq -2$.

By using (19), we obtain by a simple calculation:

$$V(t+1) - V(t) = \lambda \widetilde{d} \left(\lambda \widetilde{d} - 2\widetilde{c} \right) . \tag{39}$$

The observer gain λ still needs to be positive. In this case, $\widetilde{d} \leq -2 < 0$, so that to get a non–increasing V, λ needs to verify

$$\lambda \widetilde{d} - 2\widetilde{c} > 0 . \tag{40}$$

Since by assumption $e(t) \leq e_M$ (see (23)), the estimation error $\widetilde{c}$ verifies

$$\widetilde{c} < -m_n , \tag{41}$$

with

$$m_n(t) = \Delta T \sum_{s=d(t)+1}^{\hat{d}(t)-1} e(t-s) \geq -\Delta T(\widetilde{d}+1)e_M . \tag{42}$$

Then, from (40), we get

$$\lambda \widetilde{d} - 2\widetilde{c} > \lambda \widetilde{d} + 2m_n , \tag{43}$$

$$> \lambda \widetilde{d} - 2\Delta T(\widetilde{d}+1)e_M . \tag{44}$$

Thus, any choice of λ in the range $0 < \lambda \leq \lambda^*$, with λ^* given by (22), will result in $V(t+1) < V(t)$. In this case also, $\lambda = \lambda^*$ corresponds to the maximum guaranteed rate of decrease for V.

Third Case: $\widetilde{d}(t) = 1$ *or* $\widetilde{d}(t) = -1$ *or* $\widetilde{d}(t) = 0$.

Consider first the case $\widetilde{d} = 1$, so that (19) becomes

$$\widetilde{c}(t+1) = \widetilde{c}(t) - \lambda(t) . \tag{45}$$

From the definition of the candidate Lyapunov function V, we get

$$V(t+1) - V(t) = \widetilde{c}(t+1)^2 - \widetilde{c}(t)^2 , \tag{46}$$

$$= \lambda^2 - 2\lambda(t)\widetilde{c}(t) . \tag{47}$$

In this case, (30) provides the only available information on the estimation error $\widetilde{c}(t)$, namely that this unknown quantity is positive and lies somewhere between zero and the upper bound defined by $2\Delta T e_M$. As a result, the only way to guarantee that $V(t+1) - V(t)$ is non–increasing is to take $\lambda(t) = 0$, so that $V(t+1) = V(t)$ and $\widetilde{c}(t+1) = \widetilde{c}(t)$.

Reasoning along the same lines, one shows that $\lambda(t) = 0$ is also the appropriate choice when $\widetilde{d} = -1$ and $\widetilde{d} = 0$. □

Starting from the definition of the observation function h_t, and taking advantage of the fact that the prediction error $\widetilde{d}$ takes only integer values, we have proven that for a sufficient large prediction error $|\widetilde{d}(t)| \geq 2$, the candidate Lyapunov function $V(t) = \widetilde{c}(t)^2$ is decreasing. For small values of the prediction error, more precisely when $|\widetilde{d}(t)| \leq 1$, the candidate Lyapunov function $V(t) = \widetilde{c}(t)^2$ and the estimation error $\widetilde{c}(t)$ are constant. In addition, we have shown that the lower bound for $|\widetilde{c}(t)|$ is equal to $2\Delta T e_M$, where e_M is the maximum admission rate and ΔT the sampling period. At best, one could expect to obtain a non–zero value for the convergence value of the error $\widetilde{c}(t)$.

The radius of the convergence neighbourhood for $\widetilde{c}$, which is equal to $2\Delta T e_M$, is due to the structure of the observation function $h_t(t)$ – more precisely, to the fact that this non–linear function is piecewise constant. Because an observer is ultimately a contraption designed to invert the system's state to output map, no observer based on a piecewise constant observation function, however cleverly designed, can possibly be expected to guarantee the convergence of the estimation error towards zero. Or to put it in another way, an observer based on a piecewise observation function necessarily exhibits a limited resolution.

5 Dealing with Delayed Measurements of Congestion Delay

Let us now assume that the measurements of the source–to–destination transmission delay d and the losses l are available to the control algorithm after a possibly variable destination-to-source delay $T_m(t)$ (see Fig. 2).

In other words, at time t, the information available at the source can be described as

$$\mathcal{Y}(t) = (\widehat{c}(0), d(0), \ldots, d(t - T_m(t)), l(0), \ldots, l(t - T_m(t))) \ . \tag{48}$$

In this more realistic scenario, the following iterative two-step estimation procedure should be applied at each time t:

Observer update. When $\mathcal{Y}(t) \neq \mathcal{Y}(t-1)$, *i.e.* when new measurements have been received at time t, update the delayed observer using formula (16) up to time $s = t - T_m(t)$, yielding $\widehat{c}(t - T_m(t))$; otherwise, do nothing.

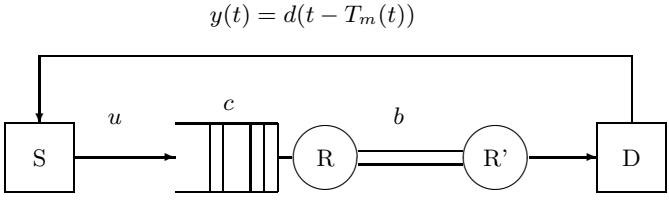

Fig. 2. Single link network with delayed measurement of d

Predictor update. Compute a predicted value of c by performing $T_m(t)$ prediction steps, leading to

$$\widehat{c}(t \mid \mathcal{Y}(t)) = \widehat{c}(t - T_m(t)) + \Delta T \sum_{s=t-T_m(t)}^{t-1} \left(u(s) - \widehat{l}(s \mid \mathcal{Y}(t)) - \widehat{b}(s \mid \mathcal{Y}(t)) \right), \tag{49}$$

where $\widehat{l}(s \mid \mathcal{Y}(t))$ and $\widehat{b}(s \mid \mathcal{Y}(t))$ are the best estimates of $l(s)$ and $b(s)$ available at time t.

In this way, the estimation algorithm keeps in store two different estimates: $\widehat{c}(t - T_m(t))$, which can be computed according to the procedure in the previous section, and to which the results in proposition 1 therefore apply; and $\widehat{c}(t \mid \mathcal{Y}(t))$, which can be expected not to stay too far from $c(t)$ if the estimates of missing values of l and b are reasonably accurate. More precisely, it immediately follows from (49) that

$$\begin{aligned} |\widetilde{c}(t \mid \mathcal{Y}(t)) - c(t)| \leq |\widetilde{c}(t - T_m(t))| + \Delta T \sum_{s=t-T_m(t)}^{t-1} \left| l(s) - \widehat{l}(s \mid \mathcal{Y}(t)) \right| \\ + \Delta T \sum_{s=t-T_m(t)}^{t-1} \left| b(s) - \widehat{b}(s \mid \mathcal{Y}(t)) \right| . \end{aligned} \tag{50}$$

6 Observer-Based Control

As indicated in the introduction, our motivation for constructing this non–linear observer is to implement an observer-based control scheme. In the full information scenario, the observer–based version of the feedback plus feedforward control defined by (10), (11), (12) would be

$$u(t) = \frac{c^r(t+1) - c^r(t)}{\Delta T} + \widehat{l}(t \mid \mathcal{Y}(t)) + \widehat{b}(t \mid \mathcal{Y}(t)) - k\left(\widehat{c}(t \mid \mathcal{Y}(t)) - c^r(t)\right) . \tag{51}$$

It is immediately checked that the dynamics of the tracking error become

$$\begin{aligned} \Delta c(t+1) = (1-k)\,\Delta c(t) + \left(-l(t) + \widehat{l}(t \mid \mathcal{Y}(t)) \right) \Delta T \\ + \left(-b(t) + \widehat{b}(t \mid \mathcal{Y}(t)) \right) \Delta T + k\left(c(t) - \widehat{c}(t \mid \mathcal{Y}(t)) \right) . \end{aligned} \tag{52}$$

A trivial but important corollary is that the control loop stability is guaranteed as long as the estimation errors for l and b can be bounded by quantities independent of c. However, since the estimation error cannot be shown to converge toward zero even under the most favorable assumptions, one should expect at best limited precision in the tracking of the reference trajectory.

7 Conclusion and Perspectives

Taking advantage of the fact that the congestion delay should be regarded as a system output, we have introduced a new delay-based non-linear observer dedicated *in fine* to the control of congestion in networks. The delay induced by the congestion in the link is computed from acknowledgement informations of the network. Then the buffer congestion is rebuilt taking into account realistic source-to-destination transmission delays.

It has been shown that the observation error converges at best to a non–zero value depending on the sampling period and on the maximum admission rate in the buffer. If the sampling period is chosen small, it is clear that the convergence neighbourhood would become closer to zero. However our model is based on averages of the link bandwidth and the effective admission rate over successive sampling intervals. As the sampling period ΔT goes to zero, the convergence of those average rates towards corresponding instantaneous rates is, at best, highly questionable, because all data processing in a network is ultimately performed by a collection of (usually non–synchronised) automata, *i.e.* computer chips and similar electronic gizmos. Thus, choosing the sampling period is perforce a sensitive design trade–off, since ΔT should be both small enough to ensure sufficient observer resolution, yet large enough so that the average rates in the underlying model retain sufficient regularity.

These theoretical results have been obtained for a simple network scheme: one source, one destination and one link. But they can be extended to more complex and realistic topologies combining several sources and destinations sharing a single congested link. Indeed, packets actually admitted in the buffer are assumed to be stored in a FIFO way. Then packets for each source undergo the same congestion delay through the FIFO buffer. If each flow is assumed to be differentiated from the other ones, the observer presented here for a single flow can be extended to a multi-flow configuration by applying observer equations to each separate flow sharing the same congestion delay. From a practical point of view, one could expect this flow differentiation to be realizable since control and observation schemes are applied to each source in a decentralized manner.

References

1. Augé A., Aspas J. (1998) TCP/IP over wireless links: performance evaluation. In Proceedings of IEEE 48^{th} VTC'98
2. Balk A., Gerla M., Maggiorini D., Sanadidi M. (2004) Adapative video streaming: pre-encoded MPEG-4 with bandwith scaling. Computer Networks 44:415–439
3. Chatté F., Ducourthial B., Niculescu S. I. (2002) Robustness issues of fluid approximation for congestion detection in best-effort networks. In Proceedings of the ISCC2002
4. Feamster N., Bansal D., Balakrishnan H. (2001) On the interactions between layered quality adaptation and congestion control for streaming video. In Proceedings of the 11^{th} International Packet Video Workshop
5. Floyd S., Handley M., Padhye J., Widmer J. (2000) Equation-based congestion control for unicast applications. ACM SIGCOMM

6. Jacobs S., Eleftheriadis A. (1996) Providing videoservices over networks without quality of services guarantees. World Wide Web Consortium Workshop on Real-Time Multimedia and Web
7. Jacobson V. (1988) Congestion Avoidance and Control. In Proceedings of SIGCOMM'88, Stanford, California
8. Padhye J., Kurose D., Towsley R. (1999) A model based tcp-friendly rate control protocol. Proceedings International Workshop on Network and Operating Systems Support for Digital Audio and Video
9. Raynaud H.-F., Hammi R., Kulcsár C. (2003) Towards a State-Space Approach to Congestion and Delay Control in Communication Networks. 7th European Control Conference (ECC'03), Cambridge
10. Raynaud, H.-F., Kulcsár C., Hammi R. (2003) In Communication Networks, There Are Delay, Delays... and Delays. IFAC Workshop on Time-Delay Systems, Rocquencourt
11. Raynaud, H.-F., Kulcsár C., Hammi R. (2004) Advances in Communication Control Networks. In Lecture Notes in Control and Information Sciences, Editors Tarbouriech S., Chaouki A., Chiasson J., Springer-Verlag, Vol. 308, Chapter 9:177–198
12. Rejaie R., Handley M., Estrin D. (1999) Rap: An end-to-end rate based congestion control mechanism for real-time streams in the Internet. Proceedings IEEE Infocom
13. Schulzrinne H., Casner S., Frederick R., Jacobson V. (1996) RTP: a transport Protocol for real-time applications, RFC1889
14. Sisalem D., Wolisz A. (2002) LDA$^+$ tcp-friendly adaptation: A measurement and comparison study. Proceedings International Workshop on Network and Operating Systems Support for Digital Audio and Video
15. Srikant R. (2004) The Mathematics of Internet Congestion Control. Birkhauser
16. The Stream Control Transmission Protocol (SCTP). RFC 2960. Available from `http://www.ietf.otg.rfc/rfc2960.txt`
17. Wang J., Zhou M., Zhou H. (2004) Clock synchronization for Internet measurements: a clustering algorithm. Computer Networks 45:731–741

On the Use of State Predictors in Networked Control Systems

Emmanuel Witrant, Didier Georges, Carlos Canudas-de-Wit, and Mazen Alamir

Laboratoire d'Automatique de Grenoble, ENSIEG, B.P. 46,
38 402 Saint Martin d'Hères, France
{witrant,georges,ccanudas,alamir}@lag.ensieg.inpg.fr

Summary. Without pretending to be exhaustive, the aim of this chapter is to give an overview on the use of the state predictor in the context of time-delay systems, and more particularly for the stabilisation of networked control systems. We show that the stabilisation of a system through a deterministic network can be considered as the stabilisation of a time-delayed system with a delay of known dynamics. The predictor approach is proposed, along with some historical background on its application to time-delayed systems, to solve this problem. Some simulation results are also presented.

Keywords: Networked controlled systems, predictive control, time-delay systems.

1 Introduction

The networked control systems (NCS) constitute a particular class of control problems, where the communication channel influence is crucial in the stabilisation of the remote system and cannot be neglected. The control setup is shown in Figure (1), where the system considered can be open-loop unstable. The sensor, actuator and system are remotely commissioned by a controller that interchange measurements and control signals through a communication network. This network is used by multiple systems and a packet management law (router, switch, priority level ...) is introduced to distribute the information. A Transfer Protocol (TP) is implemented to allow users to send and receive data over the network. The impact of such network is to introduce a *time-varying* delay in the data transmission between the system and the controller, due to the multiple users interaction.

The time-varying delay makes the problem more difficult since the time-translation is not reversible and the results established in the frequency domain cannot be used (like the Smith predictor [1]). Most of the existing control methods (like the Lyapunov-Krasovskii approaches) result in a LMI formulation based on a *constant time-delay*, or a known upper bound on it (see for example [2] or [3]). The case of time-varying or state-dependent delays can be treated along with the solutions presented in [4], and [5] as long as the system is open-loop stable. These solutions do not allow for a direct use of the time-delay dynamics in the design of the control law and naturally yield to conservative results.

J. Chiasson and J.J. Loiseau (Eds.): Appl. of Time Delay Systems, LNCIS 352, pp. 17–35, 2007.
springerlink.com

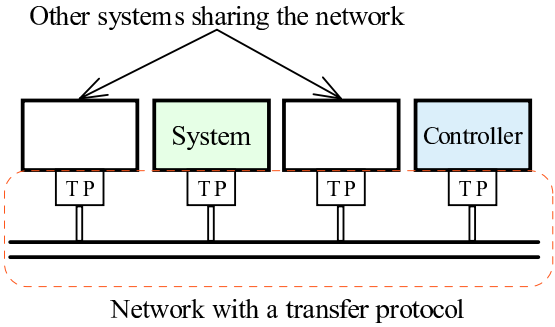

Fig. 1. Closed-loop network controlled system

The state predictor approach is particularly efficient to stabilize a delayed (possibly open-loop unstable) system since it results in the pole placement (finite spectrum assignment) of the closed-loop system. It can be applied to the case of time-varying delays by considering a predictor with a time-varying horizon, thus explicitly including the dynamics of a deterministic network in the control synthesis.

This chapter is organized as follows. The first part details the specificities introduced by the use of a deterministic network in the communication channel, along with the characteristics of the induced time delay and a description of the controlled system. The second section presents some historical key points on the use of the state predictors to assign a finite spectrum to time-delayed systems. In the third section, the state predictor is combined with some other control and analysis tools in order to design a robust control scheme, possibly with an explicit use of the network dynamics or based on a state observer. Some issues on the related numerical problems are also considered and an application example is finally proposed.

2 Problem Statement: Control Through TP Networks

The networked controlled systems are characterized by some specific transmission protocol dynamics that can be explicitly used in the design of the control feedback. This dynamics induces a *time-varing* delay which depends on the interaction of multiple users on the network.

A transfer protocol is set between the emitters and the network to manage the exchange of packets (emission and reception). The TP determines the emitter's window size and manages the reception of packets. Considering the class of *secure networks* we can guarantee that there is no loss of information in the communication process (all the lost packets are re-emitted), which results in a bounded transmission delay. Examples of such protocols (a detailed description can be found in [6]) are the Transfer Control Protocol (TCP) and Sequenced Packet Exchange (SPX) schemes. An other example is a dedicated network used to control a supply chain or an embedded system; in that case, the TP can be freely designed to ensure the desired properties.

The delay induced by the network is then the delay experienced by the control and measurement signals. Therefore, the lossless property of the network ensures that the delays are bounded and cannot increase as fast as the time (since it is the delay measured from the system or the control law sites). This motivates the following property.

H1) The time-delay $\tau(t)$ induced by the communication network satisfies, for all $t \geq 0$,

$$0 \leq \tau(t) \leq \tau_{max} \quad \textit{and} \quad \dot{\tau}(t) < 1,$$

where $\tau_{max} \geq 0$ is an upper bound on the delay.

Note that this hypothesis is generally used to ensure the stability or the controllability of time-delay systems.

The time-delay dynamics induced by a TP network can be described in a continuous, discrete or hybrid framework. For analysis purposes, we chose the continuous formulation but the proposed results can easily be extended to the other kinds of models. The induced delay is then described by the general class of systems that write as

$$\dot{z}(t) = f(z(t), u_d(t)), \quad z(0) = z_0, \tag{1}$$
$$\tau(t) = h(z(t), u_d(t)), \tag{2}$$

where

- $z(t)$ is the internal state of the network (with initial state z_0) , that describes the time evolution of the emitters window size $W_i(t)$ (for $i = 1 \dots N$ sources connected to the network) and the router's queue length $q(t)$, for example. In that case, the state writes as $z(t) = [W_1(t) \ \dots \ W_N(t) \ q(t)]^T$,
- $u_d(t)$ is the exogenous input to the system, which is the number of users $N(t)$ and the link capacity $C(t)$, if both are time-varying. We then have $u_d(t) = \{N(t), C(t)\}$,
- $f(z(t), u_d(t))$ describes the internal dynamics of the network, set by the TP on the window sizes and by the queue management scheme on the queue length, if a buffer is used to manage the packets,
- $h(z(t), u_d(t))$ gives the resulting delay $\tau(t)$ from the whole model.

Note that (1)-(2) describes an autonomous system with an exogenous input $u_d(t)$. This input is assumed to be known over a certain range of time ahead of the present time (equal to the maximum delay expected τ_{max}) in order to use the predictive approach. This would be the case for periodic systems or if the transfer protocol is set to declare to the network that its source will emit and wait during τ_{max} before starting the emission. An appropriate robustness analysis focused on the predictor sensitivity with respect to the time-delay model can be used to remove this hypothesis.

The remotely controlled system writes as:

$$\dot{x}(t) = Ax(t) + Bu(t - \tau(t)), \quad x(0) = x_0, \tag{3}$$
$$y(t) = Cx(t), \tag{4}$$

where $x \in R^n$ is the internal state, $u \in R^l$ is the control input, $y \in R^m$ is the system output, and A, B, C are matrices of appropriate dimensions. The pairs (A, B) and (A, C) are assumed to be controllable and observable, respectively, but no assumption is made on the stability of A.

3 Historical Background

After a short recall on the concept of commandability in the case of the systems with a delayed input, we present in this section the main results obtained in the years 1970-1980 concerning the state predictor. More precisely, the concepts of finite spectrum assignment, system reduction and the use of the predictor to stabilize systems with a delayed input if this delay is time-varying are detailed. The state is supposed to be completely known to establish the control law.

3.1 Controllability

The controllability of linear systems with time delays in control is not trivial and was specifically studied in [7]. We consider the general class of systems described on $[t_0, t_1]$ by

$$\dot{x}(t) = A(t)x(t) + \sum_{i=0}^{k} B_i(t)u(t - \tau_i), \tag{5}$$

where $A(t)$, $B_i(t)$ are bounded measurable matrices of size $n \times n$ and $n \times l$, respectively, and $0 = \tau_0 < \tau_1 < \ldots < \tau_k$ are real numbers. The controllability of the complete state is usually defined as follows

Definition 1. *The complete state of the process (5) at time t is the set $x_c(t) = \{x(t), v(t, s)\}$, where $v(t, s) = u(s)$, $s \in [t - \tau_k, t)$.*

Definition 2. *The complete state $x_c(t_0)$ is said to be controllable on $[t_0,\ t_1]$ if there exists a control u such that $x(t_1) = 0$.*

Definition 3. *The complete state $x_c(t_0)$ is said to be absolutely controllable on $[t_0, t_1]$ if there exists a control u such that $x_c(t_1) = 0$ (both $x(t_1) = 0$ and $v(t_1, s) = 0$).*

Definition 4. *The system (5) is said to be (absolutely) controllable on $[t_0, t_1]$ if and only if every complete state is (absolutely) controllable on this interval.*

These definitions show the influence of the delay on the concept of state and commandability. Indeed, we do not consider an instantaneous state but an evolution on a time-dependent horizon: the control law $u(\cdot)$ must be known on the horizon $[t - \max_k \tau_k, t]$ to compute the value of $\dot{x}(t)$. This comes from the fact that, if two control laws have the same value at a given instant t but a different history then the system trajectories will be different.

This principle is equivalent to the one used in the definition of the dynamics of a time-delay system writing as

$$\dot{x}(t) = A_n\, x(t) + A_d\, x(t-\tau),$$

where a proper initial condition is expressed in [2] as

$$x(t_0+\theta) = \phi(\theta), \quad \theta \in [-\tau,\, 0], \quad (t_0,\, \phi) \in \mathbb{R}^+ \times \mathcal{C}^{\nu}_{n,\,\tau}$$

with $\mathcal{C}^{\nu}_{n,\,\tau} = \{\phi \in \mathcal{C}_{n,\,\tau} : ||\phi||_c < \nu\}$, where ν is a positive real number, $||\phi||_C = \sup_{-\tau \le t \le 0} ||\phi||$, $||\cdot||$ refers to the euclidian norm and $\mathcal{C}_{n,\tau} = \mathcal{C}([-\tau,\, 0], \mathbb{R}^n)$ indicates the Banach space of the continuous vector functions projecting the interval $[-\tau,\, 0]$ in $\mathbb{R}^n$ with a uniformly convergent topology.

The concept of complete state of the first definition is thus introduced to take into account the history of the control law. The previous definitions are an application of the concept of commandability, in the traditional sense, to the class of systems considered. We take into account the fact that the control law history has to be known before the system initialization (at time t_0) and then kept in memory on the time interval $[t - \max_k \tau_k, t]$ to ensure the uniqueness of the trajectory described by (5).

Remark 1. For simplicity sake, we will consider that the values of the control law preceding the system initialization are null and that their history is preserved on the necessary horizon. The initial conditions of the system are thus reduced to $x(t_0)$ and the traditional concepts of commandability can be applied directly.

The use of the the state predictor allows, because of the infinite dimension of the resulting control law, to obtain a closed-loop system of finite dimension. This transformation of a system described by a functional differential equation into a system described by an ordinary differential equation is limited by the computation precision of the integral term. Indeed, the resulting system can be non-robust with respect to arbitrarily small uncertainties at this level. A more complete discussion on this subject is available in [8] and the resulting performance limitation of is close to the one induced by an error in the delay estimation, which is studied in [9].

The solution of the differential equation (5), along with the previous definitions, is used to establish the following theorem on absolute controllability.

Theorem 1. *If the matrices $A(t)$, $B_i(t)$ are analytic on $[t_0, t_1]$, $[t_0, t_1 + \tau_k]$, respectively, then the process (5) is controllable absolutely on $[t_0, t_1]$ if and only if rank $[D(t), LD(t), \ldots, L^{n-1}D(t)] = n$ for all but isolated points of $[t_0, t_1 - \tau_k]$. The function $D(s)$ and the operator L are defined as*

$$D(s) \doteq \sum_{i=0}^{k} \Phi(s, s+\tau_i) B_i(s+\tau_i) \text{ and } LD(t) \doteq (d/ds) D(s)|_{s=t} - A(t) D(t),$$

where $\Phi(t, t_0)$ is the transition matrix of $A(t)$.

Remark 2. For the specific case where the process is described by (3) with a constant delay, $D(s) = e^{-A\tau}B$ and the absolute stability of this system is ensured if and only if *rank* $[e^{-A\tau}B, Ae^{-A\tau}B, \ldots, A^{n-1}e^{-A\tau}B] = n$.

3.2 Finite Spectrum Assignment

It is well known that the use of a linear feedback on a dynamic system with delayed control generally yields a closed-loop system described by a retarded functional differential equation with an *infinite spectrum*. Assigning a finite spectrum to such system is not practically feasible with a state feedback control law. The aim of this section is to present the results derived in [10], where it is shown that the state predictor can be used to obtain a *finite* closed-loop spectrum for the class of systems considered in this paper.

Consider the system with a time delayed input and a non-delayed one

$$\dot{x}(t) = Ax(t) + B_0u(t) + B_1u(t-\tau), \tag{6}$$

where A, B_0 and B_1 are some matrices of appropriate dimensions. The feedback is given by

$$u(t) = Kx(t) + K\int_{-\tau}^{0} e^{-(\tau+\theta)A}B_1u(t+\theta)d\theta, \tag{7}$$

where K is a $l \times n$ matrix that specifies the location of the closed-loop spectrum. The finite spectrum of the closed-loop system is then ensured by the following theorem.

Theorem 2. *The spectrum of the closed-loop system (6), (7) coincides with the spectrum of the matrix*

$$A + [B_0 + e^{-A\tau}B_1]K.$$

Moreover, assuming controllability (respectively stabilizability) of the pair $(A, B_0 + e^{-A\tau}B_1)$ *the spectrum of the system (6), (7) can be placed at any pre-assigned self-conjugate set of n points in the complex plane (respectively the unstable eigenvalues of A can be arbitrarily shifted) by a suitable choice of the matrix K.*

Proof (Outline). Assuming that the solutions of (6) can be expressed as $x(t) = e^{At}\kappa(t)$, where $\kappa(t)$ is a continuously differentiable function, we have that

$$x(t+\tau) = e^{A\tau}\left[x(t) + \int_{-\tau}^{0} e^{-(\tau+\theta)A}[B_0u(t+\theta+\tau) + B_1u(t+\theta)]d\theta\right].$$

Substituting (7) in the previous equation, solving for $u(t)$ and looking for the delayed input, we obtain

$$u(t-\tau) = K\left[e^{-A\tau}x(t) - \int_{-\tau}^{0} e^{-(\tau+\theta)A}[B_0u(t+\theta)d\theta\right]. \tag{8}$$

The expression for $u(t)$ from (7) and the one for $u(t-\tau)$ from (8) can now be substituted in (6). Note that the integral terms cancel each other and we have the closed-loop result

$$\dot{x}(t) = (A + B_0K + B_1Ke^{-A\tau})x(t).$$

This completes the proof. □

The original result in [10] was given for the more general class of systems governed by

$$\dot{x}(t) = Ax(t) + \int_{-\tau}^{0} d\beta(\theta)u(t+\theta), \tag{9}$$

where $\beta(.)$ is an $n \times l$ matrix function of bounded variation which is a sum of an absolutely continuous function and a finite number of jump discontinuities. We restricted the class of processes considered to (6) for sake of simplicity and to remain in the scope of this chapter. The original use of Lebesgue-Stieltjes integration in [10] includes some measurement considerations, allowing for some non-uniformly distributed measurements.

Remark 3. The sensitivity of the design to the plant and control parameter variations is also considered in [10]. It is shown that, even if the desired finite spectrum is not preserved, the closed-loop system remains stable for arbitrarily small perturbations.

For the specific case where the process is described by (3) with a constant delay ($B_0 = 0$), the controllability condition of the previous theorem is equivalent to the condition expressed in *Remark 2*.

A similar stability result was also established in [11], where the receding horizon regulator is used to solve the fixed terminal energy problem.

3.3 Reduction of Systems

The previous works are generalized in [12], where an absolute continuity condition for the reduction of systems with delayed controls is proposed. This allows for the transformation of a linear system with delayed control into an ordinary measure-differential control system (system reduction). This transformation is performed as follows.

Theorem 3. *Consider the class of systems described by (6) and define*

$$p(t) \doteq x(t) + \int_{t-\tau}^{t} e^{(t-\theta-\tau)A} B_1 u(\theta) d\theta.$$

Then $\{x(t), u(t)\}$ *is admissible for (6) if and only if* $\{p(t), u(t)\}$ *is admissible for*

$$\dot{p}(t) = Ap(t) + \hat{B}(t)u, \tag{10}$$

with $\hat{B}(t) \doteq B_0 + e^{-A\tau} B_1$.

For the case of systems with a time-varying delay in the input

$$\dot{x}(t) = Ax(t) + Bu(t - \tau(t)),$$

with $\eta(t) \doteq t - \tau(t)$ absolutely continuous and $\dot{\tau}(t) \neq 1$ for almost every t, the equivalent system is obtained, for almost every t, using

$$\hat{B}(t) = \sum_{s \in \eta^{-1}(t)} e^{A(t-s)} B |1 - \dot{\tau}(s)|^{-1}.$$

where $\eta^{-1}(t) \doteq \{s | \eta(s) = t\}$.

The classical techniques of stabilization, optimization and controllability can be directly applied to the reduced system using the following result.

Theorem 4. *Let $u(t) = K(t)p(t)$ be a feedback stabilisation scheme for (10) and suppose that $K(t)$ is bounded. Then the system (6) is stabilized by the feedback scheme*

$$u(t) = K(t) \left[x(t) + \int_{t-\tau}^{t} e^{(t-\theta-\tau)A} B_1 u(\theta) d\theta \right].$$

Remark 4. The original theorems in [12] are derived for the more general class of systems governed by (9) (the particular case (6) is introduced as an illustrative exemple).

3.4 Horizon Computation for the Time-Varying Delay Case

The finite spectrum assignment control scheme is applied more specifically to systems with time-varying delayed control in [13], where it is used to design an adaptive algorithm which ensures the output convergence and global stability. The specificities induced by this delay and the design of the time-varying predictor horizon are described in this section.

The first-order system considered in [13] writes as

$$\dot{x}(t) = ax(t) + u(t - \tau(t)), \tag{11}$$

with a an unknown positive constant and $\tau(t)$ satisfying the conditions stated in section 2 ($\tau(t)$ bounded and $\dot{\tau} < 1$).

The goal is to express (11) in the form

$$\frac{dx}{d\zeta(t)}(\zeta(t)) = ax(\zeta(t)) + u(t),$$

where $\zeta(t) \doteq t + \delta(t)$ is the predicted time. This is achieved if $\delta(t)$ satisfies $\delta(t) - \tau(t + \delta(t)) = 0$. The desired pole placement on the closed-loop system is obtained using the non-causal control law (since we need to predict the state evolution)

$$u(t) = \kappa x(\zeta(t)) + \bar{u}(t),$$

where $\bar{u}(t)$ is a bounded reference input, κ is a negative constant such that $a + \kappa < 0$, and $x(\zeta(t))$ is obtained from the lemma:

Lemma 1. *The prediction $x(t + \delta(t))$ is given by the equation*

$$x(t + \delta) = F(\zeta(t), t) \left[x(t) + \int_{t-\tau(t)}^{t} F(t, \zeta(s)) \dot{\zeta}(s) u(s) ds \right],$$

where F is the state transition function of the system (11), i.e. $F(t, \sigma) = e^{a(t-\sigma)}$.

The previous lemma shows that we are able to set the proposed control law, since the predicted state $x(t+\delta)$ is computed from $x(t)$ and $u(s)$ with $s \in [t-\tau, t]$. Expressing (11) in the time-shifted coordinates, we have that

$$\frac{dx}{d\zeta(t)}(\zeta(t)) = ax(\zeta(t)) + u(t+\delta-\tau(t+\delta)) = ax(\zeta(t)) + u(t)$$

from the definition of $\delta(t)$. Introducing the proposed control law, we are able to set the pole of the closed-loop time-shifted system since it writes as

$$\frac{dx}{d\zeta(t)}(\zeta(t)) = (a+\kappa)x(\zeta(t)) + \bar{u}(t),$$

where κ is the control gain.

This method is extended to the stabilization of n-dimensional SISO systems [14] and a control scheme with a state estimator is proposed. It is also applied to non-minimum phase systems, in the case of constant delays, in [15].

4 Other Approaches

The state predictor can be combined or studied with other approaches in order to determine the robustness and performance of the closed-loop system. First, the problem of robustness with respect to the knowledge of the delay can be tackled by the frequency approach, in the case of a constant delay. Then, the H^∞ synthesis is used to reject a disturbance on the state, by partially taking into account the time variation of the delay. A control scheme using explicitely the network dynamics and an observer-based control law are presented in the third subsection. To finish, we consider some elements of numerical analysis to compensate for the instabilities induced by the computation of the integral term in the state predictor.

4.1 Robustness with Respect to the Delay Estimation: A Frequency Approach

A robustness criterium is proposed in [16], where the robustness of the state predictor with respect to delay uncertainties is investigated. The system considered is a dynamic system with a delayed input such as the one described by (3), with a constant delay. The robustness problem is formulated by introducing the maximum deviation of the delay $\Delta \doteq \tau - \hat{\tau}$, where τ is the delay induced by the network and $\hat{\tau}$ is the delay used for the prediction (measured, observed or estimated). The goal is then to find the maximum value $\overline{\Delta}$ of Δ which ensures the stability of the closed-loop system for $|\Delta| \in [0, \overline{\Delta})$. The consideration of a constant delay makes it possible to solve this problem using a frequency approach, detailed below.

The estimated delay is used to establish the control law

$$u(t) = -Ke^{A\hat{\tau}}\left[x(t) + e^{At}\int_{t-\hat{\tau}}^{t} e^{-A\theta}Bu(\theta)d\theta\right] \tag{12}$$

which writes, in the frequency domain, as

$$(I_l + K(sI_n - A)^{-1}[I_n - e^{-\hat{\tau}(sI_n - A)}]B)u(s) = -Ke^{\hat{\tau}A}x(s),$$

where I_n is the identity matrix of size $n \times n$ and s is the Laplace operator. The system (3) is described by

$$(sI_n - A)x(s) = Be^{-\tau s}u(s)$$

and the characteristic matrix of the closed-loop system is

$$\begin{aligned} &det\begin{pmatrix} sI_n - A & Be^{-\tau s} \\ -Ke^{\hat{\tau}A} & I_l + K(sI_n - A)^{-1}[I_n - e^{-\hat{\tau}(sI_n - A)}]B \end{pmatrix} \\ &= det\left(sI_n - A + [I_n - e^{\hat{\tau}A}(e^{-\hat{\tau}s} - e^{-\tau s})]BK\right). \end{aligned}$$

Remark 5. When the delay is perfectly known, $\Delta = 0$ and the closed-loop spectrum is identical to that of the non-delayed equivalent systems described previously.

The previous discussion makes it possible to establish the following proposition.

Proposition 1. *Consider the system described by (3) with a constant delay τ, controlled by (12). If the estimated delay $\hat{\tau}$ is different from the one experienced by the control input and Δ describes the deviation of this delay, then the characteristic-equation of the closed-loop system is*

$$det\left(sI_n - A + BK - e^{\hat{\tau}A}e^{-\hat{\tau}s}(1 - e^{-\Delta s})BK\right).$$

Remark 6. This result shows the correlation between the choice of the controller gain K, the estimated delay and the maximum acceptable deviation of this delay. This illustrates the necessary compromise between a high gain control scheme (broad bandwidth) and the robustness with respect to the uncertainties on the delay (sensitivity of the closed-loop system).

The maximum value of the acceptable deviation on the delay can then be computed, in an analytical way for the monovariable case (analysis based on continuity arguments) or in a numerical way for the multivariable case (frequency sweeping). The major disadvantage of this method in the context of stabilisation through networks is that it cannot be applied to the case of variable time-delays, which is of major importance in the communication networks since the delays experience strong variations according to the load.

4.2 H^∞ Control with a Time-Varying Delay

The receding horizon predictor is included in a H^∞ control scheme for a system with a time-varying delay in the control in [17]. The plant and the sensor channel are described, respectively, by

$$\dot{x}(t) = Ax(t) + Bu(t - \tau(t)) + Dv(t), \tag{13}$$
$$y(t) = x(t - \psi(t)), \tag{14}$$

where $v(t)$ is the disturbance vector, $y(t)$ is the measured output, and both delays $\tau(t)$ and $\psi(t)$ are some positive continuous functions with their time-derivative less than one. This means that the full state, delayed by $\psi(t)$, is available to establish the control law. The predictive state formulation $p(t) = x(t + \delta(t))$ is similar to the one proposed in [18] and writes as

$$\dot{p}(t) = \tilde{A}(\dot{\delta}(t))p(t) + \tilde{B}(\dot{\delta}(t))u(t) + \tilde{D}(\psi(t), \dot{\psi}(t), \delta(t))v(t - \psi(t)), \quad p(0) = 0$$

with

$$\tilde{A}(\theta) \doteq (1 + \theta)A, \quad \tilde{B}(\theta) \doteq (1 + \theta)B \quad \textit{and} \quad \tilde{D}(\psi, \theta, \delta) \doteq (1 - \theta)e^{A(\psi+\delta)}D,$$

where θ denotes the variable of the function considered. Let $z(t)$ be the controlled output defined by $z(t) \doteq Fp(t)$, where the constant matrix F is used to estimate the effect of disturbances. The effect of the disturbance $v(t)$ is compensated if the following criterion is verified

$$\int_0^\infty z^T(t)z(t)dt \leq \gamma^2 \int_0^\infty v^T(t)v(t)dt,$$

for any disturbance $v(t)$ in $L_2[0, \infty)$, the space of square integrable functions on $[0, \infty)$. From this formulation, the solution of the H^∞ control problem is established in the form of LMIs (linear matric inequalities) for two different cases:

- the delay is supposed to be known at any time (i.e. it can be predicted) and the solution is expressed in the form of time-varying LMIs,
- only past and present informations are available; the solution is then established using the upper bounds on the delays and their derivatives.

The case of output feedback is also considered, as well as the case when some sensor noises are present in the output $y(t)$.

The fact that this solution requires to solve LMI at every time to explicitly use the value of the delay reduces considerably the field of application of this method. Indeed, the NECS problems as considered here relate to systems with fast dynamics, where the network has a dominating influence. The synthesis of a controller implying the resolution of LMI in real time is thus not conceivable in this case. Nevertheless, this H^∞ solution is well suited for perturbed dynamical systems when the induced time-delay exhibits slow variations.

4.3 Explicit Use of the Network Dynamics and Observer-Based Control

The relationship between the predictor's horizon $\delta(t)$ and the delay $\tau(t)$ is studied more closely in [19], where a dynamic explicit solution is proposed to compute

$\delta(t)$. This solution directly involves the delay dynamics defined in (1)-(2) for $\tau(t)$, which can be obtained from a network model, and is included explicitly in the control's formulation. This is expressed in the following theorem, established for the non-delayed state feedback problem.

Theorem 5. *Consider the system described by (3) and assume that the delay dynamics (1)-(2) is such that H1) holds. Then the state feedback control law*

$$\begin{aligned}
u(t) &= -Ke^{A\delta(t)}\left[x(t) + e^{At}\int_{t}^{t+\delta(t)} e^{-A\theta}Bu(\theta-\tau(\theta))d\theta\right],\\
\dot{\delta}(t) &= -\frac{\lambda}{1-d\tau(\zeta)/d\zeta}\delta(t) + \frac{d\tau(\zeta)/d\zeta + \lambda\tau(\zeta)}{1-d\tau(\zeta)/d\zeta},\\
\frac{d\tau}{d\zeta}(\zeta) &= \frac{dh}{d\zeta}(z(\zeta), u_d(\zeta)),\\
\frac{dz}{d\zeta}(\zeta) &= f(z(\zeta), u_d(\zeta)), \quad z(0) = z_0,
\end{aligned}$$

with $\zeta(t) = 1 + \delta(t)$, λ is a positive constant and $\delta(0) = \delta_0$, ensures that the system trajectories converge exponentially to zero.

The stability of the resulting time-shifted closed-loop system

$$\frac{dx}{d\zeta}(\zeta) = (A - BK)x(\zeta) \tag{15}$$

is studied in details in [20] and a direct relationship is established between the system's stability and the delays properties. More precisely, the stability analysis resulted in some precise bounds on the allowable variations of $\delta(t)$. It is also shown that the exponential convergence of (3) can be deduced from the one of (15) if $H1$ holds and with bounded initial conditions.

The problem of remote output stabilization via two channels with time-varying delays is investigated in [20], considering the class of linear systems that write as (3)-(4). A dynamic model for both delays, satisfying the boundness conditions on the delays and their derivatives is supposed to be given from (1)-(2). The following result is obtained for the case of observer-based control when a time-varying delay is experienced on both communication channels ($\psi(t)$ on the sensor measurements and $\tau(t)$ on the control signals) and only the system output is available to establish the control law.

Theorem 6. *Consider the system described by (3)-(4). Assume that the delay dynamics (1)-(2) is such that H1 holds for both delays, and that*

H2) $1 > \dot{\psi}(t) > -1, \ \forall t \geq 0$[1]

[1] This hypothesis is satisfied if the data packets used to establish the control law are first organized in the proper order and is often used in teleoperation (see [21] for example).

Then, the observer-based feedback control law

$$u(t) = -Ke^{A(\delta(t)+\psi(t))}\hat{\tilde{x}}(t) - Ke^{A(t+\delta(t))}\int_{t-\psi(t)}^{t+\delta(t)} e^{-A\theta}Bu(\theta-\tau(\theta))d\theta,$$
$$\dot{\hat{\tilde{x}}}(t) = A\hat{\tilde{x}}(t) + Bu(t-\psi-\tau(t-\psi)) + H\{y(t) - C\hat{\tilde{x}}(t)\},$$

with $\hat{\tilde{x}}(t) \doteq \hat{x}(t-\psi(t))$ *ensures that the system trajectories converge exponentially to zero.*

4.4 Numerical Problems Induced by the Computation of the Integral Term

The computation of the predictive control law is typically carried out thanks to a finite approximation of the integral part. This leads to a discrete version which can induce some numerical instabilities. Three studies, carried out for the case of the constant delays, are quickly described here:

- The implementation by numerical quadrature methods is studied in [22], where it appears that the most precise methods give the worst results (they induce more oscillations). Compared to the other traditional approaches, the backward rectangular method gives the most satisfactory result (neither oscillations nor overshoot).
- An approximation of the control law with distributed delays by one with only specific delays using a set of block-pulse functions is proposed in [23]. The advantage of this method is that the nature of the closed-loop system remains unchanged, but its robustness is not studied.
- A last approximation method is proposed in [8], which also uses a finite number of specific delays. A low-pass filter introduced in the control loop (in an implicit way) induces a closed-loop quasi-polynomial of delayed type instead of the original neutral type (source of instabilities), which prevents the numerical instability.

When the delay is time-varying, the problem is more complex since in this case the discretization leads to a discrete controller with *variable dimension*. The resulting closed-loop system has a variable number of poles and zeros, which makes it difficult to study the correlation between numerical instabilities and the sampling period or the discretization method. This problem would clearly require a more thorough study but we will be satisfied here to use the method of the backward rectangular rule to approximate the integral. This choice is motivated by the simplicity of this approach and its relative robustness in the case of constant time-delays.

The integration step is chosen to be fixed and equal to the sampling period T_s. The number of steps $n_k = n(t_k)$ necessary to estimate the integral at a given instant $t = t_k$ then depends on $\hat{\delta}_k = \hat{\delta}(t_k)$ and is defined by $n_k \doteq \hat{\delta}_k/T_s$. This leads to the following approximation of the integral term, for $k = 1, 2, 3, \ldots$

$$I_k = I(t_k) \doteq e^{At_k} \int_{t_k}^{t_k+\hat{\delta}(t_k)} e^{-A\theta} Bu(\theta - \tau(\theta))d\theta,$$

$$\approx T_s \sum_{i=0}^{n_k-1} e^{-iAT_s} Bu(k+i-\frac{\tau(k+i)}{T_s}),$$

where the delay is supposed to be a multiple of the sampling period. This assumption is not too restrictive if the sampling period is sufficiently small compared to the delay, so that the fractional part $\frac{\tau(k+i)}{T_s}$ can be neglected in the approximation of the integral.

The predictive part of the control law proposed in *Theorem 5* can then be expressed in a discrete way

$$u_k = -Ke^{A\delta_k}(x_k + I_k).$$

The matrix exponent term can be computed in an approximate way by using the method of Krylov [24] or in an exact way by the method of the components of matrices [25].

5 Application Example: Control of an Inverted Pendulum Through a TCP Network

The application example presented in this section is the system proposed in [26], where an "T-shape" inverted pendulum is controlled through a simulated TCP network. This pendulum dynamics is 4^{th} order, nonminimum phase, open loop unstable and with coupled nonlinearities. Its linearized model writes as

$$\dot{x}(t) = \begin{bmatrix} 0 & 1 & 0 & 0 \\ -21.54 & 0 & 14.96 & 0 \\ 0 & 0 & 0 & 1 \\ 65.28 & 0 & -15.59 & 0 \end{bmatrix} x(t) + \begin{bmatrix} 0 \\ 8.10 \\ 0 \\ -10.31 \end{bmatrix} u(t-\tau(t)),$$

$$y(t) = x(t).$$

The behavior of the network considered is set by the average deterministic model established in [27], where a TCP model with a proportional Active Queue Management (AQM) policy (set on the router's site) is proposed. The AQM is introduced with a packet discard function $p(x)$ and acts as a feedback from the router on the emitter's window size; the proportional scheme is shown to be stable in [28]. The network equations then write as

$$\frac{dW_i(t)}{dt} = \frac{1}{R_i(t)} - \frac{W_i(t)}{2}\frac{W_i(t-R_i(t))}{R_i(t-R_i(t))}p_i(t), \tag{16}$$

$$\frac{dq(t)}{dt} = -C_r + \sum_{i=1}^{N} \frac{W_i(t)}{R_i(t)}, \quad q(t_0) = q_0, \tag{17}$$

where $R_i(t) \doteq \frac{q(t)}{C_r} + T_{pi}$ is the round trip time, $p_i(t) = K_p q(t - R_i(t))$ and T_{pi} is the constant propagation delay. The induced time-delay is $\tau_i = \frac{1}{2} R_i(t)$ and the router output link capacity is supposed to be constant.

Example 1. The network consists of one router and two TCP flows (the one used by the system and the controller, and a disturbing one, acting between $t = 10s$ and $t = 25s$). Its parameters are such that the time-delay is obtained from the following dynamics

$$\frac{dW_1(t)}{dt} = \frac{1}{R_1(t)} - \frac{W_1(t)}{2} \frac{W_1(t - R_1(t))}{R_1(t - R_1(t))} p_1(t),$$

$$\frac{dW_2(t)}{dt} = \frac{1}{R_2(t)} - \frac{W_2(t)}{2} \frac{W_2(t - R_2(t))}{R_2(t - R_2(t))} p_2(t),$$

$$\frac{dq(t)}{dt} = -300 + \sum_{i=1}^{2} \frac{W_i(t)}{R_i(t)}, \quad q(0) = 5,$$

$$\tau(t) = R_1(t)/2,$$

with $R_1(t) \doteq \frac{q(t)}{300} + 0.001$, $R_2(t) \doteq \frac{q(t)}{300} + 0.0015$, $p_i(t) = 0.005 \times q(t - R_i(t))$, $i = 1, 2$, and $W_1(0) = W_2(0.25) = 10$ packets. The behavior of the network internal states $q(t)$, $W_1(t)$ and $W_2(t)$ is presented on figure 2.

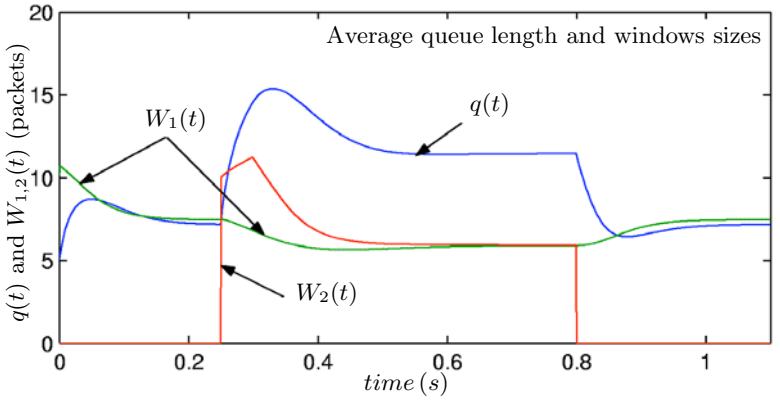

Fig. 2. Behavior of the network internal states

We now detail how the TCP model is used in the computation of the predictor horizon $\delta(t)$ to set the control law established in Theorem 5. From the definition of $R_i(t)$, we have that

$$\tau(\zeta) = \frac{1}{2} \left[\frac{q(\zeta)}{C_r} + T_{pcs} \right]. \tag{18}$$

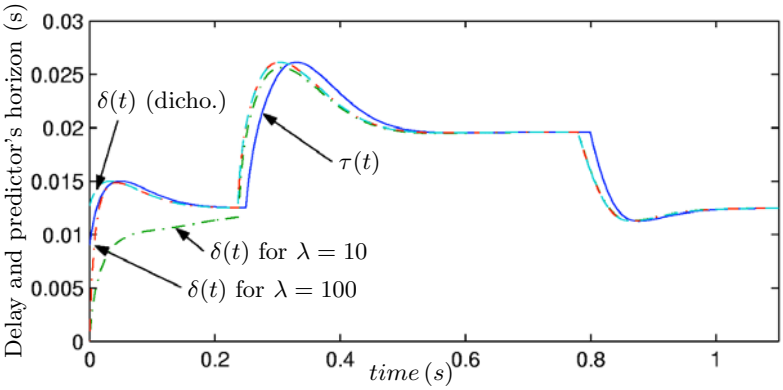

Fig. 3. Computation of the predictor's horizon

Deriving the previous equation along with (17), it follows that

$$\frac{d\tau}{d\zeta}(\zeta) = \frac{1}{2C_r}\left[\sum_{i=1}^{N(\zeta)} \frac{W_i(\zeta)}{R_i(\zeta)} - C_r\right], \tag{19}$$

where $R_i(\zeta)$ is obtained from $q(\zeta)$ and $N(\zeta)$ is assumed to be known. Both $W_i(\zeta)$ and $q(\zeta)$ are obtained from the dynamics (16)-(17): this is done by continuously computing the solutions of (16)-(17) up to the time $t + \tau_{max}$. (18)-(19) can now be substituted in (15) to obtain the dynamics $\dot{\delta}(t)$.

Example 2. Considering the delay induced by the network corresponding to the previous example, the predictor's horizon is computed for two different values of λ and compared with the exact value (computed using dichotomy) in figure 3.

This simulation shows the effectiveness of the proposed estimation to compute the time-varying horizon. The estimated horizon quickly converges toward its exact value (depending on the choice of λ).

Finally, the resulting system response is studied for four different control laws:

- state feedback,
- state predictor with a variable horizon,
- state predictor with a fixed horizon equal to the maximum delay,
- a buffer strategy, where a buffer is added at the system's input in order to make the delay constant (equal to its maximum value τ_{max}), combined with the previous predictor.

In order to compare these methods, the system response to a non-zero initial condition and with measurement noises (white vibration of power 0.01 and core [23341]) are illustrated in figure 4. The temporal evolution of the pendulum angle shows that, compared to the use of a predictor with a variable horizon:

- the simple state feedback induces an overshoot and light oscillations when the initial condition is non-zero, and significant oscillations when a measurement noise is added,

- the state predictor with a fixed horizon, although more suitable than the previous strategy, induces some oscillations and a longer settling time. It is also more sensitive to measurement noises,
- the buffer strategy exhibits a quickly compensated initial divergence (due to the increased delay) and has similar performances as the predictor with a variable horizon (peak slightly weaker). This strategy has the advantage of being simpler from the control point of view but introduces an additional complexity on the system site.

Note that the previous effects are amplified for delays of more significant amplitude and/or variation. Some experimental results [9] have shown that the state feedback can't stabilize the system in the real case and a bad transient response, due to some high frequency noise in the control signal, is obtained if the fixed horizon predictor or the buffer strategy are used.

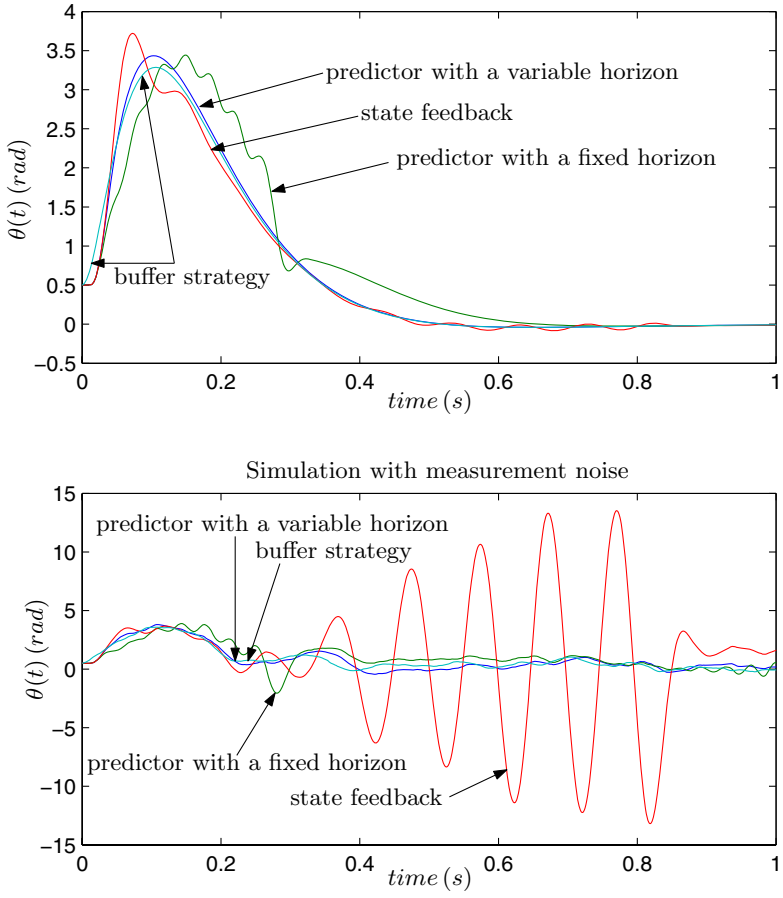

Fig. 4. Comparison between different control laws

6 Conclusion

In this chapter, the problem of stabilisation through networks has been formulated as the problem of stabilizing a system with a time-varying delay in the input. The commandability and finite spectrum assignement issues were presented, along with an overview on the use of state predictors in various control scheme. The explicit use of the network dynamics in the design of the control law was emphasized and illustrated by some simulation examples, where three predictor-based control laws are compared.

Acknowledgements

This study was realized within the NECS-CNRS projet. The authors would like to thank the CNRS for partially funding the project. The authors would also like to thank Jean-Pierre Richard and Rodolphe Sépulchre for their careful reading and constructive remarks on this document.

References

1. Smith O. (1959) Closer control of loops with dead time. Chem. Eng. Prog., 53:217–219
2. Niculescu S.-I., Verriest E., Dugard L., Dion J.-M. (1998) Stability and robust stability of time-delay systems: a guide tour. In Lecture Notes on Control and Information Sciences 228: Stability and Control of Time-delay Systems, L. Dugard and E. Verriest Eds. Springer, Berling Heidelberg New York
3. Fridman E., Shaked U. (2003) Delay-dependent stability and H_∞ control: constant and time-varying delays. Int. J. Control 76(1):48–60
4. Yu R. (1999) On stability of linear systems with time-varying delay: generalized lyapunov equation. IEEE AFRICON 1:569–574
5. Verriest E. (2002) Stability of systems with state-dependant and random delays. IMA Journal of Mathematical Control and Information 19:103–114
6. TanenbaumA.S. (1996) Computer Networks. Prentice Hall, Upper Saddle River, New Jersey
7. Olbrot A. (1972) On controllability of linear systems with time delays in the control. IEEE Trans. Automat. Contr. 16:664–666
8. Mondié S., Michiels W. (2003) A safe implementation for finite spectrum assignment: robustness analysis. In Proceedings of the 42^{nd} IEEE Conference on Decision and Control (CDC'2003), Hawaii, USA
9. Witrant E. (2005) Stabilisation des systèmes commandés par réseaux. Ph.D. dissertation, INPG/Laboratoire d'Automatique de Grenoble, Grenoble
10. Manitius A., Olbrot A. (1979) Finite spectrum assignment problem for systems with delays. IEEE Trans. Automat. Contr. 24:541–552
11. Kwon W., Pearson A. (1980) Feedback stabilization of linear systems with delayed control. IEEE Trans. Automat. Contr. 25(2):266–269
12. Artstein Z. (1982) Linear systems with delayed control: a reduction. IEEE Trans. Automat. Contr. 27(4):869–879
13. Nihtilä M. (1989) Adaptive control of a continuous-time system with time-varying input delay. Systems and Control Letters 12:357–364

14. Nihtilä M. (1991) Finite pole assignment for systems with time-varying input delays. In Proc. of the 30^{rd} IEEE Int. Conf. on Decision and Control, Brighton, England
15. Nihtilä M. (1991) Pole placement design methodology for input delay systems. In European Control Conference, Grenoble, France
16. Mondié S., Niculescu S.-I., Loiseau J.J. (2001) Delay robustness of closed loop finite assignment for input delay systems. In Proc. of the 3^{rd} IFAC Workshop on Time Delay Systems, Santa Fe, New Mexico
17. Uchida K., Misaki Y., Azuma T., and Fujita M. (2003) Predictive H^{∞} control for linear systems over communication channels with time-varying delays. In Proc. of the 4^{th} IFAC Workshop on Time Delay Systems, Rocquencourt, France
18. Uchida K., Ikeda K., Kojima A. (2000) Finite-dimensional characterizations of H^{∞} control for linear systems with delays in control input and controlled output. In Proc. of the 2^{nd} IFAC Workshop on Time Delay Systems, Ancona, Italy
19. Witrant E., Georges D., Canudas-de-Wit C., Sename O. (2005) Stabilisation of network controlled systems with a predictive approach. In Proc. of the 1^{st} Workshop on Networked Control System and Fault Tolerant Control, Ajaccio, France
20. Witrant E., Canudas-de-Wit C., Georges D. (2003) Remote output stabilization under two channels time-varying delays. In Proc. of the 4^{th} IFAC Workshop on Time Delay Systems, Rocquencourt, France
21. Hirche S., Buss M. (2004) Telepresence control in packet switched communication networks. In Proc. of the IEEE Conference on Control Applications, Taipei, Taiwan
22. Van Assche V., Dambrine M., Lafay J.-F., RichardJ.-P. (1999) Some problems arising in the implementation of distributed-delay control laws. In Proc. of the 38^{th} Conference on Decision and Control, Phoenix, Arizona
23. Fattouh A., Sename O., Dion J.-M. (2001) Pulse controller design for linear systems with delayed state and control. In Proc. of the 1^{st} IFAC Symposium on System Structure and Control, Prague, Czeck Republic
24. Sidje R.B. (1998) Expokit: a software package for computing matrix exponentials. ACM Transactions on Mathematical Software (TOMS) 24(1):130–156
25. Borne P., Dauphin-Tanguy G., Richard J.-P., Rotella F., Zambettakis I. (1992), Modélisation et identification des processus. Tome 1, série Méthodes et Pratiques de l'Ingénieur. Technip, Paris
26. Witrant E., Canudas-de-Wit C., Georges D., Alamir M. (2004) Remote stabilization via time-varying communication network delays: Application to TCP networks. In Proc. of the IEEE Conference on Control Applications, Taipei, Taiwan
27. Misra V., Gong W.-B., Towsley D. (2000) Fluid-based analysis of a network of AQM routers supporting TCP flows with an application to RED. In Proc. of ACM SIGCOMM'00, Stockholm, Sweden
28. Hollot C., Chait Y. (2001) Nonlinear stability analysis for a class of TCP/AQM networks. In Proc. of the 40^{th} IEEE Int. Conf. on Decision and Control, Orlando, Florida

Networked Control Systems: Algorithms and Experiments

Rafael Sandoval-Rodriguez[1], Chaouki T. Abdallah[1], Henry N. Jerez[1], Ivan Lopez-Hurtado[1,⋆], Oscar Martinez-Palafox[2], and Dongjun Lee[2]

[1] Electrical & Computer Engineering Department
MSC01 1100
1 University of New Mexico
Albuquerque, NM 87131-0001, USA
{rsandova,chaouki,hjerez,ilopez}@ece.unm.edu

[2] Coordinated Science Laboratory
University of Illinois at Urbana-Champaign
1308 W. Main St., Urbana IL 61801, USA
{rsandova,chaouki,hjerez,ilopez}@ece.unm.edu

1 Introduction

In this chapter we address the problem of implementing control systems using general purpose communication networks to transmit plant state information and control signals. The main idea is to expose the issues that have to be considered when implementing teleoperation and telepresence applications exploiting already deployed communication infrastructure. Some of these applications may be implemented with local controllers and remote supervisory systems, where the remote client sends set points according to the process status received, but the control loops are closed locally. Other applications however, might require gathering information from different and geographically distant agents or sensors. In such a case, loops cannot be closed locally, and the state and control signals must travel across the networks. A general purpose communication network will however introduce issues such as propagation time-delays and loss of information. Therefore, the control algorithms must now account for these issues, and they should be robust enough to guarantee a certain level of performance. We develop in this section a series of experiments to identify the issues induced by a general purpose communication network, with specific emphasis on wireless networks. We use standard operating systems and industrial hardware for data acquisition. Then, we propose compensation alternatives to cope with these issues.

2 Experimental Setup

An experimental setup was implemented in order to expose the issues induced by the network. As mentioned in Section 1, the idea is to introduce mobility into the plant,

⋆ The research of all authors is partially supported by NSF-0233205.

J. Chiasson and J.J. Loiseau (Eds.): Appl. of Time Delay Systems, LNCIS 352, pp. 37–56, 2007.
www.springerlink.com

either by physically moving the plant to new locations without the need to rewire the network, or by considering a mobile robot as the plant. A laptop computer is used as the plant's "brain", in order to connect to the building's WLAN using an 802.11b wireless card. A PCMCIA data acquisition card, DAQ 6024E from National Instruments^{TM}, is used to interface the laptop computer to the plant. The software programs used to acquire state data from the sensors, and to apply control signals to the actuators as well as to implement the communication routines, are developed in LabView® also from National Instruments^{TM}.

For the controller computer we used various configurations: A laptop computer connected to the building WLAN, a desktop computer connected to the wired building LAN, or a computer with broadband connection outside the campus LAN. The programs in the controller computer, for control and communications, were also developed using LabView®. All computers were running standard Windows XP Professional. Time stamping was used in most of our experiments, and we therefore had to synchronize the computers' clocks. For this purpose, we implemented a routine in LabView®, similar to the procedure presented in [1], as described in the following steps:

1. The plant's computer reads its millisecond timer and sets its zero mark, then sends a zero to the controller computer.
2. The controller's computer receives the zero from the plant computer, reads its millisecond timer and sets its zero mark, then sends a zero to the plant computer.
3. The plant's computer receives the zero from the controller computer, reads its millisecond timer and calculates its first round-trip time, RTT0. Then, it sends RTT0 to the controller's computer.
4. The controller's computer receives RTT0, reads its millisecond timer and calculates its first round-trip time, RTT1. Then, it sends RTT1 to the plant's computer.
5. The plant's computer receives RTT1, reads its millisecond timer and calculates its second round-trip time, RTT2. Then, it sends RTT2 to the controller computer.
6. The controller's computer receives RTT2, reads its millisecond timer and calculates its second round-trip time, RTT3.

The controller's computer calculates the time offset, t_{off}, between the zero marks in the computers using

$$t_{off} = RTT0 - \left(RTT1 - \left(RTT2 - \frac{RTT3}{2} \right) \right) \tag{1}$$

The controller's computer then estimates the current time in the plant's computer, t_p, using

$$t_p = t_c + t_{off} \tag{2}$$

where t_c is the current time in the controller's computer. Figure 1 depicts the clock synchronization procedure graphically. The clock's synchronization routine was implemented using both UDP and TCP over IP. We ran the routine at different times of the day and with the controller's computer inside and outside the building LAN. With the controller's computer inside the building LAN, (whether it is wireless or wired), and during low traffic hours, the average round-trip time was 3 *msec*. During high traffic

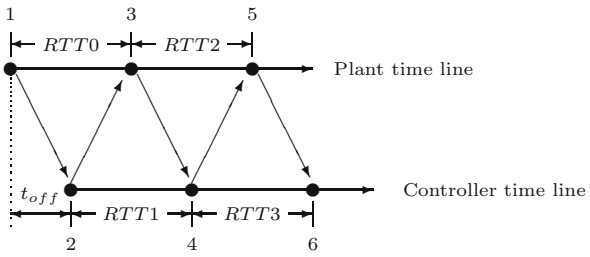

Fig. 1. Clock synchronization procedure

hours the average round-trip time was 6 *msec*. Having the controller's computer outside the campus LAN, the average round-trip time was 80 *msec*, and no significant difference in the round-trip time was observed at different times of the day. The routine was run before any experiment using time stamping. The estimated error in the clock synchronization is 1 *msec*, which is the resolution in the millisecond timers.

3 Issues Introduced by the LAN

3.1 Retention of Packets

One common application in teleoperation and telepresence is the broadcasting of the plant state's signals to controllers or supervisory monitoring systems. Such broadcasting could be, for instance, the distance to obstacles, or the current heading and speed in a mobile robot. With the purpose of measuring the difference in latency for various sizes of Ethernet packets, we ran a experiment where the plant is transmitting packets with sizes from 46 to 1500 bytes, and alternating between UDP and TCP. With the computer's controller inside the building LAN, we did not observe a significant difference in the latency when transmitting a single packet (independent of its size and using either UDP or TCP). However, when the plant broadcasts packets at a given sampling rate, a special feature in TCP limits the broadcasting rate to 200 *msec*, irrespective of the packet size. Even when the signals were sampled at a faster rate, TCP retained the packets until the next multiple of 200 *msec*. Figure 2 shows the arrival time to the controller's computer of time stamps taken at the plant every 20 *msec*; 9 packets were retained and, at the next multiple of 200 *msec*, the group of 10 packets were transmitted to the controller's computer. From Figure 2 we see that the samples with time stamps from 20 to 200 *msec* arrived to the controller's computer at $t_c = 200$ *msec*. This problem however, did not manifest itself with UDP packets which arrived every 20 *msec*, as sampled. Figure 3 shows a plot of the time stamp arrivals, with a sampling time of 200 *msec*. Now the sampling time is equal to the lower bound in the broadcasting rate induced by TCP and the packets are not retained. The retention of packets generates a later bursting of those packets. If the plant's state samples are not time stamped, confusion results at the controller's computer as the program simply can not tell the fresher samples. If bursting occurs, the program in the controller should be able to empty the incoming queue, discard old packets, and only use the last sample of the plant state. We connected the plant's laptop computer to the wired LAN, to verify that this problem

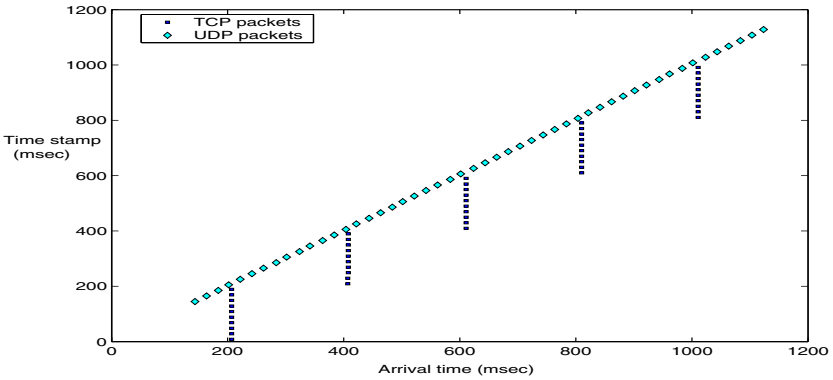

Fig. 2. Arrivals of time stamps using TCP and UDP, sampling at 20 *msec*

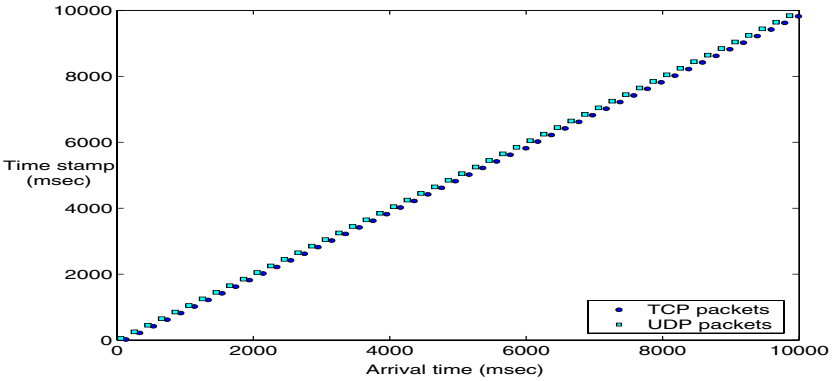

Fig. 3. Arrivals of time stamps using TCP and UDP, sampling at 200 *msec*

occurs with TCP, and not because of the wireless medium. The wired connection did generate the retention of packets when using TCP. Thus, because of this TCP-specific phenomenon, if the broadcast requires sampling times smaller than 200 *msec*, our recommendation is to use UDP, assuming inaccurate samples may be tolerated.

3.2 Disconnection from the WLAN

Another issue introduced in this case by the wireless network is the disconnection of the plant computer from the WLAN. This problem is attributed to the re-association procedure that the wireless card executes in order to find the access point with the strongest signal. We observed that the disconnection occurs on the average every 60 *secs* and lasts on the average, 1.5 *secs*. Figure 4 shows the arrival times of time stamps with a disconnection from the WLAN. The top plot shows a disconnection from the WLAN when using TCP and a sampling time of 200 *msec*. The sample with time stamp $t_p = 2410$ *msec* arrives to the controller at $t_c = 2550$ *msec*, showing a time-delay of

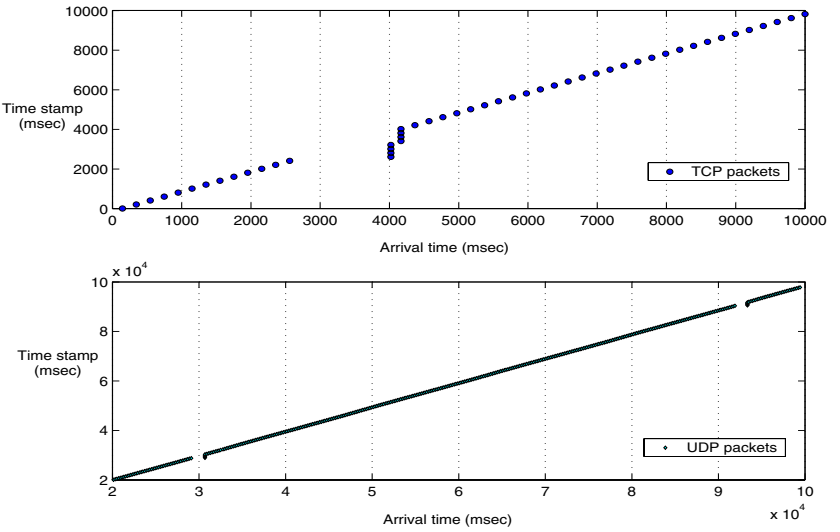

Fig. 4. Disconnection from the WLAN

$\tau = 140$ *msec*. This time delay includes the delay due to the asynchronism between the retention feature of TCP and the sampling clock in the plant, plus the propagation time-delay. The next sample with time stamp $t_p = 2610$ *msec* arrives to the controller at $t_c = 4020$ *msec*, showing a time-delay of $\tau = 1410$ *msec*. Subtracting the previous sample time-delay, results in a disconnection time of approximately 1.27 *secs*.

The bottom plot in Figure 4 shows the time between two disconnections from the WLAN when using UDP and a sampling time of 200 *msec*. The first disconnection occurred at $t_c = 29133$ *msec*, while the second disconnection occurred at $t_c = 92296$ *msec*, resulting in a time between the disconnections of approximately 63.163 *secs*. The time of disconnection, and the period between disconnections seem to be independent of the congestion control protocol and sampling time used.

3.3 Propagation Time-Delay

For this experiment the controller's computer was connected to a broadband ISP outside the building's LAN, with the purpose of emphasizing the problem of large time-delays. We again ran the experiment of reading the plant's clock as a time stamp and sending it to the controller's computer, which sends it back immediately. The plant's computer registers the arrival times and computes the round-trip times. Figure 5 shows the resulting round-trip times of 100 samples. In order to check for symmetry in the channel, we also plot the arrival times at the controller's computer, Figure 6 shows the plant-to-controller time-delay for 100 samples. We ran these experiments several times at different times of the day. The mean of the round-trip times changed slightly, but the standard deviation was relatively constant. The plant-to-controller and controller-to-plant time-delays were verified to be close, thus establishing that the propagation channel is symmetric.

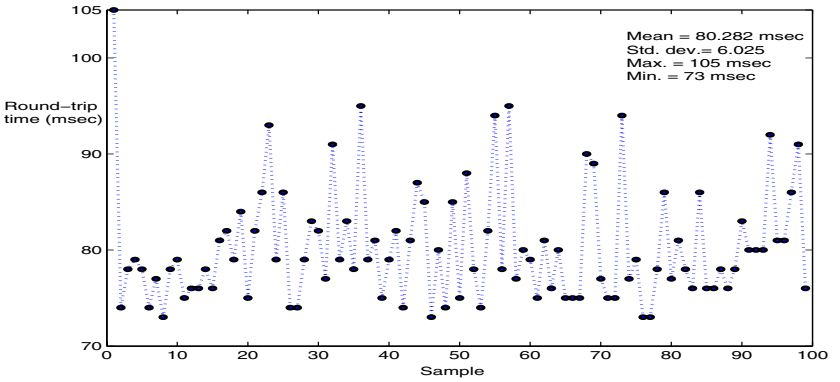

Fig. 5. Round-trip times for 100 samples

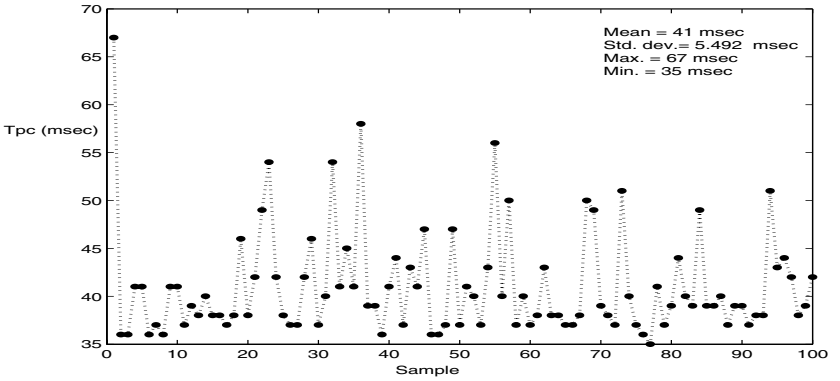

Fig. 6. Plant-to-controller time-delays for 100 samples

With the purpose of illustrating the effect of time-delay and to set a basis for the compensation schemes to be presented in Section 3.4, let us consider the scalar system

$$\dot{x} = ax + bu \tag{3}$$

where $a > 0$, and $b > 0$. Let us also consider state (in this case also output) feedback control with gain K, i.e. $u = -Kx$. The sensing is clock-driven with sampling time t_s, and the control and actuation are event-driven. This means that the controller will compute and send a control signal as soon as it receives a sample, and that the plant will immediately process any received control signal. The time-delay between the plant and the controller is denoted by τ_{pc}, while the time-delay between the controller and the plant is denoted by τ_{cp}, as depicted in Figure 7. At this time, we consider that the combined time-delay is less than the sampling time. We observe that the control signal $u = -Kx[(k-1)t_s]$ arrives to the plant at time $(k-1)t_s + \tau_{pc} + \tau_{cp}$, and is held until time $kt_s + \tau_{pc} + \tau_{cp}$, when it is replaced by the new control signal $u = -Kx[kt_s]$.

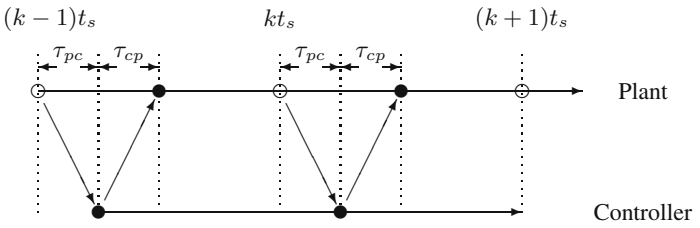

Fig. 7. Time-delay between plant and controller

Thus, two control signals are applied during the interval $kt_s \leq t \leq (k+1)t_s$. Solving for the system's state in equation (3) in the interval $kt_s \leq t \leq kt_s + \tau_{pc} + \tau_{cp}$, yields

$$x[kt_s + \tau_{pc} + \tau_{cp}] = \Phi_1 x[kt_s] + \Gamma_1 x[(k-1)t_s] \tag{4}$$

where

$$\Phi_1 = e^{a(\tau_{pc}+\tau_{cp})}$$
$$\Gamma_1 = -\frac{b}{a}K\left(e^{a(\tau_{pc}+\tau_{cp})} - 1\right)$$

Now, solving for the interval $kt_s + \tau_{pc} + \tau_{cp} \leq t \leq (k+1)t_s$, results

$$x[(k+1)t_s] = \Phi_2 x[kt_s + \tau_{pc} + \tau_{cp}] + \Gamma_2 x[kt_s] \tag{5}$$

where

$$\Phi_2 = e^{a(t_s-\tau_{pc}-\tau_{cp})}$$
$$\Gamma_2 = -\frac{b}{a}K\left(e^{a(t_s-\tau_{pc}-\tau_{cp})} - 1\right)$$

Substituting (4) into equation (5), and simplifying

$$x[(k+1)t_s] = \Psi x[kt_s] + \Upsilon x[(k-1)t_s] \tag{6}$$

where

$$\Psi = e^{at_s} - \frac{b}{a}K\left(e^{a(t_s-\tau_{pc}-\tau_{cp})} - 1\right)$$
$$\Upsilon = -\frac{b}{a}K\left(e^{at_s} - e^{a(t_s-\tau_{pc}-\tau_{cp})}\right)$$

Consider now the augmented vector

$$y[kt_s] = \begin{bmatrix} x[kt_s] \\ x[(k-1)t_s] \end{bmatrix} \tag{7}$$

leading to the augmented system

$$y[(k+1)t_s] = \Phi y[kt_s] \tag{8}$$

where

$$\Phi = \begin{bmatrix} \Psi & \Upsilon \\ 1 & 0 \end{bmatrix} \tag{9}$$

Thus, given the system parameters a and b, control gain K, and sampling time t_s, there exists an upper bound, τ^*, in the combined time-delay $\tau = \tau_{pc} + \tau_{cp}$, such that if $\tau < \tau^*$ the matrix Φ in equation (9) is Schur. In other words, the system can tolerate the combined time-delay $\tau = \tau_{pc} + \tau_{cp}$, and still converge to the origin.

3.4 Compensation Approaches

The use of time stamping in the plant's samples, along with clock synchronization between the plant and controller computers, allows the controller to estimate the time elapsed in the plant since the last received plant sample was taken. If in addition, the plant sends to the controller the last control signal applied, also time stamped, and assuming knowledge of the plant's model, the controller can estimate the current state of the plant, then generate a more accurate control signal. The following subsections present compensation approaches for the propagation time-delay and the network disconnection, assuming the conditions mentioned above.

3.5 Compensating for Plant-to-Controller Time-Delay

Assuming that the plant transmits to the controller state samples with time stamp t_{ps}, and the last control signal applied with time stamp t_{cs}, then the plant-to-controller time-delay can be obtained from

$$\tau_{pc} = t_c + t_{off} - t_{ps} \tag{10}$$

where t_c is the sample arrival time at the controller, and t_{off} is the offset time between the plant and controller clocks. For the sake of simplicity, we consider zero computation time for the control signal. Now, using the elapsed time τ_{pc}, the controller can estimate the current state of the plant, and uses that estimate to generate the control signal. Using again Figure 7, the control signal $u = -K\hat{x}[(k-1)t_s + \tau_{pc}]$ arrives at the plant at time $(k-1)t_s + \tau_{pc} + \tau_{cp}$, and is applied and held until the next control signal $u = -K\hat{x}[kt_s + \tau_{pc}]$ arrives to the plant at time $kt_s + \tau_{pc} + \tau_{cp}$. We can solve for the state of the system in equation (3) in the interval $kt_s \leq t \leq (k+1)t_s$, in the following steps:

$$x[kt_s + \tau_{pc}] = \Phi_3 x[kt_s] + \Gamma_3 x[(k-1)t_s + \tau_{pc}] \tag{11}$$

where

$$\Phi_3 = e^{a\tau_{pc}} \qquad \Gamma_3 = -\frac{b}{a}K(e^{a\tau_{pc}} - 1)$$

$$x[kt_s + \tau_{pc} + \tau_{cp}] = \Phi_4 x[kt_s + \tau pc] + \Gamma_4 x[(k-1)t_s + \tau_{pc}] \tag{12}$$

where

$$\Phi_4 = e^{a\tau_{cp}} \qquad \Gamma_4 = -\frac{b}{a}K(e^{a\tau_{cp}} - 1)$$

$$x[(k+1)t_s] = \Phi_5 x[kt_s + \tau_{pc} + \tau_{cp}] + \Gamma_5 x[kt_s + \tau_{pc}] \tag{13}$$

where

$$\Phi_5 = e^{a(t_s - \tau_{pc} - \tau_{cp})} \qquad \Gamma_5 = -\frac{b}{a}K(e^{a(t_s - \tau_{pc} - \tau_{cp})} - 1)$$

$$x[(k+1)t_s + \tau_{pc}] = \Phi_6 x[kt_s + \tau_{pc} + \tau_{cp}] + \Gamma_6 x[kt_s + \tau_{pc}] \tag{14}$$

where

$$\Phi_6 = e^{a(t_s - \tau_{cp})} \qquad \Gamma_6 = -\frac{b}{a}K(e^{a(t_s - \tau_{cp})} - 1)$$

$$x[(k+1)t_s + \tau_{pc} + \tau_{cp}] = \Phi_7 x[kt_s + \tau_{pc} + \tau_{cp}] + \Gamma_7 x[kt_s + \tau_{pc}] \tag{15}$$

where

$$\Phi_7 = e^{a(t_s)} \qquad \Gamma_7 = -\frac{b}{a}K(e^{at_s} - 1).$$

Defining now the augmented vector

$$v[kt_s] = \begin{bmatrix} x[kt_s + \tau_{pc} + \tau_{cp}] \\ x[kt_s + \tau_{pc}] \\ x[kt_s] \\ x[(k-1)t_s + \tau_{pc} + \tau_{cp}] \\ x[(k-1)t_s + \tau_{pc}] \end{bmatrix} \tag{16}$$

the augmented system becomes

$$v[(k+1)t_s] = \Phi_{pc} v[kt_s] \tag{17}$$

where

$$\Phi_{pc} = \begin{bmatrix} \Phi_7 & \Gamma_7 & 0 & 0 & 0 \\ \Phi_6 & \Gamma_6 & 0 & 0 & 0 \\ \Phi_5 & \Gamma_5 & 0 & 0 & 0 \\ 0 & \Phi_4 & 0 & 0 & \Gamma_4 \\ 0 & 0 & \Phi_3 & 0 & \Gamma_3 \end{bmatrix} \tag{18}$$

For the purpose of illustration, let us consider the following example.

Example 1. Let the system's parameters be $a = 1$, $b = 1$, $K = 2$, the sampling time $t_s = 500$ *msec*, and the propagation time-delays, $\tau_{pc} = 100$*msec* and $\tau_{cp} = 100$ *msec*. Substituting these parameters in the transition matrix of equation (9), for the original uncompensated system, its eigenvalues are found to be:$\lambda = 0.4745 \pm 0.6104i$ which lie inside the unit circle. Now let us increase the propagation time-delays to $\tau_{pc} = \tau_{cp} = 250$ *msec*, which correspond to one sample delay control. Substituting again the parameters in equation (9), the eigenvalues are found to be $\lambda = 0.8244 \pm 0.7860i$.

Note that the eigenvalues now lie outside the unit circle. Using compensation for the propagation time-delay τ_{pc}, we find the eigenvalues in equation (18) to be $\lambda = 0,\ -0.5681,\ 0, 0.5403,$ and $\pm\, 0.6614i$. All the eigenvalues now lie inside the unit circle, and in spite of the large propagation time-delays, the compensation scheme makes the system converge to the origin.

3.6 Compensating for Controller-to-Plant Time-Delay

In the previous subsection, the estimate of the plant state, $\hat{x}[kt_s + \tau_{pc}]$, was computed based on the measured time-delay τ_{pc}. The resulting control signal $u = -Kx[kt_s + \tau_{pc}]$ generated will arrive at the plant with a time-delay τ_{cp}, but unfortunately, at the time of computing the control signal, this controller-to-plant time-delay is unknown. However, assuming that we have the time stamps of the previous control signals applied to the plant, we can obtain an estimate of the next controller-to-plant time-delay. So, considering that this prediction of τ_{cp} is accurate with some degree of confidence, we can estimate the plant's state at the time of arrival of the control signal. Proceeding in a similar fashion to the previous subsection, the state of the system in equation (3), in the interval $kt_s \leq t \leq (k+1)t_s$, can be obtained in the following steps:

$$x[kt_s + \tau_{pc}] = \Phi_3 x[kt_s] + \Gamma_3 x[(k-1)t_s + \tau_{pc} + \tau_{cp}]$$

$$x[kt_s + \tau_{pc} + \tau_{cp}] = \Phi_4 x[kt_s + \tau pc] + \Gamma_4 x[(k-1)t_s + \tau_{pc} + \tau_{cp}]$$

$$x[(k+1)t_s] = \Phi_5 x[kt_s + \tau_{pc} + \tau_{cp}] + \Gamma_5 x[kt_s + \tau_{pc} + \tau_{cp}]$$

$$x[(k+1)t_s + \tau_{pc}] = \Phi_6 x[kt_s + \tau_{pc} + \tau_{cp}] + \Gamma_6 x[kt_s + \tau_{pc} + \tau_{cp}]$$

$$x[(k+1)t_s + \tau_{pc} + \tau_{cp}] = \Phi_7 x[kt_s + \tau_{pc} + \tau_{cp}] + \Gamma_7 x[kt_s + \tau_{pc} + \tau_{cp}]$$

The parameters Φ_3 to Φ_7, and Γ_3 to Γ_7, are the same as in the previous subsection. Considering again the augmented vector of equation (16), the augmented system compensating for both time-delays is given by:

$$v[(k+1)t_s] = \Phi_\tau v[kt_s] \tag{19}$$

where

$$\Phi_\tau = \begin{bmatrix} \Phi_7 + \Gamma_7 & 0 & 0 & 0 & 0 \\ \Phi_6 + \Gamma_6 & 0 & 0 & 0 & 0 \\ \Phi_5 + \Gamma_5 & 0 & 0 & 0 & 0 \\ 0 & \Phi_4 & 0 & \Gamma_4 & 0 \\ 0 & 0 & \Phi_3 & \Gamma_3 & 0 \end{bmatrix} \tag{20}$$

Again, for illustration purposes, let us use the following example.

Example 2. Let us consider the same system parameters as in example 1, but assume now the time sampling is $t_s = 700$ *msec*, and the time-delays, $\tau_{pc} = \tau_{cp} = 100$ *msec*. Substituting these parameters in the transition matrix of equation (9) for the original uncompensated system, the eigenvalues are found to be $\lambda = 0.3582 \pm 0.7757i$ which still lie inside the unit circle, despite the time-delays. Now, let us increase the propagation time-delays to $\tau_{pc} = \tau_{cp} = 200$ *msec*. Substituting again the parameters in equation (9) we obtain $\lambda = 0.6570 \pm 0.9466i$. Now, the eigenvalues lie outside the unit circle. Using compensation only for propagation time-delay τ_{pc}, we use these parameters in the transition matrix of equation (18), resulting in the eigenvalues: $\lambda = 0,\ -0.4428,\ 0,\ \text{and} 0.3582 \pm 0.7757i$. All the eigenvalues lie inside the unit circle. Let us now increase the propagation time-delays to $\tau_{pc} = \tau_{cp} = 300$ *msec*. Substituting again the parameters in the transition matrices of equations (9) and (18), we obtain the eigenvalues: $\lambda = 0.9017 \pm 1.0020i$ and $\lambda = 0,\ -0.6997,\ 0,\ \text{and} 0.5151 \pm 0.8824i$. Even with the compensation for the plant-to-controller time-delay, the complex conjugate eigenvalues lie outside the unit circle. Applying compensation for both time-delays, we substitute the parameters in the transition matrix of equation (20), resulting in the following eigenvalues $\lambda = 0,\ -0.6997,\ 0,\ 0,\ -0.0138$. All the eigenvalues lie inside the unit circle. Despite the large propagation time-delays, the compensation scheme for both time-delays makes the system converge to the origin.

3.7 Compensating for Disconnection from the WLAN

Now, consider the case of disconnection from the network, or equivalently of dropped packets. The effects of this issue on the networked-closed-loop system will depend on the stability of open-loop plant, and on the state of the plant at the time of the disconnection. In the case of an open-loop stable plant, a sufficiently large disconnection will move the plant towards an equilibrium point defined by the control signal being applied at the time of disconnection. However, in an open-loop unstable plant, the plant states will continue to increase exponentially in the direction they were moving at the time of disconnection. Fast dynamics plants may get out of control, but for some slower dynamics plants, this might be a recoverable situation. In the previous chapter, we gave upper bounds on the time that an unattended unstable system can stay inside its region of attraction, assuming saturation in the control signal. We can use those results to decide if the plant should hold the last control signal applied, or if it should apply zero control signal when a disconnection is detected.

Considering the system in equation (3), and assuming the saturation values $\pm u_{max}$ in the control signal, the region of attraction is defined by the interval

$$-x_{max} = -\frac{b}{a}u_{max} < x < \frac{b}{a}u_{max} = x_{max} \tag{21}$$

In order to find the best control action that the plant should apply in case of a disconnection, whether to hold the last control signal $u(t_d)$ or to apply zero control signal, we can use the expression of the state for system (3) and solve for the time t_e, at which the plant state leaves the region of attraction $\pm x_{max}$, given an initial condition $x(t_d)$. Considering first the case of applying zero control signal, the time t_e at which the plant state,

with initial condition $x(t_d) > 0$, will reach the positive edge, x_{max}, of the region of attraction is given by

$$t_e = \frac{1}{a} \ln \left(\frac{x_{max}}{x(t_d)} \right) \tag{22}$$

Now, considering that the plant holds the last control signal applied $u(t_d) = -Kx(t_d)$, and assuming state feedback with initial condition $x(t_d) > 0$, the time t_e at which the plant state reaches the negative edge, $-x_{max}$ is given by

$$t_e = \frac{1}{a} \ln \left(\frac{-x_{max} - \frac{aK}{b} x(t_d)}{x(t_d) - \frac{aK}{b} x(t_d)} \right) \tag{23}$$

Rearranging terms, we obtain

$$t_e = \frac{1}{a} \ln \left(\frac{x_{max}}{x(t_d)(\frac{aK}{b} - 1)} + \frac{\frac{aK}{b}}{\frac{aK}{b} - 1} \right) , \tag{24}$$

for values of $\frac{aK}{b}$ in the interval

$$2 > \frac{aK}{b} > 1 \tag{25}$$

The time t_e in equation (24) for which the system can be unattended is larger than the one in equation (22). In this case holding the last control signal will give the system a better chance to recover from the disconnection.

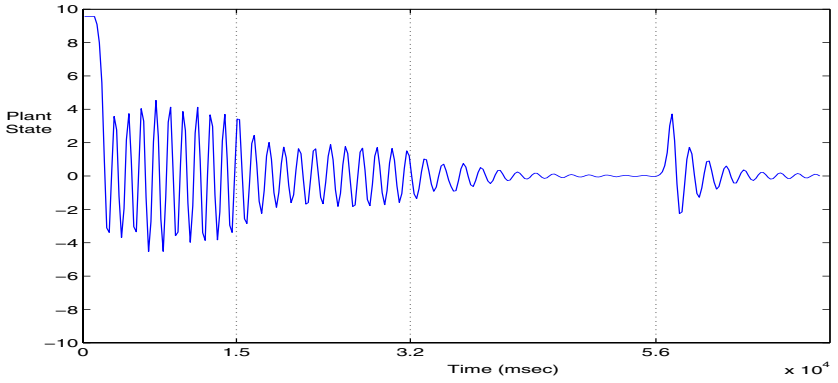

Fig. 8. Response of the plant states with time-delay, and compensations later applied

3.8 Experimental Results

In order to evaluate the performance of the time-delay compensation approaches, and considering the disconnection cases as proposed in Section 3.4, we implemented the system in equation (3) as an electronic circuit having the approximate model

$$\dot{x} = 3.2x + 3.2u \tag{26}$$

This circuit is then considered as our physical plant. We used as the controller a computer connected outside the campus LAN, and applied state feedback with gain $K = 2$. The round-trip time was on the average around 80 *msec*, as shown in Figure 5, and the one-way trips were fairly symmetric as shown in Figure 6.

In the first experiment we used a sampling time $t_s = 240$ *msec*. Figure 8 shows the response to the initial condition $x(0) = 9.6$ *volts*. For the first 15 *secs* no compensation was applied and the plant state oscillates between ± 4 *volts*. At $t = 15$ *secs* compensation for the plant-to-controller time-delay τ_{pc} is applied, which reduces the oscillations to ± 2 *volts*. At $t = 32$ *secs* compensation for the controller-to-plant time-delay τ_{cp} is also applied, and this reduces the oscillations almost to zero. At $t = 56$ *secs* a disconnection occurs, but the system is able to recover from it.

In the second experiment we used a sampling time $t_s = 220$ *msec*, but in this case the compensations for both time-delays were applied since $t = 0$. Figure 9 shows the response to the initial condition $x(0) = 9.6$ *volts*. We can see that despite the time-delay, the system converges to zero after 25 *secs*. At time $t = 55$ *secs* a disconnection occurs and the system is able to recover from it with less oscillations than in the first experiment.

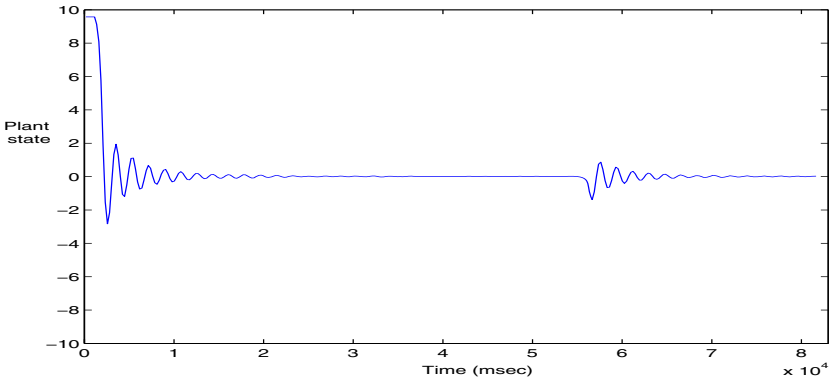

Fig. 9. Response of the plant states to time-delay, and compensations applied

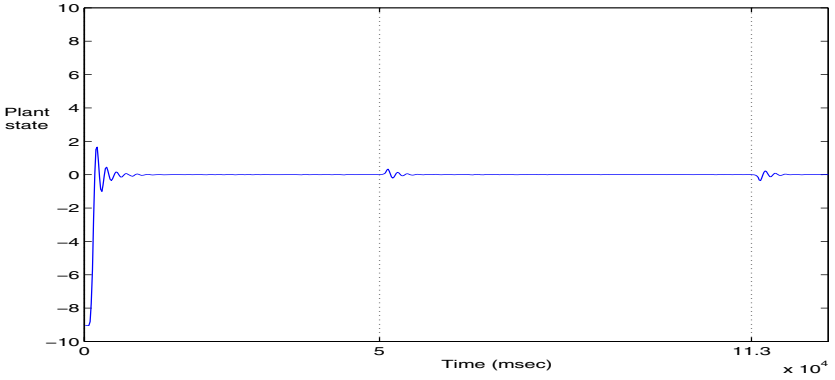

Fig. 10. Response of the plant states to time-delay, and compensations applied

In the third experiment we used a sampling time $t_s = 200$ *msec*, and the compensations for both time-delays were also applied at $t = 0$. Figure 10 shows the response to the initial condition $x(0) = -9.6$ *volts*. Two disconnections occurred, the first at $t = 50$ *secs*, and the second at $t = 113$ *secs*, but the system suffered a minimum level of disruption.

4 Teleoperation Experiment

So far, we have exposed the various issues that arise in a NCS. In this section, we focus on the time-delay issue, in a teleoperation experiment.

4.1 Experimental Setup

The teleoperation experiment was set up between a PHANToM™ Desktop haptic device as a master device, that was locally at the Coordinated Science Laboratory at the University of Illinois at Urbana Campaign, and a slave mobile robot located at the Network Control Systems Laboratory at the UNM. A laptop computer connected to the Internet through an Ethernet Card was used in the robot. A wired LAN was used instead of the WLAN in order to avoid the disconnection issue highlighted in Subsection 3.1. A PCMCIA data acquisition card, DAQ 6024E from National Instruments™, was used to interface the laptop computer to the mobile robot. The software programs used to acquire the state's measurements from the encoders and to apply control signals to the motors, as well as to implement the communication routines, were developed in LabView®, another National Instruments™ product. For the haptic device master station, a PC computer with two Pentium® 4 processors at 2.8GHz was connected to the Internet. The control and communication programs in the controller computer were developed using Microsoft™ Visual C++® ver. 6. All computers were running standard

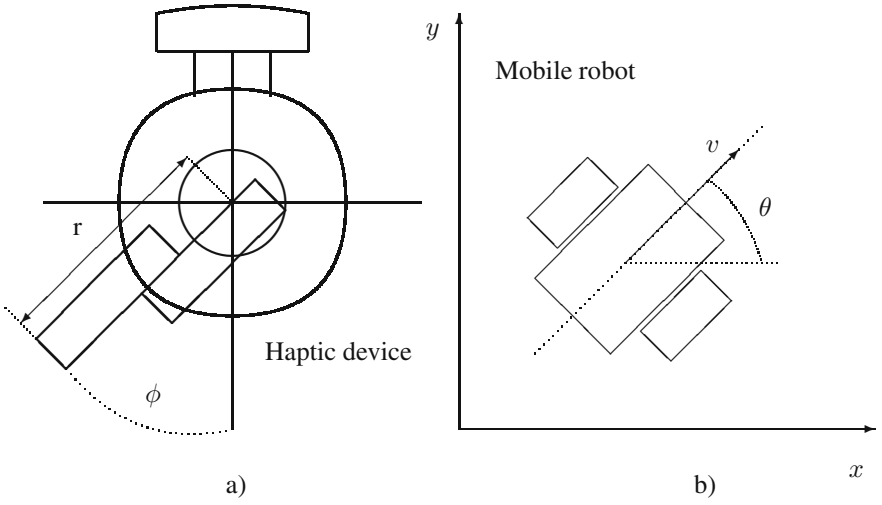

Fig. 11. a) Master r and ϕ directions, b) Slave v and θ directions

Windows® XP Professional. UDP was again the transmission protocol chosen to send and receive data from/to haptic device to/from mobile robot through the Internet, to alleviate the bursting phenomenon, described in Subsection 3.2.

4.2 Implementation

Well known is that time delay in the communication channel may cause instability in the teleoperation algorithm. For the this experiment, we use the control law proposed in [3], which, by enforcing passivity of the closed-loop teleoperator, ensures stable teleoperation with constant time-delays. Moreover, this control law also addresses kinematic/dynamic discrepancy between the master and slave systems, i.e. master haptic device is holonomic and has confined workspace, but slave mobile robot is nonholonomic and has unlimited workspace [4]. Consider the degrees of freedom defined in Figure 11. We also consider the next model for the the mobile robot

$$m\dot{v} = -\eta v + \frac{1}{r}(\tau_r + \tau_l) \tag{27}$$

$$J\dot{\omega} = -\psi\omega + \frac{l}{r}(\tau_r + \tau_l) \tag{28}$$

Where v, θ are linear velocity and heading angle, m_c, is the cart mass, J is the inertial moment, b is the the half-width of the cart, τ_r, τ_l are the torques for the right and left wheels, η is the viscous friction coefficients and ψ is the rotational friction coefficient (for simplicity, we made two assumptions: wheel inertial equal to zero and the geometrical center of the robot coincides with the center of mass). It was also considered that the robot has the pure rolling non slipping constraint $-\dot{x}sin\theta + \dot{y}cos\theta = 0$, see [5]. After some step response experiments, we determined the parameters of the robot as follows: $m_c = 25$ kg, $J = 1.03$ kgm, $l = 0.203$ m, $r = 0.101$ m, $\psi = 5.51$ kgm/s and $\eta = 133.7$ kg/s. According to [3], we sent $\hat{r}(t) := \dot{r}(t) + \lambda r(t)$ as the reference command for the linear velocity v of the slave mobile robot. Also, the angular position ϕ of the haptic interface was taken as the angular position reference for the slave mobile robot heading angle θ (Figure 11. The master control law was given by

$$T_r(t) := -B_r\dot{\hat{r}}(t) - K_r r(t) - K_{rv}(\hat{r}(t) - v(t-\tau_2)), \tag{29}$$

$$\begin{aligned} T_\phi(t) := & -B_{\phi\theta}(\dot{\phi}(t) - \dot{\theta}(t-\tau_2)) \\ & -B_\phi\dot{\phi}(t) - K_{\phi\theta}(\phi(t) - \theta(t-\tau_2)), \end{aligned} \tag{30}$$

and the slave control law was given by

$$T_v(t) := -K_{rv}(v(t) - \hat{r}(t-\tau_1)), \tag{31}$$

$$\begin{aligned} T_\theta(t) := & -B_{\phi\theta}(\dot{\theta}(t) - \dot{\phi}(t-\tau_1)) \\ & -K_{\phi\theta}(\theta(t) - \phi(t-\tau_1)). \end{aligned} \tag{32}$$

where $T_\star$ is the control command acting along the $\star$ direction, τ_1, τ_2 are the forward/backward delays, and $K_{rv}, K_r, K_{\phi\theta}, B_{\phi\theta}, B_\phi$ are (positive) control gains.

We set the control gains as follows: $B_r = 0.5$, $K_r = 0.001$, $K_{rv} = 100.0$, $B_\phi = 0.1$, $B_{\phi\theta} = 1000.0$, $K_{\phi\theta} = 2500.0$ and $\lambda = 0.04$. Here, λ was determined by trial-and-error

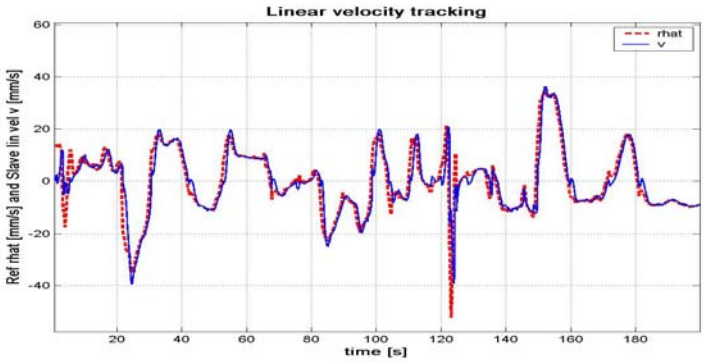

Fig. 12. Linear velocity response

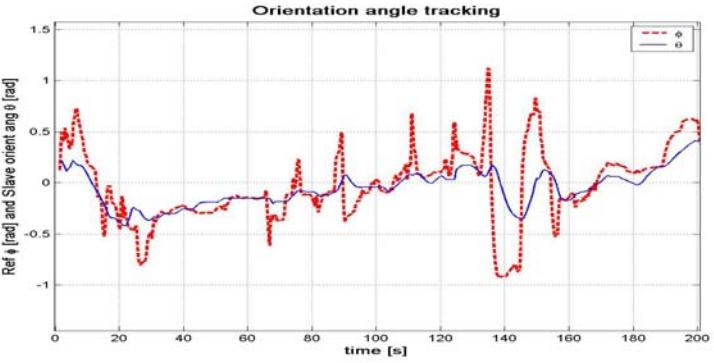

Fig. 13. Heading angle response

without master inertia identification as required in [3], while $B_{\phi\theta}$ was set with the assumption that the maximum round-trip delay can go up to 0.8 sec. For the actual implementation, the round-trip delay between the master and the slave locations was measured repeatedly, and found to have a mean of about 60 ms. In the case of the control law implemented in the robot, the gains were as follows: $K_{rv} = 100.0$, $B_{\phi\theta} = 1 \times 10^6$ and $K_{\phi\theta} = 2.5 \times 10^6$.

The force generated at the haptic interface was also scaled to achieve the bilateral power scaling, with which the different size/strength between the master and slave can be matched with each other. In [3], the control law (Equations (29)-(32)) was derived for the linear master system with constant delay. However, even with the nonlinear Phantom as the master system and time-varying delays, this control law was working fine and no unacceptable behavior (e.g. instability) was observed during this experiment. For more details on the control law (e.g. passivity proof, constraints on the master-slave dynamics and control gains), please refer to [3].

In our UDP communication scheme, each packet sent has a unique identification number. Let the packet p_i, $i \in N$ be the one received at time t_i without previously receiving p_{i-1}. If packet p_{i-1} is received a time later than t_i, then p_{i-1} is dropped to avoid time reversing.

4.3 Experimental Results

To cope with the time-varying delay, two approaches are possible: a) the estimation of the plant state that was explained in Subsection 3.3, and b) the addition of a buffer [6]. The buffer may be used to save the information that arrives from the opposite side of the teleoperation loop during a time that exceeds the maximum time delay. This information is then feed into the controllers at a constant rate to each controller. By using this method, the time delay may be kept constant at the expense of making it larger.

For the teleoperation experiment, we developed the buffer idea. However, our control law is capable of producing acceptable performance of the NCS even in the absence of the buffer, and without any other time-varying delay compensation scheme, as shown in Figures 12, and 13, which show the tracking performance of the remote slave robot.

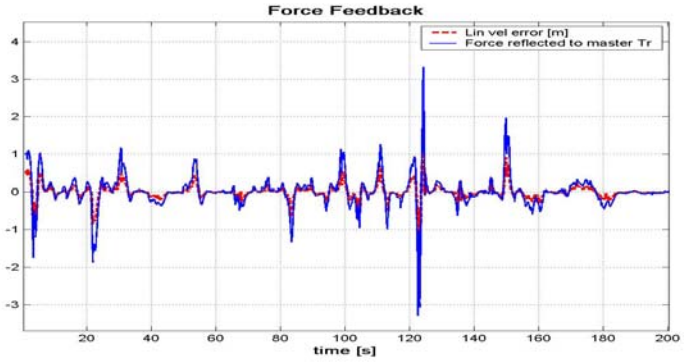

Fig. 14. Force feedback in r direction

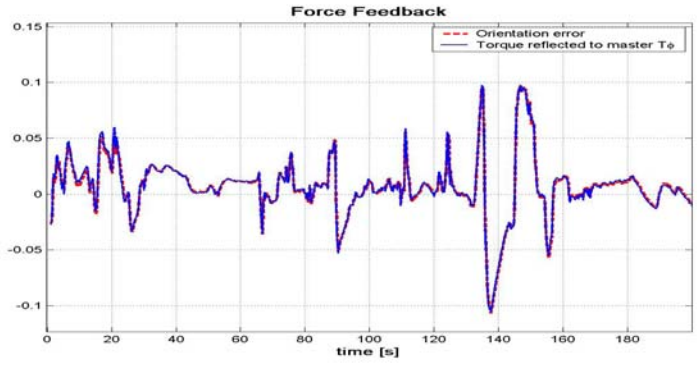

Fig. 15. Force feedback in ϕ direction

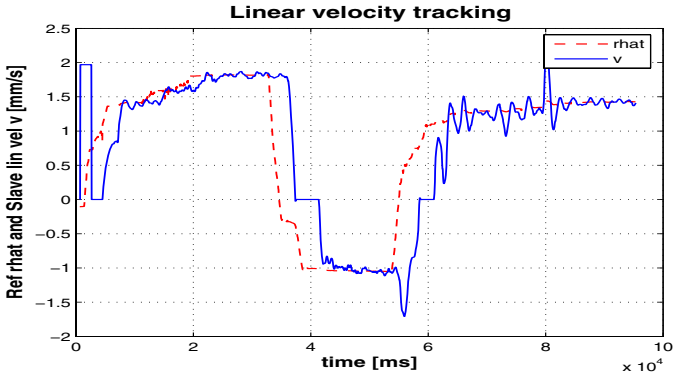

Fig. 16. Linear velocity response using the buffer

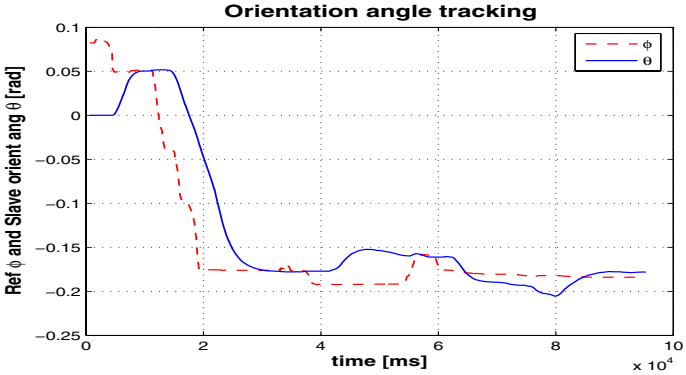

Fig. 17. Heading angle response using the buffer

The force reflected to the master in this experiment is due to the dynamics of the slave robot. In other words, even though there is no force applied to the robot from an obstacle, gravity, friction and time delays force the robot to have a settling time different from zero. This in turn produces an error between the references sent to the slave and the actual state measurements, which forms the basis for the force reflection control laws designed in Equations (29)-(32). The force reflection response is shown in Figures 14 and 15.

As we said before, the buffer idea was also implemented. The buffer size was chosen of 20, so this imply a constant time-delay in the loop of almost 20 times the average delay. This size was chosen assuming that neither the network nor the computer processing time will induced any longer delay and it worked reasonable for the experiment. Since the delay time in the loop was incremented by the buffer inclusion, the control gains were tuned again. In the case of the robot control law , the gains were as follows: $K_{rv} = 100.0$, $B_{\phi\theta} = 1 \times 10^5$ and $K_{\phi\theta} = 2.5 \times 10^6$. For the haptic device control law, the gains were: $B_r = 0.5$, $K_r = 0.001$, $K_{rv} = 100.0$, $B_\phi = 0.1$, $B_{\phi\theta} = 100.0$,

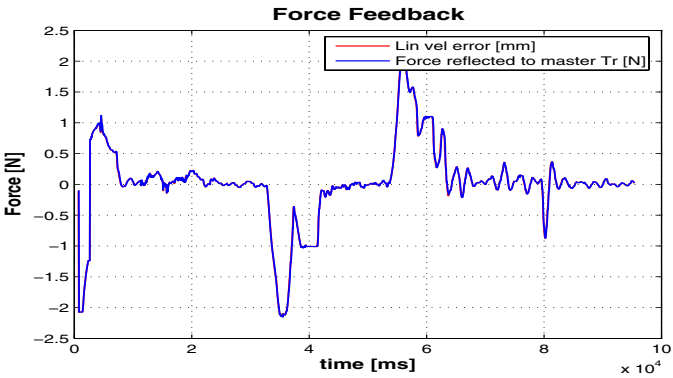

Fig. 18. Force feedback in r direction using the buffer

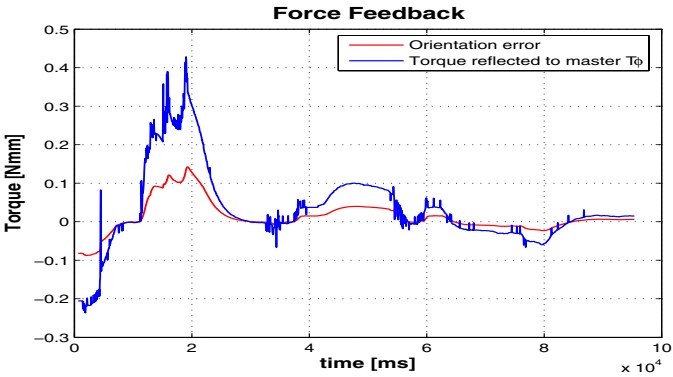

Fig. 19. Force feedback in ϕ direction using the buffer

$K_{\phi\theta} = 2500.0$ and $\lambda = 0.04$. The experimental results that we get from the application of the buffer are shown in two sets. The first set is composed of the linear velocity response and the heading angle response of the mobile robot to the reference sent from the haptic device. The second set is composed force feedback response of the haptic device.

From these results we see that the tracking in velocity and angle present a longer delay, caused by the buffer. However, the tracking in the angle is more accurate than when the buffer was not used. And this was expected since the control algorithm was designed considering a constant delay.

5 Conclusions

We have identified issues induced by a wireless network, which as far as we know had not been reported before. Teleoperation and telepresence applications involving mobile robots have to be implemented using wireless networks. The use of standard operating systems and wireless protocols would induce these or similar issues, and the control algorithms should therefore be robust enough to overcome these problems. We presented

compensation algorithms for propagation time-delay and evaluated these approaches in an experimental set-up with satisfactory results.

References

1. Mills, D. (1991) Internet time synchronization: The network time protocol. IEEE Transactions on Communications 39(10)1482–1493
2. Sandoval-Rodriguez R., Abdallah C. T., Jerez H. N., Byrne R. H. (2005) Experimental Results on the Effects of 802.11b WLAN on Networked Control System. 12^{th} Mediterranean Control and Automation Conference, Limassol, Cyprus
3. Lee D.J., Martinez-Palafox O., Spong M.W. (2006). Bilateral teleoperation of a wheeled mobile robot over delayed communication network. In Proceedings of IEEE International Conf. on Robotics & Automation, Orlando, Florida
4. Fukao T., Nakagawa H., Adachi N. (2000) Adaptive tracking control of a nonholonomic mobile robot. IEEE Transactions on Robotics and Automation 16(5):609–615
5. Fierro R., Lewis F.L. (1997) Control of a Nonholonomic Mobil Robot: Backstepping Kinematics into Dynamics. Journal of Robotics Systems 14(3):149–163
6. Nilsson J. (1998) Real-Time Control Systems with Delays. Ph.D. dissertation, Department of Automatic Control, Lund Institute of Technology, Lund

Modeling and Closed Loop Control for Resource-Constrained Load Balancing with Time Delays in Parallel Computations

Zhong Tang[1], John White[1], John Chiasson[2], and J. Douglas Birdwell[1]

[1] ECE Dept, The University of Tennessee, Knoxville, TN 37996-2100, USA
{tang,jwhite,birdwell}@lit.net
[2] EE Dept, Boise State University, Boise ID, 83725
JohnChiasson@boisestate.edu

Summary. Load balancing for parallel computations is modeled as a deterministic dynamic nonlinear time-delay system. This model accounts for the trade-off between using processor time/network bandwidth and the advantage of distributing the load evenly between the nodes to reduce overall processing time. A distributed closed-loop controller is presented to balance load dynamically at each node by using not only the local estimate of the work load of other nodes, but also measurements of the amount of work load in transit. To handle the time varying delays arising in the closed-loop load balancing, a discrete event simulation based on OPNET Modeler is presented and compared with the experiments. Results indicate good agreement between the nonlinear time-delay model and the experiments on a parallel computer network. Moreover, both simulations and experiments show a dramatic increase in performance obtained using the proposed closed loop controller.

1 Introduction

Parallel computer architectures utilize a set of interconnected computational elements (CEs) to achieve performance that is not attainable on a single processor, or CE, computer. The goal of load balancing is to minimize the execution time for a program by distributing computational loads as judiciously as possible across the available, possibly heterogeneous CE's. The effects of the communications required to distribute the work load consume both computational resources and network bandwidth. Therefore, a balanced system provides the most efficient implemenation of parallel applications taking into consideration the network topology and heterogeneity of the parallel architecture.

There are various taxonomies of load balancing algorithms existing in the literature ([1][2] etc.) Direct methods, or static balancing, examine the global distribution of computational load and assign portions of the workload to computing resources before processing begins. Iterative methods, or dynamic balancing, examine the progress of the computation and the expected utilization of resources, and adjust the workload assignments periodically as computation progresses. Assignment may be either deterministic that depends on some predefined strategy [3][4][5], or stochastic that distributes loads in some random fashion.

J. Chiasson and J.J. Loiseau (Eds.): Appl. of Time Delay Systems, LNCIS 352, pp. 57–76, 2007.
springerlink.com

A comparison of several deterministic methods is provided by Willebeek-LeMair and Reeves [6]. Approaches to modeling and iterative load balancing are given in [7][8][9][10][11][12] etc. In recent years, control theory has shown significant promise towards developement of load balancing techniques, especially for database applications and web services [13][14][15][16]. A queuing theory [17] approach is well-suited to the modeling requirements and has been used in the literature by Nelson [18], Spies [19] and others. However, whereas Spies etc. assumes a homogeneous network of CEs and models the queues in detail, the present work generalizes a queue length to an expected waiting time, normalizing to account for differences among CEs, and aggregates the behavior of each queue. Previous results by the authors appear in [20][21][22][23][24][25][27].

The advantage of dynamic load distribution is limited by diminishing returns as load distribution and task processing contend for the same resources on each CE. It is not difficult to imagine scenarios in which load distribution occurs so frequently that loads are shifted around a parallel architecture without ever being computed. It is therefore necessary to insure stability of a load balancing algorithm. Our work in [24] discusses a mathematical model that captures the constraints of a dynamic load balancing technique and proves stability. The abilities of this open loop model have been shown to perform well in both experimentation and Simulink^{TM} simulation.

There is a trade-off between using processor time/network bandwidth and the advantage of distributing the load between nodes to reduce overall processing time. Our work in [24] discusses a mathematical model to capture the processor resource constraints in load balancing. The open loop experiments and Simulink simulations correspond well. The work has been extended to the closed loop control of a load balancing network and some initial results are presented in [25]. However, Simulink does not lend itself easily to handling the time varying delays which arise in the closed loop case. This motivated the authors to develop a new discrete event simulation based on OPNET Modeler.

This work presents the nonlinear model and closed loop control of a load balancing network with time delays and processor resource constraints. The closed loop controller at each node uses not only the local estimate of the work loads of other nodes, but also measurements of the amount of work loads in transit to it. A discrete event simulation using OPNET Modeler is presented and compared with the experiments on a parallel computer network. The OPNET Modeler simulations indicate good agreement of the nonlinear time-delay model with the actual implementation. Both OPNET simulations and experimental results show the superiority of the controller based on the anticipated work loads to the controller based on the local work loads only.

Section 2 presents a model of a load balancing algorithm in the computer network that incorporates the presence of time delays in communicating between nodes and transferring tasks. Section 3 addresses the feedback control law on a local node and how a node portions out its tasks to other nodes. Feedback controllers based on the actual work load and on the *anticipated* work load are discussed in this section. Section 4 presents the OPNET model of a load balancing

system. Both simulations and experiments are presented to compare these two feedback controllers. Finally, Section 5 is a summary of the present work.

2 Mathematical Model of Load Balancing

In this section, a nonlinear continuous time model is developed to model load balancing among a network of computers. Consider a computing network consisting of n computers (nodes) all of which can communicate with each other. At start up, the computers are assigned an equal number of tasks. The change of load at each computer will lead to load imbalance, as some nodes may operate faster than others. In addition, when a node executes a particular task it can in turn generate more tasks so that very quickly the loads on various nodes become unequal. To balance the loads, each computer in the network sends its queue size $q_j(t)$ to all other computers in the network. A node i receives this information from node j *delayed* by a finite amount of time τ_{ij}; that is, it receives $q_j(t-\tau_{ij})$. Each node i then uses this information to compute its local estimate[1] of the average number of tasks in the queues of the n computers in the network. The simple estimator $\left(\sum_{j=1}^{n} q_j(t-\tau_{ij})\right)/n$, $(\tau_{ii}=0)$ which is based on the most recent observations is used. Node i then compares its queue size $q_i(t)$ with its estimate of the network average as $\left(q_i(t)-\left(\sum_{j=1}^{n} q_j(t-\tau_{ij})\right)/n\right)$ and, if this is greater than zero or some positive threshold, the node sends some of its tasks to the other nodes. If it is less than zero, no tasks are sent. Further, the tasks sent by node i are received by node j with a delay h_{ij}. The task transfer delay h_{ij} depends on the number of tasks to be transferred and is much greater than the communication delay τ_{ij}. The controller (load balancing algorithm) decides how often and fast to do load balancing (transfer tasks among the nodes) and how many tasks are to be sent to each node.

As just explained, each node controller (load balancing algorithm) has only *delayed* values of the queue lengths of the other nodes, and each transfer of data from one node to another is received only after a finite time delay. An important issue considered here is the effect of these delays on system performance. Specifically, the model developed here represents our effort to capture the effect of the delays in load balancing techniques as well as the processor constraints so that system theoretic methods could be used to analyze them.

With $q_i(t)$ the number of *tasks* on node i and t_{p_i} the average time needed to process a task on node i, the expected waiting time can be denoted by $x_i(t) = q_i(t)t_{p_i}$. In this way we generalize queue lengths to expected waiting times and use normalization to account for differencs among CEs. The basic mathematical model of a given computing node for load balancing is given by

[1] It is an estimate because at any time, each node only has the delayed value of the number of tasks in the other nodes.

$$\frac{dx_i(t)}{dt} = \lambda_i - \mu_i\left(1 - \eta_i(t)\right) - U_m(x_i)\eta_i(t) + \sum_{j=1}^{n} p_{ij}\frac{t_{p_i}}{t_{p_j}}U_m(x_j(t-h_{ij}))\eta_j(t-h_{ij}) \quad (1)$$

$$p_{ij} \geqslant 0, p_{jj} = 0, \sum_{i=1}^{n} p_{ij} = 1$$

where

$$U_m(x_i) = U_{m0} > 0 \text{ if } x_i > 0$$
$$= 0 \qquad \text{if } x_i \leq 0.$$

In this model we have

- n is the number of nodes.
- $x_i(t)$ is the *expected waiting time* experienced by a task inserted into the queue of the i^{th} node. Note that $x_j/t_{p_j} = q_j$ is the number of tasks in the node j queue. If these tasks were transferred to node i, then the waiting time transferred is $q_j t_{p_i} = x_j t_{p_i}/t_{p_j}$, so that the fraction t_{p_i}/t_{p_j} converts waiting time on node j to waiting time on node i.
- $\lambda_i \geq 0$ is the rate of generation of waiting time on the i^{th} node caused by the addition of tasks (rate of increase in x_i).
- $\mu_i \geq 0$ is the rate of reduction in waiting time caused by the service of tasks at the i^{th} node and is given by $\mu_i \equiv (1 \times t_{p_i})/t_{p_i} = 1$ for all i if $x_i(t) > 0$, while if $x_i(t) = 0$ then $\mu_i \triangleq 0$, that is, if there are no tasks in the queue, then the queue cannot possibly decrease.
- $\eta_i = 1$ or 0 is the *control input* which specifies whether tasks (waiting time) are processed on a node or tasks (waiting time) are transferred to other nodes.
- U_{m0} is the limit on the rate at which data can be transmitted from one node to another and is basically a bandwidth constraint.
- p_{ij} defines how to portion the tasks to be sent out on each sending node i. It is the probability that a certain waiting time to be transferred from node j to node i with $p_{ij} \geqslant 0, \sum_{i=1}^{n} p_{ij} = 1$ and $p_{jj} = 0$.
- $p_{ij}U_m(x_j)\eta_j(t)$ is the rate at which node j sends waiting time (tasks) to node i at time t. That is, the transfer from node j of expected waiting time $\int_{t_1}^{t_2} U_m(x_j)\eta_j(t)dt$ in the interval of time $[t_1, t_2]$ to the other nodes is carried out with the i^{th} node being sent the fraction $p_{ij}\int_{t_1}^{t_2} U_m(x_j)\eta_j(t)dt$ of this waiting time. As $\sum_{i=1}^{n}\left(p_{ij}\int_{t_1}^{t_2} U_m(x_j)\eta_j(t)dt\right) = \int_{t_1}^{t_2} U_m(x_j)\eta_j(t)dt$, this results in removing *all* of the waiting time $\int_{t_1}^{t_2} U_m(x_j)\eta_j(t)dt$ from node j to the other nodes.
- The quantity $p_{ij}U_m(x_j(t-h_{ij}))\eta_j(t-h_{ij})$ is the rate of transfer of the expected waiting time (tasks) at time t from node j by (to) node i where h_{ij} ($h_{ii} = 0$) is the time delay for the task transfer from node j to node i.
- The factor t_{p_i}/t_{p_j} converts the waiting time from node j to waiting time on node i.

In this model, all rates are in units of the *rate of change of expected waiting time*, or *time/time* which is dimensionless. As $\eta_i = 1$ or 0, node i can only send tasks to other nodes and cannot initiate transfers from another node to itself. A delay is experienced by transmitted tasks before they are received at the other node. Model (1) is the basic model, the p_{ji} defines how to portion the tasks to be transferred on each sending node i. One approach is to choose them as constant and equal

$$p_{ij} = 1/(n-1) \text{ for } j \neq i \text{ and } p_{ii} = 0 \tag{2}$$

where it is clear that $p_{ij} \geqslant 0, \sum_{j=1}^{n} p_{ij} = 1$. Another approach is to base them on the estimated state of the network; this approach is given in the next section.

The non-negativity and conservation of queue lengths and a stability analysis of this model is given in [24]. The model is shown to be self consistent in that the queue lengths are always nonnegative and the total number of tasks in all the queues and the network are conserved (i.e., load balancing can neither create nor lose tasks). The model is only (Lyapunov) stable, and asymptotic stability must be insured by judicious choice of the feedback.

3 Feedback Control

The feedback law at each node i was based on the value of $x_i(t)$ and the *delayed* values $x_j(t - \tau_{ij})$ $(j \neq i)$ from the other nodes in [23]. Here τ_{ij} $(\tau_{ii} = 0)$ denote the time delays for communicating the expected waiting time x_j from node j to node i. These communication delays τ_{ij} are much smaller than the corresponding data transfer delays h_{ij} of the actual tasks. Define

$$x_{i\_avg} \triangleq \left(\sum_{j=1}^{n} x_j(t - \tau_{ij}) \right) / n \tag{3}$$

to be the *local average* which is the i^{th} node's *estimate* of the average of all the nodes. (This is only an estimate due to the delays). Further, define

$$y_i(t) \triangleq x_i(t) - x_{i\_avg}(t) = x_i(t) - \frac{\sum_{j=1}^{n} x_j(t - \tau_{ij})}{n} \tag{4}$$

to be the expected waiting time relative to the estimate of the network average by the i^{th} node.

The control law considered here is

$$\eta_i(t) = h\left(y_i(t)\right) \tag{5}$$

where $h(\cdot)$ is a function given by

$$h(y) = \begin{cases} 1 \text{ if } y \geqslant 0 \\ 0 \text{ if } y < 0. \end{cases}$$

The control law basically states that if the i^{th} node waiting time $x_i(t)$ is above the estimate of the network average $\left(\sum_{j=1}^{n} x_j(t-\tau_{ij})\right)/n$, then it sends data to the other nodes; while if it is less than its estimate of the network average, nothing is sent. The hysteresis loop is inserted to prevent chattering.

The p_{ij} defines how to portion the tasks to be transferred on each sending node i. It is useful to use the local values of the waiting times $x_i(t), i = 1, .., n$ to set their values. Recall that p_{ij} is the fraction of $\int_{t_1}^{t_2} U_m(x_j)\eta_j(t)dt$ in the interval of time $[t_1, t_2]$ that node j allocates (transfers) to node i and conservation of the tasks requires $p_{ij} \geqslant 0, \sum_{i=1}^{n} p_{ij} = 1$ and $p_{jj} = 0$. The quantity $x_i(t-\tau_{ji}) - x_{j\_avg}$ represents what node j estimates the waiting time in the queue of node i to be relative to node j's estimate of the network average. If the queue of node i is above the network average as estimated by node j, then node j does not send any tasks to it. Define a saturation function by

$$\text{sat}(x) = \begin{cases} x \text{ if } x > 0 \\ 0 \text{ if } x \leq 0. \end{cases}$$

Then $\text{sat}(x_{j\_avg} - x_i(t-\tau_{ji}))$ is node j's estimate of how much node i is *below* the network average. Node j then repeats this computation for all the other nodes and portions out its tasks among the other nodes according to the amounts they are *below* its estimate of the network average, that is,

$$p_{ij} = \frac{\text{sat}\left(x_{j\_avg} - x_i(t-\tau_{ji})\right)}{\sum\limits_{i \ni i \neq j} \text{sat}\left(x_{j\_avg} - x_i(t-\tau_{ji})\right)}. \tag{6}$$

However, there is additional information that can be made available to the nodes. Specifically, the information of the tasks that are in the network being sent to the i^{th} node q_{net_i} or equivalently, the waiting time $x_{net_i} \triangleq t_{p_i} q_{net_i}$. It is proposed in [25] to base the controller not only on the local queue size q_i, but also use information about the number of tasks q_{net_i} being sent to node i. The node j sends to each node i in the network information on the number of tasks $q_{net_{ij}}$ it has decided to send to each of the other nodes in the network. This way the other nodes can take into account this information (without having to wait for the actual arrival of the tasks) in making their control decision. The communication of the number of tasks $q_{net_{ij}}$ being sent from node j to node i is much faster than the actual transfer of the tasks. Furthermore, each node i also broadcasts its total (anticipated) amount of tasks, i.e., $q_i + q_{net_i}$ to the other nodes so that they have a more current estimate of the tasks on each node (rather than have to wait for the actual transfer of the tasks). The information that each node has will be a more up to date estimate of the state of network using this scheme.

Define

$$z_i \triangleq x_i + x_{net_i} = t_{p_i}\left(q_i + q_{net_i}\right) \tag{7}$$

which is the *anticipated* waiting time at node i. Further, define

$$z_{i\_avg} \triangleq \left(\sum_{j=1}^{n} z_j(t - \tau_{ij}) \right) / n \tag{8}$$

to be the i^{th} node's estimate of the average anticipated waiting time of all the nodes in the network. This is still an estimate due to the communication delays. Therefore,

$$w_i(t) \triangleq x_i(t) - z_{i\_avg}(t) = x_i(t) - \frac{\sum_{j=1}^{n} z_j(t - \tau_{ij})}{n} \tag{9}$$

to be the expected waiting time relative to the estimate of average (anticipated) waiting time in the network by the i^{th} node. By using expected waiting time $x_i(t)$ rather than $z_i(t)$ in (9) we avoid trying to send nonexistent tasks (due to incorrect/delayed information) from a node when its load is above the average anticipated waiting time. A control law based on the anticipated waiting time is chosen as

$$\eta_i(t) = h\left(w_i(t)\right). \tag{10}$$

The difference between (10) and (5) will be illustrated in Section 4.

Similarly, the p_{ij} can be specified using the anticipated waiting time z_j of the other nodes. The quantity $z_{j\_avg} - z_i(t - \tau_{ji})$ represents what node j estimates the network's average anticipated waiting time is relative to its estimate of the anticipated waiting time in the queue of node i. If the estimate of the queue of node i (i.e., $z_i(t - \tau_{ji})$) is above what node j estimates the network's average (i.e., z_{j_avg}) is, then node j sends tasks to node i. Otherwise, node j sends no tasks to node i. Therefore $\mathrm{sat}(z_{j\_avg} - z_i(t - \tau_{ji}))$ is a measure by node j as to how much node i is *below* the local average. Node j then repeats this computation for all the other nodes and then portions out its tasks among the other nodes according to the amounts they are below its estimate of the network average, that is,

$$p_{ij} = \frac{\mathrm{sat}\left(z_{j\_avg} - z_i(t - \tau_{ji})\right)}{\sum_{i \ni i \neq j} \mathrm{sat}\left(z_{j\_avg} - z_i(t - \tau_{ji})\right)}. \tag{11}$$

It is obvious that $p_{ij} \geqslant 0, \sum_{i=1}^{n} p_{ij} = 1$ and $p_{jj} = 0$. All p_{ij} are defined to be zero, and no load is transferred if the denominator is zero.

4 Experimental Results

A parallel machine has been built and used as an experimental facility for evaluation of load balancing strategies. A root node communicates with several groups of networked computers. Each of these groups is composed of n nodes (hosts) holding identical copies of a portion of the database. Any pair of groups correspond to different databases, which are not necessarily disjoint. In the experimental facility, all machines run the Linux operating system. Our interest here is in the load balancing in any one group of n nodes. The database is implemented as

a set of queues with associated search engine threads, typically assigned one per node of the parallel machine. The search engine threads access tree-structured indices to locate database records that match search or store requests. Search requests that await processing may be placed in any queue associated with a search engine, and the contents of these queues may be moved arbitrarily among the processing nodes of a group to achieve a balance of the load.

The OPNET Modeler [26] is a tool suite for the creation and analysis of discrete event simulations of computer networks. A network in OPNET Modeler is built of many components including network models, node models, link models, packet formats, and process models. By configuring specific parameters for each of these components and writing C code to describe the behavior of the component, a model was created to simulate the load balancing algorithm behavior with time-varying delays over different network topologies.

Figure 1 shows the top level of the OPNET model hierarchy. The three nodes are connected by a model of a gigabit switch. Each node simulates the load balancing algorithm with a given set of initial conditions. Figure 2 shows the process model at each node, which is the lowest level of the OPNET model hierarchy. A process is modeled as a finite state machine in which events trigger changes between states. In the load balancing process, the system oscillates between the idle and processing states, receiving and sending node statistics to other nodes. A load balance event scheduled in the initial process causes the process to begin the actual load balancing algorithm after 1 millisec, and then the process sends jobs to other nodes.

4.1 Open-Loop Experiments on the Parallel Machine

Experiments are presented to indicate the effects of time delays in load balancing. In this set of experiments, the load balancing is performed *once at a fixed time*

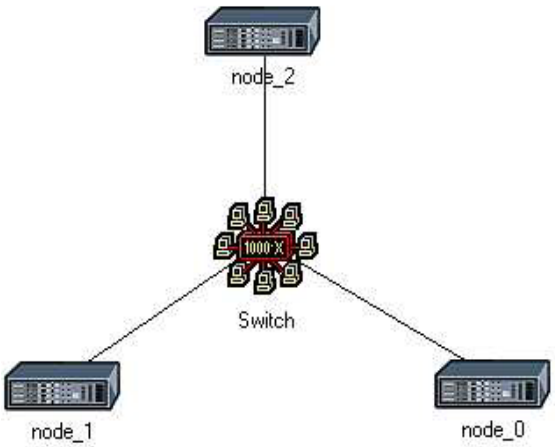

Fig. 1. OPNET simulation: node model in a load balancing system

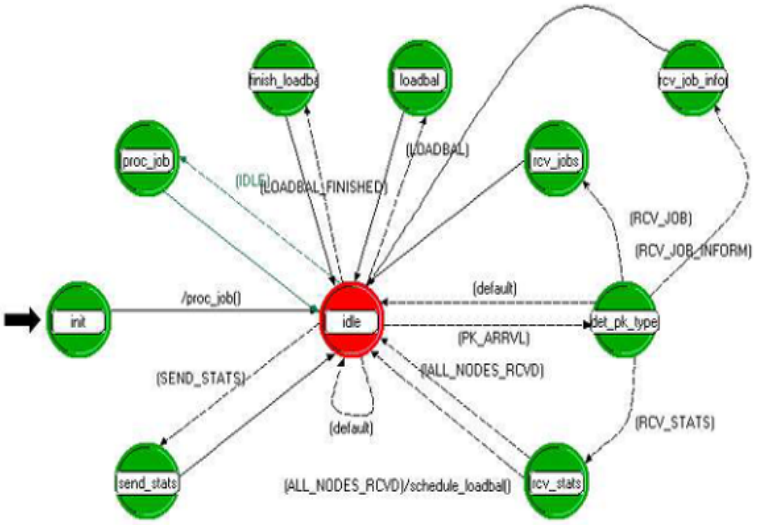

Fig. 2. OPNET simulation: process model in a load balancing system

and is referred to as an "open loop" run. This open loop experiment is done only to facilitate an explanation of the system dynamics with the effects of the delays. The open loop experiments are done for two cases. The first case uses the p_{ij} specified by (6) which are based on the x_i and the second case uses the p_{ij} specified by (11) which are based on the z_i. The initial queue distribution is $q_1(0) = 600$ tasks, $q_2(0) = 200$ tasks and $q_3(0) = 100$ tasks. The average time to do a search task is $t_{p_i} = 400\ \mu$sec, and the inputs were set as $\lambda_1 = 0, \lambda_2 = 0, \lambda_3 = 0$.

Case 1 - p_{ij} Based on x_i

In this open loop experiment, the software was written to execute the load balancing algorithm at $t_0 = 1$ millisec using the p_{ij} as specified by (6). Figure 3 is a plot of the queue size relative to its estimate of the network average, i.e.,

$$q_{i\_diff}(t) \triangleq q_i(t) - q_{i\_avg}(t) \triangleq q_i(t) - \left(\sum_{j=1}^{n} q_j(t - \tau_{ij}) \right) / n$$

for each of the nodes. All time symbols for this experimental run are shown on the figure. Note the effect of the delay in terms of what each local node *estimates* as the queue average and therefore whether it computes itself to be above or below it.

In Figure 3, at the time of load balancing $t_0 = 1$ millisec, node 1 computes its queue size *relative* to its estimate of the network average q_{1_diff} to be 300, node 2 computes its queue size *relative* to its estimate of the network average q_{2_diff} to be -100 and node 3 computes q_{3_diff} to be -200. Node 1 sends tasks out according to (6), which transfers about 100 and 200 tasks to node 2 and node 3 respectively.

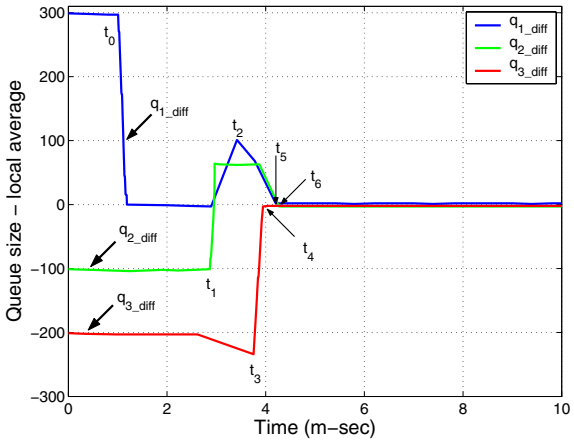

Fig. 3. Plot of $q_{i\_diff}(t) = q_i(t) - \left(\sum_{j=1}^{n} q_j(t - \tau_{ij})\right)/n$ for $i = 1, 2, 3$ using p_{ij} specified by (6)

The transfer of 200 tasks to node 3 takes more time than that of 100 tasks to node 2. It is the task transfer delay that delays node 2's receipt of the new queue size of node 3 at time t_1, and that delays node 3's receipt of the tasks until $t_4 > t_3$. At time t_1, node 2 updates its queue size relative to the estimate of the network average to be $q_{2\_diff} \approx 300 - 233 = 67 > 0$. It is the communication delay that delays node 1's receipt of the new queue size of node 2 at time t_2. At time t_2 the task transfers from node 1 are still on the way to node 2 and 3. Thus, node 1's estimate of its queue size relative to the estimate of the network average is now $q_{1\_diff} \approx 300 - 200 = 100 > 0$.

The effect of both delays could cause unnecessary transfers for node 2 at time t_1 and for node 1 at time t_2 if the load balancing were closed loop. However, this can be avoided by using available information about tasks in transit.

Case 2 - p_{ij} Based on z_i

The node that transfers tasks computes the amounts to be sent to other nodes according to how far below the network average its estimate of each recipient node's queue is. Therefore, it is feasible to send the amounts of its next task transfers to each of other nodes before actually transferring tasks. Such communications are efficient; the communication delay of each transferred measurement is much smaller than the actual task transfer delays. A key finding of this research is that knowledge of the anticipated queue sizes can be used to compensate the effect of delays.

In this experiment, the nodes have the same initial conditions. Note that $q_{i\_avg}^{est}(t) \triangleq z_{i\_avg}(t)/t_{p_i}$ (see (8)). The load balancing algorithm was executed at $t_0 = 1$ millisec using the p_{ij} as specified by (11). Figure 4 is a plot of the queue size relative to the local average, i.e.,

$$q^{est}_{i\_diff}(t) \triangleq q_i(t) - q^{est}_{i\_avg}(t) \triangleq q_i(t) - \left(\sum_{j=1}^{n} q^{est}_j(t - \tau_{ij}) \right) /n$$

for each of the nodes. Note the effect of the delay in terms of what each local node *estimates* as the queue average and therefore determines if it is above or below the network average is greatly diminished. Compared with Figure 3, the tracking differences are near or below zero, and no further unnecessary transfers are initiated.

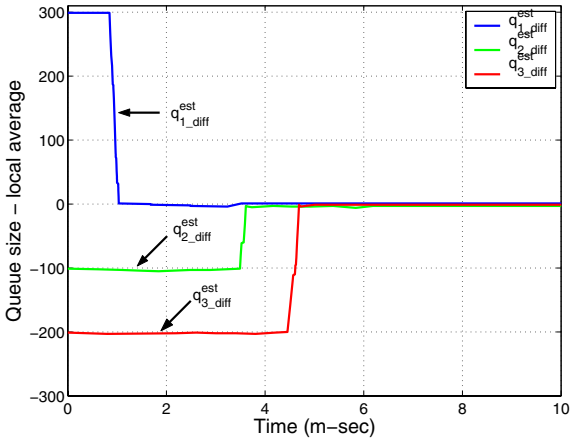

Fig. 4. Plot of $q^{est}_{i\_diff}(t) = q_i(t) - \left(\sum_{j=1}^{n} q^{est}_j(t - \tau_{ij}) \right) /n$ for $i = 1, 2, 3$ using p_{ij} specified by (11)

4.2 Closed Loop Load Balancing

OPNET Simulation

The OPNET Model is configurated as follows to match the characteristics of the load balancing experiments with an initial queue distribution of $q_1(0) = 600$, $q_2(0) = 200$ and $q_3(0) = 100$ tasks. The average time to do a search task is 400 μ sec, and the inputs are set as $\lambda_1 = 0, \lambda_2 = 0, \lambda_3 = 0$. An important point is that the actual delays experienced by the network traffic in the parallel machine are *random*. Experiments were performed and the resulting time delays were measured and analyzed. Those values were used in the simulation for comparison with the experiments.

Figures 5 shows the OPNET simulation for three nodes using p_{ij} based on x_i. As previously pointed out, the load balancer on each node has only delayed values of the queue lengths of the other nodes, and each transfer of data from one node to another is received only after a finite time delay. As shown in Figure 5, those delays result in the transient behaviors of transferring loads back and forth. It takes relatively long for the system to settle to the balance and causes

the completion time larger. Figure 6 shows the OPNET results of a 3-node load balancing using p_{ij} based on the anticipated waiting times z_i. The load balancer on each node uses the anticipated queue sizes which include both the queue information of other nodes and the task information in network transit. As the communication delay of each transferred measurement is much smaller than the actual task transfer delays, the node controller gets more up to date information to make decision for balancing. As shown on Figure 6, such a closed loop controller limits unnecessary transfers and results in faster settling time.

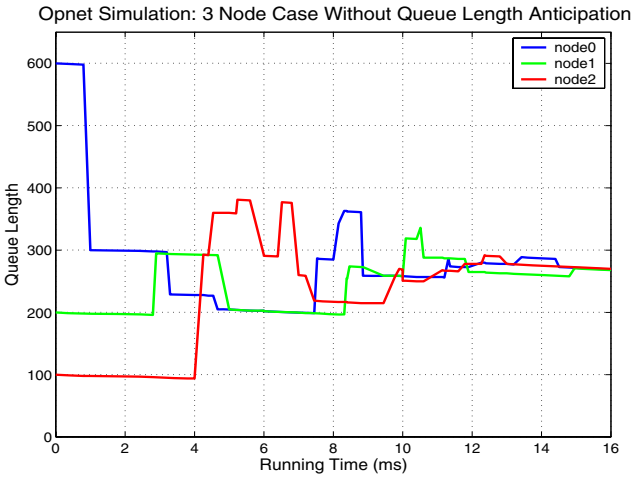

Fig. 5. OPNET simulation: 3-node load balancing using (5) and (6)

Closed-Loop Experiments on the Parallel Machine

In this set of experiments, the closed loop controller (5) with the p_{ij} specified by (6) is compared with the closed loop controller (10) with the p_{ij} specified by (11).

The following experiments show the responses using closed loop load balancing with an initial queue distribution of $q_1(0) = 600$ tasks, $q_2(0) = 200$ tasks and $q_3(0) = 100$ tasks. The average time to do a search task is 400 μsec. In these experiments the inputs were set as $\lambda_1 = 0, \lambda_2 = 0, \lambda_3 = 0$. After initial communications, the closed loop load balancing algorithm (see Section 3) was initiated using the p_{ij} as specified by (6) and by (11), respectively.

Figures 7 and 8 show the responses of the queues versus time using the p_{ij} specified by (6) and by (11), respectively. Note the substantial difference in the load balancing performance between these two schemes. In Figure 7, there are unnecessary exchanges of tasks back and forth among nodes. Although the system reaches a balanced condition at around $t = 14$ millisec, those additional transfers cost processing time and prolong the completion time. In Figure 8, the system reaches the balanced state much faster by using the anticipated waiting

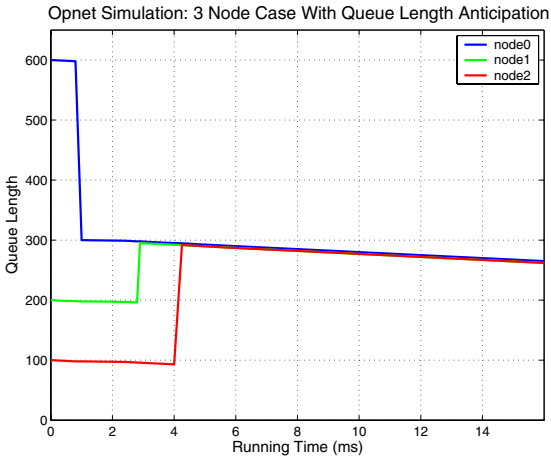

Fig. 6. OPNET simulation: 3-node load balancing using (10) and (11)

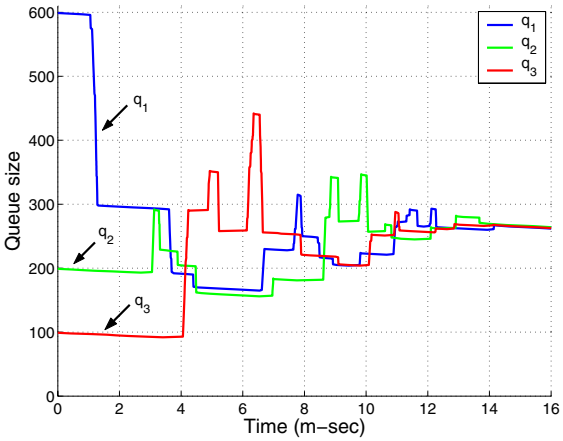

Fig. 7. Plot of queue sizes using (5) and (6)

times. Although all trajectories contain random effects and therefore can not be compared point to point directly, the qualitative behaviors of the OPNET simulation and the experiment are quite similar.

Figure 9 shows node 2's estimates of the queue sizes in the network using closed loop load balancing with the p_{ij} based on the x_i. Node 2 estimates the network average using only the delayed information from other nodes, and its controller based on its queue size relative to the estimated average causes those unnecessary exchanges of tasks back and forth, as shown in Figure 7. Figure 10 shows node 2's estimates of the anticipated queue sizes in the network using

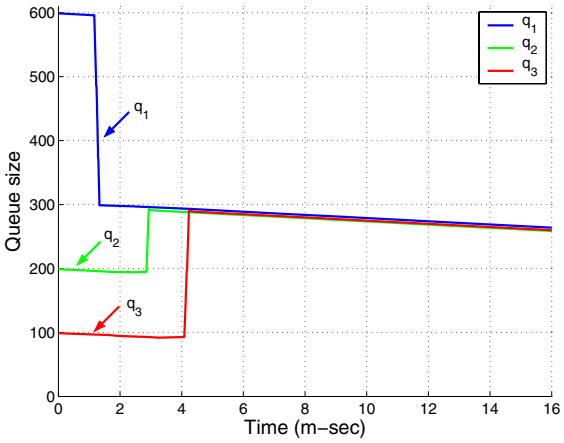

Fig. 8. Plot of queue sizes using (10) and (11)

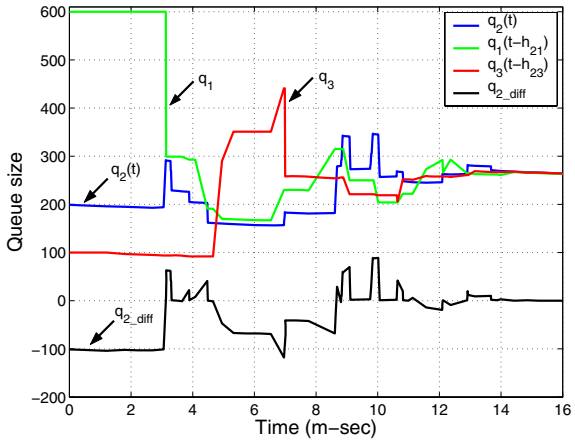

Fig. 9. Estimated queue sizes by node 2 in closed loop load balancing using (5) and (6)

closed loop load balancing with the p_{ij} based on the z_i. Node 1 sends the numbers of tasks before actually transferring tasks to the other nodes. Node 2 receives the anticipated estimate of node 3's queue size, and its controller is based on its queue size relative to the anticipated estimate of network average. This doesn't cause any unwanted transfer (as the amount is below zero). From the Figure 10, we can see that the anticipated estimates are used to compensate the effect of delays of task transfers so that there are no unnecessary task transfers initiated. This method quickly balances computational workloads across all nodes and results in a shorter job completion time.

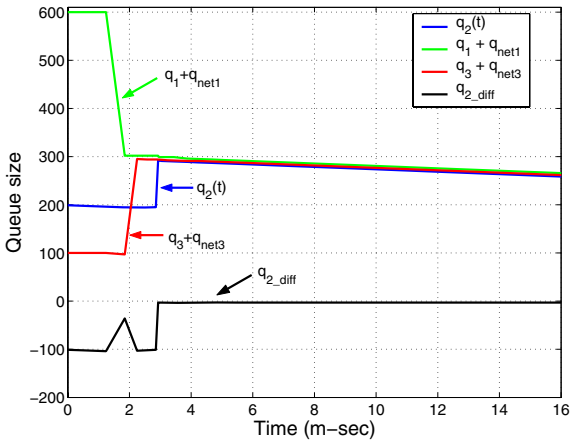

Fig. 10. Estimated queue sizes by node 2 in closed loop load balancing using (10) and (11)

Tasks Generated on Node 1

The initial queue distribution is $q_1(0) = 600$ tasks, $q_2(0) = 200$ tasks and $q_3(0) = 100$ tasks. The average time to do a search task is $t_{p_i} = 400\ \mu$ sec, and the inputs were set as $\lambda_1 = 3, \lambda_2 = 0, \lambda_3 = 0$.

Figures 11 and 12 show the responses of the queues versus time using the p_{ij} specified by (6) and by (11), respectively, with tasks being generated on node 1. The staircase-like increases of queue size corresponds to the task generation on node 1 at $\lambda_1 = 3$. Note the difference in the load balancing performance between these two schemes. In Figure 11, unnecessary transfers cause tasks exchanged back and forth among nodes, those transfers cost additial processing time and prolong the completion time. In Figure 12, the system settles to the balance much faster by using the anticipated waiting times.

4.3 Multiple Nodes: $n = 6$

Initial Tasks Only

The initial queue distribution is $q_1(0) = 650$ tasks, $q_2(0) = 50$ tasks, $q_3(0) = 50$ tasks, $q_4(0) = 50$ tasks, $q_5(0) = 100$ tasks and $q_6(0) = 50$ tasks. The average time to do a search task is $t_{p_i} = 400\ \mu$ sec, and the inputs were set as $\lambda_1 = 0, \lambda_2 = 0, \lambda_3 = 0, \lambda_4 = 0, \lambda_5 = 0, \lambda_6 = 0$.

Figures 13 and 14 show the responses of the queues versus time using the p_{ij} specified by (6) and by (11), respectively, in a network of $n = 6$ nodes. In Figure 13, the controller based the delayed values of queue sizes on other nodes causes exchanges of tasks back and forth among nodes. Those unnecessary transfers cost processing time and prolong the completion time. In Figure 14, the system

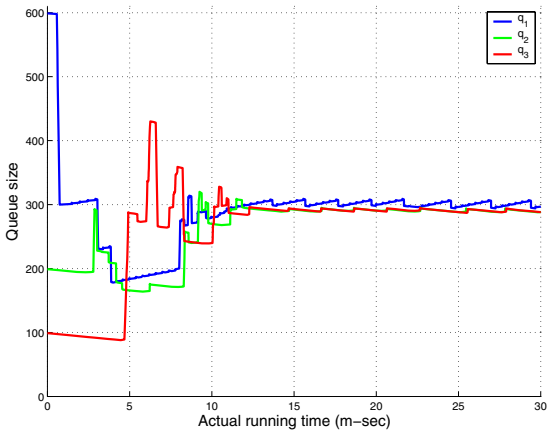

Fig. 11. Plot of queue sizes using (5) and (6)

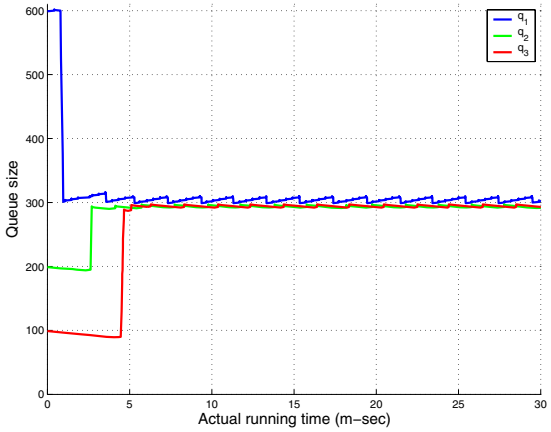

Fig. 12. Plot of queue sizes using (10) and (11)

reaches the balanced state much faster by using the anticipated waiting times and has a shorter completion time.

Tasks Generated on Node 1

The initial queue distribution is $q_1(0) = 650$ tasks, $q_j(0) = 50$ tasks on node j where $j = 2, 3, 4, 5, 6$. The average time to do a search task is $t_{p_i} = 400\ \mu$sec, and the inputs were set as $\lambda_1 = 6, \lambda_j = 0$ where $j = 2, 3, 4, 5, 6$.

Figures 15 and 16 show the responses of the queues versus time using the p_{ij} specified by (6) and by (11), respectively, with tasks generated on node 1 for a network of $n = 6$ nodes. Note the difference in the load balancing performance

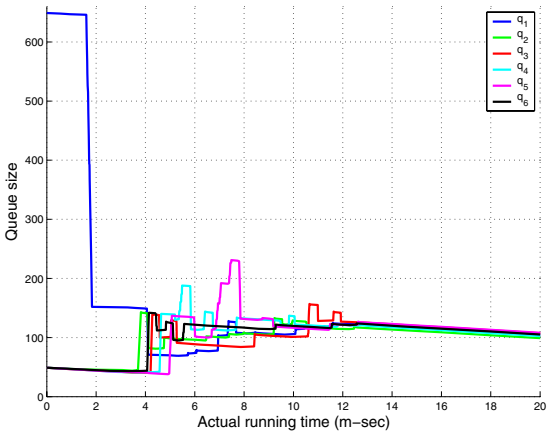

Fig. 13. Plot of queue sizes using (5) and (6)

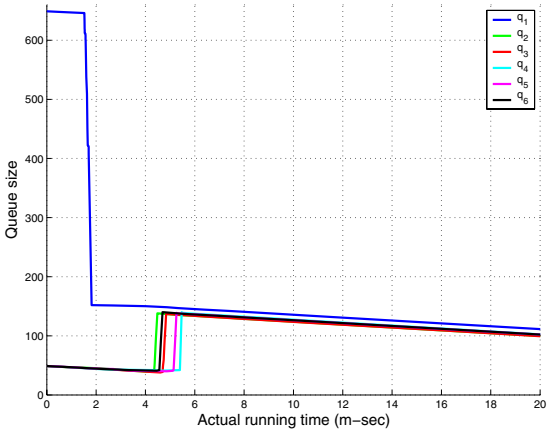

Fig. 14. Plot of queue sizes using (10) and (11)

between these two schemes. The staircase-like increases of queue sizes on the figures correspond to the tasks generated on node 1 with $\lambda_1 = 6$. In Figure 15, the controller based only on the delayed values of queue sizes on other nodes and causes exchanges of tasks back and forth among nodes. The unnecessary transfers need additional balancing operations and cost more processing time. In Figure 16, as the controller based on the anticipated queue sizes on other nodes, the system settles much faster and that results in shorter completion time.

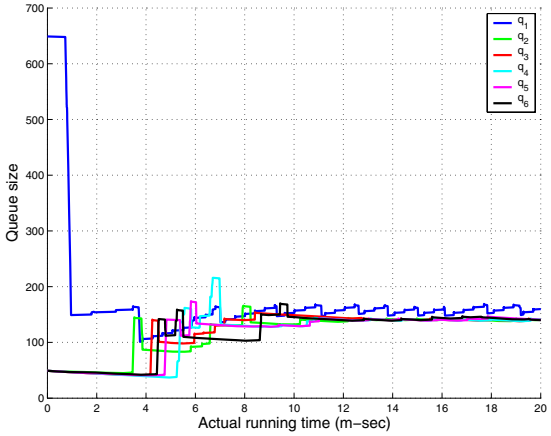

Fig. 15. Plot of queue sizes using (5) and (6)

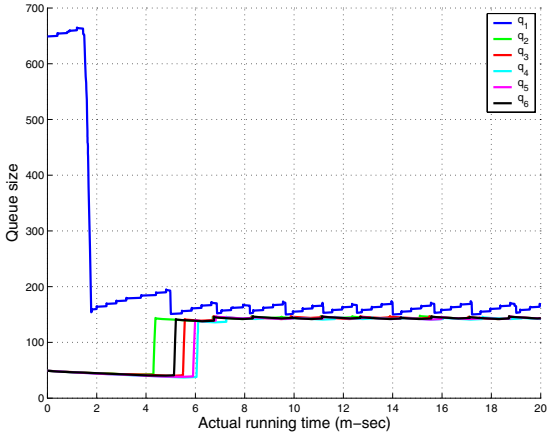

Fig. 16. Plot of queue sizes using (10) and (11)

5 Summary

In this work, a load balancing algorithm for parallel computing was modeled as a nonlinear dynamic system in the presence of time delays and processor resource constraints. A closed loop controller was presented based on the local queue size and an estimate of the tasks being sent to the queue from other nodes. The proposed control law used not only its estimate of the queue sizes at other nodes, but also measurements of the number of tasks in transit to it. The system achieved a faster settling time by using this information to avoid unnecessary transfers. An OPNET simulation model was presented to include the time varying delays arising in the closed-loop load balancing process. The OPNET simulations

indicated good agreement of the nonlinear time delay model with the actual implementation. Both simulations and experimental results showed a substantial improvement in performance obtained using the closed loop controller based on anticipated queue sizes..

Acknowledgements

The work of J. D. Birdwell, J. Chiasson, Z. Tang and J. White was supported by the National Science Foundation grant number ANI-0312182. The views and conclusions contained in this document are those of the authors and should not be interpreted as necessarily representing the official policies, either expressed or implied, of the U.S. Government.

References

1. Rotithor H.G. (1994) Taxonomy of dynamic task scheduling schemes in distributed computing systems. IEE Proceedings of Computer Digital Technology 141(1):1–10
2. Senar M.A., Corteś A., Ripoll A., Hluchý L., Astalos J. (2001) Dynamic load balancing. In Parallel Program Development for Cluster Computing, J. C. Cunha, P. Kacsuk, and S. C. Winter, eds., pp. 69–95, Nova Science Publishers, New York.
3. Xu C.Z., Lau F.C. (1992) Analysis of the generalized dimension exchange method for dynamic load balancing. Journal of Parallel and Distributed Computing 16(1):385–393
4. Corradi A., Leonardi L., Zambonelli F. (1999) Diffusive load-balancing policies for dynamic applications. IEEE Concurrency 7(1):22–31
5. Lin H., Keller R. (1987) The gradient model load balancing method. IEEE Trans. Software Engineering 13(1):32–38
6. Willebeek-LeMair M.H., Reeves A.P. (1993) Strategies for dynamic load balancing on highly parallel computers. IEEE Transactions on Parallel and Distributed Systems 4(9):979–993
7. Kameda H., El-Zoghdy Said Fathy I.R., Li J. (2000) A performance comparison of dynamic versus static load balancing policies in a mainframe. In Proceedings of the 39th IEEE Conference on Decision and Control, pp. 1415–1420, Sydney, Australia
8. Altman E. Kameda H. (2001) Equilibria for multiclass routing in multi-agent networks. In Proceedings of the 40th IEEE Conference on Decision and Control, pp. 604–609, Orlando, Florida
9. Kalé L.V. (1988) Comparing the performance of two dynamic load distribution methods. In Proc. International Conf. Parallel Processing, pp. 8–12
10. Cybenko G. (1989) Dynamic load balancing for distributed memory multiprocessors. Journal of Parallel and Distributed Computing 7(2):279–301
11. Lin H., Raghavendra C.S. (1992) A dynamic load-balancing policy with a central job dispatcher (LBC). IEEE Trans. Software Engineering 18(2):148–158
12. Ghosh B., Leighton F.T., Maggs B.M., Muthukrishnan S., Plaxton C.G., Rajaraman R., Richa A.W. (1999) Tight analysis of two local load balancing algorithms. SIAM Journal on Computing 29(1):29–764
13. Hellerstein J.L. (2004) Challenges in control engineering of computing systems. In Proceedings of the 2004 American Control Conference, pp. 1970–1979, Boston, Massachusetts

14. Diao Y., Hellerstein J.L., Storm A.J., Surendra M., Lightstone S., Pareky S., Garcia-Arellano C. (2004) Using mimo linear control for load balancing in computing systems. In Proceedings of the 2004 American Control Conference, pp. 2045–2050, Boston, Massachusetts
15. Robertsson A., Wittenmark B., Kihl M., Andersson M. (2004) Design and evaluation of load control in web server systems. In Proceedings of the 2004 American Control Conference, pp. 1980–1985, Boston, Massachusetts
16. Abdelzaher T., Lu Y., Zhang R., Henriksson D. (2004) Practical application of control theory to web services. In Proceedings of the 2004 American Control Conference, pp. 1992–1997 Boston, Massachusetts
17. Kleinrock L. (1975) Queuing Systems Vol I : Theory. John Wiley & Sons, New York
18. Nelson R.D., Philips T.K. (1993) An approximation for the mean response time for shortest queue routing with general interarrival and service times. Performance Evaluation 17:123–139
19. Spies F. (1996) Modeling of optimal load balancing strategy using queuing theory. Microprocessors and Microprogramming 41:555–570
20. Abdallah C.T., Alluri N., Birdwell J.D., Chiasson J., Chupryna V., Tang Z., Wang T. (2003) A linear time delay model for studying load balancing instabilities in parallel computations. The International Journal of System Science 34:563–573
21. Birdwell J.D., Chiasson J., Tang Z., Abdallah C.T., Hayat M., Wang T. (2003). Dynamic Time Delay Models for Load Balancing Part I: Deterministic Models. CNRS-NSF Workshop: Advances in Control of Time-Delay Systems, pp. 355–370, Keqin Gu and Silviu-Iulian Niculescu eds., Springer-Verlag, Berlin
22. Hayat M., Abdallah C.T., Birdwell J.D., Chiasson J. (2003) Dynamic Time Delay Models for Load Balancing Part II: A Stochastic Analysis of the Effect of Delay Uncertainty. CNRS-NSF Workshop: Advances in Control of Time-Delay Systems, pp. 371–385, Keqin Gu and Silviu-Iulian Niculescu eds., Springer-Verlag, Berlin
23. Birdwell J.D., Chiasson J., Abdallah C.T., Tang Z., Alluri N., Wang T. (2003) The effect of time delays in the stability of load balancing algorithms for parallel computations. In Proceedings of the 42nd IEEE Conference on Decision and Control, pp. 582–587, Maui, Hawaii
24. Tang Z., Birdwell J.D., Chiasson J., Abdallah C.T., Hayat M.M. (2004) A time delay model for load balancing with processor resource constraints. In Proceedings of the 43rd IEEE Conference on Decision and Control, Paradise Island, Bahamas.
25. Tang Z., Birdwell J.D., Chiasson J., Abdallah C.T., Hayat M.M. (2004) Closed loop control of a load balancing network with time delays and processor resource constraints. Lecture Notes in Control an Information Sciences: Advances in Communication Control Networks, S. Tarbouriech, C.T. Abdallah and J. Chiasson, eds., pp. 245–268, Springer-Verlag, Berlin
26. OPNET (2004) http://www.opnet.com/products/modeler/home.html
27. J. Chiasson, Z. Tang, J. Ghanem, C. T. Abdallah, J. D. Birdwell, M. M. Hayat, H. Jerez, The Effect of Time Delays in the Stability of Load Balancing Algorithms for Parallel Computations, IEEE Transactions on Control Systems Technology, vol. 13, No. 6, November 2005, pp. 932-942.

Stability of Load Balancing Control

Frédéric Gouaisbaut, Isabelle Queinnec, and Sophie Tarbouriech

LAAS-CNRS, 7 Avenue du Colonel Roche, 31077 Toulouse cedex 4, France
{fgouaisb,queinnec,tarbour}@laas.fr

Summary. In this chapter, the control design problem of dynamic model of load balancing is considered. The system under consideration may be represented by a continuous-time delay system subject to both amplitude saturation and additive disturbance. To deal with the control design problem, different systematic methods allowing to derive the feedback gain and the maximal admissible bounds on the delays are described. The methods are placed in a context of delay-dependent stability and are mainly based on the use of adequate functionals. Two main ways are investigated: the first one is based on the use of the Leibniz-Newton formula associated to some overbounds of the time-derivative of the Lyapunov-Krasovskii functionals; The second class of methods is based on the use of a descriptor form of the system and of Finsler's Lemma which allows to introduce new variables (named multipliers) into the conditions and therefore to increase the degrees of freedom in the synthesis problem. All these methods are evaluated and compared in the context of the dynamic model of load balancing considered.

Keywords: Time-delay, stability, load balancing, parallel computation, Lyapunov-Krasovskii approach, Finsler's lemma.

1 Introduction

During recent years, a large amount of attention has been paid to the problem of stability analysis and stabilization of linear systems with state delays [12], [16]. Several delay-dependent stabilization conditions have been proposed involving various model transformations, various weighted cross-products and various Lyapunov-Krasovskii functionals. To some extend, all these approaches are only compared numerically and generally no proof of some methods oversizing others are proposed.

In parallel, communication networks represent very solvable applications to evaluate delay-dependent (or delay-independent) stability analysis and stabilization techniques.

In this work, a parallel computer architecture communicating through a shared network is used to discuss and evaluate various stability analysis (and/or stabilization) techniques of linear time-delay systems. The dynamical load balancing model used in this chapter has been previously proposed by [2], [1], [3] in a version with a nonlinear implemented control law. In the present case, we consider a slightly modified load-balancing model but which remains self-consistent in that the queue lengths cannot become negative and the total number of tasks

J. Chiasson and J.J. Loiseau (Eds.): Appl. of Time Delay Systems, LNCIS 352, pp. 77–95, 2007.
springerlink.com

in all the queues of the network are conserved (i.e. load balancing can neither create nor lose tasks).

The chapter is organized as follows. Section 2 presents some general aspects of the load balancing algorithm involving the communication delays and the transferring tasks delays between the nodes. Some preliminaries are then stated in Section 3 such as to finally formulate the stability analysis and stabilization problems we intend to solve. Section 4 investigates various Lyapunov-Krasovskii based approaches with various model transformations before to propose a simple stability criterion and discuss the equivalence of some results. Finally, a numerical evaluation of the networks on the load balancing algorithms is proposed in Section 5 before to conclude the chapter.

Nomenclature: The notation used in the chapter is standard. $\Re_+$ is the set of non-negative real numbers. For any vector $x \in \Re^n$, $x_{(i)}$ denotes the ith component of x. $A_{(i)}$ denotes the ith row of matrix A. For two symmetric matrices, A and B, $A > B$ means that $A - B$ is positive definite. A' and $trace(A)$ denote the transpose and the trace of A, respectively. $\langle A \rangle$ stands for the symmetric matrix $\langle A \rangle = A + A'$. I_m denotes the m-order identity matrix. 1_m denotes in $\Re^m$ the vector $\begin{bmatrix} 1 \dots 1 \end{bmatrix}'$. $\mathcal{C}_\tau = \mathcal{C}([-\tau, 0], \Re^n)$ denotes the Banach space of continuous vector functions mapping the interval $[-\tau, 0]$ into $\Re^n$ with the topology of uniform convergence. $\| \cdot \|$ refers to either the Euclidean vector norm or the induced matrix 2-norm. $\| \varphi \|_c = \sup_{-\tau \le t \le 0} \| \varphi(t) \|$ stands for the norm of a function $\varphi \in \mathcal{C}_\tau$. When the delay is finite then "sup" can be replaced by "max". $\mathcal{C}_\tau^v$ is the set defined by $\mathcal{C}_\tau^v = \{\varphi \in \mathcal{C}_\tau \ ; \ \| \varphi \|_c < v, \ v > 0\}$.

2 Dynamic Model of Load Balancing Algorithm

Let us consider the mathematical model of a set of n computing nodes for load balancing, for which it is assumed that the communication delay between two different nodes is τ and the transmission delay between two different nodes is h. The state-space description of this model is given by:

$$\begin{aligned} \dot{x}(t) &= u(t) + B_h u(t-h) + d(t) \\ y(t) &= \tfrac{n-1}{n} x(t) + C_\tau x(t-\tau) \end{aligned} \tag{1}$$

where

$$B_h = \begin{bmatrix} 0 & -p_{12} & \cdots & -p_{1n} \\ -p_{21} & 0 & & \vdots \\ \vdots & & \ddots & -p_{n-1n} \\ -p_{n1} & \cdots & -p_{nn-1} & 0 \end{bmatrix}, \quad C_\tau = \begin{bmatrix} 0 & -\frac{1}{n} & \cdots & -\frac{1}{n} \\ -\frac{1}{n} & 0 & & \vdots \\ \vdots & & \ddots & -\frac{1}{n} \\ -\frac{1}{n} & \cdots & -\frac{1}{n} & 0 \end{bmatrix}$$

and $p_{ij} \ge 0$, $p_{jj} = 0$, $\sum_{i=1}^{n} p_{ij} = 1$.

The initial conditions verify

$$x(t_0+\theta)=\varphi(\theta),\ \forall\ \theta\in[-\tau-h,\ 0], t_0\in\Re_+,\ \varphi\in\mathcal{C}^v_{\tau+h} \tag{2}$$

The i^{th} component of the state $x(t)$ is the expected waiting time experienced by a task inserted into the queue of the i^{th} node. The i^{th} component of $u(t)$ is the rate of removal (transfer) of the tasks from (to) node i at time t. The i^{th} component of the output information $y(t)$ represents the difference between the expected waiting time at node i and the estimate of the average waiting time of the network viewed by node i. The i^{th} component of $d(t)$ is the difference between the rate of generation of waiting time caused by the addition of tasks and the rate of reduction in waiting time caused by the service of tasks at the i^{th} node.

Assumption 1. *$d(t)$ is such that*

$$\sum_{i=1}^{n} d_i = 0$$

This assumption allows to ensure the existence of some equilibrium point for system (1).

In matrix B_h, p_{ij} represents the fraction of waiting time sent by node j to node i. That is, $\sum_{i=1}^{n} p_{ij} = 1$ signifies that the p_{ij} represent the repartition on other nodes of the waiting time that must be removed from overloaded node j. In the sequel, one considers:

$$\begin{aligned} &p_{ij} = \tfrac{1}{n-1} \text{ for } i \neq j \\ &p_{ii} = 0 \end{aligned}$$

which signifies that the waiting time transferred from node j is fairly distributed among the other nodes.

This chapter considers the load balancing control as an output feedback memoryless control law given by:

$$u(t) = -Ky(t), \quad K = \begin{bmatrix} k_1 & 0 & \dots & 0 \\ 0 & k_2 & \dots & 0 \\ \vdots & & \ddots & \vdots \\ 0 & \dots & 0 & k_n \end{bmatrix} \tag{3}$$

Remark 1. In others cases, a saturated output function has been considered as $u(t) = -\text{sat}(Ky(t))$, where the saturation function of vector y is defined component by component as:

$$\text{sat}(y_i(t)) = \begin{cases} y_i(t) & \text{if } \ y_i(t) \geq 0 \\ 0 & \text{if } \ y_i(t) < 0 \end{cases} \tag{4}$$

This saturation function would express the fact that when $y_i(t) < 0$, i.e. when the expected waiting time at node i is lower than local waiting time average of the network viewed by node i, this local node does not initiate any transfer of tasks.

This model and more general ones have been fully described: see, in particular, [3] and references therein.

3 Preliminaries

3.1 General Problem Formulation

The closed-loop system derived from (1), (3) is:

$$\dot{x}(t) = -Ky(t) - B_h K y(t-h) + d(t) \tag{5}$$

which can be equivalently written as:

$$\begin{aligned} \dot{x}(t) = &-K\tfrac{n-1}{n}x(t) - KC_\tau x(t-\tau) - B_h K \tfrac{n-1}{n}x(t-h) \\ &-B_h K C_\tau x(t-\tau-h) + d(t) \end{aligned} \tag{6}$$

Hence, the generic problem to be solved may be summarized as follows.

Problem 1. Determine some diagonal matrix gain $K \in \Re^{n\times n}$, for given communication delay $\tau^\star$ and transmission delay $h^\star$, such that, in the load variation-free case ($d(t) = cst$, $\sum_{i=1}^{n} d_i(t) = 0$), the closed-loop system (6) is stable for any initial condition satisfying $\|\varphi\|_c \leq \nu$, $\forall\ \theta \in [-\tau - h, 0]$, with any finite ν.

3.2 Structural Analysis of the System

System (6) can be completely analyzed with respect to stability. Moreover, such a system allows to capture the oscillatory behavior of $y_i(t)$. Some results in terms of stability analysis have been presented in [2].

First, consider some preliminaries about the closed-matrix A_{cl} for system (6) without delay:

$$A_{cl} = -\frac{n-1}{n}K - KC_\tau - \frac{n-1}{n}B_h K - B_h K C_\tau$$

Lemma 1. *Whatever the diagonal matrix K is, there exists a null eigenvalue for system (6) without delay ($\tau = h = 0$).*

Proof: The closed-loop dynamic matrix for system (6) without delay defined above equivalently reads:

$$A_{cl} = -\frac{n-1}{n}K - \frac{1}{n}KE - \frac{1}{n}EK - \frac{1}{n}\frac{1}{n-1}EKE$$

with $E = \begin{bmatrix} 0 & -1 & \cdots & -1 \\ -1 & 0 & & \vdots \\ \vdots & & \ddots & -1 \\ -1 & \cdots & -1 & 0 \end{bmatrix}$.

While $E = E'$ and $K = K'$, one obtains after some mathematical manipulations:

$$A_{cl} = -\frac{1}{n}\left((n-1)I_n + E\right)\frac{K}{n-1}\left((n-1)I_n + E\right)$$

which kernel, if it exists, is directly related to the kernel of matrix $(n-1)I_n + E$. That is, if there exists a null eigenvalue for matrix $(n-1)I_n + E$, then this is also true for matrix A_{cl}. By denoting $\mu_i(E)$ the n eigenvalues of matrix E, it follows that the eigenvalues of matrix $(n-1)I_n + E$ are:

$$\lambda_i = \mu_i(E) + n - 1 \ , \quad i = 1, \cdots, n$$

According to the structure of matrix E, it may be shown that the eigenvalues of E are:

$$\sigma(E) = \{-(n-1) \ , \ 1 \ , \ \cdots \ , \ 1\} \tag{7}$$

that is

$$\sigma((n-1)I_n + E) = \{0 \ , \ n \ , \ \cdots \ , \ n\}$$

and finally A_{cl} possesses a null eigenvalue. □

Lemma 2. *Whatever the diagonal matrix K is, matrices $-KC_\tau$ and $-B_h K\frac{n-1}{n}$ possess an unstable eigenvalue.*

Proof: It directly follows from the expression of the spectrum of matrix E given in (7), multiplied by the diagonal positive matrix K. □

What follows from Lemma 1 is that, to evaluate the stability of system (6) by Lyapunov-related approaches, one should consider some model reduction in order to remove the uncontrollable null eigenvalue, such as to consider that the undelayed closed-loop dynamics matrix A_{cl} is asymptotically stable [20]. But we have no right to do such an operation, since the internal matrices $-KC_\tau$ and $-\frac{n-1}{n}B_h K$ have an unstable mode, which is the mode which is put off the reduced model. Then the unstable modes still remain in the dynamics of the eliminated state, which results that the analysis of the reduced system has no sense with respect to the whole system.

3.3 Model Modifications

At this stage, we propose to modify the problem such as to deal with the uncontrollable null eigenvalue. Let us first consider the following state transformation:

$$\begin{bmatrix} y_{avg} \\ z \end{bmatrix} = Tx \ , \quad T = \begin{bmatrix} \frac{1}{n} & \frac{1}{n} & \cdots & \frac{1}{n} & \frac{1}{n} \\ 1-\frac{1}{n} & -\frac{1}{n} & \cdots & -\frac{1}{n} & -\frac{1}{n} \\ -\frac{1}{n} & 1-\frac{1}{n} & & \vdots & \vdots \\ \vdots & & \ddots & -\frac{1}{n} & \vdots \\ -\frac{1}{n} & \cdots & -\frac{1}{n} & 1-\frac{1}{n} & -\frac{1}{n} \end{bmatrix} \ , \quad z \in \Re^{n-1} \ , \ y_{avg} \in \Re$$

which signifies that $y_{avg}(t) = \frac{1}{n}\sum_{i=1}^{n} x_i(t)$, i.e., y_{avg} represents the true expected average waiting time of the network (which is not known due to the communication delays), and $z_i(t) = x_i(t) - y_{avg}(t), i = 1, \cdots, n-1$. Note that:

$$T^{-1} = \begin{bmatrix} 1 & 1 & 0 & \cdots & 0 \\ \vdots & 0 & \ddots & \ddots & \vdots \\ \vdots & \vdots & \ddots & \ddots & 0 \\ \vdots & 0 & \cdots & 0 & 1 \\ 1 & -1 & \cdots & \cdots & -1 \end{bmatrix}$$

It then follows that:

$$\begin{aligned} \begin{bmatrix} \dot{y}_{avg}(t) \\ \dot{z}(t) \end{bmatrix} &= \begin{bmatrix} \lambda & \Lambda_0 \\ V_0 & A_0 \end{bmatrix} \begin{bmatrix} y_{avg}(t) \\ z(t) \end{bmatrix} + \begin{bmatrix} -\lambda & \Lambda_\tau \\ -V_0 & A_\tau \end{bmatrix} \begin{bmatrix} y_{avg}(t-\tau) \\ z(t-\tau) \end{bmatrix} \\ &+ \begin{bmatrix} -\lambda & -\Lambda_0 \\ V_h & A_h \end{bmatrix} \begin{bmatrix} y_{avg}(t-h) \\ z(t-h) \end{bmatrix} + \begin{bmatrix} \lambda & -\Lambda_\tau \\ -V_h & A_{\tau h} \end{bmatrix} \begin{bmatrix} y_{avg}(t-\tau-h) \\ z(t-\tau-h) \end{bmatrix} \quad (8) \\ &+ \begin{bmatrix} 0 \\ \tilde{d}(t) \end{bmatrix} \end{aligned}$$

with

$$\Lambda_0 = \begin{bmatrix} -\frac{n-1}{n^2}(k_1 - k_n) & \cdots & -\frac{n-1}{n^2}(k_{n-1} - k_n) \end{bmatrix} \ , \quad \Lambda_\tau = \begin{bmatrix} \frac{k_n - k_1}{n^2} & \cdots & \frac{k_n - k_{n-1}}{n^2} \end{bmatrix}$$

$$V_0 = \begin{bmatrix} -\frac{n-1}{n}(k_1 - \frac{1}{n}\sum_{i=1}^{n} k_i) \\ \vdots \\ -\frac{n-1}{n}(k_{n-1} - \frac{1}{n}\sum_{i=1}^{n} k_i) \end{bmatrix} \ , \ V_h = \begin{bmatrix} -\frac{k_1}{n} + \frac{1}{n^2}\sum_{i=1}^{n} k_i \\ \vdots \\ -\frac{k_{n-1}}{n} + \frac{1}{n^2}\sum_{i=1}^{n} k_i \end{bmatrix} \ , \ \lambda = -\frac{n-1}{n^2}\sum_{i=1}^{n} k_i$$

$Td(t) = \begin{bmatrix} 0 \\ \tilde{d}(t) \end{bmatrix}$ and A_0, A_τ, A_h, $A_{\tau h}$ are appropriate matrices following the state transformation. Thanks to the particular form of such a model two different cases may be considered.

Model with $K = kI_n$

When $K = kI_n$, $\Lambda_0 = \Lambda_\tau = V_0' = V_h' = \begin{bmatrix} 0 \cdots 0 \end{bmatrix}$, $\lambda = -\frac{n-1}{n}k$, the model (8) reads:

$$\begin{cases} \dot{y}_{avg}(t) = \lambda y_{avg}(t) - \lambda y_{avg}(t-\tau) - \lambda y_{avg}(t-h) + \lambda y_{avg}(t-\tau-h) & (9) \\ \dot{z}(t) = A_0 z(t) + A_\tau z(t-\tau) + A_h z(t-h) + A_{\tau h} z(t-\tau-h) + \tilde{d}(t) & (10) \end{cases}$$

The stabilization problem stated in Problem 1 is then recast as follows.

Problem 2. Determine some diagonal matrix gain $K = kI_n$, for given communication delay $\tau^\star$ and transmission delay $h^\star$, such that, in the load variation-free case ($d(t) = cst$, $\sum_{i=1}^{n} d_i(t) = 0$),

(i) the subsystem (9) is stable,
(ii) the subsystem (10) is asymptotically stable,

for any initial condition satisfying $\|\varphi\|_c \leq \nu$ with any finite ν, $\forall\ \theta \in [-\tau - h, 0]$.

Delayed Model

Let us now introduce a slightly modified systems as follows. Instead of considering the output described in system (1), we propose to consider the following system:

$$\begin{aligned} \dot{x}(t) &= u(t) + B_h u(t-h) + d(t) \\ \overline{y}(t) &= \tfrac{n-1}{n} x(t-\tau) + C_\tau x(t-\tau) = \overline{C}_\tau x(t-\tau) \end{aligned} \tag{11}$$

where

$$\overline{C}_\tau = \begin{bmatrix} \frac{n-1}{n} & -\frac{1}{n} & \cdots & -\frac{1}{n} \\ -\frac{1}{n} & \frac{n-1}{n} & & \vdots \\ \vdots & & \ddots & -\frac{1}{n} \\ -\frac{1}{n} & \cdots & -\frac{1}{n} & \frac{n-1}{n} \end{bmatrix}$$

This signifies that, even if the value of $x_i(t)$ is known, one prefers to compute the difference between the expected waiting time at node i and the estimate of the average waiting time of the network, to use the past value of the waiting time at time $t-\tau$, i.e. $x_i(t-\tau)$, such as to compare the waiting time at node i at the instant where the information relative to the network has been evaluated. In such a case, the closed-loop system (8) becomes:

$$\begin{aligned} \begin{bmatrix} \dot{y}_{avg}(t) \\ \dot{z}(t) \end{bmatrix} &= \begin{bmatrix} 0 & \Lambda_0 + \Lambda_\tau \\ 0 & A_0 + A_\tau \end{bmatrix} \begin{bmatrix} y_{avg}(t-\tau) \\ z(t-\tau) \end{bmatrix} \\ &\quad + \begin{bmatrix} 0 & -\Lambda_0 - \Lambda_\tau \\ 0 & A_h + A_{\tau h} \end{bmatrix} \begin{bmatrix} y_{avg}(t-\tau-h) \\ z(t-\tau-h) \end{bmatrix} + \begin{bmatrix} 0 \\ \tilde{d}(t) \end{bmatrix} \end{aligned} \tag{12}$$

and the stabilization problem 1 for the modified load-balancing problem (12) is recast as follows.

Problem 3. Determine some diagonal matrix gain K, for given communication delay $\tau^\star$ and transmission delay $h^\star$, such that, in the load variation-free case ($\tilde{d}(t) = cst$, $\sum_{i=1}^{n} \tilde{d}_i(t) = 0$),

(i) the subsystem $\dot{y}_{avg}(t) = (\Lambda_0 + \Lambda_\tau)z(t-\tau) - (\Lambda_0 + \Lambda_\tau)z(t-\tau-h)$, where the right-hand term is viewed as a vanishing disturbance, is stable,
(ii) the subsystem $\dot{z}(t) = (A_0 + A_\tau)z(t-\tau) + (A_h + A_{\tau h})z(t-\tau-h) + \tilde{d}(t)$ is asymptotically stable,

for any initial condition satisfying $\|\varphi\|_c \leq \nu$ with any finite ν, $\forall\ \theta \in [-\tau - h, 0]$.

3.4 Overview of the Stability and Stabilization Problem Formulated

According to Problem 2, the stability analysis and stabilization approaches to be investigated have to answer to the following set of standard problems:

(i) Stability analysis of a system

$$\dot{y}_{avg}(t) = \lambda y_{avg}(t) - \lambda y_{avg}(t-\tau) - \lambda y_{avg}(t-h) + \lambda y_{avg}(t-\tau-h)\ , \quad \lambda < 0;$$

(ii) Stabilization of a system

$$\dot{z}(t) = A_0 z(t) + A_\tau z(t-\tau) + A_h z(h) + A_{\tau h} z(t-\tau-h) + \tilde{d}(t)$$

where matrices A_0, A_τ, A_h and $A_{\tau h}$ are asymptotically stable whatever the matrix gain K is.

The stability analysis of the generic system *(i)* is not an easy task since for the delay free case, the system is not asymptotically stable but just stable. No Lyapunov functional could be found. Moreover, the classical stability tests in the frequency domain often require that the delay are commensurate and even in that case, to our best knowledge, no test could be provided relative to the simple stability of such a system.

This is the main reason why, in the sequel, we consider only Problem 3. The stability analysis and stabilization approaches have to answer to the following standard problems:

*(iii)*Stability analysis of a system

$$\dot{y}_{avg}(t) = \Lambda z(t-\tau) - \Lambda z(t-\tau-h)$$

where $\Lambda z(t)$ is a constant disturbance;
(iv) Stabilization of a system

$$\dot{z}(t) = (A_0 + A_\tau)z(t-\tau) + (A_h + A_{\tau h})z(t-\tau-h) + \tilde{d}(t)$$

i.e., without non-delayed dynamics, where matrices $A_0 + A_\tau$ and $A_h + A_{\tau h}$ are asymptotically stable whatever the matrix gain K is.

If one proves that the system *(iv)* is asymptotically stable then the system *(iii)* only involves vanishing disturbances. This signifies that when the system has converged to steady state, i.e. $z(t-\tau) = z(t-\tau-h) = constant$, the true expected average waiting time of the network also becomes a constant value.

Then, in the following, we are concerned with the stabilization problem *(iv)* which is generically expressed as:

$$\dot{z}(t) = A_1 z(t) + A_2 z(t-\tau) + A_3 z(t-\tau-h) + \tilde{d}(t) \tag{13}$$

with $A_1 = 0, A_2 = A_0 + A_\tau, A_3 = A_h + A_{\tau h}$.

Remark 2. The stabilization problem *(ii)* may be directly extended from the stabilization of (13) by considering the case with three delayed states instead of two.

4 Overview of the Different Methods Investigated

Concerning the way to ensure the closed-loop stability of the original system, we will focus on approaches based on a Lyapunov-Krasovskii functional [17] and we will study the stability of the system:

$$\dot{x}(t) = A_1 x(t) + A_2 x(t-\tau) + A_3 x(t-\tau-h) \tag{14}$$

Remark 3. In the case of load variation free case ($\tilde{d}(t)$=cst) and assuming that $A_1 + A_2 + A_3$ is non singular, a simple change of variable applied to system (13), like $x(t) = z(t) - z_e$, with $z_e = -(A_1 + A_2 + A_3)^{-1}\tilde{d}(t)$, leads to system (14).

Indeed, during the last decade, a great number of works have been devoted to the construction of Lyapunov functions and functionals to prove the stability of time-delay systems like (14) (see [19] and references therein). These methods generally lead to an optimization scheme to find the parameters of the controller. The problem of optimization is expressed in terms of Linear Matrix Inequalities (LMIs), easily solved by efficient solvers based, for example, on Interior Point techniques.

4.1 Introduction of a Stable Matrix $A_1 + A_2 + A_3$

In order to prove the delay-dependent stability of system (14), the first technic introduces the stable matrix $A_1 + A_2 + A_3$ in the system by using the well-known Leibnitz-Newton formula (see [20] and references therein):

$$x(t) - x(t-h) = \int_{t-h}^{t} \dot{x}(\nu) d\nu \tag{15}$$

We then derive a new system to be analyzed:

$$\begin{cases} \dot{x}(t) = (A_1 + A_2 + A_3)x(t) \\ \qquad -A_2 \int_{t-\tau}^{t} (A_1 x(s) + A_2 x(s-\tau) + A_3 x(s-\tau-h)) ds \\ \qquad -A_3 \int_{t-\tau-h}^{t} (A_1 x(s) + A_2 x(s-\tau) + A_3 x(s-\tau-h)) ds \end{cases} \tag{16}$$

The matrix $A_1 + A_2 + A_3$ has to be stable and the last two terms are viewed as perturbations. By using a Lyapunov-Krasovskii functional of the form

$$\begin{aligned} V(t) = x(t)'Px(t) + \int_{t-\tau}^{t} x(\theta)'Q_2x(\theta)d\theta + \int_{t-\tau-h}^{t} x(\theta)'Q_3x(\theta)d\theta \\ + \int_{t-\tau}^{t}\int_{s}^{t} x(\theta)'R_2x(\theta)d\theta ds + \int_{t-\tau-h}^{t}\int_{s}^{t} x(\theta)'R_3x(\theta)d\theta ds \end{aligned} \tag{17}$$

a convex optimization problem may be derived (see [20, 12, 16]) in order to find the best τ and h which ensure the asymptotic stability of system (16).

The main problem relies on the crossing terms which appear when we express the time-derivative of $V(t)$ along the trajectories of (16). Indeed, the time-derivative of the first term $V_1(t) = x(t)'Px(t)$ is :

$$\begin{aligned} \dot{V}_1(t) = x(t)'((A_1 + A_2 + A_3)'P + P(A_1 + A_2 + A_3))x(t) \\ -2x(t)'PA_2 \int_{t-\tau}^{t} (A_1x(s) + A_2x(s-\tau) + A_3x(s-\tau-h))ds \\ -2x(t)'PA_3 \int_{t-\tau-h}^{t} (A_1x(s) + A_2x(s-\tau) + A_3x(s-\tau-h))ds \end{aligned} \tag{18}$$

The last two terms involve several crossing terms like $-2x(t)'Hy(t)$. The first idea (see [20, 12] and references therein) is to bound theses terms using a classical inequality :

$$-2x'y \leq x'Nx + y'N^{-1}y, \tag{19}$$

where N is a free symmetric definite positive matrix to be optimized.

Nevertheless, the overall technique has to face with two important sources of conservatism:

- First of all, the new system induced by the Leibnitz-Newton formula is not equivalent to system (14) in terms of stability. As proven by [10], [12], [13], this transformation introduces some undesired dynamics and possibly significant conservatism.
- Secondly, the classical inequality may be very conservative since we bound a possibly negative product $2x'y$ by the sum of two positive numbers.

Then, this approach can be extended by using some integral inequalities (see [11], [18]) based on the following inequality:

$$-2x'y \leq \min_{X,Y,Z} \begin{bmatrix} x \\ y \end{bmatrix}' \begin{bmatrix} X & Y - I \\ Y' - I & Z \end{bmatrix} \begin{bmatrix} x \\ y \end{bmatrix} \tag{20}$$

where

$$\begin{bmatrix} X & Y \\ Y' & Z \end{bmatrix} \geq 0$$

It allows to reduce the inherent conservatism of the proposed techniques by introducing some extra variables to upperbound cross-terms. Inequality (19) is indeed a particular case of (20) with $X = N, Y = I, Z = N^{-1}$.

4.2 Introduction of a New Variable

In order to cope with the additional dynamics introduced by the formulation (16) following the transformation (15), some authors [12] have proposed to transform the system into:

$$\dot{x}(t) = (A_1 + A_2 + A_3)x(t) - A_2 \int_{t-\tau}^{t} \dot{x}(s)ds - A_3 \int_{t-\tau-h}^{t} \dot{x}(s)ds \tag{21}$$

In comparison with system (16), the time-derivative $\dot{x}(t)$ is not developed. It is now considered as a new variable. Note that equation (21) is proved to be equivalent to system (14) in terms of stability. Logically, the chosen Lyapunov-Krasovskii functional uses this new variable as follows:

$$\begin{aligned} V(t) = x(t)'Px(t) + \int_{t-\tau}^{t} x(\theta)'Q_2x(\theta)d\theta + \int_{t-\tau-h}^{t} x(\theta)'Q_3x(\theta)d\theta \\ + \int_{t-\tau}^{t}\int_{s}^{t} \dot{x}(\theta)'R_2\dot{x}(\theta)d\theta ds + \int_{t-\tau-h}^{t}\int_{s}^{t} \dot{x}(\theta)'R_3\dot{x}(\theta)d\theta ds \end{aligned} \tag{22}$$

Coupled with the Moon's inequality (20), this approach leads to an improvement of the bound of the delay.

Moreover, in the case of one delay, some extensions of the model transformation have been proposed by Han et al [15] as follows:

$$\dot{x}(t) = (A_1 + C)x(t) + (A_2 - C)x(t-h) - C \int_{t-h}^{t} \dot{x}(s)ds \tag{23}$$

This technic, originally proposed by [9], introduces a free parameter C to be optimized. The term (A_1+C) is a stable matrix, A_2-C is understood as a "delay-independent dynamics" and the last term as a "delay-dependent dynamics". This technic provides a way to find the best weighting matrix C, but in practice, it is worth to choose the matrix a priori (as it has been done in the article of [15]).

4.3 Method of Fridman et al

The approach proposed by Fridman et al [7], [8] is an interesting improvement of the last proposed technic. It highlights the introduction of this new variable $\dot{x}(t)$ by transforming the system as:

$$\begin{cases} \dot{x}(t) = y(t) \\ \quad 0 = -y(t) + A_1x(t) + A_2 \int_{t-\tau}^{t} y(\nu)d\nu + A_3 \int_{t-\tau-h}^{t} y(\nu)d\nu \end{cases}$$

Obviously, it is the same idea than transforming the original system into system (21), but technically the system is now transformed into a descriptor system form:

$$E\dot{\bar{x}}(t) = \bar{A}_1\bar{x}(t) + \bar{A}_2 \int_{t-\tau}^{t} \bar{x}(\nu)d\nu + \bar{A}_3 \int_{t-\tau-h}^{t} \bar{x}(\nu)d\nu \tag{24}$$

where $\bar{x}(t) = \begin{bmatrix} \dot{x}(t) \\ x(t) \end{bmatrix}$, $A_1 = \begin{bmatrix} 0 & 0 \\ 0 & A_1 \end{bmatrix}$, $A_2 = \begin{bmatrix} 0 & 0 \\ A_2 & 0 \end{bmatrix}$, $A_3 = \begin{bmatrix} 0 & 0 \\ A_3 & 0 \end{bmatrix}$ and $E = \begin{bmatrix} I_n & 0 \\ 0 & 0 \end{bmatrix}$. Since this transformation is equivalent to the original system [7], we expect some better bounds on the size of the delays h and τ. The Lyapunov-Krasovskii functional which involves the new variables $\bar{x}(t)$ and $y(t) = \dot{x}(t)$ has the form:

$$\begin{aligned} V(t) = \bar{x}(t)'EP\bar{x}(t) + \int_{t-\tau}^{t} x(\theta)'S_2x(\theta)d\theta + \int_{t-\tau-h}^{t} x(\theta)'S_3x(\theta)d\theta \\ + \int_{t-\tau}^{t}\int_{s}^{t} y(\theta)'R_2y(\theta)d\theta ds + \int_{t-\tau-h}^{t}\int_{s}^{t} y(\theta)'R_3y(\theta)d\theta ds \end{aligned} \tag{25}$$

Note that this Lyapunov-Krasovskii functional is a straightforward adaptation of the Lyapunov function for a linear descriptor system $E\dot{x}(t) = Ax(t)$ to the case of descriptor time-delay system.

4.4 A Simple Stability Criterion

In this paragraph, we develop some criteria based on Finsler's Lemma, which has been proved to be a very efficient and elegant tool to find conditions for stabilizing systems by introducing some extra matrices called multipliers (see, for example, [6] in the delay free linear case and [4] in the case of delay-independent stabilization for linear time delay systems).

Following the idea of [7], [8], we propose to introduce some new variables and a general descriptor form useful to reduce the conservatism of Lyapunov-Krasovskii techniques through the following theorem:

Theorem 1. *The system (14) is asymptotically stable for all delays $h < h_{max}$ and $\tau < \tau_{max}$ if there exit 5 positive definite matrices P, Q_2, Q_3, R_2, R_3 and two positive scalars h_{max}, τ_{max} solution to the optimization problem:*

$$\begin{aligned} h_{max} &= \max_{P,Q,R,h,\mu} (h) \\ \tau_{max} &= \max_{P,Q,R,\tau,\mu} (\tau) \end{aligned} \tag{26}$$

subject to

$$\mathcal{B}^{\perp\prime} \begin{bmatrix} \tau R_2 + (h+\tau)R_3 & P & 0 & 0 & 0 & 0 \\ P & Q_2+Q_3 & 0 & 0 & 0 & 0 \\ 0 & 0 & -Q_2 & 0 & 0 & 0 \\ 0 & 0 & 0 & -Q_3 & 0 & 0 \\ 0 & 0 & 0 & 0 & -\frac{R_2}{\tau} & 0 \\ 0 & 0 & 0 & 0 & 0 & -\frac{R_3}{h+\tau} \end{bmatrix} \mathcal{B}^{\perp} < 0$$

$$\text{with } \mathcal{B}^{\perp} = \begin{bmatrix} A_1 & A_2 & A_3 \\ I_n & 0 & 0 \\ 0 & I_n & 0 \\ 0 & 0 & I_n \\ I_n & -I_n & 0 \\ I_n & 0 & 0 \end{bmatrix}.$$

Proof: Let us introduce two new variables $z_1(t) = x(t) - x(t-h)$ and $z_2(t) = x(t) - x(t-h-\tau)$. The system can then be written as :

$$\begin{cases} \dot{x}(t) = A_1 x(t) + A_2 x(t-\tau) + A_3 x(t-\tau-h) \\ z_1(t) = x(t) - x(t-\tau) \\ z_2(t) = x(t) - x(t-\tau-h) \end{cases} \tag{27}$$

or equivalently

$$\mathcal{B}\zeta = 0$$

with

$$\zeta = \begin{bmatrix} \dot{x}(t) \\ x(t) \\ x(t-h) \\ x(t-h-\tau) \\ z_1(t) \\ z_2(t) \end{bmatrix}, \quad \mathcal{B} = \begin{bmatrix} -I_n & A_1 & A_2 & A_3 & 0 & 0 \\ 0 & I_n & -I_n & 0 & I_n & 0 \\ 0 & I_n & 0 & -I_n & 0 & I_n \end{bmatrix} \tag{28}$$

Note that the original system is now constrained to be on $B\zeta = 0$. Let us choose the following Lyapunov-Krasovskii functional:

$$\begin{aligned} V(t) = x(t)'Px(t) + \int_{t-\tau}^{t} x(\theta)'Q_2x(\theta)d\theta + \int_{t-\tau-h}^{t} x(\theta)'Q_3x(\theta)d\theta \\ + \int_{t-\tau}^{t}\int_{s}^{t} \dot{x}(\theta)'R_2\dot{x}(\theta)d\theta ds + \int_{t-\tau-h}^{t}\int_{s}^{t} \dot{x}(\theta)'R_3\dot{x}(\theta)d\theta ds \end{aligned} \tag{29}$$

The time-derivative of $V(t)$ along the trajectories of systems (14) then follows as:

$$\begin{aligned} \dot{V}(t) = 2x(t)'P\dot{x}(t) + x(t)'(Q_2+Q_3)x(t) - x(t-\tau)'Q_2x(t-\tau) \\ -x(t-\tau-h)'Q_3x(t-\tau-h) + \dot{x}(t)'(\tau R_2 + (h+\tau)R_3)\dot{x}(t) \\ - \int_{t-\tau}^{t} \dot{x}(\theta)'R_2\dot{x}(\theta)d\theta - \int_{t-\tau-h}^{t} \dot{x}(\theta)'R_3\dot{x}(\theta)d\theta \end{aligned} \tag{30}$$

The last two terms can be upperbounded as follows (called Jensen's inequality [12]):

$$-\int_{t-\tau}^{t} \dot{x}(\theta)'R_2\dot{x}(\theta)d\theta < -\left(\int_{t-\tau}^{t} \dot{x}(\theta)'d\theta\right)\frac{R_2}{\tau}\left(\int_{t-\tau}^{t} \dot{x}(\theta)d\theta\right)$$

and

$$-\int_{t-\tau-h}^{t} \dot{x}(\theta)' R_3 \dot{x}(\theta) d\theta < -\left(\int_{t-\tau-h}^{t} \dot{x}(\theta)' d\theta\right) \frac{R_3}{h+\tau} \left(\int_{t-\tau-h}^{t} \dot{x}(\theta) d\theta\right)$$

Using the expression of $z_1$and z_2, we get finally :

$$\dot{V}(t) < \zeta' \mathcal{M} \zeta$$

with

$$\mathcal{M} = \begin{bmatrix} \tau R_2 + (h+\tau) R_3 & P & 0 & 0 & 0 & 0 \\ P & Q_2 + Q_3 & 0 & 0 & 0 & 0 \\ 0 & 0 & -Q_2 & 0 & 0 & 0 \\ 0 & 0 & 0 & -Q_3 & 0 & 0 \\ 0 & 0 & 0 & 0 & -\frac{R_2}{\tau} & 0 \\ 0 & 0 & 0 & 0 & 0 & -\frac{R_3}{h+\tau} \end{bmatrix} \tag{31}$$

Finally, we conclude that the original system (14) is asymptotically stable if for all ζ such that $\mathcal{B}\zeta = 0$, inequality $\zeta' \mathcal{M} \zeta < 0$ holds. Using Finsler lemma, it is equivalent to ${\mathcal{B}^{\perp}}' \mathcal{M} \mathcal{B}^{\perp} < 0$ where $\mathcal{B}^{\perp}$ is a right orthogonal complement of $\mathcal{B}$. A candidate for $\mathcal{B}^{\perp}$ could be calculated as: $\mathcal{B}^{\perp} = \begin{bmatrix} A_1 & A_2 & A_3 \\ I_n & 0 & 0 \\ 0 & I_n & 0 \\ 0 & 0 & I_n \\ I_n & -I_n & 0 \\ I_n & 0 & 0 \end{bmatrix}$. □

Remark 4. Compared with the stability condition in [8], we can remark that the LMI involves fewer variables than those in [8]. Lemma 1 from [8] and its Corollary 1 need respectively $\frac{17n(n+1)}{2}$ and $\frac{11n(n+1)}{2}$ variables. Using Theorem 1, one only needs $\frac{5n(n+1)}{2}$ variables.

4.5 Comparisons

Let us consider the system:

$$\dot{x}(t) = A_1 x(t) + A_2 x(t-h_1) + A_2 x(t-h_2) \tag{32}$$

The aim of this subsection is to prove that Theorem 1 is equivalent to the result published in [8] that is recalled in the following Lemma.

Lemma 3. *System (32) is asymptotically stable if there exist $n \times n$ matrices $0 < P_1, P_2, P_3, S_i, Y_{i1}, Y_{i2}, Z_{i1}, Z_{i2}, Z_{i3}$ and $R_i > 0, i = 1, 2$ that satisfy the following linear matrix inequalities (LMIs):*

$$\Gamma = \begin{bmatrix} \Psi & P' \begin{bmatrix} 0 \\ A_2 \end{bmatrix} - Y_1' & P' \begin{bmatrix} 0 \\ A_3 \end{bmatrix} - Y_2' \\ \star & -S_1 & 0 \\ \star & \star & -S_2 \end{bmatrix} < 0 \tag{33}$$

$$\begin{bmatrix} R_i & Y_i \\ \star & Z_i \end{bmatrix} \geq 0, i = 1, 2$$

$$P = \begin{bmatrix} P_1 & 0 \\ P_2 & P_3 \end{bmatrix},\ P_1 > 0,\ Y_i = [Y_{i1}, Y_{i2}],\ Z_i = \begin{bmatrix} Z_{i1} & Z_{i2} \\ \star & Z_{i3} \end{bmatrix} \text{ and}$$

$$\Psi = P' \begin{bmatrix} 0 & I_n \\ A_1 & -I_n \end{bmatrix} + \begin{bmatrix} 0 & I_n \\ A_1 & -I_n \end{bmatrix}' P + \sum_{i=1}^{2} h_i Z_i + \begin{bmatrix} \sum_{i=1}^{2} h_i S_i & 0 \\ 0 & \sum_{i=1}^{2} h_i R_i \end{bmatrix} + \sum_{i=1}^{2} \begin{bmatrix} Y_i \\ 0 \end{bmatrix} + \begin{bmatrix} Y_i \\ 0 \end{bmatrix}'$$

Proposition 1. *Any solution of (33), with $h_1 = \tau, h_2 = \tau + h$, is a solution of (26).*

Proof: First of all note that the inequality $\Gamma < 0$ could be written as:

$$\Theta + \left\langle \begin{bmatrix} P_2' \\ P_3' \\ 0 \\ 0 \end{bmatrix} \begin{bmatrix} A_0 & -I_n & A_1 & A_2 \end{bmatrix} \right\rangle + \begin{bmatrix} \sum_{i=1}^{2} h_i Z_i + \sum_{i=1}^{2} \left\langle \begin{bmatrix} Y_i \\ 0 \end{bmatrix} \right\rangle & -Y_1' & -Y_2' \\ \star & 0 & 0 \\ \star & \star & 0 \end{bmatrix} < 0$$

with

$$\Theta = \begin{bmatrix} \sum_{i=1}^{2} S_i & P_1 & 0 & 0 \\ \star & \sum_{i=1}^{2} h_i R_i & 0 & 0 \\ \star & \star & -S_1 & 0 \\ \star & \star & \star & -S_3 \end{bmatrix}$$

First of all simple manipulations show that

$$\begin{bmatrix} R_1 & Y_1 \\ \star & Z_1 \end{bmatrix} \geq 0$$

implies that

$$\begin{bmatrix} h_1 Z_1 + \left\langle \begin{bmatrix} Y_1 \\ 0 \end{bmatrix} \right\rangle + \begin{bmatrix} \frac{R_1}{h_1} & 0 \\ 0 & 0 \end{bmatrix} - \begin{bmatrix} Y_1' & 0 \end{bmatrix} - \begin{bmatrix} \frac{R_1}{h_1} & 0 \\ 0 & 0 \end{bmatrix} \\ \star \qquad\qquad \begin{bmatrix} \frac{R_1}{h_1} & 0 \\ 0 & 0 \end{bmatrix} \end{bmatrix} \geq 0$$

and that

$$\begin{bmatrix} R_2 & Y_2 \\ \star & Z_2 \end{bmatrix} \geq 0$$

implies that

$$\begin{bmatrix} h_2 Z_2 + \left\langle \begin{bmatrix} Y_2 \\ 0 \end{bmatrix} \right\rangle + \begin{bmatrix} \frac{R_2}{h_2} & 0 \\ 0 & 0 \end{bmatrix} - \begin{bmatrix} 0 & Y_2' \end{bmatrix} - \begin{bmatrix} 0 & \frac{R_2}{h_2} \\ 0 & 0 \end{bmatrix} & \\ \star & \begin{bmatrix} 0 & 0 \\ 0 & \frac{R_2}{h_2} \end{bmatrix} \end{bmatrix} \geq 0$$

Finally, we get that $\Gamma < 0$ implies that:

$$\Xi + \left\langle \begin{bmatrix} P_2' \\ P_3' \\ 0 \\ 0 \end{bmatrix} \begin{bmatrix} A_0 & -I_n & A_1 & A_2 \end{bmatrix} \right\rangle < 0 \tag{34}$$

with

$$\Xi = \begin{bmatrix} \sum_{i=1}^{2} \left(S_i - \frac{R_i}{h_i} \right) & P_1 & \frac{R_1}{h_1} & \frac{R_2}{h_2} \\ \star & \sum_{i=1}^{2} h_i R_i & 0 & 0 \\ \star & \star & -S_1 - \frac{R_1}{h_1} & 0 \\ \star & \star & \star & -S_3 - \frac{R_2}{h_2} \end{bmatrix}$$

Applying Finsler's lemma to (34) concludes the proof. □

Moreover, it has also been proved that method from [18] is a particular case of the descriptor method and then also of Theorem 1. Furthermore, it can also be proved that [12], [15], [18] are particular cases of Theorem 1 (see [14]).

5 Evaluation of These Methods in the Context of Load Balancing Model

To evaluate the solution given by the different methods presented in the previous section, we will consider the original system with representative values established by [5] for a Fast Ethernet network. In the particular case with three nodes, $\tau = 200\mu sec$ and $h = 2\tau = 400\mu sec$, but with the original system (1)-(3), Abdallah *et al* [1] have shown that for any $K < K_{max} = \frac{5\pi}{4\tau \sin \pi/3} = 22672$, the system is asymptotically stable and for $K = K_{max}$ the system will have poles on the $j\omega$ axis.

Using theorems explained below, one proposes some results for different number of nodes n and different delays h and τ reported in table 1.

Remark 5. It is interesting to give some insights of the computations involved in the optimisation scheme. The numbers of variables and numbers of constraints are summarized in the table 2.

Remark 6. Obviously, results presented here are conservative compared with methods proposed by [1] in the frequency domain. Nevertheless, theses techniques are straightforward and could be used for different delays and different numbers of nodes.

Table 1. Maximum allowable gain K for different delays h and τ

n	3	5	5	5	5	5	10
τ	200	200	200	200	200	100	200
h	400	200	300	400	500	200	400
[16]	1999	3340	3070	2850	2655	5710	3740
Corollary 1[8]	3770	4585	4640	4585	4529	9175	4920
Lemma 1[8]	3340	4305	4250	4205	4165	7600	4900
Theorem 1	4350	5460	5440	5429	5420	10930	6050

Table 2. Numbers of constraints and variables involved for the different techniques

techniques	nb. variables	nb. constraints	**n=10**, nb. variables	**n=10**, nb. constraints
[16]	$\frac{2n(n+1)}{2}$	2n (LMI or Riccati equation)	110	20
Corollary 1[8]	$\frac{11n(n+1)}{2}$	$5n$	605	50
Lemma 1[8]	$\frac{17n(n+1)}{2}$	$7n$	935	70
Theorem 1	$\frac{5n(n+1)}{2}$	$3n$	275	30

Remark 7. It has been proved that results provided by Theorem 1 are theoretically exactly the same as results proposed by [8]. Nevertheless, the numerical experiments shows that our method gives better results than previously published papers using descriptors methods and bounding techniques [8]. It may be due to the huge number of useless variables which have to be optimized which could misguide the solver and lead it in a wrong direction for looking to the optimal values of useless variables. Furthermore, this fact could also explain why the first condition of Corollary 1 from [8] gives currently better results on examples than Lemma 1 from [8] whereas Corollary 1 is a direct extension of Lemma 1 where particular matrices are chosen and set to zero. Finally, it appears also that these observations are excessively dependent on the choice of the solver.

Remark 8. All simulations have been performed using SeDuMi, a Matlab toolbox for solving semi-definite optimization problems [21].

6 Conclusion

In this chapter, we have been interested in the problem of stabilization of the load balancing control scheme by using Lyapunov techniques. A new LMI formulation has been proposed to cope with this problem and it has been compared with previously published papers. Nevertheless, many issues remain open. In particular, it should be interesting to extend the evaluation of the different techniques developed in this chapter when a saturated output feedback is considered. In this case, the characterization of the region of stability associated to the closed loop saturated system constitutes an important challenge. To study this problem, a

representation of the saturated term via generalized sector nonlinearities could be used [22]. Such considerations will be advised in a forthcoming issue.

Acknowledgement. This research was partially granted by a CNRS-NSF PICS exchange program and developed during the visit of Sophie Tarbouriech and Isabelle Queinnec at the University of Tennessee, Knoxville (Tennessee, USA). These two authors would like to thank Professors J. Douglas Birdwell and John Chiasson for valuate discussions and insightful comments with respect to this problem.

References

1. Abdallah CT, Alluri N, Birdwell JD, Chiasson J, Chupryna V, Tang Z, Wang TW (2001) A linear time delay model for studying load balancing instabilities in parallel computations. In: Proceedings of the 3rd IFAC workshop on time delay systems, Sante Fe NM
2. Abdallah CT, Alluri N, Birdwell JD, Chiasson J, Chupryna V, Tang Z, Wang T (2003) A Linear Time Delay Model for Studying Load Balancing Instabilities in Parallel Computations. Int. J. of Systems Sciences, 34(10-11):563-573
3. Birdwell JD, Chiasson J, Tang Z, Abdallah CT, Hayat MM, Wang T (2004) Dynamic time delay models for load balancing. Part I: deterministic models. In: Niculescu SI, Gu K (eds) Advances in time-delay systems. LNCSE. Springer
4. Castelan EB, Queinnec I, Tarbouriech S (2003) Delay-independent Robust Stability Conditions of neutral linear time-delay systems. In: Proceedings of the 4th IFAC workshop on time delay systems, Rocquencourt France
5. Dasgupta P, Birdwell JD, Wang TW (2001) Timing and congestion studies under pvm. In: Tenth SIAM conference on parallel processing for scientific computation, Porthmouth VA
6. De Oliveira MC, Skelton RE (2001) Stability tests for constrained linear systems. In: Perspectives in Robust Control, Lecture notes in control and information sciences, Springer, Berlin
7. Fridman E (2001) New Lyapunov-Krasovskii functionals for stability of linear retarded and neutral type systems. Systems and Control Letters 43(4):309-319
8. Fridman E, Shaked U (2002) An improved stabilization method for linear time delay systems. IEEE Trans. on Automatic Control 47(11):1931 - 1937
9. Goubet-Bartholomeus A, Dambrine M, Richard JP (1997), Stability of perturbed systems with time-varying delays. Systems and Control Letters 31:155-163
10. Gu K, Niculescu SI (1999) Additional dynamics in transformed time-delay systems. In: Proceedings of the 38th IEEE conference on decision and control, Phoenix AZ
11. Gu K (2000) An integral inequality in the stability problem of time-delay systems. In: Proceedings of the 39th IEEE conference on decision and control, Sydney Australia
12. Gu K, Kharitonov VL, Chen J (2003) Stability of time-delay Systems. Control Engineering Series, Birkhauser, Boston
13. Gu K, Niculescu SI (2001) Further remarks on additional dynamics in various model transformations of linear delay systems. IEEE Trans. on Automatic Control 46(3):497-500

14. Gouaisbaut F, Peaucelle D (2006) A note on the stability for time-delay systems, In: Proceedings of the 5th IFAC Symposium on Robust Control Design (ROCOND'06), Toulouse France
15. Han QL (2004) A descriptor system approach to robust stability of uncertain neutral systems with discrete and distributed delays. Automatica 40:1791-1796
16. Kolmanovskii V, Richard JP (1999) Stability of some linear systems with delays. IEEE Trans. on Automatic Control 44:984-989
17. Krasovskii NN (1963) Stability of motion. Stanford University Press, Stanford CA
18. Moon YS, Park P, Kwon WH, Lee YS (2001) Delay-dependent robust stabilization of uncertain state-delayed systems. Int. J. of Control 74:1447-1455
19. Richard JP (2003) Time-delay systems: an overview of some recent advances and open problems. Automatica 39(10):1667-1694
20. Niculescu SI (2001) Delay Effects on Stability. A Robust Control Approach, Springer-Verlag, Berlin Germany
21. Sturm J.F. (1999), Using SeDuMi 1.02, a MATLAB toolbox for optimization over symmetric cones, Optimization Methods and Software 11-12:625-653.
22. Tarbouriech S, Gomes da Silva Jr. JM, Garcia G (2004) Delay-dependent anti-windup strategy for linear systems with saturating inputs and delayed outputs. Int. J. of Robust and Nonlinear Control 14:665-682

Part II

Teleoperation

Robust H_∞ Control of Bilateral Teleoperation Systems Under Communication Time-Delay

Olivier Sename[1] and Anas Fattouh[2]

[1] Laboratoire d'Automatique de Grenoble (LAG),
ENSIEG, BP 46, 38402 Saint Martin d'Hères Cedex, France
Olivier.Sename@inpg.fr

[2] Department of Automatic Control and Automation,
Faculty of Electrical and Electronic Engineering,
University of Aleppo, Aleppo, Syria
fattouh@gmail.com

Summary. In this chapter we consider the problem of robust control of bilateral teleoperation systems subject to communication time-delay. The stability of system under consideration is firstly analyzed and a sufficient condition for delay-independent stability is provided. Then the robustness issue is considered, and the problem of controller design that robustly stabilizes the system independently of time-delay w.r.t environment uncertainties is formulated as an H_∞ problem which can be solved using efficient algorithms. When delay independent stability cannot be achieved, a method to determine the maximal allowed time-delay is provided for which the system stability is guaranteed. Simulation results point out the interest of the proposed approach.

1 Introduction

This work deals with bilateral teleoperation systems via communication network. In this system, local manipulator's position is sent to the remote side and the contact force with the environment sensed at the remote side is reflected back to the local side to provide a good fidelity to the human operator. The incurred communication time delay may destabilize this system [1]. Many control schemes have been proposed in the literature to overcome the instability due to communication time delay in bilateral teleoperation systems. Some of these approaches are briefly described below.

Passivity theory have been largely used to ensure the stability of time-delay teleoperation systems [1, 2]. If a system is passive then the input-output stability of this system is guaranteed [3]. Based on this principle energy dissipating elements should be added to the system such that the passivity condition is ensured. Many approaches were proposed in the literature to choose such energy dissipating elements, see for example [1, 4, 5, 6, 7, 8, 9]. However, as pointed by [10] non-perfection can violate passivity. Moreover cautious digital implementations are necessary as passivity may be lost if no specific mechanism is done to handle missing packets [11].

In [12, 13], frequency sweeping test is used to derive conditions on PI-type controller such that the global system is asymptotically stable. The study cannot

J. Chiasson and J.J. Loiseau (Eds.): Appl. of Time Delay Systems, LNCIS 352, pp. 99–116, 2007.
springerlink.com

be directly generalized for other types of controller. Authors have also proposed in [14] finite spectrum controller for bilateral teleoperation systems. However, the time-delay must be known and robustness is difficult to be analyzed.

Leung *et al.* [15] have used μ-analysis and synthesis to design robust controllers for bilateral teleoperation systems. In this approach the local and remote manipulators are both stabilized locally under the assumption that there is no contact with the environment. In the case where there is a contact with the environment, a third controller is added in order to guarantee the stability of the closed-loop system. However, the time delay is treated as a disturbance on the system and not as a system parameter. This work has been extended (in the H_2 framework) in [16] by considering a Padé approximation of a constant delay, thus allowing to do a classical H_∞ control design for the third controller. However the results do not apply for uncertain and/or time-varying delays. In the H_∞ framework, the authors have designed an H_∞ impedance controller for bilateral teleoperation systems considering the delay as an uncertainty [17]. However these approaches lead in general to conservative results.

In this work, an H_∞ approach is proposed for designing robust controller for bilateral teleoperation systems in the presence of environment and communication time-delay uncertainties. This approach allows us to design a controller that ensures robust stability w.r.t environment impedance uncertainties and for any finite time delay (constant or time-varying). When such a solution cannot be obtained, a graphical Nyquist-type procedure in the presence of environment uncertainties is provided to determine the maximal delay uncertainty (on a constant one) that preserves the stability of the teleoperation system. Note that a preliminary version of this work has been presented in [18].

The outline of this chapter is as follows. A general representation of teleoperation systems is given in Section 2, followed by a stability analysis of the nominal system in Section 3. The robustness of bilateral teleoperation system is studied in Section 4. Section 5 presents simulation results that support the theoretical work and conclusion is drawn in Section 6.

2 System Representation

A bilateral teleoperation system can be represented by the block diagram of Fig. 1 and it consists of five subsystems: the human operator, the master manipulator, the communication channel, the slave manipulator and the environment. The variables of the system are: F_h is the force applied by human operator, F_e is the contact force with the environment and X_m, X_s are the position of master and slave manipulators respectively.

The operator commands the position of the slave through the master and the communication channel. The contact force with the environment is transmitted back to the human operator through the communication channel. Notice that, since the teleoperator is controlled bilaterally, the arrows in Fig. 1 can be reversed. In this case the operator commands force forward to the environment and environment's position is sent back to the master.

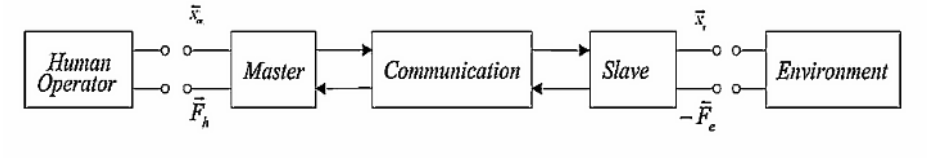

Fig. 1. Block diagram of bilateral teleoperation system

Generally, three controllers are designed for this system: two local controllers for master and slave manipulators in order to achieve desired master and slave compliance and second slave controller such that, in steady state, the slave position X_s is equal to the master position X_m and the global system is asymptotically stable. In this work, both local controllers are assumed to be already designed and integrated in the master and slave transfer functions. Only the design and robustness of the second slave controller is thus tackled.

3 Stability Analysis

In view of previous section, let P_m and P_s be the stable transfer functions of master and slave manipulators including the local controllers, Z_e be the environment impedance, $h_1 \geq 0$ and $h_2 \geq 0$ be time delays of communication forward and backward channels respectively and C be the second slave controller. With these notations, block diagram of Fig. 1 can be redrawn as shown in Fig. 2.

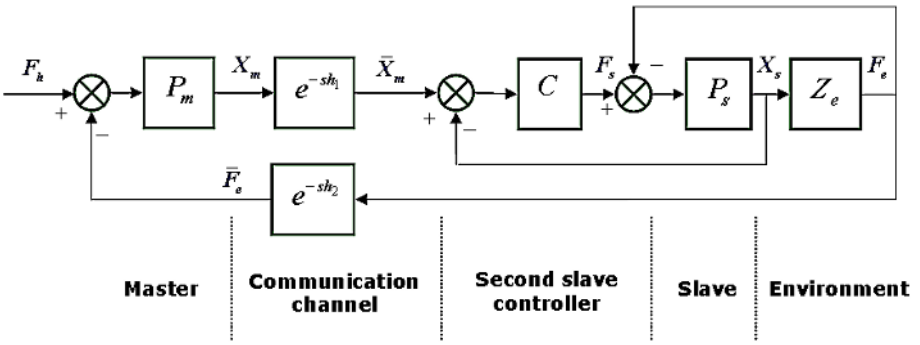

Fig. 2. Considered structure of bilateral teleoperation system

Let us firstly give a definition for asymptotic stability of the system in Fig. 2.

Definition 1. *Consider the bilateral teleoperation system of Fig. 2. This system is said to be asymptotically stable if:*

1. *The transfer function from $\bar{X}_m$ to X_s is asymptotically stable with unitary gain, and*

2. The transfer function from F_h to X_m is asymptotically stable for any time-delay.

Now both conditions of the above definition are analyzed and some criteria are provided to test these conditions.

3.1 Analysis of Condition 1 in Definition 1

The control scheme for the slave side is shown in Fig. 3 where $W_1(s)$ is a weighting function reflecting the desired tracking performance.

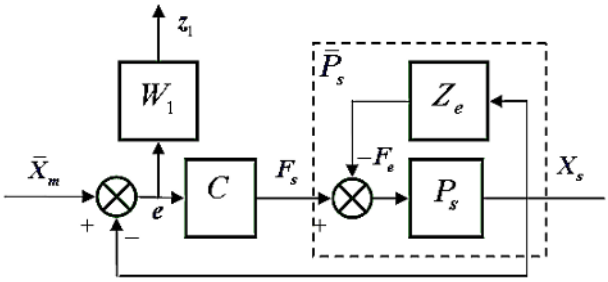

Fig. 3. Master → Slave positions system

Noting $\bar{P}_s = \frac{P_s}{1+P_s Z_e}$, the sensitivity and complementary sensitivity functions are given by

$$S_s := \frac{1}{1+C\bar{P}_s}; \quad T_s := \frac{X_s}{\bar{X}_m} = \frac{C\bar{P}_s}{1+C\bar{P}_s} \tag{1}$$

Using an ad hoc choice of the weighting function W_1, the condition 1 can be expressed as the following H_∞ problem: *find a controller C that ensures internal stability of the system in Fig. 3 and such that*

$$\|W_1 S_s\|_\infty < 1 \tag{2}$$

3.2 Analysis of Condition 2 in Definition 1

From figures 2 and 3, the transfer function from F_h to X_m can be described as shown in Fig. 4 where $h = h_1 + h_2$.

From this figure it is easy to show that

$$T_m := \frac{X_m}{F_h} = \frac{P_m}{1 + P_m T_s Z_e e^{-sh}} \tag{3}$$

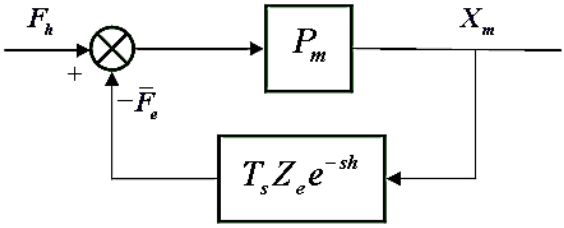

Fig. 4. Operator force → Master position system

Delay-Independent Case: An H_∞ Design

Our objective now is to provide a condition that ensures asymptotically stability of system (3) for any time delay h. To this end, let us first recall the following result [19, 20], for constant time-delays.

Lemma 1. *Let $P(s)$ and $Q(s)$ be two polynomials in complex variable s satisfying $Q(s)$ is stable, and $\deg_s[P(s)] < \deg_s[Q(s)]$. Then, the polynomial $Q(s) + P(s)e^{-s\tau}$ is stable for all $\tau \geq 0$ if and only if*

$$|Q(j\omega)| > |P(j\omega)|, \forall \omega \in \Re \tag{4}$$

In order to apply the above lemma on the system in Fig. 4, let

$$P_m(s) = \frac{N_m(s)}{D_m(s)}, \quad T_s(s) = \frac{N_s(s)}{D_s(s)}, \quad W_2 = P_m Z_e \tag{5}$$

Then the transfer function T_m given in equation (3) can be rewritten as follows

$$T_m = \frac{N_m D_s}{D_m D_s + N_m N_s Z_e e^{-sh}} \tag{6}$$

Under the assumption that P_m and T_s are stable and such that $deg_s(N_m N_s Z_e) < deg_s(D_m D_s)$, then by Lemma 1 the transfer function T_m given in (6) is asymptotically stable for any finite time delay h if and only if

$$|D_m D_s(j\omega)| > |N_m N_s Z_e(j\omega)|, \forall \omega \in \Re \tag{7}$$

which is equivalent to

$$\|W_2 T_s\|_\infty < 1 \tag{8}$$

where W_2 and T_s are given in (5).

The previous result can also be obtained through the small gain theorem. Indeed the scheme in Fig 4 can be represented as in Fig 5.

Applying the small gain theorem using $\Delta(s) = e^{-sh}$ leads to the following result, which, as explained in [21], is also true for time-varying delays.

Lemma 2. *The closed-loop system represented in figure 5 is stable for all $\Delta(s)$ s.t. $\|\Delta(s)\|\infty < 1$ if and only if $\|P_m T_s Z_e\|_\infty < 1$, i.e. $\|W_2 T_s\|_\infty < 1$.*

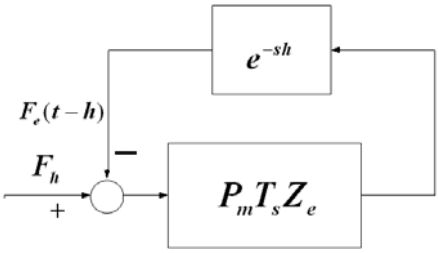

Fig. 5. Small gain approach

In view of (2) and Lemma 2, the following proposition can be obtained.

Proposition 1. *Consider the bilateral teleoperation system in Fig. 2 with transfer functions (1) and (5). Assume that P_m, T_s and $P_m T_s Z_e$ are proper and stable (i.e. belong to RH_∞), then the system is asymptotically stable in the sense of Definition 1 if there exists a controller C which internally stabilize T_s and such that*

$$\left\| \begin{matrix} W_1 S_s \\ W_2 T_s \end{matrix} \right\|_\infty < 1 \tag{9}$$

Proposition 1 gives an H_∞ problem for nominal performance and stability of system in Fig. 2. Robust stability will be analyzed in the next section.

Analysis of the Delay-Dependent Case w.r.t Time-Varying Delays

Here, the result of [22] is used to give a stability test when time-varying bounded delay is considered. The following proposition states this result.

Proposition 2. *[22] Consider the closed-loop system in Fig 4 where h is time-varying. The system is stable for any time-varying delay $0 \leq h(t) \leq \delta_{max}$ if*

$$\left| \frac{N_m N_s Z_e}{D_m D_s + N_m N_s Z_e} \right| < \frac{1}{\delta_{max} \omega}, \forall \omega \in [0, \infty] \tag{10}$$

4 Robust Analysis and Design

In this section, robustness w.r.t environment and communication time-delay uncertainties is analyzed. We assume here that the environment impedance Z_e belongs to some admissible set Ξ, and that the time-delay is constant and defined as $h = h_0 + \tau$ where h_0 is known and constant and τ represents the unknown delay uncertainty.

First, according to Fig. 3, T_s is only subject to environment uncertainties (not delay one). The environment impedance is assumed to belong to a set Ξ of multiplicative input uncertainties, defined as:

$$\Xi = \{Z_e = Z_e^0 (1 + W_e \Delta_e)\} \tag{11}$$

where Δ_e is the uncertainty matrix s.t $\|\Delta_e\|_\infty < 1$, and W_e is the uncertainty weight. Now, define the following set of transfer functions:

$$\tilde{P}_s = \left\{ \bar{P}_s : Z_e \in \Xi \right\} \tag{12}$$

The set Ξ is said to be admissible, if $\tilde{P}_s^0$ (for nominal impedance Z_e^0) and $\tilde{P}_s$ have the same unstable poles.

Our aim is to find conditions s.t T_s and T_m given in (1) and (3) are robustly stable for all $Z_e \in \Xi$ in both following cases: first for any finite time-delay h, and otherwise for a maximal delay uncertainty τ_{max} (up to a nominal one h_0) s.t T_m remains stable for all $Z_e \in \Xi$.

The following proposition provides a test condition for robust stability of the system in Fig. 3.

Proposition 3. *Consider the system of Fig. 3 with the family of transfer functions (12) and such that Ξ is admissible. Assume that the system is internally stable for nominal impedance Z_e, then the system is internally stable for all $Z_e \in \Xi$ if*

$$\|W_I T_s\|_\infty < 1 \tag{13}$$

where W_I is a weighting transfer function satisfying

$$|W_I(j\omega)| \geq \max_{Z_e \in \Xi} \left| \frac{\tilde{P}_s(j\omega)}{\tilde{P}_s^0(j\omega)} - 1 \right|, \quad \forall \omega \in \Re \tag{14}$$

and $\tilde{P}_s^0 = \tilde{P}_s$ for nominal impedance Z_e.

Proof. Using (14), the family of transfer functions (12) can be written as follows:

$$\tilde{P}_s = \tilde{P}_s^0 (1 + W_I \Delta_I) \tag{15}$$

where $\tilde{P}_s^0 = \tilde{P}_s$ for nominal impedance Z_e and Δ_I is a variable stable transfer function satisfying $\|\Delta_I\|_\infty < 1$.

From (15) and robust control theory [23], the robust stability condition for T_s w.r.t multiplicative input uncertainties is given by (13).

4.1 Robust Design w.r.t Environment Uncertainties

In view of (9) and (13), the following theorem is the main result of this work which provides criteria for nominal performance and robust stability.

Theorem 1. *Consider the system of Fig. 2 with the family of transfer functions (12) and such that Ξ is admissible. Define the uncertainty weight as:*

$$|W_4(j\omega)| = \max \left\{ |W_I(j\omega)|, \max_{Z_e \in \Xi} |W_2(j\omega)| \right\}, \quad \forall \omega \in \Re \tag{16}$$

The teleoperation system is robustly asymptotically stable for any time-delay according to Definition 1 if there exists a controller C that ensures internal stability of T_s and such that

$$\left\| \begin{matrix} W_1 S_s \\ W_4 T_s \end{matrix} \right\|_\infty < 1 \tag{17}$$

Proof. If (17) is satisfied, then

$$\|W_1 S_s\|_\infty < 1 \quad \text{and} \quad \|W_2 T_s\|_\infty < 1, \ \ \forall Z_e \in \Xi \tag{18}$$

and

$$\|W_I T_s\|_\infty < 1 \tag{19}$$

As (18) is satisfied and C internally stabilize T_s, then by Proposition 1 the system is stable for any finite time delay. In addition, as (19) is satisfied, then by Proposition 3 the system is asymptotically stable for all $Z_e \in \Xi$. Therefore, the system is asymptotically stable for all $Z_e \in \Xi$ and for any finite time delay. This ends the proof of Theorem 1.

Notice that (17) can be solved as a mixed sensitivity problem using μ-analysis and synthesis toolbox of MATLAB® [24].

4.2 Robustness Analysis w.r.t Environment and Time-Delay Uncertainties

In this subsection we consider the case where the robust design problem (17) cannot be achieved. We assume that a controller C has been designed for T_s to achieve nominal H_∞ performance and stability (9).

The environment uncertainties are considered of the form (11) and the delay is s.t $h = h_0 + \tau$, where τ represents the uncertain part of the delay.

Now, as the delay uncertainties only affect T_m, a robust stability analysis is performed to determine the maximal delay uncertainty τ_{max} that preserves stability of the teleoperation scheme in Fig. 2 and Fig. 4 in the presence of environment uncertainties. A graphical method based on the Nyquist plot is considered here. To this end, let us define the following transfer functions:

$$W_\tau = P_m T_s Z_e e^{-sh} \text{ and } W_0 = P_m T_s Z_e^0 e^{-sh_0}$$

Then:

$$W_\tau = W_0(1 + W_e \Delta_e) e^{-s\tau}$$

Following the method in [25], the procedure to determine the maximal allowed delay uncertainty can be summarized in the following proposition.

Proposition 4. *[25] Let us considered the teleoperation scheme of Fig 4. Assume that Z_e is subject to uncertainty of the form (11) and the time delay h is also subject to uncertainty of the following form $h = h_0 + \tau$. Then, the maximal allowed delay τ_{max} that preserves stability can be determined as follows:*

Step 1: Draw the Nyquist plot of the nominal system W_0.
Step 2: Define the uncertainty circles as:

$$\mathcal{Z}(w) = \mathcal{C}[W_0(j\omega), |W_0(j\omega)||W_e(j\omega)|], \forall\omega \in \Re$$

and plot the "blurred" Nyquist plot.
Step 3: Define Ω *the set of* ω *s.t.* $\mathcal{Z}(w)$ *intersects* $\mathcal{C}[0,1]$ *and compute the minimum angle* $\theta(\omega)$ *from the intersections to the negative real axis. Then:*

$$\tau_{max} = \min_{\omega\in\Omega} \frac{\theta(\omega)}{\omega}$$

5 Illustrative Example

Consider the following dynamics of the master and the slave manipulators

$$\begin{cases} M_m\dot{v}_m = F_h + u_m \\ M_s\dot{v}_s = -F_e + u_s \end{cases} \tag{20}$$

where v_m and v_s are the angular velocities for the master and the slave respectively, u_m and u_s are the respective motor torques, M_m and M_s are the respective inertias, F_h is the operator torque and F_e is the environment torque.

In order to stabilize the above system, [1] have proposed the following PI control law

$$\begin{cases} u_m = -B_m v_m - B_{s_1}(v_m - v_s) - K_s\int(v_m - v_s)dt \\ u_s = -B_{s_2}v_s - \alpha_f F_e + B_{s_1}(v_m - v_s) + K_s\int(v_m - v_s)dt \end{cases} \tag{21}$$

where $M_m = 0.4kg$, $M_s = 1kg$ $B_m = 3N/m$, $B_{s_2} = 0.2N/m$, $Z_e = 1$, $\alpha_f = 0.5$ and K_s and B_{s_1} are the parameter of the PI controller which must be chosen such that the closed-loop system is stable.

In the presence of communication time delay $h \geq 0$, [12] have ensured that for $K_s = 5$ and $B_{s_1} = 2.8$, the closed-loop system is stable for all $h > 0$. However, when the admittance of the environment changes to $Z_e = 2$, the system becomes unstable. In this case, choosing $K_s = 12$ and $B_{s_1} = 2.8$, the closed-loop system is proved to be stable for all $h < 0.3027$ sec.

Based on the above discussion, the master and slave transfer functions with local controllers are given by

$$P_m = \frac{1}{0.4s^2 + 3s + 5}, \quad P_s = \frac{1}{s^2 + 0.2s + 2.8} \tag{22}$$

The impedance of the environment is modelled as follows

$$Z_e = B_e s + K_e \tag{23}$$

Two cases of environment impedance are considered, both including the free motion:

Case 1: $0 \leq B_e \leq 2$ and $0 \leq K_e \leq 4$ (the nominal value is $Z_e = s + 2$)
Case 2: $0 \leq B_e \leq 6$ and $0 \leq K_e \leq 10$ the nominal value is $Z_e = 3s + 5$).

The nominal round-trip communication time-delay is chosen as $h_0 = 1.5sec.$

In the following the H_∞ control design is presented. Note that, in order to be more realistic and to avoid large controller gain, in particular in high frequencies, a weighting function has been added on the control input, in addition to the weighting functions presented before.

5.1 Robust Design for Case 1

The H_∞ problem to be solved is given by (17). First the tracking weight W_1 is chosen as : $W_1(s) = \frac{s/M_s + wb}{1 + wb\epsilon}$ with $\epsilon = 10^{-4}$, $M_s = 1$ and $wb = 0.25$.

Then the weight W_4, representing the robust stability constraint (see (17)), is chosen as represented in Fig 6.

Performance and Robustness Analysis

Solving the H_∞ problem (17) leads to a controller C of order 5 where the solved mixed sensitivity problem is represented in Fig 7.

As seen on fig 7, the sensitivity function S_s satisfies quite well the performance requirement. The stability condition for T_s w.r.t any delay (8) is also satisfied (see the right high frame), and the uncertainty weight $1/W_4$ as well (see the left bottom frame). The function KS represents the control input behavior (i.e. too large gains are avoided).

Stability Analysis w.r.t Time-Varying Delay

Applying the result in Proposition 2, it is shown that the teleoperation scheme in Fig 4 remains stable for all time-varying delay s.t. $0 \leq h(t) \leq 2.8sec.$, as shown in Fig 8.

Simulation Results

Here, simulations in time-domain are provided. The communication time-delay is here time-varying and s.t. $0.5 \leq h(t) \leq 2$ (i.e. $0.25 \leq d(t) \leq 1$ for each side). A step disturbance of magnitude 0.2 is applied at time $t = 60sec.$ that represents an increase of the external force (i.e of the contact at the environment).

Figures 9 show master and slave positions for variable communication time delay and null, nominal, maximal environment impedance as well as for the case where $Z_e = 2Z_{e\ max}$, i.e. outside the robustness specification. The results prove the robustness of the proposed scheme. Note that in all these cases the slave position pursuits the master position, with a tracking error that increases according to the environment impedance, as usual in teleoperation. Also a good disturbance attenuation property is obtained.

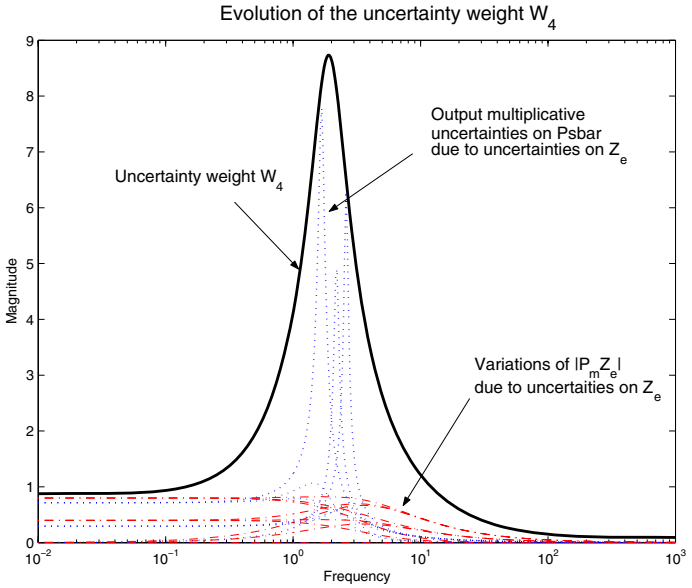

Fig. 6. Uncertainty weight W_4 - Case 1

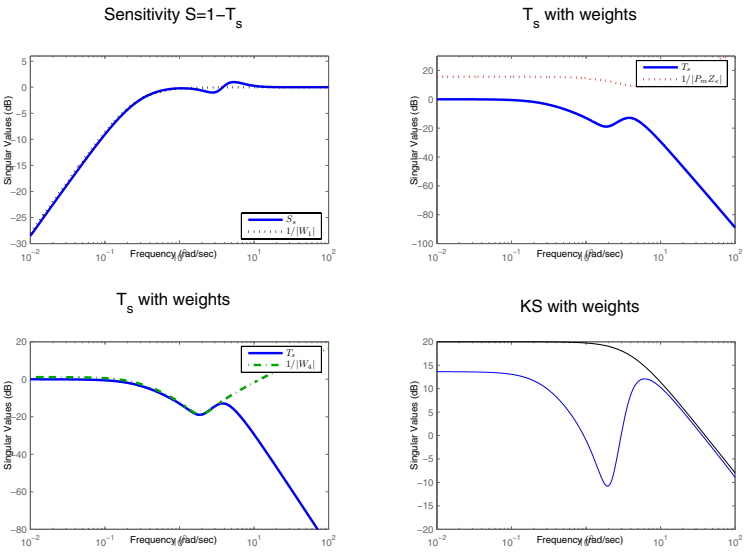

Fig. 7. Sensitivity functions S_s and T_s with weights

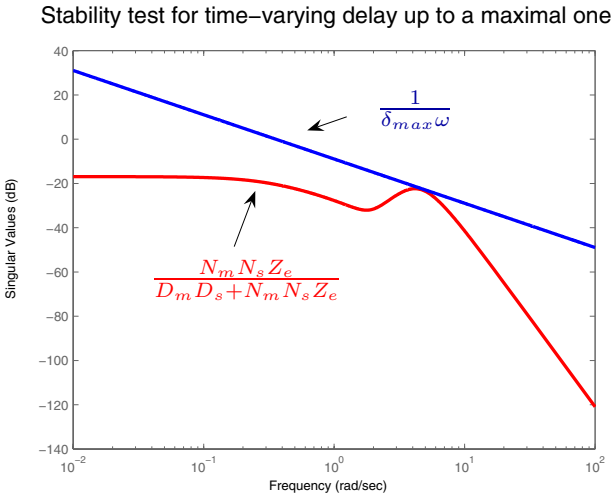

Fig. 8. Stability test w.r.t time-varying delays

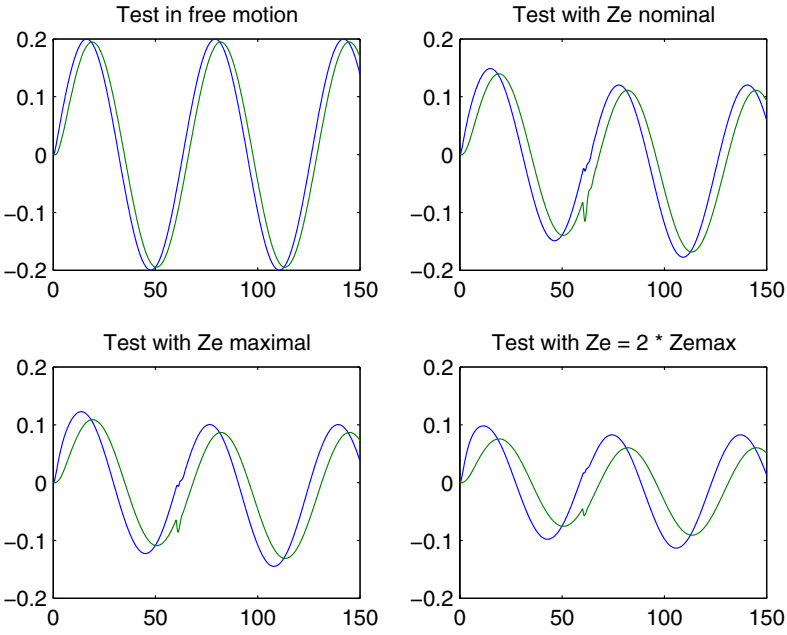

Fig. 9. Master - Slave positions: case 1

5.2 Robust Design for Case 2 and w.r.t Time-Delay Uncertainties

In this subsection we consider the case where the delay independent stability condition (9) is not satisfied, e.g. when the environment impedance is chosen as $Z_e = B_e s + K_e$ with $0 \leq B_e \leq 6$ and $0 \leq K_e \leq 10$.

Try of Robust Design

Due to the hard constraints on the environment, the control input constraint has been a few relaxed in this part, i.e. larger controller gain is accepted.

The weight W_4, representing the robust stability constraint (see (17)), is chosen as represented in Fig 10.

Solving the H_∞ problem (17) leads to a controller C of order 5 where the solved mixed sensitivity problem is represented in Fig 11.

As seen on fig 11, the sensitivity function S_s almost satisfies the performance requirement. The stability condition for T_s w.r.t any delay (8) is also satisfied, but the robustness condition is not satisfied as $|T| > 1/|W_4|$ (see the left bottom frame).

As the controller C is satisfying w.r.t to the tracking performance and nominal stability for any delay, it is kept.

Note also that, applying the result in Proposition 2, it is shown that the teleoperation scheme in Fig 4 remains stable for all time-varying delay s.t. $0 \leq h(t) \leq 0.7sec.$, as shown in Fig 12.

Robustness Analysis

Now, using the procedure described in Proposition 4, it will be shown that the system is stable for any time-delay s.t.

$$h = h_0 + \tau_{max},$$

where τ_{max} is the delay uncertainty. In Fig 13 the Nyquist plot of the nominal model W_0 is plotted as well as the uncertainty circles (w.r.t environment uncertainties) with the "stability" circle $\mathcal{C}[0, 1]$.

Using the method described in Proposition 4, the maximal delay uncertainty that ensures robust stability (w.r.t environment uncertainties) is given by:

$$\tau_{max} = 5.28sec,$$

which proves that the teleoperation scheme will remain stable for all delays up to $h = 6.78sec$.

Let us notice that, applying the previous Proposition 4 with a nominal delay equal to $6sec$ leads to a maximal delay uncertainty that preserves stability equal to $\tau_{max} = 0.8sec$, which proves that this methods is quite independent of the prespecified nominal delay value.

Simulation Results

Here, simulations in time-domain are provided, in the same conditions as previously.

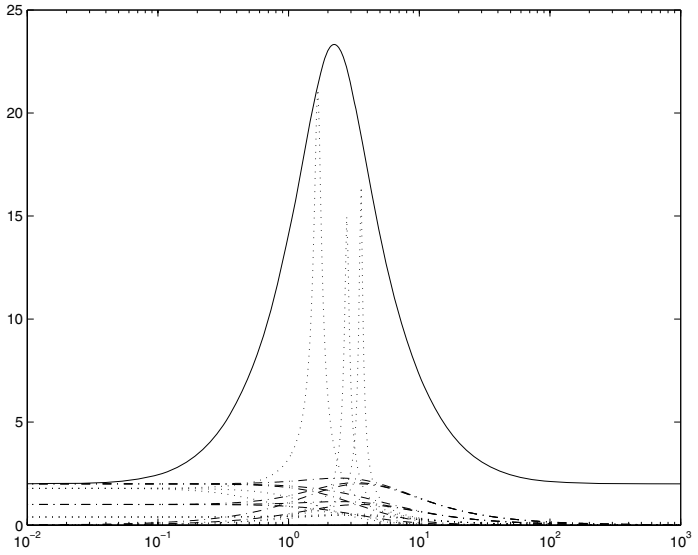

Fig. 10. Uncertainty weight W_4 - Case 2

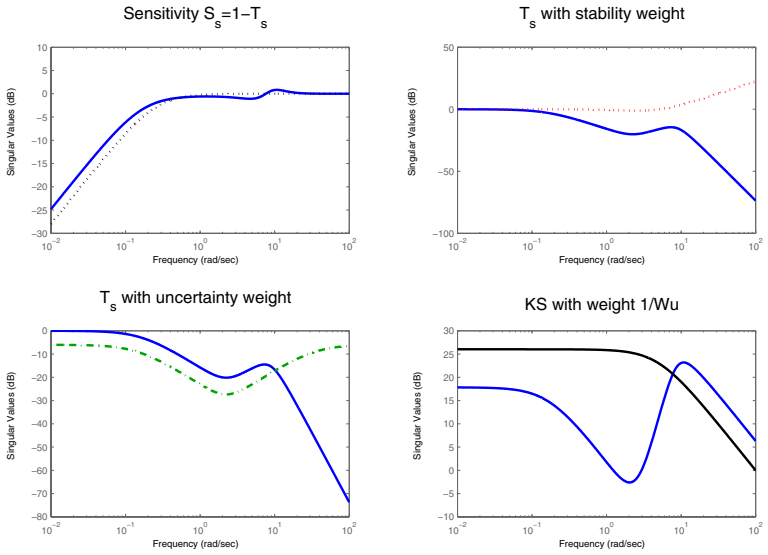

Fig. 11. Sensitivity functions S_s and T_s with weights

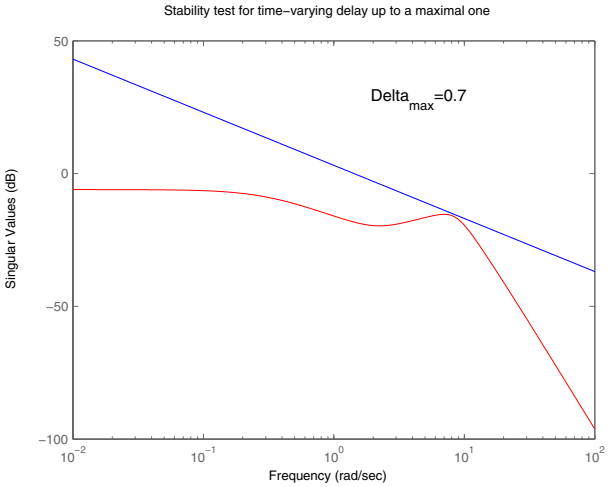

Fig. 12. Stability test w.r.t time-varying delays

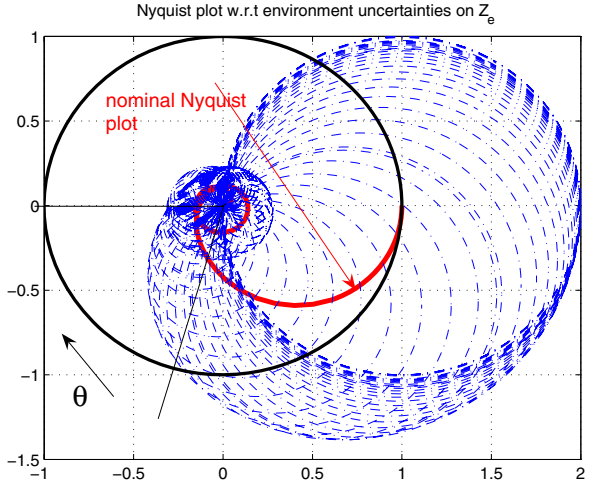

Fig. 13. "Blurred" Nyquist plot of W_τ

Figures 14 show master and slave positions for variable communication time delay and different environment impedances, which proves the robustness of the proposed scheme. Note that in all these cases the slave position pursuits the master position, with a larger tracking error than previously, due to the important increase of the environment impedance.

These simulation test emphasize the interest of the proposed approach, where uncertainties in the environment impedance and in the communication time-

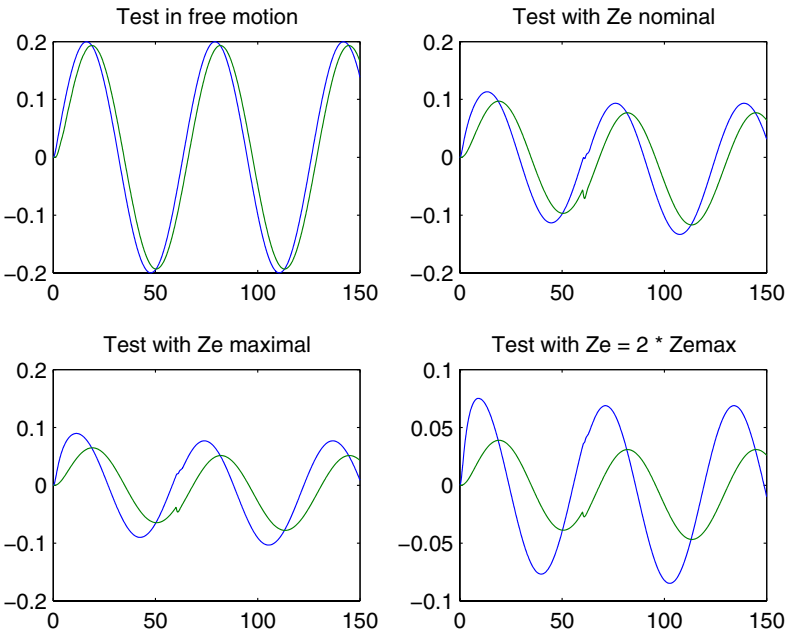

Fig. 14. Master - Slave positions: case2

delay are taken into account to design a robust teleoperation scheme. As a trade-off the teleoperation system behaves slowly.

6 Conclusion

In this work the problem of robust control design of a bilateral teleoperation system for any finite communication time delay and in the presence of environment uncertainties has been solved as an H_∞ mixed-sensitivity problem. When delay independent design is not achieved, the maximal uncertainty (upon a constant communication delay) that keeps stability has been obtained using a Nyquist graphical method.

The natural extension of this work would be to provide an H_∞ design for bounded time-varying delays, which will surely lead to a performance improvement.

References

1. Anderson RJ, Spong MW (1989) Bilateral control of teleoperators with time delay. IEEE Trans. on Automatic Control 34(5):494–501
2. Niemeyer G, Slotine JJE (1998) Towards force-reflecting teleoperation over the internet. IEEE Int. Conference on Robotics & Automation pp. 1909–1915
3. Desoer CA, Vidyasagar M (1975) Feedback systems: Input-Output properties. New York: Academic Press.

4. Kim WS, Hannaford B, Bejczy AK (1992) Force-reflecting and shared compliant control in operating telemanipulators with time delay. IEEE Trans. on Robotics and Automation vol.8, pp. 176–185
5. Shi M, Tao G, Graves S, Downs JH (1998) Positive realness and tracking of teleoperation systems. Proc. 37th IEEE Confer. on Decision & Control, Tampa, Florida, USA, pp. 2527–2532
6. Eusebi A, Melchiorri C (1998) Force reflecting telemanipulators with time-delay: stability analysis and control design. IEEE Trans. on Automatic Control, 14(4), pp. 635–640
7. Park JH, Cho HC (1999) Sliding-mode controller for bilateral teleoperation with varying time delay. Proc. of the 1999 IEEE/ASME Int. Conf. on Advanced Intelligent Mechatronics, Atlanta, USA, pp. 311–316
8. Bajcinca N, Koeppe R, Ackermann J (2002) Design of robust stable master-slave systems with uncertain dynamics and time-delay. IFAC 15th Triennial World Congress, Barcelona, Spain.
9. Hashtrudi-Zaad K, Salcudean SE (2002) Transparency in time-delayed systems and effect of local force feedback for transparent teleoperation. IEEE Trans. on Robotics and Automation, 18(1), pp. 108–114
10. Tanner NA, Niemeyer G (2004) Pratical limitations of wave variable controllers in teleoperation. IEEE Conference on Robotics, Automation and Mechatronics
11. Berestesky P, Chopra N, Spong M (2004) Theory and experiments in bilateral teleoperation over internet. Proc. of the 2004 IEEE International Conference on Control Applications, Taipei, Taiwan
12. Niculescu SI, Taoutaou D, Lozano R (2002) On the closed-loop stability of a teleoperation control scheme subject to communication time-delays. Proc. 41st IEEE Conference on Decision & Control, Las Vegas, Nevada, USA pp. 1790–1795
13. Taoutaou D, Niculescu SI, Gu K (2003) Robust stability of teleoperation schemes subject to constant and time-varying communication delays. Proc. 42nd IEEE Conference on Decision & Control, Hyatt Regency Maui, Hawaii, USA pp. 5579–5584
14. Fattouh A, Sename O (2003) Finite spectrum assignment controller for teleoperation systems with time delay. Proc. 42nd IEEE Conference on Decision & Control, Hyatt Regency Maui, Hawaii, USA
15. Leung GMH, Francis BA, Apkarian J (1995) Bilateral controller for teleoperators with time delay via μ-synthesis. IEEE Trans. on Robotics and Automation 11:105–116
16. Boukhnifer M, Ferreira, A (2004) H_2 optimal controller design for micro-teleoperation with delay. IEEE/RSJ International Conference on Intelligent Robots and Systems. sept 28-oct 02, Sendai, Japan
17. Fattouh A, Sename O (2003) H_∞-based impedance control of teleoperation systems with time delay. 5th IFAC Workshop on Time Delay Systems, INRIA, Rocquencourt, France
18. Sename O, Fattouh, A (2005) Robust $\mathcal{H}_\infty$ control of a Bilateral Teleoperation System under Communication Time-Delay. IFAC World Congress, Prague, Czech Republic
19. El'sgol'ts LE, Norkin SB (1973) Introduction to the theory and applications of differential equations with deviating arguments. vol. 105 of Mathematics in Science and Engineering. Academic Press, New York.
20. Niculescu SI (2001) Delay effects on stability. A robust control approach. Springer-Verlag, Heidelbeg
21. Gu K. and Kharitonov V.L. and Chen J. (2003) Stability of Time-Delay Systems, Birkhäuser, Boston

22. Kao, C-Y and B. Lincoln (2004) Simple stability criteria for systems with time-varying delay. Automatica, 40, pp1429–1434.
23. Zhou K, Doyle JC, Glover K (1996) Robust and optimal control. Prentice-Hall Inc.
24. Balas GJ, Doyle JC, Glover K, Packard A, Smith R (2001) μ-Analysis and synthesis toolbox for use with MATLAB. The MathWorks, Inc.
25. Tsypkin YZ, Fu M (1993) Robust stability of time-delay systems with an uncertain time-delay constant. Int. Journal of Control 57(4):865–879

Web Remote Control of Mechanical Systems: Delay Problems and Experimental Measurements of Round Trip Time

Jean Vareille, Philippe Le Parc, and Lionel Marcé

Lisyc (formerly EA2215) Département d'Informatique UBO 20 avenue Le Gorgeu
29200 BREST France
<firstname.lastname>@univ-brest.fr

Summary. The aim of this paper is to show that the web remote control of mechanical system is nowadays not only possible but also efficient due to the improvements, in terms of reliability and bandwidth, of the networks. Nevertheless, as the internet network do not guaranty any quality of services, the possible pertubations (variable delays, failure...) have to be taken into account while developping such systems. We also present some experimental results indicating a relative stability of internet connections in terms of round trip time.

1 Introduction

Currently, the control of mechanical systems is mainly local. With the development of new e-technologies, this control will become remote and made over long distance networks. The problem is to design remote control applications taking into account the following objectives:

- The aims of the industries are to increase the Value Added, to reduce the costs and to transform time into value. So the remote control of machines presents a great interest, particularly for the remote maintenance [2].
- The remote control of machines has to be reliable, fast, easy, protected against attacks or intrusions.[27]
- The used communication technology has to be cheap although it has to offer sufficient bandwidth and small delays.

How to find a good compromise to satisfy these various seemingly incompatible points ?

Our work is based on an Internet approach of the remote control of real machines, a choice of cheap client/server solutions with common operating systems and free software. We want to evaluate the ability of Internet, which is known not to provide reliability, to allow the remote control of mechanical systems in nearly real-time for applications like e-learning, e-practice work, telemaintenance and further e-manufacturing. It corresponds well to the target of the European program "Information Society Technologies" [11], which is to offer "anywhere anytime natural access to Information Society Technologies services for all", and at one fundamental rule of the "Sustainable development" that is to "Rather prefer data transmission than displacement of people or/and matter".

J. Chiasson and J.J. Loiseau (Eds.): Appl. of Time Delay Systems, LNCIS 352, pp. 117–132, 2007.
springerlink.com

In this paper we propose a cheap methodology to solve the problem of the lack of reliability of the network. Then we focus on the description of our experiments and on results of round trip time (RTT) measurements.

2 Teleoperation and WEB Remote Control

The main concerns of such a control will be introduced through a historical point of view. The wireless remote control at long distance had been the principal theme of the work of the French physicist and doctor Edouard Branly from 1890 to 1905. The French author Jules Verne [30] wrote in 1875 a speech "une ville idéale, Amiens en l'an 2000" (an ideal city, Amiens in the year 2000) about the city where he lived, and where Edouard Branly was born. One item of this text described the retransmission by remote control in real time of a music concert between concert halls located in Amiens, London, Vienna, Rome and Saint-Petersburg, etc. The work of Samuel F.B. Morse in 1837 on the telegraph was former, but the invention of the telephone by Graham Bell (1874, patented in 1876) was contemporary. Edouard Branly knew the theory of the electromagnetic waves, and the equations of James Clerk Maxwell established between 1860 and 1864. The speed of the light had been calculated by Olaus Roemer in 1675 with a wide error, but measured with accuracy by Hippolyte Fizeau in 1849, as well as the phase speed of electrical waves in conductor wires by Kirchoff in 1857. The propagation velocities of these three kinds of waves are very close and they exceed much those of the material waves in the continuous mediums, e.g. the speed of sound in air measured by Pierre Louis Dulong about 1820, in water measured by Charles Sturm in 1827 and the elastic waves in the rigid bodies. The ratio is near 1,000,000 for the sound and 60,000 for the elastic waves.

The idea germinated of transmit commands to distant systems using electromagnetic or electric waves considering the interest of their high speed. Edouard Branly invented the first electromagnetic waves receiver, the Branly's coherer, opened the way for the invention of the antenna Popov (1897) and the starting of the radio-communication Marconi (1898).

In 1905 Edouard Branly made a successful public presentation of remote control experiments named "télémécanique" (telemechanic) in Paris in the Trocadéro's palace.

The technologies for coding, to transmit and of restitution of information increased considerably during the 20th century. In the second half the computer was born and developed.

The teleoperation became unavoidable during the second world war when started the "Manahattan Project" of production of nuclear weapons. So began in the late fortieth the work about teleoperation performed by Goertz in the Argonne National Laboratory. [6]

The convergence of the information technologies and the communication allowed the birth of Internet and after 1989 the development of the WEB.

During the Nineties, several projects appeared of mechanical systems control using Internet as communication network with varied objectives: the Mercury

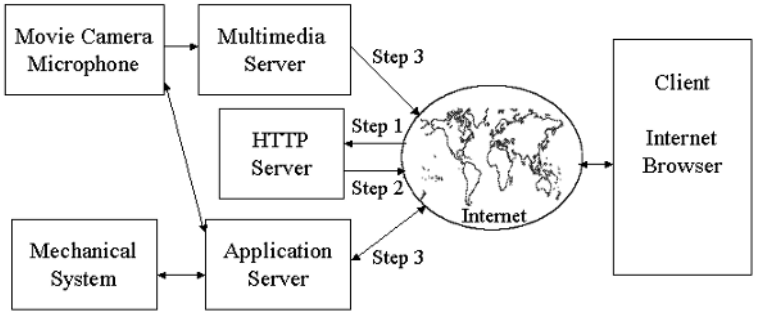

Fig. 1. General Architecture

project to prove the feasibility Goldberg and al. [7], the Australian telerobot for the interaction with the user by Taylor and al. [28], Rhino by Burgard and al.[3], Xavier by Simmons [25], Puma-Paint by Stein [26], mobile robotics Khep-OnTheWeb by Saucy and al. [23], augmented reality by Otmane Ariti [22], etc.

From the study of these experiments on Internet, a common frame can be described about the operational aspects of an application of e-manufacturing (figure 1). The user, through his Internet navigator, addresses a request to a Web server (step 1) and downloads an application on his work station such as for example a Java applet (step 2). A connection is then established towards the application server in charge of the machines's and client's management (step 3). After checks, the user is able to take the remote control of the remote device. In parallel to step 3, other connections are also established towards multi-media servers broadcasting signals (video, sound) of the system to be controlled.

Even if the general scheme is the same in most applications, no study proposes to develop a generic software architecture. More the unforeseeable nature of network (Internet) was not really taken into account with all its consequences.

In the following part we will propose a solution to these problems and we will present then various applications.

3 Methodology

We have analysed the problem with a discrete events methodology, applied to the run and stop procedures, and we have used a description tool, common in the French industry, the GEMMA [1]. It may be seen as a generic Statechart [10], an empty chart is presented on the figure 9 on appendix.

To take into account the unreliable behaviour of the network, it was necessary to improve the GEMMA. A new form: the GEMMA-Q (Quality of service GEMMA, [20]) have been introduce. 6 levels of quality of communication Q1-Q5 and Qz based on the RTT values have been defined. The state of the system is determined on the level of quality and the server can switch from, for example, the normal production state to a stop procedure when the quality is decreasing, in respect of the transitions specified in the GEMMA-Q, see figure 2.

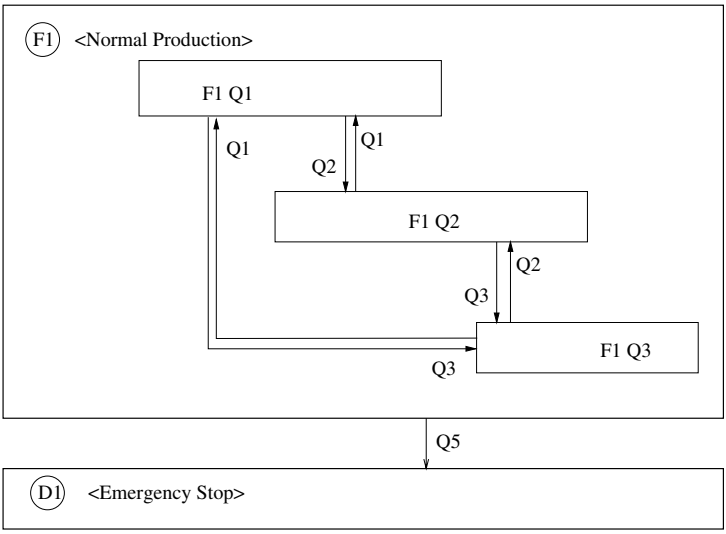

Fig. 2. Substate of the GEMMA F1 and D1

The Gemma-Q is a tool to help the developper while building his application. It forces him to think of the possible problems that may occurs due to network lack of quality of services and to propose solutions depending on the pre-defined quality levels. For example, in the case of a robotic arm, the speed of the movement may be decreased or increased according to the RTT to ensure a proper remote control in any case. More, in case of network failure (connection close), stopping the system is not all the time the best solution. The Gemma-Q offers some specific states (bottom left rectangle on figure 9) to manage defect modes and to describe the procedure to apply in such a case.

States A1 to A7, F1 to F6 and D1 to D3 are the classical states of the Gemma Model. They are all describing some specific activities that may be encounter in production systems like initialisation (A1), production (F2), test (F4 to F6) or emergency (D1). In our proposal, all these states are splitted in substates taking into account the quality of the network. A system can then be on a production mode (F1) with a good (Q1) or a rather good (Q2) or a medium (Q3) quality of the network. Quality Q4 (bad) and Q5 (no connection) forces the system to move automatically to defect mode (D1 to D3).

Developpers will first specify their Gemma-Q while giving an informal description of each state and substates. Then, these states will be instantiated with programs and the whole system is implemented on the machine side. Transitions between states will depend either on external condition (sensors) or on network conditions (quality level). Transition between sub-states only depends on network conditions. The remote user is permanently informed of the situation of the Gemma and of transition between states thanks to our underlying software architecture [21].

This architecture is implemented in java language, and involves few bonds for data- transmissions between the linked threads. This insures a rather good efficiency of the client- server system despite we don't use real time operating systems and true-time clocks. The used operating system for the server is today Windows XP®, but the server runs under Linux as well too. The downloaded code by the client is involved in applets, no plugin is needed. To add new machines we have adopted a plug and play approach, only the driver of the machine on the left side of the figure 3, and the human machine interface on the right side have to be developped. The rest of the system acts as a kernel of transmission services.

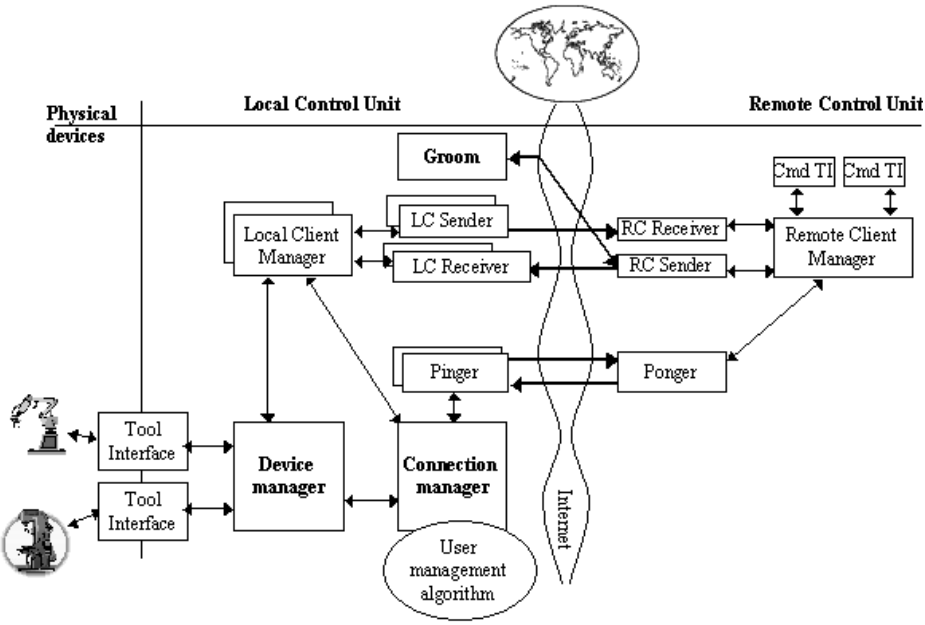

Fig. 3. Architecture of SATURN

4 Applications

Some implementations have been performed:

- a teaching arm manipulator Ericc with 5 degrees of freedom,
- a small milling machine 3d for rapid prototyping,
- a SONY camera (EVI D31) with variable pan tilt and zoom [16],
- a camera with variable pan tilt and zoom in Océanopolis, an oceanographical museum of Brest, for the observation of penguins [14].

Our system measures every second the Round Trip Time (RTT) between the connected clients and the server software, and stores these measures. The measurement procedure cannot be compared with the ICMP ping command, because this last command is just limited at the border of the operating system

Fig. 4. The robot arm Ericc and the milling machine

at either end, the Ethernet cards, and the net. The ping command sends a frame to the target machine through the net, immediately sent back by the target.

Our measures start at the application level on the server, go to the application level inside the client and come back to the server application level. It seems that the periodicities of the tasks of the operating system and the Ethernet cards and their drivers have a strong effect on the collected values e.g. the figure 7, these aren't continuously but discretely distributed. We choose the TCP-IP protocol [19] because, it's behaviour for long distance transmissions is better than with the other protocols: it improves the reliability but it is also considered as less efficient as other ones. So our values are higher than the values collected with a common ping (or a traceroute), but we are able to communicate between protected machines even when the ping command is unusable. More, the exchanged frames contain usable data for the control.

The figure 5 shows our human interface for the remote command of the robot arm. On the right side of the top, the interface displays an indicator of the ping-pong quickness, and draws a bar graph over colored stripes. Each colored stripe matches to a specific level of quality of the communication. The limit values of the levels are based on the reaction time of a worker in front of the machine inside the workshop, e.g. if the distance between the machine and him is close to 1 m, his travel speed in the factory is near 1 m/s, so his reaction time is greater than one second.

In the next section of this article we present our results of measured RTT. They show that today the reaction quickness of a qualified worker far from the

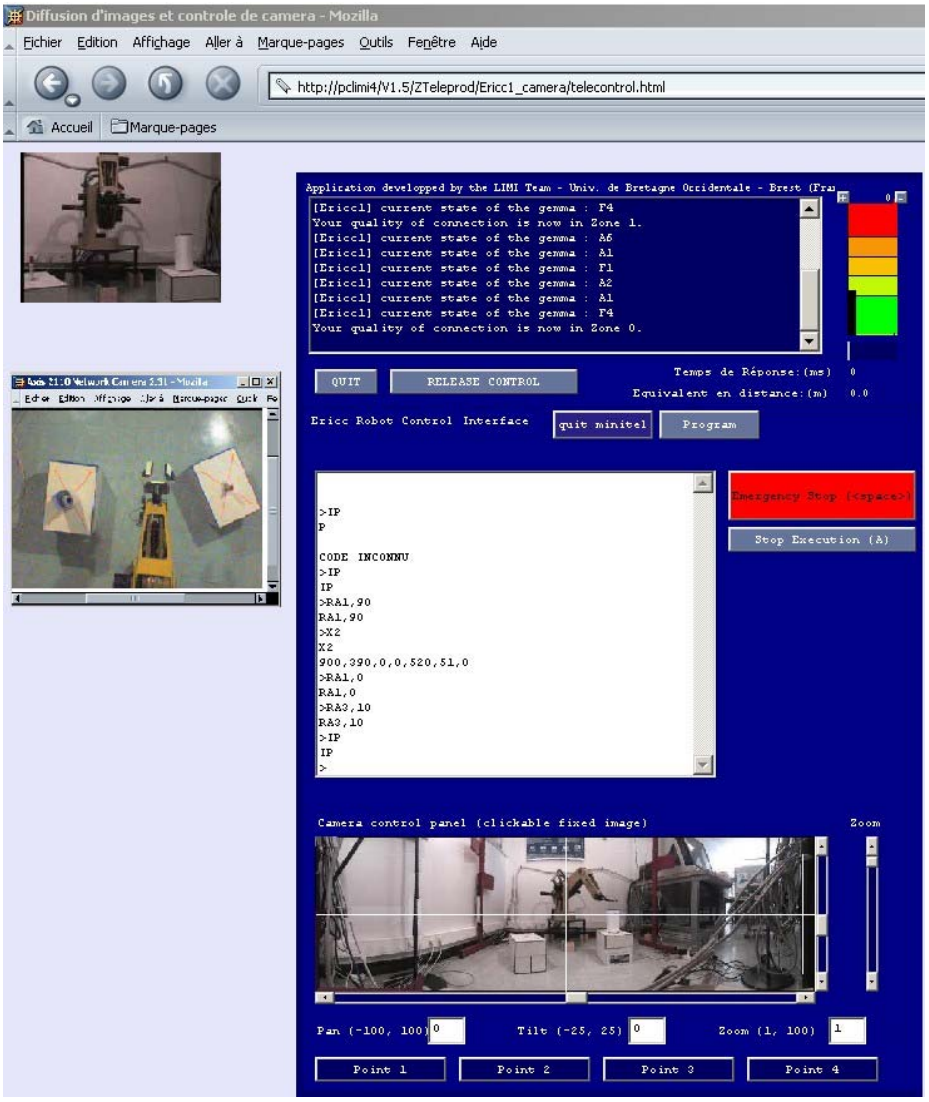

Fig. 5. The client interface

machine but well connected to Internet could be better than those of a worker in front of the machine.

5 Results

Since 2001 we have stored the data of more than 14 000 connections of more than one minute. During the last three years the performances of Internet have been increased dramatically.

We collect the values of each RTT of each connection in html files on our server, so we can access from every where to the data. Each month we transfer all the data on a MySql data base manager and we have written some typical requests to analyse the quality of the connections.

Table 1. Mean measured RTT and durations by kind of connection

	global	from France	from other countries	56k modem from France (Wanadoo)	ADSL from France (Wanadoo)
number of connections	12530	8493	4037	1468	2567
mean duration (s)	240	247	225	214	250
mean RTT (ms)	519	473	602	1023	214
standard deviation (ms)	140	140	35	669	29

The first table shows the collected values between 2001 and 2003, the two last columns display the values corresponding to the french Internet provider Wanadoo. The observed RTT values depend strongly on the kind of the connection on the side of the remote user, with Modem Lines: RTT = 1023 ms, but with Adsl lines from France to France: RTT = 214 ms, always Average values (world wide): RTT = 537 ms. Only 3% of the measured values of the RTT are over 100% of the average value. Although our RTT cannot be compared with ICMP pings, the results of measures performed during the CAIDA project [4] are similar in terms of RTT time. The figure 6 shows the evolution of the quality since august 2001 to november 2004, the percentage of the connections staying in the limit of the pic value under 100% of the mean value was only 10% at the beginning and reaches 40% at the end. We can expect that before the end of this decade less than 10% of the connection will not achieve this criterium of quality. The two bargraphs show the RTT over 50% of the average, and the RTT over 100%, it appears that the stability of the connections are increasing, today we have less than 3% of the connection with abnormal RTT higher than 100% of the average.

More, we also have observed a lot of remote connections like the one presented in figure 7 (connection from France to Japan) where the average RTT is equal to 349 ms and all the value are comprised between 270 ms and 490 ms. This connection has a duration of more than 20 minutes.

All the previous results seems to show the relative stability of the Internet network. According to us, this stability is the consequence of two main factors:

- We are using the TCP/IP protocol which has been defined to limit, as much as possible, congestion. This protocol uses different strategies, like slow start, fast retransmit or fast recovery, to try to insure a constant rate of the trafic between partners.

- Networks are now a key point of the new economy and the operators have a lot of pressure from their customers to offer the best service. The infrastructure of backbones is generally oversized to be able to manage even the worst case.

This property of relative stability can be used in the context of remote control, first of all to inform the user about the quality of the connection between him and the system he is controlling. It makes it possible to have some prospective idea of what he could do with the system. More, if several users can gained the control of the system, the one who has the best quality should be the one who will get the control.

The second aspect shown by these results is the fact that the average RTT is very small. It opens new perspectives to the remote control, to switch from nice demonstrations of feasebility to real use in the industry.

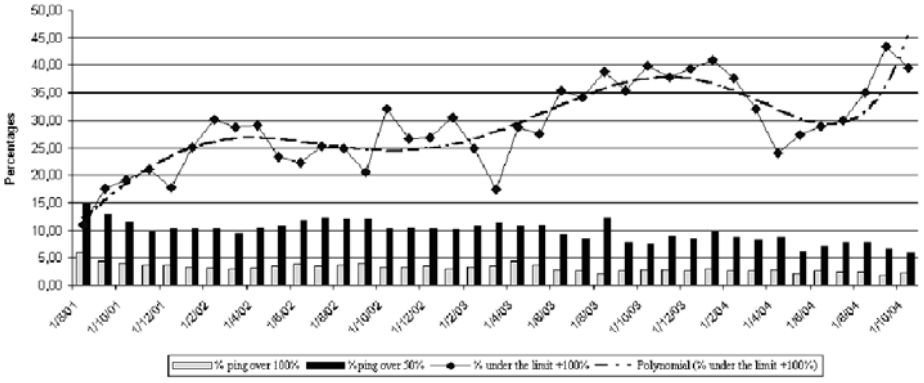

Fig. 6. Evolution of the quality

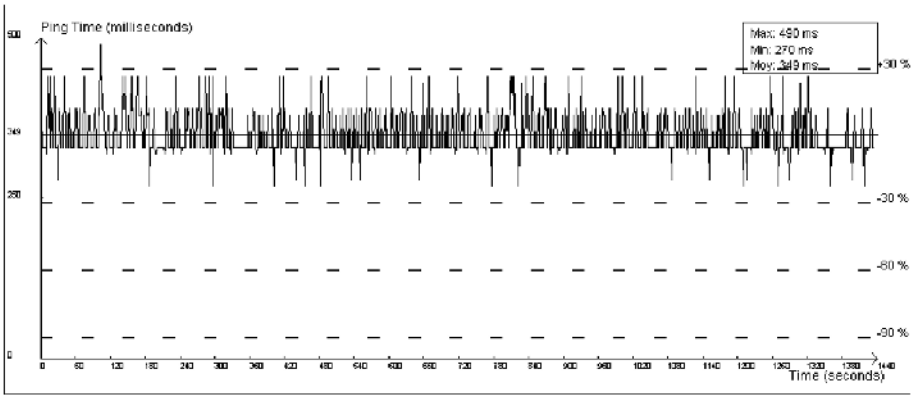

Fig. 7. Trace of a connection between Brest and a remote user situated in Japan

Nevertheless, these results also show that from time to time, depending on web factors[1](users, providers, operators, international news...), this nice stability and slow delays hypothesis are no longer true. As, the controlled system are mechanical, are moving or making movements, we have to assume security constraints. Our discrete approach with the Gemma-Q is then efficient, because the failure of the transmission occurs only accidentally. Indeed a break of the data transmission remains ever possible and for such a remote control we have to take into account that the data are transmitted to a long distance without intermediate control nor quality of service guaranteed.

It seems that the periodicities of the tasks of the operating system and the Ethernet cards and their drivers have a strong effect on the collected values e.g. the figure 7, these aren't continuously but discretely distributed.

To evaluate the velocity of Internet today we have tested with some ICMP pings the connection from Brest (France) to Auckland (New-Zealand), one of the antipodes city. Each RTT packet covers a bigger distance than 39,000 km. We have reported in the appendix two tables of typical measures of RTT and traceroute, the RTT is not stable, but the values are mostly under 400 ms.

The problem remains of the forecasts of the performance in terms of delay and bandwidth of the net, some tools about are developed about e.g. "NWS" by the Network Weather Service (NWS) [5, 18].

6 Conclusion

Our work started few years ago from a scaling concept based on the observation of the quick increasing of the performances of the IP network, and the standardization of the WEB technologies. We have developped a generic architecture and a specific sensor to measure and evaluate statistically the improvement of the net. The results are better than expected, the RTT values are small and the stability satisfactory. It appears that active remote control is feasible today on a world scale [8, 9, 31], with a rather good reliability and that the whole Internet- world is today within less than one half second for the users having "high speed connections". The physical limit of the speed is the light velocity, we are today between 5 or 10 times lower. If it should be possible to reach the limit in the future, New Zealand will be only at 200 ms RTT of Europe, such a small delay would permit an effective teleoperation [13, 29] with force feed-back on the whole earth! This perspective open the door of networked closed-loop system, where the stabilization problem of the variable time-delay would be solved. [17]

[1] The problem remains of the forecasts of the performance in terms of delay and bandwidth of the net, some tools about are developed about e.g. "NWS" by the Network Weather Service (NWS) [5, 18].

References

1. ADEPA. GEMMA : guide d'études des modes de marche et d'arrêt.
2. Bicchi A., Coppelli A., Quarto F., Rizzo L., Turchi F., Balestino A. (2001) Breaking the lab's walls telelaboratories at the university of pisa. In: Proceedings of the 2001 IEEE International Conference on Robotics and Automation, Seoul, Korea
3. Burgard W., Cremers A.B., Fox D., Hähnel D., Lakemeyer G., Schulz D., Steiner W., Thrun S (1995) The mobile robot Rhino. AI Magazine 16(2):31–38
4. CAIDA the Cooperative Association for Internet Data Analysis, see http://www.caida.org/
5. Gaidioz B., Wolski R., Tourancheau B. (2000) Synchronizing Network Probes to avoid Measurement Intrusiveness with the Network Weather Service. In: Proceedings of 9th IEEE High-performance Distributed Computing Conference, pp. 147-154
6. Goertz R. C. (1952) Fundamentals of General-Purpose Remote Manipulators. Nucleonics 10-11:36-45
7. Goldberg K., Gentner S., Sutter C., and Wiegley J. (1999) The Mercury project: a feasibility study for Intemet robotics. IEEE Robotics and Automation Magazine 3:35-40
8. Goldberg K., Santarromana J., The Telegarden, htttp ://telegarden.aec.at/
9. Goldberg K., Siegwart R. (2001) Beyond Webcams : an introduction to online robots. The MIT Press, Cambridge
10. Harel, D. (1987) STATECHARTS : A visual formalism for complex systems. In: Science of Computer programming 8(3):231–274
11. IST Information Society Technologies Programme, see http://www.cordis.lu/ist/activities/activities-d.htm
12. Krommenacker N., Georges J., Rondeau E., Divoux T. (2002) Designing, Modelling and Evaluating Switched Ethernet Networks in Factory Communication Systems. 1st International Workshop on Real-Time LANs in the Internet Age, Vienne, Autriche
13. Kuusik A., Hisada T., Suzuki S., Furuta K. (2004) Cellular Network Telecontrolled Robot Vehicle. In: Proc. TA2004, 1st IFAC Symposium on Telematics Applications in Automation and Robotics, pp 125-130, Helsinki, Finland
14. Laboratoire LIMI-E3883, Oceanopolis and IRVI-Progeneris (2001) The penguin project. http://www.oceanopolis.com/visite/visite.htm
15. Michaut F., Lepage F. (2002) A tool to Monitor the Network Quality of service. IFIP-IEEE conference on Network Control and Engineering (CON'2002), Paris, France,
16. Le Parc P., Ogor P., Vareille J., Marcé L. (1999). Robot control from the limi lab. http://similimi.univ-brest.fr
17. Niculescu S.I., Gu K., Abdallah C.T. (2003) Some Remarks on the Delay Stabilizing Effect in SISO systems. American Control Conference, Denver, Colorado
18. NWS, see http://nws.cs.ucsb.edu/
19. Oboe, R., Fiorini P. (1997) Issues on internetbased teleoperation. In: Syroco 97, pp. 611–617, Nantes, France
20. Ogor, P. (2001) Une architecture générique pour la supervision sûre à distance de machines de production avec Internet. PhD thesis. Université de Bretagne Occidentale, Brest
21. Ogor, P., Le Parc P., Vareille J., Marcé L. (2001) Control a robot on internet. In: 6th IFAC Symposium on Cost Oriented Automation, Berlin, Germany

22. Otmane S., Mallem M., Kheddar A., Chavand F. (2000) ARITI : an Augmented Reality Interface for Teleoperation on the Internet. Advanced Simulation Technologies Conference High Performance Computing HPC'2000, pp. 254 - 261 Washington D.C., USA
23. Saucy P., F.Mondada. (2000) KhepOntheWeb : Open access to a mobile robot on the Internet. IEEE robotics and automation magazine 7(1):41-47
24. Sheridan T. (1992) Telerobotics, automation and human supervisory control. The MIT Press, Cambridge
25. R. Simmons. (1998) Xavier : An autonomous mobile robot on the WEB. International Workshop On Intelligent Robots and Systems (IROS), Victoria, Canada
26. Stein M. (1998) Painting on the world wide web : the PumaPaint project. In Proceeding of the IEEE IROS'98 Workshop on Robots on the Web, Victoria, Canada
27. Strandén L., Hedberg J., Sivencrona H. (2002) Machine Control via Internet - a holistic approach. Report, 2002, Swedish National Testing and Research Institute
28. Taylor K., Trevelyan J. (1995) A telerobot on the world wide web. National Conference of the Australian Robot Association, Melbourne, Australia
29. Thompson D., Burks B. and Killough S. (1993) Remote excavation using the telerobotic small emplacement excavator. In: Proc. 5th ANS Int. Topical Meeting Robotics and Remote Systems, pp 465-470, Knoxville, Tennessee
30. Verne J. (1875) Une ville idéale. (First a speech, transformed into a novell). Ed. du Millénaire CDJV, Amiens (1999), or see
http://www.phys.uu.nl/ gdevries/etexts/index.html and
http://www.phys.uu.nl/ gdevries/etexts/ville/ville.html
31. Wang L., Orban P., Cunningham A., Lang S. (2004) Remote real-time CNC machining for web-based manufacturing. Robotics and Computer-Integrated Manufacturing 20:563-571

Appendix

In 2003 we have computed averages for some countries with values extracted from our measurements. It appears that the geographical distance as no significant influence on the RTT, and that the performances are near the interessant RTT value of 300 ms considered as a threshold compatible with the IP telephony.

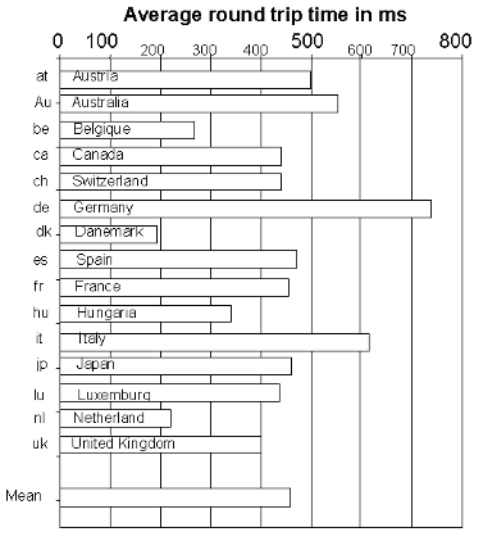

Fig. 8. Measured RTT: mean value versus the country

To evaluate the velocity of Internet today we have tested with some ICMP pings the connection from Brest (France) 48°23′ N ⊕ 4°30′ W to Auckland (New-Zealand) 37°00′ S ⊕ 174°47′ E., one of the antipodes city. Each RTT packet covers a bigger distance than 39,000 km. We have reported in the appendix two tables of typical measures of RTT and traceroute, the RTT is not stable, but the values are mostly under 400 ms.

The great-circle distance between these two towns is about 19,500 km. Each RTT packet travels more than 39,000 km. We have reported here two tables of typical measures of RTT and traceroute, clearly the RTT is not stable, the max value is approximately four times greater than the average value, but the values are mostly under 400 ms. So the operational velocity of the data is close to 100,000 km/s the half of the light speed in optic fibers !

This means that the delays induced by the equipments like switches or routers are become very small for the long distance communications on Internet.

Table 2. Sample of ICMP RTT between Brest(fr) and Auckland(nz)

```
lepouldu[4] ping -s www.auckland.ac.nz
PING www.auckland.ac.nz: 56 data bytes
64 bytes from www.auckland.ac.nz (130.216.191.67): icmp_seq=0. time=390. ms
64 bytes from www.auckland.ac.nz (130.216.191.67): icmp_seq=1. time=2154. ms
64 bytes from www.auckland.ac.nz (130.216.191.67): icmp_seq=2. time=1154. ms
64 bytes from www.auckland.ac.nz (130.216.191.67): icmp_seq=3. time=389. ms
64 bytes from www.auckland.ac.nz (130.216.191.67): icmp_seq=4. time=387. ms
64 bytes from www.auckland.ac.nz (130.216.191.67): icmp_seq=5. time=443. ms
64 bytes from www.auckland.ac.nz (130.216.191.67): icmp_seq=6. time=391. ms
64 bytes from www.auckland.ac.nz (130.216.191.67): icmp_seq=7. time=391. ms
64 bytes from www.auckland.ac.nz (130.216.191.67): icmp_seq=8. time=389. ms
64 bytes from www.auckland.ac.nz (130.216.191.67): icmp_seq=9. time=386. ms
64 bytes from www.auckland.ac.nz (130.216.191.67): icmp_seq=10. time=392. ms
64 bytes from www.auckland.ac.nz (130.216.191.67): icmp_seq=11. time=388. ms
64 bytes from www.auckland.ac.nz (130.216.191.67): icmp_seq=12. time=387. ms
64 bytes from www.auckland.ac.nz (130.216.191.67): icmp_seq=13. time=393. ms
^ C
—-www.auckland.ac.nz PING Statistics—-
14 packets transmitted, 14 packets received, 0% packet loss
round-trip (ms) min/avg/max = 386/573/2154
lepouldu[5]
```

Table 3. Sample of traceroute between Brest(fr) and Auckland(nz)

```
lepouldu[6] traceroute www.auckland.ac.nz
traceroute to www.auckland.ac.nz (130.216.191.67), 30 hops max, 40 byte packets
 1 193.52.16.16 (193.52.16.16) 0.721 ms 0.420 ms 0.291 ms
 2 172.31.1.19 (172.31.1.19) 0.593 ms 1.987 ms 1.382 ms
 3 193.50.69.249 (193.50.69.249) 2.310 ms 2.565 ms 2.131 ms
 4 193.48.78.197 (193.48.78.197) 134.774 ms 110.455 ms 111.106 ms
 5 PAO-Rennes2-TR.rrb.ft.net (195.101.145.25) 116.580 ms 115.974 ms 57.848 ms
 6 peering-GIP.rrb.ft.net (195.101.145.6) 19.283 ms 18.024 ms 115.293 ms
 7 rennes-g3-1-10.cssi.renater.fr (193.51.181.126) 37.090 ms 52.776 ms 78.339 ms
 8 caen-pos1-0.cssi.renater.fr (193.51.180.17) 128.701 ms 21.718 ms 20.487 ms
 9 rouen-pos1-0.cssi.renater.fr (193.51.180.22) 39.375 ms 28.154 ms 22.034 ms
10 nri-a-pos6-0.cssi.renater.fr (193.51.179.21) 20.082 ms 32.574 ms 29.953 ms
11 193.51.185.1 (193.51.185.1) 32.696 ms 24.649 ms 23.975 ms
12 P11-0.PASCR1.Pastourelle.opentransit.net (193.251.241.97) 30.294 ms 24.603 ms 19.522 ms
13 P2-0.AUVCR2.Aubervilliers.opentransit.net (193.251.128.117) 21.410 ms 22.717 ms 27.937 ms
14 P6-0.NYKCR2.New-york.opentransit.net (193.251.243.234) 94.401 ms 107.672 ms 113.035 ms
15 P4-0.SJOCR1.San-jose.opentransit.net (193.251.242.2) 180.001 ms 175.272 ms 175.997 ms
16 P8-0.PALCR1.Palo-alto.opentransit.net (193.251.243.121) 176.130 ms 175.997 ms 175.436 ms
17 134.159.62.5 (134.159.62.5) 175.075 ms 177.357 ms 176.800 ms
18 i-11-0.paix-core01.net.reach.com (202.84.251.21) 182.981 ms 180.188 ms 177.993 ms
19 i-13-0.wil-core01.net.reach.com (202.84.143.61) 186.890 ms 187.118 ms 186.342 ms
20 202.84.219.102 (202.84.219.102) 662.074 ms 517.804 ms 675.547 ms
21 ge0-2-0-2.xcore1.sym.telstraclear.net (203.98.4.2) 402.907 ms 389.516 ms 389.461 ms
22 ge-0-2-0-21.jcore2.acld.clix.net.nz (203.98.50.8) 397.587 ms 388.412 ms 389.480 ms
23 218.101.61.11 (218.101.61.11) 543.061 ms 455.813 ms 496.482 ms
24 clix-uofauckland-nz-1.cpe.clix.net.nz (203.167.226.42) 388.648 ms 391.259 ms 399.452 ms
25 * * *
26 * * *
27 * * *
28 ^ C lepouldu[7]
```

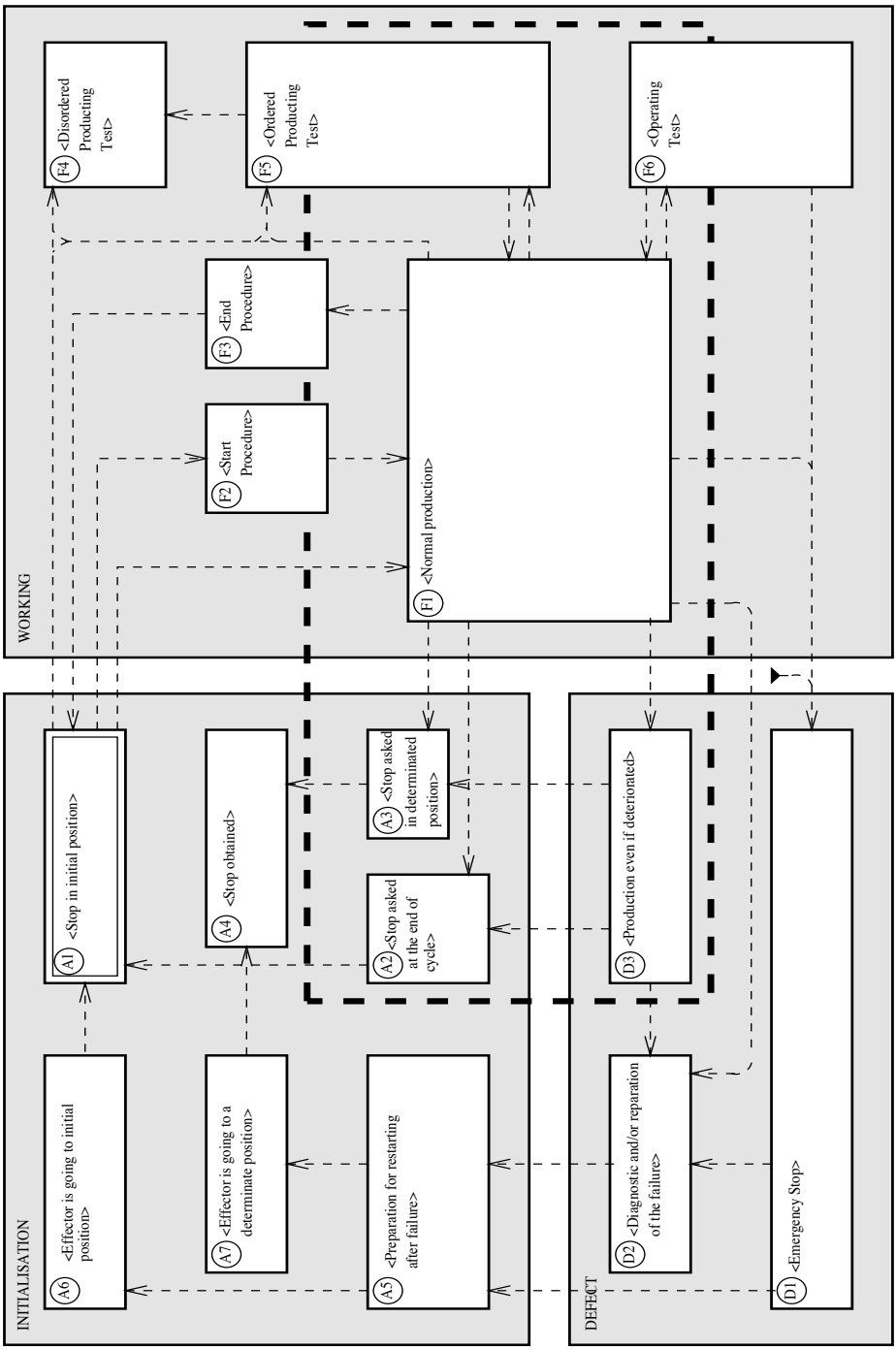

Fig. 9. Classical GEMMA

PDE Approach for Time Delays in Robotized Teleoperation

Youssoufi Touré, Laurence Josserand, Gérard Poisson, and Fabrice Babet

LVR UPRES EA 2078, Université d'Orléans, 63 avenue de Lattre de Tassigny, 18020 Bourges Cedex, France
Youssoufi.Toure@bourges.univ-orleans.fr,
Laurence.Josserand@bourges.univ-orleans.fr,
Gerard.Poisson@bourges.univ-orleans.fr,
Fabrice.Babet@bourges.univ-orleans.fr

Summary. Semigroup and spectrum perturbations are suitable for control synthesis of distributed parameter systems described by partial differential equation (PDE). The representation and processing of delay in tele-operated systems have a major scientific interest. In this contribution, the aim is to show that infinite dimensional representation of the delay by PDE can be suitable for control synthesis where the objective is that the tele-operated system tracks the master system. The Internal Model Boundary Control (IMBC) structure is used to achieve closed loop tele-operated characterization.

Keywords: Partial Differential Equation, Infinite Dimensional System, Teleoperation, C_0-semigroup.

1 Introduction

This paper presents a draft synthesis of tele-operated controlled system where time delays are defined by Partial Differential Equation (PDE). The idea is to test if this approach could be an easy way to deal with the control problem.

Indeed, the state space representation of PDE in infinite dimensional systems and the semigroup approach are well suited for the control synthesis and analysis [2], [3], [4]. The well-known concepts like open loop or closed loop design, stability, regulation, ... can be done [1][12][13][6]. In this approach, the closed loop system is studied using the fact that it can be viewed as a perturbation of the open loop system, perturbation of the semigroup and perturbation of the spectrum, in Kato sense [5].

The closed loop system stability is achieved using the spectral and semigroup perturbation theory. Consequently, the design conditions can be established for the controller to achieve tracking or for a regulation aim, using the properties stability of the semigroup and the spectrum.

This approach has been already used for classic PDE systems associated to Internal Model Boundary Control, for parabolic systems [3], [4], [7], or hyperbolic open loop stable systems [8], [9].

In this contribution, the approach is extended to tele-operated systems and more specifically to an experimental and almost industrial robotized tele-echography

J. Chiasson and J.J. Loiseau (Eds.): Appl. of Time Delay Systems, LNCIS 352, pp. 133–144, 2007.
springerlink.com

system [10]. The main contribution is the description of the teleoperation global system as the open loop system part of an appropriate form of the Internal Model Control structure. For example, the transfer between the slave and master systems are represented in a direct form instead of a "material closed loop" like system, i.e. the direct transfer between the master system and the slave system and the reverse transfer from the slave system to the master system. So it is easy to show that the practical objective of "transparency" between the "expert" operator and the slave system, the "patient", can be achieved by the internal model control structure and the control design by perturbation theory in infinite dimensional system approach.

2 Model

The overall tele-operated system has three main parts: the master station generating the operation, a slave station remotely operated by the master system and a communication link (transfer system) in between.

In the tele-echography system, the operation generator is a one degree-of-freedom (DOF) hand free device, also called fictive probe, moved by the medical expert. This fictive probe helps the medical expert to remotely control the distant ultrasound probe holder robot positioned on the patient. It doesn't acquire any image but only supply the setpoint trajectory for the real echographic probe.

The patient station sends back to the master station ultrasound images and haptic information which allow the medical expert to propose a preliminary diagnosis.

In a medical routine use, the global objective of the tele-echography chain is for the slave station to transfer locally acquired information (e.g force) for an efficient rendering at the master station.

One of the specific aspects of this chain is the existence, at various levels, of time delays which values and effects vary according to the type of use of the system. There are also various dynamic behaviours difficult to manage. These delays are represented by hyperbolic PDE.

The tele-operated system is represented in the following figure Fig. 1 by different sub-systems: the expert (master) and patient (slave) systems and the transfer links in between:

Remark: The transfer between expert station and patient station is an action link. The reverse link is a feedback information but not a feedback like action.

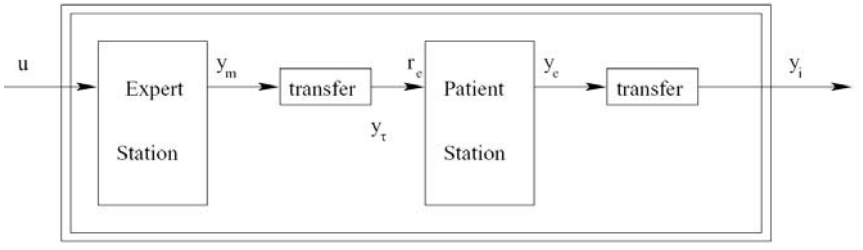

Fig. 1. Tele-operated system

2.1 Description

The description of these elements is as follows:

• **The master station**
It is a one DOF hands free mechanical device (called the fictive probe), generating the operations trajectory and giving the reference points.

$$\begin{cases} \dot{x}_m(t) = A_m x_m(t) + B_m u(t) \quad t > 0 \\ x_m(0) = x_m^0 \\ y_m(t) = C_m x_m(t) \end{cases}$$

$$x_m(t) \in I\!R^{n1} \quad u(t) \in I\!R^{m1} \quad y_m(t) \in I\!R^{p1}$$

• **The slave station**
Where the operation is performed.

$$\begin{cases} \dot{x}_e(t) = A_e x_e(t) + B_e r_e(t) \quad t > 0 \\ x_e(0) = x_e^0 \\ y_e(t) = C_e x_e(t) \end{cases}$$

$$x_e(t) \in I\!R^{n2} \quad r_e(t) \in I\!R^{m2} \quad y_e(t) \in I\!R^{p2}$$

• **Transfer master-slave**
Reference points are transferred to the slave station including variable delays modelled by transport equation with boundary control.

$$\begin{cases} \frac{\partial x_\tau}{\partial t} = -v_\tau \frac{\partial x_\tau}{\partial z} \qquad z \in \Omega_1 = (0\ L_1) \quad t > 0 \\ x_\tau(t,0) = y_m(t) \\ x_\tau(t,L_1) = r_e(t) \\ x_\tau(0,z) = x_\tau^0 \qquad z \in \ \bar{\Omega}_1 = [0,\ L_1] \end{cases} \tag{1}$$

• **Transfer slave-master**
The feedback information from slave station to master station includes also variable time delays which can be represented by a PDE.

$$\begin{cases} \frac{\partial x_i}{\partial t} = -v_i \frac{\partial x_i}{\partial z} \qquad z \in \Omega_2 = (0\ L_2) \quad t > 0 \\ x_i(t,0) = y_e(t) \\ x_i(t,L_2) = y_i(t) \\ x_i(0,z) = x_i^0 \qquad z \in \ \bar{\Omega}_2 = [0,\ L_2] \end{cases} \tag{2}$$

Remark 1. Notice that in classical delay representation, L_1/v_τ is the delay of master-slave transfer and L_2/v_i is the feedback information delay.

• **Boundary control semigroup formulation for delay systems**
The above state space models (1) and (2) of communication links, can be summarized as following:

$$\begin{cases} \dot{x}_k(t) = A_d^k x_k(t) \quad \text{on} \quad \Omega_k,\ t > 0 \\ F_b x_k(t) = B_b u_k(t) \quad \text{on} \quad \Gamma = \partial\Omega_k,\ t > 0 \\ x_k(0) = x_k^0 \quad \text{in} \quad \mathcal{D}(A_d^k) \end{cases} \tag{3}$$

the output is given by:

$$y_k(t) = C_b x_k(t), \quad t \geq 0$$

with

$$x_k(t) \in X_k = \left[L^2(\Omega_k)\right]^{p_k}$$

$$\mathcal{D}(A_d^k) = \{x_k \in X_k, x_k \ a.c, \frac{dx_k}{dz} \in \left[L^2(\Omega_k)\right]^{p_k}\}$$

Each operator F_b, B_b and C_b is taken as a bounded operator:

$$F_b \in L(X_k, I\!R^{p_k}) \quad B_b \in L(I\!R^{p_k}, I\!R^{p_k}) \quad C_b \in L(X_k, I\!R^{m_k})$$

The index k is chosen such that:

- for system (1): $x_k = x_\tau$, $u_k = y_m$, $\Omega_k = \Omega_1$, $p_k = p_1$, $m_k = m_1$ and $A_d^k x_k = -v_\tau \frac{\partial x_\tau}{\partial z}$
- for system (2): $x_k = x_i$, $u_k = y_e$, $\Omega_k = \Omega_2$, $p_k = p_2$ and $m_k = m_2$ and $A_d^k x_k = -v_i \frac{\partial x_i}{\partial z}$.

These boundary control systems may be formulated in the classical state space abstract boundary control system [11], [3], [14]:

$$\begin{cases} \dot{\varphi}_k(t) = A_k \varphi_k(t) - D_k \dot{u}_k(t), \quad \varphi_k(t) \in \mathcal{D}(A_{\mathrm{d}}^k), t > 0, \\ \varphi_k(0) = x_k(0) - D_k u_k(0) \end{cases} \tag{4}$$

where

- A_k is the "extension operator" of A_{d}^k, which means $A_k \varphi_k(t) = A_{\mathrm{d}}^k \varphi_k(t)$ for all $\varphi_k \in \mathcal{D}(A_k)$ and $\mathcal{D}(A_k) = \{\varphi_k \in \mathcal{D}(A_{\mathrm{d}}^k) \mid F_{\mathrm{b}}^k \varphi_k = 0\}$, A_k is assumed closed and densely defined in X_k.
- D_k is the bounded "distribution operator" describing the action of the boundary control on the state: $D_k \in L(U_k, X_k)$, the set of bounded operators from U_k in X_k such that $D_k u_k \in \mathcal{D}(A_{\mathrm{d}}^k)$, $F_{\mathrm{b}}^k(D_k u_k) = B_{\mathrm{d}}^k u_k, \forall u_k \in U_k$, and D_k is choosen such that it leaves the operator A_d^k unchanged (i.e., $\mathrm{im}(D_k) \subset \ker(A_d^k)$).
- The change of variables is:

$$x_k(t) = \varphi_k(t) + D_k u_k(t)$$

According to (3), the abstract boundary control (4) has the following classical solution:

$$\varphi_k(t) = T_{A_k}(t)\varphi_k(0) - \int_0^t T_{A_k}(t-s) D_k \dot{u}_k(s)\, \mathrm{d}s$$

where $\dot{u}$ is continuous and where the operator A_k is assumed to be an infinitesimal generator of the semigroup T_{A_k}.

2.2 Teleoperation Global System

The open loop system:

$$\begin{pmatrix} \dot{x}_m(t) \\ \dot{\varphi}_\tau(t) \\ \dot{x}_e(t) \\ \dot{\varphi}_i(t) \end{pmatrix} = \begin{pmatrix} A_m & 0 & 0 & 0 \\ -D_\tau C_m A_m & A_\tau & 0 & 0 \\ 0 & B_e C_\tau & A_e & 0 \\ 0 & -D_i C_e B_e C_\tau & -D_i C_e A_e & A_i \end{pmatrix} \begin{pmatrix} x_m(t) \\ \varphi_\tau(t) \\ x_e(t) \\ \varphi_i(t) \end{pmatrix} + \begin{pmatrix} B_m \\ -D_\tau C_m B_m \\ 0 \\ 0 \end{pmatrix} u(t)$$

can be summarized by the following model:

$$\dot{\tilde{x}}(t) = \tilde{A}\tilde{x} + \tilde{B}u(t) \qquad \tilde{x}(0) = \tilde{x}_0$$

where

$$\tilde{x} = (x_m\ \varphi_\tau\ x_e\ \varphi_i)^T \in \tilde{X} = I\!R^{n_1} \oplus X_1 \oplus I\!R^{n_2} \oplus X_2$$
$$\tilde{B} \in L[I\!R^{m_1}, \tilde{X}]$$

2.3 Robotic Tele-Echographic Case

In a practical point of view, the loop is closed thanks to expert image analysis. As the expert is not "controllable", he cannot be included in the global model, but rather be seen as a trajectory generator using spatial positions and orientations of the fictive probe. Therefore, its corresponding block diagram can be taken out of the global system and considered as an external trajectory generator block, which leads to the following representation:

Consequently, the global model is the following:

$$\begin{pmatrix} \dot{\varphi}_\tau(t) \\ \dot{x}_e(t) \\ \dot{\varphi}_i(t) \end{pmatrix} = \begin{pmatrix} A_\tau & 0 & 0 \\ B_e C_\tau & A_e & 0 \\ -D_i C_e B_e C_\tau & -D_i C_e A_e & A_i \end{pmatrix} \begin{pmatrix} \varphi_\tau(t) \\ x_e(t) \\ \varphi_i(t) \end{pmatrix} + \begin{pmatrix} -D_\tau & 0 \\ 0 & B_e C_\tau D_\tau \\ 0 & -D_i C_e B_e C_\tau D_\tau \end{pmatrix} \begin{pmatrix} \dot{u}(t) \\ u(t) \end{pmatrix} \tag{5}$$

and it can be summarized as follow:

$$\dot{\tilde{x}}(t) = \tilde{A}\tilde{x} + \tilde{B}\mathrm{U}(t) \quad t > 0, \quad \tilde{x}(0) = \tilde{x}_0$$

with:

$$\tilde{x} = (\varphi_\tau\ x_e\ \varphi_i)^T \in \tilde{X} = X_1 \oplus I\!R^{n_2} \oplus X_2$$
$$\mathrm{U} = (\dot{u}(t)\ u(t))^T$$

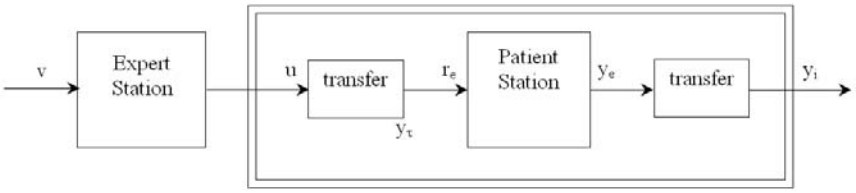

Fig. 2. Robotic tele-echographic system

and

$$\tilde{A} = \begin{pmatrix} A_\tau & 0 & 0 \\ B_e C_\tau & A_e & 0 \\ -D_i C_e B_e C_\tau & -D_i C_e A_e & A_i \end{pmatrix} \tag{6}$$

$$\tilde{B} = \begin{pmatrix} -D_\tau & 0 \\ 0 & B_e C_\tau D_\tau \\ 0 & -D_i C_e B_e C_\tau D_\tau \end{pmatrix}$$

defined by:

$$\tilde{A} \in \tilde{X} = X_1 \oplus I\!R^{n_2} \oplus X_2$$
$$\tilde{B} \in L[I\!R^{m_1}, \tilde{X}]$$

$\tilde{X}$ is an Hilbert space with the inner product:

$$< \tilde{x}_l \ , \ \tilde{x}_m >_{X_i} = \int_{\Omega_i} \tilde{x}_l \tilde{x}_m \ d\Omega_i$$

and the norm:

$$\|\tilde{x}\|^2_{\tilde{X}} = < \tilde{x} \ , \ \tilde{x} >_{\tilde{X}} = < \varphi_\tau \ , \ \varphi_\tau >_{\tilde{X}_\tau} + < x_e \ , \ x_e >_{I\!R^{n_2}} + < \varphi_i \ , \ \varphi_i >_{\tilde{X}_i} .$$

The global output of the system is $y(t) = y_i(t) \in I\!R^{n_2}$.

3 Characterization of the Open Loop Operator

3.1 Open Loop Semigroup

According to the previous part, the open loop characterization concerns the following system:

$$\begin{cases} \dot{\varphi}(t) = \tilde{A}\varphi(t) \quad t > 0 \\ \varphi(0) = \varphi_0 \in \mathcal{D}(\tilde{A}) \end{cases} \tag{7}$$

whose classical solution is $\varphi(t) = T_{\tilde{A}}(t)\varphi(0) \in \mathcal{D}(\tilde{A})$, where the operator $\tilde{A}$ is assumed to be generator of the C_0semigroup $T_{\tilde{A}}$ and

$$\mathcal{D}(\tilde{A}) = \{\tilde{x} \in \tilde{X}, \ \tilde{x} \ a.c, \ \varphi_\tau^{'} \in L^2(\Omega_\tau) \ , \varphi_i^{'} \in L^2(\Omega_i) \ , \varphi_\tau(0) = 0 \ , \varphi_i(0) = 0\}$$

Proposition 1. *The open loop teleoperation system semigroup is a contraction semigroup.*

Proof. By the formulation of the open loop operator (6), it can be seen that $\tilde{A} = A_1 + A_2$ with:

$$A_1 = \begin{pmatrix} A_\tau & 0 & 0 \\ 0 & 0 & 0 \\ 0 & 0 & A_i \end{pmatrix}$$

$$A_2 = \begin{pmatrix} 0 & 0 & 0 \\ B_e C_\tau & A_e & 0 \\ -D_i C_e B_e C_\tau & -D_i C_e A_e & 0 \end{pmatrix}$$

The operator A_2 is a bounded operator. So $\tilde{A}$ is a bounded perturbation of A_1 and its C_0-semigroup property follows the C_0-semigroup generation of A_1 (see theorem 3.2.1 p.110 [15]).

A_1 is a generator of a contraction C_0-semigroup from direct calculations of its dissipativity properties (see corollary 2.2.2 p.33 [15]), which is obtained by those of A_τ and A_i:

$$< A_\tau \varsigma, \varsigma >_{X_\tau} = -\frac{v_\tau}{2} \int_0^{L_2} \varsigma' \varsigma \, \mathrm{d}\zeta = -\frac{v_\tau}{2} \varsigma^2(L_2)$$

$$< A_\tau \varsigma, \varsigma >_{X_\tau} \leq 0.$$

The calculations are the same for A_τ^*, A_i and A_i^*. □

3.2 Stability of the Open Loop System

Corollary 1. *If the patient station system is an exponentially stable system then the global open loop system is an exponentially stable semigroup*

Proof. • The patient station is an exponentially stable system:

$$< A_e \varphi_e, \varphi_e >_{X_e} \leq -\rho_e \left\| \varphi_e \right\|_{X_e}^2 \tag{8}$$

where ρ_e is the smallest absolute eigenvalue of A_e.

• Now, let us consider the following quantity:

$$V(t) = \frac{1}{2} \left\| \varphi \right\|_{\tilde{X}}^2 \qquad \text{for } t > 0$$

then

$$\dot{V}(t) = \frac{1}{2} \frac{\left\| \varphi \right\|_{\tilde{X}}^2}{dt} = < \tilde{A}\varphi, \varphi >_{\tilde{X}} \tag{9}$$

with

$$\begin{aligned} < \tilde{A}\varphi, \varphi >_{\tilde{X}} &= < A_i \varphi_i \ , \ \varphi_i >_{X_i} + < A_\tau \varphi_\tau \ , \ \varphi_\tau >_{X_\tau} + < A_e \varphi_e \ , \ \varphi_e >_{X_e} \\ &= -\frac{v_\tau}{2} \varphi_\tau^2(L_1) - \frac{v_i}{2} \varphi_i^2(L_2) + < A_e \varphi_e \ , \ \varphi_e >_{X_e} \end{aligned}$$

- Using the fact that:

$$\|\varphi_\tau\|^2_{X_\tau} \geq \varphi^2_\tau(L_1) \quad \text{and} \quad \|\varphi_i\|^2_{X_i} \geq \varphi^2_i(L_2)$$

and the property (8), its leads to :

$$< \tilde{A}\varphi, \varphi >_{\tilde{X}} \leq -\frac{v_\tau}{2}\|\varphi_\tau\|^2_{X_\tau} - \frac{v_i}{2}\|\varphi_i\|^2_{X_i} - \rho_e \|\varphi_e\|^2_{X_e}$$

- Now, set $\rho = min\left\{\frac{v_i}{2}, \frac{v_\tau}{2}, \rho_e\right\} > 0$, then

$$< \tilde{A}\varphi, \varphi >_{\tilde{X}} < -\rho\|\varphi\|^2_{\tilde{X}} < 0.$$

- According to (9), it follows:

$$\begin{aligned} \frac{1}{2}\frac{\|\varphi\|^2_{\tilde{X}}}{dt} &< -\rho\|\varphi\|^2_{\tilde{X}} \\ ln\|\varphi\|^2_{\tilde{X}} &< -2\rho + const \\ \|\varphi\|_{\tilde{X}} &< c_o e^{-\rho t} \end{aligned}$$

with some constant c_o. Using the formal solution $\varphi(t) = T_{\tilde{A}}\varphi(0)$ of the open loop system (7), one has:

$$\|T_{\tilde{A}}\varphi(0)\|_{\tilde{X}} < c_o e^{-\rho t} \qquad \text{for} \quad t > 0$$

$$\|T_{\tilde{A}}\varphi(0)\|_{\tilde{X}} < \|\varphi(0)\|_{\tilde{X}} e^{-\rho t}$$

$$\|T_{\tilde{A}}\|_{\tilde{X}} < e^{-\rho t} \qquad \text{for} \quad t > 0$$

which means that it is an exponentially stable contraction semigroup. □

4 Internal Model Boundary Control Structure: Closed Loop System

The Internal Model Boundary Control (IMBC) structure is used as a closed loop control synthesis method. It is a slightly modified form of the classical IMC structure with some finite dimensional filters for tracking finite boundary output measurements with finite boundary control variables:

Tracking model M_r and low pass filter M_f are finite dimensionnal stable systems:

$$\begin{cases} \dot{x}_r(t) = A_r x_r(t) + B_r v(t) & \text{with } v(t) \in I\!R^{n_2} \\ r(t) = C_r x_r(t) \quad \text{and} \quad x_r(0) = 0 & \text{with } r(t) \in I\!R^{n_2} \end{cases}$$

$$\begin{cases} \dot{x}_f(t) = A_f x_f(t) + B_f e(t) & \text{with } e(t) \in I\!R^{n_2} \\ y_f(t) = C_f x_f(t) \quad \text{and} \quad x_f(0) = 0 & \text{with } y_f(t) \in I\!R^{n_2} \end{cases}$$

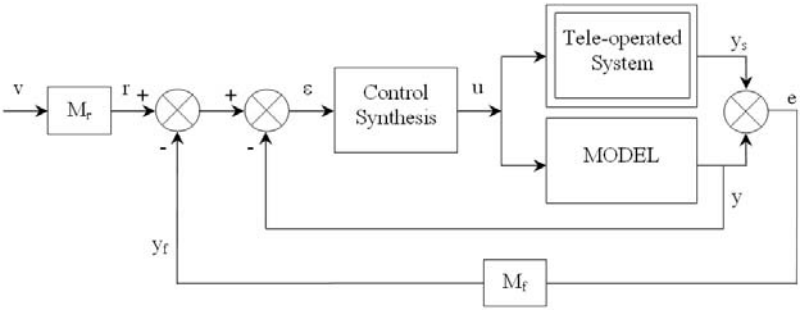

Fig. 3. Internal Model Boundary Control Structure

A multivariable integral feedback control is proposed for the control law:

$$\begin{aligned} u(t) &= \alpha \mathrm{K}_I \int \varepsilon(s)\mathrm{d}s \\ &= \alpha \mathrm{K}_I \zeta \end{aligned} \tag{10}$$

with $\dot{\zeta} = \varepsilon$ and with α a real positive tuning constant and K_I a tuning matrix from $\mathbb{R}^{n_2}$ to $\mathbb{R}^{n_2}$.

As it is seen in figure Fig. 3: $\varepsilon = r(t) - y_f(t) + y(t)$ where $r(t)$ and $e(t)$ are supposed non persistant.

Let $x = (x_\tau \ x_e \ x_i)^T$, $\tilde{x} = (\varphi_\tau \ x_e \ \varphi_i)^T$ and the following bounded operators:

$$\tilde{\mathcal{D}} = \begin{pmatrix} 0 & 0 & 0 \\ 0 & 0 & 0 \\ 0 & D_i C_e & 0 \end{pmatrix} \qquad \tilde{D}_\tau = \begin{pmatrix} D_\tau \\ 0 \\ 0 \end{pmatrix}$$

then

$$x = \tilde{x} + \tilde{D}_\tau u + \tilde{\mathcal{D}} x \tag{11}$$

Considering the following extended state space $X_a(t) = (x_r \ x_f \ \tilde{x} \ \zeta)^T$, and using relations (5)(10)(11), the IMBC closed loop system can be written as:

$$\dot{X}_a(t) = \mathcal{A}(\alpha) X_a(t) + \mathcal{B} \begin{pmatrix} v(t) \\ e(t) \end{pmatrix} \quad t > 0 \tag{12}$$

with $\mathcal{B} = \begin{pmatrix} B_r & 0 \\ 0 & B_f \\ 0 & 0 \\ 0 & 0 \end{pmatrix}$ and

$$\mathcal{A}(\alpha) = \mathcal{A} + \alpha \mathcal{A}^{(1)} + \alpha^2 \mathcal{A}^{(2)}$$

where

$$\mathcal{A} = \begin{pmatrix} \overbrace{\begin{pmatrix} A_r & 0 & 0 \\ 0 & A_f & 0 \\ 0 & 0 & \tilde{A} \end{pmatrix}}^{\bar{A}} & \begin{matrix} 0 \\ 0 \\ 0 \end{matrix} \\ \begin{matrix} C_r & -C_f & -C(I-\tilde{\mathcal{D}})^{-1} \end{matrix} & 0 \end{pmatrix}$$

$$\mathcal{A}^{(1)} = \begin{pmatrix} 0 & 0 & 0 & 0 \\ 0 & 0 & 0 & 0 \\ -\tilde{D}_\tau K_I C_r & \tilde{D}_\tau K_I C_f & \tilde{D}_\tau K_I C(I-\tilde{\mathcal{D}})^{-1} & \mathcal{B}K_I \\ 0 & 0 & 0 & -C(I-\tilde{\mathcal{D}})^{-1}\tilde{D}_\tau K_I \end{pmatrix}$$

$$\mathcal{A}^{(2)} = \begin{pmatrix} 0 & 0 & 0 & 0 \\ 0 & 0 & 0 & 0 \\ 0 & 0 & 0 & \tilde{D}_\tau K_I C(I-\tilde{\mathcal{D}})^{-1}\tilde{D}_\tau K_I \\ 0 & 0 & 0 & 0 \end{pmatrix}$$

Operators $\mathcal{A}^{(1)}$ and $\mathcal{A}^{(2)}$ are bounded. This follows from the definition of the operators they are composed of.

Now $\alpha\mathcal{A}^{(1)} + \alpha^2\mathcal{A}^{(2)}$ can be interpreted as an additive bounded perturbation of $\mathcal{A}$ and the already framework in [3][4][6][9] can be used:

- For every finite α in the formula

$$\mathcal{A}(\alpha) = \mathcal{A} + \alpha\mathcal{A}^{(1)} + \alpha^2\mathcal{A}^{(2)} \tag{13}$$

  the operator $\mathcal{A}(\alpha)$ generates a semigroup of the same class as $\mathcal{A}$.
- The spectrum of $\mathcal{A}(\alpha)$ is a perturbation of the spectrum of $\mathcal{A}$: by construction, the spectrum of $\mathcal{A}$ is $\sigma(\mathcal{A}) = \sigma(\bar{A}) \cup \{0\}$, where $\sigma(\bar{A}) \subset C^-$, because $\bar{A}$ generates an exponentially stable semigroup (open loop system). As a consequence, the eigenvalue 0 can be separated from the remainder $\sigma(\bar{A})$ of the spectrum by a vertical straight line:

$$\exists \sigma_e \in I\!R^- \text{ s.th. } \forall \lambda \in \sigma(\bar{A}), \Re(\lambda) < \sigma_e.$$

  In the context of perturbation theory, as established by Kato in the seventies [5], $\mathcal{A}$ is said to share the spectrum decomposition property, which means that a closed curve Γ in the complex plane can be used to separate the spectrum into two parts.
  As the operator $\mathcal{A}(\alpha)$ depends on the parameter α (according to (13)), there exists a value of α such that this property is no longer given [3][6]:

$$\alpha < \alpha_{\max} = \min_{\gamma \in \Gamma} \left(a \|(\gamma I - \mathcal{A})^{-1}\|_X + 1 \right)^{-1}$$

  where $a = \max\left(\mathcal{A}^{(1)}, \mathcal{A}^{(2)}\right)$. The point 0 being isolated in the interior of the curve Γ, it should be moved to the left without leaving Γ. In case the

spectrum separation property is given, this can be achieved if the system (with p inputs and p_2 outputs) satisfies the controllability condition [1]

$$\text{Rank } (C(I - \tilde{\mathcal{D}})^{-1}\tilde{D}_\tau) = p_2$$

Then it is sufficient to choose the matrix K_I in such a way that

$$\Re(\sigma(-C(I - \tilde{\mathcal{D}})^{-1}\tilde{D}_\tau K_I)) < 0$$

for all $\alpha < \alpha_{\max}$.

5 Conclusion

The main objective of this contribution is to show that the infinite dimensional description and study of the delay parts in tele-operated system can be suitable by using semigroup and spectrum perturbation theory. No approximation is made and an already control structure like internal model control, extended in a Hilbert space, is used without major technical difficulties. The open loop characterization which is the key in this approach, seems to be simpler than the same study performed with others parabolic or hyperbolic boundary control systems.

References

1. Pohjolainen, S.A. (1982) Robust Multivariable PI-Controller for Infinite Dimensional Systems. IEEE Trans. Automat. Control 27:17–30
2. Pohjolainen, S.A. (1985) Robust Controller for Systems with Exponentially Stable Strongly Continuous Semigroups. J. of Math. Anal. and Appl. 111:622–636.
3. Touré Y., & Josserand L. (1997) An Extension of IMC to Boundary Control of Distributed Parameter Systems. Proc. of the *IEEE SMC-CCS*, 3, pp. 2426–2431, Orlando, Forida
4. Touré Y., & Rudolph J. (2002) Controller Design for Distributed Parameter Systems. Encyclopedia of LIFE Support on Control Systems, Robotics and Automation, I, 933–979, Eolss Publishers, Oxford
5. Kato T. (1976) Perturbation Theory for Linear Operators. Springer Verlag, Berlin.
6. Josserand L., Touré, Y. (1996) PI-controller in IMC Structure for Distributed Parameter Systems. In Proc. of the CESA IMACS/IEEE-SMC Multiconference, pp. 1168–1172, Lille, France
7. Josserand L. (1996) Commande Frontière par Modèle Interne de Systèmes à Paramètres Distribués. Application à un double Echangeur de Chaleur. PhD Thesis, University Claude Bernard Lyon 1
8. Dos Santos V., Touré Y. (2003) On the Regulation of Irrigation Canals: Internal Model and Boundary Control Approach. Second International Conference on Signals, Decision and Information Technology (SSD'03), IEEE, n° SSD-03-A-MD-50, Tunisie
9. Dos Santos V., Touré Y. (2003) Regulation of Irrigation Canals: Multivariable Boundary Control Approach by Internal Model. Second IFAC Conference on Control Systems Design (CSD'03), Pologne

10. Vieyres P., Poisson G., Mérigeaux O., Arbeille P. (2003) The TERESA Project: from space research to ground tele-echography. Industrial Robot: an International Journal 30(1):77–82
11. Fattorini H.O. (1968) Boundary Control Systems. SIAM J. Control and Optimization 6(3):349–385
12. Schumacher J.M. (1983) Finite-dimensional Regulators for a Class of Infinite-dimensional Systems. Systems & Control Letters 3:7–12
13. Ukai H., Iwazumi T. (1985) General Servomechanism Problems for Distributed Parameter Systems. Int. J. of Control 4:1195–1212.
14. Washburn D. (1979) A Bound on the Boundary Input Map for Parabolic Equations with Application to Time Optimal Control. SIAM J. Control and Optimization, 17(5):654-671.
15. Curtain R.F., Zwart H. (1995) An Introduction to Infinite Dimensional Linear Systems Theory. Springer Verlag, Berlin Heidelberg New York

Part III

Emerging Methodologies

From Time Delay to Distributed Parameter Systems in Communications

Hugues Mounier, Véronique Vèque, and Linda Zitoune

Département AXIS
Institut d'Électronique Fondamentale
Bât. 220, Université Paris-Sud
91405 Orsay, France
hugues.mounier@ief.u-psud.fr, veronique.veque@ief.u-psud.fr,
lynda.zitoune@ief.u-psud.fr

Summary. Two applications of time delay systems to the telecommunications area are envisionned under the trajectory tracking angle. Methods form differential flatness and π-freenees are used, allowing a simple and natural solving of the underlying problems.

1 Introduction

We will here describe recent works on the control tracking of delay systems relevant to the communications area.

Our philosophy is guided by two major concerns: the first one (*practical concern*) is to discover structural properties that occur most frequently in practical applications; the second one (*simplicity concern*), related to the previous one, is to obtain the simplest properties for each class of applications.

The practical concern has led us to a new property, called π*-flatness*, which allows the tracking of a reference trajectory in a way which bears some analogy with flat finite dimensional nonlinear systems (*see* [4, 5] and the references therein).

Through the simplicity concern, we discovered a novel class named quasi-finite delay systems, the controllability and stabilization of which is very simple, and quite analogous to the one of systems without delays. Quasi-finite systems are, roughly speaking, systems where the only variable that is delayed is the input. This class seems to encompass nearly all technological examples of linear delay systems. To our knowledge, the only important practical class that does not belong to the quasi-finite one comprises systems modeled by the wave equation without damping [19].

We shall here describe techniques used at two levels : the first one at the physical layer (wave propagation) and the second one at the session layer (TCP transfer). More specifically, we consider the wave equation, useful for propagation purposes (in free space or in media like optical fibers), and a simplified TCP/RED model. These models are shown to be δ-free for the linear wave equation and δ-flat for the non linear TCP models.

J. Chiasson and J.J. Loiseau (Eds.): Appl. of Time Delay Systems, LNCIS 352, pp. 147–156, 2007.
springerlink.com

2 Session Layer: Models

2.1 Original TCP/RED Model

Suppose we are given a source and a destination linked through a TCP[1] session. Consider the heaviest loaded node crossed by the connection, and denote its (supposedly unique) queue length by $Q(t)$.

We take the model for TCP/RED[2] established in [17]:

$$\dot{W}(t) = \frac{1}{R(t)} - \frac{W(t)W(t-R(t))}{2[R(t-R(t))]}\,P(t-R(t)) \tag{1}$$

$$\dot{Q}(t) = \frac{W(t)}{R(t)}\,N(t) - C \tag{2}$$

where the various quantities are

$W(t)$ the length of the TCP window
$R(t)$ the round trip time (RTT[3])
$Q(t)$ the queue length at the heaviest loaded node
$P(t)$ the packet discard function, *taken as control input*
$N(t)$ the number of connections at the bottleneck node, *considered as an external input*
C the average link capacity

and where the round trip time $R(t)$ is related to the queue length through:

$$R(t) = T + \frac{Q(t)}{C}$$

where T is the round trip propagation time. Note that this model has an infinite queue length. In practice, the queue length $Q(t)$ has a maximum Q_M (i.e., if $Q(t) > Q_M$, there is a packet loss of $Q(t) - Q_M$).
The packet discard function chosen for RED is (see [17])

$$p(\theta(t)) = \begin{cases} 0 & \text{for } 0 \leqslant \theta(t) \leqslant \theta_{min} \\ \dfrac{\theta(t) - \theta_{min}}{\theta_{MAX} - \theta_{min}}\,p_{MAX} & \text{for } \theta_{min} \leqslant \theta(t) \leqslant \theta_{MAX} \\ 1 & \text{for } \theta_{MAX} \leqslant \theta(t) \end{cases}$$

where θ_{min}, θ_{MAX} and p_{MAX} are configurable parameters.

Remark 1. In the above formulae, the number of connections $N(t)$ is assumed to be known (an external input). Either it should be measured or a model is needed for it.

[1] Tansfer Control Protocol: the most used transport protocol in the Internet, with acknowledgments and flow control.
[2] Random Early Discard: a protocol that throws away packets to force TCP to retransmit data.

2.2 Simplified TCP/RED Models

Some simplifications have been made on the previous original model. A first possible simplification is to assume the round trip time (RTT) $R(t)$ to be a constant R, supposing the round trip time is dominated by the propagation delay. The "constant RTT model" is then:

$$\dot{W}(t) = \frac{1}{R} - \frac{W(t)W(t-R)}{2R} P(t-R) \tag{3}$$

$$\dot{Q}(t) = \frac{W(t)}{R} N(t) - C \tag{4}$$

Further simplifications consist in neglecting the delay effect in the multiplicatively decreasing part, when the window size is sufficiently large: $W \gg 1$ (see [13]), and supposing the load $N(t)$ constant: N (the number of TCP flows varies only slowly). These simplifications yield the following "simple constant RTT model":

$$\dot{W}(t) = \frac{1}{R} - \frac{(W(t))^2}{2R} P(t-R) \tag{5}$$

$$\dot{Q}(t) = \frac{W(t)}{R} N - C \tag{6}$$

2.3 Flatness Briefly Recalled

Let us briefly recall the meaning of the flatness notion. A nonlinear system is described by a (finite) set of differential equations

$$F_l(\boldsymbol{z}, \ldots, \boldsymbol{z}^{(i)}, \ldots, \boldsymbol{z}^{(\nu_l)}) = 0, \qquad l = 1, \ldots, N.$$

Broadly speaking, the notion of flatness (see [4], [5]) corresponds to the following: a nonlinear system is called *flat* if there exists a collection $\boldsymbol{y} = (y_1, \ldots, y_m)$ (where m is the number of independent inputs in the system) of functions, called a *flat output*, with the following three properties:

1. The components of $\boldsymbol{y}$ can be expressed in terms of the system variables $\boldsymbol{z}$ via differential relations of the type

   $$y_i = P_i(\boldsymbol{z}, \ldots, \boldsymbol{z}^{(\rho_i)})$$

   for $i = 1, \ldots, m$.
2. The components of y are differentially independent, i.e. they are not related by any (non-trivial) differential equation

   $$Q(\boldsymbol{y}, \ldots, \boldsymbol{y}^{(\alpha)}) = 0.$$

3. Every variable z_i used to describe the system, for instance states or inputs, are directly expressed from $\boldsymbol{y}$ using only differentiations. In other words, any such z_i satisfies a relation of the type

   $$z_i = R(\boldsymbol{y}, \ldots, \boldsymbol{y}^{(\gamma)}).$$

The third property yields a simple solution to the problem of tracking the collection of reference trajectories $\boldsymbol{y}_r(t) = (y_{1r}(t), \ldots, y_{m_r}(t))$. The second property ensures that the different components of $\boldsymbol{y}_r(t)$ can be chosen independently.

This notion can thus be defined, for the case of systems with a state $\boldsymbol{x}$ and controls $\boldsymbol{u}$ by

Definition 1. *The system*

$$\dot{\boldsymbol{x}} = f(\boldsymbol{x}, \boldsymbol{u}) \tag{7}$$

with $\boldsymbol{x} \in \mathbb{R}^n$ *and* $\boldsymbol{u} \in \mathbb{R}^m$ *is* differentially flat *if there exists a set of variables, called a* flat output*,*

$$\boldsymbol{y} = h(\boldsymbol{x}, \boldsymbol{u}, \dot{\boldsymbol{u}}, \ldots, \boldsymbol{u}^{(r)}), \qquad \boldsymbol{y} \in \mathbb{R}^m, r \in \mathbb{N} \tag{8}$$

such that

$$\boldsymbol{x} = A(\boldsymbol{y}, \dot{\boldsymbol{y}}, \ldots, \boldsymbol{y}^{(\rho_x)}) \tag{9}$$

$$\boldsymbol{u} = B(\boldsymbol{y}, \dot{\boldsymbol{y}}, \ldots, \boldsymbol{y}^{(\rho_u)}) \tag{10}$$

with q *an integer, and such that the system equations*

$$\frac{dA}{dt}(\boldsymbol{y}, \dot{\boldsymbol{y}}, \ldots, \boldsymbol{y}^{(q+1)}) = f(A(\boldsymbol{y}, \dot{\boldsymbol{y}}, \ldots, \boldsymbol{y}^{(q)}), B(\boldsymbol{y}, \dot{\boldsymbol{y}}, \ldots, \boldsymbol{y}^{(q+1)}))$$

are identically satisfied.

2.4 A Word of Methodology

The preceding notion will be used to obtain so called "open loop" controls, that is control laws which will ensure the tracking of the reference flat outputs when the *model is assumed to be perfect* and *the state initial conditions are assumed to be exactly known*. Since this is never the case in practice, one needs some feedback schemes that will ensure asymptotic convergence to zero of the tracking errors. Our framework can thus be decomposed in two steps :

1. Design of the reference trajectory of the flat outputs; off-line computation of the open loop controls.
2. Inline computation of the complementary closed loop controls in order to stabilize the system around the reference trajectories.

Why is this two step design better suited than a classical stabilization scheme? The first step obtains a first order solution to the tracking problem, while *following the model* instead of forcing it (like in a usual pure stabilization scheme). The second step is a refinement one, and the error between the actual values and the tracked references will be much smaller than in the pure stabilization case.

In some cases of delay systems (i.e. systems governed by differential-difference equations), such as the ones dealt with in the sequel, the flatness property becomes the so-called δ-flatness; the properties remain the same as in (7), (8), and (8) apart that delays and advances may appear.

2.5 Flatness of TCP/RED Models

The models shown for TCP/RED are flat with $Q(t)$ as a flat output. Let us begin with the simplest one, (5)-(6), for the sake of simplicity. Recall its equations:

$$\dot{W}(t) = \frac{1}{R} - \frac{(W(t))^2}{2R} P(t-R)$$
$$\dot{Q}(t) = \frac{W(t)}{R} N - C$$

The last equation (6) yields:

$$W(t) = \frac{R(\dot{Q}(t) + C)}{N}$$

and the first equation (5) gives:

$$P(t-R) = \frac{2R}{(W(t))^2} \left(\frac{1}{R} - \dot{W}(t) \right)$$
$$= \frac{2(1 - R\dot{W}(t))}{(W(t))^2}$$

Then, replacing $W(t)$ with its value:

$$P(t-R) = 2 \left(1 - \frac{R^2 \ddot{Q}(t)}{N} \right) \frac{N^2}{(R\dot{Q}(t) + C)^2}$$
$$= \frac{2N(N - R^2\ddot{Q}(t))}{(R\dot{Q}(t) + C)^2}$$

Thus, when a choice is made for a reference trajectory $Q_r(t)$, the following packet discard function

$$P(t) = \frac{2N(N - R^2\ddot{Q}_r(t+R))}{(R\dot{Q}_r(t+R) + C)^2}$$

ensures the open loop tracking of Q_r. Of course, as mentioned in subsection 2.4, some closed loop scheme must be added to ensure tracking in a practical case.

The model (3)-(4) can be shown to be flat as easily as what has just been done (the calculations are just a little more lengthy); the original model (1)-(2) also satisfies a form of flatness but requires the invertibility of the map $t \mapsto t - T - Q(t)/C$ with respect to composition of functions (see [18]).

3 Physical Layer: Towards Distributed Parameter Systems

3.1 The Wave Equation

Consider [19] the wave equation with a load.

$$\sigma^2 \frac{\partial^2 q}{\partial \tau^2}(\tau, z) = \frac{\partial^2 q}{\partial z^2}(\tau, z) \tag{11}$$
$$\frac{\partial q}{\partial z}(\tau, 0) = -u(\tau),\ \frac{\partial q}{\partial z}(\tau, L) = -J\frac{\partial^2 q}{\partial \tau^2}(\tau, L)$$
$$q(0, z) = q_0(z),\ \frac{\partial q}{\partial \tau}(0, z) = q_1(z)$$

Here $q(\tau, z)$ denotes the displacement from the unexcited position at a point $z \in [0, L]$ at time $\tau \geqslant 0$. L is the length, σ the inverse of the wave propagation speed, J a quantity homogeneous to an inertia, $u(\tau)$ the control and q_0, q_1 describe the initial displacement and velocity, respectively.

3.2 Delay System Model

As well known, the general solution of (11) may be written

$$q(\tau, z) = \phi(\tau + \sigma z) + \psi(\tau - \sigma z)$$

where ϕ and ψ are one variable functions. The control objective will be to assign a trajectory to the angular position of the mass; the output is thus

$$y(\tau) = q(\tau, L)$$

Set $t = (\sigma/J)\tau$, $v(t) = (2J/\sigma^2)u(t)$ and $T = \sigma L$. Easy calculations (*see* [19] for details) yield the following delay system :

$$\dddot{y}(t) + \ddot{y}(t - 2T) + \dot{y}(t) - \dot{y}(t - 2T) = v(t - T) \tag{12}$$

3.3 Controllability for Tracking: δ-Freeness

The following notion, which in a sense generalizes the existence of a controller canonical form of finite dimensional systems, is especially useful for tracking purposes.

Consider a linear time invariant delay system modelled as

$$E_0(\delta)\boldsymbol{w} + E_1(\delta)\dot{\boldsymbol{w}} + \cdots + E_\sigma(\delta)\boldsymbol{w}^{(\sigma)} = 0 \tag{13}$$

with $\boldsymbol{w} = (w_1, \ldots, w_\gamma)$, $E_i \in (\mathbb{R}[\delta])^{\beta \times \gamma}$. This system, written $E(d/dt, \delta)w = 0$ for short (with $E(d/dt, \delta) = \sum_i E_i(\delta)d^i/dt^i$) is called *$\delta$-free* if there exists a $\boldsymbol{\omega} = (\omega_1, \ldots, \omega_m)$, called a *$\delta$-basis* of the system, with the following properties:

1. It is possible to express $\boldsymbol{\omega}$ as a linear combination of the system variables $\boldsymbol{w}$ and their derivatives:

$$\omega = N_0(\delta)\boldsymbol{w} + N_1(\delta)\dot{\boldsymbol{w}} + \cdots + N_\alpha(\delta)\boldsymbol{w}^{(\alpha)}$$

$N_i(\delta) \in \mathbb{R}[\delta]^{m \times \gamma}$, $i = 0, \ldots, \alpha$.

2. There does not exist any differential relation between the components of ω:

$$M_0(\delta)\boldsymbol{\omega} + M_1(\delta)\dot{\boldsymbol{\omega}} + \cdots + M_\mu(\delta)\boldsymbol{\omega}^{(\mu)} = 0 \quad \Longrightarrow \quad M_i(\delta) = 0$$

with $M_i(\delta) \in \mathbb{R}[\delta]^{q\times m}$, $i = 0, \ldots, \mu$.

3. through The system variables $\boldsymbol{w}$ can be calculated from ω using differentiation, delays and the inverse of delays, called *advances*:

$$\boldsymbol{w} = P_0(\delta, \delta^{-1})\boldsymbol{\omega} + P_1(\delta, \delta^{-1})\dot{\boldsymbol{\omega}} + \cdots + P_\nu(\delta, \delta^{-1})\boldsymbol{\omega}^{(\nu)} \tag{14}$$

with $P_i(\delta, \delta^{-1}) \in \mathbb{R}[\delta, \delta^{-1}]^{\gamma\times m}$, $i = 0, \ldots, \nu$.

The δ-freeness simplifies open-loop tracking of a reference trajectory $\boldsymbol{\omega}_{\mathrm{r}}(t)$ of $\boldsymbol{\omega}(t)$. For, an equation of the type (14) also exists for the input $\boldsymbol{u}$. With this, the open loop control $\boldsymbol{u}_{\mathrm{r}}$ applied to track the reference $\boldsymbol{\omega}_{\mathrm{r}}(t)$ is

$$\boldsymbol{u}_{\mathrm{r}} = Q_0(\delta, \delta^{-1})\boldsymbol{\omega}_{\mathrm{r}} + Q_1(\delta, \delta^{-1})\dot{\boldsymbol{\omega}}_{\mathrm{r}} + \cdots + Q_\nu(\delta, \delta^{-1})\boldsymbol{\omega}_{\mathrm{r}}^{(\kappa)} \tag{15}$$

Notice that the use of advances in (15) is not an impediment since the reference $\boldsymbol{\omega}_{\mathrm{r}}(t)$ can be planned in advance.

Proposition 1. *The system* (13) *is δ-free if and only if*

$$\forall s \in \mathbb{C}, \forall z \in \mathbb{C}\backslash\{0\} : \ rk_{\mathbb{C}}\, E(s, z) = n \tag{16}$$

The following implications hold true:

$$\delta\text{-freeness} \Longrightarrow \text{spectral controllability} \Longrightarrow \text{weak controllability.}$$

Example 1. The system $\dot{x}(t) = u(t-1)$ is a δ-free system, x is a δ-basis. The system $\dot{x}(t) = u(t) + u(t-1)$ is spectrally controllable but not δ-free.

It seems that δ-free systems are quite frequently encountered in practice. The concept is useful for tracking, and stabilization may be achieved using distributed delays.

3.4 Tracking

One readily has

$$v = (\delta^{-1} + \delta)\ddot{y} + (\delta^{-1} - \delta)\dot{y} \tag{17}$$

which implies

Proposition 2. *System* (12) *is δ-free, with basis y.*

Equation (17), yields the open loop control

$$v_d(t) = \ddot{y}_d(t+T) + \ddot{y}_d(t-T) + \dot{y}_d(t+T) - \dot{y}_d(t-T)$$

The displacements of the other points of the rod can be obtained as (*see* [19])

$$q_d(z,t) = \frac{1}{2}\Big[y_d(t-z+T) + \dot{y}_d(t-z+T) + y_d(t-T+z) - \dot{y}_d(t-T+z)\Big]$$

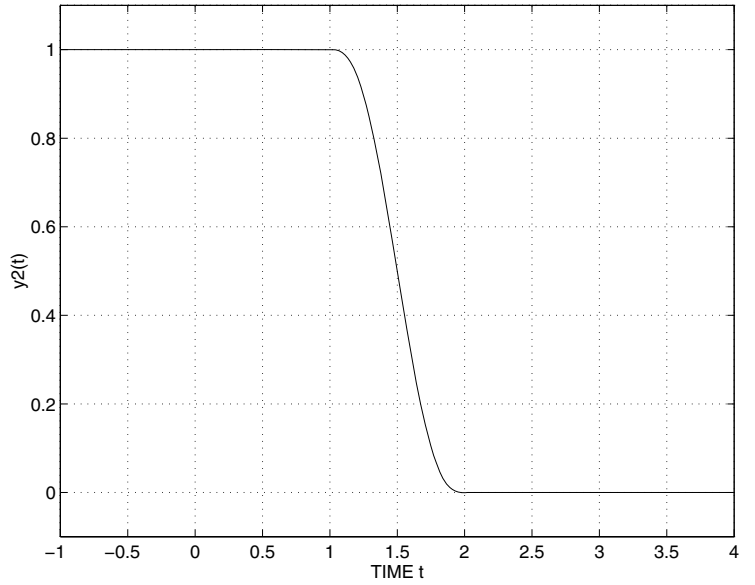

Fig. 1. Reference trajectory $y_r(t)$

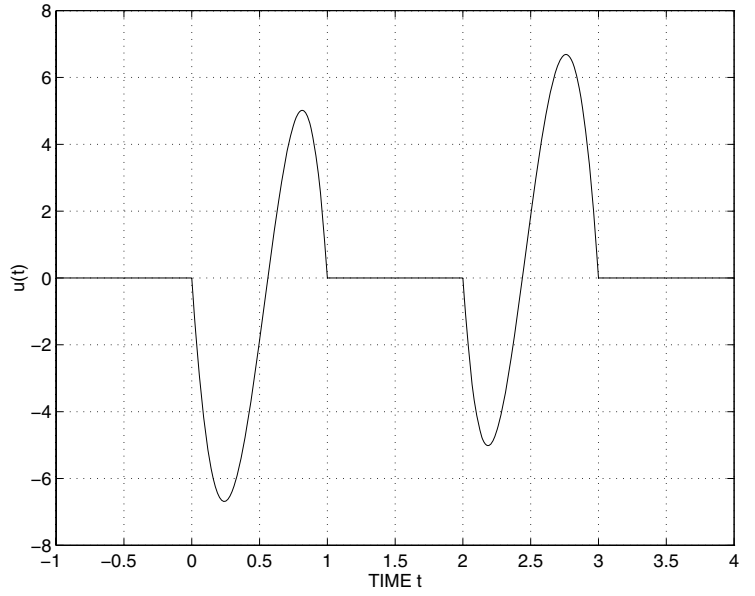

Fig. 2. Open loop control $u_r(t)$

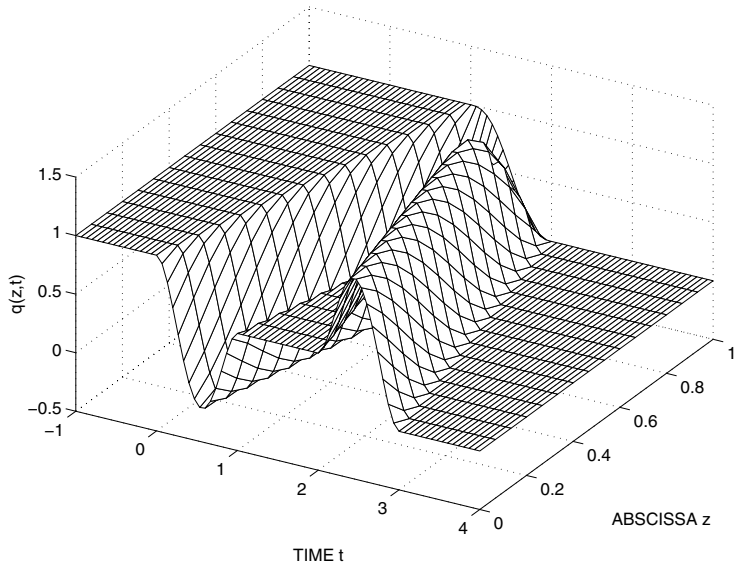

Fig. 3. Other points $q_r(z,t)$

4 Conclusion

We have presented techniques using differential flatness and π-freeness for two types of systems relevant in the domain of telecommunications. The first session layer class models are additive increase/multiplicative decrease ones, typical of the transfer control protocol (TCP) in the Internet. The physical layer model, although very simple, is yet symptomatic of how to deal with propagative phenomena.

The same underlying philosophy serves the linear and infinite dimensional non linear models, namely deriving first open loop control using the above mentionned structural properties, and second stabilize around the previously derived reference trajectories.

The advocated techniques can be useful in the session layer case for pricing operations in typical scenarii an Internet provider can have. For the physical layer model, similar techniques have been used in [6] for distortion attenuation and pre compensation on a telegraph equations model.

References

1. Altman E., Başar T., Srikant R. (1999) Congestion control as a stochastic control problem with action delays. Automatica 35:1937–1950
2. Bolot J.-C., Shankar A.U. (1992) Analysis of a fluid approximation to flow control dynamics. In Proc. IEEE INFOCOM'92, pp. 2398–2407, Florence, Italy
3. Chatté F., Ducourthial B., Nace D., Niculescu S.I. (2003) Fluid modelling of packets switched networks: perspectives for congestion control. International J. Systems Science 34:10–11

4. Fliess M., Lévine J., Martin P.,Rouchon P. (1995) Flatness and defect of non-linear systems: introductory theory and applications. International J. Control 61:1327–1361
5. Fliess M., Lévine J., Martin P.,Rouchon P. (1999) A Lie-Bäcklund approach to equivalence and flatness of nonlinear systems. IEEE Transactions on Automatic Control 44:922–937
6. Fliess M., Martin P., Petit N., Rouchon P. (1998) Commande de l'équation des télégraphistes et restauration active d'un signal. Traitement du Signal 15:619–625
7. Fliess M., Marquez R., Mounier H. (2002) An extension of predictive control, PID regulators and Smith predictors to some linear delay systems. International J. Control 75:728–743
8. Fliess M., Mounier H. (1998) Controllability and observability of linear delay systems: an algebraic approach. ESAIM COCV 3:301–314
URL: http://www.emath.fr/Maths/Cocv/cocv.html
9. Fliess M., Mounier H. (1998) Quasi-finite linear delay systems: theory and applications. In Proc. IFAC Workshop Linear Time Delay Systems, pp. 211–215, Grenoble, France
10. Floyd S., Padhye J., Widmer J. (2000) Equation-based congestion control for unicast applications, In Proc. SIGCOMM'00, Stockholm, Sweden
11. Guerin R., Peris V. (1999) Quality of service in packet networks : basic mechanisms and directions. Computer Networks 31:169–189
12. Hollot C.V., Misra V., Gong W.B., Towsley D. (2000) On Designing Improved Controllers for AQM Routers Supporting TCP Flows. In Proc. IEEE Infocom'00, Tel Aviv, Israel
13. Hollot C.V., Misra V., Towsley D., Gong W.B. (2000) C.V. Hollot, V. Misra, D. Towsley, and W.B. Gong, Analysis and design of controllers for aqm routers supporting tcp flows. IEEE Transactions on Automatic Control 47(6):945–959
14. Jacobson V. (1988) Congestion avoidance and control. In Proc. SIGCOMM'88, pp. 314–329, Palo Alto, California
15. Liu B., Figuereido D.R., Guo Y., Kurose J., Towsley D. (2001) A study of networks simulation effciency: fluid simulation vs. packet-level simulation. In Proc. IEEE INFOCOM'01, Anchorage, Alaska
16. Mascolo S. (1999) Congestion control in high-speed communication networks using the Smith principle. Automatica 35:1927–1935
17. Misra V., Gong W.B.,Towsley D. (2000) Fluid-based Analysis of a Network of AQM Routers Supporting TCP Flows with an Application to RED. In Proc. SIGCOMM'00, Stockholm, Sweden
18. Mounier H., Bastin G., Guffens V., Vèque V. (2003) Round trip time tcp tracking: a first step towards QoS pricing. International J. Systems Science 34:607–614
19. Mounier H., Rouchon P., Rudolph J. (1997) Some examples of linear systems with delays. J. Européen de Systèmes Automatisés 31:911–925
20. Mounier H., Rudolph J. (1998) Flatness based control of nonlinear delay systems: Example of a class of chemical reactors. International J. Control 71:871–890
21. Padhye J.D. (2000) Model based approach to TCP-friendly congestion control. PhD thesis, University of Massachusets, Amherst

Computing Maximum Delay Deviation Allowed to Retain Stability in Systems with Two Delays

Keqin Gu[1], Silviu-Iulian Niculescu[2], and Jie Chen[3]

[1] Department of Mechanical and Industrial Engineering, Southern Illinois University at Edwardsville, Edwardsville, Illinois 62026-1805, USA
kgu@siue.edu

[2] Laboratoire des Signaux et Systemes (L2S), CNRS-Supelec, 3, rue Joliot Curie, 91190, Gif-siu-Yvette, France
Silviu.Niculescu@lss.supelec.fr

[3] Department of Electrical Engineering, University of California, Riverside, CA 92521, USA
jchen@ee.ucr.edu

Summary. This chapter discusses the calculation of maximum delay deviation without losing stability for systems with two delays. This work is based on our previous work on the properties of the stability crossing curves in the delay parameter space. Based on the results, an algorithm to calculate the maximum radius of delay deviation without changing the number of right hand zeros of the characteristic quasipolynomial can be devised. If the nominal system is stable, then the system remains stable when the delays do not deviate more than this radius.

1 Introduction

Time delays exist in many practical systems in biology, ecology, chemistry, physics, and numerous engineering disciplines. It has naturally attracted substantial attention in the scientific community. Indeed, time-delay systems have been the topic of many books in the last few decades, see, for example, [1][3][5][6][9][10][11].

A common misconception about time-delay systems is that the increase of delay makes the system less stable. As demonstrated by Cooke and Grossman [2] through a number of simple systems, for an arbitrary integer N, it is possible to construct a system such that it switches from being stable to unstable and back to stable at least N times as delay increases. It is also well-known in industrial practice that the value of delay is rather difficult to identify. It is, therefore, of interest to consider the maximum deviation of delays allowed that do not destabilize a nominally stable system.

Consider a system with two delays described by the equation

$$\sum_{l=0}^{2}\sum_{k=0}^{n} p_{lk}\frac{d^k x(t-\tau_l)}{dt^k} = 0, \tag{1}$$

where the coefficients p_{lk}, $l = 0, 1, 2$; $k = 0, 1, 2, ..., n$ are real, and $\tau_0 = 0$. The stability of such a system is completely determined by the zeros of its characteristic quasipolynomial

J. Chiasson and J.J. Loiseau (Eds.): Appl. of Time Delay Systems, LNCIS 352, pp. 157–164, 2007.
springerlink.com

$$p_{\tau_1,\tau_2}(s) = p_0(s) + p_1(s)e^{-\tau_1 s} + p_2(s)e^{-\tau_2 s}, \tag{2}$$

where

$$p_l(s) = \sum_{k=0}^{n} p_{lk} s^k.$$

If all the coefficients p_{lk} are known, [7] provided a procedure to describe the regions in the delay parameter (τ_1, τ_2) space such that the system is stable. A number of other results are also available to determine the stability regions for some special classes of such systems [8][12][13].

In this chapter, we consider the problem of robust stability under delay deviation of the above system. Specifically, if it is already known that the nominal system with the characteristic quasipolynomial (2) with $(\tau_1, \tau_2) = (\tau_{10}, \tau_{20})$ is stable, we want to find the maximum deviation d such that the system is stable for any (τ_1, τ_2) satisfying

$$\begin{aligned} \tau_1 &\geq 0 \\ \tau_2 &\geq 0 \\ \sqrt{(\tau_1 - \tau_{10})^2 + (\tau_2 - \tau_{20})^2} &< d \end{aligned}$$

In other words, the system is stable as long as the delays (τ_1, τ_2) stay within the intersection of the first quadrant and the disk with the center at (τ_{10}, τ_{20}) and the radius d.

2 Preliminary

Our notation is rather standard. $\mathbb{R}$ denotes the set of real numbers, and $\mathbb{R}_+$ denotes the set of nonnegative real numbers. $\mathbb{R}^n$ and $\mathbb{R}^n_+$ are the sets of n-dimensional vectors with components in $\mathbb{R}$ and $\mathbb{R}_+$, respectively.

Our analysis is based on the results of our previous article [7]. In this section, we will review some basic concepts relevant to the discussions in this article.

2.1 Stability Crossing Curves

Let $\mathcal{T}$ denote the set of (τ_1, τ_2) in $\mathbb{R}^2_+$ such that $p_{\tau_1,\tau_2}(s)$ has at least one zero on the imaginary axis. Any $(\tau_1, \tau_2) \in \mathcal{T}$ is known as a *crossing point*. The set $\mathcal{T}$, which is the collection of all the crossing points, is known as the *stability crossing curves*. Correspondingly, let Ω denote the *crossing set*, which is defined as the set of all $\omega > 0$ such that there exists a pair $(\tau_1, \tau_2) \in \mathbb{R}^2_+$ to satisfy

$$p_{\tau_1,\tau_2}(j\omega) = p_0(j\omega) + p_1(j\omega)e^{-j\omega\tau_1} + p_2(j\omega)e^{-j\omega\tau_2} = 0. \tag{3}$$

We will also restrict ourselves to systems that satisfy the following assumptions.

I. Existence of principal term:

$$\deg(p_0(s)) \geq \max\{\deg(p_1(s)), \deg(p_2(s))\}. \tag{4}$$

II. Zero frequency

$$p_0(0) + p_1(0) + p_2(0) \neq 0. \tag{5}$$

III. The polynomials $p_0(s)$, $p_1(s)$ and $p_2(s)$ do not have any common zero.

IV. Restriction on difference operator:

$$\lim_{s\to\infty} (|p_1(s)/p_0(s)| + |p_2(s)/p_0(s)|) < 1. \tag{6}$$

V. Nondegeneracy

$$p_l(j\omega) \neq 0 \text{ for all } \omega \in \Omega \text{ and } l = 0, 1, 2. \tag{7}$$

Assumptions I to IV are made mainly to avoid trivial cases. Assumption V is made to simplify the presentation, and an extension to the case without this assumption is straightforward. Under these assumptions, Ω consists of a finite number of intervals of finite length,

$$\Omega = \bigcup_{k=1}^{N} \Omega_k.$$

Here, we order these intervals of finite length Ω_k from left to right as k increases.

We will write (3) as

$$a(s, \tau_1, \tau_2) = 1 + a_1(s)e^{-\tau_1 s} + a_2(s)e^{-\tau_2 s} = 0, \tag{8}$$

where

$$a_l(s) = p_l(s)/p_0(s),\ l = 1, 2.$$

Obviously $a(j\omega, \tau_1, \tau_2) = 0$ if and only if $p_{\tau_1,\tau_2}(j\omega) = 0$.

Taken as vectors in the complex plane, the three terms 1, $a_1(s)e^{-\tau_1 s}$ and $a_2(s)e^{-\tau_2 s}$ need to form a triangle in order for (8) to hold. It follows that, for any $\omega > 0$, $\omega \in \Omega$ if and only if it satisfies the following constraints,

$$|a_1(j\omega)| + |a_2(j\omega)| \geq 1, \tag{9}$$

$$-1 \leq |a_1(j\omega)| - |a_2(j\omega)| \leq 1. \tag{10}$$

The corresponding points in $\mathcal{T}$ can be calculated as follows,

$$\tau_1 = \tau_1^{u\pm}(\omega) = \frac{\angle a_1(j\omega) + (2u-1)\pi \pm \theta_1}{\omega} \geq 0, \tag{11}$$

$$u = u_0^{\pm}, u_0^{\pm} + 1, u_0^{\pm} + 2, ...,$$

$$\tau_2 = \tau_2^{v\pm}(\omega) = \frac{\angle a_2(j\omega) + (2v-1)\pi \mp \theta_2}{\omega} \geq 0, \tag{12}$$

$$v = v_0^{\pm}, v_0^{\pm} + 1, v_0^{\pm} + 2, ...,$$

where $\theta_1, \theta_2 \in [0, \pi]$ can be calculated as

$$\theta_1 = \cos^{-1}\left(\frac{1 + |a_1(j\omega)|^2 - |a_2(j\omega)|^2}{2|a_1(j\omega)|}\right), \tag{13}$$

$$\theta_2 = \cos^{-1}\left(\frac{1 + |a_2(j\omega)|^2 - |a_1(j\omega)|^2}{2|a_2(j\omega)|}\right). \tag{14}$$

Let

$$\mathcal{T}_{u,v}^{\pm k} = \{(\tau_1^{u\pm}(\omega), \tau_2^{v\pm}(\omega)) \mid \omega \in \Omega_k\},$$

and make $\angle a_1(j\omega)$ and $\angle a_2(j\omega)$ continuous functions of ω within each Ω_k (which is always possible under our standing assumptions), then for each fixed k, u and v, $\mathcal{T}_{u,v}^{+k}$ and $\mathcal{T}_{u,v}^{-k}$ are continuous curves. We further denote

$$\mathcal{T}^k = \bigcup_{u=-\infty}^{\infty} \bigcup_{v=-\infty}^{\infty} \left(\mathcal{T}_{u,v}^{+k} \cup \mathcal{T}_{u,v}^{-k}\right) \cap \mathbb{R}_+^2.$$

Then,

$$\mathcal{T} = \bigcup_{k=1}^{N} \mathcal{T}^k.$$

2.2 Types of Crossing Set and the Shapes of Stability Crossing Curves

Let the left end of interval Ω_k be ω_k^l, and the right end be ω_k^r. With Assumptions I to V, $\Omega_k = [\omega_k^l, \omega_k^r]$ if $\omega_k^l \neq 0$ (which is always valid for $k > 1$), and $\Omega_1 = (0, \omega_k^r]$ if $\omega = 0^+$ satisfies (9) and (10). Obviously, $\omega_k^l \neq 0$ or ω_k^r must satisfy one and only one of the following three equations,

$$|a_1(j\omega)| - |a_2(j\omega)| = 1, \tag{15}$$

$$|a_2(j\omega)| - |a_1(j\omega)| = 1, \tag{16}$$

$$|a_1(j\omega)| + |a_2(j\omega)| = 1. \tag{17}$$

Accordingly, we classify all the end points of Ω_k, ω_k^l or ω_k^r, into four categories: an end point satisfying (15), (16) and (17) is known as of type 1, 2, and 3, respectively. $\omega_1^l = 0$ is known as of type 0. An interval Ω_k is known as of type lr if the corresponding ω_k^l is of type l and ω_k^r is of type r.

The shape of $\mathcal{T}^k$ is intimately related to the type of Ω_k. If Ω_k is of type 11, 22 or 33, then $\mathcal{T}^k$ is a series of closed curves. If Ω_k is of type 12 or 21, then $\mathcal{T}^k$ is a series of spiral-like curves with axes oriented diagonally. If Ω_k is of type 13 or 31, then $\mathcal{T}^k$ is a series of spiral-like curves with axes oriented vertically. Corresponding to Ω_k of type 12 or 21, $\mathcal{T}^k$ is a series of spiral-like curves with axes oriented horizontally. An Ω_k of type 01, 02 or 03 corresponds to a $\mathcal{T}^k$ in the shape of a series of open-ended curves.

2.3 Tangent and Smoothness

The tangenet of $\mathcal{T}^k$ can be expressed as

$$\frac{d\tau_2}{d\tau_1} = \frac{I_0 R_1 - R_0 I_1}{R_0 I_2 - I_0 R_2}, \tag{18}$$

where

$$\begin{aligned} R_0 = \frac{1}{\omega} \operatorname{Re}([a_1'(j\omega) - \tau_1 a_1(j\omega)]\, e^{-j\tau_1\omega} \\ +[a_2'(j\omega) - \tau_2 a_2(j\omega)]e^{-j\tau_2\omega}), \end{aligned} \tag{19}$$

$$\begin{aligned} I_0 = \frac{1}{\omega} \operatorname{Im}([a_1'(j\omega) - \tau_1 a_1(j\omega)]\, e^{-j\tau_1\omega} \\ +[a_2'(j\omega) - \tau_2 a_2(j\omega)]e^{-j\tau_2\omega}), \end{aligned} \tag{20}$$

and

$$R_l = \operatorname{Re}\left(a_k(j\omega)e^{-j\tau_k\omega}\right), \tag{21}$$

$$I_l = \operatorname{Im}\left(a_k(j\omega)e^{-j\tau_k\omega}\right), \tag{22}$$

for $l = 1, 2$. Furthermore, the curve is smooth everywhere except the points corresponding to the following degenerate cases:

Case 1. $s = j\omega$ is a multiple solution of $a(s) = 0$.
Case 2. ω is a type 3 end point of Ω_k, and $\frac{d}{d\omega}\left(|a_1(j\omega)| + |a_2(j\omega)|\right) = 0$.
Case 3. ω is a type 1 or type 2 end point of Ω_k, and $\frac{d}{d\omega}\left(|a_1(j\omega)| - |a_2(j\omega)|\right) = 0$.

Especially, $\mathcal{T}^k$ is generally smooth at $\omega = \omega_k^l$ and ω_k^r even though the parameterization of $\mathcal{T}^k$ in terms of ω reverses direction.

3 Maximum Delay Deviation Problem

3.1 Problem Setup

We now consider the main problem of the article. Given the nominal delay τ_{10}, τ_{20}, such that the system with the characteristic quasipolynomial

$$p_{\tau_{10},\tau_{20}}(s) = p_0(s) + p_1(s)e^{-\tau_{10}s} + p_2(s)e^{-\tau_{20}s}$$

is stable, find the maximum deviation d such that for any

$$\tau_1 \geq 0, \tau_2 \geq 0,$$

the system with the characteristic quasipolynomial

$$p_{\tau_1,\tau_2}(s) = p_0(s) + p_1(s)e^{-\tau_1 s} + p_2(s)e^{-\tau_2 s}$$

is stable as long as

$$\sqrt{(\tau_1 - \tau_{10})^2 + (\tau_2 - \tau_{20})^2} < d.$$

The special case of $\tau_{10} = \tau_{20} = 0$ has the interpretation of the minimum delay to destabilize a stable nominal system without delay.

An equivalent statement of the problem is to find the minimum distance between (τ_{10}, τ_{20}) and $\mathcal{T}$. Since

$$\mathcal{T} = \bigcup_{k=1}^{N} \bigcup_{u=-\infty}^{\infty} \bigcup_{v=-\infty}^{\infty} \left(\mathcal{T}_{u,v}^{+k} \cup \mathcal{T}_{u,v}^{-k}\right) \cap \mathbb{R}_+^2,$$

we have

$$d = \min\{d_{u,v}^{+k}, d_{u,v}^{-k} \mid u, v \text{ integers}, k \text{ positive integers}\},$$

where

$$d_{u,v}^{\pm k} = \min\left\{ \sqrt{(\tau_1 - \tau_{10})^2 + (\tau_2 - \tau_{20})^2} \,\middle|\, (\tau_1, \tau_2) \in \left(\mathcal{T}_{u,v}^{\pm k} \cap \mathbb{R}_+^2\right) \right\}.$$

3.2 Calculating $d_{u,v}^{\pm k}$

If $\mathcal{T}_{u,v}^{\pm k}$ is smooth, then the minimum distance between (τ_{10}, τ_{20}) and $\mathcal{T}_{u,v}^{\pm k} \cap \mathbb{R}_+^2$ can only be reached at one of the following points:

i) The point (τ_1, τ_2) in $\mathcal{T}_{u,v}^{\pm k} \cap \mathbb{R}_+^2$ where the tangent of $\mathcal{T}_{u,v}^{\pm k}$ is perpendicular to the vector $(\tau_1 - \tau_{10}, \tau_2 - \tau_{20})$;
ii) The intersection of $\mathcal{T}_{u,v}^{\pm k}$ with τ_1-axis;
iii) The intersection of $\mathcal{T}_{u,v}^{\pm k}$ with τ_2-axis;
iv) The point (τ_1, τ_2) in $\mathcal{T}_{u,v}^{\pm k}$ corresponding to ω_k^l or ω_k^r.

The points in items ii) to iv) are independent of (τ_{10}, τ_{20}) and can be easily found. The crucial step in finding $d_{u,v}^{\pm k}$, therefore, is to identify points in item i). With the expression of the tangent in (18), it is easily seen that such points must satisfy

$$f(\omega) = (\tau_1 - \tau_{10})(R_0 I_2 - R_2 I_0) + (\tau_2 - \tau_{20})(R_0 I_1 - R_1 I_0) = 0, \qquad (23)$$

and

$$\tau_1 \geq 0, \tau_2 \geq 0.$$

Therefore, in order to find points in case i) above, one only needs to sweep ω through the interval Ω_k to identify the points corresponding to a change of sign of $f(\omega)$. A rather coarse gridding is sufficient in the first sweep. A refined gridding can be introduced near the points where f changes sign.

It should be pointed out that the three degenerate cases discussed at the end of last section are automatically accommodated in the above procedure. Indeed, for case 1, (23) is satisfied. Case 2 and 3 belong to the item iv) above.

3.3 Bounding the Range of $d_{u,v}^{\pm k}$

While there are an infinite number of $d_{u,v}^{\pm k}$ due to an infinite number of u and v, most of them can be quickly eliminated from consideration. Let

$$\begin{aligned}
\theta_{l\,\max}^{k} &= \max_{\omega\in\Omega_k} \theta_l, \\
\theta_{l\,\min}^{k} &= \min_{\omega\in\Omega_k} \theta_l, \\
\angle a_{l\,\max}^{k} &= \max_{\omega\in\Omega_k} \angle a_l(j\omega), \\
\angle a_{l\,\min}^{k} &= \min_{\omega\in\Omega_k} \angle a_l(j\omega).
\end{aligned}$$

Then, a bound of $\mathcal{T}_{u,v}^{+k}$ can be easily found to be

$$\begin{aligned}
\tau_{1\,\min} &= \frac{\angle a_{1\,\min}^{k} + (2u-1)\pi + \theta_{1\,\min}^{k}}{\omega_k^r}, \\
\tau_{1\,\max} &= \frac{\angle a_{1\,\max}^{k} + (2u-1)\pi + \theta_{1\,\max}^{k}}{\omega_k^l}, \\
\tau_{2\,\min} &= \frac{\angle a_{2\,\min}^{k} + (2v-1)\pi - \theta_{2\,\max}^{k}}{\omega_k^r}, \\
\tau_{2\,\max} &= \frac{\angle a_{2\,\max}^{k} + (2v-1)\pi - \theta_{2\,\min}^{k}}{\omega_k^l},
\end{aligned}$$

and a bound of $\mathcal{T}_{u,v}^{-k}$ can be found to be

$$\begin{aligned}
\tau_{1\,\min} &= \frac{\angle a_{1\,\min}^{k} + (2u-1)\pi - \theta_{1\,\max}^{k}}{\omega_k^r}, \\
\tau_{1\,\max} &= \frac{\angle a_{1\,\max}^{k} + (2u-1)\pi - \theta_{1\,\min}^{k}}{\omega_k^l}, \\
\tau_{2\,\min} &= \frac{\angle a_{2\,\min}^{k} + (2v-1)\pi + \theta_{2\,\min}^{k}}{\omega_k^r}, \\
\tau_{2\,\max} &= \frac{\angle a_{2\,\max}^{k} + (2v-1)\pi + \theta_{2\,\max}^{k}}{\omega_k^l}.
\end{aligned}$$

With these bound, we can eliminate $\mathcal{T}_{u,v}^{\pm k}$ for some u and v from consideration in searching for d. First, if $\tau_{1\,\max} < 0$ or $\tau_{2\,\max} < 0$, then $\mathcal{T}_{u,v}^{\pm k}$ does not have to be considered in searching for d since it is outside of $\mathbb{R}_+^2$.

Second, if we have already known the distance from (τ_{10}, τ_{20}) to a point (τ_1, τ_2) in $\mathcal{T}$ is d_0, then, obviously, $d \le d_0$. In this case, for certain $\mathcal{T}_{u_0,v_0}^{+k}$, if $\tau_{1\,\min} \ge \tau_{10} + d_0$, then $\mathcal{T}_{u,v}^{+k}$ for any $u \ge u_0$ can be eliminated from consideration in searching for d. Similarly, if $\tau_{2\,\min} \ge \tau_{20} + d_0$, then $\mathcal{T}_{u,v}^{+k}$ for $v \ge v_0$ can be eliminated from consideration. The same idea applies for $\mathcal{T}_{u,v}^{-k}$.

This process typically allows us to consider only very few u and v in searching for d.

4 Conclusions

For systems with two delays, a method to calculate the maximum deviation of delays without losing stability is developed. The method is based on the properties of stability crossing curves discussed in our previous paper.

References

1. Bellman R. E., Cooke K. L. (1963) Differential-Difference Equations, Academic Press, New York, 1963
2. Cooke K. L., Grossman Z. (1982) Discrete delay, distributed delay and stability switches. J. Mathematical Analysis and Applications 86:592–627
3. Diekmann O., van Gils S. A., Verduyn-Lunel S. M., Walther H. -O. (1995) Delay Equations, Functional-, Complex and Nonlinear Analysis. Appl. Math. Sciences Series 110, Springer-Verlag, Berlin Heidelberg New York
4. El'Sgol'ts L. E., Norkin S. B. (1973) Introduction to the Theory and Application of Differential Equations with Deviating Arguments. Academic Press, New York
5. Górecki H., Fuksa S., Grabowski P., Korytowski A. (1989) Analysis and Synthesis of Time-Delay Systems. Polish Scientific Publishers, Warszawa
6. Gu K., Kharitnov V. L., Chen J. (2003) Stability of Time-Delay Systems, Birkhauser, Boston
7. Gu K., Niculescu S.-I., Chen J. (2005) On stability crossing curves for general systems with two delays, J. Mathematical Analysis and Applications 311:231–253
8. Hale J. K., Huang W. (1993) Global geometry of the stable regions for two delay differential equations. J. Mathematical Analysis and Applications 178:344–362
9. Hale J. K., Verduyn Lunel S. M. (1993) Introduction to Functional Differential Equations. Applied Math. Sciences 99, Springer-Verlag, Berlin Heidelberg New York
10. Kolmanovskii V. B., Nosov V. R. (1986) Stability of Functional Differential Equations. Mathematics. Science and Eng. 180, Academic Press, New York
11. Niculescu S. I., Delay Effects on Stability—A Robust Control Approach. LNCS 269, Springer-Verlag, Berlin Heidelberg New York
12. Stépán G. (1989) Retarded Dynamical Systems: Stability and Characteristic function. Wiley, New York
13. Stépán G. (1998) Delay-differential equation models for machine tool chatter. In: F. C. Moon, Eds., Dynamics and Chaos in Manufacturing Process, pp. 165-192, Wiley, New York

On Exact Controllability of Linear Time Delay Systems of Neutral Type

Rabah Rabah[1] and Grigory Sklyar[2]

[1] Institut de Recherche en Communications et Cybernétique de Nantes, École des Mines de Nantes, 4 rue Alfred Kastler BP 20722 44307 Nantes Cedex 3, France
rabah@emn.fr

[2] Institute of Mathematics, University of Szczecin, Wielkopolska 15, 70451 Szczecin, Poland
sklar@sus.univ.szczecin.pl

Summary. The problem of exact null controllability is considered for linear neutral type systems with distributed delay. A characterization of this problem is given. The minimal time of controllability is precised. The results are based on the analysis of the Riesz basis property of eigenspaces in Hilbert space. Recent results on the moment problem and properties of exponential families are used.

1 Introduction

The problem of controllability for delay systems was considered by several authors in different framework. One approach is based on the analysis of time delay system in a module framework (space over ring, see [8]). In this case the controllability problem is considered in a formal way using different interpretations of the Kalman rank condition. Another approach is based on the analysis of time delay systems in vector spaces with finite or infinite dimension. A powerful tool is to consider a delay system as a system in a Banach functional space, this approach was developed widely in [5]. Because the state space for delay systems is a functional space, the most important notion is the function space controllability. A first important contribution in the characterization of null functional controllability was given by Olbrot [10] by using some finite dimensional tools as (A, B)-invariant subspaces for an extended system. For retarded systems one can refer to [7] (and references therein) for the analysis of function space controllability in abstract Banach spaces. The case of neutral type systems with discrete delay was also considered in such a framework (see O'Connor and Tarn [9] and references therein). A general analysis of the time delay systems in infinite dimensional spaces is given in the book [3] where several methods and references are given.

The problem considered in this paper is close to that studied in [9]. In this work the exact controllability problem was considered for neutral type systems with discrete delay using a semigroup approach in Sobolev spaces $W_2^{(1)}$ and a boundary control problem.

We consider the problem of controllability for distributed delay system of neutral type in the space $M_2(-h, 0; \mathbb{C}^n) = \mathbb{C}^n \times L_2(-h, 0; \mathbb{C}^n)$ which is natural for

J. Chiasson and J.J. Loiseau (Eds.): Appl. of Time Delay Systems, LNCIS 352, pp. 165–171, 2007.
springerlink.com

control problems. The semigroup theory developed here is based on the Hilbert space model introduced in [4]. One of our result is a generalization of the result in [9]. The main non trivial precision is the time of controllability. We generalize the results given [6] for the case of a single input and one localized delay (see also [2, 14]). The approach developed here is different from that of [9]. Our main results are based on the characterization of controllability as a moment problem and using some recent results on the solvability of this problem (see [1] for the main tools used here). Using a precise Riesz basis in the space $M_2(-h,0;\mathbb{C}^n)$ we can give a characterization of null-controllability and of the minimal time of controllability.

The present paper contains only the main idea of the approach and the formulations of the main results on exact controllability. A complete presentation of this approach is the subject of our extensive work which is to be published. One can also find the detailed proofs in the the preprint [11].

2 The Model and the Controllability Problem

We study the following neutral type system

$$\dot{z}(t) = A_{-1}\dot{z}(t-h) + \int_{-h}^{0} A_2(\theta)\dot{z}(t+\theta)\mathrm{d}\theta + \int_{-h}^{0} A_3(\theta)z(t+\theta)\mathrm{d}\theta + Bu, \quad (1)$$

where A_{-1} is constant $n \times n$-matrix, $\det A_{-1} \neq 0$, A_2, A_3 are $n \times n$-matrices whose elements belong to $L_2(-h,0)$, $h > 0$ is a constant delay. We consider the operator model of the neutral type system (1) introduced by Burns and al. in product spaces. The state space is $M_2(-h,0;\mathbb{C}^n) = \mathbb{C}^n \times L_2(-h,0;\mathbb{C}^n)$, shortly M_2, and (1) is rewritten as

$$\frac{\mathrm{d}}{\mathrm{d}t}\begin{pmatrix} y(t) \\ z_t(\cdot) \end{pmatrix} = \mathcal{A}\begin{pmatrix} y(t) \\ z_t(\cdot) \end{pmatrix} + \mathcal{B}u \quad (2)$$

where the operator $\mathcal{A}$ is given by

$$\mathcal{A}\begin{pmatrix} y(t) \\ z_t(\cdot) \end{pmatrix} = \begin{pmatrix} \int_{-h}^{0} A_2(\theta)\dot{z}_t(\theta)\mathrm{d}\theta + \int_{-h}^{0} A_3(\theta)z_t(\theta)\mathrm{d}\theta \\ \mathrm{d}z_t(\theta)/\mathrm{d}\theta \end{pmatrix}$$

with the domain

$$\mathcal{D}(\mathcal{A}) = \left\{(y, z(\cdot)) : z \in H^1(-h,0;\mathbb{C}^n), y = z(0) - A_{-1}z(-h)\right\} \subset M_2.$$

The operator $\mathcal{A}$ is the infinitesimal generator of a C_0-group. The operator $\mathcal{B}$ is defined by $\mathcal{B}u = (Bu, 0)$. The relation between the solutions of the neutral type system (1) and the system (2) is given by the substitutions

$$y(t) = z(t) - A_{-1}z(t-1), \quad z_t(\theta) = z(t+\theta).$$

The reachability set at time T is defined by

$$\mathcal{R}_T = \left\{ \int_0^T e^{\mathcal{A}t}\mathcal{B}u(t)dt : u(\cdot) \in L_2(0,T;\mathbb{C}^n) \right\}$$

It is easy to show that $\mathcal{R}_{T_1} \subset \mathcal{R}_{T_2}$ as $T_1 < T_2$. An important result is that $\mathcal{R}_T \subset \mathcal{D}(\mathcal{A}) \subset M_2$. This non-trivial fact permits to formulate the null-controllability problem in the following setting:

i) To find maximal possible set $\mathcal{R}_T$ (depending on T);

ii) To find minimal T for which the set $\mathcal{R}_T$ becomes maximal possible, i.e. $\mathcal{R}_T = \mathcal{D}(\mathcal{A})$.

Definition 1. *The system (2) is said null-controllable at the time T if $\mathcal{R}_T = \mathcal{D}(\mathcal{A})$*

The main tool is to consider the null-controllability problem as a problem of moments.

2.1 The Moment Problem

In order to formulate the moment problem we need a Riesz basis in the Hilbert space M_2. We recall that a Riesz basis is a basis which may be transformed to an orthogonal basis with respect to another equivalent scalar product. Each Riesz basis possesses a biorthogonal basis. Let $\{\varphi\}$ be a Riesz basis in M_2 and $\{\psi\}$ the corresponding biorthogonal basis. Then for each $x \in M_2$ we have $x = \sum_{\varphi\in\{\varphi\}} \langle x, \psi\rangle\varphi$. In a separable Hilbert space there always exists a Riesz basis.

A state $x = \begin{pmatrix} y \\ z(\cdot) \end{pmatrix} \in M_2$ is reachable at time T by a control $u(\cdot) \in L_2(0,T;\mathbb{C}^r)$ iff the steering condition

$$x = \begin{pmatrix} y \\ z(\cdot) \end{pmatrix} = \int_0^T \mathrm{e}^{\mathcal{A}t}\mathcal{B}u(t)\mathrm{d}t. \tag{3}$$

holds. This steering condition may be expanded using the basis $\{\varphi\}$. A state x is reachable iff

$$\sum_{\varphi\in\{\varphi\}} \langle x, \psi\rangle\varphi = \sum_{\varphi\in\{\varphi\}} \int_0^T \langle \mathrm{e}^{\mathcal{A}t}\mathcal{B}u(t), \psi\rangle \mathrm{d}t\varphi,$$

for some $u(\cdot) \in L_2(-h, 0; \mathbb{R}^r)$. Then the steering condition (3) can be substituted by the following system of equalities

$$\langle x, \psi\rangle = \int_0^T \langle \mathrm{e}^{\mathcal{A}t}\mathcal{B}u(t), \psi\rangle \mathrm{d}t, \quad \psi \in \{\psi\}. \tag{4}$$

Let $\{b_1, \ldots, b_r\}$ be an arbitrary basis in $\mathrm{Im}B$, the image of the matrix B and $\mathbf{b}_i = \begin{pmatrix} b_i \\ 0 \end{pmatrix} \in M_2,\ i = 1, \ldots, r$. Then the right hand side of (4) takes the form

$$\int_0^T \langle \mathrm{e}^{\mathcal{A}t}\mathcal{B}u(t), \psi\rangle \mathrm{d}t = \sum_{i=1}^{r} \int_0^T \langle \mathrm{e}^{\mathcal{A}t}\mathbf{b}_i, \psi\rangle u_i(t)\mathrm{d}t. \tag{5}$$

Effectiveness of the proposed approach becomes obvious if we assume that the operator $\mathcal{A}$ possess a Riesz basis of eigenvector. This situation is characteristic, for example, for control systems of hyperbolic type when $\mathcal{A}$ is skew-adjoint ($\mathcal{A}^* = -\mathcal{A}$) and has a compact resolvent (see, for example, [1], [16], [17]). Let in this case $\{\varphi_k\}$, $k \in \mathbb{N}$, be a orthonormal eigenbasis with $\mathcal{A}\varphi_k = i\lambda_k\varphi_k$, $\lambda_k \in \mathbb{R}$. Assuming for simplicity $r = 1$, $b_1 = b = \sum_k \alpha_k\varphi_k$, $\alpha_k \neq 0$, we have from (4), (5)

$$\frac{x_k}{\alpha_k} = \int_0^T e^{-i\lambda_k t}u(t)dt, \quad k \in \mathbb{N}, \tag{6}$$

where $x = \sum_k x_k\varphi_k$. Equalities (6) are a non-Fourier trigonometric moment problem whose solvability is closely connected with the property for the family of exponentials $e^{-i\lambda_k t}$, $k \in \mathbb{N}$, to form a Riesz basis on the interval $[0, T]$ ([1]). In particular, if $e^{-i\lambda_k t}$ forms a Riesz basis of $L_2[0, T_0]$ then one has

$$\mathcal{R}_T = \left\{ x : \sum_k \left(\frac{x_k}{\alpha_k}\right)^2 < \infty \right\} \quad \text{for all } T \geq T_0. \tag{7}$$

Obviously formula (7) gives the complete answer to the both items of the controllability problem. Returning now to neutral type systems we observe that the operator $\mathcal{A}$ given in (2) is not skew-adjoint and, moreover, does not possess a basis even of generalized eigenvectors. So the choice of a proper Riesz basis in context of formulas (4), (5) is an essentially more complicated problem.

2.2 The Choice of Basis

In order to design the needed basis for our case we use spectral the properties of the operator $\mathcal{A}$ obtained in [13]. Let $\mu_1, \ldots, \mu_\ell$, $\mu_i \neq \mu_j$ be eigenvalues of A_{-1} and let the integers p_m be defined as : $\dim(A_{-1} - \mu_m I)^n = p_m$, $m = 1, \ldots, \ell$. Denote by

$$\lambda_m^{(k)} = \frac{1}{h}\left(\ln|\mu_m| + \mathrm{i}(\arg\mu_m + 2\pi k)\right), \ m = 1, \ldots, \ell; \ k \in \mathbb{Z},$$

and let $L_m^{(k)}$ be the circles of the fixed radius $r \leq r_0 = \frac{1}{3}\min|\lambda_m^{(k)} - \lambda_i^{(j)}|$ centered at $\lambda_m^{(k)}$.

Let $\{V_m^{(k)}\}_{\substack{k \in \mathbb{Z} \\ m = 1, \ldots, \ell}}$ be a family of $\mathcal{A}$-invariant subspaces given by

$$V_m^{(k)} = P_m^{(k)}M_2, \qquad P_m^{(k)} = \frac{1}{2\pi\mathrm{i}}\int_{L_m^{(k)}} R(\mathcal{A}, \lambda)d\lambda.$$

The following theorem plays an essential role in our approach

Theorem 1. *[12] There exists N_0 large enough such that for any $N \geq N_0$*
i) $\dim V_m^{(k)} = p_m$, $k \geq N$,
ii) the family $\{V_m^{(k)}\}_{\substack{|k| \geq N \\ m=1,\dots,\ell}} \cup \widehat{V}_N$ *forms a Riesz basis (of subspaces) in* M_2,
where $\widehat{V}_N$ *is a finite-dimensional subspace (*$\dim \widehat{V}_N = 2(N+1)n$*) spanned by all generalized eigenvectors corresponding to all eigenvalues of* $\mathcal{A}$ *located outside of all circles* $L_m^{(k)}$, $|k| \geq N$, $m = 1, \dots, \ell$.

Using this theorem we construct a Riesz basis $\{\varphi\}$ of the form

$$\left\{\varphi_{m,j}^k, |k| > N; m = 1, \dots, l; j = 1, \dots, p_m\right\} \cup \left\{\hat{\varphi}_j^N, j = 1, \dots, 2(N+1)n\right\}$$

where for any $m = 1, \dots, l$, and $k : |k| > N$ the collection $\{\varphi_{m,j}^k\}_{j=1,\dots,p_m}$ is in a special way chosen basis of $V_m^{(k)}$ and $\{\hat{\varphi}_j^N\}_{j=1,\dots,2(N+1)n}$ is a basis of $\hat{V}_N$. In this basis equalities (4) with regard to (5) turns into a moment problem with respect to a special collection of quasipolynomials. Analyzing the mentioned moment problem by means of the methods given in [1] we obtain our main results concerning the null-controllability problem.

3 The Main Results

The characterization of the null-controllability is given by the following Theorem.

Theorem 2. *The system (2) is null-controllable by controls from* $L_2(0,T)$ *for some* $T > 0$ *iff the following two conditions hold:*
i) $\operatorname{rank}[\Delta_{\mathcal{A}}(\lambda)\ B] = n$, $\forall \lambda \in \mathbb{C}$; *where*

$$\Delta_{\mathcal{A}}(\lambda) = -\lambda I + \lambda \mathrm{e}^{-\lambda h} A_{-1} + \lambda \int_{-h}^{0} \mathrm{e}^{\lambda s} A_2(s) \mathrm{d}s + \int_{-h}^{0} \mathrm{e}^{\lambda s} A_3(s) \mathrm{d}s.$$

ii) $\operatorname{rank}[B\ A_{-1}B \cdots\ A_{-1}^{n-1}B] = n$.

The main results on the time of controllability are as follows.

Theorem 3. *Let the conditions i) and ii) of Theorem 2 hold. Then*

i) The system (2) is null-controllable at the time T as $T > nh$;
ii) If the system (2) is of single control ($r = 1$), then the estimation of the time of controllability in i) is exact, i.e. the system is not controllable at time $T = nh$.

For the multivariable case, the time depends on some controllability indices. suppose that $\dim B = r$. Let $\{b_1, \dots, b_r\}$ be an arbitrary basis noted β. Let us introduce a set integers. We denote by $B_i = \left(b_{i+1}, \dots, b_r\right)$, $i = 0, 1, \dots, r-1$, which gives in particular $B_0 = B$ and $B_{r-1} = \left(b_r\right)$ and we put formally $B_r = 0$. Let us consider the integers

$$n_i^\beta = \operatorname{rank}\left[B_{i-1}\ A_{-1}B_{i-1}\ \cdots\ A_{-1}^{n-1}B_{i-1}\right],\ i = 1, \ldots, r,$$

corresponding to the basis β. We need in fact the integers

$$m_i^\beta = n_{i-1}^\beta - n_i^\beta,$$

Let us denote by

$$m_{\min} = \max_\beta m_1^\beta \qquad m_{\max} = \min_\beta \max_i m_i^\beta,$$

for all possible choice of a basis β.

The main result for the multivariable case is the following Theorem.

Theorem 4. *Let the conditions i) and ii) of the Theorem 2 hold, then*

i) The system (2) is null-controllable at the time $T > m_{\max}h$;
ii) The system (2) is not null-controllable at the time $T < m_{\min}h$.

The proofs are based on the construction of a special Riesz basis of $\mathcal{A}$-invariant subspaces in the space M_2 according to [12] and on the analysis of the properties of some quasi-exponential functions to be a Riesz basis in $L_2(0,T)$ depending of the time T [1].

4 Final Conclusions

For the delayed system of neutral type (1) we have the following results:

i) All the reachable states $z(t), t \in [T-1, T]$ from 0 are elements of $H^1[T-1,T]$ (independently of T).
ii) If $T > m_{\max}h$ then the set of reachable states on $[0,T]$ coincides with $H^1[T-1,T]$.
iii) If $T < m_{\min}h$ then the set of reachable states is an essential subspace of $H^1[T-1,T]$.

If $r = 1$, this gives $m_{\max} = m_{\min} = n$ and then

iv) For $T = n$ the reachable states form a subspace in $H^1[T-1,T]$ of finite codimension; for $T < n$ there exists an **infinite-dimensional** subspace in $H^1[T-1,T]$ of unreachable states.

Acknowledgements. This work was realized with the partial financial support of the French-Polish grant Polonium No 07599VH.

References

1. Avdonin S. A., Ivanov S. A. (1995) Families of exponentials. The method of moments in controllability problems for distributed parameter systems. Cambridge University Press, Cambridge
2. Banks H. T., Jacobs Marc Q., Langenhop C. E. (1975) Characterization of the controlled states in $W_2^{(1)}$ of linear hereditary systems. SIAM J. Control 13

3. Bensoussan A., Da Prato G., Delfour M. C., Mitter S. K. (1992) Representation and control of infinite-dimensional systems. Vol. 1. Systems & Control: Foundations & Applications. Birkhäuser Boston
4. Burns, John A., Herdman, Terry L., Stech, Harlan W. (1983) Linear functional-differential equations as semigroups on product spaces. SIAM J. Math. Anal. 14(1):98–116.
5. Hale J., Verduyn Lunel S. M. (1993) Theory of functional differential equations, Springer-Verlag, Berlin Heidelberg New York
6. Jacobs M. Q., Langenhop C. E. (1976) Criteria for function space controllability of linear neutral systems. SIAM J. Control and Optimization 14(6)1009–1048.
7. Manitius A. and Triggiani R. (1978) Function space controllability of linear retarded systems: A derivation from abstract operator conditions, SIAM J. on Control and Optimization 16:599–645.
8. Morse A. S. (1976) Ring models for delay differential equation. Automatica 12:529-531
9. O'Connor D. A., Tarn T. J. (1983) On the function space controllability of linear neutral systems. SIAM J. Control Optim. 21(2):306–329
10. Olbrot A. W. (1973) On degeneracy and related problems for linear time lag systems. Ricerche di Automatica 3:203–220
11. Rabah R., Sklyar G. M. (2005) The analysis of exact controllability of neutral type systems by the moment problem approach. Preprint IRCCyN/École des Mines de Nantes, No 8, Nantes
12. Rabah R., Sklyar G. M. and Rezounenko A. V. (2003) Generalized Riesz basis property in the analysis of neutral type systems. C.R. Acad. Sci. Paris Ser. I 337:19–24
13. Rabah R., Sklyar G. M. and Rezounenko A. V. (2005) Stability analysis of neutral type systems in Hilbert space. J. Differential Equations 214(2):391–428
14. Rivera R.H., Langenhop C. E. (1978) A sufficient condition for function space controllability of a linear neutral system. SIAM J. Control and Optimization 16(3):429–435

Part IV

New Computational Methods

Applied Interval Computation: A New Approach for Time-Delays Systems Analysis

Michael Di Loreto[1], Massa Dao[2], Luc Jaulin[3], Jean-François Lafay[1], and Jean Jacques Loiseau[1]

[1] IRCCyN, Institut de Recherche en Communications et Cybernétique de Nantes, UMR CNRS 6597, 44321 Nantes Cedex 3, France
Michael.Di-Loreto@irccyn.ec-nantes.fr,
Jean-Francois.Lafay@irccyn.ec-nantes.fr,
Jean-Jacques.Loiseau@irccyn.ec-nantes.fr

[2] LISA, CNRS-FRE-2656, Université d'Angers, 62 Avenue Notre Dame du Lac, 49000 Angers, France
dao@istia.univ-angers.fr

[3] Laboratoire E3I2, ENSIETA, 2 rue François Verny, 29806 Brest Cedex 9, France
jaulinlu@ensieta.fr

Summary. This paper deals with interval analysis applied to linear time-delays systems. With basic examples, we describe some applications to solve various control problems, and to show that interval computation is an effective tool for time-delays systems analysis.

Keywords: Interval analysis, set inversion, constraint propagation, subpaving, neutral and retarded time-delays systems, quasipolynomial, robust stability, stabilization, frequency domain analysis, disturbance attenuation, model tracking.

1 Introduction

Time-delays systems are dead-time or aftereffect systems, hereditary systems, or systems governed by differential-difference equations, and are described by functional differential equations [2], [10], [11], [17], [26].

The analysis of time-delays systems has attracted much interest in the literature over this half century, especially in the last decade. A recurring subject of research is the stability or robust stability, and has undergone a notable development both conceptually and computationally (see *e.g.* [4], [9], [14], [15], [23], [26], [29], and references therein). Using different theoretical approaches, numerical methods and algorithms obtained are generally semi-analytic, with sometimes difficulties of implementation.

Another recurring subject of research is around optimal control, in particular H_∞ control, with a conceptual tools development adapted to time-delays systems and an extension of existing results for linear systems [8], [16], [19], [24].

Interval analysis has been a very active field in scientific computation for the last 20 years [7], [13], [20], and [25]. Interval computation leads naturally to

J. Chiasson and J.J. Loiseau (Eds.): Appl. of Time Delay Systems, LNCIS 352, pp. 175–197, 2007.
springerlink.com

numerous applications in varied fields, as applied and numerical mathematics, data processing, control systems, robotics or estimation theory [13], [21], [31].

A fundamental advantage of interval analysis is that it gives guaranteed results to a well posed problem. A small number of key concepts are at the core of interval computation and its implementation.

Briefly, consider a box $[\mathbf{x}]$ of $\mathbb{IR}^n$, $n \in \mathbb{N}$, a function f from $\mathbb{IR}^n$ to $\mathbb{IR}$, and a subset $\mathbb{S}$ of $\mathbb{IR}^n$ defined by a series of constraints. Three fundamental operations can be implemented by interval analysis. The first one is the notion of *inclusion function*, *i.e.* computing an interval that contains the image of $[\mathbf{x}]$ by f. The second operation is the *inclusion test*, *i.e.* testing when $[\mathbf{x}]$ belongs to $\mathbb{S}$, or more precisely whether $[\mathbf{x}] \subset \mathbb{S}$ or whether $[\mathbf{x}] \cap \mathbb{S} = \emptyset$. The third notion introduced is the *contraction*, *i.e.* the substitution of $[\mathbf{x}]$ by a smaller box $[\mathbf{z}] \subset [\mathbf{x}]$ such that $[\mathbf{z}] \cap \mathbb{S} = [\mathbf{x}] \cap \mathbb{S}$. If $\mathbb{S}$ defines the feasibility set for the solution of some problem, and if $[\mathbf{z}]$ turns out to be empty, then $[\mathbf{x}]$ can be eliminated from the list of boxes that may contain this solution. When no conclusion can be reached about a given box, we can do a *bisection* to obtain subboxes, and each of them can also be studied in turn. These key concepts allow to solve complex problems, with guaranteed and global solutions. All these concepts were inserted in the solver Proj2D[1]. We will see in section 3 that interval computation constitute a whole of adequate tools to analyze some fundamental properties of time-delays systems.

This paper is organized as follows. Section 2 is devoted to interval analysis. In section 3, we apply interval computation to solve some control problems for time-delays systems, like robust stability, robust stabilization, disturbance attenuation or approximtive model tracking. Illustrative examples are done troughout the paper.

2 Interval Computation

In this section, we carry out a short recall on interval computation. We start by presenting some basic concepts and definitions; After that, we analyze the contraction operation and the constraint propagation, for finally describing the set inversion algorithm, which is commonly used in control problems.

2.1 Preliminaries

Denote $\mathbb{IR}$ the field of real numbers.

Definition 2.1. *[20] A real interval* $[\mathbf{x}_0]$ *is a connected subset of* $\mathbb{IR}$. *The lower* (*upper*) *bound of an interval* $[\mathbf{x}_0]$ *is denoted by* $\underline{\mathbf{x}}_0$ ($\overline{\mathbf{x}}_0$ *respectively*).

The width of any non-empty interval $[\mathbf{x}_0]$ *is* $w([\mathbf{x}_0]) \doteq \overline{\mathbf{x}}_0 - \underline{\mathbf{x}}_0$.

The classical set-theoretic operations (union, intersection, cartesian product, ...) can be applied to intervals [20]. In the same manner, the four classical operations

[1] Available at http://www.istia.univ-angers.fr/∼dao/Proj2DV3.zip

of real arithmetic, namely addition (+), substraction (−), multiplication (∗) and division (÷) can be extended to intervals. For any such binary operator, denoted by ($\diamond$), performing the operation associated with $\diamond$ on the intervals $[\mathbf{x}_0]$ and $[\mathbf{y}_0]$ means computing

$$[\mathbf{x}_0] \diamond [\mathbf{y}_0] = [\{x \diamond y \in \mathbb{R} \,|\, x \in [\mathbf{x}_0],\, y \in [\mathbf{y}_0]\}]\,, \tag{1}$$

where $[\mathbb{A}]$ is the smallest interval that contains the set $\mathbb{A}$. For example,

$$\begin{array}{l} [\mathbf{x}_0] + [\mathbf{y}_0] = [\underline{\mathbf{x}}_0 + \underline{\mathbf{y}}_0, \overline{\mathbf{x}}_0 + \overline{\mathbf{y}}_0] \\ [\mathbf{x}_0] - [\mathbf{y}_0] = [\underline{\mathbf{x}}_0 - \overline{\mathbf{y}}_0, \overline{\mathbf{x}}_0 - \underline{\mathbf{y}}_0] \end{array}.$$

Elementary functions such as exp, log, tan, sin, cos, ... can be defined for interval computation. If f_0 is a function from $\mathbb{R}$ to $\mathbb{R}$, then its interval counterpart $[\mathbf{f}_0]$ is defined by

$$[\mathbf{f}_0]([\mathbf{x}_0]) \doteq [\{f_0(x) \,|\, x \in [\mathbf{x}_0]\}]. \tag{2}$$

These basic notions can be extended to the multivariable case [13], [20], [22].

Definition 2.2. *A real interval vector (or box)* $[\mathbf{x}]$ *is a subset of* $\mathbb{R}^n$ *which is defined by the Cartesian product of n closed intervals. It will be written as*

$$[\mathbf{x}] = [\mathbf{x}_1] \times \ldots \times [\mathbf{x}_n],\ \textit{with}\ [\mathbf{x}_i] = [\underline{\mathbf{x}}_i, \overline{\mathbf{x}}_i],\ \textit{for}\ i = 1, \ldots, n. \tag{3}$$

Its ith *interval component* $[\mathbf{x}_i]$ *is the projection of* $[\mathbf{x}]$ *onto the* ith *axis.*

The lower bound $\underline{\mathbf{x}}$ *of a box* $[\mathbf{x}]$ *is the punctual vector consisting of the lower bounds of its interval components* $\underline{\mathbf{x}} \doteq (\underline{\mathbf{x}}_1\ \ldots\ \underline{\mathbf{x}}_n)^T$. *Similarly, the upper bound* $\overline{\mathbf{x}}$ *of a box* $[\mathbf{x}]$ *is the punctual vector* $\overline{\mathbf{x}} \doteq (\overline{\mathbf{x}}_1\ \ldots\ \overline{\mathbf{x}}_n)^T$.

The width of the box $[\mathbf{x}] = ([\mathbf{x}_1]\ \ldots\ [\mathbf{x}_n])^T$ *is* $w([\mathbf{x}]) \doteq \max\limits_{1 \le i \le n} w([\mathbf{x}_i])$.

The set of all n-dimensional boxes will be denoted by $\mathbb{IR}^n$. The concept of inclusion function is fundamental for interval arithmetic.

Definition 2.3. *[20] Consider a function* $f : \mathbb{R}^n \to \mathbb{R}^m$. *The interval function* $[\mathbf{f}]$ *from* $\mathbb{IR}^n$ *to* $\mathbb{IR}^m$ *is an inclusion function for* f *if*

$$\forall [\mathbf{x}] \in \mathbb{IR}^n,\ f([\mathbf{x}]) \subset [\mathbf{f}]([\mathbf{x}]). \tag{4}$$

One of the purposes of interval computation is to provide, for a large class of functions f, inclusion functions that can be evaluated reasonably quickly and such that $[\mathbf{f}]([\mathbf{x}])$ is not too large.

Property 2.4. *[20] An inclusion function* $[\mathbf{f}]$ *for* f *is* thin *if, for any punctual interval vector* $[\mathbf{x}] = x$, $[\mathbf{f}](x) = f(x)$.

The inclusion function $[\mathbf{f}]$ *is* minimal *if for any* $[\mathbf{x}]$, $[\mathbf{f}]([\mathbf{x}])$ *is the smallest box that contains* $f([\mathbf{x}])$. *The minimal inclusion function for* f *is unique.*

To build an inclusion function for a function $f : \mathbb{R}^n \to \mathbb{R}$, we can apply the following theorem.

Theorem 2.5. *[20], [22] Consider a function*

$$f : \begin{cases} \mathbb{IR}^n \to \mathbb{IR} \\ (x_1, \ldots, x_n) \mapsto f(x_1, \ldots, x_n) \end{cases} \tag{5}$$

A thin inclusion function $[\mathbf{f}] : \mathbb{IIR}^n \to \mathbb{IIR}$ *for* f *is obtained by replacing each real variable* x_i *by an interval variable* $[\mathbf{x}_i]$ *and each operator or elementary function by its interval counterpart. This function is called the natural inclusion function of* f*.*

However, natural inclusion functions are not minimal in general [13], [22].

Example 2.6. *Consider the real function* $f : \mathbb{IR}^2 \to \mathbb{IR}$ *defined by*

$$f(x_1, x_2) = \frac{x_2}{x_1 + x_2} + \sin(x_1)\cos(x_1), \text{ with } x_1 \in [-1, 2] \text{ and } x_2 \in [3, 5]. \tag{6}$$

The natural inclusion function $[\mathbf{f}]_1$ *for* f *is obtained by replacing each real variable by an interval variable, and each real operation by its interval counterpart, i.e.*

$$[\mathbf{f}]_1([\mathbf{x}_1], [\mathbf{x}_2]) = \frac{[\mathbf{x}_2]}{[\mathbf{x}_1] + [\mathbf{x}_2]} + \sin([\mathbf{x}_1])\cos([\mathbf{x}_1]).$$

We have $[\mathbf{f}]_1([-1, 2], [3, 5]) = \frac{[3,5]}{[-1,2]+[3,5]} + \sin([-1, 2])\cos([-1, 2]) = [-0.42, 3.5]$*. A second interval extension* $[\mathbf{f}]_2$ *can be obtained rewriting* f *such that the variables appear at least twice:*

$$[\mathbf{f}]_2([\mathbf{x}_1], [\mathbf{x}_2]) = \frac{1}{1 + [\mathbf{x}_1]/[\mathbf{x}_2]} + \frac{\sin(2\,[\mathbf{x}_1])}{2}.$$

We obtain $[\mathbf{f}]_2([-1, 2], [3, 5]) = \frac{1}{1+[-1,2]/[3,5]} + \frac{\sin([-2,4])}{2} = [0.1, 2]$*. Evidently,* $[\mathbf{f}]_1$ *and* $[\mathbf{f}]_2$ *are both interval extensions of* f*. However,* $[\mathbf{f}]_2$ *is more accurate than* $[\mathbf{f}]_1$*, which suffers from the dependency effect. The interval computed by* $[\mathbf{f}]_2$ *is minimal, and thus equal to the image set* $f([-1, 2], [3, 5])$*.*

As seen, intervals and boxes form an attractive class of wrappers. However, these wrappers are not enough general to describe all types of sets under interest, which are of course not restricted to intervals and boxes, and include for instance unions of disconnected subsets.

The idea is to introduce the notion of subpaving, useful for the generalization and the implementation of set computation [13], [20].

A subpaving of a box $[\mathbf{x}] \subset \mathbb{IR}^n$ is an union of non-overlapping subboxes of $[\mathbf{x}]$ with non zero width. Subpavings can also be employed to approximate compact sets in a guaranteed way. Thus, for any full compact set $\mathbb{X}$, it is possible to find two finite subpavings $\underline{\mathbb{X}}$ and $\overline{\mathbb{X}}$ such that $\underline{\mathbb{X}} \subset \mathbb{X} \subset \overline{\mathbb{X}}$. For interval computation, the notion of subpaving plays a fundamental role, as described below with the bisection operation.

Definition 2.7. *[13] Consider the box* $[\mathbf{x}] = [\mathbf{x}_1] \times \ldots \times [\mathbf{x}_n]$*, and take the index* j *of its first component of maximum width, i.e.*

$$j = \min\{i \,|\, w([\mathbf{x}_i]) = w([\mathbf{x}])\} \tag{7}$$

The bisection of the box $[\mathbf{x}]$ *is the operation which generates two boxes* $L[\mathbf{x}]$ *and* $R[\mathbf{x}]$*, defined by*

$$\begin{cases} L[\mathbf{x}] \doteq [\mathbf{x}_1] \times \ldots \times [\underline{\mathbf{x}}_i, m([\mathbf{x}_i])] \times \ldots \times [\mathbf{x}_n] \\ R[\mathbf{x}] \doteq [\mathbf{x}_1] \times \ldots \times [m([\mathbf{x}_i]), \overline{\mathbf{x}}_i] \times \ldots \times [\mathbf{x}_n] \end{cases}, \tag{8}$$

where $m([\mathbf{x}_i]) = \frac{\overline{\mathbf{x}}_i + \underline{\mathbf{x}}_i}{2}$ *is the midpoint of* $[\mathbf{x}_i]$*.* $L[\mathbf{x}]$ *is the left child of* $[\mathbf{x}]$*, and* $R[\mathbf{x}]$ *is the right child of* $[\mathbf{x}]$*.*

L and R may be viewed as operators from $\mathbb{IIR}^n$ to $\mathbb{IIR}^n$. The two boxes $L[\mathbf{x}]$ and $R[\mathbf{x}]$ are siblings. A subpaving of $[\mathbf{x}]$ is regular if each of its boxes can be obtained from $[\mathbf{x}]$ by a finite succession of bisections and selections (see [13] and references therein).

2.2 Constraint Propagation

In this section, we present the concepts of constraint propagation and contractors [3], [5], [7], [13].

Consider n_f relations or constraints, with n_x variables $x_i \in \mathbb{R}$, $i = 1, \ldots, n_\mathrm{x}$, of the form

$$f_j(x_1, \ldots, x_{n_\mathrm{x}}) = 0,\ j = 1, \ldots, n_\mathrm{f}. \tag{9}$$

Each variable x_i is known to belong to an interval (or a union of intervals) $[\mathbf{x}_i]$. Define the vector

$$x = (x_1, \ldots, x_{n_\mathrm{x}})^T$$

and the prior domain $[\mathbf{x}]$ for x as $[\mathbf{x}] = [\mathbf{x}_1] \times \ldots \times [\mathbf{x}_{n_\mathrm{x}}]$. Let f be the function whose coordinate functions are the f_js. Equation (9) can be written in the form $f(x) = 0$. This corresponds to a constraint satisfaction problem (CSP) $\mathcal{P}$, which can be formulated as

$$\mathcal{P}:\ (f(x) = 0,\ x \in [\mathbf{x}]). \tag{10}$$

The solution set of $\mathcal{P}$ is $\mathbb{S} = \{x \in [\mathbf{x}] \,|\, f(x) = 0\}$. Such CSPs may involve equality and inequality constraints. Contracting $\mathcal{P}$ means replacing $[\mathbf{x}]$ by a smaller domain $[\mathbf{x}']$ such that the solution set $\mathbb{S}$ remains unchanged, *i.e.* $\mathbb{S} \subset [\mathbf{x}'] \subset [\mathbf{x}]$. There exists a unique optimal contraction of $\mathcal{P}$, which corresponds to replacing $[\mathbf{x}]$ by the smallest box that contains $\mathbb{S}$. A contractor for $\mathcal{P}$ is any operator that can be used to contract it.

Numerous basic contractors exist. Some of them are interval counterparts of classical point algorithms like Gauss elimination, Gauss-Seidel and Newton algorithms [5], [13], [18]. We describe here only the contractors based on constraint propagation, contractors which are implemented in the solver Proj2D.

These contractors permit to contract the domains of the CSP $\mathcal{P}$ by taking into account any one of the n_f constraints in isolation, say $f_j(x_1, \ldots, x_{n_\mathrm{x}}) = 0$. Assume that each constraint has the form $f_j(x_1, \ldots, x_{n_\mathrm{x}}) = 0$, where f_j can be decomposed into a sequence of operations involving elementary operators and

functions like $(+, -, *, \div, \sin, \cos, \ldots)$. It is then possible to decompose this constraint into primitive constraints. Roughly speaking, a primitive constraint is a constraint involving a single operator or a single function. A method for contracting $\mathcal{P}$ with respect to a constraint is to contract each of the primitive constraints until the contractors become inefficient. This is the principle of constraint propagation [7], [13].

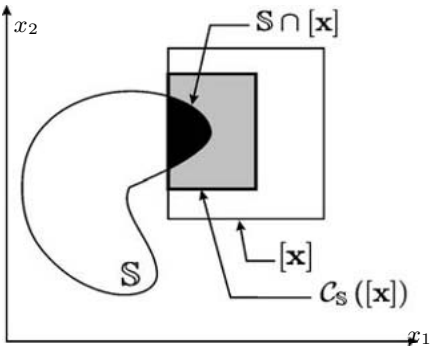

Fig. 1. Contraction of the box $[\mathbf{x}] = [\mathbf{x}_1] \times [\mathbf{x}_2]$ for the set $\mathbb{S}$, with $x_1 \in [\mathbf{x}_1]$ and $x_2 \in [\mathbf{x}_2]$

Definition 2.8. *[13] Let $\mathbb{S}$ be a set of $\mathbb{R}^n$. The operator $\mathcal{C}_{\mathbb{S}} : \mathbb{IR}^n \to \mathbb{IR}^n$ is a contractor for $\mathbb{S}$ if it satisfies*

$$\forall [\mathbf{x}] \in \mathbb{IR}^n, \begin{cases} \mathcal{C}_{\mathbb{S}}([\mathbf{x}]) \subset [\mathbf{x}] & \text{(contractance)}, \\ [\mathbf{x}] \cap \mathbb{S} \subset \mathcal{C}_{\mathbb{S}}([\mathbf{x}]) & \text{(correctness)}. \end{cases} \tag{11}$$

A contractor is minimal if $[\mathbf{x}] \cap \mathbb{S} = \mathcal{C}_{\mathbb{S}}([\mathbf{x}])$.

We give here a useful theorem for a contractor's construction based on the constraint propagation.

Theorem 2.9. *[5], [7] Let $f : \mathbb{R}^{n_\mathrm{x}} \to \mathbb{R}^{n_\mathrm{f}}$ a constraint function. Consider the solution set $\mathbb{S}$ in (10) of vectors x that verify $f(x) = 0$. Suppose there exist some functions g_i, $i = 1, \ldots, n_\mathrm{x}$, such that*

$$f(x) = 0 \Longleftrightarrow x_i = g_i({}^i x),\ \forall i \in \{1, \ldots, n_\mathrm{x}\}, \tag{12}$$

where ${}^i x = (x_1, \ldots, x_{i-1}, x_{i+1}, \ldots, x_{n_\mathrm{x}})^T$. Denote $[\mathbf{g}_i]$ an inclusion function for g_i, $i = 1, \ldots, n_\mathrm{x}$. A contractor for the set $\mathbb{S}$ is given by

$$\mathcal{C}_{\mathbb{S}}([\mathbf{x}_i]) = [\mathbf{x}_i] \cap [\mathbf{g}_i]([{}^i\mathbf{x}]),\ \forall i \in \{1, \ldots, n_\mathrm{x}\}, \tag{13}$$

with $[{}^i\mathbf{x}] = ([\mathbf{x}_1], \ldots, [\mathbf{x}_{i-1}], [\mathbf{x}_{i+1}], \ldots, [\mathbf{x}_{n_\mathrm{x}}])^T$. Furthermore, if g_i is continuous and $[\mathbf{g}_i]$ is minimal, then the contractor defined in (13) is minimal.

Example 2.10. *Let* $\mathbb{S}$ *be the set defined by*

$$\mathbb{S} = \{(x_1, x_2, x_3) \in \mathbb{R}^3 \,|\, x_3 = x_1 + x_2\}, \tag{14}$$

and the box $[\mathbf{x}] = [\mathbf{x}_1] \times [\mathbf{x}_2] \times [\mathbf{x}_3]$*, with* $[\mathbf{x}_1] = [-1, 2]$*,* $[\mathbf{x}_2] = [0, 3]$ *and* $[\mathbf{x}_3] = [4, 8]$*. For* $(x_1, x_2, x_3) \in [\mathbf{x}]$*, we obtain by applying Theorem 2.9:*

$$\begin{array}{l} x_1 \in [\mathbf{x}_1] \cap ([\mathbf{x}_3] - [\mathbf{x}_2]) = [1, 2] \\ x_2 \in [\mathbf{x}_2] \cap ([\mathbf{x}_3] - [\mathbf{x}_1]) = [2, 3]\,. \\ x_3 \in [\mathbf{x}_3] \cap ([\mathbf{x}_1] + [\mathbf{x}_2]) = [4, 5] \end{array} \tag{15}$$

The box obtained after contraction of $[\mathbf{x}]$ *for* $\mathbb{S}$ *is:*

$$\mathcal{C}_{\mathbb{S}}([\mathbf{x}]) = [1, 2] \times [2, 3] \times [4, 5],$$

which is minimal [7].

2.3 Set Inversion Algorithm

In this section, we analyze the set computation implementation, and more particularly the set inversion algorithm which we will use to solve control problems with guaranteed solutions.

The set inversion operation is the computation of the reciprocal image of a regular subpaving. The approximation is realized by a subpaving with a fixed size to guarantee a desired precision. This set inversion is realized in the algorithm SIVIA (Set Inverter Via Interval Analysis) we describe now [13], [20].

Consider a continuous function f from $\mathbb{R}^n$ to $\mathbb{R}^m$, $[\mathbf{y}]$ a box of $\mathbb{R}^m$ and $[\mathbf{x}]$ a box of $\mathbb{R}^n$. The set inversion algorithm SIVIA allows to approximate with a subpaving the set $\mathbb{S}_{\mathbf{x}}$ described by

$$\mathbb{S}_{\mathbf{x}} = \{x \in [\mathbf{x}] \,|\, f(x) \in [\mathbf{y}]\} = [\mathbf{x}] \cap f^{-1}([\mathbf{y}]). \tag{16}$$

This approximation is realized with an inner and outer subpavings, respectively $\underline{\mathbb{S}}$ and $\overline{\mathbb{S}}$, such that $\underline{\mathbb{S}} \subset \mathbb{S}_{\mathbf{x}} \subset \overline{\mathbb{S}}$. We give in Table 1 a recursive version of the set inversion algorithm for a set of equations. We suppose to have a contractor $\mathcal{C}_{\mathbb{S}_{\mathbf{x}}}$ for the set $\mathbb{S}_{\mathbf{x}}$, as described in Section 2.2. In the solver Proj2D, the contractor

Table 1. Algorithm SIVIA for solving a set of constraints

	SIVIA(in: $[\mathbf{x}]$, $\mathcal{C}_{\mathbb{S}_{\mathbf{x}}}$, ε; inout: $\mathcal{L}$)
1	$[\mathbf{x}] := \mathcal{C}_{\mathbb{S}_{\mathbf{x}}}([\mathbf{x}])$;
2	if $([\mathbf{x}] = \emptyset)$ then return;
3	if $(w([\mathbf{x}]) < \varepsilon)$ then $\mathcal{L} := \mathcal{L} \cup \{[\mathbf{x}]\}$; return;
4	bisection of $[\mathbf{x}]$ into $L([\mathbf{x}])$ and $R([\mathbf{x}])$;
5	SIVIA$(L([\mathbf{x}]), \mathcal{C}_{\mathbb{S}_{\mathbf{x}}}, \varepsilon, \mathcal{L})$; SIVIA$(R([\mathbf{x}]), \mathcal{C}_{\mathbb{S}_{\mathbf{x}}}, \varepsilon, \mathcal{L})$.

used in SIVIA is based on the constraint propagation. $\mathcal{L}$ is a boxes list, initialized as an empty list, and ε is a precision parameter.

The union of all boxes in the list $\mathcal{L}$ returned by SIVIA contains the set $\mathbb{S}_x$. The subpaving $\Delta\mathbb{S}$ consisting of all boxes of $\overline{\mathbb{S}}$ that are not in $\underline{\mathbb{S}}$ is called the uncertainty layer. It is a regular subpaving, where all internal boxes have a width smaller than ε.

3 Control Applications

The aim of this section is to introduce the application of interval techniques presented in Section 2 to solve some control problems for time-delay systems.

Interval computation allows, with an another point of view, to solve control problems, with guaranteed solutions. All results presented in Section 3 were obtained with the solver Proj2D, that uses the algorithm SIVIA and the constraint propagation technique. This solver presents solutions of a problem in a graphical form, with a colored subpaving to distinguish boxes characteristics. To solve a problem of the form (16), we obtain three classes of boxes. The first one is a box solution, *i.e.* $\mathbb{X}_{\mathrm{r}} = \{x \in [\mathbf{x}] \,|\, \forall z \in [\mathbf{z}],\ f(x,z) \in [\mathbf{y}]\}$, and its complementary set $\mathbb{X}_{\mathrm{r}}^{\mathrm{c}} = \{x \in [\mathbf{x}] \,|\, \exists z \in [\mathbf{z}],\ f(x,z) \notin [\mathbf{y}]\}$. The second one is a no–solution box, *i.e.* $\mathbb{X}_{\mathrm{b}} = \{x \in [\mathbf{x}] \,|\, \forall z \in [\mathbf{z}],\ f(x,z) \notin [\mathbf{y}]\}$, and its complementary set $\mathbb{X}_{\mathrm{b}}^{\mathrm{c}} = \{x \in [\mathbf{x}] \,|\, \exists z \in [\mathbf{z}],\ f(x,z) \in [\mathbf{y}]\}$. Finally, the last one is the uncertainty layer where all its boxes have the same desired fixed size (see Section 2.3). This characterization is sufficient to solve numerous control problems, as we will describe in the next subsections.

3.1 Frequency-Domain Analysis

We present interval analysis based procedures to construct the well known frequency-domain plots, as Bode, Nyquist or Nichols diagrams. The proposed procedures can be used to construct the plots reliably and with a prescribed accuracy over a finite user specified frequency range.

For transfer functions having a rational form, procedures are available in Matlab or Scilab. However, these procedures have several limitations. In fact, the number of grid points required to obtain a specified accuracy is unknown, as well as the amount of error present for a given frequency response plot, *i.e.* no error estimates are available. These limitations show up particularly severely when the frequency responses exhibit single or multiple sharp peaks or dips, that often happens with time-delays systems.

Interval analysis allows to supply this limitation. Consider a transfer function $H(s)$ including time-delays. We denote by $|H(j\omega)|$ and $\angle H(j\omega)$, the magnitude and phase expressions respectively of $H(s)$ on the imaginary axis, where ω is the frequency variable.

Construct natural interval extensions g and a for $|H(j\omega)|$ and $\angle H(j\omega)$ respectively. The interval frequency range is denoted by Ω.

For a Bode diagram, we consider the set in (16) defined by

$$\mathbb{S}_{\mathrm{x}} = \{(\omega, g) \in \Omega \times [\mathbf{g}] \,|\, |H(j\omega)| - g = 0\} \tag{17}$$

for the magnitude plot, and

$$\mathbb{S}_{\mathrm{x}} = \{(\omega, a) \in \Omega \times [\mathbf{a}] \,|\, \angle H(j\omega) - a = 0\} \tag{18}$$

for the phase plot. By the set inversion algorithm (Section 2.3), it is enough to plot $20\log10(g(\omega))$ for the magnitude, and $a(\omega)$ for the phase. The precision parameter ε in SIVIA ensures the control of boxes width that include the exact frequency plot.

Evidently, this method can be applied without difficulty to the Nyquist and Nichols diagrams. Indeed, consider again the transfer function $H(s)$ of a time-delays systems. Decompose this last one in real and imaginary parts, as

$$H(j\omega) = \mathrm{Re}(H(j\omega)) + j\,\mathrm{Im}(H(j\omega)). \tag{19}$$

We note $H_{\mathrm{R}}(\omega) = \mathrm{Re}(H(j\omega))$ and $H_{\mathrm{I}}(\omega) = \mathrm{Im}(H(j\omega))$. Denote by h_{R} and h_{I} the natural interval extensions of $H_{\mathrm{R}}(\omega)$ and $H_{\mathrm{I}}(\omega)$ respectively. We solve with SIVIA the problem

$$\mathbb{S}_{\mathrm{x}} = \{(\omega, h_{\mathrm{R}}, h_{\mathrm{I}}) \in \Omega \times [\mathbf{h}_{\mathrm{R}}] \times [\mathbf{h}_{\mathrm{I}}] \,|\, H_{\mathrm{R}}(\omega) - h_{\mathrm{R}} = 0 \text{ and } H_{\mathrm{I}}(\omega) - h_{\mathrm{I}} = 0\} \tag{20}$$

and we plot the results in the $(h_{\mathrm{R}}, h_{\mathrm{I}})$ plane to obtain the Nyquist diagram. For the Nichols diagram, we solve

$$\mathbb{S}_{\mathrm{x}} = \{(\omega, g, a) \in \Omega \times [\mathbf{g}] \times [\mathbf{a}] \,|\, |H(j\omega)| - g = 0 \text{ and } \angle H(j\omega) - a = 0\} \tag{21}$$

with the notations of (17) and (18), and the solution is reported in the (a, g) plane.

The main advantage of the plots described here is that the frequency diagram obtained is guaranteed, advantage we don't have with Matlab or Scilab. Furthermore, these plots have a numerical interest, as for example the determination of $\sup_{\omega \in \mathbb{IR}} |H(j\omega)|$.

Example 3.1. *Consider the system of transfer function*

$$H(s) = \mathrm{e}^{-s\tau} - 1, \tag{22}$$

with $\tau = 0.1$. The Magnitude Bode diagram of (22) is reported on Figure 2, thanks to equation (17).

Example 3.2. *Consider the system of transfer function*

$$H(s) = \frac{1 - \mathrm{e}^{1-s}}{s - 1}, \tag{23}$$

which is analytic for all $s \in \mathbb{C}$ and corresponds to a distributed delay. The magnitude plot $|H(j\omega)|$ when $\omega \in [-100, 100]$ is reported on Figure 3.

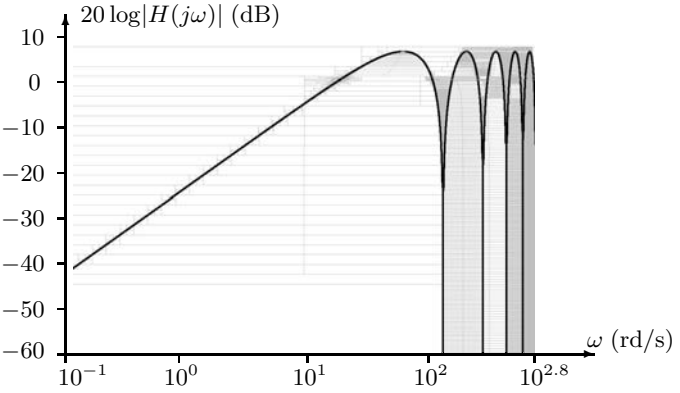

Fig. 2. Magnitude Bode diagram of $H(s)$ in (22)

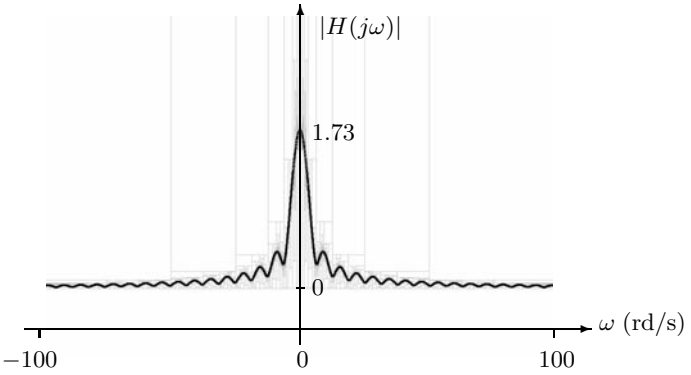

Fig. 3. Magnitude diagram $|H(j\omega)|$ for (23)

3.2 Robust Stability Analysis

The stability of time-delays systems is a problem of recurring interest in the last twenty years, thanks to the possibility to destabilize a system with the existence of a small delay.

In the literature, two classes of stability criteria for linear time-delays systems occur, according to their dependence with respect to the size of delays. The corresponding methods can be cast into two classes: frequency-domain and time-domain based methods. In the first one, we can include the approach based on the small gain theorem, two variables polynomials approach, or a generalized eigenvalues approach. In the second one, we can include the matrix measure approach, the Lyapunov stability approach combined with Lyapunov equations, Riccati equations or linear matrix inequalities, to apply techniques as the Lyapunov-Razumikhin function approach or the Lyapunov-Krasovkii functional

approach. For further informations, the reader is referred to [10], [11], [26], and references therein.

A central rule of stability analysis is played by quasipolynomials associated with the characteristic equation of a time-delays systems. We distinguish two general classes of quasipolynomials, associated with retarded or neutral time-delays systems.

A retarded quasipolynomial can be written as

$$f(s) = a_0(s) + \sum_{k=1}^{m} a_k(s)\mathrm{e}^{-\tau_k s}, \tag{24}$$

where $\tau_0 = 0 < \tau_1 < \ldots < \tau_m$, and $a_k(s)$, for $k = 0$ to m, are real polynomials described by

$$\begin{aligned} a_0(s) &= s^n + \sum_{i=0}^{n-1} a_{0,i}s^i, \\ a_k(s) &= \sum_{i=0}^{n-1} a_{k,i}s^i,\ k = 1, \ldots, m. \end{aligned} \tag{25}$$

The corresponding time-delays systems are given by

$$x^{(n)}(t) + \sum_{i=0}^{n-1}\sum_{k=0}^{m} a_{k,i}x^{(i)}(t - \tau_k) = 0. \tag{26}$$

The quasipolynomial (24) is said to be stable if $f(s) \neq 0, \forall s \in \mathbb{C}_+ = \{s \,|\, \mathrm{Re}(s) \geq 0\}$. It is said to be stable independent of delay if this condition holds for all $\tau_k,\ k = 1, \ldots, m$. A neutral time-delays system is governed by a functional differential equation of the form

$$x^{(n)}(t) + \sum_{k=1}^{m} a_{k,n}x^{(n)}(t - \tau_k) + \sum_{i=0}^{n-1}\sum_{k=0}^{m} a_{k,i}x^{(i)}(t - \tau_k) = 0, \tag{27}$$

with its characteristic equation

$$f(s) = s^n\left(1 + \sum_{k=1}^{m} a_{k,n}\mathrm{e}^{-s\tau_k}\right) + \sum_{i=0}^{n-1} a_{0,i}s^i + \sum_{k=1}^{m} a_k(s)\mathrm{e}^{-\tau_k s}, \tag{28}$$

where $a_k(s)$ are given in (25). The system (27) is said to be stable if there exists $\alpha > 0$ such that $f(s) \neq 0$ for all $s \in \mathbb{C}$ with $\mathrm{Re}(s) > -\alpha$. A large number of results is well developed for quasipolynomials analysis, with different levels of difficulty for their implementation. We can cite for instance [4], [9], [12], [28] or [30]. A difficulty issued from these results is for instance to characterize the robust stability of a given system for constant uncertain parameters and delays, which lie in known bounded intervals. Here, interval computation brings some new elements and responses. By interval computation, the localization of quasipolyomials roots in a compact set is reduced to an easy set inversion problem, solvable with the algorithm SIVIA.

We shall focus attention on robust stability and robust control problems for uncertain systems that can be described by parametric models, the unknown parameters of which are assumed to lie between known finite bounds. We begin with the problem of roots localization of quasipolynomials.

Problem 3.1. *Consider a retarded or a neutral time-delays system of the form (26) or (27) with $f(s)$ its characteristic equation, and a given box $\mathbb{X}$ of $\mathbb{C}$. We want to solve $f(s) = 0$, for $s \in \mathbb{X}$.*

Writing $s = x + jy$, $(x, y) \in \mathbb{R}^2$, the set $\mathbb{X}$ is decomposed as a Cartesian product of real intervals $\mathbb{X} = [\mathbf{x}] \times [\mathbf{y}]$, with $x \in [\mathbf{x}]$ and $y \in [\mathbf{y}]$. The Problem 3.1 is equivalent to the set inversion problem

$$\mathbb{S} = \{(x, y) \in [\mathbf{x}] \times [\mathbf{y}] \,|\, f(x + jy) = 0\} = ([\mathbf{x}] \times [\mathbf{y}]) \cap f^{-1}(0), \tag{29}$$

that can be performed by SIVIA, described in Section 2.3. Note that results obtained in (29) are guaranteed, so that we are ensured of the absence or presence of quasipolynomials roots in the box $[\mathbf{x}] \times [\mathbf{y}]$.

A direct application of the Problem 3.1 is the characterization of stability of a retarded quasipolynomial with known and constant parameters. In fact, for retarded time-delays systems, we can compute a positive born $R < \infty$ such that all unstable roots of the characteristic equation lie in the box $[0, R] \times [-R, R]$ [27]. We are also able to calculate all the unstable roots with the solutions of Problem 3.1.

For neutral systems, the conclusion is less obvious. The presence of zeros asymptotic directions of (28) required non-bounded search boxes, and an estimation of a larger born for the module of unstable zeros is not always realizable. However, interval computation allows to give some important and guaranteed indications.

For a robust stability analysis of time-delays systems, we can apply a similar reasoning. Consider a system of characteristic equation (24) or (28), *i.e.* of a general form

$$g(s, q, \tau) = \sum_{i=0}^{n} \sum_{k=0}^{m} q_{ik} s^i \mathrm{e}^{-\tau_k s}, \tag{30}$$

with $q = (q_{ik}) \in \mathbb{R}^{(n+1)\times(m+1)}$, $\tau = (\tau_0, \ldots, \tau_m)^T$, and $\tau_0 = 0 < \ldots < \tau_m$. The coefficients q_{ik} and delays τ_k are constant but uncertain. They are supposed to lie in closed intervals with known finite bounds:

$$\begin{cases} q_{ik} \in [\underline{\mathbf{q}}_{ik}, \overline{\mathbf{q}}_{ik}] = [\mathbf{q}_{ik}], \text{ for } i = 0, \ldots, n \text{ and } k = 0, \ldots, m, \\ \tau_k \in [\underline{\mathbf{d}}_k, \overline{\mathbf{d}}_k] = [\mathbf{d}_k], \quad \text{for } k = 0, \ldots, m. \end{cases}$$

with $[\mathbf{d}_k] \subset \mathbb{R}_+$, for $k = 0, \ldots, m$. Denote

$$\begin{cases} [\mathbf{q}] = \{[\mathbf{q}_{ik}], \text{ for } i = 0, \ldots, n \text{ and } k = 0, \ldots, m\} \\ [\mathbf{d}] = \{[\mathbf{d}_k], \text{ for } k = 0, \ldots, m\} \end{cases}, \tag{31}$$

the vectors of the parameters and the delays uncertainties intervals respectively. The quasipolynomials family

$$\mathcal{G} = \{g(s, q, \tau) \,|\, q \in [\mathbf{q}],\ \tau \in [\mathbf{d}]\},\ s \in \mathbb{C}, \tag{32}$$

is said to be robustly stable if for all $q \in [\mathbf{q}]$ and $\tau \in [\mathbf{d}]$,

$$g(s, q, \tau) \neq 0,\ \forall s \in \mathbb{C}_+. \tag{33}$$

It is robustly stable independent of delays if (33) holds for all $\tau \in \mathbb{R}_+^{n+1}$.

Problem 3.2. *Consider a time-delays system of characteristic equation of the form (30). We want to characterize robust stability of quasipolynomials family $\mathcal{G}$ in (32), using interval computation and property (33).*

To solve Problem 3.2, we use the set inversion algorithm applied to the set $\mathbb{S}$

$$\mathbb{S} = \{(s, q, \tau) \in [\mathbf{s}] \times [\mathbf{q}] \times [\mathbf{d}] \,|\, g(s, q, \tau) = 0\} = ([\mathbf{s}] \times [\mathbf{q}] \times [\mathbf{d}]) \cap g^{-1}(0), \tag{34}$$

where $[\mathbf{s}]$ is an interval variation of $s \in \mathbb{C}$. In practice, we will decompose in real and imaginary parts $s = x + jy$ to obtain $[\mathbf{s}] = [\mathbf{x}] \times [\mathbf{y}]$, with $[\mathbf{x}]$ and $[\mathbf{y}]$ real intervals, and we can test the absence of solutions in regions of the right half complex plane.

For retarded time-delays systems, the solution obtained for Problem 3.2 is a proof of robust stability, thanks to the existence of a finite larger bound of unstable roots modules of (24).

Problem 3.2 applied to neutral time-delays systems does not allow, without any other assumption, a conclusion on robust stability, but it provides significant indications.

Finally, note that the solution of Problem 3.2 can be projected onto a parametric plane, where only the values of coefficients $q \in [\mathbf{q}]$ and delays $\tau \in [\mathbf{d}]$ are reported. Then, we can analyze parametric regions for which the robust stability is ensured, and those for which we loose this robust property. This kind of plot brings an invaluable help for dynamics analysis.

An another interesting problem is the stabilization or robust stabilization of time-delays systems. Here, interval computation presents two limits. The first one is the restricted number of parameters, to avoid significant computing times. The second one is the necessity to choose a feedback with a predefined structure. The idea is in fact to reduce the problem of (robust) stabilization to a (robust) stability problem, treated with Problems 3.1 and 3.2, with some additional quasipolynomial coefficients to be determined which depend on the feedback structure.

Consider a time-delays system (Σ), with input u and output x. No assumption is made on the delays localization. Denote by $\hat{u}(s)$ and $\hat{x}(s)$ the Laplace transforms of u and x respectively, and by $H(s) = \frac{\hat{x}(s)}{\hat{u}(s)}$ the transfer of (Σ). Finally, denote by $k(s)$ a stabilizing feedback for Σ such that $\hat{u}(s) = k(s)\hat{x}(s)$. Interval computation allows to choose simple predefined structures for $k(s)$, as for example proportional, proportional-integral or proportional-integral-derivative controllers, or generalized feedbacks which take into account delayed state, and eventually delayed state derivatives or integrals, as for example

$$k(s) = \sum_{i=0}^{h} \sum_{l=0}^{r} k_{il} s^{i-p} \mathrm{e}^{-s\tau_l}, \tag{35}$$

with $(p, h, r) \in \mathbb{N}^3$, $k_{il} \in \mathbb{R}$ (with $r \leq m$ and $p \leq n$ for a system (Σ) of the form (30)). In practice, since the number of parameters is restricted, we will consider controllers with a maximum of 2 or 3 coefficients parameters k_{il}. The expression of $k(s)$ in (35) is not enough general; the choice of feedbacks structure is directly related to systems dynamics. The predefined structure of $k(s)$ is then to adapt to the considered problem.

Problem 3.3. *Consider an unstable time-delays system with transfer function $H(s)$, and a feedback $k(s)$ with unknown coefficients. How to ensure stability in closed loop by the choice of coefficients of $k(s)$?*

To answer Problem 3.3, note that in closed loop, the characteristic equation is of the form (30), where coefficients q_{ik} depend on the controllers coefficients k_{il} in (35). Then, in closed loop, the characteristic equation is given by a quasipolynomial of the form

$$g(s, \mathbf{k}) = \sum_{i} \sum_{l} q_{il}(\mathbf{k}) s^i \mathrm{e}^{-s\tau_l} \tag{36}$$

where $\mathbf{k}$ is the coefficients vector of the feedback $k(s)$. We are reduced to solve

$$\mathbb{S} = \{(s, \mathbf{k}) \in [\mathbf{s}] \times [\mathbf{k}] \,|\, g(s, \mathbf{k}) = 0,\ \mathrm{Re}(s) < 0\}, \tag{37}$$

where $[\mathbf{k}]$ is an admissible values interval for $\mathbf{k}$. Applying algorithm SIVIA, we obtain the guaranteed results, *i.e.* the values $\mathbf{k} \in [\mathbf{k}]$ of the feedback coefficients such that the stability is guaranteed in closed loop, at least for retarded time-delays systems. For neutral time-delays systems, we can obtain only indications, that we can verify in a second time.

A more complex problem is the robust stabilization by feedback. For this problem, we take notations of Problems 3.1 and 3.2.

Problem 3.4. *Consider a time-delays system, with uncertain and constant parameters, which lie in closed intervals with known bounds. With an appropriate feedback to determine, we want to ensure the robust stability in closed loop.*

In closed loop, the characteristic equation becomes

$$g(s, q, \tau, \mathbf{k}) = \sum_{i} \sum_{l} q_{il}(\mathbf{k}) s^i \mathrm{e}^{-s\tau_l}, \tag{38}$$

where (q, d) are defined in (31), and $\mathbf{k}$ in (36). The Problem 3.4 is reduced to the set inversion problem

$$\mathbb{S} = \{(s, q, \tau, \mathbf{k}) \in [\mathbf{s}] \times [\mathbf{q}] \times [\mathbf{d}] \times [\mathbf{k}] \,|\, g(s, q, \tau, \mathbf{k}) = 0,\ \mathrm{Re}(s) < 0\}, \tag{39}$$

where solutions given by SIVIA ensure the closed loop stability of the quasipolynomials family (38), at least for retarded systems.

Example 3.5. *Let the retarded time-delay system [23], [26],*

$$\dot{x}(t) = -ax(t) - bx(t-\tau) \tag{40}$$

with $(a, b, \tau) \in \mathbb{R} \times \mathbb{R} \times \mathbb{R}_+$ *constant uncertain parameters, which lie in* $[-1, 1] \times [2, 3] \times [0, 0.5]$ *respectively. Its characteristic equation is* $s + a + b\mathrm{e}^{-s\tau} = 0$. *We verify with interval methods if this system is robustly stable. We report solutions in the parametric plane* (a, b) *on the Figure 4. The white region ensures robust*

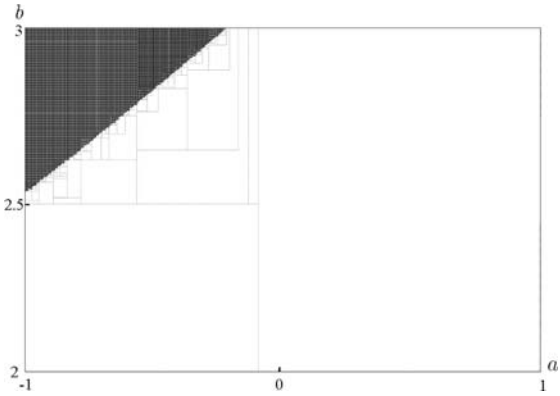

Fig. 4. Robust stable or unstable regions in the parametric plane (a, b) of (40)

stability, for all $\tau \in [0, 0.5]$. *The grey region does not guarantee robust stability, i.e. in each grey box, there exists at least one value of* (a, b, τ) *such that (40) becomes unstable. We find again the well known results on the stability of (40).*

Example 3.6. *Consider the system, with an appropriate initialization, described by*

$$x(t) = \frac{3}{4}x(t-1) - \frac{3}{4}x(t-\tau), \tag{41}$$

with its associated characteristic equation $f(s) = 1 - \frac{3}{4}\mathrm{e}^{-s} - \frac{3}{4}\mathrm{e}^{-s\tau} = 0$. *If we take* $\tau = 2$, *the solutions of this equation are stable, since denoting* $\lambda = \mathrm{e}^s$, *we have two solutions in* λ *which are* $\lambda_{1,2} = \frac{3}{8} \pm j\frac{\sqrt{39}}{8}$, *and* $|\lambda_{1,2}| < 1$. *Now, taking the delay* τ *in* $[\mathbf{d}] = [2, 3]$, *the system (41) becomes unstable, as shown in Figure 5, where the roots localization of the characteristic equation (41) is reported. For more precisions on this example and the loss of stability, see [11].*

Suppose now that we want to stabilize (41), i.e.

$$x(t) + u(t) = \frac{3}{4}x(t-1) - \frac{3}{4}x(t-\tau), \tag{42}$$

with $u(t)$ *the control variable and* $\tau \in [2, 3]$. *We want to stabilize (42) with a control law of the form*

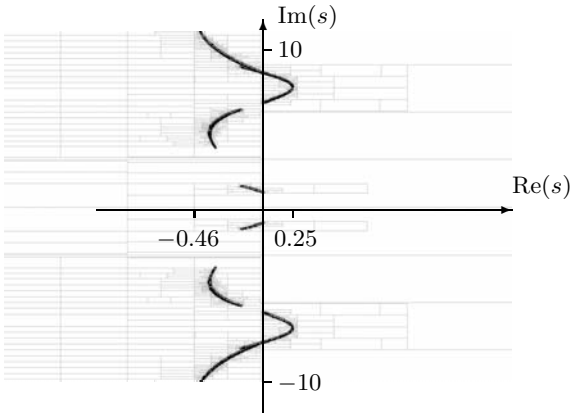

Fig. 5. Roots localization of the characteristic equation of (41), for $\tau \in [2, 3]$

$$u(t) = k_1 x(t) + k_2 x(t-1), \tag{43}$$

with $(k_1, k_2) \in [-5, 5] \times [-3, 3]$ *parameters to be determined (Problem 3.4). Applying the algorithm* SIVIA*, we guarantee the absence of roots with positive real part of the closed loop characteristic equation. In the parametric plane* (k_1, k_2)*, we obtain Figure 6. The white zone is a stable zone of (42) and (43), for all* $\tau \in [2, 3]$*. The dark-grey zone is a non robust stable zone, i.e. in each boxes, there exists at least one value of* (k_1, k_2, τ) *such that the closed loop system (42) and (43) is unstable.*

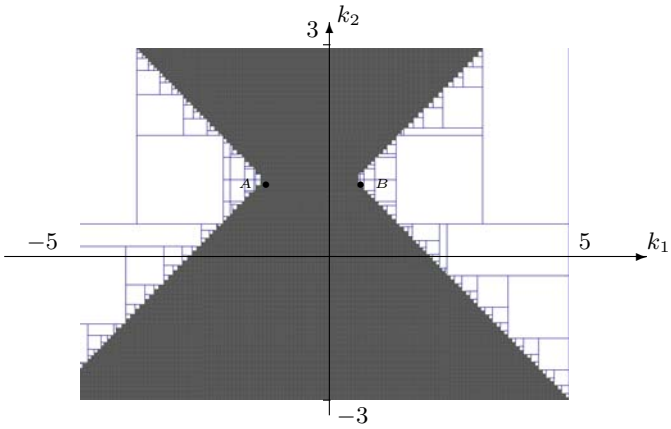

Fig. 6. Parametric regions (k_1, k_2) which ensure robust stability (white zone) of (42) and (43) in closed loop, for $\tau \in [2, 3]$, with $A = (-1.75, 0.75)$ and $B = (-0.25, 0.75)$

3.3 Other Control Problems

We are interested in this section by some other important control problems: the disturbance attenuation problem and the approximative tracking model for time-delays systems.

We choose these two control problems to show the potentiality of interval methods. The objective of this section is to pose simple problems, without establishing theoretical links with existing methods, as for instance H_∞-control. For these methods, the reader is referred to [16], [19], [26], and in references therein.

Consider a time-delays system with transfer function $H(s)$, and the control loop in Figure 7. Denote by u the control law, x the output, w a disturbance acting on u, r a reference trajectory and e the tracking error. The Laplace transforms of these signals are noted $\hat{(\cdot)}(s)$.

Denote by $\mathbf{k}$ the set of all parameters of the feedback $k(s)$ to be determined.

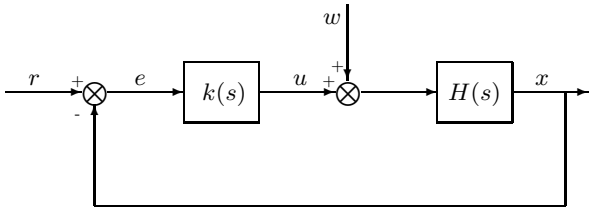

Fig. 7. Control loop of a time-delays system $H(s)$ with a feedback $k(s)$ to be determined

We have

$$\begin{array}{lll} S(s,\mathbf{k}) & = \frac{\hat{e}(s)}{\hat{r}(s)} & = \frac{1}{1+H(s)k(s)} \\ T(s,\mathbf{k}) & = \frac{\hat{x}(s)}{\hat{r}(s)} & = \frac{H(s)k(s)}{1+H(s)k(s)} \\ T_{wx}(s,\mathbf{k}) & = \frac{\hat{x}(s)}{\hat{w}(s)} & = \frac{H(s)}{1+H(s)k(s)} \end{array} . \tag{44}$$

A performance specification can be expressed succinctly by $\|S(s,\mathbf{k})\|_\infty \leq \varepsilon$, or in a more generally form as $\|S(s,\mathbf{k})W_1(s)\|_\infty \leq 1$, where $W_1(s)$ is a weighting function whose magnitude is frequency dependent. A similar reasoning allows to establish inequalities on the transfer $T_{wx}(s,\mathbf{k})$ and $T(s,\mathbf{k})$, with direct applications, respectively to an attenuation disturbance problem and a robust stabilization problem. Furthermore, we have the property of internal stability if all transfer functions in (44) are stable (if others disturbances actuate in the closed loop, all internal transfers must be stable). We solve these frequency inequalities using interval computation.

Problem 3.7. *Let $T_{wx}(s,\mathbf{k})$ be given in (44). We want to find the set parameters $\mathbf{k}$ of $k(s)$ such that*

$$\forall \omega \in \Omega,\ |T_{wx}(j\omega,\mathbf{k})| \leq \frac{1}{|W(j\omega)|},\ \textit{and } T_{wx}(s,\mathbf{k}) \textit{ be stable}, \tag{45}$$

with $\Omega \subset \mathbb{IR}$ a given finite frequency range and $W(s)$ a weighting function.

For example, we can take $W(j\omega) = \frac{1}{\varepsilon}$, $\forall \omega \in \Omega$, with $\varepsilon > 0$ a predefined attenuation parameter. For time-delays systems, as for systems without delays, this condition is often too restrictive [8]. A variable weighting function $W(s)$ allows to attenuate disturbance effects in function of frequency values.

In terms of interval computation, we suppose that $\mathbf{k}$ lie in an acceptable known box $[\mathbf{k}]$, and we are reduced to solve the set inversion problem

$$\mathbb{S} = \left\{ \mathbf{k} \in [\mathbf{k}] \,\middle|\, \forall \omega \in \Omega,\ |T_{wx}(j\omega, \mathbf{k}) W(j\omega)| \leq 1,\ \text{with stability} \right\}. \tag{46}$$

The solution of Problem 3.7 is given by the algorithm SIVIA, and we will choose the coefficients $\mathbf{k}$ of $k(s)$ which guarantee the disturbance attenuation Problem 3.7. The stability is verified in Section 3.2.

With a similar reasoning, we can ensure a disturbance attenuation for an uncertain plant $H(s)$, whose constant uncertain coefficients lie in given bounded intervals.

An interesting point, directly related to an optimal disturbance attenuation, is to find $\mathbf{k_o} \in [\mathbf{k}]$, if it exists, such that

$$\sup_{\omega \in \Omega} |T_{wx}(j\omega, \mathbf{k_o})| = \min_{\mathbf{k} \in [\mathbf{k}]} \sup_{\omega \in \Omega} |T_{wx}(j\omega, \mathbf{k})|,\ \textit{and}\ T_{wx}(s, \mathbf{k_o})\ \textit{be stable.} \tag{47}$$

This kind of problem can be solved with interval methods, as described in Example 3.9.

An another basic problem, although similar to the previous one, is the approximative tracking model.

Problem 3.8. *Let $H(s)$ be a given stable plant, and $H_M(s)$ a stable model transfer function for $H(s)$. The approximate tracking problem is to solve, with the choice of a stable feedback $k(s)$, the inequality*

$$\forall \omega \in \Omega,\ |H_M(j\omega) - H(j\omega)k(j\omega)| \leq \frac{1}{|W(j\omega)|}, \tag{48}$$

with $\Omega \subset \mathbb{R}$ a given finite frequency range and $W(s)$ a given weighting function.

Problem 3.8 is written in a similar form of Problem 3.7, *i.e.*

$$\mathbb{S} = \left\{ \mathbf{k} \in [\mathbf{k}] \,\middle|\, \forall \omega \in \Omega,\ |(H_M(j\omega) - H(j\omega)k(j\omega))W(j\omega)| \leq 1 \right\}, \tag{49}$$

with $k(s)$ be stable. A robust approximate tracking model can be defined and solved with interval methods for uncertain plants. Only the number of parameters to be determined is increased, and the methodology is the same that the previous one.

Example 3.9. *Let a transfer function between a disturbance $w(t)$ and an output $x(t)$:*

$$H(s) = \frac{\hat{x}(s)}{\hat{w}(s)} = \frac{1}{s + a\mathrm{e}^{-s\tau} + b}, \tag{50}$$

with $\tau = 1$, $a = b = 1$. The transfer $H(s)$ is stable (see Section 3.2).

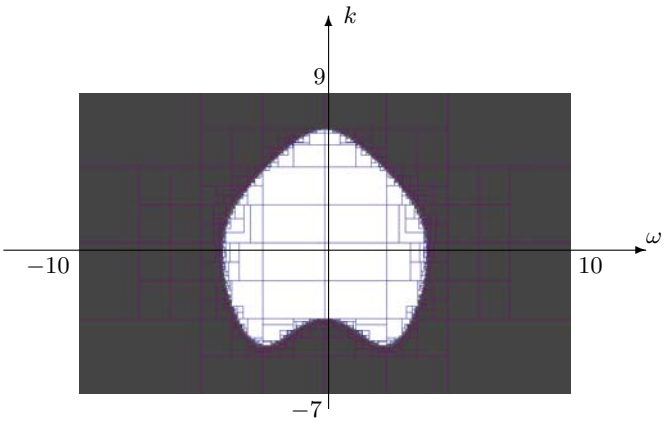

Fig. 8. Set solution $k \in [\mathbf{k}]$ of Example 3.9. Frequencies ω are reported in x-coordinates, and coefficients k in y-coordinates. The size of the white central zone is almost $[-4.1, 4.1] \times [-4.5, 7]$.

We take a feedback $k(s)$ of proportional type, i.e. $\hat{u}(s) = k\hat{x}(s)$, where k is a coefficient to be determined. We want to guarantee

$$\forall \omega \in \Omega,\ |T_{wx}(j\omega, k)| \leq \varepsilon,\ \textit{and}\ T_{wx}(s, k)\ \textit{be stable},$$

where $\Omega = [-1000, 1000]$, $\varepsilon = 0.2$, and $T_{wx}(s, k)$ is given by

$$T_{wx}(s, k) = \frac{1}{s + a\mathrm{e}^{-s\tau} + b - k} \tag{51}$$

For $k \in [\mathbf{k}] = [-7, 9]$, we solve the Problem 3.7 of set inversion by SIVIA*, to obtain the set solution $k \in [\mathbf{k}]$ reported on Figure 8, in function of $\omega \in \Omega$. The white central zone is a no-solution zone, i.e. for a given $k \in [-4.5, 7]$, $\forall \omega \in [-4.1, 4.1]$, $|T_{wx}(j\omega, k)| > \varepsilon$. In the dark-grey zone, the inequality $|T_{wx}(j\omega, k)| \leq \varepsilon$ holds. Then, if we take $k \in [-4.5, 7]$, the norm constraint is not satisfied, and a more complex feedback must be choosen.*

Solutions $k \in [\mathbf{k}]$ are also included in $[-7, -4.5] \cup [7, 9]$. The stability analysis in closed loop implies that $k < -2$, i.e. the set solution is $[-7, -4.5]$.

Take for example $k = -5$. The transfer function (51) is stable, and a Bode magnitude plot is reported on Figure 9. We verify that

$$\sup_{\omega \in \mathbb{IR}} (20 \log 10 |T_{wx}(j\omega)|) = -14 < 20 \log 10(\varepsilon) = -13.98$$

A similar analysis can be done with uncertain constant parameters (a, b, τ).

Consider now the problem of optimal attenuation, i.e. of finding $k_o \in [\mathbf{k}]$ such that

$$\sup_{\omega \in \Omega} |T_{wx}(j\omega, k_o)| = \min_{k \in [\mathbf{k}]} \sup_{\omega \in \Omega} |T_{wx}(j\omega, k)|,\ \textit{and}\ T_{wx}(s, k_o)\ \textit{be stable}. \tag{52}$$

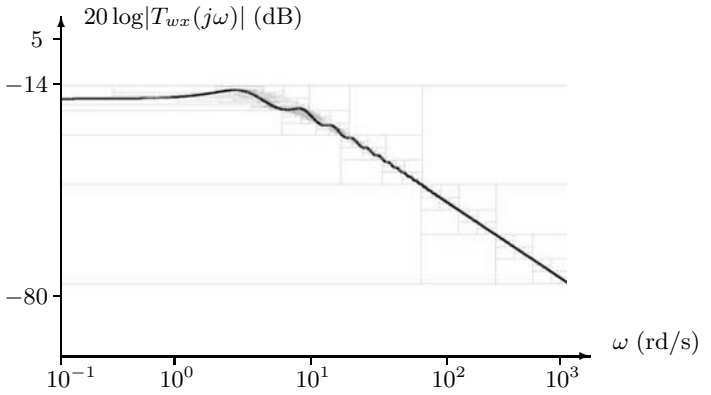

Fig. 9. Bode magnitude plot of (51), with $k = -5$

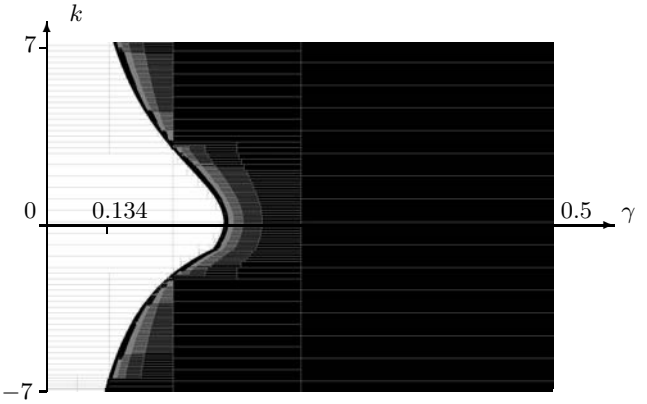

Fig. 10. Set solution (γ, k) of (53)

To solve this optimization problem, we use SIVIA *to analyze the set*

$$\mathbb{S} = \{(k, \gamma) \in [\mathbf{k}] \times \Upsilon \,|\, \forall \omega \in \Omega,\ |T_{wx}(j\omega, k)| \leq \gamma\},$$

Solutions of this problem are given in Figure 10, in the plane (γ, k)*, with* $\gamma \in \Upsilon = [0, 0.5]$ *and* $k \in [-7, 7]$*. The white zone* (γ, k) *is a no-solution zone, i.e. exists* $\omega \in \Omega$ *such that* $|T_{wx}(j\omega, k)| > \gamma$*. The black zone is a solution zone, i.e.* $\forall \omega \in \Omega$, $|T_{wx}(j\omega, k)| \leq \gamma$*. Moreover, on Figure 10, we can determine* k_o *in (52). In fact, it corresponds to*

$$k_o = \min_{\gamma \in \Upsilon} \{k \,|\, \forall \omega \in \Omega,\ |T_{wx}(j\omega, k)| \leq \gamma\},$$

that is in our case $k_o = -7$*. The optimal value of disturbance attenuation is*

$$\sup_{\omega \in \Omega} |T_{wx}(j\omega, k_o)| = 0.134.$$

Example 3.10. *Let* $H(s) = \frac{e^{-s}}{s+s_0}$ *a uncertain plant with* $s_0 \in [0.5, 1.5]$, $H_M(s) = \frac{e^{-s}}{s+2}$ *a model transfer function for* $H(s)$. *We want to ensure a robust approximative model tracking with a controller* $k(s)$ *of the form* $k(s) = \frac{p(s+q)}{s+2}$, *such that*

$$\forall \omega \in \Omega = [-1000, 1000],\ |E(j\omega, \mathbf{k})| = |H_M(j\omega) - H(j\omega)k(j\omega)| \leq 0.2, \quad (53)$$

for $s_0 \in [0.5, 1.5]$ *and* $\mathbf{k} = (p, q) \in [-10, 10] \times [-10, 10]$ *which are the parameters to be determined.*

We are analyzing a problem of type 3.6. The solutions plot is reported in the parametric plane (p, q) *on Figure 11. The grey zone is the solution set of* (p, q) *such that* $\forall(\omega, s_o) \in \Omega \times [0.5, 1.5]$, $|E(j\omega, \mathbf{k})| \leq 0.2$. *The white zone is the*

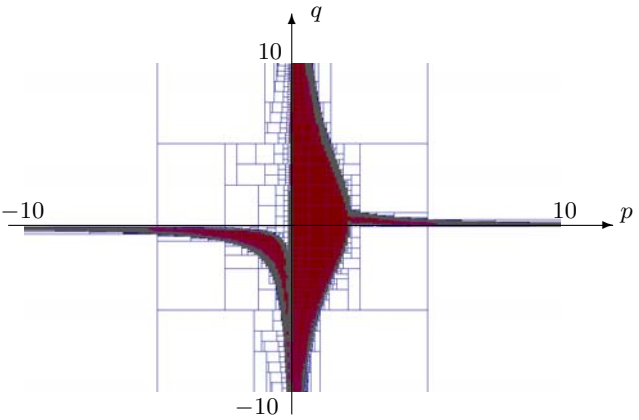

Fig. 11. Set solution (p, q) of (53). The grey zone is the solution set

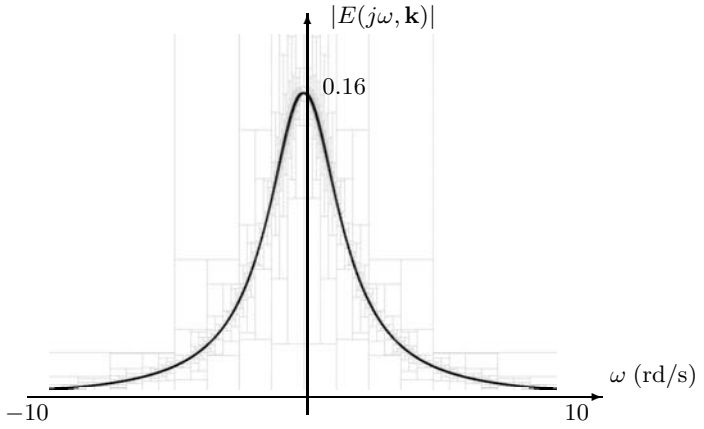

Fig. 12. Magnitude plot of $|E(j\omega, \mathbf{k})|$, for $s_o = 1.5$, and $\mathbf{k} = (p, q) = (1, 1)$

no-solution set of (p, q) *such that* $\exists(\omega, s_o) \in \Omega \times [0.5, 1.5]$ *with* $|E(j\omega, \mathbf{k})| > 0.2$. *For example, taking* $s_0 = 1.5$, $p = 1$ *and* $q = 1$, *we are in the grey zone. A plot of the magnitude* $|E(j\omega, \mathbf{k})|$ *with respect to* ω *is reported on Figure 12. We verify that* $\sup_{\omega \in \Omega} |E(j\omega, \mathbf{k})| = 0.16 < 0.2$. *A choice of* $\mathbf{k}$ *can be made to ensure a minimal tracking error, as seen in the previous example.*

4 Conclusion

In this paper, we apply interval computation to time-delays systems, to solve some control problems, as robust stability, stabilization, or disturbance attenuation by feedback. Basic illustrative examples are reported, to clarify interval methods.

In spite of a limit on the parameters number, interval computation allows to obtain guaranteed solutions for a large number of control problems, and that in an original way for time-delays systems. Graphical solutions allow an easy interpretation of physical phenomena.

References

1. Barmish B. R., Hollot C. V., Kraus F. J., Tempo R. (1992) Extreme Points Results for Robust Stabilization of Interval Plants with First Order Compensators. IEEE Transactions on Automatic Control 37:707–714
2. Bellman R., Cooke K. L. (1963) Differential–difference equations, Academic Press, New York
3. Benhamou F., Goualard F., Granvilliers L., Puget J. F. (1999) Revising Hull and Box Consistency. In Proc. Int. Conf. Logic Programming, Las Cruces, New Mexico
4. Chen J., Niculescu S. I. (2004) Robust Stability of Quasipolynomials: Vertex–Type Tests and Extensions. In Proc. ACC, pp. 4159–4164, Boston, Massachussets
5. Cleary J. G. (1987) Logical arithmetic, Future Computing Systems 2:125–149
6. Dao M., Di Loreto M., Jaulin L., Lafay J. F., Loiseau J. J. (2004) Application du calcul par intervalles aux systèmes à retards. In Proc. CIFA, Douz, Tunisia
7. Davis E. (1987) Constraint propagation with interval labels. Artificial Intelligence 32:281–331
8. Doyle J., Francis B., Tannenbaum A. (1992) Feedback Control Theory, Macmillan, Houndmills
9. Engelborghs K., Roose D. (2002) On stability of LMS–methods and characteristic roots of delay differential equations. SIAM J. Numerical Analysis 40:629–650
10. Gu K., Kharitonov V. L., Chen J. (2002) Stability of time–delay systems. Birkhauser, Boston
11. Hale J. K., Verduyn Lunel S. M. (1993) Introduction to Functional Differential Equations. Springer–Verlag, Berlin Heidelberg New York
12. Hohenbichler N., Ackermann J. (2003) Computing stable regions in parameter spaces for a class of quasipolynomials. In Proc. 4th IFAC TDS, Rocquencourt, France
13. Jaulin L., Kieffer M., Didrit O., Walter E. (2001) Applied interval analysis, Springer, Berlin Heidelberg New York

14. Kamen E. W. (1982) Linear systems with commensurate time delays: Stability and stabilization independent of delay. IEEE Transactions on Automatic Control 27:367–375
15. Kharitonov V. L, Zhabko A. (1994) Robust Stability for Time–Delay Systems. IEEE Transactions on Automatic Control 39:2388–2397
16. Kojima A., Ishijima S. (2001) H_∞ control for preview and delayed strategies. In Proc. 40th IEEE Conf. Decision Control, pp. 991–996, Orlando, Florida
17. Kolmanovskii V., Myshkis A. (1992) Applied theory of functional differential equations, Kluwer Academic Publishers, Dordrecht
18. Lhomme O. (1993) Consistency techniques for numeric CSPs. Proc. Int. Conf. Artificial Intelligence, pp. 232–238, Chambéry, France
19. Meinsma G., Zwart H. (2000) On H_∞ control for dead–time systems. IEEE Transactions on Automatic Control 45:272–285
20. Moore R. E. (1966) Interval Analysis. Prentice–Hall, Englewood Cliffs
21. Moore R. E. (1979) Methods and Applications of Interval Analysis. SIAM, Philadelphia
22. Moore R. E., Ratschek H. (1988) Inclusion function and global optimization. Mathematical Programing 41(3):341–356
23. Mori T., Kokame H. (1989) Stability of $\dot{x}(t) = Ax(t)+Bx(t-\tau)$. IEEE Transactions on Automatic Control 34:460–462
24. Nagpal K., Ravi R. (1997) H_∞ control and estimation problems with delayed measurements: State space solutions. SIAM J. Control Optimization 35:1217–1243
25. Neumaier A. (1990) Interval Methods for Systems of Equations. Cambridge University Press, Cambridge
26. Niculescu S. I. (2001) Delay Effects on Stability: A Robust Control Approach. Springer, Berlin Heidelberg New York
27. Santos J., Mondié S., Kharitonov V. (2003) Robust stability of time delay systems and the finite inclusions theorem. In Proc. 4th IFAC TDS, Rocquencourt, France
28. Tzypkin Y. Z., Fu M. (1993) Robust stability of time–delay systems with an uncertain time–delay constant. International J. Control 57:865–879
29. Verriest E. I., Fan M., Kullstam J. (1993) Frequency domain robust stability criteria for linear delay systems. In Proc. 32nd IEEE Conf. Decision Control, pp. 3473–3478, San Antonio, Texas
30. Vyhlídal T., Zítek P. (2003) Quasipolynomial mapping based rootfinder for analysis of time delay systems. In Proc. 4th IFAC TDS, Rocquencourt, France
31. Walter E., Jaulin L. (1994) Guaranteed characterization of stability domains via set inversion. IEEE Transactions on Automatic Control 39:886–889

Mathematical and Computational Tools for the Stability Analysis of Time-Varying Delay Systems and Applications in Mechanical Engineering

Wim Michiels[1], Koen Verheyden[1], and Silviu-Iulian Niculescu[2]

[1] Department of Computer Science, K.U. Leuven, Celestijnenlaan 200A, B-3001 Heverlee, Belgium
{Wim.Michiels,Koen.Verheyden}@cs.kuleuven.be
[2] HEUDIASYC (UMR CNRS 6599), Université de Technologie de Compiègne, Centre de Recherche de Royallieu, BP 20529, 60205, Compiègne, cedex, France
Silviu.Niculescu@hds.utc.fr

Summary. An overview of eigenvalue based tools for the stability analysis of linear periodic systems with delays is presented. It is assumed that both the system matrices and the delays are periodically varying. First the situation is considered where the time-variation of the periodic terms is fast compared to the system's dynamics. Then averaging techniques are used to relate the stability properties of the time-varying system with these of a time-invariant one, which opens the possibility to use frequency domain tools. As a special characteristic the averaged system exhibits distributed delays if the delays in the original system are time-varying. Both analytic and numerical tools for the stability analysis of the averaged system are discussed. Special attention is paid to the characterization of situations where a variation of a delay has a stabilizing effect. Second, the assumption underlying the averaging approach is dropped. It is described how exact stability information of the original, periodic system can be directly computed. The two approaches are briefly compared with respect to generality, applicability and computational efficiency. Finally the results are illustrated by means of two examples from mechanical engineering. The first example concerns a model of a variable speed rotating cutting tool. Based on the developed theory and using the described computational tools, both a theoretical explanation and a quantitative analysis are provided of the beneficial effect of a variation of the machine speed on enhancing stability properties, which was reported in the literature. The second example concerns the stability analysis of an elastic column, subjected to a periodic force.

Keywords: time-delay systems, linear periodic systems, averaging, collocation, stability of variable speed machines.

Introduction

We discuss mathematical and computational tools for the stability analysis of linear time-varying delay systems of the form

J. Chiasson and J.J. Loiseau (Eds.): Appl. of Time Delay Systems, LNCIS 352, pp. 199–216, 2007.
springerlink.com

$$\dot{x}(t) = A(\omega t)\ x(t) + B(\omega t)\ x(t - \tau(t)), \tag{1}$$
$$\tau(t) = \tau_0 + \delta f(\Omega t), \tag{2}$$

under appropriate initial conditions. We assume that $x \in \mathbb{R}^n$, $A : \mathbb{R} \to \mathbb{R}^{n\times n}$ and $B : \mathbb{R} \to \mathbb{R}^{n\times n}$ are bounded periodic functions with period 2π, $f : \mathbb{R} \to [-1,\ 1]$ is a periodic function with zero mean and period 2π, $\max f = 1$ and $\min f = -1$. Further, we have $\delta, \tau_0, \omega, \Omega \in \mathbb{R}_0^+$ and $\delta \leq \tau_0$. In this way, the parameters δ and Ω determine the amplitude and frequency of the delay variation, while ω determines the frequency of the variation of A and B . We do not a priori require that ω and Ω are correlated, although such a correlation exists in many applications.

The problem under consideration is inspired by applications in mechanical engineering. More precisely, in the manufacturing literature one encounters models of the form (1) for the dynamics of rotating cutting and milling machines, see e.g. [19, 40] and the references therein. In cutting machines, a workpiece rotates and the cutting inserts have a fixed position, while in milling machines the workpiece is fixed and the cutting inserts are mounted on a rotating axis. In both cases the time-delay represents the time taken for one revolution of the workpiece or cutting inserts. Therefore, it is proportional to the inverse of the rotational speed of the machine. In models for cutting machines the system matrices are typically constant, whereas they are periodically varying in models for milling machines, due to the varying angle between the cutting inserts and the workpiece. The nominal behavior of the machines corresponds to an asymptotically stable steady state solution. A loss of stability is undesired as it leads to chatter, that is, unwanted oscillations which cause irregularities in the surface of the workpiece to be processed. A typical approach to enlarge the stability region of the steady state solution of such rotating machines in a relevant parameter space consists of *fast modulating* the speed around the nominal value [19, 39]. Such a modulation of the speed precisely corresponds to a modulation of the time-delay in the model (1) of the form (2). Note that an analysis of this stabilization approach calls for mathematical tools which are also capable to characterize situations where a variation of a delay has a stabilizing effect.

If the time-variation of a delay is fast compared to the system's dynamics, then rather its distribution than its precise dependence upon time determines the stability properties of the system, as we shall see in the Section 1. This makes some of the described results directly applicable to the emerging field of network controlled systems also, since the varying delays in communication networks are typically of a stochastic nature, yet knowledge is available about their distribution, see, for instance, [36, 41] and the references therein.

This chapter is devoted to a presentation of *eigenvalue based techniques* for the stability analysis of the system (1)-(2). As an advantage w.r.t. most time-domain approaches, they lead to non-conservative results, in the sense that exact stability information is available (in terms of eigenvalues of appropriate operators), instead of sufficient stability conditions. Furthermore, the combination with a detection of critical eigenvalues and a continuation facility allows to compute the boundaries of stability regions in parameter spaces in a (numerically tractable) efficient and semi-automatic way. For systems with time-varying delay an

additional advantage lies in the fact that stabilizing effects of a delay variation can be investigated, which is not possible with approaches where a variation of the delay around a nominal value is explicitly or implicitly treated as uncertainty. Notice that time-integration (simulation), see [2] for an overview of methods, can in principle also be used to determine stability of (1)-(2) and stability regions in parameter spaces, yet it is time-consuming and boundaries of stability regions are hard to determine accurately.

The structure of the chapter is as follows: Section 1 is devoted to the case where the time-variation of the periodic terms is fast compared to the system's dynamics, while Section 2 deals with the general case. Two practical examples are presented in Section 3. The conclusions are formulated in Section 4.

1 Fast Varying Coefficients

Using averaging techniques it is shown first how the stability analysis problem of the system (1)-(2) for large values of ω and Ω can be reduced to the stability analysis of a *time-invariant* system exhibiting distributed delays. Next, computational and analytical tools for the averaged system are briefly discussed.

1.1 Averaging of the Periodic System

As an indication that the system (1)-(2) with parameters ω and Ω is suitable for averaging, observe that the upper bound in the estimate

$$\|\dot{x}(t)\| \leq \left(\max_s \|A(s)\| + \|B(s)\|\right) \max_{s\in[t-\tau_0-\delta,\ t]} \|x(s)\|$$

does not depend on the values of ω and Ω. This suggests that, on compact time-intervals, the trajectories of the system have a limit as $\omega, \Omega \to \infty$. In fact, due to the filtering property of the integration process, the parameters ω and Ω regulate the separation between time-scale associated with the periodically varying coefficients and the time-scale associated with the long-term behavior of the solutions, which forms the backbone of the averaging approach.

Averaging methods for periodic systems described by ordinary differential equations with a fast varying right-hand side are discussed in e.g. [38] and extended to delay differential equations with constant delays in [21]. Averaging methods for time-varying delays are treated in [28]. Their combination leads to the following result, which slightly generalizes [28, Theorem 1]:

Theorem 1. *Consider the system (1) and (2). Let the integrable function*[1] $w : [-1,\ 1] \to \mathbb{R}^+$ *be defined by the relation:*

$$\int_{-1}^{1} \alpha(t)w(t)dt = \frac{1}{2\pi}\int_0^{2\pi} \alpha(f(t))dt, \quad \forall \alpha \in \mathcal{C}([-1,\ 1],\ \mathbb{R}), \tag{3}$$

[1] More precisely, w represents a positive density measure.

and let

$$\bar{A} = \frac{1}{2\pi}\int_t^{t+2\pi} A(s)\ ds,\ \bar{B} = \frac{1}{2\pi}\int_t^{t+2\pi} B(s)\ ds. \tag{4}$$

If the averaged system

$$\dot{x}(t) = \bar{A}x(t) + \bar{B}\int_{t-\tau_0-\delta}^{t-\tau_0+\delta} \frac{w((t-\tau_0-\theta)/\delta)}{\delta} x(\theta)d\theta. \tag{5}$$

is asymptotically stable, then there exists a threshold ω_c such that the system (1) and (2) is globally uniformly asymptotically stable for all $\Omega > \omega_c$ and $\omega > \omega_c$.

Sketch of the proof. The existence of an integrable function w satisfying (3) follows from a change of measure and the Radon-Nikodym theorem (see [37]).

The proof of the stability assertion is based on an application of the *trajectory based proof technique*, developed in e.g. [30] for the stability analysis of ordinary differential equations and extended and applied to classes of delay differential equations in [31]. It relates closeness results for trajectories (in the sense of uniform convergence of trajectories on compact time-intervals) with stability results (which involve the behavior of trajectories on infinite time-intervals). The main steps are as follows:

1. One proves that trajectories of (1)-(2) and (5) with matching initial conditions uniformly converge to each other on *compact time-intervals* as the parameters ω and Ω tend to infinity. This is done by estimating the deviation between the solutions of (1)-(2) and (5) at time-instants later than the initial time, and involves the application of a generalization of the celebrated Gronwall Lemma.
2. This closeness result of trajectories of (5) and (1)-(2) is linked with stability assertions. By a slight generalization of [30, Theorem 1], one can conclude from the exponential stability of (5) and the closeness result that the null solution of system (1)-(2) is practically uniformly asymptotically stable (see [28] for a precise definition).
3. Practical uniform asymptotic stability of the null solution of (1)-(2) implies global uniform asymptotic stability by a scaling property of its solutions. □

Remark 1. Under the conditions of the theorem the asymptotic stability of (1)-(2) is only guaranteed if Ω and ω are sufficiently large. An explicit bound ω_c may be obtained from theoretical considerations, see for instance the discussion in [29], but such bounds are typically conservative. Therefore, it is advised to determine a threshold based on numerical simulation (if desired), and to switch to the methods described in the next section if there are indications that the separation of time-scales may not be sufficient.

Remark 2. From the definition (3) the weight function w can be interpreted as the probability distribution of $f(\zeta)$, where ζ is uniformly distributed over the interval $[0,\ 2\pi]$. This interpretation is often very useful to compute the function w out of f and offers an alternative for using the definition (3) directly. It also lays the basis for an extension of the theorem to classes of systems where the time-delay is a random variable with a known probability density function.

The importance of a reduction to a time-invariant system lies in the fact that frequency domain techniques become applicable. For instance, the stability of the averaged system (5) is determined by its rightmost eigenvalues. These are the roots of the characteristic equation, which can be written in the form

$$\det\left(sI - \bar{A} - \bar{B}e^{-s\tau_0}g(s\delta)\right) = 0, \tag{6}$$

where

$$g(s) = \int_{-1}^{1} e^{-st}w(t)dt. \tag{7}$$

Notice that the $g(s)$ can be interpreted as a correction of $e^{-s\tau_0}$, corresponding to the mean delay value τ_0, and takes all the effects of the delay *variation* into account. As an illustration, several tuples (f, w, g), characterizing the varying part of the delay, are displayed in Table 1.

Table 1. For three examples of f in (2), the corresponding weight function w of the distributed delay comparison system (5), as well as the correction term $g(s)$ in the characteristic equation (6) are shown. $J_0(.)$ denotes the Bessel function of the first kind of order zero, $h(.)$ is the Dirac impulse function. Notice that w can be seen as the probability density function of the image of f

f	w	g
$f_1(t) = \begin{cases} \frac{2}{\pi}(t - \frac{\pi}{2}), & t \in [0,\ \pi) \\ \frac{2}{\pi}(\frac{3\pi}{2} - t), & t \in [\pi,\ 2\pi) \end{cases}$ (sawtooth)	$w_1(t) = \frac{1}{2}$	$g_1(s) = \begin{cases} \frac{\sinh s}{s}, & s \neq 0 \\ 1, & s = 0 \end{cases}$
$f_2(t) = \sin(t)$	$w_2(t) = \frac{1}{\pi\sqrt{1-t^2}}$	$g_2(s) = J_0(js)$
$f_3(t) = \begin{cases} 1, & t \in [0,\ \pi) \\ -1, & t \in [\pi,\ 2\pi) \end{cases}$ (square wave)	$w_3(t) = \frac{h(t-1)+h(t+1)}{2}$	$g_3(s) = \cosh(s)$

1.2 Computational Tools

Motivated by the distributed delay in the comparison system (5), we give an overview of tools to compute the rightmost eigenvalues of integro-differential equations of retarded type, that is, delay differential equations of retarded type that contain terms of the form

$$\int_{\tau_1}^{\tau_2} K(\theta)x(t-\theta)\,\mathrm{d}\theta, \tag{8}$$

with measurable *kernel function* $K(\cdot) \in \mathbb{R}^{n\times n}$ and $\tau_1 \leqslant \tau_2$.

First, we consider the trivial case where the kernel is a constant matrix times the *Dirac impulse*, i.e., $K(\theta) \equiv Kh(\theta - \tau_0)$ with $\tau_1 \leqslant \tau_0 \leqslant \tau_2$. Then, the integral (8) equals $K\,x(t-\tau_0)$ and the integro-differential equation reduces to an equation with a point-wise delay. Various methods for determining the rightmost

eigenvalues of systems with point-wise delays have been proposed in the literature. These include, but are not limited to, methods based on discretizing the solution operator associated with the equation (see, for instance, [12]) and methods based on discretizing its infinitesimal generator [4]. The stability routine for equilibria, contained in the software package DDE-BIFTOOL [10, 11], is based on the former approach.

Integro-differential equations with a constant kernel or a *gamma distribution* kernel, that is

$$K(\theta) = K\theta^j \mathrm{e}^{-\alpha\theta}, \tag{9}$$

where j is a positive integer, are treated in [24]. It is shown how a bifurcation analysis of this type of equations can be done using computational tools for point-wise delay equations. In [23, 25] the numerical stability analysis of scalar equations with more general bounded kernels is discussed. The equations are discretized using a linear multi-step method and a quadrature method, based on Lagrange interpolation and a Gauss-Legendre quadrature rule.

Finally, we consider an integro-differential equation where the term (8) takes the form

$$K \int_{\tau_1}^{\tau_2} \frac{1}{\sqrt{1-(\theta-\tau_\mathrm{m})^2/\delta^2}} x(t-\theta)\,\mathrm{d}\theta, \tag{10}$$

with $\tau_\mathrm{m} := (\tau_1 + \tau_2)/2$ and $\delta := (\tau_2 - \tau_1)/2$. The kernel function corresponds to $w_2(\cdot)$ in the second row of Table 1, and goes to infinity at the boundaries of the integration interval. A natural way to handle this problem is to expand the (perturbed) trajectories in terms of the polynomials that are orthogonal w.r.t. the weighted $\mathcal{L}_2$ inner product $\langle p_1, p_2 \rangle := \int w_2 p_1 p_2$. In this way one arrives at the well-known *Chebyshev polynomials*, used frequently in spectral collocation methods [42].

1.3 Analytical Tools

Determining analytically the sensitivity of eigenvalues with respect to parameters is a useful tool for characterizing stabilizability properties. Following this approach, the effects of constant delays on stability have been thoroughly analyzed in the literature, see e.g. [6, 33, 32, 27]. Here, we examine the effects of a fast *variation* of parameters around a nominal value.

As follows from (4) and an application of the trajectory based proof technique, an exponentially unstable system of the form (1)-(2), with constant A, B and τ, cannot be stabilized by introducing a fast modulation of the matrices A and B, as long as their mean value remains the same. Therefore, we restrict ourselves to the stabilizability by means of a fast delay variation. By virtue of Theorem 1, the latter is implied by the stabilizability by means of a delay 'distribution'. In this way, we arrive at investigating how the eigenvalues of (5), or equivalently, the zeros of

$$H(s, g(s\delta)) := \det\left(sI - \bar{A} - \bar{B}e^{-s\tau_0} g(s\delta)\right) \tag{11}$$

behave for small values of $\delta \geq 0$. For $\delta = 0$, this expression simplifies to

$$\det\left(sI - \bar{A} - \bar{B}e^{-s\tau_0}\right), \tag{12}$$

the characteristic quasiploynomial of the constant delay system.

Because g is a smooth function, the zeros of (11) are continuous at each value of parameter $\delta \geq 0$. For a given zero s_0 of (12) with multiplicity one, this implies the existence of a root function $r(\delta)$ of (11), satisfying $r(0) = s_0$ and

$$H(r(\delta), g(r(\delta)\delta)) = 0. \tag{13}$$

To compute the sensitivity of the zero s_0 w.r.t. δ, we differentiate (13), leading to

$$r'(0) = 0, \tag{14}$$

$$r''(0) = -\frac{\frac{\partial H}{\partial g}(s_0, 1)}{\frac{\partial H}{\partial s}(s_0, 1)}\, g''(0)s_0^2, \tag{15}$$

where $g''(0) = \int_{-1}^{1} t^2 w(t)dt > 0$. A stability related corollary is:

Proposition 1. *Assume that the rightmost eigenvalues of (12) are simple and on the imaginary axis. Denote them by* $j\omega_i,\ i = 1, m$. *If*

$$\Re\left\{\frac{\frac{\partial H}{\partial g}(j\omega_i, 1)}{\frac{\partial H}{\partial s}(j\omega_i, 1)}\right\} < 0, \quad i = 1, \ldots, m, \tag{16}$$

then the system (5) is asymptotically stable for small values of δ.

In Section 3 we will discuss a *parameterized* system, for which condition (16) is always satisfied[2] in case of eigenvalues on the imaginary axis. This means that stability regions in the parameter space become *larger* when increasing δ from zero. Indeed, internal points of a stability region in the parameter space correspond to *asymptotic* stability of the system, which is preserved by increasing δ from zero (continuity argument), whereas points on the boundaries of a stability region, if any, correspond to a system having its rightmost eigenvalues on the imaginary axis, which becomes asymptotically stable under the conditions of Proposition 1. Notice that parameter values corresponding to a *zero* eigenvalue are invariant w.r.t. δ, following from $g(0) = 1$.

Compared to the numerical tools described in the § 1.2, which allow to compute stability information of (5) for all values of the parameters, analytical tools such as the ones described above are less powerful in the sense that they are suitable for asymptotic results only (e.g. stability assertions for small δ in Proposition 1). However, they are more powerful in the sense that they allow us for instance to make assertions about stabilizability by means of a delay variation, *independently* of the precise in which the delay is varied (notice that the condition (16) is independent of the choice of g and, thus, of f). This illustrates the *complementarity* of analytical and numerical methods.

[2] Such a situation is likely to occur, as motivated in [28].

2 General Case

In this section, no assumptions are made on the size of the frequencies ω and Ω in system (1)–(2). First, the *collocation* scheme for computing solutions of (1)-(2) is outlined. Next, the computation of stability determining eigenvalues corresponding to the zero solution is described, as well as the computation of the boundaries of stability regions. Then a special case is commented on, where a reduction to a time-invariant system is still possible. Finally, a comparison with the averaging based approach of the previous section is made.

For technical reasons it is assumed throughout the section that ω and Ω are rationally dependent, and that the functions f, A and B in (1)-(2) are smooth.

2.1 Collocation Scheme

By means of the system (1)-(2) we explain the collocation scheme to compute a trajectory of a periodic systems with delays for a given initial condition. This collocation variant is based on [45,44] (see also [9]).

Denote by T the least common multiple of $2\pi/\omega$ and $2\pi/\Omega$. Hence there exist integers k and K so that $T\omega = 2\pi k$ and $T\Omega = 2\pi K$. For simplicity, we call T the *period* of the system (1)–(2). Instead of solving the latter system, we rescale the time variable by $1/T$ such that the period is one in the transformed time. The transformed system is

$$\dot{x}(t) = TA(2\pi kt)x(t) + TB(2\pi kt)x(t - \sigma(t)), \tag{17}$$

$$\sigma(t) = \frac{\tau_0}{T} + \frac{\delta}{T} f(2\pi Kt). \tag{18}$$

We represent a trajectory $x(t)$ of (17)–(18) by a continuous piecewise polynomial, or *spline*. The mesh used for this *discrete* approximation is constructed as follows. First, let $\{0 = t_0 < t_1 < \ldots < t_m = 1\}$ be a mesh on $[0, 1]$ with m mesh intervals. Next, this mesh is periodically extended to the left to obtain a mesh on $[t_{-\ell}, 1]$ with $\ell + m$ intervals. For notational convenience, we use the variable $x(t)$ also for the piecewise polynomial approximation on this extended mesh. Since it is desirable that the trajectory $x(t)$ for $t > 0$ can be obtained by time-stepping if $x(t)$ on the initial interval $[t_{-\ell}, 0]$ is given, we choose ℓ such that $t_{-\ell} \leq \sigma_{\min} < t_{-\ell+1}$, where $\sigma_{\min}$ is the minimal value of $t - \sigma(t)$ for $t \in [0, 1]$. Note that the discrete approximation has $n((\ell + m)d + 1)$ degrees of freedom, where d is the dimension of the spline.

For ease of implementation, the piecewise polynomial is represented as a linear combination of basis functions $\phi_{i+\frac{j}{d}}(t)$ that are only "locally" non-zero. More specifically, the restriction of the unknown trajectory to the interval $[t_i, t_{i+1}]$ can be written as

$$\sum_{j=0}^{d} c_{i+\frac{j}{d}} \phi_{i+\frac{j}{d}}(t), \tag{19}$$

with unknown coefficients $c_{i+\frac{j}{d}} \in \mathbb{R}^{n\times 1}$.

Next, we write down the conditions that determine the discrete approximation. Firstly, *collocation requirements* are imposed, i.e., the equations (17)–(18) have to be satisfied in a number of points, i.e.

$$\dot{x}(c_{i,\nu}) = TA(2\pi k c_{i,\nu})x(t) + TB(2\pi k c_{i,\nu})x(c_{i,\nu} - \sigma(c_{i,\nu})), \tag{20}$$

$$\sigma(c_{i,\nu}) = \frac{\tau_0}{T} + \frac{\delta}{T} f(2\pi K c_{i,\nu}). \tag{21}$$

The so-called *collocation points*,

$$c_{i,\nu} := t_i + \Delta t_i z_\nu, \quad \text{for } i = 0, \ldots, m-1 \text{ and } \nu = 1, \ldots d, \tag{22}$$

where $\Delta t_i := t_{i+1} - t_i$, are obtained by scaling and shifting the set of *collocation parameters* $z_\nu \in [0, 1]$. In the case of *Gauss-Legendre collocation*, one chooses z_ν as the zeros of the *Legendre polynomial* of degree d on $[0, 1]$; see, e.g., the bifurcation packages AUTO [7] (for ordinary differential equations) and DDE-BIFTOOL [11, 10] (for delay differential equations). In our implementation, on the contrary, we choose the collocation parameters to be the zeros of the *Radau polynomial* of degree d, which is defined as the difference between the Legendre polynomials of degree d and degree $d-1$. By construction, the Radau polynomial vanishes at the right endpoint, so that $z_d = 1$ is a collocation parameter. Consequently, the equations (17)–(18) are satisfied at the mesh points t_i. Secondly, besides the md collocation requirements (20)-(21), $n(\ell d + 1)$ additional requirements are imposed. These can be used to specify the initial condition, see Section 2.2 and 2.3.

The resulting nonlinear system of equations can be solved by using Newton iterations. In each iteration, a linearized system is solved. A typical structure for this matrix is shown in [45, Fig. 1]. In general, the Newton iterations converge if the initial guess is "close enough" to the exact solution.

2.2 Computation of the Stability Determining Eigenvalues

A complex number s is an eigenvalue, or *(characteristic) root*, of (17)-(18) if and only if there exists a 'perturbation' of the zero solution of the form

$$x(t) = \mathrm{e}^{st} p(t), \tag{23}$$

where $p(t)$ is 1-periodic. This particular solution satisfies $x(t+1) = \mathrm{e}^s x(t)$ for all t, where e^s is called a *(characteristic) multiplier*. It follows that the multipliers are the eigenvalues of the linear map between the restriction of a trajectory $x(t)$ on the time intervals $[t_{-\ell}, 0]$ and $[t_{-\ell} + 1, 1]$. This map is called the *monodromy operator* if the system (17)–(18) *before* discretization is considered. *After* discretization, the map becomes finite-dimensional and is called the *monodromy matrix*.

The monodromy matrix of (17)-(18) is readily obtained from the collocation requirements (20)-(21). Indeed, the $\ell d + 1$ remaining degrees of freedom can be used to specify the solution on $[t_{-\ell}, 0]$. By solving the resulting system of equations, the corresponding solution on $[t_{-\ell} + 1, 1]$ is recovered.

The eigenvalues of the monodromy matrix can be computed by the QR algorithm, a reliable procedure that returns the all eigenvalues of a matrix. Note that only the rightmost ones are good approximations to the exact eigenvalues of the system (1)–(2) (before discretization). However, precisely these eigenvalues determine the stability of the system. If the monodromy matrix is "large", then it is much more efficient to use large-scale eigenvalue solvers, such as the *Arnoldi method* or the *Jacobi-Davidson method*, cf. [1]. These methods rely on matrix-vector products only, which can efficiently computed, and return only the small number of stability-determining eigenvalues. The monodromy matrix of the example in Section 3 is of moderate size, so that the QR method could be used. The choice of the large-scale methods to be considered depend on different factors (see, e.g. the structure and spectrum of the matrix). Finally, note that other numerical methods to compute the eigenvalues are described in e.g. [18,5].

2.3 Computation of Stability Regions

When parameters are changes, a loss of stability of the zero solution of (17)-(18) is associated with an eigenvalue s that crosses the imaginary axis. In that case, $|\mathrm{e}^s| = 1$, i.e., $s = \mathrm{i}\vartheta$ with $\vartheta \in \mathbb{R}$. Two cases can be distinguished :

- $|\mathrm{e}^{\mathrm{i}\vartheta}| = 1$ and ϑ/π is integer,
- $|\mathrm{e}^{\mathrm{i}\vartheta}| = 1$, but ϑ/π is *not* integer.

The latter case, which generically occurs, corresponds to a *torus bifurcation point*. This paragraph discusses the computation of curves of torus bifurcation points in a parameter space. By using this procedure, stability regions can be traced efficiently and in a semi-automatic way.

First, we treat the computation of one torus bifurcation point, which requires that one model parameter, say η, is freed. The unknowns are the bifurcation value of η and the trajectory $x(t) := p(t)\exp(i\vartheta t)$ corresponding to the multiplier on the unit circle, see (23). Remark that $p(t)$ is complex-valued, since the eigenvalue s is complex. Hence $p(t)$ has $2n((\ell+m)d+1)$ real degrees of freedom and the total number of degrees of freedom is $2n((\ell+m)d+1)+2$. There are nmd complex (or $2nmd$ real) collocation requirements (20)–(21). Additionally, we impose $n(\ell d+1)$ complex (or $2n(\ell d+1)$ real) requirements that specify the boundary value problem, namely requirements that express the periodicity of $p(t)$. Finally, the *normalization* of the unknown $x(t)$ gives one complex requirement (or two real ones). Typically, one requires that the (complex) inner product of $x(t)$ and a given $c(t) \approx x(t)$ equals one. In summary, the total number of (real) requirements and unknowns are both $2n((\ell+m)d+1)+2$ and Newton's method can be used to solve this system of equations.

Next, we make free a second parameter, say ζ, and outline the continuation of a curve of torus bifurcations in the two-parameter space (η, ζ). To compute a new point of the curve, an extra condition has to be added to the defining system of equations, in order to ensure uniqueness, and a starting value for the Newton iterations needs to be generated. A good starting value $(\hat{x}(t), \hat{\vartheta}, \hat{\eta}, \hat{\zeta})$ can be computed using the previous points on the curve. The easiest procedure to do

so, the *secant predictor*, constructs an initial guess along the the direction defined by the two previous points on the curve. Since it is desirable that the continuation procedure does not fail if the curve is not single-valued w.r.t. parameter η nor ζ, e.g. a closed curve, we add a *pseudo-arclength* steplength condition [8] to the equations to specify completely the new point search for, that is,

$$w_\vartheta(\vartheta - \hat{\vartheta})\dot{\vartheta} + w_p \left[\, \eta - \hat{\eta}\ \zeta - \hat{\zeta}\, \right] \begin{bmatrix} \dot{\eta} \\ \dot{\zeta} \end{bmatrix} = 0, \tag{24}$$

where $(\dot{\vartheta},\ \dot{\eta},\ \dot{\zeta})$ is the direction of the secant predictor. Here the *weights* w_ϑ and w_p are usually chosen to be one.

2.4 Special Case

If the time-dependence of $A(\cdot)$ and $B(\cdot)$ and $\tau(\cdot)$ can be replaced by a dependence on a *finite* number of harmonics,

$$c_j := \cos\left(\frac{2\pi j}{T}t\right) \quad \text{and} \quad s_j := \sin\left(\frac{2\pi j}{T}t\right), \quad j = 1, \ldots l, \tag{25}$$

then the system (1)–(2) can be transformed into a *time-invariant* system with state-dependent delay [43]. The latter takes the form (with a slight abuse of notation):

$$\begin{aligned} \dot{x}(t) &= A(c_1, s_1)\ x(t) + B(c_1, s_1)\ x(t - \tau(c_1, s_1)), \\ \dot{c}_1(t) &= -\tfrac{2\pi j}{T} s_1(t) + \gamma c_1(t)\left(1 - c_1(t)^2 - s_1(t)^2\right), \\ \dot{s}_1(t) &= \tfrac{2\pi j}{T} j c_1(t) + \gamma s_1(t)\left(1 - c_1(t)^2 - s_1(t)^2\right), \end{aligned} \tag{26}$$

where $\gamma > 0$ and $(c_j, s_j),\ j > 1$, are expressed as a function of c_1 and c_2 by means of trigonometric formulae [3]. In this way the stability analysis of the zero solution of (1)-(2) is reduced to the local stability analysis of the periodic solution

$$(x(t), c_1(t), s_1(t)) = \left(0, \cos\left(\frac{2\pi}{T}t\right), \sin\left(\frac{2\pi}{T}t\right)\right)$$

of (26), which can be performed directly with the package DDE-BIFTOOL [11]. Notice that stability is not affected by the transformation as the (decoupled) second and third equation of (26) generate a *stable* periodic solution, which corresponds to (25).

2.5 Comparison with the Averaging Based Approach

The main advantages of the approach outlined in this section are: its general applicability and the computation of exact stability information. No underlying assumptions on parameters need be taken, in contrast to the averaging based

[3] It is necessary to include these explicit links between all harmonics, since otherwise an arbitrary phase difference would occur.

results of Section 1, which are only valid for a sufficiently high frequency of variation of the periodic coefficients. Notice that in general a threshold on this frequency depends on other system's parameters. As a consequence, the validity of the averaged model should always be questioned if parameters are changed (e.g. when computing stability regions in parameter spaces out of the averaged model).

On the other hand, since the averaging approach reduces the stability analysis problem to that of a steady state solution of a time-invariant system, the computational cost of the determination of stability information, the detection and the continuation of bifurcations is reduced a lot, especially if a discretization of distributed delays in stability computations can be avoided (see § 1.2). Furthermore, the classical frequency domain controller design methods and the analytical approaches based on the sensitivity of the eigenvalues can easily be adapted to systems with a fast varying time-delay, because all the information about the varying part of a delay can be concentrated in a correction of the exponential term corresponding the mean delay value (see expression (6)).

3 Examples

The results of the previous sections are applied to two examples from mechanical engineering. An example with a periodic delay function is discussed in § 3.1, an example with periodic system coefficients in § 3.2.

3.1 Variable Spindle Speed Cutting Machine

The following equation, taken from [19]:

$$\ddot{x}(t) + 2\xi\omega_n\dot{x}(t) + \omega_n^2 x(t) = \frac{k}{m}\left(x(t-\tau(t)) - x(t)\right), \quad x \in \mathbf{R}, \tag{27}$$

models one mode of a mechanical rotational cutting process, where x represents the deflection of the machine tool and/or workpiece, ω_n the natural frequency, ξ the damping ratio and m the modal mass. The term $k(x(t-\tau(t)) - x(t))$, with $k > 0$ the cutting force coefficient, models the cutting force, which depends on the time τ, taken by the cutting insert for one revolution of the workpiece. Clearly the time-delay is inversely proportional to the rotational speed of the machine. In [19] one assumes that this speed is varied around a nominal value in a periodic way, which corresponds to a modulation of the time-delay in (27) of the form

$$\tau(t) = \tau_0 + \delta f(\Omega t). \tag{28}$$

Based on the theory developed in the chapter and the model (27) we now give an explanation for the beneficial effect of a high frequency modulating of the machine speed on increasing stability regions.

The characteristic equation of the averaged system is given by

$$H(s, g(s)) := s^2 + 2\xi\omega_n s + \omega_n^2 + \frac{k}{m}(1 - e^{-s\tau} g(s\delta)) = 0.$$

Applying the sensitivity formula (15) to an imaginary root $j\omega$ yields

$$\Re\left(r''(0)^{-1}\right) = -\frac{1}{g''(0)\ \omega^2}\left(\tau + 2\xi\omega_n^2 \frac{\omega^2 + (\omega_n - k/m)^2}{(\omega^2 - (\omega_n^2 + k/m))^2 + 4\xi^2\omega_n^2\omega^2}\right),$$

which is *strictly negative* for *any* value of the system parameters and *any* delay forcing function f. Therefore, the stability region of the steady state solution can always be enlarged by 'distributing' the point-wise delay over an interval, or, by virtue of Theorem 1, by modulating the point-wise delay (speed).

To illustrate this, we consider a delay modulation of the form

$$\tau(t) = \tau_0 + \delta f_1(\Omega t), \tag{29}$$

where $f_1(t)$ is the sawtooth function described in Table 1, and use the tools of Section 2 to compute the exact stability limits of the system (27)-(29) in the (τ_0, k)-plane, for $m = 100, \omega_n = 632.45$, $\xi = 0.039585$, $\delta = 0.05\tau_0$ and $\Omega = 2\pi/\tau_0$. We use $m = 12$ mesh intervals and a piecewise polynomial of degree $d = 3$. The results are shown in Fig. 1 (solid line). For comparison, this figure also shows the stability limits when the delay is fixed at its mean value, i.e., when $\delta = 0$ in (29). In the latter case, the computations can be done using the DDE-BIFTOOL package [11]. Note that the parameter k depends on the width of the cutting tool and on the nominal depth of cut. Therefore, the variation of the rotating speed allows to use a larger tool and/or to remove more material at once, especially at lower speed (i.e. larger delay).

The stability limits for the averaged system corresponding to (27)-(29) are shown in [28, Fig. 4]. With the delay function (29), the kernel function of the distributed delay of the averaged system is a constant. Consequently, as explained in [24], we can also use the DDE-BIFTOOL package for the computations. The resulting stability limits are very close to these of the original system (27) with (29).

Remark that in a preliminary step before the actual computations, we rescaled system (27) in order to avoid numerical problems. Here in particular, the time variable was multiplied by 10^2, so that the system could be transformed to a form with — among others — a "new" variable k that is 10^2 times smaller. Additionally, k and m were both divided by 10^3. In the post-processing step after the computations, the numerical values were re-transformed to restore the original meaning of the variables.

3.2 Forced Elastic Column

We consider a variation of the model of an elastic column studied in [45]. A column of height H is subjected to a time periodic force at the top and clamped at the bottom. Shear and inertia effects are neglected and the damping is assumed to be linear. We are interested in the local stability about the zero steady state and consider the following linear model for the displacement y at height h :

$$\alpha y_{hhhh}(h,t) + (\phi_1 + \phi_2\cos(2\pi t))y_{hh}(h,t) + y_{tt} + \kappa y_t(h,t) = 0, \tag{30}$$

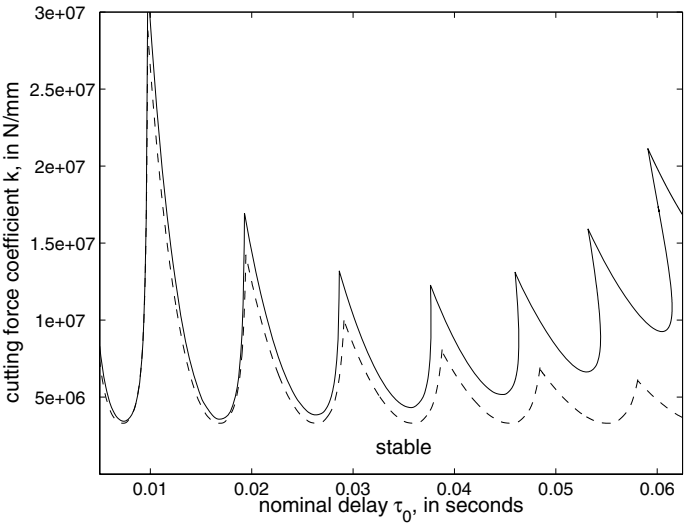

Fig. 1. The solid curve separates the stable and unstable regions in the (τ_0, k)-space for the system (27) and (29). The dashed curve separates the stable and unstable regions for the system with $\delta = 0$.

with boundary conditions

$$y(0,t) = 0, \quad y_h(0,t) = 0, \quad y_{hh}(H,t) = 0 \tag{31}$$

and

$$y_{hhh}(H,t) + (\phi_1 + \phi_2 \cos(2\pi t))(y_h(H,t) - \beta y_h(H,t-\tau)). \tag{32}$$

Note that here the delay only appears in the boundary condition (32).

In a preliminary step, this partial differential equation is discretized in space to obtain a large system of delay differential equations. First, the column is divided into k intervals of height $\Delta h := H/k$ and $x(t) \in \mathbb{R}^{2k\times 1}$ is defined by

$$\begin{aligned} x_i(t) &:= y_t(i\Delta h, t), \quad \text{for } i = 1, \ldots, k, \\ x_{k+i}(t) &:= y(i\Delta h, t), \quad \text{for } i = 1, \ldots, k. \end{aligned} \tag{33}$$

In the next step, we choose other *finite difference* formula than [45], in order to obtain a differential system without algebraic conditions. Specifically, we now discretize (32) by a one-sided finite difference formula. For brevity, the intermediate calculations are omitted, since they are straightforward. The resulting system has the form $\dot{x}(t) = A(t)x(t) + B(t)x(t-\tau)$, where

$$A(t) := \begin{bmatrix} -\kappa I_k & C(t) \\ I_k & 0 \end{bmatrix}. \tag{34}$$

Here, $C(t)$ is an $k \times k$ band matrix with bandwidth five. The matrix $B(t)$ is zero, except for the last three elements in the k^{th} row. These non-zero entries stem

from the discretization of the boundary condition (32). We choose $k = 32$; hence the size of the DDE system $n = 2k = 64$. In the computations, we use $m = 12$ mesh intervals and piecewise polynomial of degree $d = 3$, as for the previous example.

Figure 2 shows the stability region of the zero solution of (30)-(32) in the (κ, β)-space for $\alpha = 1$, $\phi_1 = \phi_2 = 1$, $\tau = 0.4$ and $H = 1$, as well as the stability region of the corresponding averaged system (obtained by setting $\phi_2 = 0$).

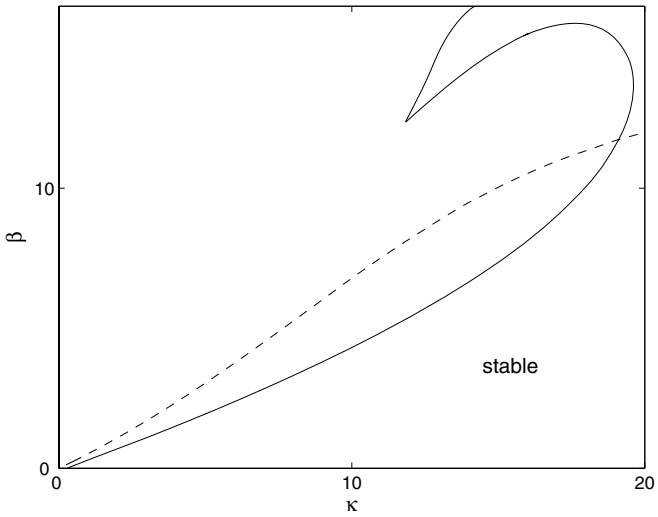

Fig. 2. The solid curve separates the stable and unstable regions in the (κ, β)-space for the forced system (30)-(32). The dashed curve separates the stable and unstable regions for the corresponding averaged system.

4 Conclusions

Both analytical methods and computational tools for the stability analysis of periodic systems with time-varying delays have been described and compared. Their applicability has been illustrated with examples from mechanical engineering.

Acknowledgements

This chapter presents results of the Research Project IUAP P5, funded by the Interuniversity Poles of Attraction of the Belgian Federal Science Policy Office. The scientific responsibility rests with its authors. W. Michiels is a Postdoctoral Fellow and K. Verheyden a Research Assistant of the Fund for Scientific Research -Flanders (Belgium).

References

1. Bai Z., Demmel J., Dongarra J., Ruhe A., van der Vorst, H. Eds. (2000) Templates for the Solution of Algebraic Eigenvalue Problems: A Practical Guide. Software, Environments, and Tools, vol. 11, SIAM, Philadelphia
2. Bellen A., Zennaro M. (2003) Numerical methods for delay differential equations. Oxford University Press, London
3. Breda D. (2004) Numerical computation of characteristic roots for delay differential equations. PhD thesis, Department of Mathematics and Computer Science, University of Udine
4. Breda D., Maset S. Vermiglio R. (2004) Computing the characteristic roots for delay differential equations. IMA J. Numerical Analysis 24(1):1-19.
5. Butcher E.A., Ma H., Bueler E., Averina V., Szabo, Z. (2004) Stability of linear time-periodic delay-differential equations via Chebyshev polynomials. International J. Numerical Methods in Engineering 59:895–922
6. Cooke K. L. Grossman Z. (1982) Discrete delay, distributed delay and stability switches. J. Mathematical Analysis and Applications 86:592-627
7. Doedel E.J., Champneys A.R., Fairgrieve T.J., Kuznetsov Y.A., Sandstede B., Wang X.-J. (1998) AUTO97: Continuation and bifurcation software for ordinary differential equations. Technical report, Dept. of Computer Science, Concordia University
8. Doedel E.J., and Kernévez J.P. (1986) AUTO: Software for continuation and bifurcation problems in ordinary differential equations. Applied Mathematics Report, California Institute of Technology, Pasadena, U.S.A.
9. Engelborghs K., Luzyanina T., in 't Hout K., Roose, D. (2000) Collocation methods for the computation of periodic solutions of delay differential equations *SIAM J. Sci. Comput.* 22:1593–1609
10. Engelborghs K., Luzyanina T., Roose D. (2002) Numerical bifurcation analysis of delay differential equations using DDE-BIFTOOL. ACM Transactions on Mathematical Software 28(1):1-21
11. Engelborghs K., Luzyanina T., Samaey G. (2001) DDE-BIFTOOL v. 2.00: a Matlab package for bifurcation analysis of delay differential equation. T.W. Report 330, Department of Computer Science, K.U. Leuven
12. Engelborghs K. and Roose D. (2002) On stability of LMS methods and characteristic roots of delay differential equations. SIAM J. Numerical Analysis 40(2):629-650
13. Fox L., Parker I. B. (1972) Chebyshev polynomials in numerical analysis. Oxford mathematical handbooks, Oxford University Press, London
14. Goubet-Bartholoméüs A., Dambrine M., Richard J. -P. (1997) Stability of perturbed systems with time-varying delays. Systems & Control Letters 31:155-163
15. Gu K., Kharitonov V.L., Chen, J. (2003) Stability of time-delay systems. Birkhauser, Boston
16. Hale J. K., Verduyn Lunel S. M. (1993) Introduction to Functional Differential Equations. Applied Math. Sciences, vol. 99, Springer Verlag, Berlin Heidelberg New York,
17. Halmos P. (1966) Measure Theory. The university series in higher mathematics, Van Nostrand Princeton
18. Insperger T., Stepan B. (2002) Semi-discretization method for delayed systems. International J. for Numerical Methods in Engineering 55(5):3-18
19. Jayaram S., Kapoor S.G., DeVor, R.E. (2000) Analytical stability analysis of variable spindle speed machines. J. of Manufacturing and Engineering 122:391-397

20. Kharitonov, V.L. and Niculescu, S.-I.: On the stability of linear systems with uncertain delay. *IEEE Trans. Automat. Contr.* **48** (2003) 127-133
21. Lehman B., Bentsman J., Verduyn Lunel S., Verriest, E.I. (1994) Vibrational Control of Nonlinear Time Lag Systems with Bounded Delay: Averaging Theory, Stabilizability, and Transient Behavior. IEEE Transactions on Automatic Control 39:898-912
22. Louisell J. (1992) Growth estimates and asymptotic stability for a class of differential-delay equation having time-varying delay. J. Mathematical Analysis and Applications 164:453-479
23. Luzyanina T., Engelborghs K., Roose, D. (2003) Computing stability of differential equations with bounded distributed delays. Numerical Algorithms 34(1):41–66
24. Luzyanina T., Roose, D. (2004) Equations with distributed delays: bifurcation analysis using computational tools for discrete delay equations. Functional Differential Equations 11:87–92
25. Luzyanina T., Roose D., Engelborghs K. (2004) Numerical stability analysis of steady state solutions of integral equations with distributed delays. Applied Numerical Mathematics 50:75–92
26. Michiels W., Engelborghs K., Roose D., Dochain, D. (2002) Sensitivity to infinitesimal delays in neutral equations. SIAM Journal of Control and Optimization 40(4):1134-1158
27. Michiels W., Niculescu S.-I., Moreau, L. (2004) Using delays and time-varying gains to improve the output feedback stabilizability of linear systems: a comparison. IMA Journal of Mathematical Control and Information 21(4):393-418
28. Michiels W., Van Assche V., Niculescu, S.-I. (2005) Stabilization of time-delay systems with a controlled, time-varying delay and applications. IEEE Transactions on Automatic Control 50(4):493-504
29. Moreau L., Aeyels D. (1999) Trajectory-based global and semi-global stability results. In Modern Applied Mathematics Techniques in Circuits, Systems and Control, N.E. Mastorakis, Ed., pp.71-76, World Scientific and Engineering Society Press 71-76
30. Moreau L., Aeyels, D. (2000) Practical stability and stabilization. IEEE Transactions on Automatic Control 45(8):1554–1558
31. Moreau L., Michiels W., Aeyels D., Roose D. (2002) Robustness of nonlinear delay equations w.r.t. bounded input perturbations: a trajectory based approach. Math. Control Signals Systems 15(4):316–335
32. Niculescu S.-I. (2001) Delay effects on stability: A robust control approach. LNCIS, vol. 269, Springer, Berlin Heidelberg New York
33. Niculescu S.-I., Gu K., Abdallah, C.T. (2003) Some remarks on the delay stabilizing effect in SISO systems. In Proc. 2003 American Control Conference, Denver, Colorado
34. Niculescu S. -I., de Souza C. E., Dion J. -M., Dugard, L. (1998) Robust exponential stability of uncertain systems with time-varying delays. IEEE Transactions on Automatic Control 43:743-748
35. Richard J.-P. (2003) Time-delay systems: an overview of recent advances and open problems. Automatica 39(10):1667-1694
36. Roesch O., Roth H., Niculescu S.-I. (2005) Remote coontrol of mechatronic systems over communication networks. In Proc. 2005 IEEE Int. Conf. Mechatronics & Automation, Niagara Falls, Canada
37. Rudin W. (1966) Real and complex analysis. McGraw Hill, New York

38. Sanders J.A., Verhulst F. (1985) Averaging Methods in Nonlinear Dynamical Systems. Applied Mathematical Sciences, vol. 59, Springer Verlag, Berlin Heidelberg New York
39. Sexton J., Stone B. (1978) The stability of machining with continuously varying spindle speed. Ann. CIRP 27:321-326
40. Sridhar R., Hohn R.E., Long G.W. (1968) A general formultion of the milling process equation. ASME J. Engineering for Industry 90:317-324
41. Tarbouriech S., Abdallah C.T., Chiasson, J.N. eds. (2005) Advances in Communication Control Networks. LNCIS, vol. 308, Springer Verlag, Berlin Heidelberg New York
42. Trefethen L.N. (2000) Spectral methods in Matlab. Software, Environments, and Tools, vol. 10, SIAM, Philadelphia
43. Van Assche V., Ganguli A., Michiels W. (2004) Practical stability analysis of systems with delay and periodic coefficients. In Proc. 5th IFAC Workshop on Time-Delay Systems, Leuven, Belgium
44. Verheyden K., Lust, K. (2005) A Newton-Picard collocation method for periodic solutions of delay differential equations. BIT 45:605–625
45. Verheyden K., Lust K., Roose D. (2005) Computation and stability analysis of solutions of periodic delay differential algebraic equations. In Proc. of ASME International Design Engineering Technical Conferences and Computers and Information in Engineering Conference, Long Beach, USA
46. Verheyden K., Luzyanina T., Roose D. (2004) Efficient computation of characteristic roots of delay differential equations using LMS methods. T.W. Report 383, Department of Computer Science, K.U. Leuven
47. Verheyden K., Roose D. (2004) Efficient numerical stability analysis of delay equations : a spectral method. In Proc. 5th IFAC Workshop on Time-Delay Systems, Leuven, Belgium

Diffusive Representation for Operators Involving Delays

Gérard Montseny

LAAS/CNRS, 7 avenue du Colonel Roche, 31077 Toulouse cedex 4 - France
montseny@laas.fr

1 Introduction

The theory of diffusive representation (DR) is essentially devoted to state-space realizations of integral operators of complex nature encountered in many concrete or theoretical situations. This approach has allowed to construct efficient solutions of non trivial problems in various fields (see [13, 9, 10]). Under their standard form, these state realizations are diffusive, which straightforwardly leads to cheap numerical approximations as well as dissipative properties useful for analysis or control purposes. This diffusive nature however imposes a restriction: the so-realized operators are pseudodifferential, which excludes in particular delay operators and so any operator involving delays.

This short study is an attempt to extend the DR approach to such operators. The only assumption to be dropped is the so-called "sectorial condition" about the spectrum γ of the state realizations, in fact at the origin of their purely diffusive characteristics. Then, the set of γ-realizable operators becomes an algebra including in particular pseudodifferential, rational and delay operators. Some essential properties for analysis as well as numerical realizations are nevertheless preserved when replacing this sectorial condition by a suitable new one, compatible with both delay operators and high frequency dissipation (in a weakened sense).

The underlying topological questions are of course essential in any approach related to infinitedimensional problems. They are not broached in this preliminary work limited to formal aspects only and will be studied in a more deepened paper.

2 Integral Operators, Symbols and State-Space Realizations

N.B.: For simplicity, we only consider in the sequel the case of scalar operators. For most of the notions introduced here-after, vector, matrix or even functional extensions are performed with minor technical adaptations [12].

2.1 Integral Operators, Pseudodifferential Operators, Delay Operators

Linear integral time-operators are defined by the general expression: $(\mathcal{H}u)(t) = \int_{\mathbb{R}} \mathbf{h}(t,s)\, u(s)\, ds = \int_{\mathbb{R}} h(t,s)\, u(t-s)\, ds$, where the *kernel* $\mathbf{h}$ and the so-called

J. Chiasson and J.J. Loiseau (Eds.): Appl. of Time Delay Systems, LNCIS 352, pp. 217–232, 2007.
springerlink.com

impulse response h are linked by $h(t,s) = \mathbf{h}(t, t-s)$. When such an operator $\mathcal{H}$ is time-invariant[1], then $\mathbf{h}(t,s) = h(t-s)$ and the impulse response is therefore depending on one time variable only; finally $\mathcal{H}$ is *causal* when it can be expressed by:

$$u \mapsto \mathcal{H}u := \int_{-\infty}^{t} \mathbf{h}(t,s)\, u(s)\, ds = \int_{0}^{+\infty} h(t,s)\, u(t-s)\, ds. \tag{1}$$

By extension to generalized functions, (1) can express any linear causal operator encountered in concrete problems[2]; for example, the derivative operator ∂_t^n is obtained by $h(t,s) = \delta^{(n)}(t-s)$ with δ the Dirac measure. Elementary delay operators defined by $u \mapsto u(t-\tau)$ are obtained with:

$$h(t,s) = \delta(s-\tau),\ \mathbf{h}(t,s) = \delta(t-s-\tau),\ \tau \in \mathbb{R}. \tag{2}$$

Note that the delay is time-variable if τ is depending on t and that such an operator is causal if and only if $\tau \geqslant 0$ for any t. The identity operator is obviously a particular delay operator with $\tau = 0$.

Definition 1. *The operator $\mathcal{H}$ is local if and only if* $\operatorname{supp} h(t,.) \subset \{0\}$.

When limited to the space of distributions [16], the impulse response $h(t,.)$ of a local operator is necessarily of the form: $h(t,s) = \sum_{n=0}^{N} k_n(t)\, \delta^{(n)}(s)$; so, $\mathcal{H}$ is a differential operator: $\mathcal{H} = \sum_{n=0}^{N} k_n(t)\, \partial_t^n$. Note that the Laplace transform[3] of $h(t,.)$ is $(\mathfrak{L}h(t,.))(p) = H(t,p) = \sum_{n=0}^{N} k_n(t)\, p^n$, so that we can write symbolically: $\mathcal{H} := H(t, \partial_t)$ (through the notion of symbol, such a property will be extended to the general case).

Definition 2. *[4, 17] The operator $\mathcal{H}$ is pseudodifferential (PDO) if and only if*[4] *$h(t,.)$ is of regularity C^∞ on $\mathbb{R}^*$.*

On the one hand, many of the operators encountered in physical problems are pseudodifferential. In particular, differential ops., rational ops. are particular PDO. Fractional operators [14], defined by $h(t,s) = k\ \mathbf{1}_{\mathbb{R}^+}(s)\, s^{-\alpha}$, $\alpha \in \mathbb{C}$, are also PDO. On the contrary, delay ops are not PDO if $\tau \neq 0$, likewise composition of delays with PDOs. This last point makes PDO and delay operators rather different from many points of view and is at the origin of specific representation tools.

[1] That is invariant under any translation: $(\mathcal{H}u)(t+t_0) = (\mathcal{H}u(.+t_0))(t)$.

[2] From the Schwartz's kernel theorem [15].

[3] In the sense of distributions and with respect to the second variable s.

[4] In fact this simplified definition is slightly different than the one given in [17]; but it is sufficient for our purpose. Note that PDO are said "pseudolocal operators" in the sense that the *singular support* of $h(t,.)$ (that is the set where $h(t,.)$ is not of regularity C^∞) is at most $\{0\}$.

On the other hand, the set $\mathcal{O}_+$ of linear integral causal operators is an algebra[5] when equipped with the standard composition product $(\mathcal{H}_1 \circ \mathcal{H}_2)(u) := \mathcal{H}_1(\mathcal{H}_2 u)$, and the subsets of causal PDOs, of local operators, etc. are sub-algebras of $\mathcal{O}_+$. Constant causal delay operators obviously constitute a group $\mathcal{D} \subset \mathcal{O}_+$, but of course not a vector space. From the topological point of view, the vector space generated by causal delay ops. is[6] $\mathcal{O}_+$: this makes useful (otherwise necessary), in practice, to consider $\mathcal{O}_+$ when delay operators can be involved in a problem simultaneously with PDOs, particularly in the quite general situation where solutions involve complex integral operators non reducible to delay nor pseudodifferential ones. Suitable (and if possible convenient) representation tools must therefore be elaborated to efficiently tackle such problems. The notions of symbol and state-space representation, which together run into the general *Diffusive Representation* approach, are devoted to this context.

2.2 Symbol of an Integral Operator [17]

In the sequel, all the integral operators are supposed to be *causal*. Various extensions, in particular to the non causal or even n-dimensional cases, will be found in [12].

Definition 3. *The symbol*[7] *of an integral operator $\mathcal{H}$ defined by its impulse response $h(t,s)$ is the function H defined on $\mathbb{R}_t \times \mathbb{C}$ by:*

$$H(t,.) = \mathfrak{L}h(t,.)\ \forall t. \tag{3}$$

It results from this definition that $H(t,p)$ is analytic (with respect to p) and can be viewed as a time-frequency representation of $\mathcal{H}$. Furthermore, $\mathcal{H}$ is symbolically expressed with no ambiguity: $\mathcal{H} = H(t,\partial_t)$. For example, rational, fractional and elementary delay operators are respectively expressed: $N(\partial_t)\left[D(\partial_t)\right]^{-1}$ with N, D polynomials, $k\,\partial_t^{\alpha}$, $\alpha \in \mathbb{C}$ and $e^{-\tau\partial_t}$ (with possible variations of coefficients k, α, τ with respect to time t). Another (non standard) example is given by the operator $-\partial_t^{-1}(\gamma + \ln(\partial_t))$, with impulse response $h(t,s) = \ln s$ [11].

The algebra $\mathcal{O}_+$ is isomorphic to an algebra of symbols with internal product denoted by $\sharp$; in the sub-algebra of invariant operators, this product is commutative and reduces to the ordinary one: $H \sharp K = H.K$.

We have the fundamental property:

Proposition 1. *for any $H(t,\partial_t) \in \mathcal{O}_+$ and any u with Laplace transform*[8] *U:*

[5] Note that in this algebra, the derivative operator ∂_t has a unique inverse ∂_t^{-1} defined by $(\partial_t^{-1}u)(t) = \int_{-\infty}^{t} u(s)\,ds$.

[6] We do not precize here these toplogical questions (see [12]); let us mention only that any operator of $\mathcal{O}_+$ can be reached with arbitrary accuracy by discrete sums of delays, as suggested by quadratures of (1).

[7] In the sense of the Laplace transform. In the general sense, the symbol is the Fourier transform of the impulse response.

[8] We in fact consider the Fourier-Laplace transform: $(\mathfrak{L}u)(p) = \int_{-\infty}^{+\infty} e^{-pt}\,u(t)\,dt$.

$$H(t,\partial_t)\,u = \mathfrak{L}^{-1}\left[H(t,.)\,U\right]_{|t}. \tag{4}$$

Proof. By denoting $*_s$ the convolution with respect to the time variable s:

$$(H(t,\partial_t)\,u)(t) = \int_0^{+\infty} h(t,s)\,u(t-s)\,ds = (h(t,.)\,*_s\,u)_{|s=t} =$$
$$= (\mathfrak{L}_s^{-1}\mathfrak{L}[h(t,.)\,*_s\,u])_{|s=t} = (\mathfrak{L}^{-1}[\mathfrak{L}_s h(t,.).\mathfrak{L}u])_{|s=t}.$$

The following result is a direct consequence of the causality of $\mathcal{H}$. It is the corner stone of state representations introduced in section 2.3. For any u, we denote $\varphi(t,s) := \mathbf{1}_{]-\infty,t]}(s)\,u(s)$ and:

$$\Psi(t,p) := \int_{\mathbb{R}} e^{p(t-s)}\varphi(t,s)\,ds \tag{5}$$

(note that we have also: $\Psi(t,p) = \int_{-\infty}^{t} e^{p(t-s)}u(s)\,ds = \int_0^{+\infty} e^{ps}\,u(t-s)\,ds = e^{pt} * u$). Then:

Proposition 2. *for any u such that $\mathcal{H}\,u$ is well-defined and for any $a \geqslant 0$:*

$$\mathcal{H}\,u = \frac{1}{2i\pi}\int_{a+i\mathbb{R}} H(.,p)\,\Psi(.,p)\,dp. \tag{6}$$

Proof. First remark that thanks to causality of $\mathcal{H} = H(t,\partial_t)$, for any t, $(H(t,\partial_t)\,u)(t)$ does not depend on $u_{|]t,+\infty[}$ (the future of u). Therefore:

$$(H(t,\partial_t)\,u)(t) = \mathfrak{L}^{-1}\left[H(t,.)\,\mathfrak{L}u\right]_{|t} = \mathfrak{L}^{-1}\left[H(t,.)\,\mathfrak{L}\varphi(t,.)\right]_{|t} =$$
$$= \left[\frac{1}{2i\pi}\int_{a+i\mathbb{R}} e^{p\tau}H(t,p)\int_{\mathbb{R}} e^{-ps}\varphi(t,s)\,ds\,dp\right]_{|\tau=t} =$$
$$= \frac{1}{2i\pi}\int_{a+i\mathbb{R}} H(t,p)\int_{\mathbb{R}} e^{p(t-s)}\varphi(t,s)\,ds\,dp.$$

In expression (6), $H(t,\partial_t)\,u$ appears as a duality product between the symbol $H(t,p)$ of the operator $\mathcal{H}$ on the one hand, and a particular time-frequency representation Ψ of the object u (on which the operator acts) on the other hand. Note that in (6), the time variable t appears in some sense as a *frozen* parameter: this enables the construction of various suitable topological duality spaces convenient (in particular from the point of view of numerical approximations) for such representations [12].

2.3 State-Space Realizations of Integral Operators

Under their integral form (1), nonlocal operators are generally not well-adapted to concrete (numerical) realizations due to the excessive cost inherent to quadratures of the integral. From the only point of view of analysis, it is also preferable to express such operators from some state-space realizations, that is $\mathcal{H}u$ is the output of a Cauchy problem (in general of infinite dimension) with input u:

$$\begin{cases} \partial_t \psi = A\psi + Bu,\ \psi(-\infty) = 0 \\ \mathcal{H}u = C\psi + Du, \end{cases} \tag{7}$$

where A, B, C are suitable linear local (with respect to the t variable) operators on a (topological) state-space $E \ni \psi(t, .)$.

Considering the so-called *history* of u, defined on $\mathbb{R}^2$ by $\mathbf{u}(t, s) := u(t - s)$, it is obvious that $\mathbf{u}$ is solution of the transport equation:

$$\partial_t \mathbf{u}(t, s) = -\partial_s \mathbf{u}(t, s) + u(t) \otimes \delta(s), \tag{8}$$

and so, a trivial (and universal!) state representation of $\mathcal{H}$ is obtained with the following output:

$$y(t) = \int_0^{+\infty} h(t, s)\, \mathbf{u}(t, s)\, ds. \tag{9}$$

Note that in opposite to classical rational state representations (in which $E \equiv \mathbb{R}^n$), operators of any order (not necessarily proper) admit the representation(8,9).

In the case of pure delay operators, defined by (2), this state representation is naturally adapted (the transport equation is indeed inherent to delays, the output being reduced to $(\mathcal{H}u)(t) = \psi(t, \tau)$). In other cases (such as PDO or even combinations of PDO and delays), more specific state representations are in general possible. They can offer a great amount of additional properties intimately associated to the differential formulation (7) which can be chosen in adequation with the particular problems under consideration [12]. Such properties are most of time useful for analysis, control or approximation (numerical realizations) purposes.

In this context, time-frequency state realizations reveal to be powerful, thanks namely to the non dependence between the two variables (in opposite to "time-time" representations such as (8,9) in which t and s are of same nature). They are the main objective of the diffusive representation approach, introduced later in a simplified way.

3 Some Physical Problems Involving Operators of Mixed Pseudodifferential and Delay Nature

Many operational problems need specific representation tools suitable for both pseudodifferential and delay operators. In several situations indeed, solutions cannot be decomposed into clearly separated pseudodifferential and delay parts and therefore cannot be correctly broached with standard tools, in particular when numerical realizations are searched for concrete implementation. As a basic example, we can of course mention the (robust) stabilization of dynamic systems with delays. In the linear case, such systems can be represented by transfer functions of the form $H(p) = \frac{D(p, e^{-\tau_1 p}, \ldots, e^{-\tau_n p})}{N(p, e^{-\tau_1 p}, \ldots, e^{-\tau_n p})}$; nevertheless, feedback solutions $K(p)$, which implicitly involve delays, are not always expressible as rational functions of the symbolic variables p and $e^{-\tau_k p}$. This is particularly the case when optimality is searched in a Hilbert space of controllers [10].

We present here-after two other typical examples, relating to standard physical problems.

3.1 Modeling of Transmission Lines with Losses

The voltage $V(t,x)$ and the current $I(t,x)$ in a transmission line of length l can be modeled by the following partial pseudodifferential system [1, 2] defined on $x \in [0,l]$:

$$\begin{cases} \partial_x V = Z(\partial_t)\, I \\ \partial_x I = Y(\partial_t)\, V, \end{cases} \tag{10}$$

with additional boundary conditions:

$$V(t,0) = V_0(t)\text{: voltage source applied at the beginning of the line,} \tag{11}$$

$$V(t,l) = Z_l(\partial_t)\, I(t,l)\text{: load at the end of the line with impedance } Z_l. \tag{12}$$

In (10), the impedances Z and $\frac{1}{Y}$ depend on the dielectric and the physical characteristics of the line. The so-called characteristic impedance and propagation coefficient of the line are given respectively by:

$$Z_c(p) = \sqrt{\frac{Z(p)}{Y(p)}}, \quad \gamma(p) = \sqrt{Z(p)\, Y(p)}. \tag{13}$$

From the only input-output point of view and by denoting $(V_0, I_0) := (V,I)_{x=0}$, $(V_l, I_l) = (V,I)_{x=l}$, it can be shown that system (10) is equivalent to the following operational formulation, of the form $V_l = H(\partial_t)\, V_0$ with $H(\partial_t)$ depending on the terminal impedance[9] Z_l [1, 18]:

$$\begin{cases} V_l = e^{-l\,\gamma(\partial_t)}\, V_0 - Z_c(\partial_t)\, I_l \\ I_0 = Z_c(\partial_t)^{-1} V_0 + e^{-l\,\gamma(\partial_t)} (I_l - Z_c(\partial_t)^{-1} V_l) \end{cases} \tag{14}$$

When $Z(p) = Lp$ and $Y(p) = Cp$, no dissipation occurs (the line is perfect); so (10) reduces to the well-known classical wave equation $\partial_t^2 V = \frac{1}{CL} \partial_x^2 V$, and $e^{-l\,\gamma(\partial_t)} = e^{-l\sqrt{LC}\,\partial_t}$ is a pure delay. When dielectric losses are taken into account, Z and Y can be of various type. In the ideal case studied in [6], $Z(p) = Lp + R$, $Y(p) = Cp + G$; so the operator $H(\partial_t)$ involves both pseudodifferential and delay-like components. In particular, the main operator $e^{-l\,\gamma(\partial_t)}$ with symbol:

$$e^{-l\sqrt{(Lp+R)(Cp+G)}} \underset{|p|\to\infty}{\sim} e^{-l\sqrt{LC}\,p} \tag{15}$$

clearly behaves at high frequencies as a pure delay, while it also presents some pseudodifferential nature (of the type $e^{-\sqrt{\partial_t}}$) at middle frequencies. In physical situations, such delay-like operators can become rather complex, all the more so that actual dielectric impedances Z and $\frac{1}{Y}$ are not rational (well-known pseudodifferential dielectric models of Cole-Davidson, Cole-Cole, Havriliak-Negami, etc. [5]).

[9] Note that in (14), $V_l = Z_l(\partial_t) I_l$ and so $I_l - Z_c(\partial_t)^{-1} V_l = 0$ if $Z_l = Z_c$: no reflexion occurs at end of the line when the impedance Z_l is matched.

3.2 Vibrations and Impedance Problems

As a simple example, first consider the ideal 2D wave equation in infinite domain $\mathbb{R}^2$, controlled at point 0, with measured output at point $\mathbf{x}_0 \in \mathbb{R}^2$ and distributed perturbations $q(t, \mathbf{x})$ (we suppose for simplicity that initial conditions are null):

$$\begin{cases} \partial_t^2 \varphi - \triangle \varphi = u(t)\, \delta(\mathbf{x}) + q(t, \mathbf{x}) \\ z(t) = \varphi(t, \mathbf{x}_0); \end{cases} \tag{16}$$

for such a system, the transfer operator $z = H(\partial_t)\, u$ is of the form [3]:

$$H(\partial_t) = k\, \partial_t^{-\frac{1}{2}} \circ e^{-\|\mathbf{x}_0\|\, \partial_t}\,; \tag{17}$$

the delay term $e^{-\|\mathbf{x}_0\|\, \partial_t}$ is obviously a consequence of the finite speed of propagation of such a system, while the pseudodifferential component $\partial_t^{-\frac{1}{2}}$ is due to the even dimension of the propagation domain.

In the general case where boundary conditions are added to a wave propagation problem in a nD domain, it is also obvious that the transfer operator necessarily involves some delay components, but a separable expression such as (17) is no more possible and the transfer function H then becomes much more complex. It furthermore depends on a continuous variable θ when the control is distributed on a part of the boundary. For example, when a high frequency pre-stabilization is performed on a regular part of the boundary from impedance matching techniques, then the model involves, in addition of delays, some pseudodifferential non local components such as [7]:

$$K(\partial_t, \partial_\theta) = \sqrt{\partial_t^2 - \partial_\theta^2}^{-1}\,. \tag{18}$$

In such cases, control problems (for example active low frequency control) needs suitable state-representation tools in order to construct and concretely implement efficient solutions.

From a quite general point of view, complex operators with delay-like components must be expected in most of vibration problems relating to propagative properties, namely in flexible structures with a high number of significant modes.

4 Diffusive Representation [12]

From definition (5), it can be shown that Ψ is the solution of the following well-posed Cauchy problem parameterized by $p \in \mathbb{C}$:

$$\partial_t \Psi = p\Psi + u,\ \Psi(-\infty, p) = 0; \tag{19}$$

with $p = a + i\omega,\ \omega \in \mathbb{R}$, (19,6) is a state realization of $\mathcal{H}$. Such a realization is not asymptotically stable ($a \geqslant 0$), in particular at high frequencies: from a practical point of view, this is a major shortcoming. Under suitable hypothesis, high frequency-asymptotically stable realizations can be built following the way described in sections 4.1, 4.2.

Definition 4. *[12] The diffusive representation of u is the restriction of the function $\Psi(t,p)$ defined by (19) to $p \in \mathbb{R}^{*-} + i\mathbb{R}$.*

Remark 1. From an abstract point of view, the operator of "diffusive representation", denoted $\mathfrak{R}$d, is the resolvent in the algebra of causal operators $\mathcal{L}_+(L^2(\mathbb{R}))$ of the operator ∂_t (whose spectrum is then $\mathbb{R}^+ + i\mathbb{R}$).

4.1 Diffusive Realizations of PDOs

Let us consider $\xi \mapsto \gamma(\xi)$ a continuous almost everywhere differentiable and injective function from $\mathbb{R}$ to $\mathbb{R}^{*-} + i\mathbb{R}$ with derivative γ' such that $0 < \alpha \leqslant |\gamma'| \leqslant \beta < +\infty$. It defines a simple oriented arc yet denoted γ closed at infinity[10]. For various mathematical reasons not recalled here, γ is located, in the standard DR approach, inside a cone as shown in Fig. 1; this is called the "sectorial condition".

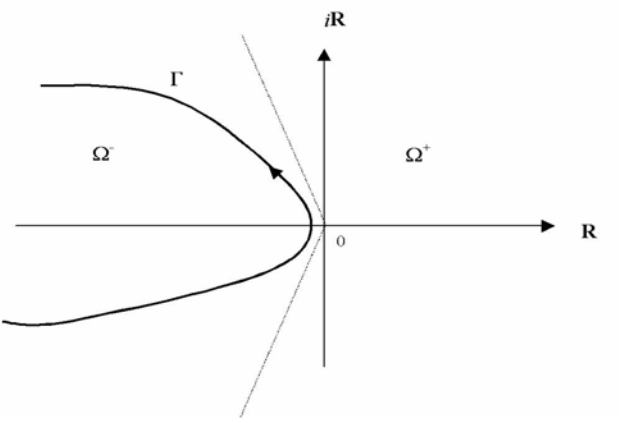

Fig. 1. Spectral arc γ for PDO

Under suitable assumptions stated in theorem 1 here-after, we obtain from Cauchy theorem:

$$\int_{a+i\mathbb{R}} H(t,p)\,\Psi(t,p)\,dp = \int_{\gamma} H(t,p)\,\Psi(t,p)\,dp. \tag{20}$$

For simplicity, we suppose that $H(t,.)$ has no singularity on γ; then, with $p = \gamma(\xi)$, $\xi \in \mathbb{R}$ and by denoting:

$$\mu(t,\xi) := \frac{\gamma'(\xi)}{2i\pi} H(t,\gamma(\xi)) \tag{21}$$

[10] The approach presented hereafter may also be formulated with a *bounded* arc γ parameterized on $\mathbb{R}/2\pi\mathbb{R} \equiv [0, 2\pi[$ instead of $\mathbb{R}$. Up to minor technical adpatations, all the results of this section remain valid after changing $\mathbb{R}$ by $\mathbb{R}/2\pi\mathbb{R}$. Note also that the domain Ω_γ^- can be empty (for example when $\gamma(\xi) = -|\xi|$).

and $< f, g > := \int_{\mathbb{R}} f\, g\, d\xi$, we deduce the following state representation[11] of $\mathcal{H}$:

$$\begin{cases} \partial_t \psi = \gamma\, \psi + u,\ \psi(-\infty, \xi) = 0 \\ \mathcal{H} u = < \mu, \psi > . \end{cases} \tag{22}$$

This state representation is stable and asymptotically stable (dissipative) at high frequencies; it is called the (diffusive[12]) γ-realization of $\mathcal{H}$.

Definition 5. *The distribution*[13] $\mu(t,.)$ *is called the (canonical*[14]*)* γ*-symbol of the operator* $H(t, \partial_t)$*; the (regular) function* $\psi(t,.)$ *is called the* γ*-representation of* u*.*

An operator $\mathcal{H}$ *which admits a* γ*-symbol for some* γ *as described above is called diffusive (in the strict sense). The operator* $\mathcal{H}$ *is diffusive in the extended sense when* $\partial_t^{-n} \circ \mathcal{H}$ *is strictly diffusive for some* $n \in \mathbb{N}$*.*

It can be shown that any diffusive operator is pseudodifferential. The following result is a sufficient condition to characterize diffusive operators. More general results can be found in [12].

Theorem 1. *[12] For a given arc* γ*, a causal operator* $\mathcal{H} = H(t, \partial_t)$ *admits a* γ*-symbol if the two following conditions are fulfilled:*

(i) the Laplace-symbol $H(t,p)$ *is holomorphic on* Ω_γ^+*;*

(ii) $H(t,p)$ *vanishes when* $|p| \to \infty$ *in* $\mathbb{C}^- \cap \Omega_\gamma^+$ *uniformly with respect to* $\arg p$*.*

For information, we give in Fig. 2 the general diagrams (extract from [12]) associated to the diffusive representation.

4.2 γ-Realizations of Operators Involving Delays

Even under its weakened formulations [12], condition (ii) of theorem 1 prohibits delay operators as soon as the sectorial condition on γ is fulfilled (recall that the symbol of the elementary delay operator is $e^{-\tau p}$, $\tau > 0$): delay operators are not diffusive. In some sense, they appear as a limit case, in fact at the boundary of the set of PDO. This last point implies on the one hand that in their standard form, diffusive realizations are not adapted to delay operators, on the other hand that delay operators can possibly be handled from diffusive representation up to replacing the sectorial condition on γ by another one. This condition should preserve some dissipativity at high frequencies, in order to conserve suitable

[11] From a rigorous point of view, the scalar product $< .,. >$ defines a topological duality between two spaces $\Delta_\gamma \ni \psi(t,.)$ and $\Delta'_\gamma \ni \mu(t,.)$ (called the algebra of γ-symbols). These spaces are widely described in [12].

[12] From the sectorial condition on γ, the state equation $\partial_t \psi = \gamma\, \psi + u$ is of diffusive nature [19].

[13] In the general case where $H(t,.)$ can be singular on γ, the expression (21) must be understood as the right trace on γ in the sense of distributions.

[14] The γ-symbol of an operator is in fact a class of equivalence of distributions [12].

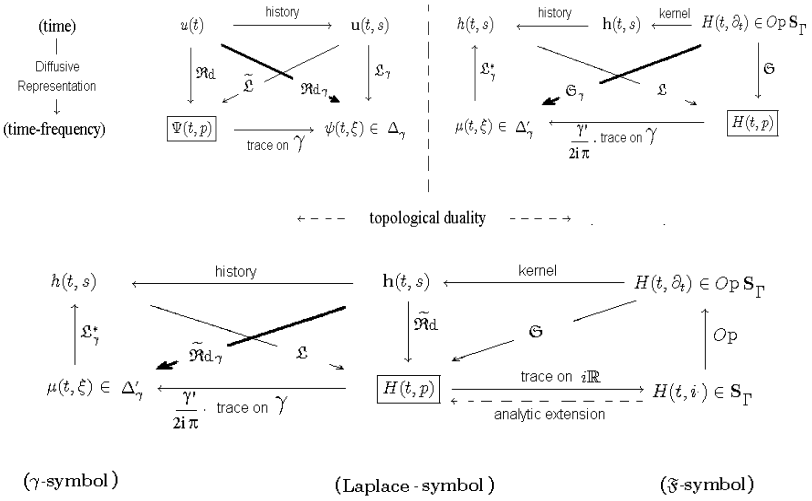

Fig. 2. The diffusive representation diagrams [12]

features for analysis and numerical approximation purposes. In such a case and up to suitable precautions, the diffusive representation approach will remain legitimate for problems involving delay and/or pseudodifferential operators.

Let us consider a spectral arc γ such as in Fig. 3 (we suppose $\gamma(0) = 0$):

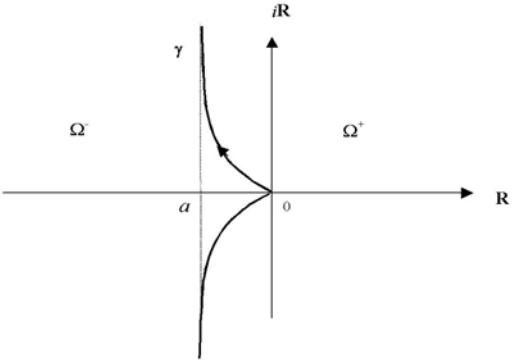

Fig. 3. Spectral arc γ for delay operators (and PDO)

With μ defined by (21) and γ such as in Fig. 3, we have the following general result:

Proposition 3. *A causal operator $\mathcal{H} = H(t, \partial_t)$ admits the γ-realization*

$$\begin{cases} \partial_t \psi = \gamma\, \psi + u,\ \psi(-\infty, \xi) = 0 \\ \mathcal{H}u = < \mu, \psi > \end{cases} \tag{23}$$

if the two following conditions are fulfilled:
(i) the Laplace-symbol $H(t,p)$ is holomorphic on Ω_γ^+;
(ii) $H(t,p)$ vanishes when $|p| \to \infty$ in $\mathbb{C}^- \cap \Omega_\gamma^+$ uniformly with respect to $\mathrm{Re}\, p$.

Proof. It suffices to show that $\int_{i\mathbb{R}} H(t,p)\,\Psi(t,p)\,dp = \int_\gamma H(t,p)\,\Psi(t,p)\,dp$; this is a consequence of Cauchy theorem and Jordan lemma (see [12] for details).

Corollary 1. *For any $\tau > 0$, the delay operator $\partial_t^{-1} \circ e^{-\tau\partial_t}$ is γ-realizable.*

Proof. (i) The symbol $p^{-1}e^{-\tau p}$ is holomorphic in $\mathbb{C}^*$. (ii) When $|p| \to \infty$ in $\mathbb{C}^- \cap \Omega_\gamma^+$, $p = x + iy$ with $x, y \in \mathbb{R}$ and $|y| \to \infty$, $a \leqslant x \leqslant 0$; it obviously results that $|p^{-1}e^{-\tau p}| \to 0$ uniformly with respect to x.

Consequently, the elementary delay operator $e^{-\tau\partial_t} = \partial_t^{-1} \circ e^{-\tau\partial_t} \circ \partial_t$ admits the following state realization[15]:

$$\begin{cases} \partial_t \psi(t,\xi) = \gamma(\xi)\,\psi(t,\xi) + \partial_t u(t),\ \psi(-\infty,\xi) = 0 \\ (\mathcal{H}u)(t) = \displaystyle\int_{-\infty}^{+\infty} \mu(\xi)\,\psi(t,\xi)\,d\xi, \end{cases} \tag{24}$$
$$\text{with } \mu(\xi) = \mathrm{fp}\tfrac{\gamma'(\xi)\,e^{-\tau\,\gamma(\xi)}}{2i\pi\,\gamma(\xi)} + k\,\delta(\xi).$$

More complex operators can be realized in the same way. For example, $e^{-\tau(t)\partial_t} \circ \partial_t^{-\alpha}$, $0 < \alpha < 1$, $\tau(t) \geqslant 0$ (the composition of a time-invariant PDO and a time-varying delay operator) is realized by (23) with $\mu(t,\xi) = \frac{\gamma'(\xi)\,e^{-\tau(t)\,\gamma(\xi)}}{2i\pi\,\gamma(\xi)^\alpha}$. Note that such an operator is γ-realizable thanks to the fact that $\mathbb{R}^{-*} \subset \Omega_\gamma^-$, so the symbol $p^\alpha\,e^{-\tau p}$ is holomorphic in Ω_γ^+.

4.3 Remarks

By changing the sectorial condition by the above one, the main lost property is[16] $h(t,s) =< \mu(t,.), e^{\gamma s} >$ (while $H(t,p) =< \mu(t,.), \frac{1}{p-\gamma} >$ remains true). This suggests that contrarily to the case of strictly diffusive realizations (where any distribution u with support in some $[t_0, +\infty[$ is admissible), the space of admissible u for (23) should be reduced in some sense. Up to this restriction, the diagrams of Fig. 2 remains valid.

Numerical *diagonal* approximations can be performed from discretization of the ξ variable and quadratures of the output integral (see some examples in

[15] Here, $\mu(t,.)$ is defined as the right trace on γ in the sense of distributions. The value of k depends on $\gamma'(0^+) - \gamma'(0^-)$.

[16] Because for any $s > 0$, $e^{\gamma(\xi)\,s} \notin \Delta_\gamma$ when the sectorial condition is not satisfied [12]. Note however that the property $h = \int \mu\,e^{\gamma s}\,d\xi$ remains true in a suitable modified sense, by involving adapted duality spaces:

$$< \int \mu(t,\xi)\,e^{\gamma(\xi)s}\,d\xi, \varphi >_s =< \mu(t,.), \int \varphi(s)\,e^{\gamma s}\,ds >_\xi .$$

section 5). Thanks to high frequency dissipativity of (24), it is possible to get numerical realizations with *infinite horizon* [12] and reasonable cost. From this point of view, a correct choice of parameter a (which determines the high frequency behavior of (24)) should be decisive. Some parasitic oscillations similar to the well-known *Gibbs phenomenon* can be expected from truncation of γ to a bounded arc; as usual, such problems should be solved by implementing soft truncations.

From the point of view of numerical cost, the dimension of approximate γ-realizations is in practice about a few tens when $\gamma(\xi) \sim -|\xi|$, a few hundreds when $\gamma(\xi) \sim |\xi|\, e^{ik\ \mathrm{sign}\,\xi}$ and a few thousands when $\gamma(\xi) \sim i\xi$. In comparison, the numerical realization (8,9) (shift register) in general necessitates several tens of thousands state variables for similar accuracy, and much more when $H(\partial_t)$ involves long memory behaviors.

5 Some Numerical Examples

For simplicity, γ is simply defined by $\gamma(\xi) = -1 + i\xi$. Two discretizations of the ξ variable have been chosen (Matlab code):

$$\mathcal{X}_{\mathrm{lin}} := \{\xi_k^1\} \texttt{=linspace((}\xi_{\min}\texttt{),(}\xi_{\max}\texttt{),}N\texttt{)}$$
$$\mathcal{X}_{\log} := \{\xi_k^2\} \texttt{=logspace(log10(}\xi_{\min}\texttt{),log10(}\xi_{\max}\texttt{),}N\texttt{)}$$

with:

$$\xi_{\min} = 10^{-3}$$
$$\xi_{\max} = 10^{3}$$

The quadrature of the output integral is defined by:

$$\int_0^{+\infty} \mu\, \psi\, d\xi \simeq \sum_{k=1}^{N} \mu_k\, \psi(., \xi_k), \tag{25}$$

$$\mu_k = \mu(\xi_k) \int_0^{+\infty} \Lambda_k(\xi)\, d\xi \tag{26}$$

where Λ_k is the standard piecewise linear "hat function" with support $[\xi_{k-1}, \xi_{k+1}]$, such that $\Lambda(\xi_k) = 1$. So, with $\gamma_k := \gamma(\xi_k)$ and from symmetry, we get the approximate rational state realization of $H(\partial_t)$ (of dimension N):

$$\begin{cases} \dot{\psi}_k = \gamma_k\, \psi_k + u,\ \psi_k(-\infty) = 0,\ k = 1, N \\ y = 2\,\mathrm{Re} \sum_{k=1}^{N} \mu_k\, \psi_k, \end{cases} \tag{27}$$

with symbol:

$$\tilde{H}(p) = \sum_{k=1}^{N} \left(\frac{\mu_k}{p - \gamma_k} + \frac{\bar{\mu}_k}{p - \bar{\gamma}_k} \right). \tag{28}$$

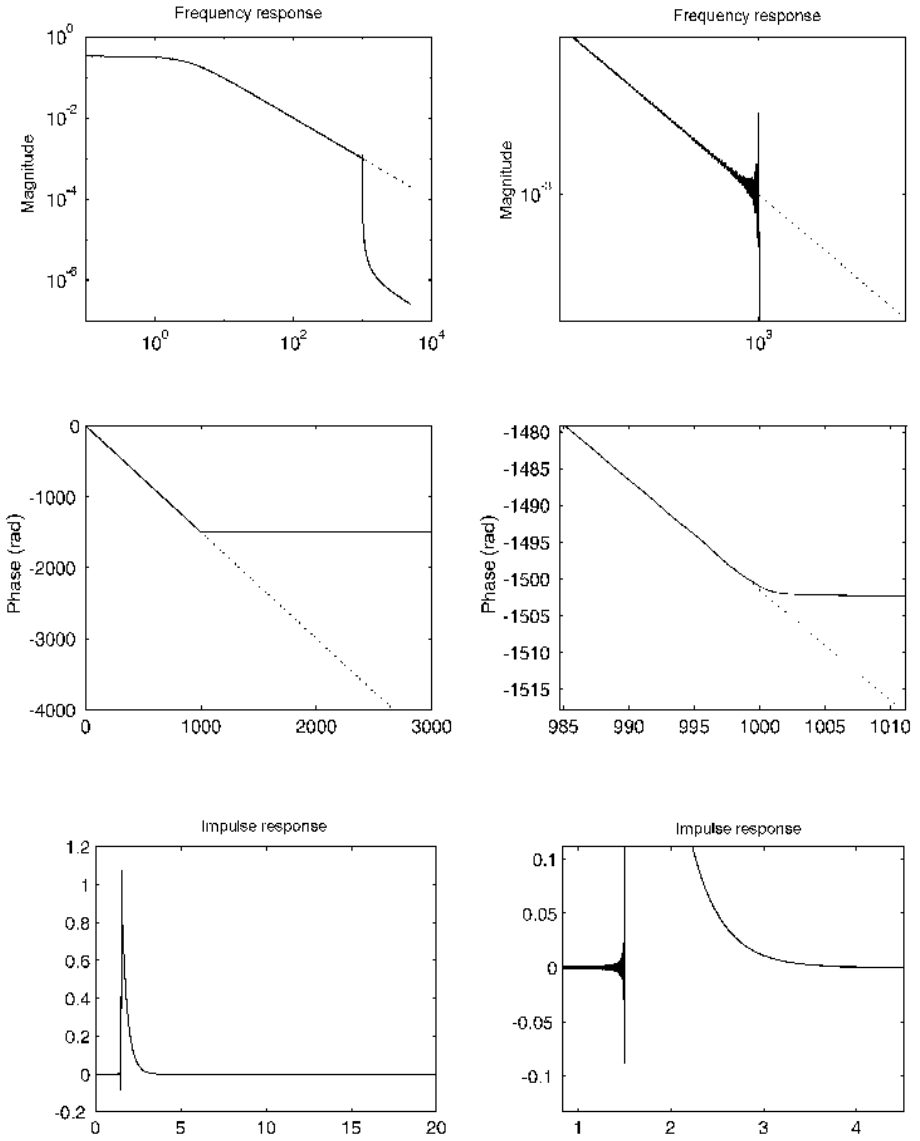

Fig. 4. Approximate realization of $H(\partial_t) = (\partial_t + 3)^{-1} \circ e^{-1.5\,\partial_t}$, lin. mesh, $N = 1000$

Remark 2. The rational state realization (27) can be interpreted as the following γ-realization (similar to (24) but with γ-symbol $\tilde{\mu}$ of measure type and with discrete support):

$$\begin{cases} \partial_t \psi(t,\xi) = \gamma(\xi)\,\psi(t,\xi) + \partial_t u(t),\ \psi(-\infty,\xi) = 0 \\ y(t) = \displaystyle\int_{-\infty}^{+\infty} \tilde{\mu}(\xi)\,\psi(t,\xi)\,d\xi, \end{cases} \tag{29}$$

$$\tilde{\mu}(\xi) = \sum_{k=1}^{N} \left(\mu_k\,\delta(\xi-\xi_k) + \bar{\mu}_k\,\delta(\xi+\xi_k)\right).$$

Some non trivial numerical results are given here-after, with operator $H(\partial_t)$ defined by the symbol:

$$H(p) = \frac{\left(e^{-\tau p}+b\right)^{\nu}}{(p-p_0)^{\alpha}},\ \tau,\nu,\alpha > 0,\ p_0 < -1; \tag{30}$$

when τ and b are such that $H(p)$ is holomorphic in $]-1,+\infty[+i\mathbb{R}$, operator $H(\partial_t)$ admits a γ-symbol μ given by:

$$\mu(\xi) = \frac{1}{2\pi}\frac{\left(e^{-\tau(-1+i\xi)}+b\right)^{\nu}}{(-1-p_0+i\xi)^{\alpha}}. \tag{31}$$

In the following Fig. 4,5,6, exact frequency responses of $H(\partial_t)$ are plotted in dotted lines (they are mostly not distinguishable of the approximate ones); impulse responses are simulated in the time domain ($\Delta t = 10^{-4}$).

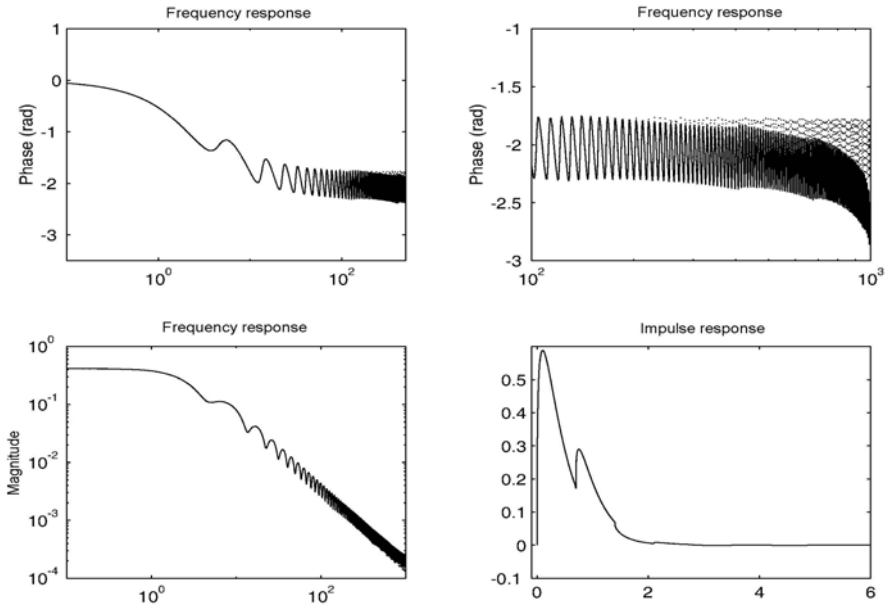

Fig. 5. Approximate realization of $H(\partial_t) = (\partial_t+3)^{-1.3} \circ \left(e^{-0.7\,\partial_t}+2\right)^{0.5}$, lin. mesh, $N = 1000$

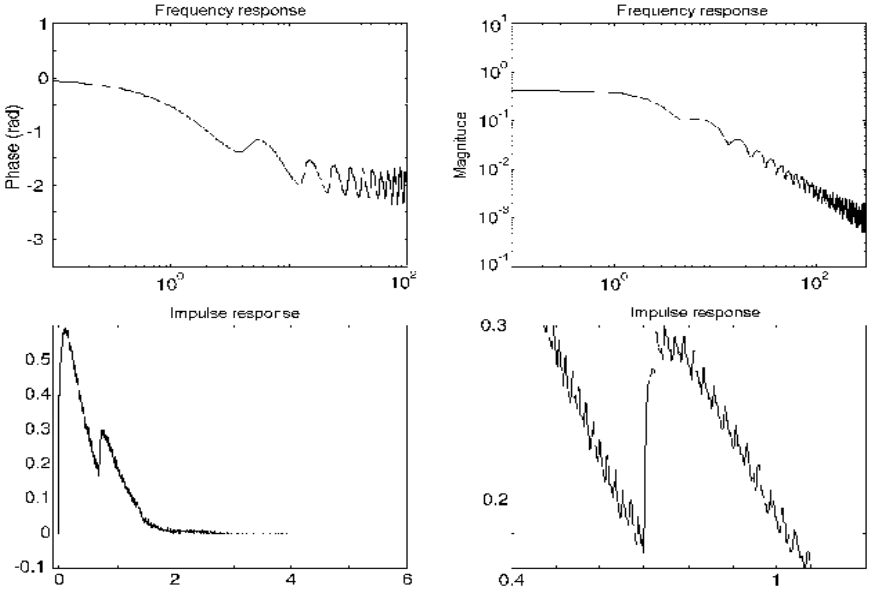

Fig. 6. Approximate realization of $H(\partial_t) = (\partial_t + 3)^{-1.3} \circ \left(e^{-0.7\,\partial_t} + 2\right)^{0.5}$, log. mesh, $N = 500$

References

1. Bidan P. (to be published) Pseudodifferential modeling of transmission lines with losses
2. Bidan P., Neacsu C., Lebey T. (2000) Pseudodifferential models for propagation and dissipation phenomena in electrical machine windings. 14th International Symposium of Mathematical Theory of Networks and Systems (MTNS'2000), Perpignan, France
3. Hardy J., Depollier C., Nicol R. (1998) Propagation dans les espaces de dimension paire. ESAIM: Proceedings 5:159-175
4. Hormander H. (1985) Linear partial differential operators. Springer Verlag, Berlin Heidelberg New York
5. Jonscher A.K. (1983) Dielectric relaxation in solids. Chelsea Dielectrics Press, London
6. Laudebat L. (2003) Modélisation et identification sous représentation diffusive de comportements dynamiques non rationnels en génie électrique. PhD thesis, Paul Sabatier University, Toulouse, France
7. Levadoux D., Montseny G. (2003) Diffusive realization of the impedance operator on circular boundary for 2D wave equation. Sixth International Conference on Mathematical and Numerical Aspects of Wave Propagation (WAVES'2003), Jyvaskyla, Finland
8. Montseny G. (1998) Diffusive representation of pseudodifferential time-operators. ESAIM: Proceedings 5:159-175

9. Montseny G. (2002) Diffusive representation: a new concept for complex dynamic problems involving pseudodifferential operators. Lecture notes of the Summer School "On the links between nonlinear physics and information sciences", Les Houches Center of Physics
10. Montseny G. (2002) Contrôle diffusif pseudo-invariant : principes et exemples. Avancées récentes en commande robuste - Applications à la mécanique des structures. Ecole CEA-EDF-INRIA Problèmes Non Linéaires Appliqués, INRIA - Rocquencourt, France
11. Montseny G. (2004) Simple approach to approximation and dynamical realization of pseudodifferential time-operators. IEEE Transactions on Circuits & Systems 51(11):613-618
12. Montseny G. (2005) Représentation diffusive. Hermès-Science, Paris
13. Montseny G. et al. Pseudodifferential operators and diffusive representation in modeling, control and signal. On-line, URL: `www.laas.fr/gt-opd`
14. Samko S.G., Kilbas A.A., Marichev O. (1987) Fractional integrals and derivatives: theory and applications. Gordon & Breach, London
15. Schwartz L. (1953, 1954) Produits tensoriels topologiques d'espaces vectoriels topologiques. Espaces vectoriels topologiques nucléaires. Applications. Séminaire Schwartz, Faculté des Sciences de Paris
16. Schwartz L. (1966) Théorie des distributions. Hermann, Paris
17. Taylor M.E. (1981) Pseudodifferential operators, Princeton University Press
18. Vander Vorst A. (1994) Electromagnétisme: champs et circuits. De Boeck University
19. Yosida K. (1965) Functional analysis. Springer, Berlin Heidelberg New York

OreModules: A Symbolic Package for the Study of Multidimensional Linear Systems

Frédéric Chyzak[1], Alban Quadrat[2], and Daniel Robertz[3]

[1] INRIA Rocquencourt, ALGO project, Domaine de Voluceau BP 105, 78153 Le Chesnay Cedex, France
frederic.chyzak@inria.fr
[2] INRIA Sophia Antipolis, CAFE project, 2004, Route des Lucioles BP 93, 06902 Sophia Antipolis Cedex, France
Alban.Quadrat@sophia.inria.fr
[3] Lehrstuhl B für Mathematik, RWTH - Aachen, Templergraben 64, 52056 Aachen, Germany
daniel@momo.math.rwth-aachen.de

1 Introduction

In the seventies, the study of transfer matrices of time-invariant linear systems of ordinary differential equations (ODEs) led to the development of the *polynomial approach* [20, 22, 44]. In particular, the univariate polynomial matrices play a central role in this approach (e.g., Hermite, Smith and Popov forms, invariant factors, primeness, Bézout/Diophantine equations).

In the middle of the seventies, while generalizing linear systems defined by ODEs to differential time-delay systems, ODEs with parameters, 2-D and 3-D filters..., one had to face the case of systems described by means of matrices with entries in multivariate commutative polynomial rings. All these new systems were called 2-D or 3-D linear systems and, more generally, *n-D systems* or *multidimensional linear systems* with constant coefficients [4, 16]. It was quickly realized that no canonical forms such as Hermite, Smith and Popov forms existed for polynomial matrices with two and three variables (i.e., with entries in $k[x_1, x_2, x_3]$, where k is a field such as $\mathbb{Q}$, $\mathbb{R}$, $\mathbb{C}$). Moreover, more than only one type of primeness was needed in order to classify n-D systems (e.g., factor/minor/zero primeness [48, 49]). Hence, it is not very surprising that, in the eighties, *Gröbner bases* were introduced in the study of multidimensional linear systems with constant coefficients [4, 16]. A Gröbner basis defines normal forms for polynomials with respect to a certain monomial ordering of the variables x_i [2, 17, 23]. Given a Gröbner basis, there is a simple algorithm to effectively compute these normal forms. In many ways, the computation of these normal forms can be seen as an extension of the Gaussian elimination algorithm to commutative polynomial rings [2, 17].

In a pioneering work, R. E. Kalman developed a *module-theoretic* approach to time-invariant ordinary differential linear systems [21]. In his PhD thesis under the supervision of R. E. Kalman, Y. Rouchaleau considered Kalman-type

J. Chiasson and J.J. Loiseau (Eds.): Appl. of Time Delay Systems, LNCIS 352, pp. 233–264, 2007.
springerlink.com

systems where the entries of (A, B, C, D) belong to a commutative ring. In particular, he studied their structural properties using module theory. Such systems are nowadays called *systems over rings* and they have been considerably studied in the literature [43] since. An extension of the *geometric approach* [46] to linear systems over rings has also been recently developed [1, 12, 18, 19]. Using effective algebra methods (Gröbner bases, *characteristic sets*), the computational aspects of the systems over rings (e.g., differential time-delay systems) were firstly studied by L. Habets in [18, 19].

In the nineties, U. Oberst developed a general module-theoretic approach to multidimensional linear systems with constant coefficients [28]. Using B. Malgrange's approach [24], in which a *finitely presented D-module M* is associated with a linear system of equations over a polynomial ring D, he showed how some structural properties of the system corresponded to algebraic properties of the D-module M. He then was able to develop a complete duality between his module-theoretic approach and the *behavioural approach* developed by J. C. Willems [30]. Based on U. Oberst's ideas, the behavioural approach to multidimensional linear systems has been successfully developed in the recent years. See [30, 29, 36, 47, 49] and the references therein.

Within a similar module-theoretic approach, the concepts of *flatness* and *π-freeness* were introduced in [15, 26] for differential time-delay linear systems with constant coefficients. As it is shown in [26, 27] on different concrete examples, the detection of such structural properties is important for the study of the motion planning problem. In the behavioural approach, the concept of flatness corresponds to the existence of an *observable image representation* for the multidimensional system [32].

In the same years as [28], J.-F. Pommaret studied underdetermined systems of partial differential equations (PDEs) coming from mathematical physics and differential geometry (e.g., elasticity, electromagnetism, hydrodynamics, general relativity). See also [3]. In particular, he showed how his mathematical approach was a generalization of U. Oberst's module-theoretic approach for multidimensional (linear) systems with varying coefficients. See [31] for more details and references. In particular, the problem of checking whether or not a multidimensional linear system described by PDEs with varying coefficients could be formally parametrized was solved within the theory of differential operators. Moreover, the work of M. Fliess on linear systems defined by ODEs with variable coefficients also illustrated the need to pass from the commutative polynomial viewpoint to the non-commutative one [14].

Based on B. Malgrange's approach [24], *algebraic analysis* has been developed in mathematics in order to study general linear systems of PDEs with variable coefficients using module theory, algebraic geometry, homological algebra and functional analysis. Algebraic analysis has recently been introduced in control theory in [38] in order to study multidimensional linear systems defined by PDEs with varying coefficients. In particular, using the formal theories of PDEs (Spencer's, Riquier-Janet's theories), it was shown in [31, 32, 33, 34, 38] how some structural properties of systems could be checked by means of constructive algorithms.

Finally, using the homological algebra approach developed in [38], we have recently shown in [9, 11] how the previous results could be generalized to some classes of multidimensional linear systems with varying coefficients encountered in the literature (e.g., ODEs, PDEs, differential time-delay systems, multidimensional discrete systems, partial differential delay systems). In order to do that, the concept of multidimensional linear systems over *Ore algebras* was introduced in [9, 11]. An Ore algebra is a ring of non-commutative polynomials in functional operators with polynomial or rational coefficients [5, 6, 7]. Characterizations of algebraic structural properties such as, for instance, controllability, parametrizability and flatness were obtained.

The recent progress of Gröbner bases over Ore algebras (i.e., over some classes of non-commutative polynomial rings) [5, 6, 7, 23] allows us to effectively test the algebraic properties of general multidimensional linear systems (e.g., controllability, observability, parametrizability, flatness, π-freeness) and compute different types of parametrizations and to propose feedback laws (motion planning, tracking, Bézout equations, optimal control).

In this paper, we shall develop the following methodology for the study of multidimensional linear systems over Ore algebras (see also [11]):

1. A linear system is defined by means of a $(q \times p)$-matrix R with entries in an Ore algebra D, i.e., it corresponds to a system of linear equations $R\,z = 0$, where z is composed of the system variables (see Section 2).
2. We associate the finitely presented left D-module $M = D^{1\times p}/(D^{1\times q}\,R)$ with the system $R\,z = 0$.
3. We develop a dictionary between the structural properties of the system and the properties of the left D-module M. Using module theory, we can then classify the properties of the left D-module M (see Section 3).
4. Homological algebra permits to check these properties of the left D-module M using *extension* and *torsion functors* (see Section 4).
5. Gröbner bases over Ore algebras allow to develop effective algorithms which check the properties of the left D-module M, and thus, of the system $R\,z = 0$ (see Section 5).
6. Implementations of these algorithms in the package OreModules for the computer algebra system Maple (see Section 6).

The purpose of this paper is to give an introduction to the package OreModules [8] for Maple which offers symbolic methods to investigate the structural properties of multidimensional linear systems over Ore algebras. The advantage of describing these properties in the language of homological algebra carries over to the implementation of OreModules: up to the choice of the domain of operators which occur in a given system, all algorithms are stated and implemented in sufficient generality such that ODEs, PDEs, differential time-delay systems, discrete systems with constant, polynomial or rational coefficients... are covered at the same time.

This paper is an extension of the congress paper [10].

2 Multidimensional Linear Systems over Ore Algebras

The mathematical framework of this paper is built on the concept of *Ore algebras* [5, 6, 7]. Ore algebras are non-commutative polynomial rings that represent linear functional operators in a natural way.

We recall that a ring with a unit 1 is a *domain* if the product of non-zero elements is non-zero. In what follows, we shall denote by A a domain which has a k-algebra structure, where k is a field.

Definition 1. 1. [25] A *skew polynomial ring* $A[\partial;\sigma,\delta]$ is a non-commutative ring consisting of all polynomials in ∂ with coefficients in A obeying the commutation rule

$$\forall\, a \in A, \quad \partial\, a = \sigma(a)\,\partial + \delta(a), \tag{1}$$

where σ is a *k-algebra endomorphism of A*, namely, $\sigma : A \longrightarrow A$ satisfies

$$\sigma(1) = 1, \quad \forall\, a, b \in A, \quad \sigma(a+b) = \sigma(a) + \sigma(b), \quad \sigma(a\,b) = \sigma(a)\,\sigma(b),$$

and δ is a *σ-derivation of A*, namely, $\delta : A \longrightarrow A$ satisfies:

$$\forall\, a, b \in A, \quad \delta(a+b) = \delta(a) + \delta(b), \quad \delta(a\,b) = \sigma(a)\,\delta(b) + \delta(a)\,b.$$

2. [5, 7] Let $A = k[x_1, \ldots, x_n]$ be a commutative polynomial ring over a field k (if $n = 0$ then $A = k$). The skew polynomial ring

$$D = A[\partial_1;\sigma_1,\delta_1]\ldots[\partial_m;\sigma_m,\delta_m]$$

is called *Ore algebra* if the σ_i's and δ_j's commute for $1 \leq i, j \leq m$ and satisfy:

$$\sigma_i(\partial_j) = \partial_j, \quad \delta_i(\partial_j) = 0, \quad j < i.$$

Example 1. In order to model an ordinary differential linear system with polynomial coefficients, we use the *Weyl algebra* $A_1(k) = k[t][\partial;\sigma,\delta]$ which is a non-commutative k-algebra generated by t and ∂. Elements of $A_1(k)$ are non-commutative polynomials in t and ∂ with coefficients in the field k (e.g., $k = \mathbb{Q}$, $\mathbb{R}, \mathbb{C}$) satisfying the following commutation rule:

$$\forall\, a \in k[t], \quad \partial\,(a\,\cdot) = a\,\partial\,\cdot + \frac{da}{dt}\,\cdot.$$

Therefore, regarding Definition 1, we have $\sigma = \mathrm{id}_{k[t]}$ and $\delta = \frac{d}{dt}$.

More generally, for the study of partial differential linear systems, we shall use the *Weyl algebra* $A_n(k) = k[x_1, \ldots, x_n][\partial_1;\sigma_1,\delta_1]\ldots[\partial_n;\sigma_n,\delta_n]$, where σ_i and δ_i are the maps on $k[x_1, \ldots, x_n]$ defined by

$$\sigma_i = \mathrm{id}_{k[x_1,\ldots,x_n]}, \quad \delta_i = \frac{\partial}{\partial\, x_i}, \quad i = 1, \ldots, n,$$

and every other commutation rule is prescribed by Definition 1. We have:

$$\partial_i\, x_j = x_j\,\partial_i + \delta_{ij}, \quad 1 \leq i, j \leq n, \quad \text{where} \quad \delta_{ij} = 1 \ \text{ if } i = j \ \text{ and } \ 0 \ \text{ else.}$$

Example 2. The algebra of *shift operators* with polynomial coefficients is another special case of an Ore algebra. For h in the field k (e.g., $k = \mathbb{Q}, \mathbb{R}$), we define $S_h(k) = k[t][\delta_h; \sigma_h, \delta]$ by:

$$\forall\, a \in k[t], \quad \sigma_h(a)(t) = a(t-h), \quad \delta(a) = 0.$$

The commutation rule $\delta_h\, t = (t-h)\, \delta_h$ represents the action of the shift operator on polynomials. Forming equations over S_h, we model time-delay (resp., time-advance) systems if $h > 0$ (resp., $h < 0$).

Example 3. For differential time-delay linear systems, we mix the constructions of the two preceding examples. For $h \in k$ (e.g., $k = \mathbb{Q}, \mathbb{R}$), we define the Ore algebra $D_h(k) = k[t][\partial; \sigma_1, \delta_1][\delta_h; \sigma_2, \delta_2]$ where:

$$\sigma_1 = \mathrm{id}_{k[t]}, \quad \delta_1 = \frac{d}{dt}, \quad \forall\, a \in k[t], \quad \sigma_2(a)(t) = a(t-h), \quad \delta_2 = 0.$$

If the considered system also involves an advance operator, then we may work with the algebra defined by

$$H_{(h,l)}(k) = k[t][\partial; \sigma_1, \delta_1][\delta_h; \sigma_2, \delta_2][\tau_l; \sigma_3, \delta_3],$$

where σ_i, δ_i, $i = 1, 2$, are as above and:

$$\forall\, a \in k[t], \quad \sigma_3(a)(t) = a(t+l), \quad \delta_3 = 0, \quad l > 0.$$

Example 4. In order to study multidimensional discrete linear systems, we can define the following Ore algebra $k[z_1, \ldots, z_n][\partial_1; \sigma_1, \delta_1] \ldots [\partial_n; \sigma_n, \delta_n]$, where σ_i and δ_i, $i = 1, \ldots, n$, are the maps on $k[z_1, \ldots, z_n]$ defined by $\delta_i = 0$ and:

$$\forall\, a \in k[z_1, \ldots, z_n], \quad \sigma_i(a)(z_1, \ldots, z_n) = a(z_1, \ldots, z_{i-1}, z_i + 1, z_{i+1}, \ldots, z_n).$$

We refer to [7] for more examples of Ore algebras using for instance the difference, the divided differences or the q-dilation functional operators.

We can "concatenate" different Ore algebras in order to combine different types of functional operators and, by this means, we get Ore algebras for most of the linear systems commonly considered in control theory. Moreover, we can also use different rings of coefficients such as the field of rational functions or the ring of analytic functions. However, as we shall develop computational aspects, we only consider here polynomial or rational coefficients over $\mathbb{Q}$. Finally, we can prove that the algebras defined in Examples 1, 2, 3 and 4 are *left* and *right noetherian rings* (namely, every left/right ideal is generated by means of a finite number of elements). Thus, they have the *left* and *right Ore properties* (namely, for any pair (a_1, a_2) of elements, there exists a non-zero pair (b_1, b_2) (resp., (c_1, c_2)) such that $b_1\, a_1 = b_2\, a_2$ (resp., $a_1\, c_1 = a_2\, c_2$)) [5, 7, 11, 25].

Linear systems studied in control theory are generally defined by means of systems of ordinary or partial differential equations, time-delay equations, recurrence equations... These equations usually come from mathematical models. Hence, we can generally write a system as $R\, z = 0$, where R is a matrix with entries in a certain Ore algebra and z contains the system variables including the inputs, the outputs, the states, the latent variables.

Example 5. • The linear system $P\left(\frac{d}{dt}\right) y = Q\left(\frac{d}{dt}\right) u$, where P and Q are two polynomial matrices in the differential operator $\frac{d}{dt}$ and with coefficients in $k[t]$, can be rewritten as $R\,z = 0$, where the entries of the matrix

$$R = \left(P\left(\frac{d}{dt}\right), \quad -Q\left(\frac{d}{dt}\right)\right)$$

belong to the Weyl algebra $A_1(k)$ and $z = (y^T,\, u^T)^T$.

- The differential time-delay linear system $\dot{x}(t) = A(t)\,x(t) + B(t)\,u(t-h)$, where A and B are two matrices with entries in $k[t]$ and $h > 0$, can be rewritten as $R\,z = 0$, where the entries of the matrix

$$R = \left(\frac{d}{dt}\,I - A(t), \quad -B(t)\,\delta_h\right)$$

belong to the Ore algebra $D_h(k)$ and $z = (x^T,\, u^T)^T$.

- The partial differential equation (heat equation)

$$\frac{\partial y(t,x)}{\partial t} = \frac{\partial}{\partial x}\left(a(x)\,\frac{\partial y(t,x)}{\partial x}\right) + u(t,\,x),$$

where the conductivity of the bar a is assumed to be polynomial in x, can be rewritten as $R\,z = 0$, where the entries of the matrix

$$R = \left(\frac{\partial}{\partial t} - \frac{\partial}{\partial x}\left(a(x)\,\frac{\partial}{\partial x}\right), \quad -1\right)$$

belong to the Weyl algebra $A_2(k)$ with $x_1 = t$, $x_2 = x$ and $z = (y,\, u)^T$.

Real systems are generally nonlinear ones, meaning that the theory developed in this paper is not directly applicable to these systems. However, using a linearization around a (generic/given) trajectory of the system, then the linearized system has varying coefficients. Therefore, we can examine the structural properties of the linearized system by means of the approach described here and use them to study the ones of the nonlinear system.

3 A Module-Theoretical Approach to Linear Systems

In what follows, we denote by D an Ore algebra. The main idea of *algebraic analysis* is to study a linear system of the form $R\,z = 0$, where $R \in D^{q\times p}$, by means of the *finitely presented (f.p.) left D-module* $M = D^{1\times p}/(D^{1\times q}\,R)$ [24]. M is associated with $R\,z = 0$ in the sense that, if we denote by z_i the residue class in M of the row vector $e_i \in D^{1\times p}$ defined by 1 in the i^{th} position and 0 elsewhere and $z = (z_1, \ldots, z_p)^T$, then M is defined by all left D-linear combinations of the system equations $R\,z = 0$. See [11, 28, 31, 47] for more details.

The use of the residue class left D-module M is natural as it is a generalization of the construction of the algebras commonly studied in algebraic or analytic

geometry and number theory (e.g., $\mathbb{C} = \mathbb{R}[x]/(x^2+1)$, $\mathbb{Z}[i\sqrt{5}] = \mathbb{Z}[x]/(x^2+5)$, $A = \mathbb{C}[x,y]/(x^2+y^2-1,\ x\,y-1)$) [17]. For instance, $A = \mathbb{C}[x,y]/I$, where I is the ideal $I = (x^2+y^2-1,\ x\,y-1)$ of $\mathbb{C}[x,y]$, can be defined by:

$$A = \mathbb{C}[x,y]/(\mathbb{C}[x,y]^{1\times 2}\,R), \quad R = \begin{pmatrix} x^2+y^2-1 \\ x\,y-1 \end{pmatrix} \in \mathbb{C}[x,y]^{2\times 1}.$$

The first main interest regarding the left D-module M instead of the system $R\,z = 0$ is that M is intrinsically well-defined in the sense that it does not depend on the choice of the representation $R\,z = 0$ of the system. Indeed, the same system can be represented in different equivalent forms having different numbers of unknowns and equations (e.g., state-space or input-output representations, Roesser or Fornasini-Marchesini models) [35, 38, 45].

The second main interest of using the finitely presented left D-module M is that we can classify the structural properties of the system by means of the module properties of M. We introduce a few definitions [25, 45].

Definition 2. Let M be a finitely generated left module over a left noetherian domain D. Then, we have the following definitions:

1. M is *free* if there exists $r \in \mathbb{Z}_+$ such that M is isomorphic to $D^{1\times r}$, a fact that we denote by $M \cong D^{1\times r}$.
2. M is *stably free* if there exist $r,\ s \in \mathbb{Z}_+$ such that $M \oplus D^{1\times s} \cong D^{1\times r}$, where $\oplus$ denotes the direct sum.
3. M is *projective* if there exist a left D-module N and $r \in \mathbb{Z}_+$ such that we have $M \oplus N \cong D^{1\times r}$. Then, the left D-module N is also projective.
4. M is *reflexive* if the following canonical D-morphism (i.e., D-linear map)

$$\varepsilon_M : M \longrightarrow \hom_D(\hom_D(M,D),D), \quad \varepsilon_M(m)(f) = f(m),$$

   – where $m \in M$ and f belongs to the right D-module $\hom_D(M,D)$ formed by the left D-morphisms from M to D – is an isomorphism (i.e., ε_M is both injective and surjective).
5. M is *torsion-free* if the left D-submodule

$$t(M) = \{m \in M \mid \exists\ 0 \neq P \in D,\ P\,m = 0\}$$

   of M is reduced to 0. $t(M)$ is called the *torsion left D-submodule* of M and the elements of $t(M)$ are the *torsion elements* of M.
6. M is *torsion* if $t(M) = M$.

We have the following important results [25, 45].

Theorem 1. *1. We have the following implications of module properties:*

$$\textit{free} \Rightarrow \textit{stably free} \Rightarrow \textit{projective} \Rightarrow \textit{reflexive} \Rightarrow \textit{torsion-free}.$$

2. Every torsion-free left module over $A_1(k)$ (resp., $k\left[\frac{d}{dt}\right]$, $k(t)\left[\frac{d}{dt}\right]$) is stably free (resp., free).

3. *Every projective module over the commutative polynomial ring $k[x_1, \ldots, x_n]$ over a field k is free (Quillen-Suslin theorem).*

In the recent years, a classification of properties of multidimensional linear systems has been established in terms of the properties of the corresponding left D-module M. Let us summarize some of them in Table 1. We refer the reader to [15, 28, 26, 29, 31, 32, 33, 34, 37, 38, 47, 49] for the precise definitions of the properties listed in the second and third column of Table 1.

Table 1. Classification of structural properties

Module M	**Structural properties**	**Optimal control**
Torsion	Poles/zeros classifications	
With torsion	Existence of autonomous elements	
Torsion-free	No autonomous elements, Controllability, Parametrizability, π-flatness	Variational problem without constraints (Euler-Lagrange equations)
Reflexive	Filter identification	
Projective	Internal stabilizability, Bézout identities, Stabilizing controllers	Computation of the Lagrange parameters without integration
Free	Flatness, Poles placement, Doubly coprime factorization, Youla-Kučera parametrization	Optimal controller

4 Homological Algebra

The main issue of checking effectively the system properties via the properties of modules defined in Section 3 was still open until recently. Only the case of multidimensional systems defined by a *full row rank* matrix R with entries in

the commutative polynomial ring $k[x_1, \ldots, x_n]$ was known using the different concepts of primeness [26, 34, 48, 49] developed in the middle of the seventies.

The concepts of *syzygy modules*, *free resolutions*, *extension* and *torsion functors*, *projective* and *homotopic equivalences*, *projective dimensions*... developed in homological algebra [45] form the basis of new algorithms checking the first column of Table 1, and thus, the system properties. These algorithms were obtained in [38] in the case of PDEs (see also [31, 32, 33, 34]).

We have recently shown in [9, 11] how these algorithms could be extended to some classes of Ore algebras including the interesting ones from the control theory point of view (e.g., ODEs, PDEs, recurrence operators, time-delay operators). The main steps of the algorithms developed in [9, 11] are:

1. Computation of *free resolutions* of f.p. left modules over an Ore algebra.
2. *Dualization* of the previous free resolutions using the $\hom_D(\cdot, D)$ *functor*.
3. Use of *involutions* in order to pass from right to left D-modules.
4. Computation of the quotient module of f.p. left D-modules.

Using the previous four points, we can then compute the *extension modules* $\text{ext}^i_D(M, D)$, $i \in \mathbb{Z}_+$, of any left D-module of the form $M = D^{1\times p}/(D^{1\times q}\, R)$. Let us explain the previous concepts. See [45] for more details.

Definition 3. We have the following definitions:

- A *complex* of left D-modules is a sequence formed by left D-modules P_i and left D-morphisms $d_i : P_i \longrightarrow P_{i-1}$ which satisfy $\text{im}\, d_{i+1} \subseteq \ker d_i$ for all $i \in \mathbb{Z}_+$. Such a complex is denoted by:

$$\ldots \xrightarrow{d_{i+2}} P_{i+1} \xrightarrow{d_{i+1}} P_i \xrightarrow{d_i} P_{i-1} \xrightarrow{d_{i-1}} P_{i-2} \xrightarrow{d_{i-2}} \ldots \tag{2}$$

- The left D-module $H(P_i) = \ker d_i/\text{im}\, d_{i+1}$ is called the *defect of exactness* of (2) at P_i. The complex (2) is said to be *exact at* P_i if $H(P_i) = 0$, i.e., $\ker d_i = \text{im}\, d_{i+1}$, and *exact* if $H(P_i) = 0$ for all $i \in \mathbb{Z}_+$.
- Let $M = D^{1\times p}/(D^{1\times q}\, R)$ be a finitely presented left D-module. A *free resolution* of M is an exact sequence of the form

$$\ldots \xrightarrow{.R_3} D^{1\times p_2} \xrightarrow{.R_2} D^{1\times p_1} \xrightarrow{.R_1} D^{1\times p_0} \xrightarrow{\pi} M \longrightarrow 0, \tag{3}$$

  where $p_0 = p$, $p_1 = q$, $R_1 = R$, $R_i \in D^{p_i\times p_{i-1}}$ and $.R_i : D^{1\times p_i} \longrightarrow D^{1\times p_{i-1}}$ is defined by $(.R_i)(\lambda) = \lambda\, R_i$ for all $\lambda \in D^{1\times p_i}$.
- Let us consider the free resolution (3) of M and the following complex

$$\ldots \xleftarrow{R_3.} D^{p_2} \xleftarrow{R_2.} D^{p_1} \xleftarrow{R_1.} D^{p_0} \longleftarrow 0, \tag{4}$$

  where $R_i. : D^{p_{i-1}} \longrightarrow D^{p_i}$ is defined by $(R_i.)(\lambda) = R_i\, \lambda$ for all $\lambda \in D^{p_{i-1}}$. Then, the defects of exactness of the complex (4) are denoted by:

$$\begin{cases} \text{ext}^0_D(M, D) = \ker(R_1.), \\ \text{ext}^i_D(M, D) = \ker(R_{i+1}.)/(R_i\, D^{1\times p_{i-1}}), \quad i \geq 1. \end{cases}$$

$\text{ext}^i_D(M, D)$ inherits a right module structure by the right action of D.

Proposition 1. *[45] The right D-module $\mathrm{ext}^i_D(M,D)$ only depends on M, i.e., we can choose any free resolution of M to compute $\mathrm{ext}^i_D(M,D)$, $i \in \mathbb{Z}_+$. Moreover, we have $\mathrm{ext}^0_D(M,D) = \mathrm{hom}_D(M,D)$.*

Coming back to the four main algorithmic steps outlined above, we recall that an *involution* θ of D is a k-linear map $\theta : D \longrightarrow D$ satisfying:

$$\forall\, a_1, a_2 \in D, \quad \theta(a_1 \cdot a_2) = \theta(a_2) \cdot \theta(a_1), \quad \theta \circ \theta = \mathrm{id}_D. \tag{5}$$

Example 6. We have the following examples of involutions:

1. If $D = k[x_1, \ldots, x_n]$ is a commutative polynomial algebra, then $\theta = id$ is a trivial involution.
2. If $D = A_n$ is the Weyl algebra and $P \in D$, then we let $\theta(P)$ be the classical *formal adjoint* of P obtained by multiplying a test function on the left of $P\,z$ and by integrating by parts [31, 33, 34]. Equivalently, θ is defined by $\theta(x_i) = x_i$ and $\theta(\partial_i) = -\partial_i$, $i = 1, \ldots, n$.
3. Let $S_h(k)$ be the Ore algebra of shift operators defined in Example 2. Then, an involution θ of $S_h(k)$ is defined by $\theta(t) = -t$ and $\theta(\delta_h) = \delta_h$.
4. If $D_h(k)$ is the Ore algebra of differential time-delay operators defined in Example 3, then an involution θ of $D_h(k)$ can be defined by $\theta(t) = -t$, $\theta(\delta_h) = \delta_h$ and $\theta(\partial) = \partial$. This last result shows that a simple involution of $D_h(k)$ exists contrary to what was written in [11] (we thank V. Levandovskyy for pointing out to us this trivial mistake).

Now, if R is a matrix with entries in an Ore algebra having an involution θ (e.g., $A_n(k)$, $S_h(k)$, $D_h(k)$), then we can define $\theta(R) = (\theta(R_{ij}))^T$ and the left D-module $\widetilde{N} = D^{1\times q}/(D^{1\times p}\,\theta(R))$. The main idea developed in [9, 11, 31, 34, 38] is that the module properties in the first column of Table 1 are characterized by the vanishing of certain $\mathrm{ext}^i_D(\widetilde{N}, D)$ as it is shown in Table 2. We refer the reader to [42] for a constructive algorithm which checks freeness and computes bases of free modules.

The last column of Table 2 explains the correspondence between module properties and primeness for a multidimensional system defined by a full row rank matrix R with entries in the commutative polynomial ring $D = k[x_1, \ldots, x_n]$ [34]. The third column generalizes the last column to multidimensional systems defined by a full row rank matrix R with entries in the ring of differential operators with rational coefficients and $d(\widetilde{N})$ denotes the *Krull dimension* of the *characteristic variety* of $\widetilde{N}$ (see [34, 39]).

5 Computation of $\mathrm{ext}^i_D(\widetilde{N}, D)$

The main difficulty in the computation of $\mathrm{ext}^i_D(\widetilde{N}, D)$ is to be able to construct a free resolution for the left D-module $\widetilde{N} = D^{1\times q}/(D^{1\times p}\,\theta(R))$ (see point 1 in the previous section), i.e., an exact sequence of the form

$$\ldots \xrightarrow{.\tilde{R}_4} D^{1\times q_3} \xrightarrow{.\tilde{R}_3} D^{1\times q_2} \xrightarrow{.\tilde{R}_2} D^{1\times q_1} \xrightarrow{.\tilde{R}_1} D^{1\times q_0} \longrightarrow \widetilde{N} \longrightarrow 0,$$

where $\widetilde{R}_1 = \theta(R)$, $q_0 = q$, $q_1 = p$ and $.\widetilde{R}_i : D^{1\times q_i} \rightarrow D^{1\times q_{i-1}}$ is defined by $(.\widetilde{R}_i)(\lambda) = \lambda\,\widetilde{R}_i$. The left D-module

$$S_i(\widetilde{N}) = \ker(.\widetilde{R}_i) = \{\lambda \in D^{1\times q_i} \mid \lambda\,\widetilde{R}_i = 0\}$$

is called the i^{th} *syzygy left D-module* of $\widetilde{N}$. If D is a noetherian ring, which is the case for a large class of algebras (e.g., A_n, S_h, D_h and $H_{(h,l)}$) [9, 11], then free resolutions always exist for finitely generated left D-modules [25, 45].

The computation of the matrix $\widetilde{R}_{i+1}$ is an *elimination problem* [2, 17]. Indeed, multiplying $\lambda \in S_i(\widetilde{N})$ on the left of the inhomogeneous system $\widetilde{R}_i\,y = u$, we then obtain $\lambda\,u = 0$. Hence, finding a family of generators for $S_i(\widetilde{N})$, i.e., $\{\lambda_j\}_{1\leq j\leq q_{i+1}}$, $\lambda_j \in D^{1\times q_i}$ satisfying $S_i(\widetilde{N}) = D\,\lambda_1 + \ldots + D\,\lambda_{q_{i+1}}$ is equivalent to finding a family of generators for the *compatibility conditions* of the inhomogeneous system $\widetilde{R}_i\,y = u$. Then, if we denote by $\widetilde{R}_{i+1} = (\lambda_1^T, \ldots, \lambda_{q_{i+1}}^T)^T$, we finally obtain $S_i(\widetilde{N}) = D^{1\times q_{i+1}}\,\widetilde{R}_{i+1}$.

Such a difficult problem has largely been studied for linear systems of PDEs since the 19^{th} century [31, 38, 39]. But, only recently some computational answers were found based on the concepts of *Janet* and *Gröbner bases* for non-commutative polynomial rings. We recall the definition of Gröbner bases for polynomial ideals. This definition can easily be extended to modules [2, 17]. The algorithmic methods used in the theory of Gröbner bases require that a monomial order is chosen to compare polynomials.

Table 2. Characterization of module properties

Module M	$\mathbf{ext}^i_D(\widetilde{N}, D)$	$d(\widetilde{N})$	**Primeness**
With torsion	$\text{ext}^1_D(\widetilde{N}, D) \cong t(M)$	$n-1$	$\emptyset$
Torsion-free	$\text{ext}^1_D(\widetilde{N}, D) = 0$	$n-2$	Minor left-prime
Reflexive	$\text{ext}^i_D(\widetilde{N}, D) = 0$, $i = 1, 2$	$n-3$	
Projective	$\text{ext}^i_D(\widetilde{N}, D) = 0$, $1 \leq i \leq n$	-1	Zero left-prime

Definition 4. 1. Let D be an Ore algebra. A *monomial order* $<$ on D is defined as a total order on the *set of monomials* $\mathrm{Mon}(D)$ satisfying the following two conditions:
   a) For all monomials $m \in \mathrm{Mon}(D)\backslash\{1\}$, we have $1 < m$.
   b) If $m_1 < m_2$ holds for two monomials $m_1, m_2 \in \mathrm{Mon}(D)$, then, for all $n \in \mathrm{Mon}(D)$, we have $n \cdot m_1 < n \cdot m_2$.
2. Given a polynomial $P \in D\backslash\{0\}$ and a monomial order $<$ on D, we can compare the monomials with a non-zero coefficient in P w.r.t. $<$. The greatest of these monomials is the *leading monomial* $\mathrm{lm}(P)$ of P.

Definition 5. [2, 17] Let D be a polynomial ring and I a (left) ideal of D. A set of non-zero polynomials $G = \{g_1, \ldots, g_t\} \subset I$ is called a *Gröbner basis* for I if for all $0 \neq f \in I$, there exists $1 \leq i \leq t$ such that $\mathrm{lm}(g_i)$ divides $\mathrm{lm}(f)$.

One consequence of the condition that defines Gröbner bases is that every polynomial f in I is *reduced* to 0 modulo G, i.e., by subtraction of suitable left multiples of the $g_i \in G$ from f, we then obtain the zero polynomial.

For the case of commutative polynomial rings, *Buchberger's algorithm* [2, 17] computes Gröbner bases of polynomial ideals. Recently, Buchberger's algorithm was extended to some non-commutative polynomial rings and, in particular, to some classes of Ore algebras [5, 7] that are important for the study of multidimensional linear systems. Hence, manipulations of (one-sided) ideals and modules over many classes of Ore algebras have been turned effective. Moreover, the Maple library *Mgfun* [6] has been developed for the symbolic manipulation of a large class of special functions and combinatorial sequences. It offers implementations of Gröbner bases for some classes of Ore algebras.

6 The Package OreModules

Using the Maple library *Mgfun*, the authors of this paper have recently been developing the package OreModules [8, 10]. OreModules as well as a library of examples are freely available at:

`http://wwwb.math.rwth-aachen.de/OreModules`.

This second release of OreModules focuses on the following problems:

- Compute free resolutions, formal adjoints, extension functors, duals and biduals of f.p. left D-modules over some classes of Ore algebras D.
- Recognize the properties of a finitely presented left D-module M (torsion-free, reflexive, projective, stably free, free).
- Decide the existence of torsion elements in the corresponding system and, if so, compute a family of generators for them.
- Compute left/right/generalized inverses of matrices with entries in D.
- Check whether or not a multidimensional linear system is controllable in the sense of [14, 15, 26, 30, 29, 31, 32, 47, 49] or compute the autonomous elements of the system [30, 31, 32, 47, 49].

- Check whether or not a multidimensional linear system is parametrizable in the sense of [11, 31, 32, 33].
- Check whether or not a multidimensional linear system is flat and, if so, compute an injective parametrization and a flat output [15, 26, 31, 33, 42].
- Check whether or not a multidimensional linear system with constant coefficients is π-free and, if so, compute the ideal of all the π-polynomials [11, 15, 26].

A list of the most important functions of OreModules is given in Table 3 (the suffix "Rat" distinguishes the procedures which deal with polynomial/rational coefficients). Detailed documentation of OreModules is available in form of Maple help pages.

7 Worked Examples Using OreModules

OreModules comes with a library of examples which demonstrates the above features by means of systems like two pendula mounted on a cart, stirred tank models, electric transmission line, wind tunnel model, Maxwell equations, Einstein equations, equations of linear elasticity, Lie-Poisson structures... We only give here four simple examples but we refer the reader to [8, 9, 11] for more sophisticated examples. All examples were run on a Pentium III, 1 GHz with 1 GB RAM using Maple 8 (OreModules is available for Maple V release 5, Maple 6, Maple 8, Maple 9 and Maple 10).

Example 7. We study a linearized bipendulum [31], i.e., a system composed of a bar, where two pendula are fixed, one of length $l1$ and one of length $l2$. The appropriate Ore algebra for this example is the Weyl algebra $Alg = A_1$, i.e., $A_1 = \mathbb{Q}(l1, l2, g)[t][\mathrm{D}]$, where $\mathrm{D} = \frac{d}{dt}$ is the differential operator w.r.t. time t:

```
> with(OreModules):
> Alg:=DefineOreAlgebra(diff=[D,t],polynom=[t],comm=[g,l1,l2]):
```

Note that we have to declare all constants appearing in the system equations (the gravitational constant g and the lengths $l1$ and $l2$) as variables that commute with D and t. Next, we enter the system matrix:

```
> R:=evalm([[D^2+g/l1, 0, -g/l1], [0, D^2+g/l2, -g/l2]]);
```

$$R := \begin{bmatrix} \mathrm{D}^2 + \frac{g}{l1} & 0 & -\frac{g}{l1} \\ 0 & \mathrm{D}^2 + \frac{g}{l2} & -\frac{g}{l2} \end{bmatrix}$$

In terms of equations, the linearized bipendulum is described by:

```
> ApplyMatrix(R, [x1(t),x2(t),u(t)], Alg) = evalm([[0],[0]]);
```

$$\begin{bmatrix} \frac{g\,\mathrm{x1}(t)}{l1} + (\frac{d^2}{dt^2}\,\mathrm{x1}(t)) - \frac{g\,\mathrm{u}(t)}{l1} \\ \frac{g\,\mathrm{x2}(t)}{l2} + (\frac{d^2}{dt^2}\,\mathrm{x2}(t)) - \frac{g\,\mathrm{u}(t)}{l2} \end{bmatrix} = \begin{bmatrix} 0 \\ 0 \end{bmatrix}$$

Table 3. List of the most important functions of OreModules

Main functions for the treatment of linear systems over Ore algebras D	
`Parametrization(Rat)`	Find parametrization of the system
`MinimalParametrization(s)(Rat)`	Find minimal parametrization(s) of the system
`AutonomousElements(Rat)`	Find a generating set of autonomous elements of the system (i.e., solve the system of equations for the torsion elements) in case of PDEs
`LeftInverse(Rat)`	Compute a left-inverse for a matrix over D
`LocalLeftInverse`	Given a $0 \neq \pi \in k[x_1, \ldots, x_n]$, compute a left inverse for a matrix over $k[x_1, \ldots, x_n, \pi^{-1}]$
`RightInverse(Rat)`	Compute a right-inverse for a matrix over D
`GeneralizedInverse(Rat)`	Compute a generalized inverse matrix over D
`PiPolynomial`	Given a system matrix over a commutative polynomial ring D and a variable $x_i \in D$, compute the ideal of all π-polynomials in x_i for the system
`FirstIntegral`	For ODEs, find first integrals of motion
`LQEquations`	Compute the Euler-Lagrange equations of a linear quadratic problem and a controllable OD system
Module theory over Ore algebras D	
`TorsionElements(Rat)`	Compute the torsion submodule of a f.p. D-module
`Exti(Rat)`	Given a f.p. left D-module M and j, compute $\mathrm{ext}^j_D(M, D)$
`Extn(Rat)`	Given a f.p. left D-module M and m, compute $\mathrm{ext}^i_D(M, D)$ for $0 \leq i \leq m$
`Quotient(Rat)`	Compute the quotient module of two left D-modules generated by the rows of matrices
`SyzygyModule(Rat)`	Compute the first syzygy module of a f.p. left D-module
`Resolution(Rat)`	Given i, compute the first i^{th} terms of a free resolution of a f.p. left D-module
`FreeResolution(Rat)`	Compute a free resolution of a f.p. left D-module
`OreRank(Rat)`	Compute the rank of a f.p. left D-module
Some low-level functions of OreModules	
`DefineOreAlgebra`	Set up an Ore algebra D in OreModules
`Involution`	Apply an involution to a matrix over D
`Factorize(Rat)`	Right-divide a matrix over D by another one
`Mult`	Multiply two or more matrices over D
`ApplyMatrix`	Apply (matrices of) operators in D to (vectors of) functions

We compute the formal adjoint of R:

```
> R_adj:=Involution(R, Alg);
```

$$R\_adj := \begin{bmatrix} \mathrm{D}^2 + \dfrac{g}{l1} & 0 \\ 0 & \mathrm{D}^2 + \dfrac{g}{l2} \\ -\dfrac{g}{l1} & -\dfrac{g}{l2} \end{bmatrix}$$

By computing $\mathrm{ext}^1_{A_1}(A_1^{1\times 2}/(A^{1\times 3}\, R\_adj), A_1)$, we check whether or not the left A_1-module $M = A_1^{1\times 3}/(A_1^{1\times 2}\, R)$ is torsion-free, i.e., whether or not the bipendulum is controllable and parametrizable:

```
> Ext:=Exti(R_adj, Alg, 1);
```

$$Ext := \left[\begin{bmatrix} 1 & 0 \\ 0 & 1 \end{bmatrix}, \begin{bmatrix} \mathrm{D}^2\, l1 + g & 0 & -g \\ 0 & \mathrm{D}^2\, l2 + g & -g \end{bmatrix}, \begin{bmatrix} l2\, \mathrm{D}^2\, g + g^2 \\ g^2 + \mathrm{D}^2\, l1\, g \\ l2\, \mathrm{D}^2\, g + l2\, l1\, \mathrm{D}^4 + \mathrm{D}^2\, l1\, g + g^2 \end{bmatrix}\right]$$

From the output, we can see that the system is *generically* controllable because $Ext[1]$ is the identity matrix which means that there are no torsion elements in the left A_1-module M associated with the system. The interpretation of this structural fact is that the system has no autonomous elements *in the generic case* (see Section 3). There may be a few configurations of the constants g, $l1$, $l2$, in which the bipendulum is not controllable. We will actually find the only configuration where it is not controllable below. Let us write down the generic parametrization $Ext[3]$ in a more familiar way with a free function ξ_1.

```
> P:=Parametrization(R, Alg);
```

$$P := \begin{bmatrix} g\,(g\,\xi_1(t) + l2\,\frac{d^2}{dt^2}\,\xi_1(t) \\ g\,(g\,\xi_1(t) + l1\,\frac{d^2}{dt^2}\,\xi_1(t) \\ g^2\,\xi_1(t) + g\,l2\,\frac{d^2}{dt^2}\,\xi_1(t) + g\,l1\,\frac{d^2}{dt^2}\,\xi_1(t) + l1\,l2\,(\frac{d^4}{dt^4}\,\xi_1(t)) \end{bmatrix}$$

Therefore, all smooth solutions of the system are parametrized by P, i.e.,

$$R\,(x_1,\, x_2,\, u)^T = 0 \;\Leftrightarrow\; (x_1,\, x_2,\, u)^T = Ext[3]\,\xi_1 = P\,\xi_1.$$

Since the bipendulum is generically a time-invariant controllable system, it is also generically a flat system. A *flat output* of the system can be computed as a left-inverse of the parametrization $Ext[3]$:

```
> S:=LeftInverse(Ext[3], Alg);
```

$$S := \left[\frac{l1}{g^2\,(l1 - l2)} \;\; -\frac{l2}{g^2\,(l1 - l2)} \;\; 0\right]$$

i.e., a flat output is defined by $\xi_1 = S\ (x_1,\ \ x_2,\ \ u)^T$, namely:

```
> xi[1](t)=ApplyMatrix(S, [x1(t),x2(t),u(t)], Alg)[1,1];
```

$$\xi_1(t) = \frac{l1\,\mathrm{x1}(t)}{g^2\,(l1-l2)} - \frac{l2\,\mathrm{x2}(t)}{g^2\,(l1-l2)}$$

We remark that this flat output is defined only if $l1 - l2 \neq 0$. In this case, let us compute the Brunovský canonical form of the system.

```
> B:=Brunovsky(R, Alg);
```

$$B := \begin{bmatrix} \dfrac{l1}{g^2\,(l1-l2)} & -\dfrac{l2}{g^2\,(l1-l2)} & 0 \\ \dfrac{\mathrm{D}\,l1}{g^2\,(l1-l2)} & -\dfrac{\mathrm{D}\,l2}{g^2\,(l1-l2)} & 0 \\ -\dfrac{1}{g\,(l1-l2)} & \dfrac{1}{g\,(l1-l2)} & 0 \\ -\dfrac{\mathrm{D}}{g\,(l1-l2)} & \dfrac{\mathrm{D}}{g\,(l1-l2)} & 0 \\ \dfrac{1}{(l1-l2)\,l1} & -\dfrac{1}{(l1-l2)\,l2} & \dfrac{1}{l1\,l2} \end{bmatrix}$$

In other words, we have the following transformation between the system variables x_1, x_2 and u and the Brunovský variables z_i, $i = 1, \ldots, 4,$ and v:

```
> evalm([seq([z[i](t)],i=1..4),[v(t)]])=ApplyMatrix(B,
> [x1(t),x2(t),u(t)], Alg);
```

$$\begin{bmatrix} z_1(t) \\ z_2(t) \\ z_3(t) \\ z_4(t) \\ \mathrm{v}(t) \end{bmatrix} = \begin{bmatrix} \dfrac{l1\,\mathrm{x1}(t)}{g^2\,(l1-l2)} - \dfrac{l2\,\mathrm{x2}(t)}{g^2\,(l1-l2)} \\ \dfrac{l1\,(\frac{d}{dt}\,\mathrm{x1}(t))}{g^2\,(l1-l2)} - \dfrac{l2\,(\frac{d}{dt}\,\mathrm{x2}(t))}{g^2\,(l1-l2)} \\ -\dfrac{\mathrm{x1}(t)}{g\,(l1-l2)} + \dfrac{\mathrm{x2}(t)}{g\,(l1-l2)} \\ -\dfrac{\frac{d}{dt}\,\mathrm{x1}(t)}{g\,(l1-l2)} + \dfrac{\frac{d}{dt}\,\mathrm{x2}(t)}{g\,(l1-l2)} \\ \dfrac{\mathrm{x1}(t)}{(l1-l2)\,l1} - \dfrac{\mathrm{x2}(t)}{(l1-l2)\,l2} + \dfrac{\mathrm{u}(t)}{l1\,l2} \end{bmatrix}$$

Let us check that the new variables z_i, $i = 1, \ldots, 4,$ and v satisfy a Brunovský canonical form:

```
> F:=Elimination(linalg[stackmatrix](B, R), [x1,x2,u],
> [seq(z[i],i=1..4),v,0,0], Alg):
> ApplyMatrix(F[1], [x1(t),x2(t),u(t)], Alg)=ApplyMatrix(F[2],
> [seq(z[i](t),i=1..4),v(t)], Alg);
```

$$\begin{bmatrix} 0 \\ 0 \\ 0 \\ 0 \\ \mathrm{u}(t) \\ \mathrm{x2}(t) \\ \mathrm{x1}(t) \end{bmatrix} = \begin{bmatrix} -(\frac{d}{dt}\, z_4(t)) + \mathrm{v}(t) \\ -(\frac{d}{dt}\, z_3(t)) + z_4(t) \\ -(\frac{d}{dt}\, z_2(t)) + z_3(t) \\ -(\frac{d}{dt}\, z_1(t)) + z_2(t) \\ g^2\, z_1(t) + (g\, l2 + g\, l1)\, z_3(t) + l1\, l2\, \mathrm{v}(t) \\ g^2\, z_1(t) + g\, l1\, z_3(t) \\ g^2\, z_1(t) + g\, l2\, z_3(t) \end{bmatrix}$$

The last three equations give u, x_1 and x_2 in terms of the z_i and v.

$l1 = l2$ describes the only case in which the bipendulum may be uncontrollable. We now turn to the case where the lengths of the pendula are equal:

```
> R_mod:=subs(l2=l1, evalm(R));
```

$$R\_mod := \begin{bmatrix} \mathrm{D}^2 + \frac{g}{l1} & 0 & -\frac{g}{l1} \\ 0 & \mathrm{D}^2 + \frac{g}{l1} & -\frac{g}{l1} \end{bmatrix}$$

```
> Ext_mod:=Exti(Involution(R_mod, Alg), Alg, 1);
```

$$Ext\_mod := \left[\begin{bmatrix} \mathrm{D}^2\, l1 + g & 0 \\ 0 & 1 \end{bmatrix}, \begin{bmatrix} 1 & -1 & 0 \\ 0 & \mathrm{D}^2\, l1 + g & -g \end{bmatrix}, \begin{bmatrix} g \\ g \\ \mathrm{D}^2\, l1 + g \end{bmatrix} \right]$$

The computation of $\mathrm{ext}^1_{A_1}(A_1^{1\times 2}/(A_1^{1\times 3}\,\theta(R_{mod})), A_1)$ gives the torsion submodule $t(M)$ of M: it is generated by the residue class of the row r of $Ext\_mod[2]$ which corresponds to the row with entry $l1\,\mathrm{D}^2 + g$ in $Ext\_mod[1]$. This means that $(l1\,\mathrm{D}^2 + g)\, r = 0$ in M, and the difference of the positions of the pendula (relative to the bar) is an autonomous element of the system. We can conclude that the bipendulum is controllable if and only if $l1 \neq l2$.

We can directly obtain the torsion elements of M as follows:

```
> TorsionElements(R_mod, [x1(t),x2(t),u(t)], Alg);
```

$$[\left[g\,\theta_1(t) + l1\,(\tfrac{d^2}{dt^2}\,\theta_1(t)) = 0 \right], \left[\theta_1(t) = \mathrm{x1}(t) - \mathrm{x2}(t) \right]]$$

We can also explicitly integrate this torsion element of M:

```
> AutonomousElements(R_mod, [x1(t),x2(t),u(t)], Alg)[2];
```

$$\left[\theta_1 = \_C1\, \sin(\frac{\sqrt{g}\, t}{\sqrt{l1}}) + \_C2\, \cos(\frac{\sqrt{g}\, t}{\sqrt{l1}}) \right]$$

The fact that there exists an autonomous element in the system is equivalent to the existence of a first integral of motion in the system. Indeed, we recall that we have a one-to-one correspondence between the torsion elements and the first integrals of motion. For more details, see [33]. We can compute this first integral of motion by using the command FirstIntegral:

```
> V:=FirstIntegral(R_mod, [x1(t),x2(t),u(t)], Alg);
```

$$
\begin{aligned}
V := &-(-(\tfrac{d}{dt}\,\mathrm{x1}(t))\,\_C1\,\sin(\frac{\sqrt{g}\,t}{\sqrt{l1}})\,\sqrt{l1} - (\tfrac{d}{dt}\,\mathrm{x1}(t))\,\_C2\,\cos(\frac{\sqrt{g}\,t}{\sqrt{l1}})\,\sqrt{l1} \\
&+ \sqrt{g}\,\mathrm{x1}(t)\,\_C1\,\cos(\frac{\sqrt{g}\,t}{\sqrt{l1}}) - \sqrt{g}\,\mathrm{x1}(t)\,\_C2\,\sin(\frac{\sqrt{g}\,t}{\sqrt{l1}}) \\
&+ (\tfrac{d}{dt}\,\mathrm{x2}(t))\,\_C1\,\sin(\frac{\sqrt{g}\,t}{\sqrt{l1}})\,\sqrt{l1} + (\tfrac{d}{dt}\,\mathrm{x2}(t))\,\_C2\,\cos(\frac{\sqrt{g}\,t}{\sqrt{l1}})\,\sqrt{l1} \\
&- \sqrt{g}\,\mathrm{x2}(t)\,\_C1\,\cos(\frac{\sqrt{g}\,t}{\sqrt{l1}}) + \sqrt{g}\,\mathrm{x2}(t)\,\_C2\,\sin(\frac{\sqrt{g}\,t}{\sqrt{l1}}))\,/\sqrt{l1}
\end{aligned}
$$

We let the reader check by himself that we have $\dot{V}(t) = 0$. For the explicit computations, see [8].

Finally, even if we have some autonomous elements in the system, we can parametrize all solutions of the system in terms of one arbitrary function ξ_1 and two arbitrary constants C_1 and C_2 (these constants can easily be computed in terms of the initial conditions of the system):

```
> P2:=Parametrization(R_mod, Alg);
```

$$
P2 := \begin{bmatrix} g\,\xi_1(t) \\ -\_C1\,\sin(\frac{\sqrt{g}\,t}{\sqrt{l1}}) - \_C2\,\cos(\frac{\sqrt{g}\,t}{\sqrt{l1}}) + g\,\xi_1(t) \\ l1\,(\frac{d^2}{dt^2}\,\xi_1(t)) + g\,\xi_1(t) \end{bmatrix}
$$

i.e., we have $R\,(x_1,\, x_2,\, u)^T = 0 \Leftrightarrow (x_1,\, x_2,\, u)^T = P_2(\xi_1, \_C1, \_C2)$. We can easily check that P_2 gives a parametrization of some solutions of the system as we have:

```
> simplify(ApplyMatrix(R_mod, P2, Alg));
```

$$
\begin{bmatrix} 0 \\ 0 \end{bmatrix}
$$

We can prove that P_2 parametrizes all smooth solutions of the system [40].

Example 8. This example demonstrates the study of structural properties of a simple linear time-varying ordinary differential system [41, 43]. See [8] for more sophisticated examples.

```
> Alg:=DefineOreAlgebra(diff=[D,t], polynom=[t]):
```

Let us consider the following matrix of ordinary differential operators:

```
> R:=evalm([[D, -t]]);
```

$$
R := \begin{bmatrix} \mathrm{D} & -t \end{bmatrix}
$$

The matrix R corresponds to the following time-varying linear system:

```
> ApplyMatrix(R, [x(t),u(t)], Alg)[1,1]=0;
```

$$(\tfrac{d}{dt}\,\mathrm{x}(t)) - t\,\mathrm{u}(t) = 0$$

Let us check whether or not this system is controllable and flat. In order to do that, let us define the formal adjoint *R_adj* of *R*.

```
> R_adj:=Involution(R, Alg);
```

$$R\_adj := \begin{bmatrix} -\mathrm{D} \\ -t \end{bmatrix}$$

We compute the first extension module $\mathrm{ext}^1_{A_1(\mathbb{Q})}(A_1(\mathbb{Q})/(A_1(\mathbb{Q})^{1\times 2}\,R\_adj), A_1(\mathbb{Q}))$ of the left *Alg*-module associated with *R_adj*:

```
> Ext:=Exti(R_adj, Alg, 1);
```

$$Ext := [\begin{bmatrix} 1 \end{bmatrix}, \begin{bmatrix} \mathrm{D} & -t \end{bmatrix}, \begin{bmatrix} -t^2 & -1 + t\,\mathrm{D} \\ -2 - t\,\mathrm{D} & \mathrm{D}^2 \end{bmatrix}]$$

Therefore, we obtain that the left A_1-module $M = A_1(\mathbb{Q})^{1\times 2}/(A_1(\mathbb{Q})\,R)$ associated with R is torsion-free, and thus, stably free as $A_1(\mathbb{Q})$ is a hereditary ring. A parametrization of the system is given by *Ext*[3]. This result can directly be obtained by using the following command:

```
> Parametrization(R, Alg);
```

$$\begin{bmatrix} -t^2\,\xi_1(t) - \xi_2(t) + t\,(\frac{d}{dt}\,\xi_2(t)) \\ -2\,\xi_1(t) - t\,(\frac{d}{dt}\,\xi_1(t)) + (\frac{d^2}{dt^2}\,\xi_2(t)) \end{bmatrix}$$

Let us notice that the previous parametrization depends on two arbitrary functions ξ_1 and ξ_2. However, the system has only 1 input, and thus, the rank of the left $A_1(\mathbb{Q})$-module M is 1. Let us check this result:

```
> OreRank(R, Alg);
```

$$1$$

Hence, we deduce that there exist some minimal parametrizations of the system which depend on 1 arbitrary function. Let us compute some of them.

```
> P:=MinimalParametrizations(R, Alg);
```

$$P := [\begin{bmatrix} -t^2 \\ -2 - t\,\mathrm{D} \end{bmatrix}, \begin{bmatrix} -1 + t\,\mathrm{D} \\ \mathrm{D}^2 \end{bmatrix}]$$

Let us check whether or not the first minimal parametrization $P[1]$ is injective.

```
> LeftInverse(P[1], Alg);
```

$$[]$$

We obtain that $P[1]$ is not an injective parametrization of the system. Let us examine the second minimal parametrization $P[2]$ in a similar way:

```
> LeftInverse(P[2], Alg);
```

$$[]$$

We find that $P[2]$ is not an injective parametrization of the system either. Therefore, we cannot conclude that the left $A_1(\mathbb{Q})$-module M associated with the system is free. In fact, we can prove that M is not a free left $A_1(\mathbb{Q})$-module, and thus, the corresponding time-varying system is not flat. See [39, 42] for more details. However, we already know that M is a stably free left $A_1(\mathbb{Q})$-module as the matrix R has full row rank and R admits a right-inverse defined by:

```
> RightInverse(R, Alg);
```

$$\begin{bmatrix} t \\ \mathrm{D} \end{bmatrix}$$

See [11] for more details. One of the main interests of the non-minimal parametrization $Ext[3]$ is that it admits a generalized inverse, namely, there exists a matrix G with entries in $A_1(\mathbb{Q})$ satisfying $Ext[3]\ G\ Ext[3] = Ext[3]$ (contrary to $P[1]$ and $P[2]$). This last result implies that the non-minimal parametrization parametrizes all the solutions of the corresponding time-varying system which belong to any left $A_1(\mathbb{Q})$-module $\mathcal{F}$ (e.g., $\mathcal{F} = C^\infty(\mathbb{R})$, $\mathbb{R}(t)$, $\mathbb{R}[t]$). Let us compute one generalized inverse of $Ext[3]$:

```
> G:=GeneralizedInverse(Ext[3], Alg);
```

$$G := \begin{bmatrix} 0 & -1 \\ -1 & 0 \end{bmatrix}$$

```
> Mult(Ext[3], G, Ext[3], Alg);
```

$$\begin{bmatrix} -t^2 & -1 + t\,\mathrm{D} \\ -2 - t\,\mathrm{D} & \mathrm{D}^2 \end{bmatrix}$$

Let us determine the obstruction of flatness. In order to do that, we study the system over the ring $\mathbb{Q}(t)\left[\frac{d}{dt}\right]$ of ordinary differential operators with rational coefficients in t. Let us compute a parametrization of the system by allowing to invert non-zero polynomials in t:

```
> Extrat:=ExtiRat(R_adj, Alg, 1);
```

$$Extrat := [\left[1\right], \left[\mathrm{D}\ -t\right], \begin{bmatrix} -t^2 \\ -2 - t\,\mathrm{D} \end{bmatrix}]$$

We obtain that the left $\mathbb{Q}(t)\left[\frac{d}{dt}\right]$-module $M' = \mathbb{Q}(t)\left[\frac{d}{dt}\right]^{1\times 2}/(\mathbb{Q}(t)\left[\frac{d}{dt}\right]\ R)$ is torsion-free, and thus, free because $\mathbb{Q}(t)\left[\frac{d}{dt}\right]$ is a left principal ideal domain.

Moreover, a (minimal) parametrization of the system is defined by $Extrat[3]$. This result can directly be obtained by using ParametrizationRat:

```
> ParametrizationRat(R, Alg);
```

$$\begin{bmatrix} -t^2\,\xi_1(t) \\ -2\,\xi_1(t) - t\,(\frac{d}{dt}\,\xi_1(t)) \end{bmatrix}$$

The fact that the left $\mathbb{Q}(t)[D]$-module M associated with R is free implies that, away from some singularities that we are going to determine, the system is flat. Let us compute a basis for this module which gives a flat output of the system.

```
> S:=LeftInverseRat(Extrat[3], Alg);
```

$$S := \begin{bmatrix} -\frac{1}{t^2} & 0 \end{bmatrix}$$

Therefore, we obtain that a basis of the left $\mathbb{Q}(t)[D]$-module M is defined by $\xi_1 = S\ (x,\ \ u)^T$ and satisfies:

$$(x,\, u)^T = Extrat[3]\, \xi_1.$$

In particular, we see that this parametrization is not defined for $t = 0$ as we have a singularity. Therefore, the system is flat except for $t = 0$. Finally, we note that, away from $t = 0$, we have another right-inverse of R defined by:

```
> RightInverseRat(R, Alg);
```

$$\begin{bmatrix} 0 \\ -\frac{1}{t} \end{bmatrix}$$

Let us compute the Brunovský canonical form:

```
> B:=BrunovskyRat(R, Alg);
```

$$B := \begin{bmatrix} -\frac{1}{t^2} & 0 \\ \frac{2}{t^3} & -\frac{1}{t} \end{bmatrix}$$

Let us check that the variables z and v defined by $(z,\ \ v)^T = B\ (x,\ \ u)^T$ satisfy a Brunovský canonical form:

```
> E:=EliminationRat(linalg[stackmatrix](B, R), [x,u], [z,v,0],
> Alg):
> ApplyMatrix(E[1], [x(t),u(t)], Alg)=ApplyMatrix(E[2],
> [z(t),v(t)], Alg);
```

$$\begin{bmatrix} 0 \\ \mathrm{u}(t) \\ \mathrm{x}(t) \end{bmatrix} = \begin{bmatrix} -(\frac{d}{dt}\,\mathrm{z}(t)) + \mathrm{v}(t) \\ -2\,\mathrm{z}(t) - t\,\mathrm{v}(t) \\ -t^2\,\mathrm{z}(t) \end{bmatrix}$$

The first equation shows that z and v satisfy a Brunovský canonical form. The last two equations give x and u in terms of z and v. We refer to [8] for more difficult examples of time-varying ordinary differential linear systems.

Example 9. Let us consider the example of a two reflector antenna [26]. We first define an Ore algebra with a differential operator Dt w.r.t. time t and a constant time-delay operator δ. Note also that the constants *K1*, *K2*, *Te*, *Kp*, *Kc* have to be declared in the definition of the Ore algebra.

```
> Alg:=DefineOreAlgebra(diff=[Dt,t], dual_shift=[delta,s],
> polynom=[t,s], comm=[K1,K2,Te,Kp,Kc], shift_action=[delta,t]):
```

Enter the matrix R of the differential time-delay linear system:

```
> R:=evalm([[Dt,-K1,0,0,0,0,0,0,0],
> [0,Dt+K2/Te,0,0,0,0,-Kp/Te*delta,-Kc/Te*delta,-Kc/Te*delta],
> [0,0,Dt,-K1,0,0,0,0,0],
> [0,0,0,Dt+K2/Te,0,0,-Kc/Te*delta,-Kp/Te*delta,-Kc/Te*delta],
> [0,0,0,0,Dt,-K1,0,0,0],
> [0,0,0,0,0,Dt+K2/Te,-Kc/Te*delta,-Kc/Te*delta,-Kp/Te*delta]]);
```

$$R := \begin{bmatrix} Dt & -K1 & 0 & 0 & 0 & 0 & 0 & 0 & 0 \\ 0 & Dt+\frac{K2}{Te} & 0 & 0 & 0 & 0 & -\frac{Kp\,\delta}{Te} & -\frac{Kc\,\delta}{Te} & -\frac{Kc\,\delta}{Te} \\ 0 & 0 & Dt & -K1 & 0 & 0 & 0 & 0 & 0 \\ 0 & 0 & 0 & Dt+\frac{K2}{Te} & 0 & 0 & -\frac{Kc\,\delta}{Te} & -\frac{Kp\,\delta}{Te} & -\frac{Kc\,\delta}{Te} \\ 0 & 0 & 0 & 0 & Dt & -K1 & 0 & 0 & 0 \\ 0 & 0 & 0 & 0 & 0 & Dt+\frac{K2}{Te} & -\frac{Kc\,\delta}{Te} & -\frac{Kc\,\delta}{Te} & -\frac{Kp\,\delta}{Te} \end{bmatrix}$$

Then, we use an involution θ of *Alg* in order to obtain $R\_adj = \theta(R)$:

```
> R_adj:=Involution(R, Alg):
```

By means of the next command, we compute the torsion-free part (if *Ext1*[1] is not the identity matrix, then the torsion submodule is generated by the rows of *Ext1*[2] modulo the module generated by the rows of R) and a parametrization of the torsion-free part in *Ext1*[3]. Equivalently, we check whether or not the two reflector antenna is controllable:

```
> st:=time(): Ext1:=Exti(R_adj, Alg, 1): time() - st;
```

0.920

```
> Ext1[1];
```

$$\begin{bmatrix} 1 & 0 & 0 & 0 & 0 & 0 \\ 0 & 1 & 0 & 0 & 0 & 0 \\ 0 & 0 & 1 & 0 & 0 & 0 \\ 0 & 0 & 0 & 1 & 0 & 0 \\ 0 & 0 & 0 & 0 & 1 & 0 \\ 0 & 0 & 0 & 0 & 0 & 1 \end{bmatrix}$$

We conclude that the first extension module $\mathrm{ext}^1_{Alg}(\widetilde{N}, Alg)$ of the *Alg*-module $\widetilde{N} = Alg^{1\times 6}/(A^{1\times 9}\,\theta(R))$ associated with $R\_adj = \theta(R)$ is the zero module. Hence, the module defined by R is torsion-free. Equivalently, R is parametrizable and *Ext1*[3] gives a parametrization of R involving three free parameters:

```
> Ext1[3];
```

$$\begin{bmatrix} K1\,\delta\,Kc & K1\,\delta\,Kc & Kp\,K1\,\delta \\ Dt\,\delta\,Kc & Dt\,\delta\,Kc & Kp\,\delta\,Dt \\ K1\,\delta\,Kc & Kp\,K1\,\delta & K1\,\delta\,Kc \\ Dt\,\delta\,Kc & Kp\,\delta\,Dt & Dt\,\delta\,Kc \\ Kp\,K1\,\delta & K1\,\delta\,Kc & K1\,\delta\,Kc \\ Kp\,\delta\,Dt & Dt\,\delta\,Kc & Dt\,\delta\,Kc \\ 0 & 0 & Dt^2\,Te + Dt\,K2 \\ 0 & Dt^2\,Te + Dt\,K2 & 0 \\ Dt^2\,Te + Dt\,K2 & 0 & 0 \end{bmatrix}$$

The same parametrization can be obtained by using Parametrization. The result involves three free functions ξ_1, ξ_2, ξ_3:

```
> Parametrization(R, Alg);
```

$$\begin{bmatrix} K1\,Kc\,\xi_1(t-1) + K1\,Kc\,\xi_2(t-1) + Kp\,K1\,\xi_3(t-1) \\ Kc\,\mathrm{D}(\xi_1)(t-1) + Kc\,\mathrm{D}(\xi_2)(t-1) + Kp\,\mathrm{D}(\xi_3)(t-1) \\ K1\,Kc\,\xi_1(t-1) + Kp\,K1\,\xi_2(t-1) + K1\,Kc\,\xi_3(t-1) \\ Kc\,\mathrm{D}(\xi_1)(t-1) + Kp\,\mathrm{D}(\xi_2)(t-1) + Kc\,\mathrm{D}(\xi_3)(t-1) \\ Kp\,K1\,\xi_1(t-1) + K1\,Kc\,\xi_2(t-1) + K1\,Kc\,\xi_3(t-1) \\ Kp\,\mathrm{D}(\xi_1)(t-1) + Kc\,\mathrm{D}(\xi_2)(t-1) + Kc\,\mathrm{D}(\xi_3)(t-1) \\ Te\,(\mathrm{D}^{(2)})(\xi_3)(t) + K2\,\mathrm{D}(\xi_3)(t) \\ Te\,(\mathrm{D}^{(2)})(\xi_2)(t) + K2\,\mathrm{D}(\xi_2)(t) \\ Te\,(\mathrm{D}^{(2)})(\xi_1)(t) + K2\,\mathrm{D}(\xi_1)(t) \end{bmatrix}$$

The two reflector antenna is not a flat system [15, 26] because $\mathrm{ext}^2_{Alg}(\widetilde{N}, Alg)$ of the Alg-module $\widetilde{N}$ is different from zero as it is shown next:

```
> st:=time(): Ext2:=Exti(R_adj, Alg, 2): time() - st;
```

$$0.750$$

```
> Ext2[1];
```

$$\begin{bmatrix} \delta & 0 & 0 \\ Dt^2\,Te + Dt\,K2 & 0 & 0 \\ 0 & \delta & 0 \\ 0 & Dt^2\,Te + Dt\,K2 & 0 \\ 0 & 0 & \delta \\ 0 & 0 & Dt^2\,Te + Dt\,K2 \end{bmatrix}$$

Since the *torsion-free degree* $i(M)$ of $M = Alg^{1\times 9}/(Alg^{1\times 6}\,R)$ is equal to 1 (i.e., M is a torsion-free but not a projective Alg-module [11, 47]), we can find a polynomial π in the variable δ such that the system is π-*free* [15, 26]:

```
> PiPolynomial(R, Alg, [delta]);
```

$$[\delta]$$

We obtain $\pi = \delta$. By definition of the π-polynomial [15, 26], this means that if we can permit the time-advance operator δ^{-1}, then the system of the two reflector antenna becomes flat, i.e., the new $D = Alg[\delta^{-1}]$-module $P = D^{1\times 9}/(D^{1\times 6}\, R)$ associated with the system is free. We shall find a basis for the D-module P below.

We note that the fact that the two reflector antenna is not a flat system (without the advance operator δ^{-1}) is coherent with the fact that the full row-rank matrix R does not admit a right-inverse. Indeed, we can prove that a full row-rank matrix R admits a right-inverse if and only if the Alg-module $M = Alg^{1\times 9}/(Alg^{1\times 6}\, R)$ is projective [11]. By the Quillen-Suslin theorem (see 3 of Theorem 1), projective modules over commutative polynomial rings are free. This remark applies to our situation as we have:

```
> SyzygyModule(R, Alg); RightInverse(R, Alg);
```

$$\mathrm{INJ}(6)$$

$$[]$$

The fact that the system is not flat is also coherent with the fact that its parametrization *Ext1*[3] does not admit a left-inverse. Indeed, a linear system is flat if and only if it admits a left-invertible parametrization [11].

```
> LeftInverse(Ext1[3], Alg);
```

$$[]$$

We finish by computing a basis of the free $D = Alg[\delta^{-1}]$-module P. In the terminology of control, such a basis is called a *flat output*. We apply LocalLeftInverse to the parametrization *Ext1*[3] by allowing to invert δ:

```
> S:=LocalLeftInverse(Ext1[3], [delta], Alg);
```

$$S := \begin{bmatrix} -\dfrac{Kc}{\delta\, K1\, \%1} & 0 & -\dfrac{Kc}{\delta\, K1\, \%1} & 0 & \dfrac{Kp+Kc}{\delta\, K1\, \%1} & 0 & 0 & 0 & 0 \\ -\dfrac{Kc}{\delta\, K1\, \%1} & 0 & \dfrac{Kp+Kc}{\delta\, K1\, \%1} & 0 & -\dfrac{Kc}{\delta\, K1\, \%1} & 0 & 0 & 0 & 0 \\ \dfrac{Kp+Kc}{\delta\, K1\, \%1} & 0 & -\dfrac{Kc}{\delta\, K1\, \%1} & 0 & -\dfrac{Kc}{\delta\, K1\, \%1} & 0 & 0 & 0 & 0 \end{bmatrix}$$

$$\%1 := Kp^2 - 2\, Kc^2 + Kp\, Kc$$

By construction, the matrix S is a left-inverse of *Ext1*[3]:

```
> Mult(S, Ext1[3], Alg);
```

$$\begin{bmatrix} 1 & 0 & 0 \\ 0 & 1 & 0 \\ 0 & 0 & 1 \end{bmatrix}$$

Therefore, $(z_1,\ z_2,\ z_3)^T = S\ (x_1, \ldots, x_6,\ u_1,\ u_2,\ u_3)^T$ is a basis of the D-module P associated with R, and thus, a flat output of the two reflector antenna. Therefore, a flat output $(z_1,\ z_2,\ z_3)^T$ of the system is defined by:

```
> evalm([seq([z[i](t)], i=1..3)])=
> ApplyMatrix(S,[seq(x[i](t),i=1..6),seq(u[i](t),i=1..3)],Alg);
```

$$\begin{bmatrix} z_1(t) \\ z_2(t) \\ z_3(t) \end{bmatrix} = \begin{bmatrix} -\dfrac{Kc\,x_1(t+1)}{K1\,\%1} - \dfrac{Kc\,x_3(t+1)}{K1\,\%1} + \dfrac{(Kc+Kp)\,x_5(t+1)}{K1\,\%1} \\ -\dfrac{Kc\,x_1(t+1)}{K1\,\%1} + \dfrac{(Kc+Kp)\,x_3(t+1)}{K1\,\%1} - \dfrac{Kc\,x_5(t+1)}{K1\,\%1} \\ \dfrac{(Kc+Kp)\,x_1(t+1)}{K1\,\%1} - \dfrac{Kc\,x_3(t+1)}{K1\,\%1} - \dfrac{Kc\,x_5(t+1)}{K1\,\%1} \end{bmatrix}$$

$$\%1 := Kp\,Kc - 2\,Kc^2 + Kp^2$$

Finally, if we substitute $(z_1,\ z_2,\ z_3)^T$ into the parametrization $Ext1[3]$ of the system, we obtain $(x_1, \ldots, x_6,\ u_1,\ u_2,\ u_3)^T = T(x_1, \ldots, x_6,\ u_1,\ u_2,\ u_3)^T$, where the matrix T is defined by:

```
> T:=Mult(Ext1[3], S, Alg);
```

$$T := \begin{bmatrix} 1, 0, 0, 0, 0, 0, 0, 0, 0 \\ \dfrac{Dt}{K1}, 0, 0, 0, 0, 0, 0, 0, 0 \\ 0, 0, 1, 0, 0, 0, 0, 0, 0 \\ 0, 0, \dfrac{Dt}{K1}, 0, 0, 0, 0, 0, 0 \\ 0, 0, 0, 0, 1, 0, 0, 0, 0 \\ 0, 0, 0, 0, \dfrac{Dt}{K1}, 0, 0, 0, 0 \\ \dfrac{Dt\,(Dt\,Te + K2)\,(Kp+Kc)}{\delta\,K1\,\%1}, 0, \%2, 0, \%2, 0, 0, 0, 0 \\ \%2, 0, \dfrac{Dt\,(Dt\,Te + K2)\,(Kp+Kc)}{\delta\,K1\,\%1}, 0, \%2, 0, 0, 0, 0 \\ \%2, 0, \%2, 0, \dfrac{Dt\,(Dt\,Te + K2)\,(Kp+Kc)}{\delta\,K1\,\%1}, 0, 0, 0, 0 \end{bmatrix}$$

$$\%1 := Kp^2 - 2\,Kc^2 + Kp\,Kc$$

$$\%2 := -\frac{Dt\,(Dt\,Te + K2)\,Kc}{\delta\,K1\,\%1}$$

We note that $(x_2,\ x_4,\ x_6,\ u_1,\ u_2,\ u_3)^T$ is expressed in terms of x_1, x_3 and x_5 only. Thus, (x_1, x_3, x_5) is also a basis of the $D = Alg[\delta^{-1}]$-module P (compare with [26]). More precisely, we have:

```
> evalm([seq([x[i](t)=ApplyMatrix(T,[seq(x[j](t),j=1..6),
> seq(u[j](t),j=1..3)],Alg)[i,1]],i=1..6)]);
```

$$\begin{bmatrix} x_1(t) = x_1(t) \\ x_2(t) = \dfrac{\mathrm{D}(x_1)(t)}{K1} \\ x_3(t) = x_3(t) \\ x_4(t) = \dfrac{\mathrm{D}(x_3)(t)}{K1} \\ x_5(t) = x_5(t) \\ x_6(t) = \dfrac{\mathrm{D}(x_5)(t)}{K1} \end{bmatrix}$$

```
> evalm([seq([u[i](t)=ApplyMatrix(T,[seq(x[j](t),j=1..6),
> seq(u[j](t),j=1..3)],Alg)[6+i,1]],i=1..3)]);
```

$$\left[u_1(t) = \frac{K2\,(Kc+Kp)\,\mathrm{D}(x_1)(t+1)}{K1\,\%1} + \frac{Te\,(Kc+Kp)\,(\mathrm{D}^{(2)})(x_1)(t+1)}{K1\,\%1}\right.$$
$$- \frac{K2\,Kc\,\mathrm{D}(x_3)(t+1)}{K1\,\%1} - \frac{Te\,Kc\,(\mathrm{D}^{(2)})(x_3)(t+1)}{K1\,\%1} - \frac{K2\,Kc\,\mathrm{D}(x_5)(t+1)}{K1\,\%1}$$
$$\left. - \frac{Te\,Kc\,(\mathrm{D}^{(2)})(x_5)(t+1)}{K1\,\%1}\right]$$

$$\left[u_2(t) = -\frac{K2\,Kc\,\mathrm{D}(x_1)(t+1)}{K1\,\%1} - \frac{Te\,Kc\,(\mathrm{D}^{(2)})(x_1)(t+1)}{K1\,\%1} + \frac{K2\,(Kc+Kp)\,\mathrm{D}(x_3)(t+1)}{K1\,\%1}\right.$$
$$\left. + \frac{Te\,(Kc+Kp)\,(\mathrm{D}^{(2)})(x_3)(t+1)}{K1\,\%1} - \frac{K2\,Kc\,\mathrm{D}(x_5)(t+1)}{K1\,\%1} - \frac{Te\,Kc\,(\mathrm{D}^{(2)})(x_5)(t+1)}{K1\,\%1}\right]$$

$$\left[u_3(t) = -\frac{K2\,Kc\,\mathrm{D}(x_1)(t+1)}{K1\,\%1} - \frac{Te\,Kc\,(\mathrm{D}^{(2)})(x_1)(t+1)}{K1\,\%1} - \frac{K2\,Kc\,\mathrm{D}(x_3)(t+1)}{K1\,\%1}\right.$$
$$- \frac{Te\,Kc\,(\mathrm{D}^{(2)})(x_3)(t+1)}{K1\,\%1} + \frac{K2\,(Kc+Kp)\,\mathrm{D}(x_5)(t+1)}{K1\,\%1}$$
$$\left. + \frac{Te\,(Kc+Kp)\,(\mathrm{D}^{(2)})(x_5)(t+1)}{K1\,\%1}\right]$$

$$\%1 := Kp\,Kc \quad 2\,Kc^2 + Kp^2$$

We refer to [26] for applications of the previous results to the motion planning and tracking problems. See also [8] for more details.

Example 10. We consider the differential time-delay system of a vibrating string with an interior mass [27]. We define the Ore algebra Alg, where D is the differential operator w.r.t. t and σ_1 and σ_2 are two non-commensurate time-delay operators. The constant parameters η_1, η_2 (composition of the mass, tensions and densities) of the system must be declared in the algebra Alg:

```
> Alg:=DefineOreAlgebra(diff=[D,t], dual_shift=[sigma1,y1],
> dual_shift=[sigma2,y2], polynom=[t,y1,y2], comm=[eta1,eta2]):
```

We only study the case of position control on both boundaries [27]. For the case of a single control, we refer to [8]. We enter the system matrix R:

```
> R:=evalm([[1,1,-1,-1,0,0],[D+eta1,D-eta1,-eta2,eta2,0,0],
> [sigma1^2,1,0,0,-sigma1,0],[0,0,1,sigma2^2,0,-sigma2]]);
```

$$R := \begin{bmatrix} 1 & 1 & -1 & -1 & 0 & 0 \\ \mathrm{D}+\eta 1 & \mathrm{D}-\eta 1 & -\eta 2 & \eta 2 & 0 & 0 \\ \sigma 1^2 & 1 & 0 & 0 & -\sigma 1 & 0 \\ 0 & 0 & 1 & \sigma 2^2 & 0 & -\sigma 2 \end{bmatrix}$$

We use an involution θ of Alg in order to obtain $R\_adj = \theta(R)$:

```
> R_adj:=Involution(R, Alg):
```

We check controllability of the system by applying Exti to R_adj:

```
> st:=time(): Ext1:=Exti(R_adj, Alg, 1): time()-st; Ext1[1];
```

$$1.191$$

$$\begin{bmatrix} 1 & 0 & 0 & 0 \\ 0 & 1 & 0 & 0 \\ 0 & 0 & 1 & 0 \\ 0 & 0 & 0 & 1 \end{bmatrix}$$

Since $Ext1[1]$ is the identity matrix, then we obtain that the Alg-module $M = Alg^{1\times 6}/(Alg^{1\times 4}\, R)$ associated with the system is torsion-free. This means that the vibrating string with interior mass is controllable and, equivalently, parametrizable. A parametrization of the system is then given by $Ext1[3]$:

```
> Ext1[3];
```

$$\begin{bmatrix} 2\,\sigma 2\,\eta 2\,,\ -\sigma 2\,\sigma 1\,\eta 2\,,\ -\eta 2\,\sigma 1+\sigma 1\,\eta 1-\sigma 1\,\mathrm{D} \\ 0\,,\ \sigma 2\,\sigma 1\,\eta 2\,,\ \eta 2\,\sigma 1+\sigma 1\,\mathrm{D}+\sigma 1\,\eta 1 \\ \sigma 2\,\mathrm{D}+\sigma 2\,\eta 2+\sigma 2\,\eta 1\,,\ -\sigma 2\,\sigma 1\,\eta 1\,,\ 0 \\ -\sigma 2\,\mathrm{D}+\sigma 2\,\eta 2-\sigma 2\,\eta 1\,,\ \sigma 2\,\sigma 1\,\eta 1\,,\ 2\,\sigma 1\,\eta 1 \\ 2\,\sigma 2\,\sigma 1\,\eta 2\,,\ \sigma 2\,\eta 2-\sigma 2\,\eta 2\,\sigma 1^2\,,\ -\eta 2\,\sigma 1^2+\eta 2+\eta 1\,\sigma 1^2-\sigma 1^2\,\mathrm{D}+\mathrm{D}+\eta 1 \\ \mathrm{D}-\mathrm{D}\,\sigma 2^2+\eta 2\,\sigma 2^2-\eta 1\,\sigma 2^2+\eta 2+\eta 1\,,\ -\sigma 1\,\eta 1+\sigma 1\,\eta 1\,\sigma 2^2\,,\ 2\,\sigma 2\,\sigma 1\,\eta 1 \end{bmatrix}$$

Therefore, the system can be parametrized by means of three free functions. We now want to check whether this parametrization is a *minimal* one [11, 33]. In order to do that, let us compute the rank of the Alg-module M.

```
> OreRank(R, Alg);
```

$$2$$

Hence, we know that there exist some parametrizations of the system with only two arbitrary functions [11, 33]. We find some minimal parametrizations:

```
> P:=MinimalParametrizations(R, Alg);
```

$$P := \left[\left[\begin{array}{cc} 2\,\sigma2\,\eta2 & -\sigma2\,\sigma1\,\eta2 \\ 0 & \sigma2\,\sigma1\,\eta2 \\ \sigma2\,\mathrm{D}+\sigma2\,\eta2+\sigma2\,\eta1 & -\sigma2\,\sigma1\,\eta1 \\ -\sigma2\,\mathrm{D}+\sigma2\,\eta2-\sigma2\,\eta1 & \sigma2\,\sigma1\,\eta1 \\ 2\,\sigma2\,\sigma1\,\eta2 & \sigma2\,\eta2-\sigma2\,\eta2\,\sigma1^2 \\ \mathrm{D}-\mathrm{D}\,\sigma2^2+\eta2\,\sigma2^2-\eta1\,\sigma2^2+\eta2+\eta1 & -\sigma1\,\eta1+\sigma1\,\eta1\,\sigma2^2 \end{array}\right],\right.$$
$$\left[\begin{array}{c} 2\,\sigma2\,\eta2\,,\ -\eta2\,\sigma1+\sigma1\,\eta1-\sigma1\,\mathrm{D} \\ 0\,,\ \eta2\,\sigma1+\sigma1\,\mathrm{D}+\sigma1\,\eta1 \\ \sigma2\,\mathrm{D}+\sigma2\,\eta2+\sigma2\,\eta1\,,\ 0 \\ -\sigma2\,\mathrm{D}+\sigma2\,\eta2-\sigma2\,\eta1\,,\ 2\,\sigma1\,\eta1 \\ 2\,\sigma2\,\sigma1\,\eta2\,,\ -\eta2\,\sigma1^2+\eta2+\eta1\,\sigma1^2-\sigma1^2\,\mathrm{D}+\mathrm{D}+\eta1 \\ \mathrm{D}-\mathrm{D}\,\sigma2^2+\eta2\,\sigma2^2-\eta1\,\sigma2^2+\eta2+\eta1\,,\ 2\,\sigma2\,\sigma1\,\eta1 \end{array}\right],$$
$$\left.\left[\begin{array}{cc} -\sigma2\,\sigma1\,\eta2 & -\eta2\,\sigma1+\sigma1\,\eta1-\sigma1\,\mathrm{D} \\ \sigma2\,\sigma1\,\eta2 & \eta2\,\sigma1+\sigma1\,\mathrm{D}+\sigma1\,\eta1 \\ -\sigma2\,\sigma1\,\eta1 & 0 \\ \sigma2\,\sigma1\,\eta1 & 2\,\sigma1\,\eta1 \\ \sigma2\,\eta2-\sigma2\,\eta2\,\sigma1^2 & -\eta2\,\sigma1^2+\eta2+\eta1\,\sigma1^2-\sigma1^2\,\mathrm{D}+\mathrm{D}+\eta1 \\ -\sigma1\,\eta1+\sigma1\,\eta1\,\sigma2^2 & 2\,\sigma2\,\sigma1\,\eta1 \end{array}\right]\right]$$

Since R has full row rank (this fact can be checked by computing SyzygyModule(R, Alg)), we know that M is projective, and thus, free if and only if R admits a right-inverse (see [11, 33] for more details).

```
> RightInverse(R, Alg);
```

$$[]$$

Hence, M is not projective, which implies that M is not free, i.e., the vibrating string with interior mass is not a flat system [27]. Another way to verify this fact is to compute $\mathrm{ext}^2_{Alg}(\widetilde{N}, Alg)$ and $\mathrm{ext}^3_{Alg}(\widetilde{N}, Alg)$ of the Alg-module $\widetilde{N} = Alg^{1\times4}/(Alg^{1\times6}\,R\_adj)$:

```
> Exti(R_adj, Alg, 2);
```

$$\left[\left[\begin{array}{ccc} 1 & 0 & 0 \\ 0 & 1 & 0 \\ 0 & 0 & 1 \end{array}\right], \left[\begin{array}{ccc} \sigma2\,\eta2 & 0 & \sigma1\,\eta1 \\ \eta2+\eta1+\mathrm{D} & -\sigma1\,\eta1 & 0 \\ 0 & \sigma2\,\eta2 & \eta2+\eta1+\mathrm{D} \end{array}\right], \left[\begin{array}{c} -\sigma1\,\eta1 \\ -\mathrm{D}-\eta2-\eta1 \\ \sigma2\,\eta2 \end{array}\right]\right]$$

```
> Exti(R_adj, Alg, 3);
```

$$\left[\left[\begin{array}{c} \sigma2 \\ \sigma1 \\ \eta2+\eta1+\mathrm{D} \end{array}\right], \left[\,1\,\right], \mathrm{SURJ}(1)\right]$$

We see that $\mathrm{ext}^2_{Alg}(\widetilde{N}, Alg)$ equals zero but $\mathrm{ext}^3_{Alg}(\widetilde{N}, Alg)$ is different from zero. Therefore, M is a reflexive but not a projective Alg-module. Indeed, we recall that M is reflexive (resp., projective) iff $\mathrm{ext}^i_{Alg}(\widetilde{N}, Alg)$ equals zero for $i = 1, 2$ (resp., $i = 1, 2, 3$). Let us find a polynomial π in the variable σ_1 such that the system is π-free [15, 26, 27].

```
> PiPolynomial(R, Alg, [sigma1]);
```

$$[\sigma 1]$$

Let us find a polynomial π in the variable σ_2 such that the system is π-free.

```
> PiPolynomial(R, Alg, [sigma2]);
```

$$[\sigma 2]$$

Hence, if we invert σ_1 or σ_2, i.e., we allow ourselves to have a time-advance operator, then, by definition of the π-polynomial, the system becomes flat. A flat output for this system can be computed from a left-inverse of the minimal parametrization P, where we allow σ_1 or σ_2 to appear in the denominators.

We compute the annihilator of the Alg-module $M_1 = Alg^{1\times 2}/(Alg^{1\times 6}\, P[1])$ of the minimal parametrization $P[1]$.

```
> Ann1:=AnnExti(linalg[transpose](P[1]), Alg, 1);
```

$$Ann1 := [\sigma 2]$$

Let us compute a left-inverse of the minimal parametrization $P[1]$ by allowing σ_2 to appear in the denominators.

```
> L1:=LocalLeftInverse(P[1], Ann1, Alg);
```

$$L1 := \begin{bmatrix} 0 & 0 & \dfrac{1}{2\,\sigma 2\,\eta 2} & \dfrac{1}{2\,\sigma 2\,\eta 2} & 0 & 0 \\ 0 & \dfrac{\sigma 1}{\sigma 2\,\eta 2} & -\dfrac{\sigma 1}{\sigma 2\,\eta 2} & -\dfrac{\sigma 1}{\sigma 2\,\eta 2} & \dfrac{1}{\sigma 2\,\eta 2} & 0 \end{bmatrix}$$

We easily check that $L1$ is a left-inverse of $P[1]$.

```
> Mult(L1, P[1], Alg);
```

$$\begin{bmatrix} 1 & 0 \\ 0 & 1 \end{bmatrix}$$

If we use σ_2^{-1}, then we obtain that a flat output of the system is defined by

$$(\xi_1,\, \xi_2)^T = L1\,(\phi_1,\, \psi_1,\, \phi_2,\, \psi_2,\, u,\, v)^T,$$

where ϕ_1, ψ_1, ϕ_2, ψ_2, u, v are the system variables [27]. Let us point out that any multiplication of $(\xi_1,\, \xi_2)^T$ by a unimodular matrix over the commutative ring $\mathbb{Q}(\eta_1, \eta_2)[\frac{d}{dt}, \sigma_1, \sigma_2,\, \sigma_2^{-1}]$ gives a new flat output of the system. For instance,we obtain the following flat output of the system [27]:

$$\xi_1' = 2\,\eta_2\,\sigma_2\,\xi_1 = \phi_2 + \psi_2, \quad \xi_2' = \eta_2\,\sigma_2(\xi_2 + 2\,\sigma_1\,\xi_1) = \sigma_1\,\psi_1 + u.$$

We can repeat the same procedure for $P[2]$ and $P[3]$.

```
> Ann2:=AnnExti(linalg[transpose](P[2]), Alg, 1);
> Ann3:=AnnExti(linalg[transpose](P[3]), Alg, 1);
```

$$Ann2 := [\eta 2 + \eta 1 + \mathrm{D}]$$

$$Ann3 := [\sigma 1]$$

The annihilator of $P[3]$ only contains σ_1. Let us compute a flat output by allowing the time-advance operator σ_1^{-1} to appear in the basis.

```
> L3:=LocalLeftInverse(P[3], Ann3, Alg);
```

$$L3 := \begin{bmatrix} 0 & 0 & 0 & \dfrac{\sigma 2}{\sigma 1\,\eta 1} & 0 & -\dfrac{1}{\sigma 1\,\eta 1} \\ 0 & 0 & \dfrac{1}{2\,\sigma 1\,\eta 1} & \dfrac{1}{2\,\sigma 1\,\eta 1} & 0 & 0 \end{bmatrix}$$

$L3$ is a left-inverse of $P[3]$ over $\mathbb{Q}(\eta_1, \eta_2)[\frac{d}{dt}, \sigma_1, \sigma_2, \sigma_1^{-1}]$ as we can check:

```
> Mult(L3, P[3], Alg);
```

$$\begin{bmatrix} 1 & 0 \\ 0 & 1 \end{bmatrix}$$

Therefore, if we use the time-advance operator σ_1^{-1}, we obtain the flat output of the system $(\xi_1,\, \xi_2)^T = L3\,(\phi_1,\, \psi_1,\, \phi_2,\, \psi_2,\, u,\, v)^T$. Using trivial linear combinations of ξ_1 and ξ_2 over the ring $\mathbb{Q}(\eta_1, \eta_2)[\frac{d}{dt}, \sigma_1, \sigma_2, \sigma_1^{-1}]$, we then obtain that $(\xi_1' = \sigma_2\,\psi_2 - v, \quad \xi_2' = \phi_2 + \psi_2)$ is another flat output of the system over $\mathbb{Q}(\eta_1, \eta_2)[\frac{d}{dt}, \sigma_1, \sigma_2, \sigma_1^{-1}]$.

We refer to [27] for applications of the previous results to the motion planning and tracking problems [26]. See also [8] for more details and examples.

8 Conclusion

We hope to have convinced the reader of the main interest of the package OreModules for the study of the structural properties of multidimensional linear systems over Ore algebras. To our knowledge, OreModules is the first implementation of homological methods with regard to applications in control theory. We hope that OreModules will become in the future a platform for the implementation of different algorithms obtained in the literature of multidimensional linear systems (see e.g., [1, 4, 13, 16, 18, 19, 20, 31, 32, 33, 34, 35, 37, 40, 43, 47, 49] and the references therein).

References

1. Assan J. (1999) Analyse et synthèse de l'approche géométrique pour les systèmes linéaires sur un anneau. PhD thesis. Ecole Centrale de Nantes, France
2. Becker T., Weispfenning V. (1993) Gröbner Bases. A Computational Approach to Commutative Algebra. Springer, Berlin Heidelberg New York
3. Bender C. M., Dunne G. V., Mead L. R. (2000) Underdetermined systems of partial differential equations. J. Mathematical Physics 41:6388–6398
4. Bose N. K. (1985) Multidimensional Systems Theory: Progress, Directions, and Open Problems. D. Reidel Publishing Company, Dordrecht

5. Chyzak F. (1998) Fonctions holonomes en calcul formel. PhD thesis, Ecole Polytechnique, France
6. Chyzak F., Mgfun Project. http://algo.inria.fr/chyzak/mgfun.html
7. Chyzak F., Salvy B. (1998) Non-commutative elimination in Ore algebras proves multivariate identities. J. Symbolic Computation 26:187–227
8. Chyza F., Quadrat, A., Robertz D. (2002) OreModules project. http://wwwb.math.rwth-aachen.de/OreModules
9. Chyzak F., Quadrat A., Robertz D. (2003) Linear control systems over Ore algebras: Effective algorithms for the computation of parametrizations. In Proc. IFAC Workshop on Time-Delay Systems TDS03, INRIA Rocquencourt, France
10. Chyzak F., Quadrat A., Robertz D. (2004) OreModules: A symbolic package for the study of multidimensional linear systems. In Proc. Symposium MTNS04, Leuven, Belgium
11. Chyzak F., Quadrat A., Robertz D. (2005) Effective algorithms for parametrizing linear control systems over Ore algebras. Applicable Algebra in Engineering, Communication and Computing (AAECC) 16:319–376
12. Conte G., Perdon A. M. (2000) Systems over rings: geometric theory and applications. Annual Reviews in Control 24:113–124
13. Cotroneo T. (2001) Algorithms in Behavioral Systems Theory. PhD thesis. University of Groningen, The Netherlands
14. Fliess M. (1991) Controllability revisited. In A. C. Antoulas ed., Mathematical System Theory. The influence of R. E. Kalman, Springer, Berlin Heidelberg New York
15. Fliess M., Mounier H. (1998) Controllability and observability of linear delay systems: an algebraic approach. ESAIM COCV 3:301–314.
16. Galkowski K., Wood J. eds. (2001) Multidimensional Signals, Circuits and Systems, Taylor and Francis, London
17. Greuel G.-M., Pfister G. (2002) A Singular Introduction to Commutative Algebra. Springer, Berlin Heidelberg New York
18. Habets L. (1994) Algebraic and computational aspects of time-delay systems. PhD thesis, University of Eindhoven, The Netherlands
19. Habets L. (1996) Computational aspects of systems over rings − reactability and stabilizability. CWI Quarterly 9:85–95.
20. Kailath T. (1980) Linear Systems. Prentice-Hall, Upper Saddle River
21. Kalman R. E., Falb P. L., Arbib M. A. (1969) Topics in Mathematical Systems Theory, McGraw-Hill, New York
22. Kučera V. (1979) Discrete Linear Control: The Polynomial Equation Approach, Wiley, London
23. Li H. (2002) Non-commutative Gröbner Bases and Filtered-Graded Transfer. Lecture Notes in Mathematics 1795, Springer, Berlin Heidelberg New York
24. Malgrange B. (1963) Systèmes à coefficients constants. Séminaire Bourbaki 1962/63, 246:1–11
25. McConnell J. C., Robson J. C. (2000) Noncommutative Noetherian Rings. American Mathematical Society, Providence
26. Mounier H. (1995) Propriétés structurelles des systèmes linéaires à retards: aspects théoriques et pratiques. PhD Thesis, University of Orsay, France
27. Mounier H., Rudolph J., Fliess M., Rouchon P. (1998) Tracking control of a vibrating string with an interior mass viewed as delay system. ESAIM COCV 3:315–321
28. Oberst U. (1990) Multidimensional constant linear systems. Acta Appl. Math. 20:1–175

29. Pillai H. K., Shankar S. (1998) A behavioral approach to control of distributed systems. SIAM J. Control and Optimization 37:388–408
30. Polderman J. W., Willems J. C. (1998) Introduction to Mathematical Systems Theory. A Behavioral Approach. TAM 26, Springer, Berlin Heidelberg New York
31. Pommaret J.-F. (2001) Partial Differential Control Theory. Kluwer, Dordrecht
32. Pommaret J.-F., Quadrat A. (1998) Generalized Bezout Identity. Applicable Algebra in Engineering, Communication and Computing 9:91–116
33. Pommaret, J.-F., Quadrat, A. (1999) Localization and parametrization of linear multidimensional control systems. Systems & Control Letters 37:247–260
34. Pommaret J.-F., Quadrat A. (1999) Algebraic analysis of linear multidimensional control systems. IMA J. Control and Optimization 16:275–297
35. Pommaret J.-F., Quadrat A. (2000) Equivalences of linear control systems. In Proc. Symposium MTNS 2000, Perpignan, France
36. Pommaret J.-F., Quadrat A. (2003) A functorial approach to the behaviour of multidimensional control systems. Applied Mathematics and Computer Science 13:7–13
37. Pommaret J.-F., Quadrat A. (2004) A differential operator approach to multidimensional optimal control. International J. Control 77:821–836
38. Quadrat A. (1999) Analyse algébrique des systèmes de contrôle linéaires multidimensionnels. PhD thesis, Ecole Nationale des Ponts et Chaussées, France
39. Quadrat A. (2005) An introduction to the algebraic theory of linear systems of partial differential equations, in preparation.
40. Quadrat A., Robertz D. (2005) Parametrizing all solutions of uncontrollable multidimensional linear systems. In Proc. 16th IFAC World Congress, Prague, Czech Republic
41. Quadrat A., Robertz D. (2005) On the blowing-up of stably-free behaviours. In Proc. CDC-ECC05, Sevilla, Spain
42. Quadrat A., Robertz D. (2005) Constructive computation of bases of free modules over the Weyl algebras. INRIA report 5181 (`www.inria.fr/rrrt/rr-5181.html`), submitted for publication.
43. Sontag E. (1976) Linear systems over commutative rings: a survey. Ricerche di Automatica 7:1–34
44. Rosenbrock H. H. (1970) State Space and Multivariable Theory. Wiley, London
45. Rotman J. J. (1979) An Introduction to Homological Algebra. Academic Press, New York
46. Wonham M. (1985) Linear Multivariable Control: a Geometric Approach. Springer, Berlin Heidelberg New York
47. Wood J. (2000) Modules and behaviours in nD systems theory. Multidimensional Systems and Signal Processing 11:11–48
48. Youla D. C., Gnavi G. (1979) Notes on n-dimensional system theory. IEEE Transactions on Circuits & Systems 26:259–294
49. Zerz E. (2000) Topics in Multidimensional Linear Systems Theory. Lecture Notes in Control and Information Sciences 256, Springer, Berlin Heidelberg New York

Part V

Predictors, Inversion and Filtering

Inversion and Tracking Problems for Time Delay Linear Systems

Giuseppe Conte[1], Anna Maria Perdon[1], and Claude H. Moog[2]

[1] Dipartimento di Ingegneria Informatica, Gestionale e dell' Automazione
Università Politecnica delle Marche
Via Brecce Bianche, 60131 Ancona, Italy
gconte@univpm.it, perdon@univpm.it
[2] IRCCyN, UMR 6597 CNRS
Claude.Moog@irccyn.ec-nantes.fr

1 Introduction

Delay differential systems play a basic role in modelling phenomena which involve transportation over non negligible distances of materials, as it happens in many industrial processes, or of information, as it happens in large communication systems. Various approaches for different problems have been developed (see [2], [13], [14] for a general introduction to this topic and the Proceedings of the IFAC Workshops on Time Delay Systems (1998, 2000, 2001, 2003) for an account of the most recent research activity).

Here, we discuss the Inversion Problem, reporting results obtained in ([5]) and ([8], and the related Tracking Problem for linear time delay systems, using algebraic and geometric tools in the line of ([6]).

In Section 2, we start by recalling how the inversion problem is dealt with in the case of delay systems and after that we investigate how a tracking problem for a SISO, linear, delay differential system can be solved by a stable compensator that, after enough time has elapsed, make the tracking error arbitrarily small, under relatively mild hypothesis. In particular, we do not assume that the state of the considered system Σ_d is measurable, neither that its initial conditions are known. In Section 3, MIMO systems are considered and the problem is tackled in much more detail, considering state feedback with or without delayed dynamics. Some concluding remarks are given in Section 4.

2 SISO Systems

Let the linear, time invariant, delay-differential, dynamical SISO system Σ_d be described by the set of equations

$$\Sigma_d = \begin{cases} \dot{x}(t) = \sum_{i=0}^{\alpha} A_i x(t-ih) + \sum_{i=0}^{\beta} b_i u(t-ih) \\ y(t) = \sum_{i=0}^{\gamma} c_i x(t-ih) \end{cases} \tag{1}$$

where, denoting by $\mathbb{R}$ the field of real numbers, $A_i,\ b_i,\ c_i$, are matrices of suitable dimensions with entries in $\mathbb{R}$, $x \in \mathbb{R}^n$, $u \in \mathbb{R}$, $y \in \mathbb{R}$ and $h \in \mathbb{R}^+$ is a given

J. Chiasson and J.J. Loiseau (Eds.): Appl. of Time Delay Systems, LNCIS 352, pp. 267–284, 2007.
springerlink.com

delay. Denoting by δ the delay operator defined by $\delta f(t) = f(t-h)$, we can define $A(\delta) = \sum_{i=0}^{\alpha} A_i \delta^i$, $b(\delta) = \sum_{i=0}^{\beta} b_i \delta^i$,$c(\delta) = \sum_{i=0}^{\gamma} c_i \delta^i$. It is possible to substitute, formally, the delay operator δ with the algebraic indeterminate Δ, thus associating to Σ_d the system Σ, defined, over the ring $R = I\!R[\Delta]$ of real polynomials in one indeterminate, by the set of equations

$$\mathbf{\Sigma} = \begin{cases} x(t+1) = A(\Delta)x(t) + b(\Delta)u(t) \\ \qquad y(t) = c(\Delta)x(t) \end{cases} \tag{2}$$

where, by abuse of notation, we denote by x an element of the free state module R^n, by u an element of the free input module R, by y an element of to the free output module R and where A, b, c are matrices with entries in $R = I\!R[\Delta]$ given respectively by $A(\Delta) = \sum_{i=0}^{\alpha} A_i \Delta^i$, $b(\Delta) = \sum_{i=0}^{\beta} b_i \Delta^i$ and $c(\Delta) = \sum_{i=0}^{\gamma} c_i \Delta^i$.

The use of models with coefficients in a ring is crucial for facilitating the introduction of a geometric point of view similar to the one described in [1] for systems without delays. In this way, in facts, one avoids the necessity of dealing with infinite dimensional vector spaces for representing the systems at issue and, in place, one can use finite dimensional modules over suitable rings. Such set up fits well with geometric techniques and, actually, it allows one to extend a number of results from the classical case to that of delay-differential systems.

Given a sufficiently regular reference output $r(t)$ and denoting by $e(t) = y(t) - r(t)$ the error signal, the *Tracking Problem* for the dynamical system Σ_d consists, from a general point of view, in the possibility of constructing a stable compensator Σ_C of the form

$$\Sigma_C = \begin{cases} \dot{z}(t) = Fz(t) + \sum_{i=0}^{\eta} g_i r^{(i)}(t) + \sum_{i=0}^{\mu} h_i e^{(i)}(t) \\ u(t) = Lz(t) + \sum_{i=0}^{\nu} g'_i r^{(i)}(t) + \sum_{i=0}^{\pi} h'_i e^{(i)}(t) \end{cases}, \tag{3}$$

where $F = \sum_{i=0}^{\bar{\alpha}} F_i \delta^i$, $g_i = \sum_{j=0}^{\bar{\eta}} g_{ij} \delta^j$, $h_i = \sum_{j=0}^{\bar{\mu}} h_{ij} \delta^j$, $L = \sum_{i=0}^{\bar{\gamma}} L_i \delta^i$, $g'_i = \sum_{j=0}^{\bar{\nu}} g'_{ij} \delta^j$, $h'_i = \sum_{j=0}^{\bar{\pi}} h'_{ij} \delta^j$ and where $r^{(i)}(t)$, $e^{(i)}(t)$ denote the i-th time derivative of the corresponding signals, such that, in response to the reference signal $r(t)$, the output $y(t)$ of the compensated system tracks asymptotically $r(t)$, that is: the error $e(t) = y(t) - r(t)$ goes to 0 as t goes to ∞.

The construction of the compensator that possibly solves the problem is based on the inversion of the system Σ, (see [4], [5] and [7]).

Given a dynamical system Σ, Left Invertibility consists, from a general point of view, in the possibility of reconstructing univocally, by means of a dynamical process, the input that has produced a given output.

Basic information about invertibility can be obtained, both in the case of linear and of nonlinear systems, by means of the so-called Inversion Algorithm.

For single input-single output (SISO) systems with coefficients in a ring, it is possible to extend in a straightforward way the classical Silverman Inversion Algorithm (see [16]). To this aim, given a system Σ of the form (2) with $m = p = 1$ and writing accordingly $\Sigma = (A, b, c)$, let us evaluate recursively $y(t+k)$, for $k \geq 1$. Since

$$y(t+k) = cA^k x(t) + \sum_{i=0}^{k-1} cA^{k-i-1} bu(t+i),$$

either

$$cA^{k-1}b = 0 \quad \text{for all} \quad k \geq 1,$$

or there exists k_0 (necessarily lesser than or equal to $dim\ \mathcal{X}$) such that

$$cA^{k-1}b = 0 \quad \text{for} \quad k < k_0 \quad \text{and} \quad cA^{k_0-1}b \neq 0.$$

In the last case the algorithm stops at step k_0, yielding

$$\begin{aligned} y(t+1) &= cAx(t) \\ y(t+2) &= cA^2x(t) \\ &\vdots \\ y(t+k_0) &= cA^{k_0}x(t) + cA^{k_0-1}bu(t). \end{aligned} \tag{4}$$

It is clear now, that Σ is invertible if the coefficient $cA^{k_0-1}b$ is an invertible element of the ring R.

Moreover, paralleling the case of linear systems with coefficients in a field, we can give the following definition.

Definition 1. *Let the single input-single output system $\Sigma = (A, b, c)$ with coefficients in the ring R be given, assume that there exists k_0 such that $cA^{k-1}b = 0$ for $k < k_0$ and $cA^{k_0-1}b \neq 0$. Then, Σ has a* finite relative degree *equal to k_0. If, in addition, $cA^{k_0-1}b$ is an invertible element of R, we say that the relative degree is* pure. *Alternatively, if $cA^{k-1}b = 0$ for all $k \geq 1$, we say that Σ has no finite relative degree.*

Assume that Σ has pure relative degree k_0, then an inverse Σ' for Σ is given by the following equations

$$\Sigma' = \begin{cases} z(t+1) = (A + b(cA^{k_0-1}b)^{-1}cA^{k_0})z(t) + \\ \qquad\qquad +b(cA^{k_0-1}b)^{-1}y(t+k_0) \\ u(t) = (cA^{k_0-1}b)^{-1}cA^{k_0}z(t) + \\ \qquad\qquad +(cA^{k_0-1}b)^{-1}y(t+k_0) \end{cases} \tag{5}$$

In facts, Σ', initialized at $z(0) = x(0)$, gives, in response to any output sequence $\{y(t)\}_{t\geq 0}$ of Σ, the input sequence $\{u(t)\}_{t\geq 0}$ of Σ that produced $\{y(t)\}_{t\geq 0}$.

On the other hand, chosen any sequence $\{y(t)\}_{t\geq 0}$, the system Σ', initialized at $z(0) = 0$ and fed with $\{y'(t)\}_{t\geq 0}$, where $y'(t) = 0$ for $t < k_0$ and $y'(t) = y(t-k_0)$ for $t \geq k_0$, gives in response a sequence $\{u(t)\}_{t\geq 0}$ which, as input of Σ, produces the output $\{y(t-k)\}_{t\geq 0}$.

Assuming that Σ has pure, finite relative degree k_0, we consider the extended system Σ_E, whose output represents the tracking error, defined by the equations

$$\Sigma_E = \begin{cases} \dot{x}(t) = Ax(t) + bu(t) \\ e(t) = cx(t) - r(t) \end{cases}$$

Mimicking the procedure employed to construct an inverse, in the ring framework, of Σ, we evaluate recursively the time derivatives of $e(t)$. We have

$$\begin{aligned} e(t) &= y(t) - r(t) = cx(t) - r(t) \\ \dot{e}(t) &= cAx(t) - \dot{r}(t) \\ &\vdots \\ e^{(k_0-1)}(t) &= cA^{k_0-1}x(t) - r^{(k_0-1)}(t) \\ e^{(k_0)}(t) &= cA^{k_0}x(t) + cA^{k_0-1}bu(t) - r^{(k_0)}(t) \end{aligned} \tag{6}$$

and, by the hypothesis on the relative degree, $m(\Delta) = c(\Delta)(A(\Delta))^{k_0-1}b(\Delta)$, is an invertible element of the ring R. In other terms, $[m(\Delta)]^{-1} = m^{-1}(\Delta)$, we have that $f(t) = m^{-1}(\delta)g(t)$ is a non-anticipative relation in the differential framework.

The stability of the compensator obtained in this way is interpreted in terms of zero dynamics of Σ (see [3], [15]).

Assume that the system Σ has pure, finite relative degree k_0, and choose the real coefficients α_i, $i = 0, \ldots, k_0 - 1$ in such a way that

$$\pi(s) = s^{k_0} + \sum_{i=0}^{k_0-1} \alpha_i s^i$$

is an Hurwitz polynomial whose roots, w.l.o.g., are real. Consider the compensator Σ_C described by the following equations.

$$\Sigma_C = \begin{cases} \dot{z}(t) = Az(t) + bu(t) \\ u(t) = -m^{-1}[cA^{k_0}z(t) - r^{(k_0)}(t)] - m^{-1}\sum_{i=0}^{k_0-1} \alpha_i e^{(i)}(t). \end{cases} \tag{7}$$

The closed loop action of the compensator Σ_C on Σ_d is described by the equations

$$\begin{cases} \dot{z}(t) = Az(t) + bu(t) \\ \dot{x}(t) = Ax(t) + bu(t) \\ y(t) = cx(t) \\ u(t) = -m^{-1}[cA^{k_0}z(t) - r^{(k_0)}(t)] - m^{-1}\sum_{i=0}^{k_0-1} \alpha_i e^{(i)}(t) \end{cases} \tag{8}$$

and the tracking error satisfies the following relation.

$$e^{(k_0)}(t) + \textstyle\sum_{i=0}^{k_0-1} \alpha_i e^{(i)}(t) = cA^{k_0}(x(t) - z(t)). \tag{9}$$

If we impose that Σ_C and Σ have identical initial conditions, that is $z(t) = x(t)$ for $t \in [-Nh, 0]$ for a suitable N, we can prove that the output of the compensated system will track asymptotically the reference signal $r(t)$.

In case it is not possible to impose the same initial conditions, assuming that the system Σ_d is globally asymptotically stable, we can prove that the module of the tracking error between the output of the compensated system and the reference can be made arbitrarily small for t sufficiently large.

Concerning the stability of the compensator Σ_C, the construction based on the inversion in the ring framework guarantees that a reduced order compensator Σ_{CR} can be obtained as

$$\Sigma_{CR} = \begin{cases} \dot{\xi}_1(t) = A_1\xi_1(t) + A_2\tilde{e}(t) + b_1(e^{(k_0)}(t) + r^{(k_0)}(t)) \\ u(t) = g_1\xi_1(t) + g_2\tilde{e}(t) + +m^{-1}(e^{(k_0)}(t) + r^{(k_0)}(t)). \end{cases} \tag{10}$$

Stability will then depends on the zero dynamics of Σ (see [3]). Assuming that the system Σ is formally a minimum phase system or, equivalently, it has a formally stable zero dynamics, then, the compensator Σ_{CR} is stable and the output $y(t)$ of Σ_d compensated by means of Σ_{CR} tracks asymptotically $r(t)$.

3 MIMO Systems

Let the linear, time invariant, delay-differential, dynamical MIMO system Σ_d be described by the set of equations

$$\begin{cases} \dot{x}(t) = \sum_{i=0}^{\alpha} A_i x(t - ih) + \sum_{i=0}^{\beta} B_i u(t - ih) \\ y(t) = \sum_{i=0}^{\gamma} C_i x(t - ih) \end{cases} \tag{11}$$

where, denoting by $\mathbb{R}$ the field of real numbers, x belongs to the state space $\mathbb{R}^n$, u belongs to the input space $\mathbb{R}^m$, y belongs to the output space $\mathbb{R}^p$, A_i, $i = 0, 1, ..., \alpha$; B_i, $i = 0, 1, ..., \beta$; C_i, $i = 0, 1, ..., \gamma$, are matrices of suitable dimensions with entries in $\mathbb{R}$ and $h \in \mathbb{R}^+$ is a given delay. As done for SISO systems, the use of the delay operator δ yields the definition of matrices

$$A(\delta) = \sum_{i=0}^{\alpha} A_i\delta^i,\ B(\delta) = \sum_{i=0}^{\beta} B_i\delta^i,\ C(\delta) = \sum_{i=0}^{\gamma} C_i\delta^i$$

and, then,

$$\Sigma_d = \begin{cases} \dot{x}(t) = A(\delta)x(t) + B(\delta)u(t) \\ y(t) = C(\delta)x(t) \end{cases} \tag{12}$$

Substituting formally the delay operator δ with the algebraic indeterminate Δ, and denoting by $A(\Delta)$, $B(\Delta)$, $C(\Delta)$ the matrices given respectively by

$$A(\Delta) = \sum_{i=0}^{\alpha} A_i\Delta^i,\ B(\Delta) = \sum_{i=0}^{\beta} B_i\Delta^i,\ C(\Delta) = \sum_{i=0}^{\gamma} C_i\Delta^i,$$

it is possible to associate to Σ_d the system Σ, defined over the ring R by the set of equations

$$\mathbf{\Sigma} = \begin{cases} x(t+1) = Ax(t) + Bu(t) \\ y(t) = Cx(t) \end{cases} \tag{13}$$

where, by abuse of notation, we denote by x an element of the free state module R^n, by u an element of the free input module R^m, by y an element of to the free output module R^p.

The Trajectory Tracking Problem we consider here for the dynamical system Σ_d is described as follows.

Problem 1. Given a sufficiently regular reference output $r(t)$ and denoting by $e(t) = y(t) - r(t)$ the difference between the output of Σ_d and the reference, the *Tracking Problem* consists in finding a compensator Σ_C of the form

$$\Sigma_C = \begin{cases} \dot{z}(t) \quad = Lx(t) + Fz(t) + \sum_{i=0}^{\eta} G_i r^{(i)}(t) + \sum_{i=0}^{\mu} H_i e^{(i)}(t) \\ Mu(t) = L'x(t) + F'z(t) + \sum_{i=0}^{\nu} G'_i r^{(i)}(t) + \sum_{i=0}^{\pi} H'_i e^{(i)}(t) \end{cases} \tag{14}$$

where

$$F = \sum_{i=0}^{\bar{\alpha}} F_i \delta^i,\ G_i = \sum_{j=0}^{\bar{\eta}} g_{ij}\delta^j,\ H_i = \sum_{j=0}^{\bar{\mu}} h_{ij}\delta^j,$$

$$L = \sum_{i=0}^{\bar{\gamma}} L_i \delta^i,\ G'_i = \sum_{j=0}^{\bar{\nu}} G'_{ij}\delta^j,\ H'_i = \sum_{j=0}^{\bar{\pi}} H'_{ij}\delta^j,$$

$$F' = \sum_{i=0}^{\bar{\alpha}} F'_i \delta^i,\ L' = \sum_{i=0}^{\bar{\gamma}} L'_i \delta^i,\ M = I + \sum_{i=1}^{\sigma} M_i \delta^i,$$

I denotes the identity matrix and $r^{(i)}(t),\ e^{(i)}(t)$ denote the i-th time derivative of the corresponding signals, such that, in response to the reference signal $r(t)$, the output $y(t)$ of the compensated system tracks asymptotically $r(t)$, that is: the error signal $e(t) = y(t) - r(t)$ goes to 0 as t goes to ∞.

To study the Tracking Problem just described, it is convenient to state it in the framework of systems with coefficients in a ring, using the formalism employed in associating Σ to Σ_d for transferring the point of view from the delay-differential framework to the ring one. As this operation is straightforward, we give it for granted. In this way, that is working in the framework of systems with coefficients in a ring, we can employ the inversion procedure and a number of related notions described in [5] and [7]. In constructing a possible solution to the Tracking Problem we can consider different solvability conditions. As these conditions become less and less restrictive, the dynamical structure of the compensators of the general form (14) we need to consider becomes more and more complex.

3.1 Special Case

Let us start by introducing the following definition.

Definition 1. *Let Σ be a system with coefficients in R of the form (13) and denote by c_i the i-th row of the matrix C. For $i = 1, ..., p$, we say that the i-th output component y_i has independent finite relative degree equal to k_i if there exists an integer k_i such that $c_i A^{k-1} B = 0$ for $k < k_i$ and $c_i A^{k_i - 1} B \neq 0$.*

If $c_i A^{k-1} B = 0$ for all k, we say that i-th output component y_i has infinite relative degree.

Remark 1. *The adjective "independent" in the above Definition is used to stress the fact that the relative degree at issue refers to each single output component by considering it separately from the others. The notion of relative degree given in [7] is different, as it depends also on the coupling of the various output components.*

State Feedback Solution

Assume that the output components of the system Σ have independent finite relative degrees k_i, for $i = 1, \ldots, p$. In that case, we denote by D the $p \times m$ matrix whose rows are given by $c_i A^{k_i - 1} B$, for $i = 1, \ldots, p$. Then, the following result holds.

Proposition 1. *Given a system Σ_d of the form (12), there exists a static state feedback compensator which solves the Tracking Problem for Σ_d if all the output components of the associated system Σ, with coefficients in the ring $R = \mathbb{R}[\Delta]$, have independent finite relative degree and the matrix D is right invertible over R.*

Proof. Working in the ring framework, let us consider, for $i = 1, \ldots, p$, the components $e_i(t) = y_i(t) - r_i(t)$ of the error signal. By the hypothesis on the relative degrees, we have, $i = 1, \ldots, p$, for $i = 1, \ldots, p$,

$$e_i(t + k_i) = c_i A^{k_i} x + c_i A^{k_i - 1} B u - r_i(t + k_i). \tag{15}$$

Let $s^{k_i} + \sum_{j=0}^{j=k_i-1} \lambda_{ij} s^j$ be Hurwitz polynomials, for $i = 1, ..., p$, and impose the conditions

$$e_i(t + k_i) + \sum_{j=0}^{k_i - 1} \lambda_{ij} e_i(t + j) = 0 \tag{16}$$

for $i = 1, ..., p$. The purpose of the above conditions is that of ensuring that the tracking error for Σ_d goes to 0 as t goes to ∞. Actually, conditions (16) can be viewed as an abstract way to formulate in the ring framework, where the notion of limit does not make sense, the requirement about the asymptotic behaviour of $e(t)$.

By (15) and (16) we can write the system of equations

$$\begin{bmatrix} c_1 A^{k_1} x(t) - r_1(t + k_1) \\ \vdots \\ c_p A^{k_p} x(t) - r_p(t + k_k) \end{bmatrix} = \\ \begin{bmatrix} -\sum_{j=0}^{j=k_1-1} \lambda_{1j} [c_1 A^j x(t) - r_1(t + j)] \\ \vdots \\ -\sum_{j=0}^{j=k_p-1} \lambda_{pj} [c_p A^j x(t) - r_p(t + j)] \end{bmatrix} - Du(t) \tag{17}$$

which, since D is right invertible, can be solved for u. The solution gives rise, in the delay-differential framework, to the static state feedback compensator

$$u(t) = D^{-1} \begin{bmatrix} c_1 A^{k_1} x(t) - r_1^{(k_1)}(t) \\ \vdots \\ c_p A^{k_p} x(t) - r_p^{(k_p)}(t)) \end{bmatrix} + D^{-1} \begin{bmatrix} \sum_{j=0}^{j=k_1-1} \lambda_{1j} [c_1 A^j x(t) - r_1^{(j)}(t)] \\ \vdots \\ \sum_{j=0}^{j=k_p-1} \lambda_{pj} [c_p A^j x(t) - r_p^{(j)}(t)] \end{bmatrix} \tag{18}$$

which solves the Tracking Problem for Σ_d.

Example 1. *Let Σ_d be the delay differential system defined by the set of equations*

$$\Sigma_d = \begin{cases} \dot{x}_1(t) = x_1(t-h) + x_2(t) + u_1(t) \\ \dot{x}_2(t) = -x_2(t) + u_2(t) \\ y_1(t) = x_1(t-h) - x_2(t) + x_2(t-h) \\ y_2(t) = x_1(t) + x_2(t) \end{cases} \tag{19}$$

The associated system Σ, with coefficients in the ring of real polynomials $R = I\!R[\Delta]$, is described by the equations

$$\Sigma = \begin{cases} x_1(t+1) = \Delta x_1(t) + x_2(t) + u_1(t) \\ x_2(t+1) = -x_2(t) + u_2(t) \\ y_1(t) = \Delta x_1(t) + (\Delta - 1)x_2(t) \\ y_2(t) = x_1(t) + x_2(t) \end{cases} \tag{20}$$

We have

$$c_1\ B = [\Delta \quad \Delta - 1]$$

and

$$c_2\ B = [1 \quad 1].$$

Therefore, both the output components y_1 and y_2 have independent finite relative degree $k_1 = k_2 = 1$. The matrix

$$D = \begin{bmatrix} \Delta & \Delta - 1 \\ 1 & 1 \end{bmatrix}$$

is invertible over the ring R, since $\det D = 1$. Let $r(t)$ be a given reference output and denote by $e_i(t) = y_i(t) - r_i(t)$ the error for $i = 1, 2$. Choosing $\lambda_{10} = \lambda_{20} = 1$, let us impose the conditions

$$e_i(t+1) + e_i(t) = 0$$

for $i = 1, 2$. Then, (17) becomes

$$\begin{bmatrix} \Delta^2 & 1 \\ \Delta & 0 \end{bmatrix}\ x(t) - r(t+1) = \begin{bmatrix} -\Delta & -\Delta + 1 \\ -1 & -1 \end{bmatrix}\ x(t) + r(t) - Du(t) \tag{21}$$

Solving for u, we have

$$u(t) = \begin{bmatrix} 1 & 1 - \Delta \\ -1 & \Delta \end{bmatrix} \begin{bmatrix} -\Delta^2 - \Delta & -\Delta \\ -\Delta - 1 & -1 \end{bmatrix}\ x(t) + \begin{bmatrix} 1 & 1 - \Delta \\ -1 & \Delta \end{bmatrix} (r(t) + r(t+1))$$

and finally

$$\begin{cases} u_1(t) = -(\Delta + 1)x_1(t) - x_2(t) + (r_1(t) + r_1(t+1)) \\ \qquad\qquad +(1 - \Delta)(r_2(t) + r_2(t+1)) \\ \\ u_2(t) = -(r_1(t) + r_1(t+1)) + \Delta(r_2(t) + r_2(t+1)). \end{cases}$$

Going back to the original delay differential framework we obtain the static state feedback compensator

$$\begin{cases} u_1(t) = -x_1(t-h) - x_1(t) - x_2(t) + r_1(t) + \dot{r}_1(t) \\ \qquad\quad +r_2(t) + \dot{r}_2(t) - r_2(t-h) - \dot{r}_2(t-h) \\ \\ u_2(t) = -r_1(t) - \dot{r}_1(t) + r_2(t-h) + \dot{r}_2(t-h) \end{cases} \tag{22}$$

It is easy to verify that the tracking error of each output component satisfies the equation $\dot{e}_i(t)+e_i(t) = 0$ *and, therefore, it goes asymptotically to* 0 *as* t *goes to* ∞.

State Feedback Solutions with Delayed Dynamics

The condition of Proposition 1 about invertibility of the matrix D is quite strong. Writing D as $D(\Delta) = D_0 + D_1\ \Delta + \cdots + D_n\ \Delta^n$, a condition weaker than right invertibility of D is that the matrix $D_0 = D(0)$ is right invertible. In such case, to solve the Tracking Problem we need to employ state feedback compensators derived from a relation of the form

$$u(t) = F\xi(t) + G_1 u(t-h) + \cdots + G_n u(t-nh).$$

A compensator of that kind is said to have a delayed dynamics and it can be realized as

$$\begin{cases} z_1(t) = u(t-h) \\ \qquad \vdots \\ z_n(t) = u(t-nh) \\ u(t) = F\xi(t) + G_1 z_1(t) + \cdots + G_n z_n(t) \end{cases} .$$

More precisely, we have the following result.

Proposition 2. *Given a system* Σ_d *of the form (12), there exists a static state feedback compensator with delayed dynamics which solves the Tracking Problem for* Σ_d *if all the output components of the associated system* Σ*, with coefficients in the ring* $R = I\!R[\Delta]$*, have independent finite relative degree and, writing* D *as* $D = D_0 + D_1\ \Delta + \cdots + D_n\ \Delta^n$*, the matrix* D_0 *is right invertible.*

Proof. As in the proof of Proposition 1, we get a relation of the form (17), which gives rise, in the delay-differential framework to the following one:

$$\begin{bmatrix} c_1 A^{k_1} x(t) - r_1^{(k_1)}(t) \\ \vdots \\ c_p A^{k_p} x(t) - r_p^{(k_p)}(t) \end{bmatrix} = \begin{bmatrix} -\sum_{j=0}^{j=k_1-1} \lambda_{1j}[c_1 A^j x(t) - r_1^{(j)}(t)] \\ \vdots \\ -\sum_{j=0}^{j=k_p-1} \lambda_{pj}[c_p A^j x(t) - r_p^{(j)}(t)] \end{bmatrix} \tag{23}$$

$$-(D_0 u(t) + D_1\ u(t-h) + \cdots + D_n\ u(t-nh))$$

Solving (23) for $u(t)$, since D_0 is right invertible, we finally get the state feedback compensator with delayed dynamics

$$\begin{cases} z_1(t) = u(t-h) \\ \quad\vdots \\ z_n(t) = u(t-nh) \\ u(t) = -D_0^{-1}\left(-\begin{bmatrix} c_1A^{k_1}x(t) - r_1^{(k_1)}(t) \\ \vdots \\ c_pA^{k_p}x(t) - r_p^{(k_p)}(t) \end{bmatrix} + \right. \\ \qquad\qquad \left. + \begin{bmatrix} \sum_{j=0}^{j=k_1-1} \lambda_{1j}[c_1A^jx(t) - r_1^{(j)}(t))] \\ \vdots \\ \sum_{j=0}^{j=k_p-1} \lambda_{pj}[c_pA^jx(t) - r_p^{(j)}(t)] \end{bmatrix}\right) + \\ \qquad\qquad -D_0^{-1}(D_1z_1(t) + \cdots + D_nz_n(t)) \end{cases} \tag{24}$$

which solves the Tracking Problem for Σ_d.

Example 2. *Let Σ_d be the delay differential system defined by the set of equations*

$$\Sigma_d = \begin{cases} \dot{x}_1(t) = x_1(t) + x_3(t) + u_1(t-h) + u_1(t) \\ \dot{x}_2(t) = x_2(t) + u_2(t) \\ \dot{x}_3(t) = x_3(t-h) + u_2(t) \\ y_1(t) = x_1(t) \\ y_2(t) = x_2(t-h) - x_2(t) \end{cases} \tag{25}$$

The associated system Σ, with coefficients in the ring of real polynomials $R = \mathbb{R}[\Delta]$, is described by the equations

$$\Sigma = \begin{cases} x_1(t+1) = x_1(t) + x_3(t) + (\Delta+1)u_1(t) \\ x_2(t+1) = x_2(t) + u_2(t) \\ x_3(t+1) = \Delta x_3(t) + u_2(t) \\ \quad y_1(t) = x_1(t) \\ \quad y_2(t) = (\Delta-1)x_2(t) \end{cases} \tag{26}$$

We have

$$c_1\ B = [\Delta+1 \quad 0]$$

and

$$c_2\ B = [0 \quad \Delta-1].$$

Therefore, both the output components y_1 and y_2 have independent finite relative degree $k_1 = k_2 = 1$. The matrix

$$D = \begin{bmatrix} \Delta+1 & 0 \\ 0 & \Delta-1 \end{bmatrix}$$

is not invertible over the ring R, since $\det D = \Delta^2 - 1$. However, writing $D = D_0 + D_1 \cdot \Delta$, with

$$D_0 = \begin{bmatrix} 1 & 0 \\ 0 & -1 \end{bmatrix}, \quad D_1 = \begin{bmatrix} 1\ 0 \\ 0\ 1 \end{bmatrix},.$$

we have that D_0 is invertible. Let $r(t)$ be a given reference output and denote by $e_i(t) = y_i(t) - r_i(t)$ the error for $i = 1, 2$. Choosing $\lambda_{10} = 2$ and $\lambda_{20} = 1$, let us impose the conditions

$$e_i(t+1) + \lambda_{i0} e_i(t) = 0$$

for $i = 1, 2$. Then, (17) becomes

$$\begin{aligned} &\begin{bmatrix} x_1(t) + x_3(t) - r_1(t+1) \\ (\Delta - 1)x_2(t) - r_2(t+1) \end{bmatrix} = \\ &= \begin{bmatrix} -2x_1(t) + 2r_1(t) \\ (\Delta - 1)x_2(t) + r_2(t) \end{bmatrix} - D_0 u(t) - D_1 \ \Delta u(t). \end{aligned} \tag{27}$$

In the delay-differential framework, this corresponds to the relation

$$\begin{aligned} &\begin{bmatrix} x_1(t) + x_3(t) - \dot{r}_1(t) \\ x_2(t) - x_2(t-h) - \dot{r}_2(t) \end{bmatrix} = \\ &= \begin{bmatrix} -2x_1(t) + 2r_1(t) \\ x_2(t-h) - x_2(t) + r_2(t) \end{bmatrix} - D_0 u(t) - D_1 u(t-h). \end{aligned} \tag{28}$$

Solving for $u(t)$, we have

$$\begin{aligned} u(t) = \begin{bmatrix} -3 & 0 & -1 \\ 0 & -2 & 0 \end{bmatrix} \ x(t) + \begin{bmatrix} 0\,0\,0 \\ 0\,2\,0 \end{bmatrix} \ x(t-h) + \begin{bmatrix} 1 & 0 \\ 0 & -1 \end{bmatrix} \dot{r}(t) + \\ + \begin{bmatrix} 2 & 0 \\ 0 & -1 \end{bmatrix} r(t) + \begin{bmatrix} -1 & 0 \\ 0 & 1 \end{bmatrix} u(t-h). \end{aligned}$$

Defining $z_1(t) = u_1(t-h)$ and $z_2(t) = u_2(t-h)$, the state feedback compensator with delayed dynamics given by the equations

$$\begin{cases} z_1(t) = u_1(t-h) \\ z_2(t) = u_2(t-h) \\ u_1(t) = -3x_1(t) - x_3(t) + \dot{r}_1(t) + 2r_1(t) - z_1(t) \\ u_2(t) = 2x_2(t-h) - 2x_2(t) - \dot{r}_2(t) + \\ \qquad\qquad -r_2(t) + z_2(t) \end{cases} \tag{29}$$

solves the Tracking Problem for Σ_d, since the components of the error signal, satisfying the equations $\dot{e}_1(t) + 2e_1(t) = 0$ and $\dot{e}_2(t) + e_2(t) = 0$, go asymptotically to 0 as t goes to ∞

3.2 General Case

In the general case nor D neither D_0 can be assumed to be invertible matrices. To handle this case, we need to introduce the following concepts (see [7]).

Definition 2. *A system Σ defined by equations of the form (2) over a ring R is said*

• *right invertible, or functionally controllable, if any function $y(t)$ can be obtained as output of Σ for a suitable choice of the input and zero initial condition, possibly with a finite delay;*

• *weakly right invertible, or weakly functionally controllable, if there exists a matrix K with entries in R such that any function of the form $Ky(t)$ can be obtained as output of Σ for a suitable choice of the input and zero initial condition, possibly with a finite delay.*

In the framework of delay-differential systems, functional controllability corresponds to the reproducibility of any sufficiently smooth output (in other terms, to the existence of a right inverse system), while the weak notion corresponds to reproducibility (under the same smoothness conditions) after some delay.

Extending in a suitable way the classical inversion algorithm to the case of MIMO systems over the ring $R = I\!R[\Delta]$, in [8] two algorithms have been introduced to check, respectively, weak functional controllability and functional controllability of a given system Σ. They are reported in Appendix and are called, respectively, Algorithm 1 and Algorithm 2.

Referring to the Appendix for the technicalities, we recall that the both the Algorithms, when applied to Σ, construct a p-vector denoted by $Y_r(t)$, whose components are linear combinations of the components the output y of Σ at different time instants, verifying a relation of the form $Y_r(t) = C_r x(t) + D_r u(t)$, where C_r and D_r are matrices with entries in R of suitable dimensions. Then, we have the following results (see [8]).

Proposition 3. *Let Σ be a system over the ring R, defined by equations of the form (1) with $m \geq p$. Then Σ is weakly functionally controllable if and only if Algorithm 1 stops at step $r \leq n$ providing*

$$Y_r(t) = C_r x(t) + D_r u(t)$$

with rank $D_r = p$.

If Algorithm 1 stops at step $r \leq n$ with *rank* $D_r < p$, Σ is not weakly functionally controllable and, as a consequence, it is not right invertible. If Σ turns out to be weakly functionally controllable, Algorithm 2 allows to check right invertibility.

Proposition 4. *Let Σ be a weakly functionally controllable system over the ring R, defined by equations of the form (1) with $m \geq p$. Then Σ is functionally controllable if and only if Algorithm 2 stops at Step $r \leq n$ providing*

$$Y_r(t) = C_r x(t) + D_r u(t)$$

with D_r right invertible over R.

The relation between these notions and the Tracking Problem we are dealing with is given in the following Propositions.

Proposition 5. *Given a system Σ_d of the form (1), there exists a dynamic state feedback compensator which solves the Tracking Problem for Σ_d if the associated system Σ is functionally controllable.*

Proof. Algorithm 2 stops at step $r \leq n$ providing

$$Y_r(t) = C_r x(t) + D_r u(t),$$

where $Y_r(t)$ is a p-vector whose components are linear combination of the components $y_i(t+j)$ of the output y of Σ for different values of j and D_r is a right invertible matrix. Letting $e_i(t) = y_i(t) - r_i(t)$, from the above relation we obtain a new one of the form

$$E_r(t) = C_r x(t) + D_r u(t) - R_r(t), \tag{30}$$

where the vectors $E_r(t)$ and $R_r(t)$ correspond to $e(t)$ and to $r(t)$ in the same way as $Y_r(t)$ corresponds to $y(t)$.

Let $s^{k_i} + \sum_{j=0}^{j=k_i-1} \lambda_{ij} s^j$ be Hurwitz polynomials, for $i = 1, ..., p$, and and impose the conditions

$$e_i(t+k_i) + \sum_{j=0}^{k_i-1} \lambda_{ij} e_i(t+j) = 0 \tag{31}$$

for $i = 1, ..., p$. By (30) and (31) we obtain a new set of equations that, as in the proof of Proposition 1, can be solved for $u(t)$, providing a dynamic state feedback compensator which, in the delay-differential framework, solves the Tracking problem for Σ_d.

Example 3. *Let Σ_d be the delay differential system defined by the set of equations*

$$\begin{cases} \dot{x}_1 = u_1(t) \\ \dot{x}_2 = u_1(t-h) + x_3(t) \\ \dot{x}_3 = u_2(t) \\ y_1 = x_1(t) \\ y_2 = x_2(t) \end{cases}$$

The associated system Σ with coefficients in the ring $R = \mathbb{R}[\Delta]$ is described by the equations

$$\begin{cases} x_1(t+1) = u_1(t) \\ x_2(t+1) = x_3(t) + \Delta u_1(t) \\ x_3(t+1) = u_2(t) \\ y_1 = x_1(t) \\ y_2 = x_2(t) \end{cases}$$

Σ does not satisfies the hypotheses of Proposition 1 and 2, since we have

$$D = \begin{bmatrix} 1 & 0 \\ \Delta & 0 \end{bmatrix}.$$

However, Algorithm 1 gives

$$\begin{aligned} y_1(t+1) &= u_1(t) \\ y_2(t+2) - \Delta y_1(t+2) &= u_2(t) \end{aligned}$$

and, so, D_2 is the identity matrix.

Let $r(t)$ be a given reference output and denote by $e_i(t) = y_i(t) - r_i(t)$ the error for $i = 1, 2$. Choosing, e.g., $\lambda_{11} = \lambda_{21} = 3$, $\lambda_{10} = \lambda_{20} = 2$, let us impose, for $i = 1, 2$ the conditions

$$e_i(t+2) + 3e_i(t+1) + 2e_i(t) = 0.$$

Then, solving for $u(t)$ the resulting set of equations, we obtain

$$\begin{aligned} &\begin{bmatrix} u_1(t) \\ u_2(t) \end{bmatrix} = \\ &= \begin{bmatrix} e_1(t+1) \\ -3e_2(t+1) - 2e_2(t) + 3\Delta e_1(t+1) + 2\Delta e_1(t) \end{bmatrix} + \\ &\quad + \begin{bmatrix} r_1(t+1) \\ r_2(t+2) - \Delta r_1(t+2) \end{bmatrix}. \end{aligned} \tag{32}$$

Going back to the original delay-differential framework we get the state feedback compensator

$$\begin{cases} u_1(t) = \dot{e}_1(t) + \dot{r}_1(t) \\ u_2(t) = -3\dot{e}_2(t) - 2e_2(t) + 3\dot{e}_1(t-h) + 2e_1(t-h) + \\ \qquad \ddot{r}_2(t) - \ddot{r}_1(t-h) \end{cases} \tag{33}$$

It is easy to verify that each component of the tracking error satisfies the equation $\ddot{e}_i(t) + 3\dot{e}_i(t) + 2e_i(t) = 0$ and, therefore, it goes asymptotically to 0 as t goes to ∞.

3.3 State Feedback Solution with Delayed Dynamics

We want now to relax the condition of Proposition 5 about functional controllability and invertibility of the matrix D_r. As already done in Section 3.1, writing D_r as $D_r(\Delta) = D_{r0} + D_{r1}\,\Delta + \cdots + D_{rn}\,\Delta^n$, a condition weaker than those just recalled is that the matrix $D_{r0} = D_r(0)$ is right invertible. In such case, to solve the Tracking Problem we need again to employ state feedback compensators which present a delayed dynamics, in the sense already illustrated in Section 3.1. More precisely, we have the following result.

Proposition 6. *Given a system Σ_d of the form (1), there exists a dynamic state feedback compensator with elayed dynamics which solves the Tracking Problem for Σ_d if the associated system Σ is weakly functionally controllable and $D_r(0)$ is a right invertible matrix.*

Proof. The proof follows from that of Proposition 5 in the same way as the proof of Proposition 2 follows from that of Proposition 1.

Example 4. *Let Σ_d be the delay differential system defined by the set of equations*

$$\begin{cases} \dot{x}_1 = u_1(t) + u_1(t-h) \\ \dot{x}_2 = u_1(t-h) + x_3(t) \\ \dot{x}_3 = u_2(t) \\ y_1 = x_1(t) \\ y_2 = x_2(t) \end{cases}.$$

The associated system Σ with coefficients in the ring $R = \mathbb{R}[\Delta]$ is described by the equations

$$\begin{cases} x_1(t+1) = (1+\Delta)u_1(t) \\ x_2(t+1) = \Delta u_1(t) + x_3(t) \\ x_3(t+1) = u_2(t) \\ y_1 = x_1(t) \\ y_2 = x_2(t) \end{cases}$$

and Algorithm 1 gives

$$\begin{bmatrix} y_1(t+1) \\ -\Delta y_1(t+2) + (1+\Delta)y_2(t+2) \end{bmatrix} = \begin{bmatrix} (1+\Delta)u_1(t) \\ (1+\Delta)u_2(t) \end{bmatrix}.$$

Then

$$D_2 = \begin{bmatrix} (1+\Delta) & 0 \\ 0 & (1+\Delta) \end{bmatrix}$$

and D_{20} is the identity matrix.

Let $r(t)$ be a given reference output and denote by $e_i(t) = y_i(t) - r_i(t)$ the error for $i = 1, 2$. Chose λ_{ij} in such a way that $s^2 + \lambda_{i1}s + \lambda_{i0}$ is an Hurwitz polynomial for $i = 1, 2$ and impose the conditions

$$e_i(t+2) + \lambda_{i1}e_i(t+1) + \lambda_{i0}e_i(t) = 0$$

for $i = 1, 2$. From

$$\begin{aligned} &\begin{bmatrix} e_1(t+1) \\ -\Delta e_1(t+2) + (1+\Delta)e_2(t+2) \end{bmatrix} = \\ &= \begin{bmatrix} -r_1(t+1) \\ -\Delta r_1(t+2) + (1+\Delta)r_2(t+2) \end{bmatrix} + \begin{bmatrix} u_1(t) \\ u_2(t) \end{bmatrix} + \\ &+\Delta \begin{bmatrix} u_1(t) \\ u_2(t) \end{bmatrix}. \end{aligned} \tag{34}$$

and from the Hurwitz conditions we get a relation which, solving for $u(t)$, gives, in the delay-differntial framework,

$$\begin{cases} u_1(t) = \dot{e}_1(t) + \dot{r}_1(t) - u_1(t-h) \\ u_2(t) = \lambda_{11}\dot{e}_1(t-h) + \lambda_{10}e_1(t-h) - \ddot{r}_1(t-h) + \\ \qquad -\lambda_{21}\dot{e}_2(t) - \lambda_{20}e_2(t) - \lambda_{21}\dot{e}_2(t-h) + \\ \qquad -\lambda_{20}e_2(t-h) + \ddot{r}_2(t) - u_2(t-h) \end{cases}.$$

By letting $z(t) = u(t-h)$, we get the feedback compensator with delayed dynamics which solves the Tracking Problem for Σ_d.

4 Conclusion

An asymptotic Tracking Problem for multi input/multi output linear, delay-differential systems has been studied, using the formalism of systems over rings,

and solutions have been found for a large class of systems. In particular, different sufficient conditions for the existence of solutions have been given and feasible synthesis methods have been described. In case where the sufficient conditions are more restrictive, the resulting compensators have a simpler dynamics. A characterization of solvability in the general case is still to be found and this, as well as a study of the stability properties of the considered dynamic compensators, will be the object of further researches.

References

1. Basile G., Marro G. (1992) Controlled and conditioned invariants in linear system theory. Prentice Hall, New York
2. Boukas E. K., Liu Z.K. (2002) Deterministic and Stochastic Time-Delay Systems. Series on Control Engineering, Birkhauser, Boston.
3. Conte G., Perdon A.M. (1984) An algebraic notion of zeros for systems over rings. In Lecture Notes in Control and Information Science 58, pp. 166–182, Springer Verlag, Berlin Heidelberg New York
4. Conte G., Perdon A.M. (1998) Systems over Rings: Geometric Theory and Applications. In Proc. IFAC Workshop on Linear Time Delay Systems, Grenoble, France
5. Conte G., Perdon A.M. (2000) Invertibility and Inversion for Systems over Rings and Applications to Delay-differential Systems. In Proc. 39th IEEE CDC, Sydney, Australia
6. Conte G., Perdon A.M. (2000) Systems over rings: Geometric theory and applications. Annual Review in Control 24(1) :113–124
7. Conte G., Perdon A.M. (2002) Functional controllability and right invertibility for systems over rings. IMA J. Mathematical Control and Information 19(1): 95–102
8. Conte G., Perdon A.M., Iachini R. (2001) Inversion problems for time-delay systems via systems over rings. In Proc. 1^{st} IFAC Symposium on System Structure and Control, Prag, Czech Republic
9. Dion J.-M., Dugard L., Fliess M. eds. (1998) Proceedings of the 1^{st} IFAC Workshop on Linear Time Delay Systems, Grenoble, France
10. Perdon A.M. ed. (2000) Proceedings of the 2^{nd} IFAC Workshop on Linear Time Delay Systems, Ancona, Italy
11. Abdallah C.T. ed. (2001) Proceedings of the 3^{rd} IFAC Workshop on Linear Time Delay Systems, Albuquerque, New Mexico
12. Bliman P.-A. ed. (2003) Proceedings of the 4^{th} IFAC Workshop on Linear Time Delay Systems, Rocquencourt, France
13. Gu K., Kahritonov V.L., Chen J. (2003) Stability of Time-Delay Systems, Series on Control Engineering. Birkhauser, Boston
14. Kolmanovskii V., Niculescu S.I., Gu K. (1999) Delay effects on stability and control: a survey. In Proc. 38th IEEE CDC, Phoenix, Arizona
15. Márquez-Martínez L.A., Moog C.H. (2001) Trajectory tracking control for nonlinear time-delay systems. Kybernetika 37(4): 370–380
16. Silverman L. (1969) Inversion of multivariable linear systems. IEEE Trans. Aut. Control, 14:141–149

Appendix

Algorithm 1

Step 1. Let $d_0 = p$, $q_0 = 0$ and define $M_0 = \begin{bmatrix} 0 & I_{d_0} \end{bmatrix}$.

Compute $M_0 \begin{pmatrix} y_0(k) \\ y_0(k+1) \end{pmatrix} = y_0(k+1) = Cx(k+1) = CAx(k) + CBu(k)$.

Assume $rank\ CB = q_1$ and denote by S_1 a nonsingular matrix such that $S_1 CB = \begin{bmatrix} D_1 \\ 0 \end{bmatrix}$, where D_1 is a $q_1 \times m$ matrix of rank q_1. If $q_1 = p$, then the algorithm stops, else define $d_1 := q_0 + d_0 - q_1$ and $Y_1(k) = S_1 M_0 \begin{pmatrix} y(k) \\ y(k+1) \end{pmatrix} = \begin{bmatrix} C_1 \\ \tilde{C}_1 \end{bmatrix} x(k) + \begin{bmatrix} D_1 \\ 0 \end{bmatrix} u(k)$.

Step i. From the previous step we have

$$Y_{i-1}(k) = \begin{bmatrix} C_{i-1} \\ \tilde{C}_{i-1} \end{bmatrix} x(k) + \begin{bmatrix} D_{i-1} \\ 0 \end{bmatrix} u(k)$$

with $dim D_{i-1} = q_{i-1} \times m$ and $d_{i-1} = q_{i-2} + d_{i-2} - q_{i-1}$.

Define $M_{i-1} = \begin{bmatrix} I_{q_{i-1}} & 0\,0 & 0 \\ 0 & 0\,0 & I_{d_{i-1}} \end{bmatrix}$ and compute $M_{i-1} \begin{pmatrix} Y_{i-1}(k) \\ Y_i i - 1(k+1) \end{pmatrix} = \begin{bmatrix} C_{i-1}x(k) \\ \tilde{C}_{i-1}x(k+1) \end{bmatrix} + \begin{bmatrix} D_{i-1}u(k) \\ 0 \end{bmatrix} = \begin{bmatrix} C_{i-1} \\ \tilde{C}_{i-1}A \end{bmatrix} x(k) + \begin{bmatrix} D_{i-1} \\ \tilde{C}_{i-1}B \end{bmatrix} u(k)$.

Assume $rank \begin{bmatrix} D_{i-1} \\ \tilde{C}_{i-1}B \end{bmatrix} = q_i$ and denote by S_i a nonsingular matrix such that $S_i \begin{bmatrix} D_{i-1} \\ \tilde{C}_{i-1}B \end{bmatrix} = \begin{bmatrix} D_i \\ 0 \end{bmatrix}$, where D_i is a $q_i \times m$ matrix of rank q_i.

If $q_i = p$, then the algorithm stops, else define $Y_i(k) = S_i M_{i-1} \begin{pmatrix} y_{i-1}(k) \\ y_{i-1}(k+1) \end{pmatrix} = \begin{bmatrix} C_i \\ \tilde{C}_i \end{bmatrix} x(k) + \begin{bmatrix} D_i \\ 0 \end{bmatrix} u(k)$.

Step n. At step n, we get $Y_n(k) = \begin{bmatrix} C_{n1} \\ \tilde{C}_n \end{bmatrix} x(k) + \begin{bmatrix} D_n \\ 0 \end{bmatrix} u(k)$ with $rank\ D_n = q_n$ and the algorithm stops.

Algorithm 2

Step 1. Let $q_0 = 0$, $d_0 = p$ and define $M_0 = \begin{bmatrix} 0 & I_{d_0} \end{bmatrix}$.

Compute $M_0 \begin{pmatrix} y(k) \\ y(k+1) \end{pmatrix} = y(k+1) = Cx(k+1) = CAx(k) + CBu(k)$.

Assume that $rank\ CB = q_1$ and denote by S_1 a matrix, if any exists, such that $S_1 CB = \begin{bmatrix} D_1 \\ 0 \end{bmatrix}$, where D_1 is a right invertible matrix of rank q_1.

If such a matrix S_1 does not exist, the algorithm stops with no outputs.
If a matrix S_1 exists and $q_1 = p$, the algorithm stops and gives as output

$$Y_1(k) = C_1 x(k) + D_1 u(k)$$

where $C_1 = S_1 CA$ and $D_1 = S_1 CB$. Else, namely if a matrix S_1 exists but $q_1 < p$, we update $q_1 = d_0 + q_o - q_1$ and we define $Y_1(k) = S_1 M_0 \begin{pmatrix} y(k) \\ y(k+1) \end{pmatrix} = \begin{bmatrix} C_1 \\ \tilde{C}_1 \end{bmatrix} x(k) + \begin{bmatrix} D_1 \\ 0 \end{bmatrix} u(k)$ and we go to the next step.

Step i. From the previous step we have

$$Y_{i-1}(k) = \begin{bmatrix} C_{i-1} \\ \tilde{C}_{i-1} \end{bmatrix} x(k) + \begin{bmatrix} D_{i-1} \\ 0 \end{bmatrix} u(k)$$

with D_{i-1} of dimension $q_{i-1} \times m$ and $d_{i-1} = q_{i-2} + d_{i-2} - q_{i-1}$.

Define $M_{i-1} = \begin{bmatrix} I_{q_{i-1}} & 0\,0 & 0 \\ 0 & 0\,0 & I_{d_{i-1}} \end{bmatrix}$ and then compute $M_{i-1} \begin{pmatrix} Y_{i-1}(k) \\ Y_{i-1}(k+1) \end{pmatrix} = \begin{bmatrix} C_{i-1} x(k) \\ \tilde{C}_{i-1} x(k+1) \end{bmatrix} + \begin{bmatrix} D_{i-1} u(k) \\ 0 \end{bmatrix} = \begin{bmatrix} C_{i-1} \\ \tilde{C}_{i-1} A \end{bmatrix} x(k) + \begin{bmatrix} D_{i-1} \\ \tilde{C}_{i-1} B \end{bmatrix} u(k)$.

Assume that $rank \begin{bmatrix} D_{i-1} \\ \tilde{C}_{i-1} B \end{bmatrix} = q_i$ and denote by S_i a matrix, if any exists, such that $S_i \begin{bmatrix} D_{i-1} \\ \tilde{C}_{i-1} B \end{bmatrix} = \begin{bmatrix} D_i \\ 0 \end{bmatrix}$, where D_i is a right invertible matrix of rank q_i. If such a matrix S_i does not exist, the algorithm stops with no output.

If a matrix S_i exists and $q_i = p$, the algorithm stops and gives as output

$$Y_i(k) = C_i x(k) + D_i u(k)$$

with $D_i = S_i \begin{bmatrix} D_{i-1} \\ \tilde{C}_{i-1} B \end{bmatrix}$. Else, namely if a matrix S_i exists and $q_i < p$, we update $d_i = d_{i-1} + q_{i-1} - q_i$ and we define $Y_i(k) = S_i M_{i-1} \begin{pmatrix} y_{i-1}(k) \\ y_{i-1}(k+1) \end{pmatrix} = \begin{bmatrix} C_{i-1} \\ \tilde{C}_{i-1} \end{bmatrix} x(k) + \begin{bmatrix} D_i \\ 0 \end{bmatrix}$.

Step n. At step n, either the algorithm stops with no output because S_n cannot be found, or we have $Y_n(k) = \begin{bmatrix} C_n \\ \tilde{C}_n \end{bmatrix} x(k) + \begin{bmatrix} D_n \\ 0 \end{bmatrix} u(k)$, with D_n a right invertible matrix of rank $q_n = p$ and the algorithm stops giving the final expression

$$Y_n(k) = C_n x(k) + D_n u(k).$$

Finite Impulse Response Systems for Almost Perfect Decoupling in Nonminimum-Phase Plants

Giovanni Marro and Elena Zattoni

Dipartimento di Elettronica, Informatica e Sistemistica, Università di Bologna, Viale Risorgimento 2, 40136 Bologna, Italy
{gmarro,ezattoni}@deis.unibo.it

Summary. This contribution focuses on decoupling of previewed signals, i.e. the problem of making the output insensitive to input signals which are known a certain amount of time in advance. Inclusion of time delays in the problem formulation enables decoupling with preview to be turned into a causal problem. The solution of this latter problem is then completely set forth in the geometric approach context. Necessary and sufficient constructive conditions for decoupling of previewed signals are provided, where self-bounded controlled invariant subspaces play a key role in connection with internal stability of the devised system. If the minimal self-bounded controlled invariant subspace satisfying the structural constraint is internally stabilizable, decoupling just requires finite preview. Otherwise, infinite preview is demanded. In this latter case, resorting to finite impulse response systems yields a practically implementable solution which approximates the theoretical one with arbitrary accuracy. The procedure is illustrated by a benchmark example consisting of a flexible mechanical structure.

1 Introduction

Perfect tracking and decoupling problems are difficult to be solved when they involve nonminimum-phase systems [1, 2, 3]. In fact, troubles concerned with internal stability can only be overcome by facing noncausal problems, where the signals to be tracked or rejected are known in advance [1, 4, 5]. Indeed, circumstances where references or disturbances are known with finite or even infinite preview often occur in practice: for instance, flight routes are planned in advance, machine-tool working profiles are scheduled a priori, altitude winds as well as underwater marine currents may be known, forecast, or measured, and so forth. Hence, a great deal of research effort has been directed towards the investigation of techniques for achieving noncausal inversion. This issue was first addressed for SISO systems in [6, 7, 8, 9] and, subsequently, for MIMO systems both in the linear [10] and in the nonlinear case [11]. In those papers, perfect tracking was achieved by means of steering-along-zeros techniques devised in the polynomial approach context. Instead, a complete treatment of noncausal inversion for multivariable discrete-time systems in the geometric framework can be found in [12].

This contribution extends steering-along-zeros techniques to decoupling with preview in multivariable discrete-time systems. As in [12], the problem is tackled

J. Chiasson and J.J. Loiseau (Eds.): Appl. of Time Delay Systems, LNCIS 352, pp. 285–299, 2007.
springerlink.com

in a strict geometric context. Following an approach typical of [13], the structural and the stabilizability conditions are considered separately. The structural condition for decoupling with preview — namely $\mathcal{H} \subseteq \mathcal{V}^* + \mathcal{S}^*$ in [14, 15], where $\mathcal{H}$ is the image of the previewed disturbance input matrix H, $\mathcal{V}^*$ is the maximal $(A, \mathcal{B})$-controlled invariant contained in the null space $\mathcal{C}$ of the output matrix C, and $\mathcal{S}^*$ is the minimal $(A, \mathcal{C})$-conditioned invariant containing the image $\mathcal{B}$ of the control input matrix B — is the natural extension of that for measurable signal decoupling ($\mathcal{H} \subseteq \mathcal{V}^* + \mathcal{B}$ in [16]), which, in turn, extends that for inaccessible signal decoupling ($\mathcal{H} \subseteq \mathcal{V}^*$ in [17]). In contrast, the stabilizability condition — namely, the condition that $\mathcal{V}_m = \mathcal{V}^* \cap \min \mathcal{S}(A, \mathcal{C}, \mathcal{B} + \mathcal{H})$ be internally stabilizable, where $\mathcal{V}_m$ is the minimal $(A, \mathcal{B})$-controlled invariant self-bounded with respect to $\mathcal{C}$ such that $\mathcal{H} \subseteq \mathcal{V}_m + \mathcal{S}^*$, already considered for inaccessible and measurable signal decoupling in [18, 19, 20, 13] — holds unmodified also for decoupling with finite preview. Consequently, on the assumption that the structural condition holds, two cases must be distinguished: i) if $\mathcal{V}_m$ is internally stabilizable, perfect decoupling can be achieved provided that a finite preview of the input signal is available; ii) if $\mathcal{V}_m$ is not internally stabilizable but it does not have unassignable internal eigenvalues on the unit circle, perfect decoupling can be achieved provided that an infinite preview of the input signal is given. In the former case, the length of the finite preview is connected to the number of steps of the conditioned invariant algorithm, i.e. the algorithm providing for $\mathcal{S}^*$ [13]. In the latter case, infinite preview is related to dynamics of the unstable internal unassignable eigenvalues of $\mathcal{V}_m$. In practice, infinite preview is not necessary: in fact, the ideal behavior can be approximated with arbitrary accuracy when the preview is finite but sufficiently greater than the greatest time constant associated to the internal unassignable eigenvalues of $\mathcal{V}_m$.

With respect to the wide available literature on decoupling, the first asset of this contribution is of a methodological nature and concerns the use of $\mathcal{V}_m$ for checking stabilizability. In fact, in [15] and [21] the controlled invariant considered for stability is $\mathcal{V}_g^*$, the maximal internally stabilizable $(A, \mathcal{B})$-controlled invariant contained in $\mathcal{C}$. Since an internally stabilizable $\mathcal{V}_m$ is contained in $\mathcal{V}_g^*$, assuming $\mathcal{V}_m$ in place of $\mathcal{V}_g^*$ has the advantage of yielding a control system with the minimum number of internal unassignable dynamics. Moreover, the analysis based on $\mathcal{V}_m$ leads to a sharper insight into the connections between nonmimum-phase plants and noncausal problems. Since $\mathcal{V}_m \subseteq \mathcal{V}^*$, $\mathcal{V}_m$ may be internally stabilizable while $\mathcal{V}^*$ is not, which is to say that nonminimum-phase systems may not require infinite preview if the unstable internal unassignable eigenvalues of $\mathcal{V}^*$ are external to $\mathcal{V}_m$.

Another remarkable feature of this work is the extension of the class of the admissible compensators to include pure convolutors, which are infinite-dimensional dynamic systems whose I/O equation is of the following type

$$u(k) = \sum_{\ell=-\infty}^{\infty} \Phi(\ell)\, h(k-\ell), \quad k = 0, 1, \ldots .$$

However, truncation of the convolution profiles is unavoidable in practice. Hence, pure convolutors are replaced by finite-dimensional dynamic systems modeled as finite impulse response systems, i.e. as systems whose I/O equation can be written as

$$u(k) = \sum_{\ell=-k_a}^{k_p} \Phi(\ell)\, h(k-\ell), \quad k = 0, 1, \ldots.$$

Moreover, in the discrete-time case, these latter systems can be model by quadruples with a special structure of the system matrix, which is nilpotent. As aforementioned, the truncation error can be made negligible if the window of the finite impulse response system, i.e. the length of the time interval $[-k_a,\ k_p]$, is sufficiently large with respect to the time constants associated with the internal dynamics of $\mathcal{V}_m$.

2 Perfect Decoupling with Finite Preview

At the beginning of this section some well-known results on disturbance and measurable signal rejection are recalled for the reader's convenience (from Problem 1 to Algorithm 1). Then, attention is drawn to perfect decoupling of input signals known with finite preview (Problem 3). The main result of this section is a necessary and sufficient constructive condition for its solution (Lemma 1 and Theorem 3).

Throughout this chapter, the discrete time-invariant linear system

$$x(k+1) = A\,x(k) + B\,u(k) + H\,h(k), \tag{1}$$

$$y(k) = C\,x(k), \tag{2}$$

will be considered, with state $x \in \mathbb{R}^n$, control input $u \in \mathbb{R}^p$, inaccessible/measurable/ previewed input $h \in \mathbb{R}^s$, and controlled output $y \in \mathbb{R}^q$.

The set of all admissible control input sequences is the set $\mathcal{U}_f$ of all bounded sequences with values in $\mathbb{R}^p$. The set of all admissible inaccessible/measurable/previewed input sequences is the set $\mathcal{H}_f$ of all bounded sequences with values in $\mathbb{R}^s$. The matrices B, H, and C are assumed to be full-rank matrices. The symbols $\mathcal{B}$, $\mathcal{H}$, $\mathcal{C}$ will be used for $\operatorname{im} B$, $\operatorname{im} H$, $\ker C$, respectively. Moreover, $\mathcal{V}^*$ or $\max \mathcal{V}(A, \mathcal{B}, \mathcal{C})$ will stand for the maximal $(A, \mathcal{B})$-controlled invariant contained in $\mathcal{C}$, $\mathcal{S}^*$ or $\min \mathcal{S}(A, \mathcal{C}, \mathcal{B})$ will denote the minimal $(A, \mathcal{C})$-conditioned invariant containing $\mathcal{B}$, and $\mathcal{R}_{\mathcal{V}^*}$ will represent the constrained reachability subspace on $\mathcal{V}^*$, i.e. $\mathcal{R}_{\mathcal{V}^*} = \min \mathcal{J}\,(A + BF, \mathcal{V}^* \cap \mathcal{B})$, where F is any real matrix such that $(A + BF)\,\mathcal{V}^* \subseteq \mathcal{V}^*$. The subspaces $\mathcal{V}^*$, $\mathcal{S}^*$, and $\mathcal{R}_{\mathcal{V}^*}$ satisfy $\mathcal{R}_{\mathcal{V}^*} = \mathcal{V}^* \cap \mathcal{S}^*$ [22].

With respect to the system (1), (2), let $\mathcal{V} \subseteq \mathcal{X}$ be an $(A, \mathcal{B})$-controlled invariant, let F be any real matrix such that $(A + BF)\,\mathcal{V} \subseteq \mathcal{V}$, and let $\mathcal{R}_{\mathcal{V}}$ be the subspace reachable from the origin on $\mathcal{V}$ (i.e., $\mathcal{R}_{\mathcal{V}} = \mathcal{V} \cap \min \mathcal{S}(A, \mathcal{V}, \mathcal{B})$). The assignable and the unassignable internal eigenvalues of $\mathcal{V}$ are respectively defined as $\sigma((A + BF)|_{\mathcal{R}_{\mathcal{V}}})$ and $\sigma((A + BF)|_{\mathcal{V}/\mathcal{R}_{\mathcal{V}}})$. The assignable

and the unassignable external eigenvalues of $\mathcal{V}$ are respectively defined as $\sigma((A+BF)|_{(\mathcal{V}+\mathcal{R})/\mathcal{V}})$ and $\sigma((A+BF)|_{\mathcal{X}/(\mathcal{V}+\mathcal{R})})$. Hence, $\mathcal{V}$ is an internally stabilizable $(A,\mathcal{B})$-controlled invariant if and only if at least one real matrix F exists, such that $(A+BF)\,\mathcal{V}\subseteq\mathcal{V}$ and $\sigma((A+BF)|_{\mathcal{V}})\subset\mathbb{C}^{\odot}$. Likewise, $\mathcal{V}$ is an externally stabilizable $(A,\mathcal{B})$-controlled invariant if and only if at least one real matrix F exists, such that $(A+BF)\,\mathcal{V}\subseteq\mathcal{V}$ and $\sigma((A+BF)|_{\mathcal{X}/\mathcal{V}})\subset\mathbb{C}^{\odot}$. It follows that if (A,B) is stabilizable, any $(A,\mathcal{B})$-controlled invariant is externally stabilizable. The unassignable internal eigenvalues of $\mathcal{V}^*$ are the invariant zeros of the triple (A,B,C) and they are denoted by $\mathcal{Z}(A,B,C)$. Let $\mathcal{V}\subseteq\mathcal{X}$ be an $(A,\mathcal{B})$-controlled invariant contained in $\mathcal{C}$, $\mathcal{V}$ is said to be self-bounded with respect to $\mathcal{C}$ if $\mathcal{V}\supseteq\mathcal{V}^*\cap\mathcal{B}$. The set of $(A,\mathcal{B})$-controlled invariants self-bounded with respect to $\mathcal{C}$ is a non-distributive lattice with respect to $\subseteq$, $+$, $\cap$, also denoted by $\Phi(\mathcal{B},\mathcal{C})$. Its supremum is $\mathcal{V}^*$. Its infimum is $\mathcal{R}_{\mathcal{V}^*}$.

Internal stabilizability and self-boundedness of $(A,\mathcal{B})$-controlled invariants are notions of primary importance in the statement of the necessary and sufficient constructive condition for inaccessible and measurable signal decoupling with stability, as briefly recalled below.

Problem 1 (Perfect Decoupling of Inaccessible Signals). Consider the system (1),(2). Let $x(0)=0$. Design a linear algebraic state feedback F such that $\sigma(A+BF)\subset\mathbb{C}^{\odot}$ and, for all admissible $h(t)$ $(t\geq 0)$, $y(t)=0$ for all $t\geq 0$.

Theorem 1 (Perfect Decoupling of Inaccessible Signals [18, 19, 20, 13]). *Consider the system (1), (2). Let (A,B) be stabilizable. Problem 1 is solvable if and only if: i) $\mathcal{H}\subseteq\mathcal{V}^*$; ii) $\mathcal{V}_m=\mathcal{V}^*\cap\min\mathcal{S}(A,\mathcal{C},\mathcal{B}+\mathcal{H})$ is internally stabilizable.*

Problem 2 (Perfect Decoupling of Measurable Signals). Consider the system (1), (2). Let $x(0)=0$. Design a linear algebraic state feedback F and a linear algebraic feedforward S of the measurable input h on the control input u such that $\sigma(A+BF)\subset\mathbb{C}^{\odot}$ and, for all admissible $h(t)$ $(t\geq 0)$, $y(t)=0$ for all $t\geq 0$.

Theorem 2 (Perfect Decoupling of Measurable Signals [13]). *Consider the system (1), (2). Let (A,B) be stabilizable. Problem 2 is solvable if and only if: i) $\mathcal{H}\subseteq\mathcal{V}^*+\mathcal{B}$; ii) $\mathcal{V}_m=\mathcal{V}^*\cap\min\mathcal{S}(A,\mathcal{C},\mathcal{B}+\mathcal{H})$ is internally stabilizable.*

Algorithm 1 (Conditioned Invariant Algorithm [13]). *The conditioned invariant subspace $\mathcal{S}^*=\min\mathcal{S}(A,\mathcal{C},\mathcal{B})$ is the last term of the sequence $\mathcal{S}_1=\mathcal{B}$, $\mathcal{S}_i=\mathcal{B}+A\,(\mathcal{S}_{i-1}\cap\mathcal{C})$, with $i=2,\ldots,\rho_M$ where ρ_M $(\leq n)$ is the least integer such that $\mathcal{S}_{\rho_M+1}=\mathcal{S}_{\rho_M}$.*

In the light of the previous results, let us focus our attention on the case where the signal to be rejected is known with finite preview. The block diagram for previewed signal decoupling with stability is shown in Fig. 1. The block Σ stands the system (1),(2), Σ_c represents the feedforward compensator defined by the quadruple (A_c,B_c,C_c,D_c), and the block 'k_p-delays' denotes a cascade of k_p unit delays inserted in the input h signal flow in order to take into account its preview of k_p steps. The problem can be formalized as follows.

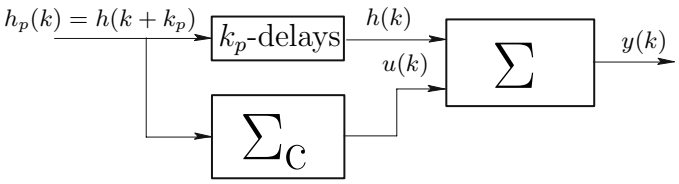

Fig. 1. Block diagram for previewed signal decoupling

Problem 3 (Perfect Decoupling with Finite Preview). Consider the system (1), (2). Let $\sigma(A) \subset \mathbb{C}^{\odot}$. Let $x(0) = 0$. Let $h(k)$ be known with preview of k_p steps, $\rho_M \leq k_p < \infty$. Design a linear dynamic feedforward compensator (A_c, B_c, C_c, D_c), having $h_p(k) = h(k + k_p)$ as input, such that $\sigma(A_c) \subset \mathbb{C}^{\odot}$ and, for all admissible $h(t)$ $(t \geq 0)$, $y(t) = 0$ for all $t \geq 0$.

A necessary and sufficient constructive condition for the solution of Problem 3 is expressed, through the following Lemma 1, by means of the following Theorem 3.

Lemma 1. *For any subspace $\mathcal{Q} \subseteq \mathbb{R}^n$, the relation*

$$\min \mathcal{S}(A, \mathcal{C}, \mathcal{B} + \mathcal{Q}) = \min \mathcal{S}(A, \mathcal{C}, \mathcal{S}^* + \mathcal{Q})$$

holds.

Proof. By construction, the subspaces generated by the standard algorithms for the minimal $(A, \mathcal{C})$-conditioned invariant subspaces respectively containing $\mathcal{B} + \mathcal{Q}$ and $\mathcal{B}$ satisfy the inclusions $\mathcal{S}'_1 = \mathcal{B} + \mathcal{Q} \supseteq \mathcal{S}_1 = \mathcal{B}$ and

$$\mathcal{S}'_i = A(\mathcal{S}'_{i-1} \cap \mathcal{C}) + \mathcal{B} + \mathcal{Q} \supseteq \mathcal{S}_i = A(\mathcal{S}_{i-1} \cap \mathcal{C}) + \mathcal{B},$$

for $i = 2, 3, \ldots, \rho_M$, where ρ_M is the number of steps for evaluating $\mathcal{S}^*$. These algorithms do not necessarily converge within the same number of steps, but the last inclusion implies $\min \mathcal{S}(A, \mathcal{C}, \mathcal{B} + \mathcal{Q}) \supseteq \mathcal{S}^*$. Hence, it implies $\min \mathcal{S}(A, \mathcal{C}, \mathcal{B} + \mathcal{Q}) \supseteq \mathcal{S}^* + \mathcal{B} + \mathcal{Q} \supseteq \mathcal{S}^* + \mathcal{Q}$. The latter inclusion means that $\min \mathcal{S}(A, \mathcal{C}, \mathcal{B} + \mathcal{Q})$ is an $(A, \mathcal{C})$-conditioned invariant containing $\mathcal{S}^* + \mathcal{Q}$, which implies

$$\min \mathcal{S}(A, \mathcal{C}, \mathcal{B} + \mathcal{Q}) \supseteq \min \mathcal{S}(A, \mathcal{C}, \mathcal{S}^* + \mathcal{Q}).$$

On the other hand, $\mathcal{B} + \mathcal{Q} \subseteq \mathcal{S}^* + \mathcal{Q}$ implies

$$\min \mathcal{S}(A, \mathcal{C}, \mathcal{B} + \mathcal{Q}) \subseteq \min \mathcal{S}(A, \mathcal{C}, \mathcal{S}^* + \mathcal{Q}),$$

which completes the proof. □

Theorem 3 (Perfect Decoupling with Finite Preview). *Problem 3 is solvable if and only if: i) $\mathcal{H} \subseteq \mathcal{V}^* + \mathcal{S}^*$; ii) $\mathcal{V}_m = \mathcal{V}^* \cap \min \mathcal{S}(A, \mathcal{C}, \mathcal{B} + \mathcal{H})$ is internally stabilizable.*

Proof. Since condition i) is well settled in the literature, this proof will focus on the sole condition ii).

If. By virtue of condition i), there exist subspaces $\mathcal{H}_{\mathcal{S}^*} \subseteq \mathcal{S}^*$ and $\mathcal{H}_{\mathcal{V}^*} \subseteq \mathcal{V}^*$ such that $\mathcal{H} = \mathcal{H}_{\mathcal{S}^*} + \mathcal{H}_{\mathcal{V}^*}$. By superposition, assuming $h(k) = e_i\,\delta(k-\rho_M)$, with $k = 0, 1, \ldots$ and e_i $(i = 0, 1, \ldots, s)$ denoting the generic i-th vector of the main basis of $\mathbb{R}^s$, does not cause any loss of generality. The input $h(k)$ is assumed to be previewed of ρ_M time instants. Let τ be defined as $\tau = H\,e_i\,\delta(k-\rho_M)$ with $k = \rho_M$, where $\delta(k)$, with $k = 0, 1, \ldots$ denotes the unit pulse sequence (i.e., $\delta(0) = 1$ and $\delta(k) = 0$ far any $k \neq 0$). Then, τ can be expressed as $\tau = \tau_{\mathcal{S}^*} + \tau_{\mathcal{V}^*}$ with $\tau_{\mathcal{S}^*} \in \mathcal{H}_{\mathcal{S}^*}$ and $\tau_{\mathcal{V}^*} \in \mathcal{H}_{\mathcal{V}^*}$. The decomposition of τ as $\tau_{\mathcal{S}^*}$ and $\tau_{\mathcal{V}^*}$ is not unique if $\mathcal{H}_{\mathcal{S}^*} \cap \mathcal{H}_{\mathcal{V}^*} \neq \{0\}$, which may occur if the system is not left-invertible: However, the arguments consiedered in this proof do not depend on the specif decomposition considered. By definition of $\mathcal{S}^*$, any state belonging to $\mathcal{H}_{\mathcal{S}^*}$ can be reached from the origin in ρ_M steps, along a trajectory in $\mathcal{C}$, therefore invisible at the output, until the last step but one. Hence, the component $\tau_{\mathcal{S}^*}$ can be zeroed by applying the control input sequence which steers the state from the origin to its opposite, $-\tau_{\mathcal{S}^*}$. As far as the component $\tau_{\mathcal{V}^*}$ is concerned, it can be maintained indefinitely on $\mathcal{V}^*$, since both the conditions of Theorem 1 are satisfied. In fact, $\mathcal{H}_{\mathcal{V}^*} \subseteq \mathcal{V}^*$ by construction, and $\mathcal{V}^* \cap \min\, \mathcal{S}(A, \mathcal{C}, \mathcal{B} + \mathcal{H}_{\mathcal{V}^*})$ is internally stabilizable since, by Lemma 1,

$$\begin{aligned}
&\mathcal{V}^* \cap \min\, \mathcal{S}(A, \mathcal{C}, \mathcal{B} + \mathcal{H}_{\mathcal{V}^*}) \\
&\quad = \mathcal{V}^* \cap \min\, \mathcal{S}(A, \mathcal{C}, \mathcal{S}^* + \mathcal{H}_{\mathcal{V}^*}) \\
&\quad = \mathcal{V}^* \cap \min\, \mathcal{S}(A, \mathcal{C}, \mathcal{S}^* + \mathcal{H}) \\
&\quad = \mathcal{V}^* \cap \min\, \mathcal{S}(A, \mathcal{C}, \mathcal{B} + \mathcal{H}) \\
&\quad = \mathcal{V}_m,
\end{aligned}$$

and $\mathcal{V}_m$ is internally stabilizable by assumption.

Only if. Assume, by contradiction, that $\mathcal{H} \not\subseteq \mathcal{V}^* + \mathcal{S}^*$. Then, the effect of any input sequence $h(k)$, with $k = 0, 1, \ldots$, cannot be made invisible at the output because of the maximality of the respective subspaces $\mathcal{V}^*$ and $\mathcal{S}^*$. In fact, $\mathcal{V}^*$ is the maximal set of initial states in $\mathcal{C}$ corresponding to trajectories indefinitely controllable on $\mathcal{C}$, while $\mathcal{S}^*$ is the maximal set of states that can be reached from the origin in a finite number of steps with all the intermediate states in $\mathcal{C}$ except the last one. □

On the basis of Theorem 3, a feedforward compensator Σ_c, defined by a quadruple (A_c, B_c, C_c, D_c), can easily be derived. Since a possible design procedure partially overlaps that for the design of the feedforward compensator solving the problem of decoupling with infinite preview, both the procedures will be illustrated in a compact form in the following section.

Before concluding this section, it is worth to briefly comment the assumption of stability of the to-be-controlled system.

Remark 1. In Theorem 3, the assumption that A has all its eigenvalues in the open unit disk is not restrictive with respect to the assumptions of stabilizability

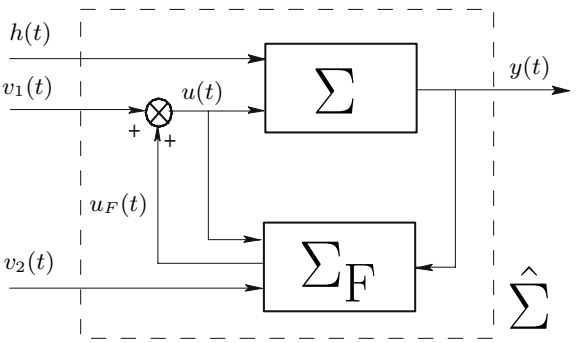

Fig. 2. Block diagram for prestabilization

of (A, B) and detectability of (A, C) which are usually considered. In fact, on those hypotheses, a stable system can always be obtained by output dynamic feedback. If, in particular, the output dynamic feedback unit receives an additional input v_2 from the feedforward unit Σ_c as is shown in the block diagram of Fig. 2, it can be proved that in the extended state space of the stabilized system, the set of the internal unassignable eigenvalues of the minimal self-bounded controlled invariant subspace satisfying the structural constraint matches that defined in the state space of the original system, thus the dynamic order of the feedforward unit is not increased by the presence of the stabilizing feedback unit [23].

3 Perfect Decoupling with Infinite Preview

In this section, we focus on a relaxed version of Problem 3, where the preview available is not necessarily finite and the precompensator Σ_c is not necessarily a standard dynamic system defined by a quadruple (A_c, B_c, C_c, D_c). By releasing those constraints, perfect decoupling with stability can be achieved also in the presence of unstable unassignable internal eigenvalues of $\mathcal{V}_m$, provided that the signal to be decoupled is completely available a priori and that $\mathcal{V}_m$ has no unassignable internal eigenvalues on the unit circle. On these assumptions, the precompensator includes not only a dynamic unit reproducing the stable dynamics of $\mathcal{V}_m$ and the sequence of impulses associated to the control strategy in $\mathcal{S}^*$, but it also incorporates a convolution unit reproducing the antistable dynamics of $\mathcal{V}_m$. However, the convolution is truncated in practice, and the additional unit working in connection with the standard dynamic unit turns out to be a finite impulse response system. Nevertheless, the theoretical solution can be approximated with arbitrary accuracy by choosing the length of the FIR system window sufficiently greater than the greatest time constant associated to the unstable unassignable internal eigenvalues of $\mathcal{V}_m$. As aforementioned, the design procedure presented in this section also encompasses the case of decoupling with finite preview as a special case.

A few fundamental concepts of the geometric approach constitute the theoretical basis of the design procedure illustrated in this section, which, in its earlier version was sketched as an algorithmic setting in [24]. In particular, in the present chapter, the presence of unassignable internal eigenvalues of $\mathcal{V}_m$ on the unit circle is excluded outrightly and the derivation of a left-invertible triple with nice properties in connection with the specific problem at issues is set forth through Theorem 4.

In order to outline the design procedure, the structural condition of Theorem 3 — namely, $\mathcal{H} \subseteq \mathcal{V}^* + \mathcal{S}^*$ — is assumed to be satisfied. Then, two different strategies are devised depending on whether the stabilizability condition — i.e., internally stabilizable $\mathcal{V}_m$ — is satisfied or not.

The subspace $\mathcal{V}_m$ is the subspace contained in $\mathcal{C}$ locus of the initial points of state trajectories which can be maintained indefinitely in $\mathcal{C}$ by suitable control actions. On the other hand, the subspace $\mathcal{S}^*$ is the maximal set of states that can be reached from the origin in ρ_M steps along trajectories with all the states in $\mathcal{C}$ except the last one. Then, let a unit pulse be applied to the input h at the time ρ_M, thus producing a component of the state $x_h \in \mathcal{H}$, which is decomposable as $x_h = x_{h,S} + x_{h,V}$, with $x_{h,S} \in \mathcal{S}^*$ and $x_{h,V} \in \mathcal{V}_m$ — note that $\mathcal{H} \subseteq \mathcal{V}_m + \mathcal{S}^*$ is implied by the structural condition (refer e.g. to [18, 19, 13]). The component $x_{h,S}$ can be zeroed by applying the control sequence that steers the state from the origin to $-x_{h,S}$ along a trajectory in $\mathcal{S}^*$. The component $x_{h,V}$ can be driven asymtotically to the origin along a trajectory lying on $\mathcal{V}_m$ by a suitable control action in the time interval $\rho_M \leq k < \infty$, if all the internal eigenvalues of $\mathcal{V}_m$ are (or have been assigned) in the open unit disk. Otherwise, the component $x_{h,V}$ must be further decomposed as $x_{h,V} = x_{h,V_S} + x_{h,V_U}$, with x_{h,V_S} belonging to the subspace of the stable internal eigenvalues of $\mathcal{V}_m$ and x_{h,V_U} belonging to that of the unstable internal eigenvalues. The former component can be driven asymptotically to the origin on $\mathcal{V}_m$, in the time interval $\rho_M \leq k < \infty$, while the latter component can theoretically be zeroed by driving the state from the origin to $-x_{h,V_U}$ with a control action, applied in the time interval $-\infty < k \leq \rho_M - 1$, along a trajectory, which, once again, is in $\mathcal{V}_m$.

As already remarked, the hypothesis that $\mathcal{V}_m$ does not have unassignable internal eigenvalues on the unit circle is implicit in the abovementioned control strategy. Moreover, the design procedure that will be illlustrated requires that the system (1),(2) be left-invertible. The following Theorem 4 deals with the squaring down procedure.

Theorem 4 (Squaring Down). *Consider the system (1),(2). Let $\mathcal{V}^* \cap \mathcal{B} \neq \{0\}$. Let F be any real matrix such that $(A + BF)\mathcal{V}^* \subseteq \mathcal{V}^*$. Let $(B^{-1}\mathcal{V}^*)^\perp \neq \{0\}$, where $B^{-1}\mathcal{V}^*$ denotes the inverse image of $\mathcal{V}^*$ through B, and let $\tilde{U}$ be a basis matrix of $(B^{-1}\mathcal{V}^*)^\perp$. Let $\tilde{A} = A + BF$, $\tilde{B} = B\tilde{U}$, $\tilde{\mathcal{V}}^* = \max \mathcal{V}(\tilde{A}, \tilde{\mathcal{B}}, \mathcal{C})$. Then, the following properties hold:*

(i) $\tilde{\mathcal{V}}^* = \mathcal{V}^*$;

(ii) $\tilde{\mathcal{V}}^* \cap \tilde{\mathcal{B}} = \{0\}$;

(iii) $\mathcal{Z}(\tilde{A},\tilde{B},C)=\mathcal{Z}(A,B,C)\uplus\sigma((A+BF)|_{\mathcal{R}_{\mathcal{V}^*}})$;

(iv) if $\mathcal{V}^*$ *is internally stabilizable and* F *is such that* $\sigma((A+BF)|_{\mathcal{R}_{\mathcal{V}^*}})\subset\mathbb{C}^{\odot}$, *then* $\tilde{\mathcal{V}}^*$ *is internally stable.*

Proof

(i) By construction, $\tilde{\mathcal{B}}\subseteq\mathcal{B}$, $\mathcal{V}^*\cap\tilde{\mathcal{B}}=\{0\}$. By definition, $\mathcal{V}^*$ is the maximal $(A,\mathcal{B})$-controlled invariant contained in $\mathcal{C}$. Hence, for any F such that $(A+BF)\mathcal{V}^*\subseteq\mathcal{V}^*$, $\mathcal{V}^*$ is the maximal $(A+BF)$-invariant contained in $\mathcal{C}$. Moreover, from $\tilde{\mathcal{B}}\subseteq\mathcal{B}$, it follows that $\mathcal{V}^*$ is also the maximal $(A+BF,\tilde{\mathcal{B}})$-controlled invariant contained in $\mathcal{C}$, namely $\mathcal{V}^*=\tilde{\mathcal{V}}^*$.

(ii) It follows from $\mathcal{V}^*\cap\tilde{\mathcal{B}}=\{0\}$ and property (i).

(iii) Due to property (ii), $\mathcal{Z}(\tilde{A},\tilde{B},C)=\sigma((\tilde{A}+\tilde{B}\tilde{F})|_{\tilde{\mathcal{V}}^*})$ for any $\tilde{F}$ such that $(\tilde{A}+\tilde{B}\tilde{F})\tilde{\mathcal{V}}^*\subseteq\tilde{\mathcal{V}}^*$. From $\tilde{A}=A+BF$, $\tilde{\mathcal{B}}\subseteq\mathcal{B}$, property (i), and property (ii), it follows that

$$\sigma((\tilde{A}+\tilde{B}\tilde{F})|_{\tilde{\mathcal{V}}^*})=\sigma((A+BF)|_{\mathcal{V}^*})=\mathcal{Z}(A,B,C)\uplus\sigma((A+BF)|_{\mathcal{R}_{\mathcal{V}^*}}).$$

(iv) It follows from property (ii) and property (iii). □

The following properties provide the control sequences suitably steering the component of the states on $\mathcal{V}_m$ and nulling the component of the states on $\mathcal{S}^*$, when the previewed input sequence is $h(k)=I\,\delta(k-\rho_M)$. This particular choice of the input sequence, which, actually, turns out to be a matrix input sequence, directly yields the FIR system convolution profiles and the matrices of the dynamic unit, due to linearity and time-invariance.

For the sake of simplicity, we will introduce a suitable state space basis transformation. Let V and S denote basis matrices of $\mathcal{V}_m$ and $\mathcal{S}^*$, respectively. Let F be any real matrix such that $(A+BF)\,\mathcal{V}_m\subseteq\mathcal{V}_m$. Perform the similarity transformation $T=[V\ S\ T_1]$. The matrices $A+BF$, B, H, C in the new basis have the structures:

$$A+BF=\begin{bmatrix}A_{11}&A_{12}&A_{13}\\O&A_{22}&A_{23}\\O&A_{32}&A_{33}\end{bmatrix},\quad B=\begin{bmatrix}O\\B_2\\O\end{bmatrix},\quad H=\begin{bmatrix}H_1\\H_2\\O\end{bmatrix},$$

$$C=\begin{bmatrix}O&C_2&C_3\end{bmatrix},\quad F=\begin{bmatrix}F_1&F_2&F_3\end{bmatrix}.$$

Then, the following property concerns the control sequence managing the component of the states on $\mathcal{S}^*$.

Property 1. Let W_i, with $i=1,\ldots,\rho_M-1$, be basis matrices of the respective subspaces $\mathcal{S}_i\cap\mathcal{C}$, with $i=1,\ldots,\rho_M-1$. Let the sequences $Q(i)$ and $U_1(i)$, with $i=1,\ldots,\rho_M-1$, be defined by

$$\begin{bmatrix}Q(\rho_M-j)\\U_1(\rho_M-j)\end{bmatrix}=\begin{bmatrix}A\,W_{\rho_M-j}&B\end{bmatrix}^{\#}W_{\rho_M-j+1}Q(\rho_M-j+1),\ j=1,\ldots,\rho_M-1,$$

with $W_{\rho_M} = S$ and $Q(\rho_M) = -H_2'$. Let $U_1(0) = B^{\#} W_1 Q(1)$. Let the sequence $X_1(i)$, $i = 1, \ldots, \rho_M$, be defined as $X_1(i) = W_i Q(i)$, with $i = 1, \ldots, \rho_M$. Then, the control sequence driving the states on $\mathcal{S}^*$ is $U_1(k)$, $k = 0, \ldots, \rho_M - 1$, and $X_1(k)$, $k = 1, \ldots, \rho_M$, is the sequence of the corresponding states.

The following property concerns the control sequence driving the state on $\mathcal{V}_m$ on the assumption of internal stabilizability.

Property 2. Let $\mathcal{V}_m$ be internally stabilizable. Let

$$X_2(\rho_M + i) = (A_{11})^i H_1, \quad i = 0, 1, \ldots,$$

and

$$U_2(\rho_M + i) = F_1 (A_{11})^i H_1, \quad i = 0, 1, \ldots.$$

Then, the sequences $X_2(\rho_M + i)$ and $U_2(\rho_M + i)$, with $i = 0, 1, \ldots$, respectively are the sequence of the states restricted to $\mathbb{R}^{n_\mathcal{V}}$, with $n_\mathcal{V} = \dim(\mathcal{V}_m)$, and the corresponding sequence of the controls.

If $\mathcal{V}_m$ is not internally stabilizable, a further state space basis transformation T' must be performed, whose aim is to separate the stable and antistable subspaces of $\mathcal{V}_m$. The matrices respectively corresponding to A_{11}, H_1 and F_1 in the new basis, have the structures

$$A_{11} = \begin{bmatrix} A_s & O \\ O & A_u \end{bmatrix}, \quad H_1 = \begin{bmatrix} H_s \\ H_u \end{bmatrix}, F_1 = \begin{bmatrix} F_s & F_u \end{bmatrix}.$$

Then, the stable component of the state H_s is managed as in the case where $\mathcal{V}_m$ is stabilizable, while a preaction, nulling the unstable component of the state H_u at the time instant ρ_M must be computed backwards through the matrix A_u. The following property concerns the control sequence driving the state on the antistable part of $\mathcal{V}_m$.

Property 3. Let

$$X_3(\rho_M - j) = -A_u^{-j} H_u, \quad j = 0, 1, \ldots,$$

and

$$U_3(\rho_M - j) = -F_u A_u^{-j} H_u, \quad j = 1, \ldots.$$

Then, the sequences $X_3(\rho_M - j)$ and $U_3(\rho_M - j)$, with $j = 1, \ldots$, respectively are the sequence of the states restricted to $\mathbb{R}^{n_u}$, with $n_u = \dim(\mathcal{V}_m^U)$, and the sequence of the corresponding controls.

The previous properties directly yield the compensator. If all the internal eigenvalues of $\mathcal{V}_m$ are stable, decoupling is achieved by means of the minimal preaction and postaction. The first can be obtained as the output of a ρ_M-step FIR system with suitable convolution profiles, the latter one can be realized as the output of a stable dynamic unit. Hence, the compensator turns out to be the parallel of a ρ_M-step FIR system and a dynamic unit. The FIR system is

$$u_F(k) = \sum_{\ell=0}^{\rho_M-1} \Phi(\ell)\, h(k-\ell), \quad k=0,1,\ldots, \tag{3}$$

with $\Phi(\ell) = U_1(\ell)$, $\ell = 0,\ldots,\rho_M - 1$. The dynamic unit is

$$w(k+1) = N\, w(k) + L\, h(k-\rho_M),\ k=0,1,.., \tag{4}$$

$$u_D(k) = M\, w(k), \tag{5}$$

where $N = A_{11}$, $L = H_1$, $M = F_1$. Hence, the control input is

$$u(k) = u_F(k) + u_D(k), \quad k=0,1,\ldots.$$

As aforementioned, in this case, the precompensator achieving perfect decoupling with stability can also be implemented as a unique standard dynamic unit (A_c, B_c, C_c, D_c) also including the FIR system. Otherwise, if antistable internal unassignable eigenvalues are also present in $\mathcal{V}_m$, infinite preview is required. The evolution of the state along the antistable unassignable internal eigenvalues of $\mathcal{V}_m$ can only be computed backwards in time and reproduced through a convolutor with an infinitely large window. In practice, an FIR system is considered, whose window should be large enough to make the truncation error negligible. The effect of the truncation error estinguishes since the system is stable and the applied control corresponds to an admissible trajectory for the system.

In conclusion, to achieve perfect decoupling with stability in the presence of unstable unassignable internal eigenvalues of $\mathcal{V}_m$ a convolutor with an infinitely large window would be required and this cannot be reduced to a standard dynamic unit (A_c, B_c, C_c, D_c). However, practical implementation requirements introduce truncation, which implies that: i) only an approximate solution is achievable in practice, although with arbitrary accuracy; ii) the convolution unit with truncated profile can be implemented as an FIR system, which, in the discrete-time case, can be reduced to a quadruple (A_c, B_c, C_c, D_c) with a peculiar structure. In this case, (3) is modified into

$$u_F(k) = \sum_{\ell=-k_a}^{\rho_M-1} \Phi(\ell)\, h(k-\ell), \quad k=0,1,\ldots, \tag{6}$$

with $\Phi(\ell) = U_1(\ell) + U_3(\ell)$, $\ell = -k_a,\ldots,\rho_M - 1$, (with a slight abuse of notation the control sequences are assumed to be zero wherever they are not explicitly defined). The dynamic unit is described by (4),(5) with $N = A_s$, $L = H_s$, $M = F_s$.

If the triple (A, B, C) is not left-invertible, the previous procedure can be applied anyhow, provided that a preliminary manipulation is performed to obtain a left-invertible triple according to Theorem 4 and the results thus obtained are adapted to fit the original system according to the following remark.

Remark 2. If the triple (A, B, C) is not left-invertible, let $\bar{U}_i(k)$ and $\bar{X}_i(k)$, with $i = 1, 2, 3$ and k consistently defined, be the sequences of controls and states provided by the Properties 1, 2, 3 applied to $(\tilde{A}, \tilde{B}, C)$. The corresponding control sequences for (A, B, C) must be computed as $U_i(k) = \tilde{U}\bar{U}_i(k) + F\bar{X}_i(k)$, $i = 1, 2, 3$.

4 A Benchmark Example

The proposed method is illustrated by an example often considered in the literature (see e.g. [25] and references therein). The system consists of two masses connected by a flexible rod (Fig. 3). The manipulable input is a force F applied to the mass with displacement x_2. In addition, we consider a disturbance W, which is a force acting on the mass with displacement x_1. Assuming $x_3 = \dot{x}_1$ and $x_4 = \dot{x}_2$, the state equations turn out to be

$$\begin{aligned} \dot{x}(t) &= A\,x(t) + B\,u(t) + H\,h(t), \\ y(t) &= C\,x(t), \end{aligned}$$

with

$$A = \begin{bmatrix} 0 & 0 & 1 & 0 \\ 0 & 0 & 0 & 1 \\ -0.0909 & 0.0909 & -0.0091 & 0.0091 \\ 0.0909 & -0.0909 & 0.0091 & -0.0091 \end{bmatrix},$$

$$B = \begin{bmatrix} 0 \\ 0 \\ -0.0070 \\ 0.0839 \end{bmatrix}, \quad H = \begin{bmatrix} 0 \\ 0 \\ -0.0839 \\ 0.0070 \end{bmatrix},$$

$$C = \begin{bmatrix} 1 & 0 & 0 & 0 \end{bmatrix}.$$

The system is stabilized by feedback of the displacement x_2 on the manipulable variable, i.e. we consider a state feedback matrix $K = [\,0 \quad -20 \quad 0 \quad 0\,]$, so that the new system matrix is $A_s = A + BK$. The poles of the stabilized system are $\sigma(A_s) = \{-0.0055 \pm 1.2653\,j,\ -0.0036 \pm 0.2775\,j\}$. A discrete-time model is derived by ZOH-sampling with $T = 0.1\,\mathrm{s}$. Hence, the sampled-data system equations are of the type of (1),(2), with

$$A = \begin{bmatrix} 0.9995 & 0.0012 & 0.0999 & 0.0001 \\ 0.0005 & 0.9921 & 0.0001 & 0.0997 \\ -0.0091 & 0.0229 & 0.9986 & 0.0021 \\ 0.0091 & -0.1582 & 0.0014 & 0.9912 \end{bmatrix},$$

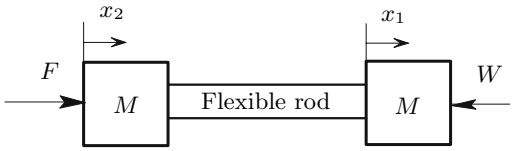

Fig. 3. Scheme of the mechanical system

$$B = \begin{bmatrix} 0 \\ 0.0004 \\ -0.0007 \\ 0.0084 \end{bmatrix}, \; H = \begin{bmatrix} -0.0004 \\ 0 \\ -0.0084 \\ 0.0007 \end{bmatrix},$$

$$C = \begin{bmatrix} 1 \; 0 \; 0 \; 0 \end{bmatrix}.$$

The sampled-data system invariant zeros are $\mathcal{Z} = \{1.1205, 0.9014, -0.9961\}$.

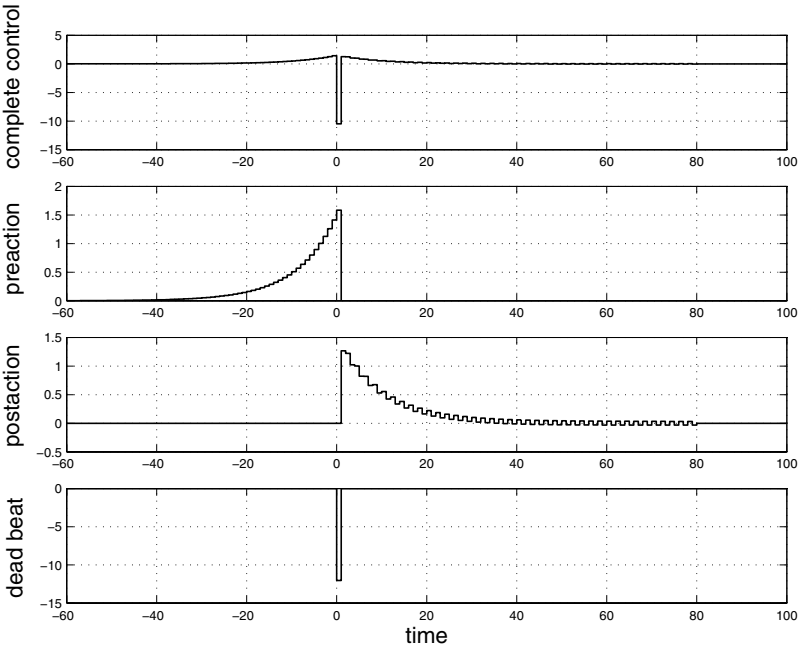

Fig. 4. Decomposition of the control sequence with a preview of 60 samples

Therefore, the system has nonminimum-phase dynamics. Standard computations provide the subspaces $\mathcal{S}^* = \mathcal{S}_1 = \mathcal{B}$ and $\mathcal{V}^* = \mathcal{V}_m = \text{im}\,[\,e_2 \; e_3 \; e_4\,]$, where e_j, with $j = 2, 3, 4$, denotes the j-th vector of the main basis of $\mathbb{R}^4$. The relative degree is $\rho_M = 1$. Hence, the finite preaction (or dead-beat control) consists of one single step. Exact decoupling requires infinite preaction, due to the unstable internal unassignable eigenvalue $z = 1.1205$ of $\mathcal{V}_m$. Stable dynamics are managed through infinite postaction. Software developed by means of the standard geometric routines[1] allows an output error amplitude of about 10^{-5} to be achieved with a 60-sample preview. The control sequence decomposed into its different contributions is shown in Fig. 4.

[1] e.g. those first published with [13] and now on-line available at http://www3.deis.unibo.it/FullProf/GiovanniMarro/downloads.htm

5 Conclusions

The problem of making the output totally insensitive to an exogenous input signal known a certain amount of time in advance has been solved in the geometric context, by exploiting the properties of the minimal self-bounded controlled invariant subspace satisfying the structural constraint. An algorithmic procedure was detailed for designing the compensator both in the case where the stabilizability condition is satisfied, and in the case where unstable internal unassignable eigenvalues of the minimal self-bounded controlled invariant are present. In the former case only the finite preview is required, while in the latter case an infinite preview is necessary. Indeed, practical implementation requires truncation of the convolution profiles, which implies an error of the actual behavior of the compensated system with respect to the ideal behavior. However, the ideal behavior can be approximated with arbitrary accuracy by choosing the length of the FIR window sufficiently greater than the longest time constant associated to the unstable internal unassignable dynamics of $\mathcal{V}_m$.

References

1. Ben Jemaa L., Davison E.J. (2003) Performance limitations in the robust servomechanism problem for discrete-time LTI systems. IEEE Transactions on Automatic Control 48(8):1299–1311
2. Davison E.J., Scherzinger B.M. (1987) Perfect control of the robust servomechanism problem. IEEE Transactions on Automatic Control 32(8):689–701
3. Qiu L., Davison E.J. (1993) Performance limitations of non-minimum phase systems in the servomechanism problem. Automatica 29(2):337–349
4. Devasia S., Chen D., Paden B. (1996) Nonlinear inversion-based output tracking. IEEE Transactions on Automatic Control 41(7):930–942
5. L.R. Hunt L.R., Meyer G., Su R. (1996) Noncausal inverses for linear systems. IEEE Transactions on Automatic Control 41(4):608–611
6. Gross E., Tomizuka M., Messner W. (1994) Cancellation of discrete time unstable zeros by feedforward control. ASME Journal of Dynamic Systems, Measurement and Control 116(1):33–38
7. Tsao T.-C. (1994) Optimal feed-forward digital tracking controller design. Journal of Dynamic Systems, Measurements and Control, 116:583–592
8. Marro G., Fantoni M. (1996) Using preaction with infinite or finite preview for perfect or almost perfect digital tracking. In Proceedings of the 8th Mediterranean Electrotechnical Conference on Industrial Applications in Power Systems, Computer Science and Telecommunications, volume 1, pp. 246–249, Bari, Italy
9. Marro G. Multivariable regulation in geometric terms: old and new results. In C. Bonivento, G. Marro, and R. Zanasi, eds., Colloquium on Automatic Control, Lecture Notes in Control and Information Sciences 215, pp. 77–138, Springer-Verlag, London
10. Zou Q., Devasia S. (1999) Preview-based stable-inversion for output tracking of linear systems. Journal of Dynamic Systems, Measurement and Control, 121:625–630
11. Zeng G., Hunt L.R. (2000) Stable inversion for nonlinear discrete-time systems. IEEE Transactions on Automatic Control 45(6):1216–1220

12. Marro G., Prattichizzo D., Zattoni E. (2002) Convolution profiles for right-inversion of multivariable non-minimum phase discrete-time systems. Automatica 38(10):1695–1703
13. Basile G., Marro G. (1992) Controlled and Conditioned Invariants in Linear System Theory. Prentice Hall, Englewood Cliffs
14. Willems J.C. (1982) Feedforward control, PID control laws, and almost invariant subspaces. Systems & Control Letters 1(4):277–282
15. Imai H., Shinozuka M., Yamaki T., Li D., Kuwana M. (1983) Disturbance decoupling by feedforward and preview control. ASME Journal of Dynamic Systems, Measurements and Control, 105(3):11–17
16. Bhattacharyya S.P. (1974) Disturbance rejection in linear systems. International Journal of Systems Science, 5(7):931–943
17. Wonham W.M., Morse A.S. (1970) Decoupling and pole assignment in linear multivariable systems: a geometric approach. SIAM Journal on Control 8(1):1–18
18. Basile G., Marro G. (1982) Self-bounded controlled invariant subspaces: a straightforward approach to constrained controllability. Journal of Optimization Theory and Applications, 38(1):71–81
19. Schumacher J.M. (1983) On a conjecture of Basile and Marro. Journal of Optimization Theory and Applications 41(2):371–376
20. Basile G., Marro G., Piazzi A. (1984) A new solution to the disturbance localization problem with stability and its dual. In Proc. '84 International AMSE Conference on Modelling and Simulation, volume 1.2, pages 19–27, Athens, Greece
21. Wonham W.M. (1985) Linear Multivariable Control: A Geometric Approach. Springer-Verlag, Berlin Heidelberg New York
22. Morse A.S. (1973) Structural invariants of linear multivariable systems. SIAM Journal of Control 11(3):446–465
23. Marro G., Zattoni E. (2005) Measurable signal decoupling through self-bounded controlled invariants: minimal unassignable dynamics of feedforward units for prestabilized systems. In Proc. 44th IEEE Conference on Decision and Control and European Control Conference, Sevilla, Spain
24. Marro G., Prattichizzo D., Zattoni E. (2000) A unified algorithmic setting for signal-decoupling compensators and unknown input observers. In Proc. 39th IEEE Conference on Decision and Control, Sydney, Australia
25. Perez H., Devasia S. (2003) Optimal output transitions for linear systems. Automatica, 39:181–192

Linearization of the Power Amplifier in Mobile Telecommunications

Sven Nõmm[1], Claude H. Moog[2], Emmanuel Cottais[3], and Yide Wang[3]

[1] Institute of Cybernetics at Tallinn University of Technology, Akadeemia tee 21, 12618, Tallinn, Estonia
sven@cc.ioc.ee

[2] Institut de Recherche en Communications et Cybernétique de Nantes (IRCCyN - UMR CNRS 6597), 1, rue de la Noë BP 92101 F-44321 Nantes Cedex 03
Claude.Moog@irccyn.ec-nantes.fr

[3] Institut de recherche en Electronique et Electrotechnique de Nantes Atlantique, Ecole polytechnique de l'université de Nantes Rue Christian Pauc - La Chantrerie BP 50609 44306 Nantes Cedex 3 - France

Summary. A nonlinear amplifier used in digital mobile telecommunications is considered. It is modelled by a nonlinear difference equation, and it is shown, that control techniques available for nonlinear discrete-time systems yield new results for managing power consumption through increasing the efficiency of digital electronic circuits. Namely an attempt is made to achieve higher efficiency of power amplifier by linearizing its characteristics (output power vs. input power). The results are illustrated by numerical simulations.

1 Introduction

Power consumption is an important issue for the digital mobile communication systems. One of the possible ways to manage the power consumption is to increase efficiency level of each device in the circuit. The main goal of this contribution is to apply control techniques available for nonlinear discrete-time systems to reduce energy consumption of power amplifier. This problem was considered in [1] and [2].

In digital mobile communications, the circuit of a typical transmitter usually contains a power amplifier and an antenna as the last two elements of the device. The schematic diagram of such a circuit is given in Figure 1. The power amplifier amplifies the modulated signal and transports it to the antenna.

Two important characteristics of the power amplifier are depicted in Figures 2 and 3. The first of them is the relation between the power of the input signal and the power of the output signal Figure 2. The second graph represents the dependance of the amplifier efficiency on the power of the input signal in Figure 3.

Here P_i is the power of input signal, P_o is the power of output signal and R_a is the efficiency of the amplifier. The domain of the characteristics where the output power is almost linear with respect to the input power is the most interesting for transmission since there is no distorsion. Unfortunately the efficiency of the

J. Chiasson and J.J. Loiseau (Eds.): Appl. of Time Delay Systems, LNCIS 352, pp. 301–312, 2007.
springerlink.com

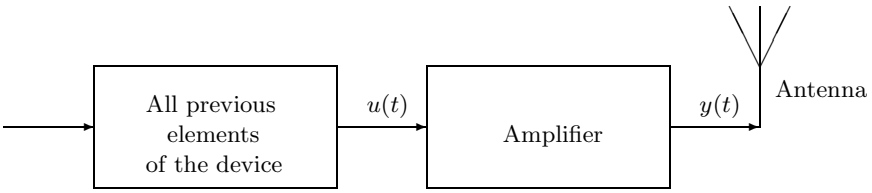

Fig. 1. Amplifier and antenna

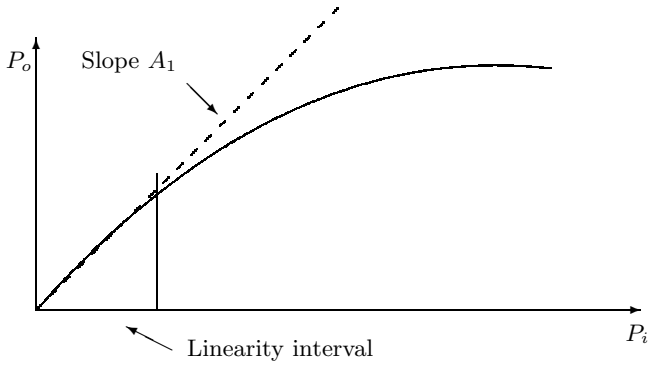

Fig. 2. Output power vs. input power

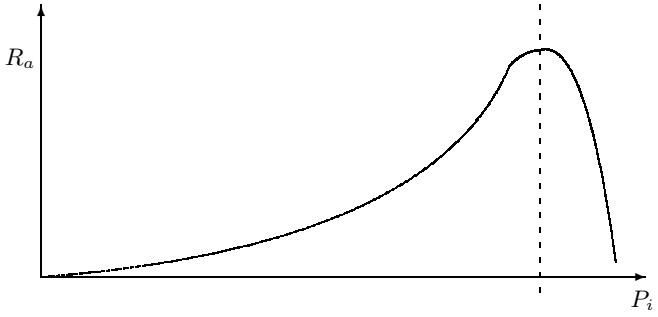

Fig. 3. Efficiency vs. input power

amplifier is very low in this region. Comparing graphs presented on Figures 2 and 3 one can easily see that the maximal efficiency of the amplifier lies out of the linearity domain of the amplifier characteristics. In the region where the efficiency is maximal, the amplifier can not be used due to the nonlinearity of the plant characteristics, the distortion of the signal is not acceptable. This results in the necessity to increase the battery capacity or to use more terrestrial base stations for the operator to limit transmission errors caused by the weakness of the signal.

One of the possible ways to overcome this problem is to enlarge the linearity interval of the characteristic function by linearizing the amplifier. This approach has already been studied in [1] and [2]. Most of the previous methods based on the adaptive predistortion, are limited to memoryless power amplifiers, that corresponds to $P = 1$ in (1). These existing results [1], [2] enlarge only locally the domain of linearity and they are based on approximations which remain arguable. The linearization technique proposed in this paper is based on the results of [3] and [4] and linearizes exactly and globally the whole characteristics of the model. The advantage is to take into account both non-linearity and the memory effect of the power amplifier which allows to eliminate totally intermodulation products and preserve the amplifier's gain. The global linearization technique results in the design of a dynamic precompensator since no static solution exists. To our best knowledge there is no general result in the literature describing this approach in the area of mobile telecommunications. Preliminary results obtained for some special cases have been published in [5], [6] and [7]. We assume that the linearizing compensator does not consume more energy than saved due to the linearization.

The chapter is organized as follows. Section 2 gives the precise problem formulation in terms of mathematical control theory. Section 3 introduces a general class of associative models [8] and discusses the issue of linearization. In section 4 analytical solution of the problem by input-output linearization by dynamic precompensation is given. Section 6 contains the simulation results. Section 6.3 contains the comparison with previous works [1] and [2]. Finally last section draws some conclusions.

2 Model of Amplifier

2.1 Input Output Model

The output signal of the amplifier is given by the following equation

$$y(t) = \sum_{k=0}^{P-1} \sum_{i=0}^{N} h'_k a_{2i+1} \mid u(t-k) \mid^{2i} u(t-k) \tag{1}$$

here P represents the memory effect and N is the order of nonlinearity, u is an input signal of the amplifier. This model is widely used in the domain of digital telecommunications [9], [10].

Equivalently the model of power amplifier can be written in a more standard way as

$$y(t+P-1) = \sum_{j=0}^{P-1} \sum_{i=0}^{N} h_j a_{2i+1} \mid u(t+j) \mid^{2i} u(t+j) \tag{2}$$

where $h_j = h'_{P-1-j}$, $y \in \mathbb{C}$ and $u \in \mathbb{C}$. The gain of the amplifier for model input power is the amplitude A_1 of a_1. Equation (2) is a special case of general associative models [8].

3 Linearization of General Associative Models

The structure of the model of the power amplifier (2) is s a special case of a generalized associative model as described in [8] . In this section, the lineariztaion theory is adapted to the latter class of systems, this will allow to apply results of present research for a larger variety of amplifiers.

3.1 Realization of General Associative Model

In order to accommodate the model of the amplifier (2) one has to include some notation which will result in the following model

$$\begin{aligned} y(t+n) = [[\ldots[f_0(y(t),u(t)) \circ_0 f_1(y(t+1),u(t+1))] \circ_2 \ldots] \\ \circ_{n-1} f_n(y(t+n),u(t+n))] \end{aligned} \tag{3}$$

where $\circ_i$ is the associative binary operator. By choosing state coordinates as follows

$$\begin{aligned} x_1(t) &= y(t+n) \diamond_{n-1} [[\ldots[f_0(y(t),u(t)) \circ_0 f_1(y(t+1),u(t+1))] \circ_2 \ldots] \\ &\quad \circ_{n-1} f_n(y(t+n-1),u(t+n-1))] \\ x_2(t) &= y(t+n-1) \diamond_{n-2} [[\ldots[f_0(y(t),u(t)) \circ_0 f_1(y(t+1),u(t+1))] \circ_2 \ldots] \\ &\quad \circ_{n-2} f_{n-2}(y(t+n-2),u(t+n-2))] \\ x_3(t) &= y(t+n-2) \diamond_{n-3} [[\ldots[f_1(y(t),u(t)) \circ_0 f_2(y(t+1),u(t+1))] \circ_2 \ldots] \\ &\quad \circ_{n-3} f_{n-3}(y(t+n-3),u(t+n-3))] \end{aligned} \tag{4}$$

$$\vdots$$

$$\begin{aligned} x_{n+2}(t) &= y(t+2) \diamond_2 [[f_0(y(t),u(t)) \circ_0 f_1(y(t+1),u(t+1))] \\ &\quad \circ_2 f_2(y(t+2),u(t+2))] \\ x_{n+1}(t) &= y(t+1) \diamond_1 [f_0(y(t),u(t)) \circ_0 f_1(y(t+1),u(t+1))] \\ x_n(t) &= y(t) \diamond_0 f_0(y(t),u(t)) \end{aligned}$$

where $\diamond_i$ is the inverse operator to $\circ_i$ one gets the following state-space equations

$$\begin{aligned} x_1(t+1) &= x_2(t) \circ_{n-1} f_1(y(t),u(t)) \\ x_2(t+1) &= x_3(t) \circ_{n-2} f_2(y(t),u(t)) \\ &\vdots \\ x_{n-1}(t+1) &= x_n \circ_1 f_{n-1}(y(t),u(t)) \\ x_n(t+1) &= f_n(y(t),u(t)) \\ y(t) &= x_1(t) \circ_0 f_0(y(t),u(t)) \end{aligned} \tag{5}$$

3.2 Linearization by Static State Feedback

By solving, with respect to u, the following equation

$$f_0(y(t), u(t)) = v(t) \diamond_0 x_1(t) \tag{6}$$

compute the static state feedback which yelds the linear closed loop system $y(t) = v(t)$.

Let us now show that in this case, linearization by dynamic precompensation is exactly the same as linearization by static estimated state feedback.

3.3 Linearization by Dynamic Precompensation

Problem Statement

Consider the following system.

$$x(t+1) = f(x(t), u(t)), \qquad t = 0, 1, 2, \ldots \tag{7}$$

$$y(t) = h(x(t), u(t)) \tag{8}$$

$x \in \mathbb{C}^n$, $u \in \mathbb{C}$ and $y \in \mathbb{C}$; find if possible a regular dynamic state feedback

$$\begin{cases} u(t) = H(\eta(t), v(t)) \\ \eta(t+1) = G(\eta(t), v(t)) \end{cases} \tag{9}$$

where $\eta \in \mathbb{C}^q$ such that the closed loop system

$$\begin{cases} x(t+1) = f(x(t), H(\eta(t), v(t)) \\ \eta(t+1) = G(\eta(t), v(t)) \\ y(t) = h(x(t), H(\eta(t), v(t)) \end{cases} \tag{10}$$

is diffeomorphic to

$$\zeta^1(t+1) = A\zeta^1(t) + bv(t) \tag{11}$$

$$\zeta^2(t+1) = \bar{f}^2(\zeta(t), v(t)) \tag{12}$$

$$y(t) = c\zeta^1(t) + \mathrm{d}v(t) \tag{13}$$

in which $\zeta^1(t) \in \mathbb{C}^{\bar{n}}$, $\zeta^2(t) \in \mathbb{C}^{n+q-\bar{n}}$, (c, A) is an observable pair.

General Form of Compensator

Given the system 3.1, define the state coordinates of the compensator as follows

$$\eta_1(t) = y(t+n) \diamond_{n-1} [[\ldots [f_0(y(t), u(t)) \circ_0 f_1(y(t+1), u(t+1))] \circ_2 \ldots] \\ \circ_{n-1} f_n(y(t+n-1), u(t+n-1))]$$

$$\eta_2(t) = y(t+n-1) \diamond_{n-2} [[\ldots [f_0(y(t), u(t)) \circ_0 f_1(y(t+1), u(t+1))] \circ_2 \ldots] \\ \circ_{n-2} f_{n-2}(y(t+n-2), u(t+n-2))]$$

$$\begin{aligned}
\eta_3(t) &= y(t+n-2) \diamond_{n-3} [[\dots [f_1(y(t),u(t)) \circ_0 f_2(y(t+1),u(t+1))] \circ_2 \dots] \\
&\quad \circ_{n-3} f_{n-3}(y(t+n-3),u(t+n-3))] \\
&\vdots \\
\eta_{n+2}(t) &= y(t+2) \diamond_2 [[f_0(y(t),u(t)) \circ_0 f_1(y(t+1),u(t+1))] \\
&\quad \circ_2 f_2(y(t+2),u(t+2))] \\
\eta_{n+1}(t) &= y(t+1) \diamond_1 [f_0(y(t),u(t)) \circ_0 f_1(y(t+1),u(t+1))] \\
\eta_n(t) &= y(t) \diamond_0 f_0(y(t),u(t))
\end{aligned} \tag{14}$$

This will lead to the following form of compensator

$$\begin{cases}
\eta_1(t+1) = \eta_2(t) \circ_{n-1} f_0(y(t),u(t)) \\
\eta_2(t+1) = \eta_3(t) \circ_{n-2} f_1(y(t),u(t)) \\
\vdots \\
\eta_{n-1}(t+1) = \eta_n \circ_1 f_{n-1}(y(t),u(t)) \\
\eta_n(t+1) = f_n(y(t),u(t)) \\
f_n(\eta(n)) = \eta_1(t) \circ_0 f_0(y(t),u(t))
\end{cases} \tag{15}$$

Linearization by Estimated State Feedback

Consider now linearization by estimated state feedback. Define the following observer.

$$\begin{aligned}
\hat{x}_1(t+1) &= \hat{x}_2(t) \circ_{n-1} f_1(y(t),u(t)) \\
\hat{x}_2(t+1) &= \hat{x}_3(t) \circ_{n-2} f_2(y(t),u(t)) \\
&\vdots \\
\hat{x}_{n-1}(t+1) &= \hat{x}_n \circ_1 f_{n-1}(y(t),u(t)) \\
\hat{x}_n(t+1) &= f_n(y(t),u(t)) \\
y(t) &= x_1(t) \circ_0 f_0(y(t),u(t))
\end{aligned} \tag{16}$$

It is easy to see, that after the first n steps, the estimated state is equal to the state of the system $\hat{x}_i = x_i \ i = 1, \dots, n$. This is why in this case, linearization by static state feedback is equivalent to the linearization by estimated state feedback.

4 Input-Output Linearization of the Amplifier

4.1 Special Case of the Amplifier

Our purpose is formulated as a control problem of feedback linearization design [3]. Consider u as the control input and y as system output. Our goal is to design

a compensator of form (9) which will provide a linear closed loop system such that the gain remains unchanged globally.

$$y(t) = Kv(t) \tag{17}$$

where $K = A_1$, is the slope in Figure 2 and denotes the gain on the whole domain of P_i. Since system input, output and all the coefficients are complex, trigonometrical or/and amplitude/phase forms can be used.

$$\begin{array}{ll} h_0 = 1 & \\ h_1 = H_1 e^{j\xi_1} = H_1(\cos\xi_1 + j\sin\xi_1) & h_2 = H_2 e^{j\xi_2} = H_2(\cos\xi_2 + j\sin\xi_2) \\ h_3 = H_3 e^{j\xi_3} = H_3(\cos\xi_3 + j\sin\xi_3) & h_4 = H_4 e^{j\xi_4} = H_1(\cos\xi_4 + j\sin\xi_4) \\ a_1 = A_1 e^{j\alpha_1} = A_1(\cos\alpha_1 + j\sin\alpha_1) & u(t) = Ue^{j\phi} = U(\cos\phi + j\sin\phi) \\ a_3 = A_3 e^{j\alpha_3} = A_3(\cos\alpha_3 + j\sin\alpha_3) & v(t) = Ve^{j\nu} = V(\cos\nu + j\sin\nu) \\ a_5 = A_5 e^{j\alpha_5} = A_5(\cos\alpha_5 + j\sin\alpha_5) & \eta(t) = Ce^{j\theta} = C(\cos\theta + j\sin\theta) \end{array} \tag{18}$$

One of requirement of practical applications is to preserve the amplifier's gain which means that from here and below we will suppose that in equation (17) $K = A_1$ ($K \in \mathbb{R}$).

5 Practical Implementation of the Linearizing Compensator

The majority of power amplifiers are easily represented by the models of the second order of nonlinearity $N = 2$. There are two possible approaches to find equations for amplitude and phase of output signal of compensator. The first approach is to transform dynamics equations of compensator into trigonometrical form and separate real and imaginary parts. By solving the obtained equations find the amplitude and phase of the signal. The second approach is based on the separation of phase and amplitude in the dynamics equations of compensator. We will concentrate our attention on the second approach.

5.1 Approach of Separation Amplitude and Phase of the Signal

This approach to find the amplitude and the phase of compensators output signal, does not require immediate usage of the trigonometrical form. In case of $P = 2$, equations (9) will take the following form

$$\begin{cases} \displaystyle\sum_{i=0}^{N} a_{2i+1}|u(t)|^2 u(t) = A_1 v(t) - \eta(t) \\ \eta(t+1) = \displaystyle\sum_{i=0}^{N} h_1 a_{2i+1}|u(t)|^2 u(t) \end{cases} \tag{19}$$

Consider the first part of equation (19), and rewrite it in the following form

$$\Big[\sum_{i=0}^{N} a_{2i+1} \mid U \mid^{2i} u(t)\Big]u(t)e^{j\phi} = Kv(t) - \eta(t) \tag{20}$$

consider now squares of modules of both sides

$$\Big|\sum_{i=0}^{N} a_{2i+1}U^{2i+1}\Big|^2 = |Kv(t) - \eta(t)|^2 \tag{21}$$

rewriting both parts into trigonometric form will lead

$$\Big|\sum_{i=0}^{N} A_{2i+1}U^{2i+1}(\cos\alpha_{2i+1} + j\sin\alpha_{2i+1})\Big|^2 = |A_1V\cos\nu + A_1Vj\sin\nu - C\cos\theta - Cj\sin\theta|^2 \tag{22}$$

simplification of both parts will give the following

$$\Big(\sum_{i=0}^{N} A_{2i+1}U^{2i+1}\cos\alpha_{2i+1}\Big)^2 + \Big(\sum_{i=0}^{N} A_{2i+1}U^{2i+1}\sin\alpha_{2i+1}\Big)^2 = |A_1^2V^2 + C^2 - 2A_1VC\cos(\nu-\theta) \tag{23}$$

The amplitude is given by real positive solution of (23); denote this solution as U_0. substitution of U_0 in to the first equation of (19) will give the phase ϕ in the following form

$$\phi = \arg\frac{A_1v(t) - \eta(t)}{h_0\Big[\sum_{i=0}^{N} a_{2i+1} \mid U \mid^{2i} u(t)\Big]} \tag{24}$$

This method is better suited to perform all calculations required by simulations because it excludes symbolic computations for $N \geq 2$ for instance. One can further increase the order of the system. For example if $P = 5$, equations (9) will take the following form

$$\begin{cases} \eta_1(t+1) = \eta_2 + \sum_{i=0}^{N} h_1a_{2i+1}|u(t)|^2u(t) \\ \eta_2(t+1) = \eta_3 + \sum_{i=0}^{N} h_2a_{2i+1}|u(t)|^2u(t) \\ \eta_3(t+1) = \eta_4 + \sum_{i=0}^{N} h_3a_{2i+1}|u(t)|^2u(t) \\ \eta_4(t+1) = \sum_{i=0}^{N} h_4a_{2i+1}|u(t)|^2u(t) \\ \sum_{i=0}^{N} a_{2i+1}|u(t)|^2u(t) = A_1v(t) - \eta_1(t) \end{cases} \tag{25}$$

Preliminary tests show that with orders $P = 5$ and $N = 2$ the model adequately represents the amplifier.

6 Computer Simulation

To see if the proposed solution is suitable for testing it on real devices, simulation in MATLAB environment was performed.

6.1 Linearization Results for P=2 and N=2

First we consider results obtained for the case $P = 2$, $N = 2$. In our case we will deal with a 2-tone signal, described by following equation.

$$v(t) = A_1\left[\cos(2\pi f_1 t) + a_2 \cos(2\pi f_2 t)\right] \tag{26}$$

$f_1 = 1\text{GHz}$ and $f_2 = 1.5\text{GHz}$. The values of coefficients of the amplifier for this simulation were chosen as follows

$$\begin{gathered} a_1 = 1.955 - i0.8794 \\ a_3 = 3.913568\,10^{-8} + i2.579951\,10^{-8} \\ a_5 = -2.917965\,10^{-4} - i9.1593110^{-15} \\ h_0 = 1 \\ h1 = 0.05208017737668 + i0.01559637151563 \end{gathered} \tag{27}$$

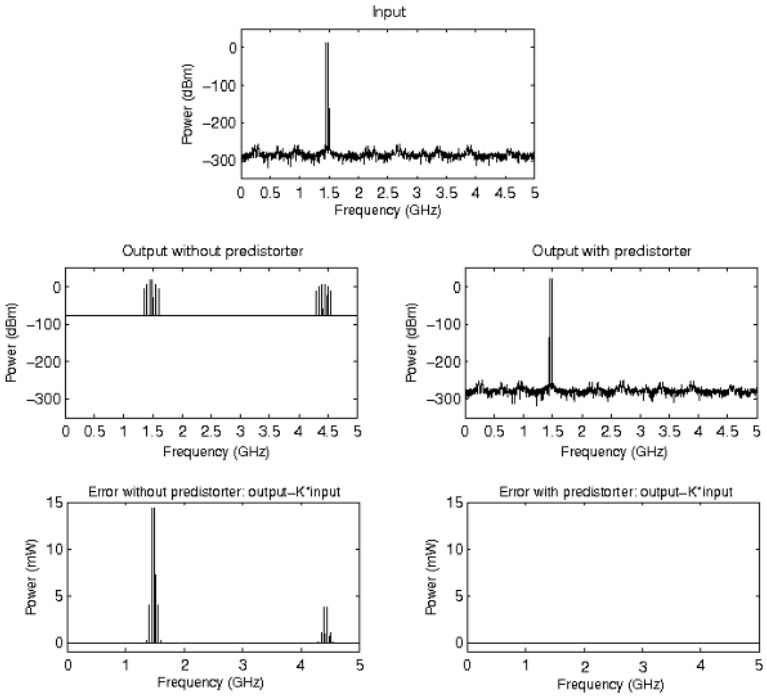

Fig. 4. Simulation results for P=2, N=2

Results of the simulation are presented on figure 4. The difference between input and output (with predistortion) signals of the linearized circuit is clearly seen. The products of the intermodulation and harmonics are eliminated. This also shows that the proposed method is suitable for application purposes.

6.2 Linearization Results for P=5 and N=2

In this case, the equation for amplitude and phase of compensator's output signal can not always be solved analytically. This causes some slowdown of the simulation program. The values of coefficients a_1, a_3, a_5, h_0 and h_1 of the amplifier for this simulation will remain the same as for the previous one (27) and values for the coefficients h_2, h_3 and h_4 are given below

$$\begin{aligned} h_2 &= -0.01317506666381 - i0.02032369105600 \\ h_3 &= 0.01662432189544 + i0.00634872216343 \\ h_4 &= -0.00546135327346 + i0.00148666118415 \end{aligned} \tag{28}$$

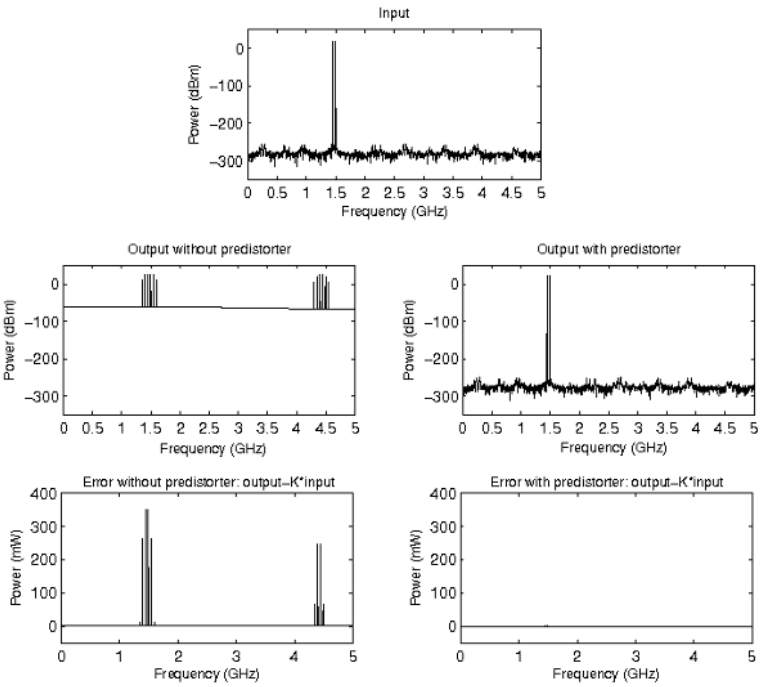

Fig. 5. Simulation results for P=5, N=2

6.3 Discussion

The value of the amplifier's gain K should be equal to A_1 which is 2.1437. The actual value of the gain K can be calculated on the basis of the following equation

$$\frac{P_o - P_i}{P_o} = \log K \tag{29}$$

by calculating the value for each frequency one can see that it varies around 2.1878 which gives an acceptable error.

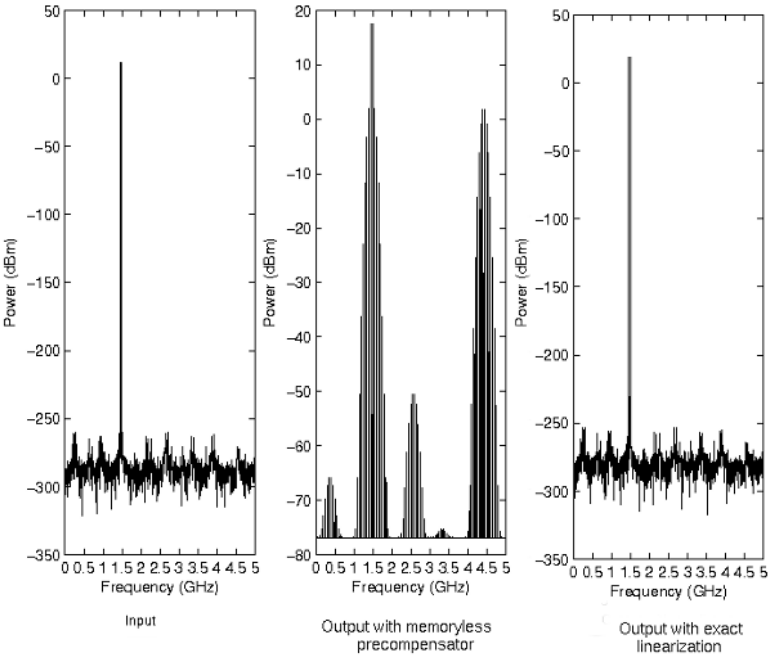

Fig. 6. Output with precompensator from [2] vs. output with the proposed precompensator

As it was stated before, the method proposed in this article has the advantage to take into account both non-linearity and memory effect of the power amplifier which allows to eliminate totally intermodulation products and preserve the amplifier's gain. Figures 4 and 5 clearly shows that the products of intermodulation and harmonics are eliminated and the signal becomes linear. Figure 6 demonstrates differences between outputs of the amplifier linearized by the present method and the amplifier linearized using the method proposed in [2]. The first graph represents the input, the graph in the center represents the output with precompensator proposed in [2] and the third graph represents the output with exact linearization .

7 Conclusions

This paper presents a new method for linearization of power amplifiers in transmitters of telecommunication devices. The main advantage of this method is

that it allows to linearize the power amplifier and to totally eliminate the intermodulation products preserving the amplifier's gain. This is achieved by taking into account both nonlinearity and memory effect of power amplifier and applying suitable linearization method. One open problem is to demonstrate that linearization does not change the characteristic function. A second open problem is to show that linearizing compensator does not consume more energy than saved due to the linearization.

Acknowledgments

This work was partially supported by the French-Estonian program in scientific and technological cooperation "Parrot", the scholarship of the French Government, the European Commission program "Marie Curie Control Training Site", Estonian Science Foundation Grant Nr 5405, and Estonian science foundation "Archimedes".

References

1. Stapleton S.T. (2001) Amplifier linearization using adaptive digital predistorsion. Applied microwave and wireless
2. Yun S.-Y. , Jeong S.-W., Jong Y.-C., Kim C.-D. (2001) A design of predistorative high power amplifier using carrier complex power series analysis. In Proc. of 31st European Microwave Conference, pp. 219–222, London, United Kingdom
3. Aranda-Bricaire E., Kotta Ü., Moog C.H. Linearization of discrete-time systems. SIAM J. Control Optimization 34:1999–2023
4. Pothin R., Kotta Ü, Moog C.H. (2000) Output feedback linearization of nonlinear discrete-time systems. In Proc. of the IFAC Conf. on Control system design, pp. 174–179, Bratislava, Slovakia
5. Cottais E., Nõmm S., Wang Y., Toutain S., Moog C. (2003) Linéarisation d'amplificateurs de puissance avec mémoire par prédistorsion adaptive. In Proc. of XIIIth national conference MICRONDES, Lille, France
6. Cottais E., Nõmm S., Wang Y., Toutain S., Moog C. (2003) Généralisation d'une nouvelle méthode de linéarisation d'amplificateurs de puissance avec mémoire par prédistorsion adaptive. In Proc. of GRETSI, Paris, France
7. Nõmm S., Moog C.H., Cottais E., Wang Y. Linearization as a new approach for the power consumption management of power amplifier. In Proc. of the 6nth IFAC Symp. on Nonlinear Control Systems, pp. 1535–1540, Stuttgart, Germany
8. Pearson R.K., Kotta Ü., Nomm S. (2002) Systems with associative dynamics. Kybernetika, 38(5):585–600
9. Launay F., Wang Y., Toutain S. (2002) Nonlinear amplifier modeling taking into account hf memory frequency. In Proc of the IEEE MTT-S International Microwave Symposium Digest, volume 2, pp. 865–868, Seattle, Washington
10. Launay F., Wang Y., Toutain S. (2002) M-ary psk signal power spectrum at the output of a nonlinear power amplifier. In *Proc of the IEEE MTT-S International Microwave Symposium Digest*, volume 3, pages 2197–2200, Seattle, Washinton

Part VI

Merging Saturations and Input Delays

Robust Sampled-Data Control: An Input Delay Approach

Emilia Fridman[1], Alexandre Seuret[2], and Jean-Pierre Richard[2,3]

[1] Department of Electrical Engineering-Systems Tel-Aviv University, Tel-Aviv 69978, Israel
emilia@eng.tau.ac.il
[2] LAGIS UMR 8146, Ecole Centrale de Lille, 59651 Villeneuve d'A scq cedex
{seuret.alexandre,jean-pierre.richard}@ec-lille.fr
[3] project ALIEN, INRIA Futurs

1 Introduction

Modelling of continuous-time systems with digital control in the form of continuous-time systems with delayed control input was introduced by Mikheev, Sobolev & Fridman [19], Astrom & Wittenmark [1] and further developed by Fridman (1992). The digital control law may be represented as delayed control as follows:

$$u(t) = u_d(t_k) = u_d(t-(t-t_k)) = u_d(t-\tau(t)), \quad t_k \le t < t_{k+1},\ \tau(t) = t-t_k, \quad (1)$$

where u_d is a discrete-time control signal and the time-varying delay $\tau(t) = t-t_k$ is piecewise-linear with derivative $\dot\tau(t) = 1$ for $t \neq t_k$. Moreover, $\tau \le t_{k+1} - t_k$. Based on such a model, for small enough sampling intervals $t_{k+1} - t_k$ asymptotic approximations of the trajectory [19] and of the optimal solution to the sampled-data LQ finite horizon problem [7] were constructed.

Since the middle of 90's years of the last century different LMI conditions for robust stability of linear systems with uncertain, but bounded constant delay with a given upper bound have been derived (see e.g. [18],[17] and [20]). For systems with time-varying delays such conditions were obtained via Lyapunov-Krasovskii functionals in the case where the derivative of the delay is less than one (see e.g. [15]). The stability issue in the cases of time-varying delay without any restrictions on the derivative of the delay has been treated mainly via Lyapunov-Razumikhin functions, which usually lead to conservative results (see e.g. [14],[16],[20] and [13]). Only recently for the first time this case was treated by Lyapunov-Krasovskii technique [11]. This became possible due to a new descriptor model representation of the delay system introduced by Fridman [8].

The main approach to the sampled-data robust stabilization problem (see e.g. [6], [21]) is based on the lifting technique ([2],[26]) in which the problem is transformed to equivalent finite-dimensional discrete problem. However, this approach does not work in the cases with uncertain sampling times or uncertain system matrices. In the present paper we suggest a new approach to the robust sampled-data stabilization. We find a solution by solving the problem for

J. Chiasson and J.J. Loiseau (Eds.): Appl. of Time Delay Systems, LNCIS 352, pp. 315–327, 2007.
springerlink.com

a continuous-time system with uncertain but bounded (by the maximum sampling interval) time-varying delay in the control input. We verify that the LMI sufficient conditions for stability of [11] are valid also in the case of piecewise-continuous delay and derive LMIs for the feedback gain. The conditions which we obtain are robust with respect to different samplings with the only requirement that the maximum sampling interval is not greater than h. As a by-product we show that for $h \to 0$ the conditions coincide with the necessary and sufficient conditions for the continuous-time stabilization. Such convergence in H_2 framework and related results were proved in [19], [4], [7], [22], [25] and [21].

For the first time the new approach allows to develop different robust control methods for the case of sampled-data control. The LMIs are affine in the system matrices and thus for the systems with polytopic type uncertainty the quadratic stabilization conditions, where the common Lyapunov functional for different vertices of the polytope is used, readily follow. We derive a parameter dependent solution, where different Lypunov functionals are used for different vertices by modifying results of (Fridman & Shaked, 2003). We also consider the regional stabilization by sampled-data saturated state-feedback, where we give an estimate on the domain of attraction. For continuous-time stabilization of state-delayed systems by saturated-feedback see e.g. [5], [24], [3] and [10].

Notation: Throughout the paper the superscript 'T' stands for matrix transposition, $\mathcal{R}^n$ denotes the n dimensional Euclidean space with vector norm $|\cdot|$, $\mathcal{R}^{n\times m}$ is the set of all $n\times m$ real matrices, and the notation $P>0$, for $P \in \mathcal{R}^{n\times n}$ means that P is symmetric and positive definite. Given $\bar{u} = [\bar{u}_1, ..., \bar{u}_m]^T,\ 0 < \bar{u}_i,\ i = 1, ..., m$, for any $u = [u_1, ..., u_m]^T$ we denote by $sat(u, \bar{u})$ the vector with coordinates $sign(u_i)min(|u_i|,\ \bar{u}_i)$. By stability of the system we understand the asymptotic stability of it.

2 Sampled-Data Stabilization of Systems with Polytopic Type Uncertainty

2.1 Problem Formulation

Consider the system

$$\dot{x}(t) = Ax(t) + Bu(t), \tag{2}$$

where $x(t) \in \mathcal{R}^n$ is the state vector, $u(t) \in \mathcal{R}^m$ is the control input.

We are looking for a piecewise-constant control law of the form $u(t) = u_d(t_k), t_k \le t < t_{k+1}$, where u_d is a discrete-time control signal and $0 = t_0 < t_1 < \cdots < t_k < \cdots$ are the sampling instants. Our objective is to find a state-feedback controller given by

$$u(t) = Kx(t_k),\ t_k \le t < t_{k+1}, \tag{3}$$

which stabilizes the system.

We represent a piecewise-constant control law as a continuous-time control with a time-varying piecewise-continuous (continuous from the right) delay

$\tau(t) = t - t_k$ as given in (1). We will thus look for a state-feedback controller of the form:

$$u(t) = Kx(t - \tau(t)). \tag{4}$$

Substituting (4) into (2), we obtain the following closed-loop system:

$$\dot{x}(t) = Ax(t) + BKx(t - \tau(t)), \quad \tau(t) = t - t_k,\ t_k \le t < t_{k+1}. \tag{5}$$

We assume that

A1 $t_{k+1} - t_k \le h\ \forall k \ge 0$.

From A1 it follows that $\tau(t) \le h$ since $\tau(t) \le t_{k+1} - t_k$. We will further consider (5) as the system with uncertain and bounded delay.

2.2 Stability of the Closed-Loop System

Similarly to [11], where the continuous delay was considered, we obtain for the case of piecewise-continuous delay the following result:

Lemma 1. *Given a gain matrix K, the system (5) is stable for all the samplings satisfying A1, if there exist $n \times n$ matrices $0 < P_1,\ P_2,\ P_3,\ Z_1,\ Z_2, Z_3$ and $R > 0$ that satisfy the following LMIs:*

$$\Psi_1 < 0, \quad \textit{and} \quad \begin{bmatrix} R & [0\ K^T B^T]P \\ * & Z \end{bmatrix} \ge 0, \tag{6}$$

where

$$P = \begin{bmatrix} P_1 & 0 \\ P_2 & P_3 \end{bmatrix}, \quad Z = \begin{bmatrix} Z_1 & Z_2 \\ * & Z_3 \end{bmatrix}, \quad \Psi_1 = \Psi_0 + hZ + \begin{bmatrix} 0 & 0 \\ 0 & hR \end{bmatrix},$$
$$\Psi_0 = P^T \begin{bmatrix} 0 & I \\ A + BK & -I \end{bmatrix} + \begin{bmatrix} 0 & I \\ A + BK & -I \end{bmatrix}^T P.$$

Proof is based on the following descriptor representation of (5) [8]:

$$\dot{x}(t) = y(t), \quad 0 = -y(t) + (A + BK)x(t) - BK \int_{t-\tau(t)}^{t} y(s)ds, \tag{7}$$

which is valid in the case of piecewise-continuous delay $\tau(t)$ for $t \ge 0$. Given a matrix K and initial condition $x(t) = \phi(t) (t \in [-h, 0])$, where ϕ is a piecewise continuous function, $x(t)$ satisfies (5) for $t \ge 0$ iff it satisfies (7). Note that the descriptor system (7) has no impulsive solutions since in (7) $y(t)$ is multiplied by the nonsingular matrix I [9].

We apply the Lyapunov-Krasovskii functional of the form:

$$V(t) = V_1 + V_2, \tag{8}$$

where

$$\bar{x}(t) = col\{x(t),\ y(t)\}, \quad E = \begin{bmatrix} I_n & 0 \\ 0 & 0 \end{bmatrix}, \quad P = \begin{bmatrix} P_1 & 0 \\ P_2 & P_3 \end{bmatrix}, \quad P_1 = P_1^T > 0, \tag{9a-d}$$

and

$$V_1 = \bar{x}^T(t)EP\bar{x}(t),\ V_2 = \int_{-h}^{0}\int_{t+\theta}^{t} y^T(s)Ry(s)dsd\theta, \tag{9e-f}$$

which satisfies the following inequalities

$$a|x(t)|^2 \leq V(t) \leq b \sup_{s\in[-h,0]} |\bar{x}(t+s)|^2, \quad a>0,\ b>0. \tag{10}$$

Differentiating $V(t)$ along the trajectories of (7) for $t \geq h$ we find (see [11]) that

$$\dot{V}(t) < \bar{x(t)}^T \Psi_1 \bar{x(t)} < -c|x(t)|^2, \quad c>0, \tag{11}$$

Provided that (6a,b) hold. Integrating (11) we have

$$V(t) - V(h) \leq -c\int_{-h}^{t} |x(s)|ds \tag{12}$$

and, hence, (10) yields $|x(t)|^2 \leq V(t)/a \leq V(h)/a < b/a \sup_{s\in[-h,0]} |\bar{x}(h+s)|^2$. Since $\sup_{s\in[-h,0]} |\bar{x}(h+s)| \leq c_1 \sup_{s\in[-h,0]} |\phi(s)|$,$c_1 > 0$ (cf. Hale & Lunel, 1993, p168) and thus $\dot{x}$, defined by the right-hand side of (5), satisfy $\sup_{s\in[-h,0]} |\dot{x(h+s)}| \leq c_2 \sup_{s\in[-h,0]} |\phi(s)|$, $c_2 > 0$, we obtain that

$$|x(t)|^2 \leq c_3 \sup_{s\in[-h,0]} |\phi(s)|^2, c_3 > 0. \tag{13}$$

Hence (5) is stable (i.e. $x(t)$ is bounded and small for small ϕ). To prove asymptotic stability we note that $x(t)$ is uniformly continuous on $[0,\infty)$ (since $\dot{x}(t)$ defined by the right-hand side of (5 is uniformly bounded). Moreover, (12) yields that $|x(t)|^2$ is integrable on $[0,\infty)$. Then, by Barbalat's lemma, $x(t) \to 0$ for $t \to \infty$ □

Consider now the continuous state-feedback

$$u(t) = Kx(t) \tag{14}$$

and the closed-loop system (2), (14)

$$\dot{x}(t) = (A+BK)x(t). \tag{15}$$

It is clear that the stability of the latter system is equivalent to the stability of its equivalent descriptor form

$$\dot{x}(t) = y(t), \quad 0 = -y(t)+(A+BK)x(t), \tag{16}$$

which coincides with (7) for $h = 0$. It is well-known ([23]) that the stability of the latter system is equivalent to the condition $\Psi_0 < 0$.

If there exists P of the form (9c,d) which satisfies $\Psi_0 < 0$, then for small enough $h > 0$ LMIs of Lemma 2.1 are feasible (take e.g. $Z = I_{2n}$ and $R = [0\ K^TB^T]P^TP[0\ K^TB^T]^T$). We, therefore, obtain the following result:

Corollary 1. *If the continuous-time state-feedback (14) stabilizes the linear system (2), then the sampled-data state-feedback (3) with the same gain K stabilizes (2) for all small enough h.*

In the case where the matrices of the system are not exactly known, we denote $\Omega = \begin{bmatrix} A & B \end{bmatrix}$ and assume that $\Omega \in \mathcal{C}o\{\Omega_j,\ j = 1, ...N\}$, namely,

$$\Omega = \sum_{j=1}^{N} f_j \Omega_j \quad \text{for some} \quad 0 \le f_j \le 1,\ \sum_{j=1}^{N} f_j = 1, \tag{17}$$

where the N vertices of the polytope are described by

$$\Omega_j = \begin{bmatrix} A^{(j)} & B^{(j)} \end{bmatrix}.$$

In order to guarantee the stability of (2) over the entire polytope one can use the result of Lemma 2.1 by applying the same matrices P_2 and P_3 for all the points in the polytope and solving (6a,b) for the N vertices only. A quadratic stability type criterion is then obtained:

Corollary 2. *Given a gain matrix K, the system (5) is stable, over the entire polytope Ω, if there exist $n \times n$ matrices $0 < P_1^{(j)},\ P_2,\ P_3,\ Z_1^{(j)},\ Z_2^{(j)}, Z_3^{(j)}$ and $R^{(j)} > 0$ that satisfy the following LMIs:*

$$\Psi_1^{(j)} < 0, \quad \textit{and} \quad \begin{bmatrix} R^{(j)} & [0\ K^T B^{(j)T}]P^{(j)} \\ * & Z^{(j)} \end{bmatrix} \ge 0,\ j = 1, ..., N, \tag{18}$$

where

$$P^{(j)} = \begin{bmatrix} P_1^{(j)} & 0 \\ P_2 & P_3 \end{bmatrix}, \quad Z^{(j)} = \begin{bmatrix} Z_1^{(j)} & Z_2^{(j)} \\ * & Z_3^{(j)} \end{bmatrix}, \quad \Psi_1^{(j)} = \Psi_0^{(j)} + hZ^{(j)} + \begin{bmatrix} 0 & 0 \\ 0 & hR^{(j)} \end{bmatrix},$$
$$\Psi_0^{(j)} = P^{(j)T} \begin{bmatrix} 0 & I \\ A^{(j)} + B^{(j)}K & -I \end{bmatrix} + \begin{bmatrix} 0 & I \\ A^{(j)} + B^{(j)}K & -I \end{bmatrix}^T P^{(j)}.$$

2.3 Quadratic Stabilization

LMIs of Lemma 2.1 are bilinear in P and K. In order to obtain LMIs we use P^{-1}. It is obvious from the requirement of $0 < P_1$, and the fact that in (6) $-(P_3 + P_3^T)$ must be negative definite, that P is nonsingular. Define

$$P^{-1} = Q = \begin{bmatrix} Q_1 & 0 \\ Q_2 & Q_3 \end{bmatrix} \quad \text{and} \quad \Delta = diag\{Q,\ I\} \tag{19}$$

Applying Schur formula to the term hR in (6a), we multiply (6a,b) by Δ^T and Δ, on the left and on the right, respectively. Denoting $\bar{R} = R^{-1}$ and $\bar{Z} = Q^T Z Q$ we obtain, similarly to [11], the following

Theorem 1. *The control law of (3) stabilizes (2) for all the samplings with the maximum sampling interval not greater than h and for all the system parameters that reside in the uncertainty polytope Ω, if there exist: $Q_1 > 0$, $Q_2^{(j)}$, $Q_3^{(j)}$, $\bar{R}$, $\bar{Z}_1^{(j)}$, $\bar{Z}_2^{(j)}$, $\bar{Z}_3^{(j)} \in \mathcal{R}^{n\times n}$, $\bar{Y} \in \mathcal{R}^{q\times n}$ that satisfy the following LMIs:*

$$\begin{bmatrix} Q_2^{(j)}+Q_2^{(j)T}+h\bar{Z}_1^{(j)} & \hat{\Xi}^{(j)} & hQ_2^{(j)T} \\ * & -Q_3^{(j)}-Q_3^{(j)T}+h\bar{Z}_3^{(j)} & hQ_3^{(j)T} \\ * & * & -h\bar{R} \end{bmatrix} < 0,$$

and nonlinear matrix inequalities

$$\begin{bmatrix} Q_1\bar{R}^{-1}Q_1 & 0 & \bar{Y}^TB^{(j)T} \\ * & \bar{Z}_1^{(j)} & \bar{Z}_2^{(j)} \\ * & * & \bar{Z}_3^{(j)} \end{bmatrix} \geq 0, \tag{20}$$

where

$$\hat{\Xi}^{(j)} = Q_3^{(j)} - Q_2^{(j)T} + Q_1A^{(j)T} + h\bar{Z}_2^{(j)} + \bar{Y}^TB^{(j)T}, \quad j = 1, 2, ..., N. \tag{21}$$

The state-feedback gain is then given by

$$K = \bar{Y}Q_1^{-1}. \tag{22}$$

For solving (20) there exist *two methods*. The *first* uses the assumption

$$\bar{R} = \epsilon Q_1, \quad \epsilon > 0, \tag{23}$$

and thus leads to $2N$ LMIs with tuning parameter ϵ:

$$\begin{bmatrix} Q_2^{(j)}+Q_2^{(j)T}+h\bar{Z}_1^{(j)} & \hat{\Xi}^{(j)} & hQ_2^{(j)T} \\ * & -Q_3^{(j)}-Q_3^{(j)T}+h\bar{Z}_3^{(j)} & hQ_3^{(j)T} \\ * & * & -\epsilon hQ_1 \end{bmatrix} < 0, \tag{24}$$

$$\begin{bmatrix} \epsilon Q_1 & 0 & \epsilon\bar{Y}^TB^{(j)T} \\ * & \bar{Z}_1^{(j)} & \bar{Z}_2^{(j)} \\ * & * & \bar{Z}_3^{(j)} \end{bmatrix} \geq 0, \tag{25}$$

where $\hat{\Xi}^{(j)}$ and j are given by (21).

Similarly to Corollary 2.2 we can show that if the system (2) is quadratically stabilizable by a continuous-time state-feedback (14), then for all small enough h the latter LMIs are feasible and the sampled-data state-feedback with the same gain stabilizes the system.

The *second* method for solving the matrix inequalities of Lemma 2.4 is based on the iterative algorithm developed recently by Gao and Wang (2003). This method is preferable in the cases of comparatively large h, since it leads to less conservative results. However it may take more computer time due to iterative

process. In the sequel we shall adopt the first method for solving the matrix inequalities of Lemma 2.4.

Example 1. We consider (2) with the following matrices:

$$A=\begin{bmatrix}1 & 0.5\\ 0 & -1\end{bmatrix},\quad B=\begin{bmatrix}1\\ -1\end{bmatrix}.$$

It is verified by using Theorem 2.4 that the system is stabilizable by a sampled-data state-feedback with the maximum sampling interval $h \leq 0.69$. Thus, for $h = 0.69$ the resulting $K = [-1.048 \;\; 0.2511]$ (with $\epsilon = 0.34$). Simulation results (for uniform samplings with the sampling interval less than 0.7) show that the closed-loop system is stable.

2.4 Parameter Dependent Stabilization

The requirement for the quadratic stabilization imposes a serious constraint on the solution, where the same matrices Q_1 should satisfy the matrix inequalities in all the vertices of the polytope. To alleviate this difficulty a parameter dependent solution with different matrices $Q_1^{(j)}$ was derived in [12] for the case of state delay. We modify the results of Corollary 4 of [12] for the case of input delay by assuming that $\bar{R} = \epsilon G_1$ and obtain

Theorem 2. *Consider the system (2) and assume that its parameters lie in the polytope $\bar{\Omega}$. The system is stabilized, over the entire polytope Ω, by the controller of (3), for all the samplings with the maximum sampling interval not greater than h, if for some tuning positive scalar parameters ϵ and α there exist $2n\times 2n$ matrices: Q_j, G_j and H_j, of the form*

$$Q_j=\begin{bmatrix}Q_1^{(j)} & 0\\ Q_2^{(j)} & Q_3^{(j)}\end{bmatrix},\; G_j=\begin{bmatrix}G_1 & 0\\ G_2^{(j)} & G_3^{(j)}\end{bmatrix},\; H_j=\begin{bmatrix}\alpha G_1 & 0\\ H_2^{(j)} & H_3^{(j)}\end{bmatrix}.$$

and $\bar{Z}_j$, $j = 1, ..., \bar{N}$, a $m\times n$ matrix $\bar{Y}$ and $n\times n$ matrix $\bar{R}$ that satisfy the following LMIs.

$$\begin{bmatrix} M_j & \begin{bmatrix}Q_2^{(j)T}\\ Q_3^{(j)T}\end{bmatrix} & Q_j^T-G_j^T+\bar{A}^{(j)}H_j+\begin{bmatrix}0\\ \alpha B^{(j)}\end{bmatrix}\begin{bmatrix}\bar{Y} & 0\end{bmatrix}\\ * & -\epsilon h^{-1}G_1 & 0\\ * & * & -H_j^T-H_j\end{bmatrix}<0 \tag{26a}$$

$$\begin{bmatrix}\epsilon G_1 & [0 \;\; \epsilon\bar{Y}^T B^{(j)T}]\\ * & \bar{Z}_j\end{bmatrix}>0,\quad j=1,...,\bar{N}. \tag{26b}$$

where

$$M_j=G_j^T\bar{A}^{(j)T}+\bar{A}^{(j)}G_j+\begin{bmatrix}\bar{Y}^T\\ 0\end{bmatrix}\begin{bmatrix}0 & B^{(j)T}\end{bmatrix}+\begin{bmatrix}0\\ B^{(j)}\end{bmatrix}\begin{bmatrix}\bar{Y} & 0\end{bmatrix}+h\bar{Z}_j,\;\; \bar{A}^{(j)}=\begin{bmatrix}0 & I\\ A^{(j)} & -I\end{bmatrix}.$$

The state-feedback gain that stabilizes the system over Ω is then given by $K = \bar{Y}G_1^{-1}$.

Example 2. We consider (2) with the following matrices taken from [10], where $h = 0$:

$$A = \begin{bmatrix} 0 & 1 \\ -1 + g_1 & -.5 \end{bmatrix}, \; B = \begin{bmatrix} -1 + g_2 \\ 1 \end{bmatrix}$$

and where $|g_1| \leq 0.53$ and $|g_2| \leq 1.7$. It was shown in [12] that the system is not quadratically stabilizable by continuous state-feedback (i.e. for $h = 0$). It is verified by using Theorem 2.5 that the system is stabilizable by a sampled-data state-feedback with the maximum sampling interval $h \leq 0.299$. Thus, for $h = 0.299$ the resulting $K = [0.0821 \quad -0.1487]$ (with $\epsilon = 3.56$ and $\alpha = 1.1$). Simulation results (see e.g. Fig.1 for the case of $g_1 = g_1(t) = 0.53 \sin t$, $g_2 = g_2(t) = 1.7 \cos t, t_{k+1} - t_k = 0.299 \; \forall k \geq 0$ and the initial condition $x(0) = [5 \quad -5]^T$) show that the resulting closed-loop solutions converge to origin.

3 Regional Stabilization by Sampled-Data Controller with Saturation

3.1 Problem Formulation

Consider the system (2) with the sampled-data control law (3) which is subject to the following amplitude constraints

$$|u_i(t)| \leq \bar{u}_i, \quad 0 < \bar{u}_i, \; i = 1, ..., m \tag{27}$$

Denote by $x(t, x(0))$ the state trajectory of (2) with the initial condition $x(0) \in R^n$. Then the domain of attraction of the origin of the closed-loop system (2), (3) is the set

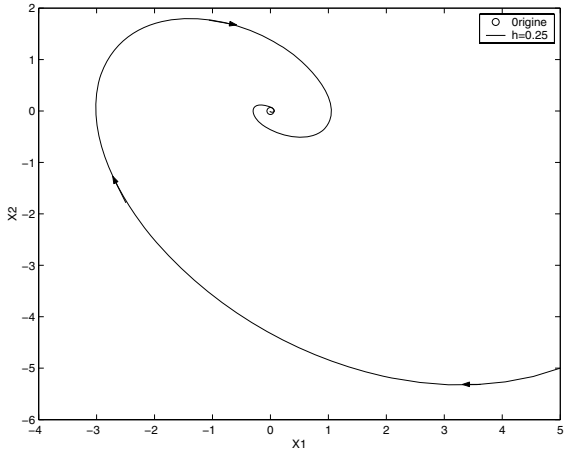

Fig. 1. State trajectories of the closed-loop system for $h = 0.299, g_1 = 0.53 \sin t$, $g_2 = 1.7 \cos t$ and $x(0) = [5 \quad -5]^T$

$$\mathcal{A} = \{x(0) \in R^n : \lim_{t\to\infty} x(t, x(0)) = 0\}.$$

We seek conditions for the existence of a gain matrix K which leads to a stable closed-loop. Having met these conditions, a simple procedure for finding the gain K should be presented. Moreover, we obtain an estimate $\mathcal{X}_\beta \subset \mathcal{A}$ on the domain of attraction, where

$$\mathcal{X}_\beta = \{x(0) \in R^n : x^T(0)P_1x(0) \le \beta^{-1}\}, \tag{28}$$

and where $\beta > 0$ is a scalar and $P_1 > 0$ is an $n \times n$ matrix.

We represent the state-feedback in the delayed form

$$u(t) = sat(Kx(t - \tau(t)), \bar{u}). \tag{29}$$

Reducing the original problem to the problem with input delay, we solve it by modifying derivations of [10], where the case of state delay was considered.

3.2 A Linear System Representation with Polytopic Type Uncertainty

Applying the control law of (29) the closed-loop system obtained is

$$\dot{x}(t) = Ax(t) + Bsat(Kx(t - \tau(t)),\ \bar{u}),\ \tau(t) = t - t_k,\ t_k \le t < t_{k+1}. \tag{30}$$

Though the closed-loop system has a delay, we keep in mind that in the case of sampled-data control the initial condition is defined in the point $t = 0$ and not on the segment $[-h, 0]$. That is why for the estimation of the domain of attraction we can restrict ourself to the following initial functions $\phi(s),\ s \in [-h, 0]$:

$$\phi(0) = x(0),\ \phi(s) = 0, s \in [-h, 0). \tag{31}$$

Denoting the i-th row by k_i, we define the polyhedron

$$\mathcal{L}(K, \bar{u}) = \{x \in \mathcal{R}^n\ : |k_i x| \le \bar{u}_i,\ i = 1, ..., m\}.$$

If the control and the disturbance are such that $x \in \mathcal{L}(K, \bar{u})$ then the system (30) admits the linear representation. Following [3], we denote the set of all diagonal matrices in $\mathcal{R}^{m\times m}$ with diagonal elements that are either 1 or 0 by Υ, then there are 2^m elements D_i in Υ, and for every $i = 1, ..., 2^m$ $D_i^- \stackrel{\Delta}{=} I_m - D_i$ is also an element in Υ.

Lemma 2. *[3] Given K and H in $\mathcal{R}^{m\times n}$. Then*

$$sat(Kx(t),\ \bar{u}) \in \mathcal{C}o\{D_iKx + D_i^-Hx,\ i = 1, ..., 2^m\}$$

for all $x \in \mathcal{R}^n$ that satisfy $|h_ix| \le \bar{u}_i,\ i = 1, ..., 2^m$.

The following is obtained from Lemma 3.1.

Lemma 3. *Given $\beta > 0$, assume that there exists H in $\mathcal{R}^{m\times n}$ such that $|h_i x| \leq \bar{u}_i$ for all $x(t) \in \mathcal{X}_\beta$. Then for $x(t) \in \mathcal{X}_\beta$ the system (30) admits the following representation.*

$$\dot{x}(t) = Ax(t) + \textstyle\sum_{j=1}^{2^m} \lambda_j(t) A_j x(t-\tau(t)) \tag{32}$$

where

$$A_j = B(D_j K + D_j^- H) \quad j = 1, ..., 2^m, \ \textstyle\sum_{j=1}^{2^m} \lambda_j(t) = 1, \ 0 \leq \lambda_j(t), \ \forall\, 0 < t, \tag{33}$$

We denote

$$\Omega_\alpha = \sum_{j=1}^{2^m} \lambda_j \Omega_j \quad \text{for all} \quad 0 \leq \lambda_j \leq 1, \ \sum_{j=1}^{2^m} \lambda_j = 1 \tag{34}$$

where the vertices of the polytope are described by $\Omega_j = \left[\, A_j \,\right], \quad j = 1, ..., 2^m$. The problem becomes one of finding $\mathcal{X}_\beta$ and a corresponding H such that $|h_i x| \leq \bar{u}_i, \ i = 1, ...2^m$ for all $x \in \mathcal{X}_\beta$ and that the state of the system

$$\dot{x}(t) = Ax(t) + A_j x(t-\tau(t)), \ \tau(t) = t - t_k, \ t_k \leq t < t_{k+1}, \tag{35}$$

remains in $\mathcal{X}_\beta$.

3.3 Regional Stabilization

Applying the descriptor model transformation and the Lyapunov-Krasovskii functional of (8) by using the first method for solving the stabilization matrix inequalities (with tuning parameter ϵ) , we obtain the following result:

Theorem 3. *Consider the system (2) with the sampled-data control law (3) which is subject to the constraints (27). The system is stable with $\mathcal{X}_\beta$ inside the domain of attraction for all the samplings with the maximum sampling interval not greater than h, if there exist $0 < Q_1$, $Q_2^{(j)}$, $Q_3^{(j)}, Z_1^{(j)}$, $Z_2^{(j)}$, $Z_3^{(j)} \in \mathcal{R}^{n\times n}$, Y, $G \in \mathcal{R}^{m\times n}$ and $\beta > 0$ that satisfy the following set of inequalities:*

$$\begin{bmatrix} Q_2^{(j)} + Q_2^{T(j)} + hZ_1^{(j)} & \Sigma_j & hQ_2^{(j)} \\ * & -Q_3^{(j)} - Q_3^{T(j)} + hZ_3^{(j)} & hQ_3^{(j)} \\ * & * & -\epsilon h Q_1 \end{bmatrix} < 0, \ j = 1, ..., 2^m \tag{36a}$$

$$\begin{bmatrix} \epsilon Q_1 & 0 & \epsilon(Y^T D_j + G^T D_j^-) B^T \\ * & Z_1^{(j)} & Z_2^{(j)} \\ * & * & Z_3^{(j)} \end{bmatrix} \geq 0 \tag{36b}$$

$$\begin{bmatrix} \beta & g_i \\ * & \bar{u}_i^2 Q_1 \end{bmatrix} \geq 0, \ i = 1, ..., m, \tag{37}$$

where

$$\Sigma_j = Q_3^{(j)} - Q_2^{T(j)} + Q_1 A^T + (Y^T D_j + G^T D_j^-) B^T + hZ_2^{(j)}. \tag{38}$$

The feedback gain matrix which stabilizes the system is given by $K = YQ_1^{-1}$.

Proof: For V given by (8) conditions are sought to ensure that $\dot{V} < 0$ for any $x(t) \in \mathcal{X}_\beta$. As in [10], the inequalities (37) guarantee that $|h_i x| \leq \bar{u}_i, \forall x \in \mathcal{X}_\beta,\ i = 1, ..., m$, where $g_i \stackrel{\Delta}{=} h_i Q_1,\ i = 1, ..., m$ and $Q_1 \stackrel{\Delta}{=} P_1^{-1}$, and the polytopic system representation of (35) is thus valid. Moreover, (36a,b) guarantee that $\dot{V} < 0$.

From $\dot{V} < 0$ it follows that $V(t) < V(0)$ and therefore for the initial conditions of the form (31)

$$x^T(t)P_1x(t) \leq V(t) < V(0) = x^T(0)P_1x(0) \leq \beta^{-1}. \tag{39}$$

Then for all initial values $x(0) \in \mathcal{X}_\beta$, the trajectories of $x(t)$ remain within $\mathcal{X}_\beta$, and the polytopic system representation (35) is valid. Hence $x(t)$ is a trajectory of the linear system (35) and $\dot{V} < 0$ along the trajectories of the latter system which implies that $\lim_{t\to\infty} x(t) = 0$.

Example 3. We consider (2) with the following matrices (taken from [3], where $h = 0$):

$$A = \begin{bmatrix} 1.1 & -0.6 \\ .5 & -1 \end{bmatrix}, \quad B_1 = \begin{bmatrix} 1 \\ 1 \end{bmatrix}$$

and where $\bar{u} = 5$. Applying Theorem 3.3 a stabilizing gain was obtained for all samplings with the maximum sampling interval $h \leq 0.75$. In order to 'enlarge' the volume of the ellipse we minimized the value of β (to improve the result we also added the inequality $Q_1 > \alpha I$ and chose such $\alpha > 0$ that enlarged the resulting ellipse). The ellipse volume increases when h decreases (see Figure 2). For, say, $h = 0.75$ we obtain $K = [-1.6964\ 0.5231]$ (with $\epsilon = 0.325$, $\beta = 0.1261, P_1 = \begin{bmatrix} 0.9132 & -0.2816 \\ -0.2816 & 0.0868 \end{bmatrix}, \alpha = 1$) and we show (see Figure 3) that a trajectory starting on

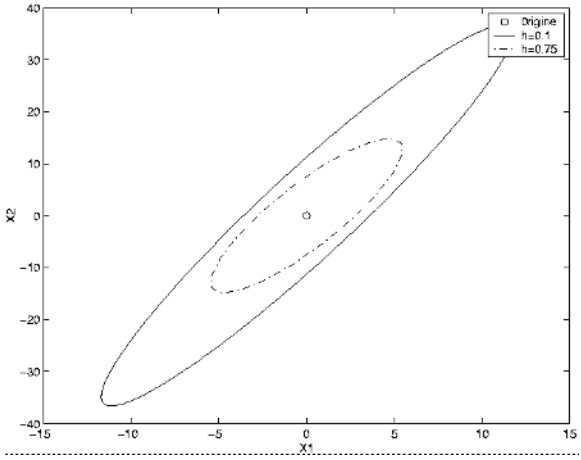

Fig. 2. Ellipsoidal bounds on the domain of attraction: line corresponds to $h = 0.1$; slash line to $h = 0.75$; point line to $h =$

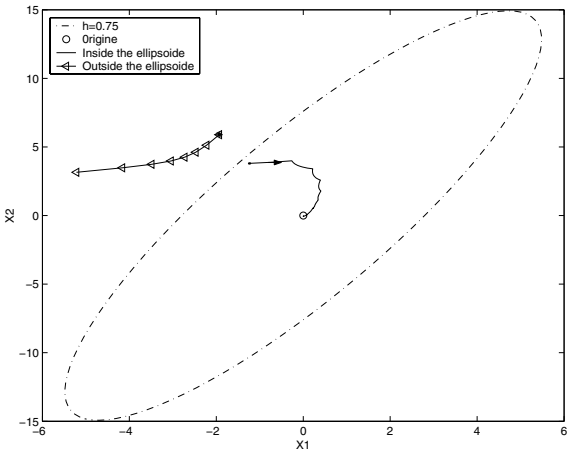

Fig. 3. Stabilization result for $h = 0.75$

the periphery of the ellipse (for the case of the uniform sampling with the sampling period $t_{k+1} - t_k = 0.75$) never leaves this ellipse and converges to the origin, while a trajectory starting not far from the ellipse remains outside the ellipse.

4 Conclusions

A new method for robust sampled-data stabilization of linear continuous-time systems is introduced. This method is based on the continuous-time model with time-varying input delay. Under assumption that the maximum sampling interval is not greater then $h > 0$, the h-dependent sufficient LMIs conditions for stabilization of systems with polytopic type uncertainty and for regional stabilization of systems with sampled-data saturated state-feedback are derived via descriptor system approach to time-delay systems.

The new approach solves the problems for comparatively small h and leads to sufficient conditions only, however these conditions are simple. The method may be applied to a wide spectrum of robust sampled-data control problems (e.g. to guaranteed cost or to $H_\infty control$).

References

1. Astrom K., Wittenmark B. (1989) *Adaptative Control.* Prentice Hall publisher, Upper Saddle River
2. Bamieh B., Pearson J., Francis B., Tannenbaum A. (1991) A lifting technique for linear periodic systems. System & Control Letters 17:79–88
3. Cao Y., Lin Z., Hu T. (2002) Stability analysis of linear time-delay systems subject to input saturation. IEEE Trans. on Circuits and Systems 49(2):233–240
4. Chen T., Francis B. (1991) h_2 optimal sampled-data control. IEEE Transactions on Automatic Control 36:387–397

5. Dambrine M., Richard J.-P., Borne P. (1995) Feedback control of time-delay systems with bounded control and state. Mathematical Problems in Engineering, 1:77–87
6. Dullerud G., Glover K. (1993) Robust stabilization of sampled-data systems to structured lti perturbations. IEEE Transactions on Automatic Control 38:1497–1508
7. Fridman E. (1992) Use of models with aftereffect in the problem of design of optimal digital control. Automation and Remote Control 53:1523–1528
8. Fridman E. New lyapunov-krasovskii functionals for stability of linear retarded and neutral type systems. System & Control Letters 43:309–319
9. Fridman E. Stability of linear descriptor systems with delay: A lyapunov-based approach. Journal of Mathematical Analysis and Applications 273(1):24–44
10. Fridman E., Pila A., Shaked U. (2003) Regional stabilization and control of time-delay systems with saturating actuators. International J. Robust Nonlinear Control 13(9):885–907
11. Fridman E., Shaked U. (2002) An improved stabilization method for linear time-delay systems. IEEE Trans. on Automatic Control 47(11):1931–1937
12. Fridman E., Shaked U. (2003) Parameter dependent stability and stabilization of uncertain time-delay systems. IEEE Transactions on Automatic Control 48(5):861–866
13. Gouaisbaut F., Dambrine M., Richard J.-P. (2002) Robust control of dealy systems: a sliding mode control design via lmi. Systems & Control Letters 46(4):219–230
14. Hale J., Lunel S. (1993) Introduction of functional differential equations. Springer-Verlag, Berlin Heidelberg New York
15. Kim J.H. (2001) Delay and its time-derivative dependent robust stability of time-delayed linear systems with uncertainty. IEEE Trans. on Automatic Control 46:789–792
16. Kolmanovskii V., Myshkis A. (1999) Applied theory of functional differential equations. Kluwer, Dordrecht
17. Kolmanovskii V., Niculescu S.I., Richard J.-P. (1999) On the lyapunov-krasovskii functionals for stability analysis of linear delay systems. Int. J. Control 72:374–384
18. Li X., de Souza C. (1997) Criteria for robust stability and stabilization of uncertain linear systems with state delay. Automatica 33:1657–1662
19. Mikheev Yu.V. , Sobolev V.A., Fridman E.M. (1988) Asymptotic analysis of digital control systems. Automation and Remote Control 49(9):1175–1180
20. Niculescu S.I. (2001) Delay effects on stability: A robust control approach. In Lecture Notes in Control and Information Sciences, Springer-Verlag, Berlin Heidelberg New York
21. Oishi Y. (1997) A bound of conservativeness in sampled-data robust stabilization and its dependence on sampling periods. Systems & Control Letters 32:11–19
22. Osborn S., Bernstein D. (1995) An exact treatement of the achievable closed-loop h_2-performance of sampled-data controllers: From continuous-time to open-loop. Automatica 31(4):617–620
23. Takaba K., Morihira N., Katayama T. (1995) A generalized lyapunov theorem for descriptor systems. Systems & Control Letters 24:49–51
24. Tarbouriech S., Gomes da Silva J. (2000) Synthesis of controllers for continuous-time delay systems with saturating controls via lmi's. IEEE transactions on Automatic Control 45(1):105–111
25. Trentelman H., Stoorvogel A. (1995) Sampled-data and discrete-time h^2 optimal control. J. Control and Optimization 33(3):834–862
26. Yamomoto Y. (1990) New approach to sampled-data control systems - a function space method. In Proc. 29th Conf. on Decision and Control, pp. 1882–1887, Honolulu, Haiwai

Stabilization and Finite-Gain Stabilizability of Delay Linear Systems Subject to Input Saturation

Karim Yakoubi and Yacine Chitour

Laboratoire des signaux et systèmes, Univ. Paris-Sud, CNRS, Supélec, 91192 Gif-sur-Yvette cedex, France
{karim.yakoubi,yacine.chitour}@lss.supelec.fr

Summary. This chapter deals with two problems on stabilization of linear systems by static feedbacks which are bounded and time-delayed, namely global asymptotic stabilization and finite gain L^p-stabilization, $p \in [1, \infty]$. Regarding the first issue, we provide, under standard necessary conditions, two types of solutions for arbitrary small bound on the control and large (constant) delay. The first solution is based on the knowledge of a static stabilizing feedback in the zero-delay case and the second solution is of nested saturation type, which extends results of [2]. For the finite-gain L^p-stabilization issue, we assume that the system is neutrally stable. We show the existence of a linear feedback such that, for arbitrary small bound on the control and large (constant) delay, finite gain L^p-stability holds with respect to every L^p-norm, $p \in [1, \infty]$. Moreover, we provide upper bounds for the corresponding L^p-gains which are delay-independent.

Keywords: Saturated feedback, Stabilization, Lyapunov functions, Time-delay systems, Linear continuous-time delay systems, Finite-gain stability.

1 Introduction

In this chapter, we address two issues relative to the stabilization for continuous-time delay linear systems subject to input saturation, of the type

$$(S) : \dot{x}(t) = Ax(t) + Bu(t-h), \tag{1}$$

where (i) $A \in \mathbb{R}^{n\times n}$ and $B \in \mathbb{R}^{n\times m}$, with n the dimension of the system and m the number of inputs; (ii) the control u verifies $\|u\| \leq r$, where $r \in (0, 1]$ only depends on (S); (iii) there is an arbitrary constant delay $h \geq 0$ appears in the input.

We use $(S)^r_h$, $r \in (0, 1]$, $h > 0$, to denote the control system (S) with input bound r and input time delay h. We omit the index r if it is equal to one and, similarly for the index h if it is equal to zero.

The first problem is that of globally asymptotically stabilizing (S) to the origin by mean of a static feedback. We then seek u as

$$u(t-h) = -r\sigma\left(F^r_h(x(t-h))\right), \tag{2}$$

J. Chiasson and J.J. Loiseau (Eds.): Appl. of Time Delay Systems, LNCIS 352, pp. 329–341, 2007.
springerlink.com

where the non-linearity σ is of "saturation" type (definitions are given in section (2)) and the function $F_h^r : \mathbb{R}^n \longrightarrow \mathbb{R}^m$ is at least locally Lipschitz (to obtain at least locally solutions).

In the zero–delay case, the stabilization of linear systems with saturating actuators has been widely investigated in the last years: static feedbacks of nested saturation type (see [11] and [12]) or based on maximal ellipsoid saturation (see [4]) can be used. It is well-known that such a global asymptotic stabilization is possible if and only if (S) satisfies

$$(C) : \begin{cases} (i) A \text{ is neutrally stable ,} \\ \\ (ii) \text{ the pair } (A, B) \text{ is stabilizable .} \end{cases}$$

It is trivial to see that condition (C) is also necessary in the case of non zero delay and it seems natural to expect condition (C) to be also sufficient. In that regard, partial results have been recently obtained by Mazenc, Mondie and Niculescu. To state the results, we define the unrestricted GAS property. We say that $(S)_h^r$ is unrestricted GAS if, for arbitrary delay $h > 0$ and any input rate $r \in (0, 1]$ small enough, $(S)_h^r$ is global asymptotic stabilizable. The nested saturation construction is used to show that $(S)_h^r$ is unrestricted GAS if A is nilpotent ([2]) and for the two-dimensional oscillator ([3]). One of our main results is to complete that line of work, namely to show that condition (C) is sufficient for unrestricted GAS.

We will actually provide two different ways to solve the GAS problem. The first one is based on the knowledge of a globally Lipschitz static stabilizing feedback F in the zero–delay case. From it, one can build a static stabilizing feedback for $(S)_{h^*}$, with $h^* > 0$ only depending on A, B, σ and K_F, the Lipschitz constant of F. If, in addition, an extra hypothesis holds on stabilizing feedbacks of $(S)^r$, for r small enough, unrestricted GAS holds. It turns out that the nested saturated feedbacks of [11] verify these hypotheses, and thus we conclude, see [14].

The second solution for unrestricted GAS directly uses the nested saturated feedbacks of [11] and can be seen as a generalization of [2, 3]. However, the argument is an extension to the non-zero delay case of that of [11]. Recall that, at the heart of the argument of [11], lies a result on finite-gain L^∞-stability for one and two dimensional neutrally stable linear systems subject to input saturation. Such an argument was first introduced in [1], where was addressed the issue of finite-gain L^p-stability of neutrally stable linear systems subject to input saturation.

It is therefore natural to consider the L^p-stability question. We extend to the non-zero delay cases results of [1]. Our objective here consists in showing that the results of [1] carry over to continuous linear time-delay systems. More specifically, we show that, for neutrally stable continuous linear time-delay systems subject to input saturation, finite-gain L^p-stabilization can be achieved by the use of linear feedbacks, for every $p \in [1, \infty]$. While many of the arguments of the present paper are conceptually similar to those of [1], there are technical aspects that are different and not obvious. Indeed, as in [1], the proof to get finite gain

L^p-stability relies on passivity techniques. We determine a suitable "storage" function V_p and establish for it a "dissipation inequality" of the form $\frac{dV_p(x_u(t))}{dt} \leq -\|x_u(t)\|^p + \lambda_p\|u(t)\|^p$, for some constant $\lambda_p > 0$ possibly depending on the input bound r and the delay h. For more discussion on passivity, see [13] for instance. Recall that the "storage function" in [1], V_p^0 is non-smooth. In the present situation, the "storage function" V_p will be the sum of a term similar to V_p^0 and a Lyapunov-Krasovskii functional, in order to take care of the delay. However, unlike in [1], the saturation in (1) needs to be multiplied by a small factor r dependent on the delay h in order to insure finite-gain L^p-stability. In addition, by choosing carefully the factor r and the linear feedback inside the saturation, we are able to provide upper bounds for the L^p-gains of $(S)_h^r$ which are *independent* of $r \in (0, 1]$ and $h > 0$. We refer to that property as the *unrestricted finite-gain L^p-stability*.

The argument corresponding to that uniformity result is specific to the non-zero delay case and constitutes the most technical part of [15]. To establish it, we first start with the single-input case where it amounts in estimating the behavior of the solution P_r of a parameterized Lyapunov equation (L_r), $r \in (0, 1]$, as the parameter r tends to zero. The multi-input case requires additional work. We first rewrite the original system as an appropriate cascade of single-input subsystems, all of them except one being perturbed by an external disturbance, appearing outside the saturation (see Theorem 5). We then proceed by an inductive argument on the number of distinct algebraic multiplicities of the eigenvalues of A.

Generally speaking, our treatment of the aforementioned issues on time-delay systems follows a common pattern. We always try to reformulate them as problems for perturbed *delay-free* systems and handle the perturbation by Lyapunov techniques. One of the reasons for which that strategy works well lies in the fact that the input saturation makes the perturbation uniformly bounded with respect to the delay.

The complete proofs of the results presented in this chapter are contained in [14] for stabilization and [15] for finite-gain stabilizability.

2 Notations and Statement of the Main Results

2.1 Notations

For $x \in \mathbb{R}^n$, $\|x\|$ and x^T denote respectively the Euclidean norm of x and the transpose of x. Similarly, for any $n \times m$ matrix K, K^T and $\|K\|$ denote respectively the transpose of K and the induced $2-$norm of K. Moreover, $\lambda_{\min}(K)$ and $\lambda_{\max}(K)$ denote the minimal and the maximal singular values of the matrix K. If $f(.)$ and $g(.)$ are two real-valued functions, we mean by $f(r) \asymp_0 g(r)$, that there are positive constants ξ_1 and ξ_2 independent of r small enough, such that the inequalities

$$\xi_1 g(r) \leq f(r) \leq \xi_2 g(r),$$

are valid. Initial conditions for delayed systems are continuous vectors-valued functions defined on $[-h, 0]$ and taking values in $\mathbb{R}^n$. For $h > 0$, let $C_h := C([-h, 0], \mathbb{R}^n)$; $x_t(\theta) := x(t + \theta)$, for $-h \leq \theta \leq 0$ and $\|x_t\|_h := \sup_{-h\leq\theta\leq 0} \|x(t + \theta)\|$.

Definition 1. *(Saturation function) We call $\sigma : \mathbb{R} \longrightarrow \mathbb{R}$ a saturation function ("S-function" for short) if there exist two real numbers $0 < a \leq K_\sigma$ such that for all $t, t' \in \mathbb{R}$*

(i) $|\sigma(t) - \sigma(t')| \leq K_\sigma \inf(1, |t - t'|)$,
(ii) $|\sigma(t) - at| \leq K_\sigma t\sigma(t)$.
(iii) $\sigma(t) = t$ *when* $|t| \leq a$.

It is assumed here that the function is normalized at the origin, i.e. $a = \sigma'(0) = 1$. The global lipschitzness of σ implies that for every real numbers x, y,

$$|x[\sigma(x + y) - \sigma(x)]| \leq K|y|.$$

For an $m-$tuple $k = (k_1, \ldots, k_m)$ of nonnegative integers, define $|k| = k_1 + \ldots + k_m$. We say that σ is an $\mathbb{R}^{|k|}-$ valued S-function if

$$\sigma = (\sigma_1, \ldots, \sigma_{|k|}) = (\sigma_1^1, \ldots, \sigma_{k_1}^1, \ldots, \sigma_1^m, \ldots, \sigma_{k_m}^m)$$

$$= \left((\sigma_i^1)_{1\leq i\leq k_1}, (\sigma_i^2)_{1\leq i\leq k_2}, \ldots, (\sigma_i^m)_{1\leq i\leq k_m}\right),$$

where, for $1 \leq j \leq m$, $(\sigma_i^j)_{1\leq i\leq k_j}$ is an $\mathbb{R}^{k_j}$-valued S-function ($i.e : (\sigma_i^j)_{1\leq i\leq k_j} = (\sigma_1^j, \ldots, \sigma_{k_j}^j)$ where each component $\sigma_i^j, 1 \leq i \leq k_j$ is an S-function and

$$(\sigma_i^j)_{1\leq i\leq k_j}(x) = \left(\sigma_1^j(x_1), \ldots, \sigma_{k_j}^j(x_{k_j})\right),$$

for $x = (x_1, \ldots, x_{k_j})^T \in \mathbb{R}^{k_j}$. Here we use $(\ldots)^T$ to denote the transpose of the vector $(\ldots)$.)

Definition 2. *Consider the functional differential equation of retarded type*

$$(\Sigma)_h : \begin{cases} \dot{x}(t) = f(x_t), \text{ for } t \geq t_0; \\ \\ x_{t_0}(\theta) = \Psi(\theta), \forall\theta \in [-h, 0]. \end{cases}$$

It is assumed that $\Psi \in C_h$, the map f is continuous and Lipschitz in Ψ and $f(0) = 0$. We say that $(\Sigma)_h$ is globally asymptotically stable (GAS for short) if the following conditions hold:

(i) for every $\varepsilon > 0$, there exists a $\delta > 0$ such that, for any $\Psi \in C_h$, with $\|\Psi\|_h \leq \delta$, there exists $t_0 \geq 0$, such that the solution $x(\Psi)$ of $(\Sigma)_h$ satisfies $\|x_t(\Psi)\|_h \leq \varepsilon$, for all $t \geq t_0$;

(ii) for all $\Psi \in C_h$, the trajectory of $(\Sigma)_h$ with the initial condition Ψ and defined on $[t_0, \infty)$ converges to zero as $t \to \infty$.

2.2 GAS Using a Stabilizing Feedback in the Zero Delay Case

Our objective is to relate the asymptotic stability properties of the system (S) with those of the delay-free system provided that it is globally asymptotically stable. The study is then extended to investigate conditions which ensure that the class of linear controllers, stabilizing the delay-free system, also stabilize (S) by stating the problem as an asymptotic stability problem. For this purpose, the delayed system (S) is considered as a perturbation of that of the delay-free system. We now state our first result.

Theorem 1. *Assume* $(\mathbf{H})_{\mathbf{0}}$: *There exists* $F : \mathbb{R}^n \longrightarrow \mathbb{R}^m$ *globally Lipschitz, with Lipschitz constant* K_F *such that the system*

$$(S)_0 : \quad \dot{x} = Ax - B\sigma(F(x)),$$

is globally asymptotically stable with respect to 0.
Then, there exists $h^* = h(A, B, \sigma, K_F) > 0$ *such that, for all* $h \in [0, h^*]$, *there exists* $F_h : \mathbb{R}^n \longrightarrow \mathbb{R}^m$ *that globally asymptotically stabilizes the system*

$$(S)_h : \dot{x} = Ax - B\sigma(F_h(x(t-h))),$$

with respect to zero.

Sketch of proof. Let $F_h(x(t)) = F(\Phi(t, t-h, x(t)))$, where Φ is the flow of the equation $(S)_0$. We rewrite $(S)_h$ as $\dot{x}(t) = Ax(t) - B\sigma(F(x(t))) - B\varepsilon(t)$, where $\varepsilon(t)$ as a perturbation of $(S)_0$. The perturbation ε may cause instability but we show that $\|\varepsilon(x(t))\| \leq \tilde{K}e^{-\lambda t}$ for some $\tilde{K}$ (that may depend on ε) and $t \geq 0$. Using Lemma 3.1 in [6], we are able to conclude.

The second result completes the stability result of Theorem 1 to get unrestricted global asymptotic stability (unrestricted GAS). It is stated as follows:

Theorem 2. *Assume* $(\mathbf{H})_{\mathbf{0}}^{\mathbf{r}}$: *For each* $r \in]0, 1]$, *there exists a globally Lipschitz function* $F^r : \mathbb{R}^n \longrightarrow \mathbb{R}^m$, *with Lipschitz constant* K_{F^r}, *such that*

(i) $\quad (S)_0^r : \quad \dot{x} = Ax - rB\sigma(F^r(x))$, is GAS with respect to zero ,

(ii) $\quad rK_{F^r} \to 0$ if $r \to 0$.

Then, for all $h \geq 0$, *there exists* $r^*(h) \in]0, 1]$, *such that for any* $r \in]0, r^*(h)]$, *a function* $F_h^r : \mathbb{R}^n \longrightarrow \mathbb{R}^m$ *exists for which the system*

$$(S)_h^r : \quad \dot{x} = Ax - rB\sigma(F_h^r(x(t-h))),$$

is globally asymptotically stable with respect to zero.

2.3 Feedbacks of Nested Saturation Type

We next determine two explicit expressions of globally asymptotically stabilizing feedbacks for general time-delay linear systems, both of nested saturation type,

according to the results of the stabilization of delay free-system. The above problem was first studied for delay-free continuous-time systems. It was shown in [11] that, under condition (C), there exists explicit expressions of globally asymptotically stabilizing feedbacks. Then, it is natural to investigate whether this technique can be extended to the case where there is a delay in the input. In this section, we will take for simplicity the initial state to be zero. We start by giving some definitions, first introduced in [11] and adapted here to the delay case.

Definition 3. *For a retarded system $\dot{x}(t) = f(x(t), u(t-h)), x \in \mathbb{R}^n, u \in \mathbb{R}^m$, we say that a feedback $u(.) = k(x(.))$ is stabilizing if zero is a globally asymptotically stable equilibrium of the system $\dot{x}(t) = f(x(t), k(x((t-h)))$.*

Definition 4. *(cf. [11]) For a square matrix A, let $N(A) = s(A) + z(A)$, where $s(A)$ is the number of conjugate pairs of nonzero purely imaginary eigenvalues of A (counting multiplicity) and $z(A)$ is the multiplicity of zero as an eigenvalue of A.*

Theorem 3. *Assume that condition (C) holds for $(S)^r_h$. Let $N = N(A)$ and $\sigma = (\sigma_1, \ldots, \sigma_N)$ be an arbitrary sequence of S-functions. Then, for all $h > 0$, there exist a number $r^*(h) \in (0, 1]$, an $m-$tuple $k = (k_1, \ldots, k_m)$ of non negative integers such that $|k| = N$ and for each $1 \leq j \leq m$, linear functions $f^j_{h,i}, g^j_{h,i} : \mathbb{R}^n \longrightarrow \mathbb{R}, 1 \leq i \leq k_j$, such that for all $r \in (0, r^*(h)]$, there are stabilizing feedbacks*

$$\begin{aligned}(*)\quad u_j(t-h) = -r\sigma^j_{k_j}\{f^j_{h,k_j}(x(t-h)) + \alpha^j_{k_j-1}\sigma^j_{k_j-1}[f^j_{h,k_j-1}(x(t-h)) + \\ + \ldots + \alpha^j_1\sigma^j_1(f^j_{h,1}(x(t-h)))\ldots]\},\end{aligned} \tag{3}$$

where $\alpha^j_i \geq 0$, for all $i \in [1, k_j - 1]$, and

$$\begin{aligned}(**)\ u_j(t-h) = -r\Big[\beta^j_{k_j}\sigma^j_{k_j}\Big(g^j_{h,k_j}(x(t-h))\Big) + \beta^j_{k_j-1}\sigma^j_{k_j-1}\Big(g^j_{h,k_j-1}(x(t-h))\Big) + \\ + \ldots + \beta^j_1\sigma^j_1\Big(g^j_{h,1}(x(t-h))\Big)\Big],\end{aligned} \tag{4}$$

where $\beta^j_1, \ldots, \beta^j_{k_j}$ are nonnegative constants such that $\beta^j_1 + \ldots + \beta^j_{k_j} \leq 1$.

Sketch of proof. The argument of proof follows the strategy of the principal result of [11]. We start therefore with the single-input case and prove the theorem by induction on the dimension of the system. In order to facilitate the analysis of the stabilizability properties by bounded feedback of $(S)^r_h$, a linear transformation is carried out in [11].

Lemma 1. *(cf. [11]) Let $(S_1)^r_h : \dot{x}(t) = Ax(t) + bu(t-h)$ be an n-dimensional linear single-input system. Suppose that (A, b) is a controllable pair and all eigenvalues of A are critical.*

(i) If 0 is an eigenvalue of A, then there exists a linear coordinate transformation $y = Sx$ which transforms $(S_1)^r_h$ into

$$\begin{cases} \dot{\bar{y}}(t) = A_1 \bar{y}(t) + (y_n(t) + u(t-h))\, b_1, \\ \dot{y}_n(t) = u(t-h), \end{cases} \tag{5}$$

where the pair (A_1, b_1) *is controllable,* y_n *is a scalar variable, and* $\bar{y} = (y_1, \ldots, y_{n-1})^T$.

(ii) If A *has an eigenvalue of the form* $i\omega$*, with* $\omega > 0$*, then there is a linear change of coordinates* $Sx = (y_1, \ldots, y_n)^T = (\bar{y}^T, y_{n-1}, y_n)^T$ *of* $\mathbb{R}^n$ *that puts* $(S_1)_h^r$ *in the form:*

$$\begin{cases} \dot{\bar{y}}(t) = A_1 \bar{y}(t) + (y_n(t) + u(t-h))\, b_1, \\ \dot{y}_{n-1}(t) = \omega y_n(t), \\ \dot{y}_n(t) = -\omega y_{n-1}(t) + u(t-h), \end{cases} \tag{6}$$

where the pair (A_1, b_1) *is controllable and* y_{n-1}, y_n *are scalar variables.*

The following lemma is the key technical point of the proof.

Lemma 2. *Let* $\rho > 0$ *and* σ *be an S-function. Then, for all* $h > 0$ *there exist* $r^*(h) \in]0, 1]$ *and an* 2×1 *matrix* F_h *such that, for any two bounded measurable functions* $\alpha(t), \beta(t)$ *converges both to zero as* $t \longrightarrow \infty$ *and for all* $r \in]0, r^*(h)]$*, the control system*

$$(S_2)_h^r : \begin{cases} \dot{x}_1(t) = \rho x_2(t) + r\alpha(t), \\ \dot{x}_2(t) = -\rho x_1(t) - r\sigma(F_h^T x(t-h) + u(t-h)) + rv(t-h) + r\beta(t), \\ x_0 = ((x_1)_0, (x_2)_0)^T = \bar{0}, \text{ on } [-h, 0], \end{cases}$$

with $\bar{0}$ *the zero function in* C_h*, and* $u, v \in L^\infty([-h, \infty), \mathbb{R})$*, with* $\|v\|_{L^\infty} \leq v^*$*,* ($v^*$ *independent of* r) *verifies:*

(i) There exists a finite constant $M_\infty > 0$ *independent of* r*, such that*

$$\limsup_{t \to \infty} \|x(t)\| \leq M_\infty \left(\|u\|_{L^\infty} + \|v\|_{L^\infty} + \|f\|_{L^\infty} \right), \tag{7}$$

where $x = (x_1, x_2)^T$, $f = (\alpha, \beta)^T$.

(ii) In the absence of u, v *and* f*, the equilibrium* $(x, y) = (0, 0)$ *is globally asymptotically stable.*

Sketch of proof. We consider the linear feedback $F_h = e^{-\rho A_0 h} b$, where $A_0 = \begin{pmatrix} 0 & 1 \\ -1 & 0 \end{pmatrix}$ and $b = (0, 1)^T$. The argument here is the simplest case of the more general result given in Proposition 1 for the single input case, see the corresponding sketch of proof below. More precisely, it corresponds to $p = 2$, $A = A_0$ and b is defined above. Note that in this case, the matrix P_r can be computed explicitly as well as $\lambda_{\max}(P_r)$ and $\lambda_{\min}(P_r)$.

2.4 Finite Gain Stabilizability

Finite-gain stability results for various $p-$norms are presented. We start with definitions.

L^p-Stability. For $p \in [1,\infty]$ and $0 \leq h$, we use L^p to denote $L^p(-h,\infty)$ and we let $\|y\|_{L^p}$ denote the L^p-norm: $\|y\|_{L^p} = \left(\int_{-h}^{\infty} \|y(t)\|^p dt\right)^{\frac{1}{p}}$, if $p < \infty$ and $\|y\|_{L^\infty} = ess\sup_{-h\leq t<\infty} \|y(t)\|$.

Consider the control system with delay in the input given by

$$(\Sigma)_h : \dot{x}(t) = f(x(t), u(t-h)), \text{ for } t \geq 0,$$

where the state x and the control u take respectively values in $\mathbb{R}^n$ and $\mathbb{R}^m$ and $f : \mathbb{R}^n \times \mathbb{R}^m \to \mathbb{R}^n$, is locally Lipschitz in (x,u), with $f(0,0) = 0$. Trajectories of $(\Sigma)_h$ starting at an initial condition $x_0 \in C_h$ and corresponding to an input $u \in L^p$ are defined for a time interval I of $\mathbb{R}^+$ (which may depend on x_0 and u) and verify the equation $(\Sigma)_h$ for almost every $t \in I$. Let $\bar{0}$ be the zero function in C_h.

Definition 5. *(L^p-stability): Given $p \in [1,\infty]$, the continuous-time delay system $(\Sigma)_h$ is said to be L^p-stable if, for every $u \in L^p$, we have $x_u \in L^p$, where x_u denotes the solution of $(\Sigma)_h$ corresponding to u with initial condition $x_0 = \bar{0}$.*

Definition 6. *(Finite-gain L^p- stability) : Given $p \in [1,\infty]$, the continuous-time delay system $(\Sigma)_h$ is said to be finite-gain L^p-stable if it is L^p-stable, and there exists a positive constant M_p such that, for every $u \in L^p$,*

$$\|x_u\|_{L^p} \leq M_p \|u\|_{L^p}.$$

Furthermore, the infimum of such numbers M_p will be called the L^p-gain of the system.

We next give our main results.

Theorem 4. *Let A, B be $n \times n, n \times m$ matrices respectively. Let σ be an $\mathbb{R}^m-$valued $S-$function. Assume that A be neutrally stable and (A,B) controllable. Then, for every $h \geq 0$, there exists an $n \times m$ matrix F_h such that the system,*

$$(S)_h^r : \dot{x} = Ax - rB\sigma(F_h^T x(t-h) + u(t-h)), \text{ for } t \geq 0,$$

has the unrestricted finite gain L^p-stability property for every $p \in [1,\infty]$, i.e., for every $h > 0$, there exists $r^*(h) \in (0,1]$ such that for every $p \in [1,\infty]$, $(S)_h^r$, $r \in (0, r^*(h)]$, is finite-gain L^p-stable.

Remark 1. In the absence of u, the equilibrium point $\bar{0}$ is globally asymptotically stable for the delayed system $\dot{x}(t) = Ax(t) - rB\sigma(F_h^T x(t-h))$.

Theorem 4 is a particular case of a stronger result given next.

Theorem 5. *With the same hypothesis on A, B and σ, consider the following delayed system (still denoted $(S)_h^r$)*

$$(S)_h^r : \dot{x}(t) = Ax(t) - rB\sigma\left(F_h^T x(t-h) + u_1(t-h)\right) + ru_2(t-h), \text{ for } t \geq 0,$$

where F_h is defined as in Theorem 4 and the input u_2 takes values in $\mathbb{R}^n$. then, there exist a constant $C_0 > 0$ and, for every $1 \leq p \leq \infty$, a constant $M_p > 0$ such that, for every $h > 0$ there is an $r^*(h) \in (0, 1]$, for which the trajectories x_{u_1,u_2} of $(S)_h^r$, $r \in (0, r^*(h)]$, starting at $\bar{0}$ and corresponding to $u_1, u_2 \in L^p$ with $\|u_2\|_{L^\infty} \leq C_0$, verify

$$\|x_{u_1,u_2}\|_{L^p} \leq M_p \left(\|u_1\|_{L^p} + \|u_2\|_{L^p}\right). \tag{8}$$

Remark 2. It will be clear from our argument that we can in fact obtain the following stronger Input-To-State-Stable (ISS for short)-like property ([9] and references there):

$$\|x^{\psi}_{u_1,u_2}\|_{L^p} \leq \theta_p(\|\psi\|_h) + M_p(\|u_1\|_{L^p} + \|u_2\|_{L^p}), \tag{9}$$

where $\psi \in C_h$ is the initial condition for the trajectory $x^{\psi}_{u_1,u_2}$ corresponding to u_1, u_2 and θ_p is a $\mathcal{K}$-function (i.e. $\theta_p : \mathbb{R}_+ \to \mathbb{R}_+$, is continuous, strictly increasing and satisfies $\theta_p(0) = 0$.).

Sketch of proof of Theorem 5. From elementary linear algebra, a neutrally stable matrix A is similar to a matrix $\begin{pmatrix} A_1 & 0 \\ 0 & A_2 \end{pmatrix}$, where A_1 is an $q \times q$ Hurwitz matrix and A_2 is an $(n-q) \times (n-q)$ skew-symmetric matrix. So, up to a change of coordinates, we may assume that A is already in this form. In this coordinates, we write $B = (B_1^T \ B_2^T)^T$, where B_2 is an $(n-q) \times m$ matrix and we write vectors as $x = (x_1^T, x_2^T)^T$ and $u_2 = (u_{21}^T, u_{22}^T)^T$.

For $r \in (0, 1]$ and $h > 0$, consider the feedback law $(0, F_h^T)$. Then system $(S)_h^r$, with this choice of F_h^T, can be written as

$$\begin{cases} \dot{x}_1(t) = A_1 x_1(t) - rB_1\sigma(F_h^T x_2(t-h) + u_1(t-h)) + ru_{21}(t-h), \\ \dot{x}_2(t) = A_2 x_2(t) - rB_2\sigma(F_h^T x_2(t-h) + u_1(t-h)) + ru_{22}(t-h). \end{cases}$$

Since A_1 is Hurwitz, it will be sufficient to show that there exists an $r^*(h) \in (0, 1]$, such that the x_2- subsystem is finite gain L^p-stable, for all $r \in (0, r^*(h)]$.

The controllability assumption on (A, B) implies that the pair (A_2, B_2) is also controllable. Therefore, the theorem is a consequence of the following proposition.

Proposition 1. *Let σ, u_1, u_2 be as in Theorem 5. Let (A, B) a controllable pair with A skew-symmetric. Then, for every $h \geq 0$, there exist an $n \times m$ matrix F_h and $r^*(h) \in (0, 1]$, such that, for every $r \in (0, r^*(h)]$, the system*

$$(S)_h^r : \dot{x}(t) = Ax(t) - rB\sigma[F_h^T x(t-h) + u_1(t-h)] + ru_2(t-h), \text{ for } t \geq 0,$$

verifies the conclusion of Theorem 5.

Sketch of proof. We start the proof by zooming on the single-input case. The general proof first starts with algebraic transformations and proceeds by induction on the number of distinct algebraic multiplicities of the eigenvalues of A.

1) The single-input case: The principal idea is to rephrase the delay systems as problems for perturbed delay-free systems and handle the perturbation by Lyapunov techniques. For this, Let $h > 0$ and consider y the solution of

$$\begin{cases} \dot{y}(t) = (A - rbb^T)y(t) + ru_2(t-h), \text{ for } t \geq 0, \\ y_0 = \bar{0}, \quad \text{on } [-h, 0]. \end{cases} \tag{10}$$

Since A is skew-symmetric, the matrix $A_r := A - rbb^T$ is Hurwitz for every $r > 0$. Then (10) is L^p-stable for any $1 \leq p \leq \infty$. Let γ_p be it is L^p-gain, so $\|y\|_{L^p} \leq \gamma_p \|u_2\|_{L^p}$.

Let x be the solution of $(S)_h^r$ starting at $\bar{0} \in C_h$ and corresponding to u_1, u_2. Set $z := x - y$. Then, z satisfies, for $t \geq 0$,

$$\begin{cases} \dot{z}(t) = Az(t) - rb\left[\sigma\left(F_h^T z(t-h) + \tilde{u}(t-h)\right) - \tilde{v}(t)\right], \\ z_0 = \bar{0}, \quad \text{on } [-h, 0]. \end{cases} \tag{11}$$

where $\tilde{u}(t-h) = F_h^T y(t-h) + u_1(t-h)$ and $\tilde{v}(t) = b^T y(t)$. From (11), we have

$$z(t) = e^{Ah} z(t-h) - r \int_{t-h}^{t} e^{A(t-\xi)} b[\sigma(F_h^T z(\xi - h) + \tilde{u}(\xi - h)) - \tilde{v}(\xi)] d\xi.$$

Then,

$$F_h^T z(t-h) + \tilde{u}(t-h) = b^T z(t) + \tilde{d}(t),$$

where

$$\tilde{d}(t) = \tilde{u}(t-h) + r \int_{t-h}^{t} b^T e^{A(t-\xi)} b[\sigma(F_h^T z(\xi - h) + \tilde{u}(\xi - h)) - \tilde{v}(\xi)] d\xi.$$

Consider the Lyapunov function defined by

$$V_{p,r}(t, z) := \lambda_{p,r} \frac{\|z(t)\|^{p+1}}{p+1} + (z^T(t) P_r z(t))^{\frac{p}{2}} + \mu_{p,r} \int_{t-2h}^{t} (\int_{s}^{t} \|z(l)\|^p dl) ds,$$

where P_r is the unique positive-definite solution to the Lyapunov equation

$$X(A - rbb^T) + (A - rbb^T)^T X = -Id_n.$$

The appropriate choice of $\lambda_{p,r}$ and $\mu_{p,r}$ requires careful estimates on P_r as r tends to zero.

We need the next lemma (in order to show ultimately the independence of M_p with respect the parameters r and h).

Lemma 3. *Let A and b be as in Proposition 1. Then, the following properties hold.*

There exists a $r^* \in (0,1]$ such that for all $t \geq 0$,

$$C_1' e^{-C_2' r t} \leq ||e^{(A-rbb^T)t}|| \leq C_1 e^{-C_2 r t}, \quad \forall r \in (0, r^*], \tag{12}$$

for some positive constants C_1, C_1', C_2 and C_2' independent of r, and

$$\lambda_{\max}(P_r) \asymp_0 \lambda_{\min}(P_r) \asymp_0 \frac{1}{r}. \tag{13}$$

We determine a dissipation inequality for $V_{p,r}$, i.e., we take the time derivative of $V_{p,r}(t, x(t))$ along trajectories of $(S)_h^r$. After some computation we get

$$\begin{aligned} \dot{V}_{p,r}(z(t)) \leq & -C_1(r)\|z(t)\|^p + C_2(r)\|z(t)\|^{p-1}[\|\tilde{u}(t-h)\| + \|\tilde{v}(t)\| + \\ & + rC_3 \int_{t-h}^{t} (\|\tilde{u}(\xi - h)\| + \|\tilde{v}(\xi)\|)\, d\xi], \end{aligned} \tag{14}$$

where $C_1(r)$, $C_2(r)$ and C_3 denote constants that are dependent and independent of r. For every $t \geq 0$, integrating (14) from 0 to t and applying Hölder's inequality, we get

$$V_p(z(t)) + C_1(r)\|z\|^p_{L^p[0,t]} \leq (1 + rhC_3)C_2(r)\|z\|^{p-1}_{L^p[0,t]} \times (\|\tilde{u}\|_{L^p} + \|\tilde{v}\|_{L^p}). \tag{15}$$

Since $V_{p,r} \geq 0$ and

$$\begin{cases} \|\tilde{v}\|_{L^p} \leq \|b\|\|y\|_{L^p} \leq \gamma_p \|b\|\|u_2\|_{L^p}, \\ \|\tilde{u}\|_{L^p} \leq \|u_1\|_{L^p} + \gamma_p \|b\|\|u_2\|_{L^p}, \\ \|z\|_{L^p} \geq \|x\|_{L^p} - \|y\|_{L^p} \geq \|x\|_{L^p} - \gamma_p \|u_2\|_{L^p}, \end{cases}$$

we get that $x \in L^p([0,\infty), \mathbb{R}^n)$ and

$$\|x\|_{L^p} \leq M_p(\|u_1\|_{L^p} + \|u_2\|_{L^p}), \tag{16}$$

where

$$M_p = \max\{\frac{C_2(r)}{C_1(r)}(1 + rhC_3), \gamma_p \left[1 + 2\|b\|\frac{C_2(r)}{C_1(r)}(1 + rhC_3)\right]\}. \tag{17}$$

A careful computation shows that

$$\frac{C_2(r)}{C_1(r)} \asymp_0 (\frac{\lambda_{\max}(P_r)}{\lambda_{\min}(P_r)})^{|\frac{p}{2}-1|} \asymp_0 1, \tag{18}$$

thanks to Lemma 3 and by choosing $rh \leq 1$. In that way, upper bound for the L^p-gain M_p is delay-independent.

2) The general case: Complete details of the argument of this case are given in [15].

Remark 3. In the single input case ($m = 1$), F_h can be chosen as $e^{-Ah}B$, which corresponds, up to the delay h, to the linear feedback law suggested by the passivity approach and used in [1]. A simple adaptation of the proof to the multi-input case shows that such a feedback can also be used to get L^p-stability but the corresponding L^p-gain is delay-independent only for single-input systems. The difference between the single and the multi-input case shows up in (13). In the multi-input case, there are n eigenvalues of $A_r = A - rBB^T$, $\lambda_1(r), \ldots, \lambda_n(r)$, defining continuous functions, which are not analytic in general. These functions, though, can be written as Puiseux series (cf. [7]),

$$\lambda_i(r) = \lambda_i(0) + \sum_{j=1}^{\infty} \alpha_j^{(i)} r^{\frac{j}{p_i}},$$

where $\lambda_i(0)$ is a root of multiplicity ξ of A and p_i is positive integers eventually larger than one. It implies that

$$\lambda_{\max}(P_r) \asymp_0 (\frac{1}{r})^{s_{\max}} \text{ and } \lambda_{\min}(P_r) \asymp_0 (\frac{1}{r})^{s_{\min}},$$

for positive constants $1 \leq s_{\min} \leq s_{\max}$. Therefore, by equation (18), upper bound for the L^p-gain M_p cannot be delay-independent.

References

1. Liu W., Chitour Y., Sontag E.D. (1996) On finite-gain stabilizability of linear systems subject to input saturation. Siam J. Control & Optimazation 34(4):1190–1219
2. Mazenc F., Mondie S., Niculescu S. (2003) Global Asymptotic Stabilization for Chains of Integrators with a Delay in the Input. IEEE Transactions on Automatic Control 48(1):57–63
3. Mazenc F., Mondie S., Niculescu S. (2002) Global Stabilization of oscillators with bounded Delayed Input. In Proc. 41th IEEE Conference on decision and control, Las Vegas, Nevada
4. Megretsky A. (1996) A gain scheduled for systems with saturation which makes the closed loop system L^2- bounded. In Proc. IFAC World Congress, San Francisco, California
5. Niculescu S.-I. (2001) Delay effects on stability: a control perspective. Lecture Notes in Control and Information, Springer-Verlag, Berlin Heidelberg New York
6. Sontag E.D., Sussmann H.J. (1990) Nonlinear output feedback design for linear systems with saturating controls. In Proc. IEEE Conf. Decision and Control, pp. 3414–3416, Honolulu, Haiwai
7. Reed M., Simon B. (1978) Methods of modern Mathematical Physics, Analysis of operators. Academic Press, New York
8. Saberi A., Hou P., Stoorvogel A. A. (2000) On simultaneous global external and global internal stabilization of critically unstable linear systems with saturating actuators. IEEE Transactions on Automatic Control 45(6):117–135
9. Sontag E.D. (1988) Comments on integral variants of ISS. Systems & Control Letters 43:93–100

10. Sontag E.D. (1994) Mathematical control theory: Deterministic Finite Dimensional systems. Springer Verlag, Berlin Heidelberg New York
11. Sussmann H.J., Sontag E.D., Yang Y. (1994) A general result on the stabilization of linear systems using bounded controls. IEEE Transactions Automatic Control 39:2411–2425
12. Teel A. (1992) Global stabilization and restricted tracking for multiple integrators with bounded controls. Systems & Control Letters 18:165–171
13. Van Der Schaft A.J. (1996) L^2-gain and passivity techniques in nonlinear control. Lecture Notes in Control and Information Sciences, Springer-Verlag, Berlin Heidelberg New York
14. Yakoubi K., Chitour Y. (2006) Linear systems subject to input saturation and time delay: Global asymptotic stabilization. Submitted
15. Yakoubi K., Chitour Y. (2006) Linear systems subject to input saturation and time delay: Finite-gain L^p-stabilization. Submitted

Global Asymptotic Stabilization of a PVTOL Aircraft Model with Delay in the Input

Rogelio Francisco[1], Frédéric Mazenc[2], and Sabine Mondié[1]

[1] Departamento de Control Automático CINVESTAV-IPN, Av. IPN 2508, A.P. 14-740, 07300 México, D.F., México
rfrancisco@ctrl.cinvestav.mx, smondie@ctrl.cinvestav.mx

[2] Projet MERE INRIA-INRA, UMR Analyse des Systèmes et Biométrie, INRA, 2, pl. Viala 34060 Montpellier, France
mazenc@helios.ensam.inra.fr

Summary. A model of PVTOL aircraft with two delayed inputs is considered. The origin of this system is globally asymptotically and locally exponentially stabilized by bounded control laws. The explicit expressions of the control laws applied are determined through recent extensions of the forwarding approach to systems with a delay in the input. In a second step, the output feedback stabilization problem consisting in globally asymptotically stabilizing the origin of the PVTOL when the variables of velocity are unmeasured is solved through a recent technique which extensively exploits the presence of positive delays in the inputs.

Keywords: stabilization, PVTOL aircraft model, nonlinear feedforward system, output feedback.

1 Introduction

The feedforward systems are nonlinear systems described by equations having a specific triangular structure which, in general, cannot be linearized. The problem of the global asymptotic stabilization by state feedback of these triangular equations in the absence of delay has been studied by many researchers [18, 8, 16, 5, 19], during the last decade. The techniques of stabilization of feedforward systems have been successfully applied to different physical devices such as, for example, ' the card-pendulum system '(see [9]), ' the Ball and beam ' with a friction term (see [16]), ' the TORA system ' (see [16]) and ' the PVTOL ' (*Planar Vertical Takeoff and Landing Aircraft*), (see [18]).

Three recent works [10, 12, 14] are devoted to the problem of designing globally asymptotically stabilizing control laws for particular families of feedforward systems with an arbitrarily large delay in the input: this problem is solved for chains of integrators in [10, 14] and for nonlinear feedforward systems admitting a chain of integrators as linear approximation at the origin in [12, 13]. The basic idea of these three papers consists in selecting, according to the value of the delay, appropriate stabilizing control laws in a family of control laws whose explicit formulae generalize those of the control laws provided by A. Teel in [17].

J. Chiasson and J.J. Loiseau (Eds.): Appl. of Time Delay Systems, LNCIS 352, pp. 343–356, 2007.
springerlink.com

In the present work we will use the aforementioned theoretical results, and especially the one of [13], to stabilize a PVTOL model, when the control inputs are subject to delays. The PVTOL aircraft model is well-known by the control community. Due to the fact that flight control is an essential control problem, this simple model, which retains main features that must be considered when designing control laws for a real aircraft, has been studied extensively by many researchers. Some of the works devoted to this system are the following. In 1992 J. Hauser et al. [2] developed for this model an approximate input-output linearization procedure which results in bounded tracking and asymptotic stability. In 1996 A. Teel [18] illustrated his nonlinear small gain theorem based approach for the stabilization of feedforward systems by applying it to the PVTOL aircraft. In 1996 P. Martin et al. [7] proposed an extension of [2] relying extensively on the concept of flatness. In 1999, F. Lin et al. [4] studied the robust hovering control of the PVTOL and designed a nonlinear state feedback by applying an optimal control approach. The recent publications by L. Marconi et al. [6] within an internal model approach and by K.D. Do et al. [1], who have solved an output feedback tracking problem, show that this system still captures the attention of researchers.

Observe that, due to the number of papers devoted to the PVTOL system, the list of works on the PVTOL aircraft we give is not exhaustive. However, to the best of our knowledge, all the theoretical results available in the literature on the asymptotic stabilization of the PVTOL assume that there is no delay in the inputs. Nevertheless, such a delay, due to sensors and information processing, is often present in practice. This is in particular the case of the experimental PVTOL setup presented in the work of Palomino et al. [15] where the position and roll angle of the system are measured with the help of a vision system that induces a delay of approximately $40ms$.

The main features of our contribution can be summarized as follows. In the first part of the work, we construct state feedbacks which globally asymptotically and locally exponentially stabilize the origin of the equations modelling the PVTOL when there are known delays in the inputs. These constructions extensively rely on the control design techniques proposed in [12], [13], [10]. The control laws obtained that way are bounded and involve a distributed term. Moreover they depend on the variables of position and velocity. In the second part of the work, we complement this result by showing that using the presence of known nonzero delays in the inputs (or by introducing artificially delays in the inputs), one can determine globally asymptotically and locally exponentially stabilizing control laws depending only on the variables of position and not on the variables of velocity, which in practice cannot be easily measured. This result is proved through ideas borrowed from the recent works [11] and [3] on the output feedback stabilization of linear systems by means of delayed feedbacks. The main feature of the original approach proposed in these works is that it does not rely on the construction of an observer or on the introduction of dynamic extensions but only on the presence of a delay. In the present paper, it is applied for the first time to a nonlinear system. This strategy of output feedback stabilization

for the PVTOL has clearly no similarity with the one adopted in [1], since the latter relies on the construction of an observer.

The paper is organized as follows. In Section 2, we recall the main theoretical result which is used to construct the control laws. The simplified PVTOL aircraft model that is analyzed in this work is presented in Section 3. The control laws and the state reconstructor for the PVTOL aircraft model are designed respectively in Sections 4 and 5. Simulation results are presented in Section 6. The paper ends with some concluding remarks in Section 7.

Technical Preliminaries

1. A function $\gamma(X)$ is of order one (resp. two) at the origin if for some $c > 0$, the inequality $|\gamma(X)| \leq c|X|$ (resp. $|\gamma(X)| \leq c|X|^2$) is satisfied on a neighborhood of the origin.
2. The argument of the functions will be omitted or simplified whenever no confusion can arise from the context. For example, we may denote $f(x(t))$ by simply $f(t)$ or $f(\cdot)$.
3. By $\sigma : \mathbb{R} \to \mathbb{R}$ we denote a saturation function which satisfies
a) $\sigma(\cdot)$ is odd, nondecreasing and of class C^1,
b) $0 \leq \sigma'(s) \leq 1$, $\forall s \in \mathbb{R}$,
c) $\sigma(s) = 1$ for all $s \geq \frac{21}{20}$ and $\sigma(s) = s$ for all $s \in \left[0, \frac{19}{20}\right]$.
4. By $\sigma_i : \mathbb{R} \to \mathbb{R}$ we denote the functions

$$\sigma_i(s) := \varepsilon_i \sigma\left(\frac{1}{\varepsilon_i} s\right), \ \varepsilon_i = \frac{1}{20^{n-i+1}}, \ i = 1, \ldots, n. \tag{1}$$

2 Theoretical Results

In this section, we recall the main stabilization result of [13] for nonlinear feedforward systems with a delay in the input and subject to vanishing perturbations. It is a generalization of the result presented in [12] for nonlinear feedforward systems in absence of vanishing perturbations, which in turn is a generalization of the recursive methodology developed in [11] to solve the problem of stabilizing chains of integrators.

Theorem 1. *[13] Consider the following feedforward system*

$$\begin{cases} \dot{x}_1(t) &= x_2(t) + h_1(x_2(t), \ldots, x_n(t)) + r_1(t), \\ \dot{x}_2(t) &= x_3(t) + h_2(x_3(t), \ldots, x_n(t)) + r_2(t), \\ \vdots & \\ \dot{x}_{n-1}(t) &= x_n(t) + h_{n-1}(x_n(t)) + r_{n-1}(t), \\ \dot{x}_n(t) &= u(t - \tau), \end{cases} \tag{2}$$

where $x_i \in \mathbb{R}$, $u \in \mathbb{R}$ is the input, $\tau \geq 0$ is the delay and where each function $h_i(\cdot)$ is a function of a class C^2 and of order 2 at the origin, that satisfies the inequality

$$|h_i(x_{i+1}, x_{i+2}, \ldots, x_n)| \leq M(x_{i+1}^2 + x_{i+2}^2 + \cdots + x_n^2) \tag{3}$$

where M is a strictly positive constant when $|x_j| \leq 1, \quad j = i+1, \ldots, n$, and where each function $r_i(\cdot)$ is a function continuously differentiable and such that, for some real-valued nonnegative and nonincreasing function $R \in L^2[0, +\infty)$ the inequalities

$$|r_i(t)| \leq R(t) \tag{4}$$

are satisfied for all $t \geq 0$. Consider the control law bounded in norm

$$\begin{aligned} u(x_1, x_2, \ldots, x_n) = & -\tfrac{L}{Mk^n}\sigma_n(p_n(k^{n-1}\tfrac{M}{L}x_n) + \ldots \\ & +\sigma_{n-1}(p_{n-1}(k^{n-2}\tfrac{M}{L}x_{n-1}, k^{n-1}\tfrac{M}{L}x_n) + \ldots \\ & +\sigma_1(p_1(\tfrac{M}{L}x_1, \ldots, k^{n-2}\tfrac{M}{L}x_{n-1}, k^{n-1}\tfrac{M}{L}x_n)))\ldots) \end{aligned} \tag{5}$$

where

$$p_i(x_i, ..., x_n) = \sum_{j=i}^{n} \frac{(n-i)!}{(n-j)!(j-i)!} x_j,$$

where the functions $\sigma_i(\cdot)$ are the functions defined in the preliminaries (see (1)) and

$$k \geq \frac{\tau}{\min\left\{\frac{1}{16n^3\left[4n\sqrt{n}(1+n^2)^{n-1}+1\right]^2}, \frac{1}{4.20^{n+1}n(n+2)}\right\}}, \tag{6}$$

$$0 < L \leq \min\left\{\frac{\eta k}{n^3(n!)^3}, \frac{Mk}{(n+1)!}, M\right\}, \tag{7}$$

$$0 \leq \eta \leq \min\left\{\frac{1}{8(1+n^2)^{n-1}}, \frac{1}{10.20^n n}\right\}.$$

Then all the trajectories of the system (2) in closed-loop with the control law (5) converge to the origin. Moreover, the origin of the system (2) in closed-loop with the control law (5) is globally uniformly asymptotically and locally exponentially stable when each function $r_i(\cdot)$ is identically equal to zero.

3 The PVTOL Model and Problem Statement

Aircraft control is a challenging field of control theory. Given the complexity of the systems describing the behavior of aircraft, it is convenient to study simplified models of them that contemplate a specific number of state variables and controls which capture the essential features of the systems for control purposes. The simplified model of PVTOL we consider in this work is the following

$$\left.\begin{aligned} \dot{x}_1 &= x_2, \\ \dot{x}_2 &= u_1(t-\tau_1)\sin\theta, \end{aligned}\right\} \tag{8}$$

$$\left.\begin{aligned} \dot{y}_1 &= y_2, \\ \dot{y}_2 &= u_1(t-\tau_1)\cos\theta - 1, \end{aligned}\right\} \tag{9}$$

$$\left.\begin{aligned} \dot{\theta} &= \omega, \\ \dot{\omega} &= u_2(t-\tau_2). \end{aligned}\right\} \tag{10}$$

The variables x_1, y_1 denote the horizontal and the vertical positions, θ is the roll angle that the aircraft makes with the horizon, u_1, u_2 are the control inputs and $\tau_2 > 0, \tau_1 > 0$ are the delays. The control input u_1 is the thrust (directed out of the bottom of the aircraft) and u_2 is the angular acceleration (rolling moment).

In the next two sections, we will address the following problems:

Problem 1: *Construct state feedbacks which globally uniformly asymptotically and locally exponentially stabilizes the system (8), (9), (10) when there are delays in the inputs.*

Problem 2: *Construct output feedbacks which globally uniformly asymptotically and locally exponentially stabilize the system (8), (9), (10) with θ, y_1, x_1 as output variables when there are delays in the inputs.*

4 Stabilization Result

This section is devoted to Problem 1. Through the result which has been recalled in section 2, we will establish the following result.

Theorem 2. *Consider the system (8), (9), (10) with the delays $\tau_1 = 0.2, \tau_2 = 0.3$. The origin of this system in closed-loop with the control laws*

$$u_1 = u_{1s}(y_2(t-\tau_1), y_1(t-\tau_1), \hat{\theta}(t-\tau_2)), \tag{11}$$

$$u_2 = u_{2s}(\omega(t-\tau_2), \theta(t-\tau_2), x_2(t-\tau_2), x_1(t-\tau_2)) \tag{12}$$

with

$$\begin{aligned} u_{2s}(\omega, \theta, x_2, x_1) = & -\tfrac{L}{Mk^4}\sigma_4(k^3\tfrac{M}{L}\omega + \sigma_3(k^3\tfrac{M}{L}\omega \\ & + k^2\tfrac{M}{L}\theta + \sigma_2(k^3\tfrac{M}{L}\omega + 2k^2\tfrac{M}{L}\theta + k\tfrac{M}{L}x_2 \\ & + \sigma_1(k^3\tfrac{M}{L}\omega + 3k^2\tfrac{M}{L}\theta + 3k\tfrac{M}{L}x_2 + \tfrac{M}{L}x_1)))), \end{aligned} \tag{13}$$

with $M = 0.6$ and $L = 6.45 \times 10^{-10}$, $k = 7.5931 \times 10^{12}$ and

$$u_{1s}(y_2, y_1, \hat{\theta}) = \frac{1 + v_{1s}(y_2, y_1)}{\cos(\sigma(\hat{\theta}))}, \tag{14}$$

with

$$v_{1s}(y_2, y_1) = -\sigma_2(y_2 + \sigma_1(y_2 + y_1)) \tag{15}$$

and

$$\begin{aligned} \hat{\theta}(t-\tau_2) = & \theta(t-\tau_2) + \tau_2\omega(t-\tau_2) \\ & - \textstyle\int_{t-\tau_2}^{t} (s-t)u_{2s}(s-\tau_2)ds \end{aligned} \tag{16}$$

is globally uniformly asymptotically and locally exponentially stable.

Remark

1. For the sake of simplicity, we have restricted our attention to the case where $\tau_1 = 0.2, \tau_2 = 0.3$. However, one can easily deduce from the proof of Theorem 2 that for any values of τ_1, τ_2, Problem 1 can be solved.

2. From a practical point of view, the smallness of the size of the control law $u_{2s}(\cdot)$ is a drawback. It is important to observe that this drawback can be overcome. Indeed, by constructing a control law by means of the key ideas of Theorem 1 but by taking advantage of the specificity of the nonlinearities of the system (21), one can obtain a control law $u_{2s}(\cdot)$ with respectively much larger and much smaller values for the parameters L and k. For the sake of simplicity, we do not have performed this simple but lengthy construction of feedback and have instead directly applied Theorem 1.

Proof. The proof splits up into three steps. In Step 1 and Step 2, we establish that the control law defined in (12) ensures that the solutions of the subsystem (10) enter in finite time a particular neighborhood of the origin. Next, we show that this property implies that the control law defined in (11) stabilizes the subsystem (9). Then the problem considered reduces to the stability analysis of a four dimensional feedforward system. This analysis is carried out in Step 3.

Step 1
In Appendix A, we establish the following result.

Lemma 1. *The control law defined in (11) is well defined. The trajectories of system (8), (9), (10) in closed-loop with the bounded feedbacks (11), (12) are defined for all $t \geq 0$. Moreover, there exists $T \geq 2\tau_2$ such that*

$$|\theta(t)| \leq \frac{\pi}{4}\ ,\ \forall t \geq T. \tag{17}$$

Step 2
One can establish that, for all $t \geq 2\tau_2$,

$$\hat{\theta}(t-\tau_2) = \theta(t), \tag{18}$$

by observing that, when $t \geq 2\tau_2$,

$$\begin{aligned}
\theta(t) &= \theta(t-\tau_2) + \textstyle\int_{t-\tau_2}^{t} \dot{\theta}(s)ds \\
&= \theta(t-\tau_2) + \textstyle\int_{t-\tau_2}^{t} \omega(s)ds \\
&= \theta(t-\tau_2) + \tau_2\omega(t-\tau_2) \\
&\quad + \textstyle\int_{t-\tau_2}^{t} [\omega(s) - \omega(t-\tau_2)]ds \\
&= \theta(t-\tau_2) + \tau_2\omega(t-\tau_2) \\
&\quad + \textstyle\int_{t-\tau_2}^{t} \left(\int_{s}^{t-\tau_2} \dot{\omega}(l)dl \right) \\
&= \theta(t-\tau_2) + \tau_2\omega(t-\tau_2) \\
&\quad - \textstyle\int_{t-\tau_2}^{t} \left(\int_{t-\tau_2}^{s} u_2(l-\tau_2)dl \right) \\
&= \theta(t-\tau_2) + \tau_2\omega(t-\tau_2) \\
&\quad - \textstyle\int_{t-\tau_2}^{t} (s-t)u_{2s}(s-\tau_2)ds.
\end{aligned}$$

Equality (18), the definition of $\sigma(\cdot)$ and Lemma 1 ensure that for all $t \geq T$,

$$u_{1s}(t-\tau_1) = \frac{1 + v_{1s}(t-\tau_1)}{\cos(\theta(t))} \tag{19}$$

which implies that for all $t \geq T$, the system (9) simplifies as

$$\begin{aligned}\dot{y}_1 &= y_2(t),\\ \dot{y}_2 &= v_1(t-\tau_1)\\ &= -\sigma_2(y_2(t-\tau_1)+\sigma_1(y_2(t-\tau_1)+y_1(t-\tau_1))).\end{aligned} \tag{20}$$

Using Theorem 1 (or the main result of [10]), one can prove that this system is globally uniformly asymptotically and locally exponentially stable.

Step 3

According to (19), the system (8), (10) in closed-loop with (11), for all $t \geq T + 2\tau_2$, is described by the equations

$$\begin{cases}\dot{x}_1 = x_2(t),\\ \dot{x}_2 = (1+v_{1s}(t-\tau_1))\tan\theta(t),\\ \dot{\theta} \;= \omega(t),\\ \dot{\omega} \;= u_{2s}(t-\tau_2),\end{cases}$$

or, equivalently, by the equations

$$\begin{cases}\dot{x}_1 = x_2(t),\\ \dot{x}_2 = \theta(t) + (\tan\theta(t)-\theta(t)) + v_{1s}(t-\tau_1)\tan\theta(t),\\ \dot{\theta} \;= \omega(t),\\ \dot{\omega} \;= u_{2s}(t-\tau_2).\end{cases} \tag{21}$$

Observe that the inequalities

$$|\tan\theta - \theta| \leq \int_0^{|\theta|} \tan^2(l)dl \leq 0.6\theta^2$$

hold for all $\theta \in [-1,1]$. It follows that the function $\tan\theta - \theta$ is of class C^2 of order 2 at the origin: it satisfies the requirement (3) imposed on the function $h_2(\cdot)$ in Theorem 1. Notice also that in (21), the functions corresponding to $h_1(\cdot)$ and $h_3(\cdot)$ in Theorem 1 are identically equal to zero. Moreover, we know that the real-valued functions $y_1(t)$, $y_2(t)$ converge exponentially to zero and that for all $t \geq T$, $|\tan\theta(t)| \leq 1$. Therefore $v_{1s}(t-\tau_1)\tan\theta(t)$ converges exponentially to zero: it follows that this function belongs to $L^2[0,+\infty)$ and thereby can be regarded as a bounded vanishing disturbance ($r_2(t)$ in Theorem 1). Then, using Theorem 1, one can check that all the trajectories of the feedforward system (21) converge to the origin and besides that the system (8), (9), (10) in closed-loop with the feedbacks (12), (15) is globally uniformly asymptotically and locally exponentially stable. (The value of the constant M, in the particular case of the system (21), is $M = 0.6$.) This concludes the proof.

5 A State Reconstructor for the PVTOL

This section is devoted to Problem 2 (see the end of Section 3). We show that one can solve the problem of stabilizing the PVTOL system when only the variables of position are available by measurement. The approach consists in evaluating the exact values of the variables of velocity through a state reconstructor for each subsystem (8), (9), (10). We show that, when the delays are known, the

knowledge of the positions and roll angle of the aircraft which correspond to the states $x_1(t)$, $y_1(t), \theta(t)$ along with the control inputs $u_1(t)$ and $u_2(t)$ at present and past time instants is sufficient to determine the derivatives $x_2(t), y_2(t), \omega(t)$. The approach draws inspiration from the ideas on output feedback stabilization used in [11] for the case of a bounded input delayed simple oscillator and in [3] for the case of multiple oscillators and chains of integrators.

Theorem 3. *Consider the system (8), (9), (10) with delays $\tau_1 = 0.2, \tau_2 = 0.3$. The origin of this system in closed-loop with the control laws*

$$u_2(t-\tau_2) = u_{2s}(\overline{\omega}(t-\tau_2), \theta(t-\tau_2), \overline{x}_2(t-\tau_2), x_1(t-\tau_2)), \tag{22}$$

$$u_1(t-\tau_1) = u_{1s}(\overline{y}_2(t-\tau_1), y_1(t-\tau_1), \overline{\hat{\theta}}(t-\tau_2)), \tag{23}$$

with

$$\begin{aligned}
\overline{x}_2(t) &= \tfrac{1}{\tau_1}\left[x_1(t) - x_1(t-\tau_1) - \right. \\
&\qquad \left. \int_{t-\tau_1}^{t} \left(\int_t^s u_{1s}(l-\tau_1)\sin\theta(l)dl \right) ds \right], \\
\overline{y}_2(t) &= \tfrac{1}{\tau_1}\left[y_1(t) - y_1(t-\tau_1) - \right. \\
&\qquad \left. \int_{t-\tau_1}^{t} \left(\int_t^s (u_{1s}(l-\tau_1)\cos\theta(l) - 1)dl \right) ds \right], \\
\overline{\omega}(t) &= \tfrac{1}{\tau_2}\left[\theta(t) - \theta(t-\tau_2) - \right. \\
&\qquad \left. \int_{t-\tau_2}^{t} \left(\int_t^s u_{2s}(l-\tau_2)dl \right) ds \right],
\end{aligned} \tag{24}$$

and

$$\overline{\hat{\theta}}(t-\tau_2) = \theta(t-\tau_2) + \tau_2\overline{\omega}(t-\tau_2) - \int_{t-\tau_2}^{t} (s-t)u_{2s}(s-\tau_2)ds, \tag{25}$$

where $u_{1s}(\cdot), u_{2s}(\cdot)$ are the functions defined respectively in (14) and (13), is globally uniformly asymptotically and locally exponentially stable.

Proof. It follows from (8) that, for all $t \geq 2\tau_1$,

$$\begin{aligned}
x_1(t) &= x_1(t-\tau_1) + \int_{t-\tau_1}^{t} \dot{x}_1(s)ds \\
&= x_1(t-\tau_1) + \int_{t-\tau_1}^{t} x_2(s)ds \\
&= x_1(t-\tau_1) + \tau_1 x_2(t) + \int_{t-\tau_1}^{t} (x_2(s) - x_2(t))\, ds \\
&= x_1(t-\tau_1) + \tau_1 x_2(t) + \int_{t-\tau_1}^{t} \left(\int_t^s \dot{x}_2(l)dl \right) ds \\
&= x_1(t-\tau_1) + \tau_1 x_2(t) \\
&\quad + \int_{t-\tau_1}^{t} \left(\int_t^s u_{1s}(l-\tau_1)\sin\theta(l)dl \right) ds.
\end{aligned}$$

Hence we obtain that the equality

$$x_2(t) = \overline{x}_2(t), \tag{26}$$

holds for all $t \geq 2\tau_1$. Similarly, it follows from (9) that, for all $t \geq 2\tau_1$,

$$y_2(t) = \overline{y}_2(t) \tag{27}$$

and from (10) that, for all $t \geq 2\tau_2$,

$$\omega(t) = \overline{\omega}(t). \tag{28}$$

It follows readily that, for all $t \geq 2(\tau_2 + \tau_1)$, the control laws (23), (22) are equal to the control laws (11), (12) used in Theorem 2. This concludes the proof.

6 Simulation Results

We have performed simulations for the system (8), (9) and (10) in closed-loop with the control laws (11) and (12) where the variables $x_2(t), y_2(t)$ and $\omega(t)$ are substituted by the right hand side of (26), (27) and (28) respectively. The initial conditions we have chosen are: $x_1(0) = x_2(0) = 0.5$, $\theta(0) = \omega(0) = 0.55$, $y_1(0) = y_2(0) = 1$. The behavior of the six state variables and the two control inputs is presented below

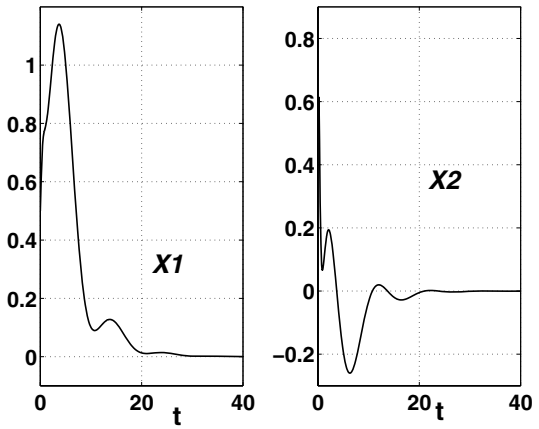

Fig. 1. Horizontal position and velocity

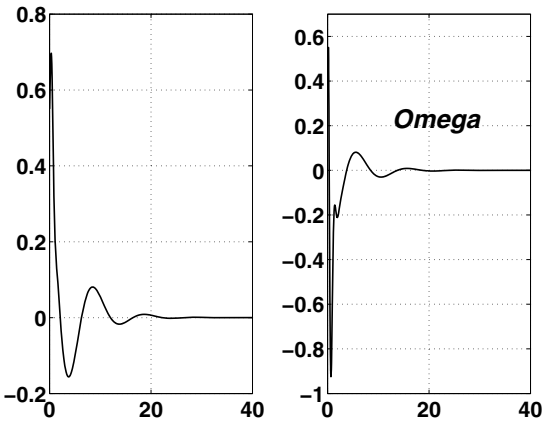

Fig. 2. Roll angle and velocity

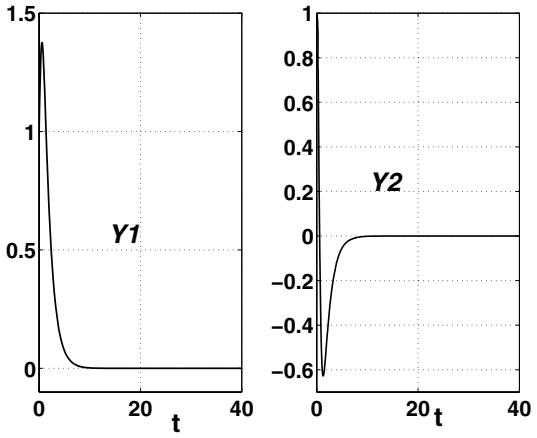

Fig. 3. Vertical position and velocity

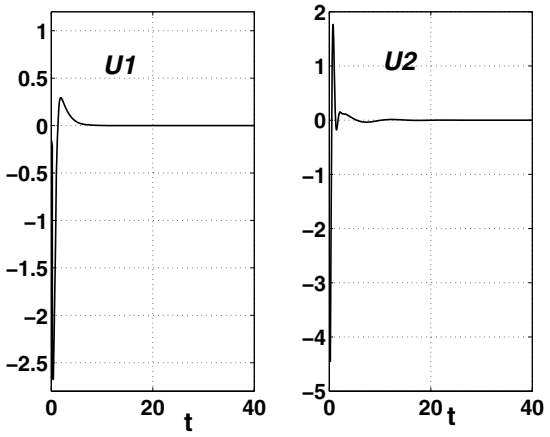

Fig. 4. Thrust and angular acceleration

7 Conclusion

In this work, two problems have been solved. First, we have achieved the global uniform asymptotic and local exponential stabilization of an aircraft PVTOL model with two delays in the inputs, using bounded state feedbacks. In a second step, we have shown how the presence of delays in the inputs can be exploited to achieve the global uniform asymptotic and local exponential stabilization of an aircraft PVTOL model when the variables of velocity are not measured. The main interest of the work is that it illustrates the possibility of applying recent theoretical results for nonlinear systems with delay to a physical system, very relevant from a practical point of view. Much remains to be done. We plan

to study the following problems: Investigating whether or not there are possible ways to modify our construction in such a way that the resulting control laws are without distributed terms, determining control laws for the PVTOL with delay using not the forwarding approach but the backstepping approach, extending our results to the case where the exact values of the delay are unknown.

Acknowledgements. This work was supported by Conacyt, Mexico, Project 41276-Y and Grant 158335.

References

1. Do D.K. , Jiang Z.P., Pan J. (2003) On Global Tracking Control of a Aircraft Without Velocity Measurement. IEEE Transactions on Automatic Control 48:2212–2217
2. Hauser J., Sastry S., Meyer G. (1992) Nonlinear Control Design for Slightly Non-minimum Phase Systems: Application to V/STOL Aircraft. Automatica 28:665–679
3. Kharitonov V.L., Niculescu S.-I., Moreno J., Michiels W. (2003) Some remarks on static output feedback stabilization problem: necessary conditions for multiple delay controllers. In Proc. ECC 2003, Cambridge, U.K
4. Lin F., Zhang W., Brandt R.D. (1999), Robust Hovering Control of a PVTOL Aircraft. IEEE Transactions on Control Systems Technology 7:343–351
5. Marconi L., Isidori A. (2000) Robust global stabilization of a class of uncertain feedforward nonlinear systems. Systems & Control Letters 41:281–290
6. Marconi L., Isidori A., Serrani A (2002) Autonomous vertical landing on an oscillating platform: an internal-model based approach. Automatica 38:21–32
7. Martin P., Devasia S., Paden B. (1996) A Different Look at Output Tracking: Control of a VTOL aircraft. Automatica 32:101–107
8. Mazenc F., Praly L. (1996) Adding an integration and global asymptotic stabilization of feedforward systems. IEEE Transactions on Automatic Control 41:559–1578
9. Mazenc F., Bowong S. (2003) Tracking trajectories of the cart-pendulum system. Automatica 39:677–684
10. Mazenc F., Mondié S., Niculescu S.-I. (2003) Global Asymptotic Stabilization for Chains of Integrators with a Delay in the Input. IEEE Transactions Automatic Control 48:57–63
11. Mazenc F., Mondié S., Niculescu S.-I. (2004) Global Stabilization of Oscillators With Bounded Delayed Input. Systems & Control Letters 53:415–422
12. Mazenc F., Mondié S., Francisco R. (2004) Global Asymptotic Stabilization of Feedforward System with Delay in the Input. IEEE Transactions Automatic Control 49:844–850
13. Mazenc F., Francisco R., Mondié S. (2004) Global Asymptotic Stabilization of Feedforward System with Delay in the Input and vanishing perturbations. In Proc. 3rd IFAC Symposium on Systems, Structure and Control, pp. 216–221, Oaxaca, Mexico
14. Michiels W., Roose D. (2001) Global stabilization of multiple integrators with time-delay and input constraints. In Proc. IFAC Workshop on Time Delay Systems, pp. 266-271, Santa Fe, New Mexico
15. Palomino A., Castillo P., Fantoni I., Lozano R., Pégard C. (2003) Control Strategy Using Vision for the Stabilization of an Experimental PVTOL Aircraft Setup. In Proc. 42th IEEE Conference on Decision and Control, Maui, Hawaii

16. Sepulchre R., Janković M., Kokotovic P.V. (1997) Constructive Nonlinear Control, Springer-Verlag, London
17. Teel A.R. (1992) Global stabilization and restricted tracking for multiple integrators with bounded controls. Systems & Control Letters 18:165-171
18. Teel A.R. (1996) A Nonlinear Small Gain Theorem for the Analysis of Control Systems with Saturation. IEEE Transactions on Automatic Control 41:1256-1270
19. Tsinias J., Tzamtzi M.P. (2001) An explicit formula of bounded feedback stabilizers for feedforward systems, Systems & Control Letters 43:247-261

A Proof of Lemma 1

The fact that $\tau_2 \geq \tau_1$ ensures that the control law $u_{1s}(\cdot)$ defined in (11) is well defined. Due to the feedforward structure of the system (8), (9), (10), it is clear that the trajectories of this system in closed- loop with the bounded feedbacks (15), (12) are defined for all $t \geq 0$ (observe in particular that the finite escape time phenomenon obviously does not occur).

The next step of the proof consists in showing that $u_{2s}(\cdot)$ defined in (12) ensures that $|\theta(t)| \leq \frac{\pi}{4}$ when t is large enough. This proof is lengthy but simple.

First observe that

$$\begin{array}{rl} \omega(t-\tau_2)-\omega(t) & = \int_t^{t-\tau_2} \dot{\omega}(s)ds \\ & = \int_{t-\tau_2}^{t} \frac{L}{Mk^4}\sigma_4(\cdot)ds. \end{array} \tag{29}$$

It follows that

$$\dot{\omega} = -\frac{L}{Mk^4}\sigma_4(k^3\frac{M}{L}\omega(t)+\mu_1(t)) \tag{30}$$

where $\mu_1(t) = k^3\frac{M}{L}(\omega(t-\tau_2)-\omega(t))+\sigma_3(\cdot)$ is a function such that, for all $t \geq 0$,

$$|\mu_1(t)| \leq \frac{\tau_2}{k}\varepsilon_4 + \varepsilon_3. \tag{31}$$

The derivative of the positive definite and radially unbounded function

$$V_1(\omega) = \frac{1}{2}\omega^2 \tag{32}$$

along the trajectories of (30) satisfies

$$\begin{array}{rl} \dot{V}_1 & \leq -\frac{L}{Mk^4}\omega(t)\sigma_4(k^3\frac{M}{L}\omega(t)+\mu_1(t)) \\ & \leq -\frac{L}{Mk^4}|\omega(t)|\varepsilon_4\sigma(\frac{1}{\varepsilon_4}(k^3\frac{M}{L}|\omega(t)| - \frac{\tau_2}{k}\varepsilon_4 - \varepsilon_3)). \end{array} \tag{33}$$

It follows that, when $|\omega(t)| \geq 2\frac{L}{Mk^3}\left(\frac{\tau_2}{k}\varepsilon_4+\varepsilon_3\right)$,

$$\dot{V}_1 \leq -2\frac{L^2\left(\frac{\tau_2}{k}\varepsilon_4+\varepsilon_3\right)\varepsilon_4}{M^2k^7}\sigma(\frac{1}{\varepsilon_4}\left(\frac{\tau_2}{k}\varepsilon_4+\varepsilon_3\right)) < 0. \tag{34}$$

It follows that there exists $T_1 \geq 0$ such that, for all $t \geq T_1$,

$$|\omega(t)| \leq 2\frac{L}{Mk^3}\left(\frac{\tau_2}{k}\varepsilon_4+\varepsilon_3\right). \tag{35}$$

Combining (31) and (35), we deduce that, for all $t \geq T_1$,

$$\frac{1}{\varepsilon_4}\left|k^3\frac{M}{L}\omega(t)+\mu_1(t)\right| \leq \left(3\frac{\tau_2}{k}+3\frac{\varepsilon_3}{\varepsilon_4}\right) \leq \frac{1}{2}. \tag{36}$$

We deduce that there exists $T_2 \geq T_1$ such that, for all $t \geq T_2$,

$$\begin{array}{l} \dot{\omega} = -\frac{L}{Mk^4}k^3\frac{M}{L}\omega(t-\tau_2) - \frac{L}{Mk^4}\sigma_3(\cdot) \\ \quad = -\frac{1}{k}\omega(t-\tau_2) - \frac{L}{Mk^4}\sigma_3(\cdot). \end{array} \tag{37}$$

It follows that the derivative of the variable

$$\gamma = k\omega + \theta \tag{38}$$

satisfies

$$\begin{array}{l} \dot{\gamma} = \omega(t) - \omega(t-\tau_2) - \frac{L}{Mk^3}\sigma_3(k^3\frac{M}{L}\omega(t-\tau_2) + k^2\frac{M}{L}\theta(t-\tau_2) + \sigma_2(\cdot)) \\ \quad = -\frac{L}{Mk^3}\sigma_3(k^3\frac{M}{L}\omega(t) + k^2\frac{M}{L}\theta(t) + \mu_2(t)) + \mu_3(t) \\ \quad = -\frac{L}{Mk^3}\sigma_3(\frac{M}{L}k^2\gamma(t) + \mu_2(t)) + \mu_3(t), \end{array} \tag{39}$$

where $\mu_2(t)$ and $\mu_3(t)$ are continuous functions such that

$$\begin{array}{l} |\mu_2(t)| \leq k^3\frac{M}{L}\left|\omega(t)-\omega(t-\tau_2)\right| + k^2\frac{M}{L}\left|\theta(t)-\theta(t-\tau_2)\right| + \varepsilon_2, \\ |\mu_3(t)| \leq \left|\omega(t)-\omega(t-\tau_2)\right|. \end{array} \tag{40}$$

From (29) and (35), we deduce that there exists $T_3 \geq T_2$ such that, for all $t \geq T_3$,

$$\begin{array}{l} |\mu_3(t)| \leq \frac{\tau_2 L\varepsilon_4}{Mk^4}, \\ |\mu_2(t)| \leq k^3\frac{M}{L}\frac{\tau_2 L\varepsilon_4}{Mk^4} + \varepsilon_2 + k^2\frac{M}{L}\int_{t-\tau_2}^{t}|\omega(s)|\,ds \\ \qquad \leq \varepsilon_2 + \frac{2\tau_2}{k}\varepsilon_3 + \left(\frac{\tau_2}{k}+\frac{2\tau_2^2}{k^2}\right)\varepsilon_4. \end{array}$$

It follows that the derivative of the positive definite and radially unbounded function

$$V_2(\gamma) = \frac{1}{2}\frac{Mk^3}{L}\gamma^2 \tag{41}$$

along the trajectories of (39) satisfies, when $t \geq T_3$

$$\begin{array}{l} \dot{V}_2 \leq -\frac{Mk^3}{L}\frac{L}{Mk^3}\gamma(t)\sigma_3(\frac{M}{L}k^2\gamma(t)+\mu_2(t)) + \gamma\frac{Mk^3}{L}\mu_3(t) \\ \quad \leq -\varepsilon_3|\gamma(t)|\sigma(\frac{1}{\varepsilon_3}(\frac{M}{L}k^2|\gamma(t)| - (\varepsilon_2 + \frac{2\tau_2}{k}\varepsilon_3 + (\frac{\tau_2}{k}+\frac{2\tau_2^2}{k^2})\varepsilon_4)))) + \frac{\tau_2\varepsilon_4}{k}|\gamma(t)|. \end{array} \tag{42}$$

It follows that when $t \geq T_3$ and when

$$|\gamma(t)| \geq 2\frac{L}{Mk^2}\left(\varepsilon_2 + \frac{2\tau_2}{k}\varepsilon_3 + \left(\frac{\tau_2}{k}+\frac{2\tau_2^2}{k^2}\right)\varepsilon_4\right),$$

the inequality

$$\dot{V}_2 \leq -\varepsilon_3|\gamma(t)|\sigma\left(\frac{1}{\varepsilon_3}\left(\varepsilon_2+\frac{2\tau_2}{k}\varepsilon_3+\left(\frac{\tau_2}{k}+\frac{2\tau_2^2}{k^2}\right)\varepsilon_4\right)\right)+\frac{\tau_2\varepsilon_4}{k}|\gamma(t)| \tag{43}$$

is satisfied. The values of the parameters present in this inequality and the properties of $\sigma(\cdot)$ imply that when $t \geq T_3$ and when

$$|\gamma(t)| \geq 2\frac{L}{Mk^2}\left(\varepsilon_2+\frac{2\tau_2}{k}\varepsilon_3+\left(\frac{\tau_2}{k}+\frac{2\tau_2^2}{k^2}\right)\varepsilon_4\right),$$

the following inequality is satisfied.

$$\begin{aligned}\dot{V}_2 &\leq -|\gamma(t)|\left(\varepsilon_2+\tfrac{2\tau_2}{k}\varepsilon_3+\left(\tfrac{\tau_2}{k}+\tfrac{2\tau_2^2}{k^2}\right)\varepsilon_4\right)+\tfrac{\tau_2\varepsilon_4}{k}|\gamma(t)| \\ &\leq -|\gamma(t)|\left(\varepsilon_2+\tfrac{2\tau_2}{k}\varepsilon_3+\tfrac{2\tau_2^2}{k^2}\varepsilon_4\right)<0.\end{aligned} \tag{44}$$

We deduce that there exists $T_4 \geq T_3$ such that, for all $t \geq T_4$,

$$|\gamma(t)| \leq 2\frac{L}{Mk^2}\left(\varepsilon_2+\frac{2\tau_2}{k}\varepsilon_3+\left(\frac{\tau_2}{k}+\frac{2\tau_2^2}{k^2}\right)\varepsilon_4\right). \tag{45}$$

This inequality, the definition of γ (see (38)) and (35) imply that, when $t \geq T_4$,

$$\begin{aligned}|\theta(t)| &\leq 2\tfrac{L}{Mk^2}\left(\tfrac{\tau_2}{k}\varepsilon_4+\varepsilon_3\right) \\ &\quad +2\tfrac{L}{Mk^2}\left(\varepsilon_2+\tfrac{2\tau_2}{k}\varepsilon_3+\left(\tfrac{\tau_2}{k}+\tfrac{2\tau_2^2}{k^2}\right)\varepsilon_4\right) \\ &\leq \tfrac{\pi}{4}.\end{aligned}$$

The result is proved.

Index

Printing: Mercedes-Druck, Berlin
Binding: Stein + Lehmann, Berlin

Lecture Notes in Control and Information Sciences

Edited by M. Thoma, M. Morari

Further volumes of this series can be found on our homepage:
springer.com

Vol. 352: Chiasson, J.; Loiseau, J.J. (Eds.)
Applications of Time Delay Systems
358 p. 2007 [978-3-540-49555-0]

Vol. 351: Lin, C.; Wang, Q.-G.; Lee, T.H., He, Y.
LMI Approach to Analysis and Control of
Takagi-Sugeno Fuzzy Systems with Time Delay
204 p. 2007 [978-3-540-49552-9]

Vol. 350: Bandyopadhyay, B.; Manjunath, T.C.; Umapathy, M.
Modeling, Control and Implementation of Smart Structures 250 p. 2007 [978-3-540-48393-9]

Vol. 349: Rogers, E.T.A.; Galkowski, K.; Owens, D.H.
Control Systems Theory
and Applications for Linear
Repetitive Processes 482 p. 2007 [978-3-540-42663-9]

Vol. 347: Assawinchaichote, W.; Nguang, K.S.; Shi P.
Fuzzy Control and Filter Design
for Uncertain Fuzzy Systems
188 p. 2006 [978-3-540-37011-6]

Vol. 346: Tarbouriech, S.; Garcia, G.; Glattfelder, A.H. (Eds.)
Advanced Strategies in Control Systems
with Input and Output Constraints
480 p. 2006 [978-3-540-37009-3]

Vol. 345: Huang, D.-S.; Li, K.; Irwin, G.W. (Eds.)
Intelligent Computing in Signal Processing
and Pattern Recognition
1179 p. 2006 [978-3-540-37257-8]

Vol. 344: Huang, D.-S.; Li, K.; Irwin, G.W. (Eds.)
Intelligent Control and Automation
1121 p. 2006 [978-3-540-37255-4]

Vol. 341: Commault, C.; Marchand, N. (Eds.)
Positive Systems
448 p. 2006 [978-3-540-34771-2]

Vol. 340: Diehl, M.; Mombaur, K. (Eds.)
Fast Motions in Biomechanics and Robotics
500 p. 2006 [978-3-540-36118-3]

Vol. 339: Alamir, M.
Stabilization of Nonlinear Systems Using
Receding-horizon Control Schemes
325 p. 2006 [978-1-84628-470-0]

Vol. 338: Tokarzewski, J.
Finite Zeros in Discrete Time Control Systems
325 p. 2006 [978-3-540-33464-4]

Vol. 337: Blom, H.; Lygeros, J. (Eds.)
Stochastic Hybrid Systems
395 p. 2006 [978-3-540-33466-8]

Vol. 336: Pettersen, K.Y.; Gravdahl, J.T.; Nijmeijer, H. (Eds.)
Group Coordination and Cooperative Control
310 p. 2006 [978-3-540-33468-2]

Vol. 335: Kozłowski, K. (Ed.)
Robot Motion and Control
424 p. 2006 [978-1-84628-404-5]

Vol. 334: Edwards, C.; Fossas Colet, E.; Fridman, L. (Eds.)
Advances in Variable Structure and Sliding Mode Control
504 p. 2006 [978-3-540-32800-1]

Vol. 333: Banavar, R.N.; Sankaranarayanan, V.
Switched Finite Time Control of a Class of Underactuated Systems
99 p. 2006 [978-3-540-32799-8]

Vol. 332: Xu, S.; Lam, J.
Robust Control and Filtering of Singular Systems
234 p. 2006 [978-3-540-32797-4]

Vol. 331: Antsaklis, P.J.; Tabuada, P. (Eds.)
Networked Embedded Sensing and Control
367 p. 2006 [978-3-540-32794-3]

Vol. 330: Koumoutsakos, P.; Mezic, I. (Eds.)
Control of Fluid Flow
200 p. 2006 [978-3-540-25140-8]

Vol. 329: Francis, B.A.; Smith, M.C.; Willems, J.C. (Eds.)
Control of Uncertain Systems: Modelling, Approximation, and Design
429 p. 2006 [978-3-540-31754-8]

Vol. 328: Loría, A.; Lamnabhi-Lagarrigue, F.; Panteley, E. (Eds.)
Advanced Topics in Control Systems Theory
305 p. 2006 [978-1-84628-313-0]

Vol. 327: Fournier, J.-D.; Grimm, J.; Leblond, J.; Partington, J.R. (Eds.)
Harmonic Analysis and Rational Approximation
301 p. 2006 [978-3-540-30922-2]

Vol. 326: Wang, H.-S.; Yung, C.-F.; Chang, F.-R.
H_∞ Control for Nonlinear Descriptor Systems
164 p. 2006 [978-1-84628-289-8]

Vol. 325: Amato, F.
Robust Control of Linear Systems Subject to Uncertain
Time-Varying Parameters
180 p. 2006 [978-3-540-23950-5]

Vol. 324: Christofides, P.; El-Farra, N.
Control of Nonlinear and Hybrid Process Systems
446 p. 2005 [978-3-540-28456-7]

Vol. 323: Bandyopadhyay, B.; Janardhanan, S.
Discrete-time Sliding Mode Control
147 p. 2005 [978-3-540-28140-5]

Vol. 322: Meurer, T.; Graichen, K.; Gilles, E.D. (Eds.)
Control and Observer Design for Nonlinear Finite and Infinite Dimensional Systems
422 p. 2005 [978-3-540-27938-9]

Vol. 321: Dayawansa, W.P.; Lindquist, A.; Zhou, Y. (Eds.)
New Directions and Applications in Control Theory
400 p. 2005 [978-3-540-23953-6]

Vol. 320: Steffen, T.
Control Reconfiguration of Dynamical Systems
290 p. 2005 [978-3-540-25730-1]

Vol. 319: Hofbaur, M.W.
Hybrid Estimation of Complex Systems
148 p. 2005 [978-3-540-25727-1]

Vol. 318: Gershon, E.; Shaked, U.; Yaesh, I.
H_∞ Control and Estimation of State-multiplicative Linear Systems
256 p. 2005 [978-1-85233-997-5]

Vol. 317: Ma, C.; Wonham, M.
Nonblocking Supervisory Control of State Tree Structures
208 p. 2005 [978-3-540-25069-2]

Vol. 316: Patel, R.V.; Shadpey, F.
Control of Redundant Robot Manipulators
224 p. 2005 [978-3-540-25071-5]

Vol. 315: Herbordt, W.
Sound Capture for Human/Machine Interfaces: Practical Aspects of Microphone Array Signal Processing
286 p. 2005 [978-3-540-23954-3]

Vol. 314: Gil', M.I.
Explicit Stability Conditions for Continuous Systems
193 p. 2005 [978-3-540-23984-0]

Vol. 313: Li, Z.; Soh, Y.; Wen, C.
Switched and Impulsive Systems
277 p. 2005 [978-3-540-23952-9]

Vol. 312: Henrion, D.; Garulli, A. (Eds.)
Positive Polynomials in Control
313 p. 2005 [978-3-540-23948-2]

Vol. 311: Lamnabhi-Lagarrigue, F.; Loría, A.; Panteley, E. (Eds.)
Advanced Topics in Control Systems Theory
294 p. 2005 [978-1-85233-923-4]

Vol. 310: Janczak, A.
Identification of Nonlinear Systems Using Neural Networks and Polynomial Models
197 p. 2005 [978-3-540-23185-1]

Vol. 309: Kumar, V.; Leonard, N.; Morse, A.S. (Eds.)
Cooperative Control
301 p. 2005 [978-3-540-22861-5]

Vol. 308: Tarbouriech, S.; Abdallah, C.T.; Chiasson, J. (Eds.)
Advances in Communication Control Networks
358 p. 2005 [978-3-540-22819-6]

Vol. 307: Kwon, S.J.; Chung, W.K.
Perturbation Compensator based Robust Tracking Control and State Estimation of Mechanical Systems
158 p. 2004 [978-3-540-22077-0]

Vol. 306: Bien, Z.Z.; Stefanov, D. (Eds.)
Advances in Rehabilitation
472 p. 2004 [978-3-540-21986-6]

Vol. 305: Nebylov, A.
Ensuring Control Accuracy
256 p. 2004 [978-3-540-21876-0]

Vol. 304: Margaris, N.I.
Theory of the Non-linear Analog Phase Locked Loop
303 p. 2004 [978-3-540-21339-0]

Vol. 303: Mahmoud, M.S.
Resilient Control of Uncertain Dynamical Systems
278 p. 2004 [978-3-540-21351-2]

Vol. 302: Filatov, N.M.; Unbehauen, H.
Adaptive Dual Control: Theory and Applications
237 p. 2004 [978-3-540-21373-4]

Vol. 301: de Queiroz, M.; Malisoff, M.; Wolenski, P. (Eds.)
Optimal Control, Stabilization and Nonsmooth Analysis
373 p. 2004 [978-3-540-21330-7]

Vol. 300: Nakamura, M.; Goto, S.; Kyura, N.; Zhang, T.
Mechatronic Servo System Control
Problems in Industries and their Theoretical Solutions
212 p. 2004 [978-3-540-21096-2]

Vol. 299: Tarn, T.-J.; Chen, S.-B.; Zhou, C. (Eds.)
Robotic Welding, Intelligence and Automation
214 p. 2004 [978-3-540-20804-4]

Vol. 298: Choi, Y.; Chung, W.K.
PID Trajectory Tracking Control for Mechanical Systems
127 p. 2004 [978-3-540-20567-8]